DIVERSITY OF FUNGI ASSOCIATED WITH GRAPEVINE, CHERRY AND BLUEBERRY IN CHINA

YUEYAN ZHOU

DOCTOR OF PHILOSOPHY

IN

BIOLOGICAL SCIENCE

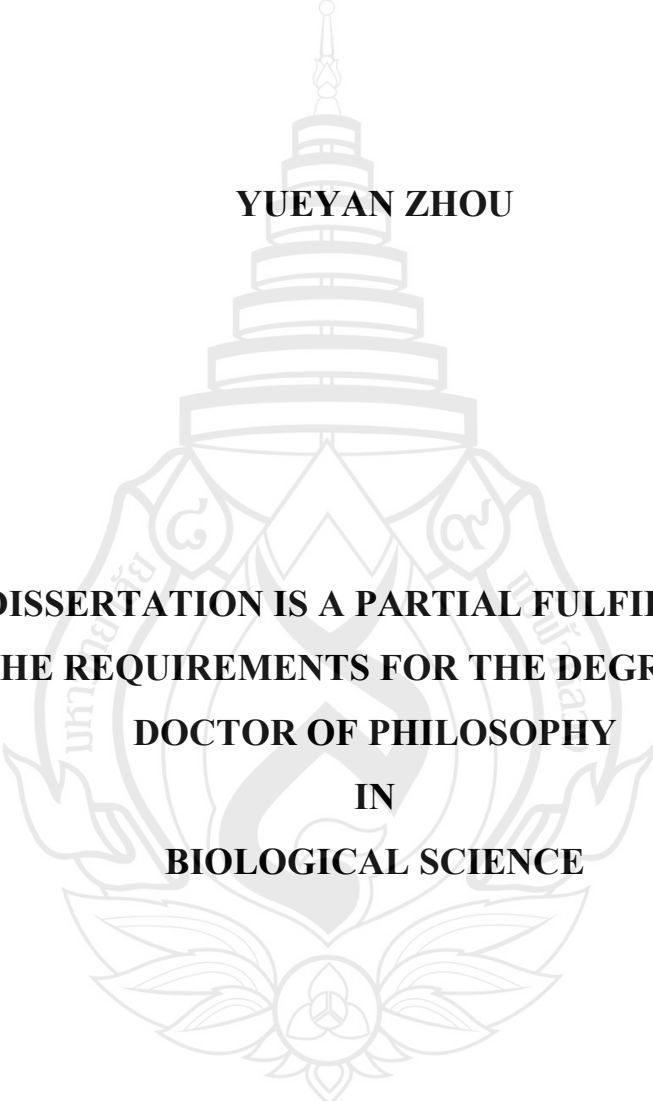SCHOOL OF SCIENCE

MAE FAH LUANG UNIVERSITY

2024

DIVERSITY OF FUNGI ASSOCIATED WITH GRAPEVINE, CHERRY AND BLUEBERRY IN CHINA

YUEYAN ZHOU

THIS DISSERTATION IS A PARTIAL FULFILLMENT OF
THE REQUIREMENTS FOR THE DEGREE OF
DOCTOR OF PHILOSOPHY
IN
BIOLOGICAL SCIENCE

SCHOOL OF SCIENCE
MAE FAH LUANG UNIVERSITY
2024

DISSERTATION APPROVAL

MAE FAH LUANG UNIVERSITY

FOR

DOCTOR OF PHILOSOPHY IN BIOLOGICAL SCIENCE

Dissertation Title: Diversity of Fungi Associated with Grapevine, Cherry and Blueberry in China
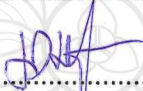
Author: Yueyan Zhou

Examination Committee:

Professor Wei Zhang, Ph. D.	Chairperson
Thilini Chethana Kandawatte Wedaralalage, Ph. D.	Member
Adjunct Professor Kevin David Hyde, Ph. D.	Member
Professor Jiye Yan, Ph. D.	Member
Mahamarakkalage Mary Ruvishika Shehali Jayawardena, Ph. D.	Member
Professor Alan John Lander Phillips, Ph. D.	Member

Advisors:

....Advisor

(Thilini Chethana Kandawatte Wedaralalage, Ph. D.)

....Co-Advisor

(Adjunct Professor Kevin David Hyde, Ph. D.)

....Co-Advisor

(Professor Jiye Yan, Ph. D.)

Dean:

....

(Professor Surat Laphookhieo, Ph. D.)

ACKNOWLEDGEMENTS

Dissertation Title   Diversity of Fungi Associated with Grapevine, Cherry and Blueberry in China

Author   Yueyan Zhou

Degree   Doctoral of Philosophy (Biological Science)

Advisor   Thilini Chethana Kandawatte Wedaralalage, Ph. D.

Co-Advisor   Adjunct Professor Kevin David Hyde, Ph. D.

Associate Professor Jiye Yan, Ph. D.

ABSTRACT

Cherry, grapevine, and blueberry are important fruit crops in China, valued for their high economic and nutritional significance. However, they are susceptible to various fungal diseases caused by multiple pathogens, which severely impact fruit production and quality, leading to significant economic losses. Although extensive research has been conducted on fungal pathogens causing these diseases, most studies have only focused on a single fungal taxon or one type of disease. Additionally, inconsistencies in identification methods and the lack of adherence to the latest fungal classification systems have led to confusing and potentially misleading results. The objectives of this study are to: (1) investigate the occurrence of important diseases affecting cherry, grapevine and blueberry across different cultivation regions in China and identify the associated fungi. This will help explore emerging and potential fungal pathogens, dominant disease-associated fungal communities, as well as the relationship between fungi, disease types and their distribution; (2) Compile fungal pathogen data by integrating results from this study with previous research, providing an updated and systematic summary that aligns with the latest fungal classification. Given their widespread occurrence and significant impact, cherry leaf spot (CLS) and grapevine trunk diseases (GTD) were selected to study their associated fungal communities; For blueberry, as emerging diseases and pathogens have been frequently reported in recent years, a comprehensive identification was conducted on fungi associated with important diseases, including fruit rot, leaf spot, stem blight and root rot. Fungal species were identified based on morphological characters and multi-locus phylogenetic analysis, and pathogenicity tests were performed on selected fungal isolates.

As a result, three *Colletotrichum* species from Beijing, seven *Fusarium* species from three provinces (including six new host records), six *Cladosporium* species from Beijing (including five new host records), as well as one *Neopestalotiopsis* and one *Diaporthe* species were identified from different symptom types of cherry leaf spot. The pathogenicity of *Colletotrichum* and *Fusarium* species was verified, and all fungal species reported as CLS pathogens were summarized. For grapevine trunk disease, forty species associated with Botryosphaeria dieback, black foot disease, and Diaporthe dieback were identified across eight provinces. These species belonged to twenty-one genera, including twelve new host records. The dominant genera included *Diaporthe*, Botryosphaeriaceae, *Cylindrocarpon*-like and *Fusarium*-like species, providing a comprehensive summary and supplementation to existing GTD studies. On blueberry, fruit rot, leaf spot, stem blight and root rot diseases were comprehensively investigated from five provinces, seven pathogens causing blueberry fruit rot were identified, and 103 species from forty fungal genera were recovered from the other three diseases. *Alternaria*, *Botryosphaeria*, *Fusarium*, *Neopestalotiopsis*, and *Pestalotiopsis* are the five most prevalent genera associated with leaf spot, stem blight and root rot, accounting for nearly 50% isolation ratio. The prevalence of the fungal genera in isolation sources and regions was preliminarily analysed. Species from the dominant genera *Neopestalotiopsis* and *Pestalotiopsis* were characterized and described, including seventeen new host records and three new species. Additionally, pathogenicity assays were conducted on seven species causing fruit rot and three species causing stem blight. Finally, a comprehensive summary of fungal pathogens associated with blueberry diseases in China was compiled. The current study is a continuation, expansion and conclusion of fungal species associated with cherry leaf spot diseases, grapevine trunk diseases and blueberry diseases in China, relevant results provide an insight into the overall occurrence of the diseases, as well as an important basis on the diagnosis and management of the diseases.

Keywords: China, Cherry Leaf Spot, Grapevine Trunk Disease, Blueberry, Pathogens, Phylogenetic Analysis, Morphological Characterization, Pathogenicity Test, Taxonomy

TABLE OF CONTENTS

TABLE OF CONTENTS

LIST OF TABLES

LIST OF FIGURES

LIST OF FIGURES

LIST OF FIGURES

LIST OF FIGURES

LIST OF FIGURES

LIST OF FIGURES

LIST OF FIGURES

CHAPTER 1

INTRODUCTION

1.1 Current Status of Cherry, Grapevine and Blueberry Cultivation in China

The cultivation of fruit crops has a long history, which can be traced back to 6000 to 3000 BCE (Janick, 2005). However, the studies on the domestication of fruit trees are much less than those on herbaceous annuals serving as food sources (Goldschmidt, 2013). Compared with annual crop plants, cultivating fruits requires more complicated technologies and long-term management (Janick, 2005). In the past decade, improvements in fruit cultivation technology have greatly accelerated the expansion of the yield of fruit crops (Rajan et al., 2021). Fruit is a good source of multiple nutrient elements, including vitamins, fibres, carbohydrates, and minerals, and can promote physical fitness in humans by reducing the risk of diseases and delaying senescence (Vicente et al., 2009).

Cherry (*Prunus*, Rosaceae) is native to Europe and Asia regions with more than 2,000 years of cultivation history and is currently an economically important fruit widely cultivated in temperate and subtropical regions of the Northern Hemisphere (Blando & Oomah, 2019; Song et al., 2024). In the past two decades, global cherry production has grown by 37% (Vignati et al., 2022). Among more than 50 species of cherry, *Prunus avium* (sweet cherry), *P. cerasus* (sour cherry), *P. pseudocerasus* (Chinese cherry) and *P. tomentosa* (Nanking cherry) are the most commonly consumed edible species, which are used for fresh eating and processed into products, such as jam, juice and dried fruits (Cao et al., 2015; Song et al., 2024). Sweet cherry (*Prunus avium* L.) is one of the most widely consumed and popular cherry species, known for its bright appearance, delicious taste, and high nutritional value. Sweet cherry is rich in essential nutrients and bioactive components, including vitamin C, fibre, minerals and polyphenols, which contribute to its anti-oxidant and anti-inflammatory properties. Additionally, sweet cherry consumption has been linked to a reduced risk of

cardiovascular diseases, diabetes, and cancer (Kelley et al., 2018). In recent years, sweet cherry production in China has grown rapidly, making the country the world's largest producer (Zhang et al., 2024a). As of 2021, the total area of sweet cherry plantations in China reached 233,334 ha, with an annual yield of 1,600,000 tons. The main production regions include Shandong, Liaoning, Shaanxi, Henan, Shanxi, Sichuan, Gansu, Hebei, and Beijing (Zhang et al., 2024b). Currently, 30 to 50 main cultivars are grown in China, such as 'Hongdeng', 'Tieton', 'Summit', 'Brooks', 'Lapins' and 'Sunburst'; and over 50 to 60 new cultivars are being tested or promoted (Zhang, 2017; Zhang et al., 2024b).

Grapevine (*Vitis* spp.) is a perennial climbing plant in the Vitaceae. Among more than 100 described species, *Vitis vinifera* L., known as the common grapevine, is the most widely planted species for its edible fruit. Other species, such as *V. rupestris*, *V. riparia* and *V. berlandieri*, are primarily used as breeding rootstock due to their resistance to pathogens (Terral et al., 2010; Gramaje et al., 2018). Grapevine is one of the longest-domesticated fruit crops, dating back to 6000 BCE in regions, including Iran, the Caucasus and Anatolia, before spreading throughout the Near East and Europe. Vine growing and winemaking have long been symbolic of human societies and civilizations (Limier et al., 2018). Nowadays, grapevines are widely cultivated in temperate and subtropical regions around the world (Terral et al., 2010). There are 6,000–10,000 different grapevine cultivars, but only 400 hold economic and commercial significance (Limier et al., 2018; Vignani & Scali, 2024). In 2022, the global vineyard area reached 7.3 million ha, with grape production totalling 80.1 million tons. Of this, 50% was used for wine production, 42% for table grapes, and 7% for dried grapes. Spain, France, China, Italy and Turkey are the top five grape-cultivation countries (OIV, 2023). Grapevine cultivation and the wine industry in China have developed rapidly over the past 30 years. Grapevines are currently cultivated in more than 20 provinces and municipalities in China, with the main production concentrated in Xinjiang, Shandong, Liaoning, and Hebei Provinces (Li et al., 2015). Among grape-cultivation countries, China ranks third in cultivation area of 785 Kha and ranks first in annual grape production, reaching 15 million tons (OIV, 2023).

Blueberry (*Vaccinium* spp.), a perennial shrub of the family Ericaceae, has been cultivated for more than 100 years. Commercial varieties of blueberry mainly include

highbush (*Vaccinium corymbosum*), lowbush (*Vaccinium angustifolium*) and Rabbiteye (*Vaccinium virgatum*) (Edger et al., 2022). Blueberries are recognized as a "superfruit" for their rich nutrients, including vitamins (C and K), minerals (calcium, iron, magnesium, manganese and zinc), dietary fibre (2.4–3.5% of fruit weight) and polyphenols (anthocyanins and flavonols) (Krishna et al., 2023). Specifically, anthocyanin flavonoids, which account for up to 60% of the total polyphenolics in ripe blueberries, may make the greatest contribution to the health benefits of blueberry in reducing risk of cardiovascular disease, death, and type 2 diabetes, as well as improving weight maintenance and neuroprotection (Kalt et al., 2020). The blueberry industry has developed rapidly in recent years, with global production more than doubling in the past decade (U.S. Department of Agriculture, 2021). According to the data issued by the International Blueberry Organization (2024), the global area for blueberry cultivation reached 262,417 hectares in 2023, with a total production of 1.78 million tons. China has been the top producer of blueberries in the world, with 77,641 hectares of growing area and 0.56 million tons of production, followed by the United States, Peru, Chile, and Canada. Blueberry was first introduced into China in the 1980s and is now planted in 26 out of 34 provinces, mainly distributed in the Northeast, Shandong province, Southeast, and Southwest of China (Yu et al., 2012; USDA, 2023).

Due to their contribution to the economy, cherries, grapevines, and blueberries are important fruit crops in China. The quality and nutrient composition of fruits are highly dependent on environmental conditions and agricultural practices, including fertilization, irrigation, and weed and pest control. Good management techniques are crucial to the sustainable development of the fruit industry (do Nascimento Nunes, 2008; Askari-Khorasgani et al., 2019; Yuan et al., 2022).

1.2 Plant Diseases and Fungal Identification

1.2.1 An Overview of Plant Diseases and Fungal Pathogens

Plants can be affected by diseases throughout their life cycle and on all parts of their organs. Of the 36.5% global total losses caused by diseases, insects, and weeds in crop production, 14.1% are caused by diseases. Plant diseases are divided into non-

infectious diseases caused by abiotic factors (such as drought, salinity, heat, cold and nutrient stress) and infectious diseases caused by biotic factors (such as fungi, bacteria, viruses and nematodes) (Atkinson & Urwin, 2012; Oliver, 2024).

As an important group of plant pathogens, fungi have a huge impact on agricultural production. There were numerous examples of severe damage caused by fungi and fungus-like organisms throughout history. The Irish Potato Famine in the 1840s, widely regarded as one of the most devastating historical events, resulted in the deaths of approximately one million individuals and forced an equal number to flee their homeland. The trigger of the disaster is potato late blight caused by *Phytophthora infestans* (Oomycetes) (Turner, 2005). Coffee rust caused by *Hemileia vastatrix* is the most destructive disease of coffee; its outbreak in 1869 in Ceylon (now Sri Lanka) destroyed Ceylon's coffee industry, forcing planters to grow tea instead (McCook & Vandermeer, 2015). Fusarium wilt on bananas, also known as Panama disease, is caused by *Fusarium oxysporum* f. sp. *cubense*. The disease destroyed 40,000 ha of the cultivar Gros Michel in Central America from the 1890s to the 1950s (Pérez-Vicente et al., 2004). Currently, around 8,000 species of fungi have been reported to cause plant diseases, affecting trees, shrubs, grasses, cereals, vegetables, and fruit crops. These pathogens can lead to 30–40% of crop losses, amounting to hundreds of billions of dollars annually (Xu, 2022). Given that fungal pathogens continue to pose a significant threat to plant biodiversity, crop production and food security, it is essential to adopt strategies, such as disease surveillance, disease-resistant breeding, improved agricultural practice, and international research collaboration (Fisher et al., 2020).

1.2.2 Common Diseases of Fruit Trees and Related Pathogens

Fungal diseases could occur on any part of the fruit trees, including the leaves, trunks (stems), roots, flowers and fruits. Some are grouped according to the plant organ they affect and symptoms they cause, such as leaf spots, blights, wilts and root rots; and some have specific names like grey mould caused by *Botrytis cinerea*, and anthracnose caused by *Colletotrichum* spp. (Dean et al., 2012; Oliver, 2024). Diseases of fruits directly influence the quality and the yield of fruits. For example, Botrytis fruit rot or grey mould is one of the most common and destructive diseases on many fruit crops such as strawberry, pear, kiwifruit, grape and blueberry, causing decay of fruits at both preharvest and postharvest stages, leading to 20–50% loss in severe case (Dwivedi et

al., 2024). Brown rot caused by *Monilinia* spp. also affects a wide range of fruits, especially *Prunus,* including almond, cherry, peach and plum, resulting in 1.7 thousand million Euro in economic loss annually (Lino et al., 2016). Moreover, post-harvest diseases of fruits also represent a significant challenge, contributing up to 50% of global fruit losses annually. *Botrytis cinerea*, *Alternaria alternata*, *Colletotrichum* spp. and *Penicillium* spp. are common fungal pathogens (Pétriacq et al., 2018).

Though diseases on fruits were studied more extensively, diseases on other organs cannot be overlooked and even have more profound implications. Foliar diseases, such as leaf spots, leaf blights, leaf rust, downy mildew and powdery mildew, are caused by various fungal species depending on the host (Jain et al., 2019). The leaf damages cause a reduction in photosynthesis and carbohydrate production, resulting in indirect yield loss (Roloff et al., 2007; Jermini et al., 2010; Gruber et al., 2012). Trunk diseases cause symptoms, such as blights, cankers, dieback, gummosis and wood rotting, leading to tree death in severe cases (Guarnaccia et al., 2023). Their causal agents mainly belong to Botryosphaeriaceae, Calosphaeriaceae, Cytosporaceae, Diaporthaceae, Diatrypaceae, Nectriaceae and Togniniaceae (Martino et al., 2024). Root diseases caused by various fungi (especially *Fusarium* and *Rhizoctonia*) and Oomycetes (especially *Pythium* and *Phytophthora*) threaten various fruits. For being underground, they are often difficult to detect in the early stages, but when aboveground parts appear to have symptoms, it may be too late to recover (Williamson-Benavides & Dhingra, 2021). In practical field conditions, symptoms induced by a pathogen are usually not confined to a specific organ, such as anthracnose caused by *Colletotrichum* presents symptoms on both leaves and fruits, and *Fusarium* can cause fruit rot, leaf spots and crown rot (Fu et al., 2019; Zakaria 2023).

Whether pome fruits (such as apples and pears), stone fruits (such as peaches, plums, and cherries), berry fruits (such as blueberries and cranberries), grapevine, citrus or mangoes, all fruit crops are susceptible to various fungal diseases. The severity of these diseases depends on factors such as host susceptibility and environmental conditions (Pétriacq et al., 2018; Jain et al., 2019; Williamson-Benavides & Dhingra, 2021; Martino et al., 2024). Effective management practices are essential to protect crops from infections, and disease resistance remains one of the main considerations in breeding programs (El-Baky & Amara, 2021).

1.2.3 Complexities of Plant-Associated Fungal Pathogens

1.2.3.1 Undetermined number. The global number of fungal species is estimated to be 2.5 million, though the exact number of plant fungal pathogens remains undetermined (Hyde et al., 2024). Some pathogens can be directly observed on the surface of plants with the naked eye or under a microscope, while most are located inside the plants and need to be examined at the margins of the affected tissues or the vascular tissues (Oliver, 2024).

1.2.3.2 Mixed infections. In the field, the occurrence of some diseases is often caused by the co-infection of multiple pathogens rather than a single pathogen, which can influence the course and severity of the disease (Abdullah et al., 2017). These factors contribute to the challenges of disease diagnosis under practical field conditions. Misdiagnosis and inaccurate identification of pathogens can result in inappropriate control measures, leading to economic loss, environmental disruption and development of resistant pathogen strains (Crous et al., 2015; Srinidhi et al., 2021). Therefore, it is crucial to properly identify the disease and the causal agents.

1.2.3.3 Life mode transfer and latent infection. Among the diverse fungi associated with plants, phytopathogens represent a relatively small proportion, while others function as endophytes or saprobes. Most endophytic fungi colonizing plants can protect their hosts by promoting plant growth and activating systemic resistance. Saprobes are typically decomposers that live on dead organic matter without causing any disease (Carris et al., 2012; Akram et al., 2023). However, some endophytes could switch to pathogens under certain conditions, such as environmental stress and host senescence or host shift (Hrycan et al., 2020; Bhunjun et al., 2024). For example, some strains of *Fusarium oxysporum* cause wilt disease on plant hosts, while others grow asymptomatically as endophytes or even enhance host resistance to other fungal pathogens (Redkar et al., 2022). Several fungi associated with grapevine trunk diseases, such as Botryosphaeria dieback, were also detected in asymptomatic grapevines, suggesting that some of these fungi may act as latent pathogens in grapevines, with their activity influenced by abiotic or biotic triggers and initial inoculum concentrations (Hrycan et al., 2020). Based on various evidence, Bhunjun et al. (2024) proposed that an endophytic lifestyle is a common strategy in most fungi, and some pathogens also have endophytic ancestors. Lifestyle switches also occur between pathogens and

saprobes. Most pathogenic fungi can survive on dead plant material as saprobes to overwinter, becoming the primary inoculum when environmental conditions are suitable for infection; some opportunistic species, also known as facultative pathogens, survive as saprobes on dead organic matter, but can also infect living organisms (Sharon & Shlezinger, 2013; Jayawardena et al., 2018). Hofstetter et al. (2012) also hypothesised that the fungal pathogens associated with esca disease, a significant threat to grapevine, are likely saprobes that accelerate the decay of senescent or dead wood caused by intensive pruning, frost or other mechanical injuries like grafting.

To sum up, the identification, infection mechanism and interactions between disease-associated fungi are complicated. Comprehensive identification of disease-associated fungi (all fungi generated from diseased plant tissues) is a necessary basis for further research on the diagnosis, epidemiology, disease mechanism, and biocontrol strategies of the plant disease.

1.2.4 Research Advances on Fungal Identification

Scientific names are crucial in studying fungi, including their ecology, applications, threats, and conservation (Cheek et al., 2020). In plant pathology, identifying and naming fungi is fundamental for determining the causal agents of disease and understanding their biology, distribution, host range, potential risk and control strategies (Crous et al., 2015; Manawasinghe et al., 2021). However, fungi remain largely unexplored due to the challenges in research, including their cryptic lifestyles, deficiency in discriminative morphological characters, and the frequent occurrence of convergent evolution. Current estimates suggest that over 50% of plant species have likely been identified, while more than 90% of fungi remain undiscovered (Cheek et al., 2020).

Traditionally, the identification of pathogenic fungi was based on morphology and host associations. However, overlapping morphological characteristics, separate names for sexual and asexual morphs, and ambiguous relationships between fungi and hosts led to species delimitation often indistinguishable and confusing (Jayawardena et al., 2021). With the development and application of DNA sequencing technology, molecular phylogenetics is gradually popularized to assess species boundaries, which resolve the cryptic species, and link asexual and sexual morphs of the same fungus, and phylogenomics derived from genomic data further advanced species delimitations and

higher-level classifications (Chethana et al., 2021; Hyde et al., 2024). In spite of this, phylogeny sometimes also has limitations that lead to misleading and inaccurate inferences. A polyphasic approach combining biology, ecology, morphology and phylogeny is necessary for species definition (Chethana et al., 2021).

1.2.5 The Relationship Between Fungal Taxonomy and Pathogenic Fungal Identification

Most phytopathogenic fungi are ascomycetes, and many of them are pleomorphic, which means that the fungi have both sexual and asexual states. In the mid-nineteenth century, people became aware of the phenomenon that different morphs of the same fungal species existed. To resolve the complex situation, a dual nomenclature system was established. Independent names were assigned to different morphs, such as *Diaporthe* (sexual) and *Phomopsis* (asexual), *Gibberella* (sexual) and *Fusarium* (asexual), and *Glomerella* (sexual) and *Colletotrichum* (asexual) (Wingfield et al., 2012; Jayawardena et al., 2021). Over the past two decades, the rapid advancement of molecular techniques has provided unprecedented insights into fungal taxonomy and systematics. However, the chaos and confusion caused by dual nomenclature led to increasing debate, eventually prompting taxonomists to consider abandoning the dual system. Since January 1st, 2013, the "one fungus-one name" rule was implemented, meaning only one name would be adopted for each fungal species (Wingfield et al., 2012; Manawasinghe et al., 2021). Most names are selected based on priority, such as *Fusarium* over *Gibberella*, and *Diaporthe* over *Phomopsis* (Rossman et al., 2013; Rossman et al., 2015). However, some younger but more commonly used names are exceptions, such as *Colletotrichum* over *Glomerella* (Jayawardena et al., 2021).

Due to the different areas of focus and expertise, plant pathologists sometimes find the ongoing changes in fungal taxonomy confusing. They face challenges in identifying and naming pathogenic fungi according to the latest classifications, while also trying to link scientific names to prior knowledge that is more familiar and acceptable to farmers or researchers working at the frontline dealing with plant pathogens (Crous et al., 2015; Manawasinghe et al., 2021). Two typical examples are as follows:

1. New pathogen name with old disease name. According to the "One fungus, one name" principle, *Diaporthe* takes precedence over *Phomopsis* by publication date (Rossman et al., 2015). However, many *Diaporthe* species were previously widely known as *Phomopsis* in books and literature (Udayanga et al., 2011; Oliver, 2024). Both *Diaporthe* (1309 epithets) and *Phomopsis* (983 epithets) have a huge number of epithets listed in Index Fungorum (https://indexfungorum.org/Names/Names.asp, Accessed in March 2025). Currently, diseases caused by *Diaporthe*, such as leaf spot, blight, and canker, are still commonly known as Phomopsis blight/ stem canker/ cane and leaf spot (Fedele et al., 2024; Goutam et al., 2024; Underwood & Misar, 2024). In addition, some *Phomopsis* species, such as *Phomopsis asparagi* and *Phomopsis longanae*, have not transferred to *Diaporthe*, which are still legitimate (Sun et al., 2024; Zheng et al., 2025).

2. Wider use of old fungal names in some pathogens. Apple Valsa canker is a devastating disease of apple around the world, which was first reported more than 100 years ago. *Valsa mali* is the dominant pathogen responsible for causing severe tree branch deaths and significant yield losses (Feng et al., 2023). Though *Valsa* is now classified under *Cytospora* based on the priority of the latter (Rossman et al., 2015), due to its long history and substantial impact, most research on the mechanisms and control of the pathogen still uses the name *Valsa mali* (Meng et al., 2024; Li et al., 2025). Additionally, some plant pathologists have discussed the conflict between the well-known name of the pathogen and its identity transformation under the "One Fungus = One Name" system (Wang et al., 2020).

Despite these challenges, given the trends toward comprehensive development of fungal research, the "One Fungus = One Name" rule serves as a simple, accurate, and efficient standard for fungal nomenclature (Hyde et al., 2024). In plant pathology, using the correct name is essential for disease diagnosis, quarantine and management, which further contributes to guaranteeing biosecurity, supporting international trade, and advancing scientific research (Jayawardena et al., 2021).

In conclusion, plant diseases represent an inevitable challenge throughout the life cycle of crops. As economically important fruit crops in China, cherry, grapevine and blueberry are subjected to various fungal pathogens, exhibiting both diversity and complexity. The identification methods and classification standards of fungal pathogens have undergone numerous changes and continue to evolve. It is crucial to understand both the disease characteristics and the organism's taxonomy. Polyphasic approaches, particularly

involving morphological characters and phylogenetic analysis, are necessary for accurate identification. Additionally, biological and ecological factors, such as host and geographical distribution, should also be considered in the identification process.

1.3 Fungal Diseases of Cherry, Grapevine and Blueberry

1.3.1 Fungal Diseases and Pathogens of Cherry

In the previous research, common fungal diseases on cherry include anthracnose (caused by *Colletotrichum* spp.), black knot (caused by *Apiosporina* spp.), brown rot (caused by *Monilinia* spp.), canker (caused by *Cytospora* spp.), crown and root rot (caused by *Armillaria* spp. and *Fusarium* spp.), fruit rot (caused by *Alternaria* spp., *Penicillium* spp., *Cladosporium* spp. and *Botrytis* spp.), leaf spot (caused by *Blumeriella* spp.) and powdery mildew (caused by *Podosphaera* spp.) (Uyemoto, 2018). In China, cherry leaf spot (Chethana et al., 2019), grey mould (Yin et al., 2018), and trunk disease (Chen et al., 2023a) are common fungal diseases, and other diseases occasionally occur under some conditions. Grey mould disease is particularly severe under greenhouse conditions and during storage, especially in high-humid environments (Elad, 2016). Other fruit diseases, such as brown rot caused by *Monilia* spp. and fruit rot caused by *Sclerotinia sclerotiorum,* were also reported in China (Ruan et al., 2023; Zhao et al., 2023). Trunk diseases on cherry were recognized to be caused by *Botryosphaeria dothidea*, known as gummosis disease (Zhang et al., 2019). Chen et al. (2023) found that *Diaporthe* species also cause branch dieback and gummosis on cherry. Due to its wide distribution in most cherry-growing areas worldwide, cherry leaf spot has been getting more attention in China in recent years. Though *Blumeriella jaapi* is regarded as the causal agent of leaf spot disease in America and Europe (Holb, 2009), the reported pathogens in China are different, which are mainly *Pruniphilomyces circumscissus* (=*Passalora circumscissa*), *Colletotrichum* spp. and *Alternaria* spp. (Chethana, 2019; Sun et al., 2022). The disease causes early defoliation, and in severe cases, eventual death of the tree (Ellis, 2016). Therefore, it is of great significance to identify the main types and pathogens of cherry leaf spot disease in order to maintain sustainable and safe cherry production in China.

1.3.2 Fungal Diseases and Pathogens of the Grapevine

Among numerous reports of grapevine diseases caused by fungi and Oomycetes, anthracnose, bitter rot, Botrytis bunch rot and blight, downy mildew, powdery mildew, Phomopsis cane and leaf spot, ripe rot, white rot, and grapevine trunk diseases occur in most grapevine cultivation regions (Wilcox et al., 2015). Some diseases are caused by common pathogens worldwide, such as downy mildew by *Plasmopara viticola* (Boso et al., 2014), black rot by *Guignardia bidwellii* (Szabó et al., 2023), and bunch rot and blight by *Botrytis cinerea* (Steel et al., 2013), while others are caused by various pathogens in different countries. For example, grapevine anthracnose is usually known to be caused by *Elsinoe ampelina*, while anthracnose was also found to be caused by *Colletotrichum* species with different symptoms in China (Yan et al., 2015; Li et al., 2021). *Coniella vitis* was the main pathogen of white rot in China rather than *Coniella diplodiella*, which was considered to be the causal agent previously (Chethana et al., 2017; Ji et al., 2021). Unlike other diseases caused by specific pathogens, grapevine trunk diseases are a group of diseases caused by multiple fungal pathogens (Mondello et al., 2018). Grapevines can be affected by one or more trunk diseases simultaneously, including Esca complex, Eutypa dieback, Botryosphaeria dieback, black foot and Phomopsis (Diaporthe) dieback caused by different pathogens belonging to *Botryosphaeriaceae, Diaporthe, Cylindrocarpon*-like fungi and others (Gramaje et al., 2018). Field symptoms have become complex due to the mixed infections caused by different pathogens (Patanita et al., 2022). Grapevine trunk diseases have become a huge threat to the sustainable development of the viticulture and viniculture industries, resulting in reduced yields and limited vineyard lifespans (Hrycan et al., 2020).

1.3.3 Fungal Diseases and Pathogens of Blueberry

As for blueberry diseases, fungal diseases also occur on the whole plants, including fruit rots caused by *Alternaria, Colletotrichum, Botrytis, Diaporthe* and *Phyllosticta* species, Armillaria root rot caused by *Armillaria*, stem blight and dieback caused by Botryosphaeriaceae and pestalotioid fungi, twig blight caused by *Gibbera* and *Diaporthe*, stem canker caused by *Botryosphaeriaceae, Fusicoccum, Gloeosporium, Diaporthe* and *Septoria* taxa, Botrytis blossom blight caused by *Botrytis* spp., Cylindrocladium rot caused by *Calonectria* spp., leaf spot caused by pestalotioid fungi, *Alternaria, Exobasidium, Septoria* and *Phyllosticta* taxa, and Powdery mildew caused by *Erysiphe* spp. (Araujo et

al., 2023; Polashock et al., 2017; Santos et al., 2022). In China, stem blight, dieback, or canker of blueberry have been frequently observed, as well as leaf spot and fruit rot (Li et al., 2023a; Zhao et al., 2022; Zheng et al., 2023). Pestalotioid fungi and Botryosphaeriaceae species are the causal agents of stem blight and leaf spot (Zhao et al., 2022; Zheng et al., 2023). *Diaporthe* has been reported to cause stem canker, leaf spot and post-harvest rot (Lai et al., 2023; Li et al., 2023b; Yu et al., 2018). Additionally, *Fusarium* species have been reported to cause root rot (Li et al., 2023c). Other common fungal pathogens, such as *Botrytis*, *Calonectria*, *Cylindrocladium* and *Nigrospora*, were also reported on blueberries in China (Luan et al., 2006; Zhang et al., 2019; Chen et al., 2023b; Li et al., 2023a).

1.4 Research Objectives

1.4.1 To investigate the occurrence of diseases of cherry, blueberry and grapevine across different cultivation regions in China

1.4.2 To identify the micro-fungi associated with the main diseases based on morphology and phylogeny analyses

1.4.3 To determine the pathogenic potential of selected fungi through inoculation experiments to assess their impact on crop health

1.4.4 To speculate the relationship between fungi, disease symptoms, isolation source and cultivation region.

1.5 Research Contents

This thesis is divided into five chapters:

Chapter 1 is the general introduction, which provides a comprehensive background on the current status of cherry, grapevine and blueberry cultivation. It presents an overview of plant diseases and fungal pathogens, highlighting the impact of plant diseases, main disease types affecting fruit trees, complexities of fungal pathogen identification, as well as fungal classification from both plant pathology and taxonomy aspects. Additionally, it offers a brief introduction to fungal diseases and pathogens associated with cherry, grapevine and blueberry.

Chapter 2 details the material and methodology used in this study, including field investigations, sample collection and fungal isolation. It also covers DNA extraction, PCR amplification and sequencing, followed by phylogenetic analyses. Additionally, the chapter describes the morphological characterization of fungal isolates and pathogenicity tests conducted on leaves, stems and fruits.

Chapter 3 investigates and identifies fungal species associated with cherry leaf spot disease in China. This verifies the primary *Colletotrichum* species responsible for leaf anthracnose and reports two newly identified types of cherry leaf spot related to *Fusarium* and *Cladosporium*. Additionally, a new host record on cherry, *Neopestalotiopsis rosae*, was described; and the new species *Diaporthe beijingensis* was introduced. Finally, it provides a summary of fungal species associated with cherry leaf spot diseases worldwide.

Chapter 4 provides a comprehensive identification of fungal species associated with grapevine trunk disease across eight provinces in China. It provides the details of the disease symptoms, fungal species, along with their isolation sources, geographical distribution, global records, as well as taxonomic descriptions. Finally, the dominant fungal genera in this study, the distribution of species, and the roles of different fungal groups in the grapevine are discussed.

Chapter 5 presents a comprehensive study on main fungal diseases (fruit rot, leaf spot, stem blight and root rot) of blueberry and associated fungal groups, which provides a list of fungal species recorded on blueberry in this study, the distribution of fungal genera, taxonomy description on important species, and pathogenicity tests on selected fungal species. A list of fungal species associated with blueberry diseases in China is also provided.

Chapter 6 summarizes the key findings of the study, highlighting the major discoveries and research advancements. It also provides recommendations for future research directions in the study of fungal pathogens associated with cherry, grapevine, and blueberry diseases.

CHAPTER 2

MATERIAL AND METHODS

2.1 Field Investigation, Sample Collection and Fungal Isolation

Fungal diseases were investigated at orchards in major cultivation regions in China. Cherry leaf spot disease samples were collected from Beijing, Shandong and Liaoning. Grapevine trunk disease samples were collected from Beijing, Fujian, Hebei, Hubei, Ningxia, Shaanxi, Shanxi and Yunnan. Blueberry disease samples were collected from Fujian, Guizhou, Heilongjiang, Jilin and Liaoning (Figure 2.1).

Figure 2.1 Collection site of cherry, grapevine and blueberry samples in China

Field symptoms of the main diseases were recorded and photographed, and samples with typical symptoms were collected in zip-lock bags with information labels (collection site, variety, temporary sample number). Samples were kept in the box with an ice bag and the stems of leaf samples were wrapped with wet tissue to preserve

moisture. After being brought to the laboratory, leaf and fruit samples were kept in the fridge, wood samples were kept in a cool place, and all samples were processed within 48 h in case the growth of saprobes.

Before isolation, photos of systemic and local symptoms (including section views of wood samples) of the samples were also taken in the lab for further studies. Lesions on samples were checked through the stereomicroscope Nikon SMZ1500 (Nikon, Japan). If fungal spore masses or fruiting bodies were observed on the surface of the lesion, they were picked or scraped using sterile needles to make slides or spore suspensions. Prepared slides were checked using the Nikon E200 compound microscope (Nikon, Japan) to preliminarily speculate the taxa of fungi according to the micromorphology, such as spore characters. If spores are in sufficient quantity, single spore isolation was conducted. Spores were suspended in sterile water, adjusted the concentration to around 1×10^4 spores/mL, and 80–100 mL suspension was added on the surface of water agar (WA) plates and evenly spread. Germinated spores were picked up with a sterilized needle and transferred onto fresh PDA plates. If few spores were observed or no spores in fruiting bodies, diseased samples were kept in high humidity to induce sporulation. For samples without spores and fruiting bodies on the lesion surface, tissue isolation was conducted. Tissues from the junction between diseased and healthy areas were cut into small pieces (5×5 mm) with sterilized scissors or blades, surface sterilized using 75% alcohol for 30 s and 2% NaClO for 2 min, and rinsed three times in sterile water. After drying on the sterilized filter paper, tissues were transferred onto potato dextrose agar (PDA) plates and incubated at 25°C. After 3–5 days of inoculation, colonies with different morphologies were counted, and the hyphal tips of selected colonies were transferred onto fresh PDA plates. After sporulation, single spore isolation was performed using the method mentioned earlier. For some non-sporulating isolates, single hyphae tip isolation was performed, and near-ultraviolet light and plant tissue (pine needle or host tissue) were also used to induce sporulation (Su et al., 2012). Pure cultures were preserved on PDA slopes at 4°C. All isolates obtained in this study were deposited in the culture collection of the Institute of Plant Protection, Beijing Academy of Agriculture and Forestry Sciences (JZB), China. Dry cultures of new species and new geographic or host records were deposited

in the herbarium of the Institute of Plant Protection, Beijing Academy of Agriculture and Forestry Sciences (JZBH), China.

2.2 DNA Extraction, PCR Amplification and Sequencing

Purified isolates were cultured on PDA plates for seven days at 25°C. Fresh mycelia grown on PDA plates were collected into 1.5 mL centrifuge tubes (500 mg), and genomic DNA was extracted using the CTAB (cetyltrimethylammonium bromide) method (Udayanga et al., 2012) or TIANcombi DNA Lyse and Det PCR Kit (Tiangen Biotech Co., Ltd., Beijing, China). Polymerase chain reactions (PCR) were performed in C1000 TouchTM Thermal Cycler to amplify different gene regions with the primers shown in Table 2.1: internal transcribed spacer region (ITS), partial translation elongation factor 1-alpha (*tef1*), β-tubulin (*tub2*), RNA polymerase II second largest subunit (*rpb2*), 28S large subunit of nuclear ribosomal RNA (LSU), histone H3 (*his3*), actin (*act*), calmodulin (*cal*), glyceraldehyde 3-phosphate dehydrogenase (*gapdh*), chitin synthase (*chs*) and heat shock protein 60 (*hsp60*). The 50 mL volume of the PCR mixture includes 44 mL of 1×Taq PCR Mix (TransGen Biotech, Beijing, China), 2 mL of each forward and reverse primer (Sangon Biotech, Shanghai, China), and 2 mL of DNA template. The PCR conditions were as follows: initial denaturation for 3 min at 95°C, followed by 34 cycles of denaturation for 30 s at 95°C, annealing for 30 s, 1 min elongation at 72°C, and final extension for 10 min at 72°C. The annealing temperatures for different primers were noted in Table 2.1. The PCR products were examined in 1.5% agarose gel under UV light after staining with ethidium bromide and sequenced at SinoGenoMax Co., Ltd. (Beijing, China). Chromatograms of generated sequences were checked with BioEdit 7.0.9.0 to confirm sequence quality. Eligible sequences of the internal transcribed spacer (ITS) region were compared with sequences in GenBank of the National Centre for Biotechnology Information (NCBI) using the BLAST tool (https://blast.ncbi.nlm.nih.gov/Blast.cgi). Other gene loci were then amplified according to the resulting genus.

Table 2.1 Primers and their annealing temperatures, with sequences and references

Locus	Primer	Sequence (5'–3')	Annealing temperature (°C)	References
ITS	ITS5	GGAAGTAAAAGTCGTAACAAGG	58	White (1990)
	ITS4	TCCTCCGCTTATTGATATGC		
tef1	EF1-728F	CATCGAGAAGTTCGAGAAGG	54	Carbone and
	EF1-986R	TACTTGAAGGAACCCTTACC		Kohn (1999)
	EF1-688F	CGGTCACTTGATCTACAAGTGC	54	Alves et al.
	EF1-1251R	CCTCGAACTCACCAGTACCG		(2008)
	EF1-983F	GCYCCYGGHCAYCGTGAYTTYAT	54	Rehner and
				Buckley (2005)
	EF1-2218R	ATGACACCRACRGCRACRGTYTG		
	EF1	ATGGGTAAGGARGACAAGAC	54	O'Donnell et al.
	EF2	GGARGTACCAGTSATCATG		(1998)
	EF1LLErev	AACTTGCAGGCAATGTGG	55	Jaklitsch et al.
				(2005)
tub2	Bt2a	GGTAACCAAATCGGTGCTGCTTTC	58	Glass and
	Bt2b	ACCCTCAGTGTAGTGACCCTTGGC		Donaldson
				(1995)
	T1	AACATGCGTGAGATTGTAAGT	58	O'Donnell and
				Cigelnik (1997)
rpb2	RPB2-5f	GAYGAYMGWGATCAYTTYGG	56	Reeb et al.
				(2004)
	RPB2-7Cr	CCCATRGCTTGYTTRCCCAT		Liu et al. (1999)
	RPB2Ffor	GATGATCGTGATCATTTCGG	55	Staats et al.
	RB2rev	CCCATAGCTTGCTTACCCAT		(2004)
LSU	LR5	TCCTGAGGGAAACTTCG	52	Vilgalys and
				Hester (1990)
	LROR	ACCCGCTGAACTTAAGC		Rehner and
				Samuels (1994)
	LR7	TACTACCACCAAGATCT	50	Vilgalys and
				Hester (1990)
his	CYLH3F	AGGTCCACTGGTGGCAAG	58	Crous et al.
	CYLH3R	AGCTGGATGTCCTTGGACTG		(2004)
	H3-1a	ACTAAGCAGACCGCCCGCAGG	58	Glass and
	H3-1b	GCGGGCGAGCTGGATGTCCTT		Donaldson
				(1995)
act	ACT-512F	ATGTGCAAGGCCGGTTTCGC	56	Carbone and
	ACT-783R	TACGAGTCCTTCTGGCCCAT		Kohn (1999)

Table 2.1 (continued)

Locus	Primer	Sequence (5'–3')	Annealing temperature (°C)	References
cal	CAL-228F	GAGTTCAAGGAGGCCTTCTCCC	55	Carbone and
	CAL-737R	CATCTTTCTGGCCATCATGG		Kohn (1999)
	CL1C	GAATTCAAGGAGGCCTTCT	58	Weir et al. (2012)
	CL2C	CTTCTGCATCATGAGCTGGAC		
gapdh	GDF	GCCGTCAACGACCCCTTCATTGA	54	Templeton et al.
	GDR	GGGTGGAGTCGTACTTGAGCATGT		(1992)
	gpd1	CAACGGCTTCGGTCGCATTG	58	Berbee et al.
	gpd2	GCCAAGCAGTTGGTTGTGC		(1999)
	G3PDHfor	ATTGACATCGTCGCTGTCAACGA	64	Staats et al.
	G3PDHrev	ACCCCACTCGTTGTCGTACCA		(2004)
chs-1	CHS-79F	TGGGGCAAGGATGCTTGGAAGAAG	58	Carbone and
	CHS-345R	TGGAAGAACCATCTGTGAGAGTTG		Kohn (1999)
hsp60	HSP60for	CAACAATTGAGATTTGCCCACAAG	55	Staats et al.
	HSP60rev	GATGGATCCAGTGGTACCGAGCAT		(2004)

Note The annealing temperature of EF1-728F/EF 2 is 56°C.

2.3 Phylogenetic Analysis

Reference sequences for phylogenetic analyses were downloaded from the GenBank, NCBI (National Centre for Biotechnology Information), following the relevant literature (Table 2.2). Each dataset was aligned in MAFFT v. 7 (https://mafft.cbrc.jp/alignment/server/) (Katoh et al., 2019) and manually adjusted in BioEdit v7.0.9.0. where necessary, and sequences of different gene regions were trimmed by trimAl (Capella-Gutiérrez et al., 2009), then aligned gene regions were concatenated using BioEdit v7.0.9.0.

Phylogenetic analyses of alignments were conducted using maximum likelihood (ML) and Bayesian inference (BI) analysis. The ML analyses were implemented on the combined alignment through the tool RAxML-HPC2 on XSEDE (v.8.2.12) (Stamatakis et al., 2008; Stamatakis, 2014) in the online platform CIPRES Science Gateway (https://www.phylo.org/portal2) (Miller et al., 2010). The model of evolution GTR + I + G with 1000 nonparametric bootstrapping iterations were applied. Bayesian posterior probabilities (BYPP) were evaluated using MrBayes v3.2.7 based

on the Markov Chain Monte Carlo sampling (BMCMC), and different evolutionary models were selected using MrModeltest v. 3.7. For the combined dataset, six simultaneous Markov chains were run for 2,000,000 generations and trees were sampled at every 1000th generation. The first 25% of the generated trees were discarded, and the remaining 75% was used to calculate posterior probabilities (PP) of the majority rule consensus tree (Ronquist & Huelsenbeck, 2003).

Phylogenetic trees were visualized in FigTree v. 1.4.0 (Rambaut, 2023) and edited in Microsoft Office PowerPoint 2016 and Adobe Illustrator 2020. Sequences generated in this study were deposited in GenBank.

2.4   Morphological Characterization

The morphological characteristics of each species were examined. For cultural features, mycelial discs (5 mm in diam.) were taken from the growing edge of 6-day-old cultures in triplicate, transferred to fresh plates of PDA, and incubated in the dark at 25°C. The shape, color and density of colonies were recorded. Colony colors were recorded following Rayner (1970), and colony diameters were measured. To observe micromorphological characters, isolates were cultured on PDA, carnation leaf agar (CLA) (for *Fusarium*), pine needle agar (PNA), as well as host tissues on agar (Su et al., 2012). After sporulation, the micromorphology of fungal structures was observed using Axio 506 color Imager Z2 photographic microscope (Carl Zeiss Microscopy, Oberkochen, Germany), and photographs and measurements were taken with ZEN Pro 2012 (Carl Zeiss Microscopy). Pictures were processed and combined into photo plates using Adobe Photoshop CS6 Extended (V13.1.2). Description and photo plates were provided for the new species and new records.

2.5   Pathogenicity Test

2.5.1   Cherry Leaf Spot

Pathogenicity was tested by inoculating detached leaves with spore suspension. Representative isolates of each species were cultured on PDA at 25°C until sporulation.

Tender, healthy-looking leaves of *P. avium* were collected from Tongzhou Experimental Station for Cherries, Beijing Academy of Forestry and Pomology Sciences, Beijing, China. Leaves were surface-sterilized with 75% ethanol for 30 s, rinsed three times with sterile water and air-dried on sterilized filter paper. Fungal spores produced on the cultures were collected into 1.5 mL centrifuge tubes using sterilized toothpicks. Spore suspensions were prepared in sterile water and adjusted to a concentration of 1.0×10^6 conidia/mL and determined with a haemocytometer. Spore suspensions were symmetrically inoculated on either side of the main leaf veins, with one side pierced by four small holes made with a sterile insect mounting needle (wound) and the other side remained unwound. Five leaves were inoculated for each isolate in plastic boxes maintained at 25°C and 80% relative humidity and a 12/12 h light/dark cycle. Control leaves were treated with sterilized water. Inoculated plants were maintained in a greenhouse at 25°C under a light/ dark cycle. Experiments were carried out three times. Disease incidence (%) [(symptomatic sites/total inoculated sites) × 100%] was calculated, and lesion diameters were measured after the appearance of symptoms. Data was subjected to two-way analysis of variance using the software IBM SPSS Statistics v21 to determine the significance of the differences. Means of different species from the pathogenicity test were separated using the least significant difference test at a $P = 0.05$ level. Symptoms were observed every day. Koch's postulates were confirmed by re-isolating the inoculated fungi, which were identified based on cultural and morphological characters, as well as molecular characteristics.

2.5.2 Blueberry Fruit Rot

Pathogenicity tests were conducted on detached fruits using spore suspension of representative isolates. Conidia were collected from fruiting bodies on the cultures, dispersed in sterile water, and adjusted to 1×10^6 conidia per mL using a hemocytometer, and 0.02% Tween-20 was added to increase surface activity. Fresh, healthy, and unwounded blueberry fruits were surface-disinfested in 75% ethyl alcohol for 2 min, rinsed three times with sterile water, and then air-dried on filter paper. Fruits were placed at the bottom of 9 mm petri dishes with moist filter paper and inoculated with 20 μL of conidial suspension on the fruit. The experiment was conducted on eight fruits for each isolate and repeated three times. The same amount of sterile water was dropped on the fruits as the control. Plates were placed in the plastic box covered with plastic

wrap to maintain the humidity and incubated at 25°C. Inoculated fruits were observed daily until they showed symptoms and photographed with a camera and stereomicroscope. To fulfil Koch's postulate, fungi were re-isolated from the diseased site and identified by morphological characters.

2.5.3 Blueberry Stem Blight

Pathogenicity tests were conducted on one-year-old green shoots of blueberry. One isolate from each of the three species was selected and inoculated onto fifteen shoots, respectively. Mycelium plugs (4 mm) were made by a disinfected hole puncher from the margin of a 5-day-old colony. The green shoots were cut to 30 cm in length and surface sterilized using 75% ethyl alcohol. Wounds with a 4 mm diameter and 2 mm depth were created using a hole puncher on the internode. Mycelium plugs were placed on the wounds and wrapped with sealing film. PDA plugs were used as controls. Inoculated green shoots were inserted into small pots with moist soil and incubated in the greenhouse at 25°C and 100% humidity; after 48 h, the sealing film was removed, and the humidity was maintained at 80%. Inoculation results were observed after three weeks, and lesions were photographed and measured. Koch's postulate was confirmed by re-isolating the inoculated fungus, which was identified based on morphological characters.

CHAPTER 3

IDENTIFICATION OF FUNGAL SPECIES ASSOCIATED WITH CHERRY LEAF SPOT DISEASE

3.1 Introduction

3.1.1 An Overview of Cherry Leaf Spot Disease

Cherry leaf spot (CLS) is a common, serious disease of sweet cherry worldwide (Holb, 2009). Leaf spots caused by various fungal pathogens lead to early defoliation and eventual death of the tree (Chethana et al., 2019). Capacity for photosynthesis in leaves is affected by cherry leaf spot, and the early leaf defoliation during summer weakens the trees and increases their susceptibility to frost, ultimately leading to considerable yield losses and a reduction of their quality (Gruber et al., 2012; Ellis, 2016). Leaf spot can be particularly damaging in severe cases; it has been reported in Israel to cause a loss of up to 40% of cherry yield (Sztejnberg, 1986), and the disease incidence rate in China can exceed 90% in severe cases (Liu, 2012). Humidity is an important factor affecting the occurrence of leaf spot disease, wet weather can cause all the leaves of infected orchards to fall off in mid-June without applying medicine (Andersen et al., 2018).

The disease was first reported in America in 1878 and later reported in Europe and other countries (Holb, 2009). *Blumeriella jaapi* was identified as the most common organism in many countries and caused brown spots with whitish-pink masses of spores on the infected leaves (Wharton et al., 2003). In the later stage, the lesions expanded and fused to form a large spot, or the middle part fell off to form a shot hole. Leaves exhibit chlorosis and fall off (Ellis, 2016). The fungi overwinter on the diseased leaves with the stroma, produce ascospores in spring, and release ascospores under humid conditions at the flowering stage for initial infection. Conidial reinfection occurs in late spring and persists into autumn (Garcia, 1993). Other studies have shown that pathogens may also overwinter on dormant buds as the primary infection source

(Joshua & Mmbaga, 2015). Though *B. jaapi* is the main pathogen in America and Europe, it has not been reported in China.

Species belonging to Mycosphaerellaceae are also causal agents of cherry leaf spot, with a long history. In 1886, Saccardo isolated *Cercospora circumscissa* from cherry leaves in Italy for the first time, and reported its sexual morph *Mycosphaerella cerasella,* in 1902. In 1974, leaf spot disease caused by *C. circumscissa* was widespread in Israel. The symptom of Cercospora leaf spot was 4-5 mm in diameter, with a light brown centre and reddish-brown edges. Lesions can occur on both the upper and lower surfaces of the leaves, and often form shot-hole or combine into large lesions in the later stages (Sztejnberg, 1986). Afterwards, *Passalora circumscissa* was isolated from cherry leaves in South Africa (Crous & Braun, 1996), and *Pseudocercospora pruni-persicicola* was reported in Korea in 2014 (Choi et al., 2014). In China, *Mycosphaerellaceae* are associated with CLS, including *Cercospora circumscissa*, *Pseudocercospora circumscissa* and *Passalora circumscissa*, with *Mycosphaerella cerasella* as the sexual morph (Sun et al., 2014). Crous et al. (2020) re-classified *Cercospora circumscissa*, *Passalora circumscissa* and *Mycosphaerella cerasella* as a new combination, *Pruniphilomyces circumscissus*, and isolated the species from the leaf spot of sour cherry. In addition to the two typical pathogens, there are other records of pathogenic fungi infecting cherry leaves, such as *Alternaria alternata* reported in Greece, causing enlarging blackish leaf spots (Thomidis & Tsipouridis, 2006); and *Colletotrichum acutatum* reported in Norway as a latent pathogen (Børve & Stensvand, 2008).

In the early studies on cherry leaf spots, fungal identifications were only based on the field experience of morphological characters. With the development of molecular techniques, mycologists have suggested that a polyphasic approach is necessary for identification of fungi at the species level. In this way, phytopathogens were identified based on morphological characteristics, phylogenetic analyses and pathogenicity tests, which enabled the identification to be more accurate (Crous et al., 2015; Chethana et al., 2019). In recent years, more fungal species associated with CLS, especially *Alternaria* and *Colletotrichum* species, have been accurately identified in China (Chethana et al., 2019; Zhou et al., 2023).

3.1.2 Common Fungal Pathogens Associated with Cherry Leaf Spot in China

3.1.2.1 *Pruniphilomyces circumscissus*

Pruniphilomyces circumscissus (syn. *Cercospora circumscissa*, *Pseudocercospora circumscissa*, *Passalora circumscissa* and *Mycosphaerella cerasella*) was previously recognized as the dominant pathogen of cherry leaf spot disease in China. Guo and Liu (1992) reported the species (as *Pseudocercospora circumscissa*) from sour cherry. Subsequently, *Cercospora circumscissa*, *Pseudocercospora circumscissa* and the sexual morph *Mycosphaerella cerasella* were reported to cause leaf spot disease, termed brown spot, on sweet cherry (Shao, 1995; Zhang, 2010). However, no morphological and molecular evidence were provided in these records. In 2012, Liu et al., identified the pathogen of brown spot as *Passalora circumscissa* by morphological characterization, and Sun et al. (2017) identified *Passalora circumscissa* through morphological identification and ITS analysis. Though Crous et al. (2020) have proposed the new combination *Pruniphilomyces circumscissus* to accommodate these species, *Passalora circumscissa* was still used in recent research (Ma et al., 2022; Sun et al., 2022).

3.1.2.2 *Alternaria* spp.

During an investigation on black spot disease, a prevalent leaf disease in Gansu Province in 2001–2002, the pathogen was identified as *Alternaria cerasi* by morphological characters (Zhu & Chang, 2004). Zhao et al. (2013) isolated *A. alternata* from cherry fruits with black spot symptoms in Liaoning Province, and inoculated on cherry leaves, resulting in weak pathogenicity. Later, *A. alternata* was frequently isolated from Beijing City, Gansu Province and Qinghai Province (Chethana et al., 2019; Liu et al., 2020). In addition, *A. tenuissima* was reported in both Gansu and Qinghai Provinces (Liu et al., 2020). Chethana et al. (2019) introduced two new species *Alternaria prunicola* and *Alternaria pseudoeichhorniae*., with *A. prunicola* as the main CLS pathogen in Beijing.

3.1.2.3 *Colletotrichum* spp.

The genus *Colletotrichum* ranked eighth among the top 10 fungal plant pathogens worldwide, causing many diseases, especially anthracnose, in a wide range of herbaceous or woody plants (Dean et al., 2012). However, reports of *Colletotrichum* associated with cherry leaf spot in China have just appeared in recent years. Chethana

et al. (2019) identified *C. aenigma* and *C. pseudotheobromicola* associated with cherry leaf spot disease in Beijing, which exhibited a higher level of virulence than the main pathogen *A. prunicola* in the study. In 2020, *Colletotrichum* species were isolated from cherry leaves in Qinghai Province, but were not identified to species level. Tang et al. (2021) reported *C. fructicola* causing cherry anthracnose in Zhejiang Province. The descriptions of symptoms of anthracnose leaf spot were similar, which appeared as small, dark red or purple pinpoint lesions on the leaves, and later the lesions enlarged to form dark brown or red brown circular lesions (Chethana et al., 2019; Liu et al., 2020; Tang et al., 2021). Zhou et al. (2023) further divided three symptom types of anthracnose leaf spot (brown spot, purple spot and leaf blight) through investigation in four provinces in China, and identified thirteen species. It was interesting that lesions showed different characters when infected by different *Colletotrichum* species, and the pathogenicity test on living plants reproduced the lesion consistent with the field symptoms.

3.1.2.4 Didymellaceae species

In 2019, Chethana et al., reported four Didymellaceae species associated with cherry leaf spot in Beijing, including *Nothophoma quercina* and *Stagonosporopsis citrulli* and two new species *Epicoccum pseudokeratinophilum* and *Nothophoma pruni*. The species showed weak virulence in the pathogenicity test, thus possible be the secondary pathogen of cherry leaf spot.

3.1.2.5 Other pathogens

Some fungi associated with other diseases of cherry were also found to cause cherry leaf spot. *Botryosphaeria dothidea*, the causal agent of cherry gummosis disease, was reported to cause large brown spots on cherry leaves, leading to leaf chlorosis, blight or defoliation (Zhou et al., 2021); *Diaporthe eres* was recorded on cherry early, while no detailed information was provided (Dai et al., 1979). Zhou et al. (2022) reported a cherry leaf spot disease showing brownish-grey lesions surrounded by yellowish halo rings caused by *D. eres*, as well as *D. sojae*.

In conclusion, though more studies on cherry leaf spot are emerging in recent years, the knowledge on the disease is still limited. In contrast to *Blumeriella jaapi*, the dominant causal agent of the disease in most European and American countries, CLS pathogens seem to be more diverse in China. However, previous fungal

identification on cherry leaf spot was usually based on morphological characters and sequences of the ITS region, which may cause inaccurate identification results; and latest research on CLS pathogens are still very few compared with other important fruit crops. Therefore, it is necessary to continue the investigation and fungal identification of cherry leaf spot disease.

3.2 Results

During the investigation of cherry leaf spot disease, different symptoms of cherry leaf spot were observed, which led to the leaf chlorosis or defoliation in the late stages (Figure 3.1).

According to the result of previous publications and data from the lab, *Alternaria*, *Colletotrichum*, *Cladosporium*, Didymellaceae species, and *Fusarium* are the top five groups of fungi associated with cherry leaf spot. *Alternaria* associated with CLS have been studied in different regions in China (Chethana et al., 2019; Liu et al., 2020; Yang et al., 2020), and Didymellaceae species were found to be weakly pathogenic (Chethana et al., 2019). Therefore, this study was focused on the other three genera. Though *Colletotrichum* species causing anthracnose leaf spot have been comprehensively identified (Chethana et al., 2019; Zhou et al., 2023), a re-investigation and identification were conducted to compare the dominant species of *Colletotrichum* with previous studies.

Figure 3.1 Symptoms of cherry leaf spot disease in the field

3.2.1 *Colletotrichum* Species Causing Cherry Leaf Spot Disease in Beijing, China

3.2.1.1 Sampling and fungal isolation

In 2021, thirteen anthracnose leaf spot samples of sweet cherry were collected from Haidian, Fangshan and Tongzhou District, Beijing, China (Figure 3.2). The symptoms present circular to subcircular, brown spots with dark-brown or purple margins, and some showed leaf blight with semicircular or irregular brown necrotic lesions at the leaf margin. The symptoms were consistent with the previous description (Zhou et al., 2023). Eighteen isolates were generated by direct single-spore isolation or tissue isolation.
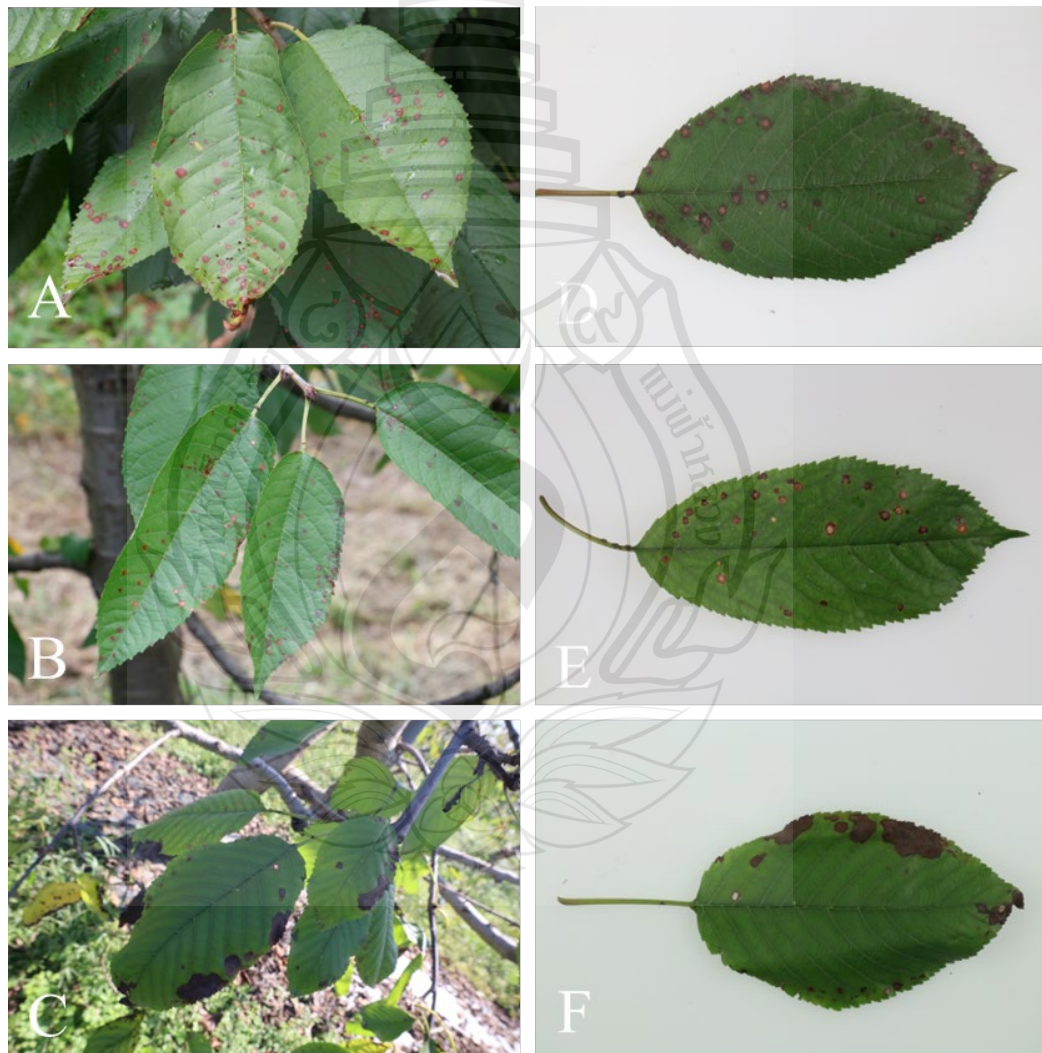
Note A–C leaf symptoms in the field. D–F leaf spot samples.

Figure 3.2 Anthracnose cherry leaf spot

3.2.1.2 Molecular and morphological identification

According to the BLAST results of the ITS region, all isolates belong to the *Colletotrichum gloeosporioides* species complex. The multi-locus phylogenetic tree of *C. gloeosporioides* species complex was constructed based on *act*, *tub2*, *cal*, *chs-1*, *gapdh* and ITS, with *C. boninense* (CBS 123755) as the outgroup (Figure 3.3). Eight isolates clustered with the ex-type of *C. gloeosporioides* (IMI 356878) with 100% ML bootstrap support value and 1.00 BYPP. Eight isolates clustered with the ex-type of *C. fructicola* (ICMP 18646) with 99% ML bootstrap support value and 1.00 BYPP. Two isolates clustered with the ex-type of *C. aenigma* (ICMP 18608) with 97% ML bootstrap support value and 1.00 BYPP.
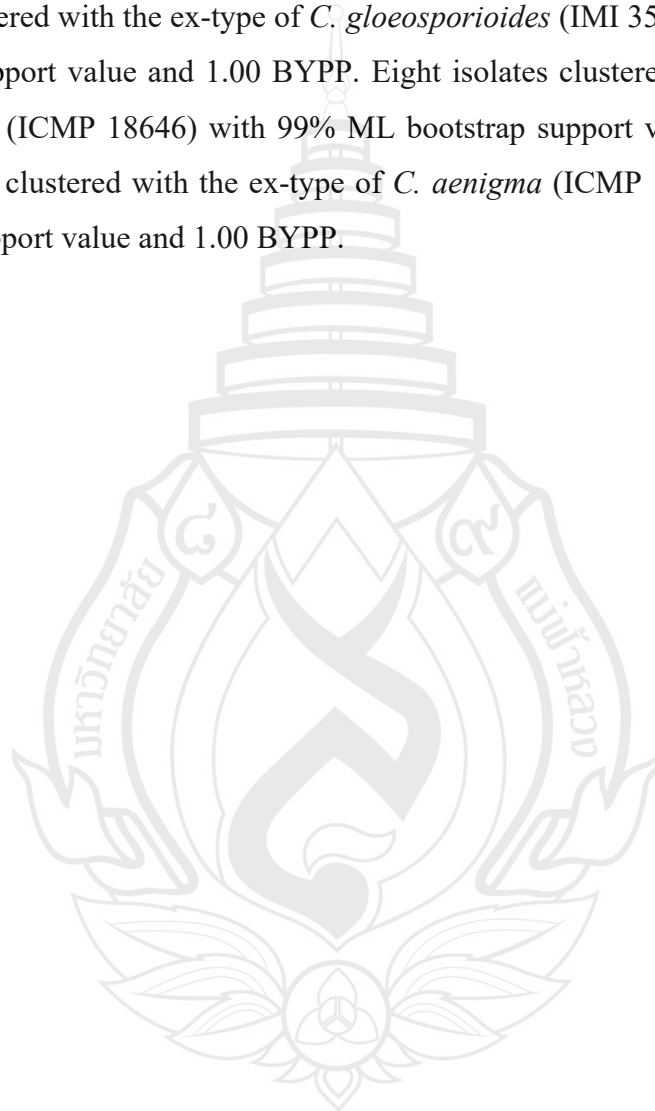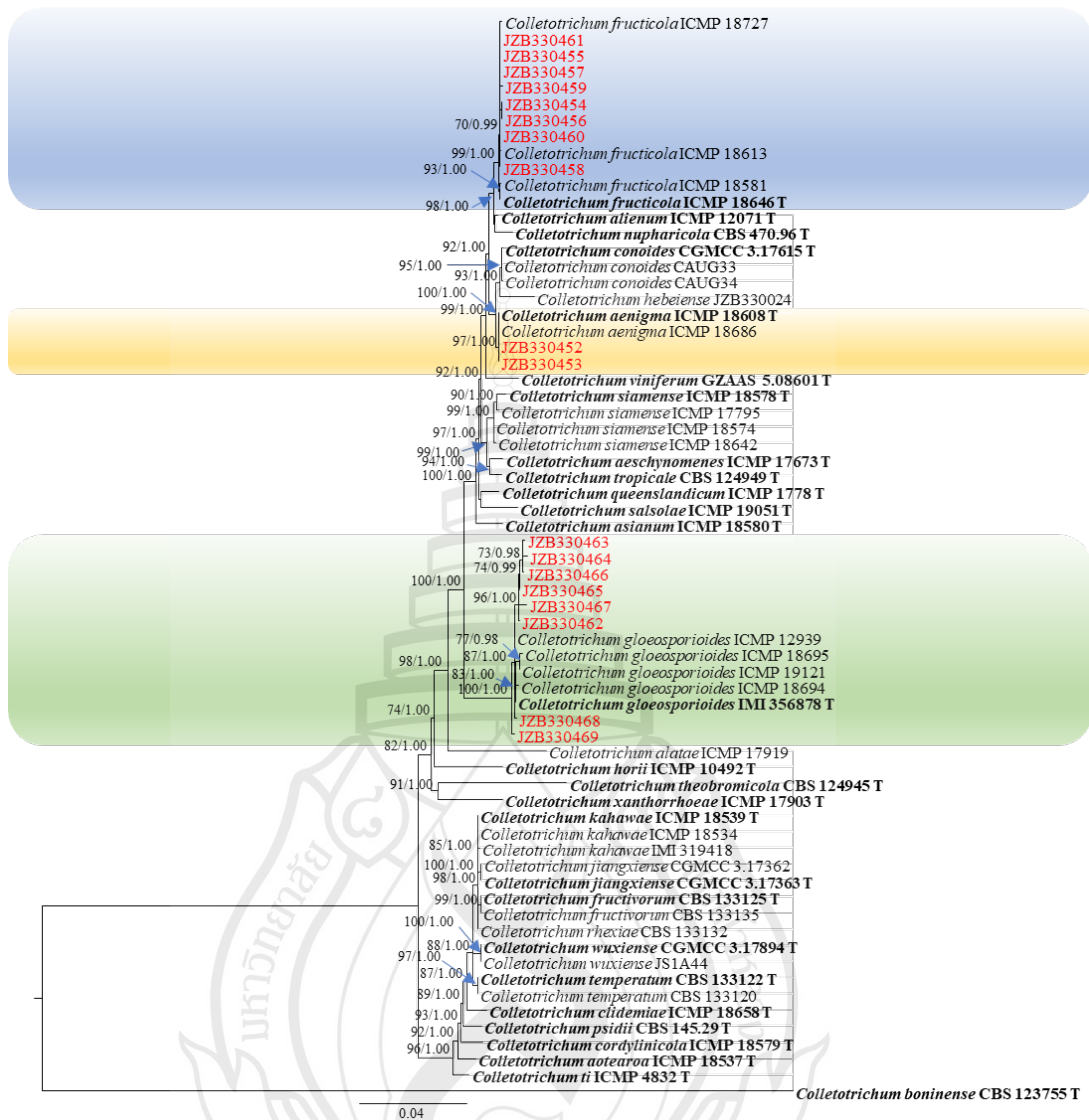
Figure 3.3 Phylogenetic tree generated by maximum likelihood analysis (RAxML) of
Colletotrichum gloeosporioides species complex based on the combined
act, *tub2*, *cal*, *chs-1*, *gapdh* and ITS sequence data

Figure 3.3 The tree is rooted with *C. boninense* (CBS 123755). The best scoring RAxML tree with a final likelihood value of -4987.801452 is presented. The matrix had 738 distinct alignment patterns, with 0.90% of undetermined characters or gaps. Estimated base frequencies were as follows: A = 0.22653, C = 0.29987, G = 0.24843, T = 0.22678; substitution rates AC = 1.00000, AG = 3.46970, AT = 1.00000, CG = 1.00000, CT = 5.77541, GT = 1.000000; gamma distribution shape parameter α = 0.40254. ML bootstrap support values ≥50% and Bayesian posterior probabilities (BYPP)≥0.95 are shown near

the nodes. The scale bar indicates 0.02 changes per site. The ex-type strains are in bold, and isolates from the current study are in red.

Morphologically, the three species conformed to the description of ex-type and previous isolates from CLS of *C. gloeosporioides*, *C. fructicola* and *C. aenigma* (Cannon et al., 2008; Prihastuti et al., 2009; Weir et al., 2012; Zhou et al., 2023) (Figure 3.4). *Colletotrichum* species within a species complex may share similar morphology, and morphological characters of a species can be changed by subculturing, different conditions of growth and differences between strains, which are insufficient to distinguish species within a species complex. The definition of species is thus mainly based on multi-gene phylogenies (Weir et al., 2021).

Therefore, *Colletotrichum* isolates generated in this study are identified as *C. gloeosporioides* (8 isolates), *C. fructicola* (8 isolates) and *C. aenigma* (2 isolates), which are also the top three groups in the previous study (Zhou et al., 2023).
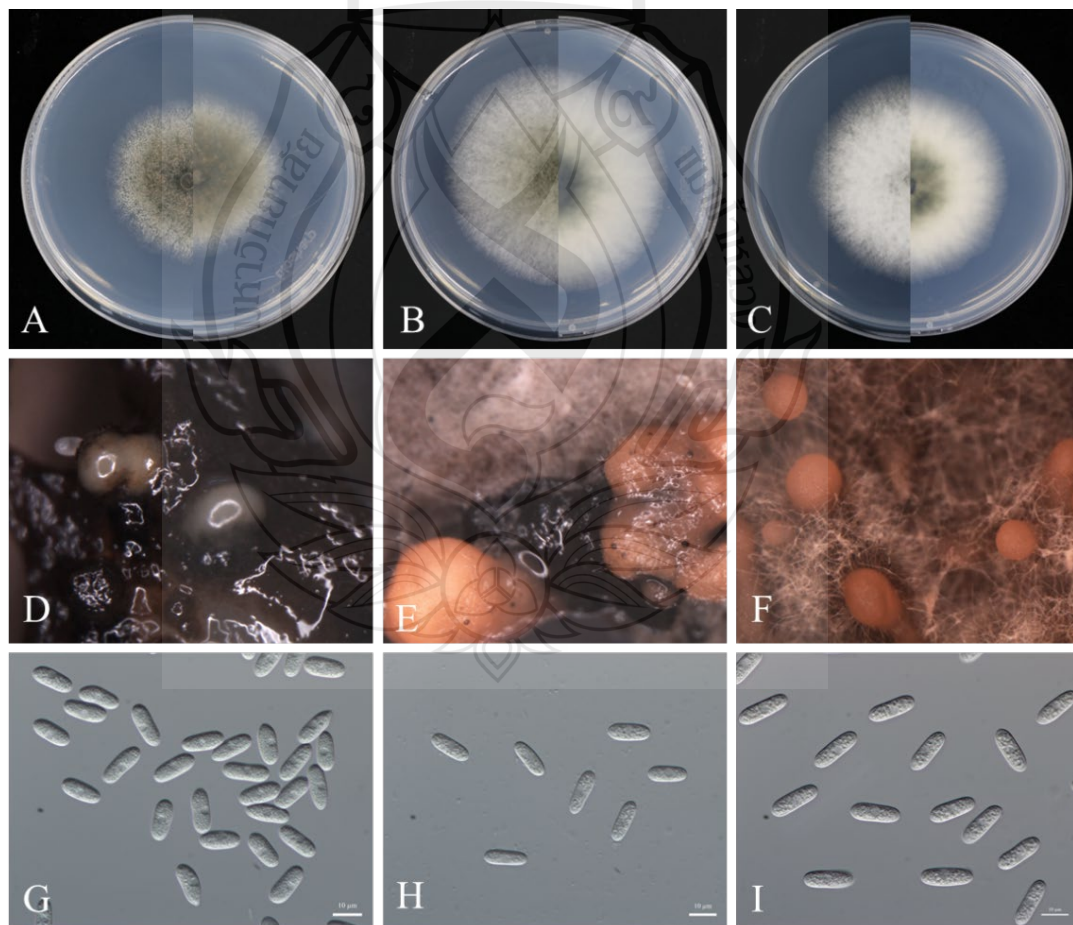
Figure 3.4 Morphological characteristics of *Collototrichum* species isolated from cherry leaf spot

Figure 3.4 A Front (left) and back (right) views of the 4-day-old colony of *C. gloeosporioides*. B Front (left) and back (right) views of the 4-day-old colony of *C. fructicola*. C Front (left) and back (right) views of the 4-day-old colony of *C. aenigma*. D Conidiomata of *C. gloeosporioides*. E Conidiomata of *C. fructicola*. F Conidiomata of *C. aenigma*. G Conidia of *C. gloeosporioides*. H Conidia of *C. fructicola*. I Conidia of *C. aenigma*. Scale bars: G–I = 10 μm.

3.2.1.3 Pathogenicity test

Three days post inoculation, all *Colletotrichum* species were pathogenic to detached cherry leaves (Figure 3.5). Leaves inoculated with *C. gloeosporioides* and *C. fructicola* showed dark brown lesions on both wounded and unwounded side, while leaves inoculated with *C. aenigma* only shown lesions in the wounded side. No symptoms were observed on the control leaves. The fungi were re-isolated from the lesions successfully and identified using morphology and molecular analyses.

Figure 3.5 Pathogenicity test of *Colletotrichum* species on detached cherry leaves (cv. Caihong) three days post inoculation

Figure 3.5 A–C Detached leaves inoculation of *C. gloeosporioides*, *C. fructicola* and *C. aenigma*, respectively. Left side of the leaf was unwounded before inoculation, right side was wounded. D Control.

3.2.1.4 Summary

Colletotrichum is a common pathogen on cherry associated with leaf spot disease. In this study, twenty *Colletotrichum* isolates from cherry leaf spot in Beijing were identified as *C. gloeosporioides*, *C. fructicola* and *C. aenigma*, which have been reported

by Zhou et al. (2023) as the top three species in terms of isolate number. Current results verified the conclusion that the three species are the main pathogens causing anthracnose leaf spot. In the pathogenicity assay, *C. gloeosporioides* and *C. fructicola* were pathogenic to both wounded and unwounded leaves, while *C. aenigma* could only cause lesions on wounded leaves. This result is different from previous studies that *C. aenigma* exhibited strong pathogenicity (Zhou et al., 2023), which may be influenced by the cherry cultivar and virulence difference between fungal isolates.

3.2.2 *Fusarium* Species Causing Cherry Leaf Spot Disease in China

3.2.2.1 Symptom observation, sample collection and fungal isolation

From 2019 to 2020, fifteen cherry leaf spot samples were collected from cherry orchards (open field) in Beijing, Liaoning and Shandong Provinces in China, with the following symptoms, (1) small purple-brownish spots which may merge with expansion (Figure 3.6. A–B); (2) circular or irregular brownish grey necrotic lesions with dark brown margin (Figure 3.6. C–D). Twenty-four *Fusarium* isolates were obtained by tissue isolation, among which thirteen were from Beijing, nine from Shandong and two from Liaoning (Table 3.1).
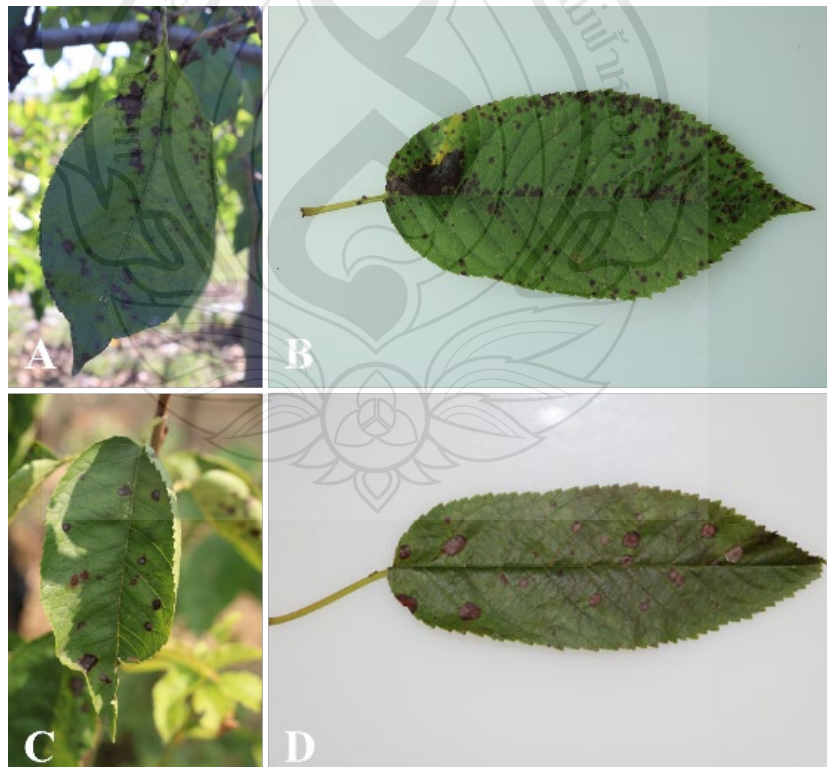
Note A, B symptom type 1. C, D symptom type 2

Figure 3.6 Symptoms of *Fusarium* leaf spot

Table 3.1 Information of *Fusarium* isolates obtained in this study

Species	Isolate number	Origin	Date collected
F. compactum	JZB3110202	Beijing	2019.7
F. compactum	JZB3110203	Beijing	2019.8
F. compactum	JZB3110204	Beijing	2019.8
F. compactum	JZB3110205	Beijing	2019.8
F. compactum	JZB3110206	Liaoning	2019.9
F. ipomoeae	JZB3110207	Beijing	2019.8
F. luffae	JZB3110208	Beijing	2019.7
F. luffae	JZB3110209	Shandong	2019.8
F. luffae	JZB3110210	Shandong	2019.8
F. luffae	JZB3110211	Shandong	2019.8
F. luffae	JZB3110212	Shandong	2019.8
F. luffae	JZB3110213	Beijing	2019.10
F. luffae	JZB3110214	Beijing	2020.9
F. citri	JZB3110215	Shandong	2019.8
F. citri	JZB3110216	Beijing	2019.10
F. nygamai	JZB3110217	Beijing	2019.8
F. nygamai	JZB3110218	Beijing	2019.8
F. lateritium	JZB3110219	Shandong	2019.8
F. lateritium	JZB3110220	Shandong	2019.8
F. lateritium	JZB3110221	Shandong	2019.8
F. lateritium	JZB3110222	Shandong	2019.8
F. lateritium	JZB3110223	Shandong	2020.9
F. lateritium	JZB3110224	Shandong	2020.9
F. curvatum	JZB3110225	Liaoning	2019.9

3.2.2.2 Molecular characterization and phylogenetic analysis

The ITS sequences of isolates showed 100% similarity to *Fusarium* spp. based on BLAST analysis. Phytogenic trees of *Fusarium incarnatum-equiseti* species complex (FIESC), *Fusarium lateritium* species complex (FLSC), *Fusarium fujikuroi*

species complex (FFSC) and *Fusarium oxysporum* species complex (FOSC) were constructed using combined sequence alignment. The sequences were deposited in GenBank, and accession numbers were obtained.

Phylogenetic analysis of FIESC was constructed based on the combined *CaM*, *rpb2* and *tef1* multi-locus dataset, with *Fusarium concolor* (CBS 961.87) as the outgroup taxon (Figure 3.7). Both maximum likelihood and Bayesian analyses resulted in the same topology. Among the ninety-six fungal isolates in the dataset, fifteen were from the current study. Seven isolates clustered with *F. luffae* in two branches with 67% ML bootstrap and 1.0 BYPP, and 70% ML bootstrap, five clustered with *F. compactum* with 81% ML bootstrap and 0.99 BYPP, two clustered with *F. citri* with 63% ML bootstrap and 0.95 BYPP, and one isolate with *F. ipomoeae* with 99% ML bootstrap and 1.0 BYPP.

Phylogenetic analysis of FLSC was constructed based on the combined *rpb2*, *tef1* and *tub2* multi-locus dataset, with *Fusarium buharicum* (CBS 796.70) as the outgroup taxon (Figure 3.8). Both maximum likelihood and Bayesian analyses resulted in the same topology. Six isolates clustered with *F. lateritium* with 94% ML bootstrap and 1.0 BYPP.

Phylogenetic analysis of FFSC was constructed based on the combined *tef1*, *rpb2*, *tub2* and *CaM* multi-locus dataset, with *Fusarium nirenbergiae* (CBS 744.97) as the outgroup taxon (Figure 3.9). Both maximum likelihood and Bayesian analyses resulted in the same topology. Two isolates clustered with *F. nygamai* with 100% ML bootstrap and 1.0 BYPP.

Phylogenetic analysis of FOSC was constructed based on the combined *rpb2*, *tef1* and *tub2* multi-locus dataset, with *Fusarium foetens* (CBS 120665) and *Fusarium udum* (CBS 177.31) as the outgroup taxa (Figure 3.10). Both maximum likelihood and Bayesian analyses resulted in the same topology. One isolate clustered with *F. curvatum* with 69% ML bootstrap and 1.0 BYPP.
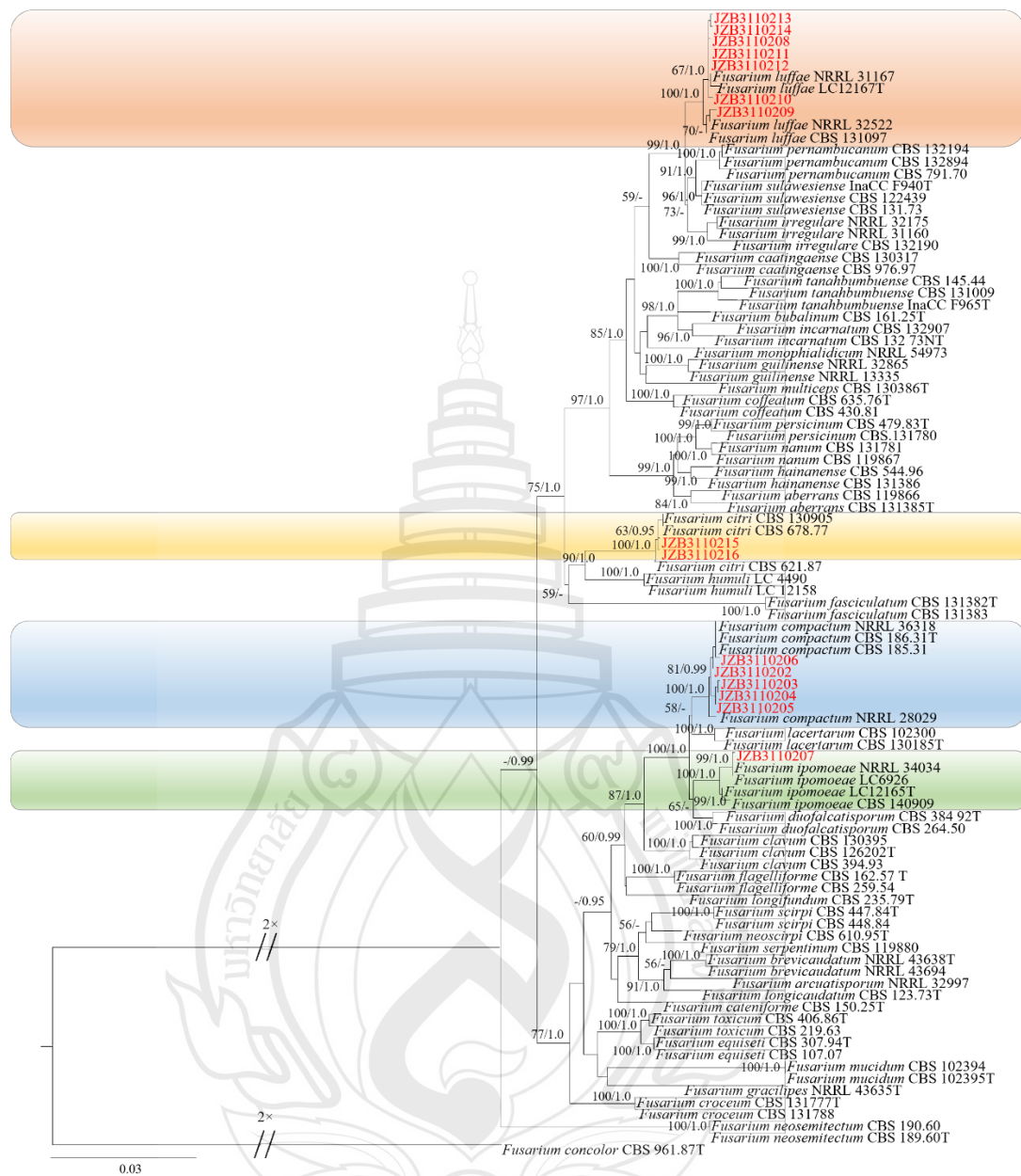
Figure 3.7 Phylogenetic tree generated by maximum likelihood analysis (RAxML) of
FIESC based on the combined *CaM*, *rpb2* and *tef1* sequence data

Figure 3.7 The tree is rooted with *Fusarium concolor* (CBS 961.87). The
best scoring RAxML tree with a final likelihood value of –11974.052080 is presented.
The matrix had 701 distinct alignment patterns, with 7.69% of undetermined characters
or gaps. Estimated base frequencies were as follows: A = 0.258901, C = 0.260331,
G = 0.245699, T = 0.235069; substitution rates AC = 1.002698, AG = 4.065670, AT =

1.349366, CG = 0.882966, CT = 10.506153, GT = 1.000000; gamma distribution shape parameter α = 0.751525. ML bootstrap support values ≥50% and Bayesian posterior probabilities (BYPP)≥0.95 are given near the nodes. The scale bar indicates 0.03 changes per site. Isolates belong to this study are given in red.
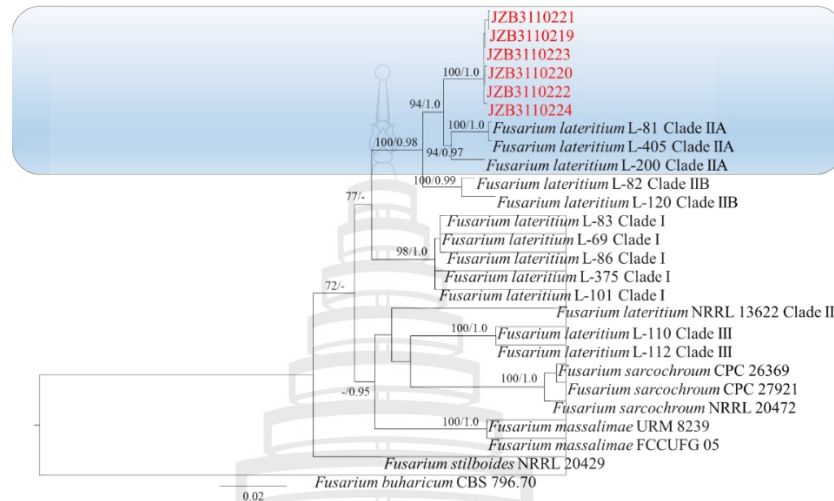
Figure 3.8 Phylogenetic tree generated by maximum likelihood analysis (RAxML) of FLSC based on the combined *rpb2*, *tef1* and *tub2* sequence data

Figure 3.8 Phylogenetic tree generated by maximum likelihood analysis (RAxML) of FLSC based on the combined *rpb2*, *tef1* and *tub2* sequence data. The tree is rooted with *Fusarium buharicum* (CBS 796.70). The best scoring RAxML tree with a final likelihood value of -5602.556442 is presented. The matrix had 358 distinct alignment patterns, with 32.15% of undetermined characters or gaps. Estimated base frequencies were as follows: A = 0.236754, C = 0.282131, G = 0.242563, T = 0.238552; substitution rates AC = 2.260928, AG = 7.239234, AT = 2.341489, CG = 1.331525, CT = 16.787035, GT = 1.000000; gamma distribution shape parameter α = 1.252177. ML bootstrap support values ≥50% and Bayesian posterior probabilities (BYPP)≥0.95 are given near the nodes. The scale bar indicates 0.02 changes per site. Isolates belong to this study are given in red.

Figure 3.9 Phylogenetic tree generated by maximum likelihood analysis (RAxML) of FFSC based on the combined *tef1*, *rpb2*, *tub2* and *CaM* sequence data

Figure 3.9 The tree is rooted with *Fusarium nirenbergiae* (CBS 744.97). The best-scoring RAxML tree with a final likelihood value of –16169.804811 is presented. The matrix had 1172 distinct alignment patterns, with 12.61% of undetermined characters or gaps. Estimated base frequencies were as follows: A = 0.246851, C = 0.265429, G = 0.243377, T = 0.244344; substitution rates AC = 1.195289, AG = 4.703565, AT = 1.258970, CG = 0.717390, CT = 9.004544, GT = 1.000000; gamma distribution shape parameter α = 0.838651. ML bootstrap support values ≥50% and Bayesian posterior probabilities (BYPP)≥0.95 are given near the nodes. The scale bar indicates 0.03 changes per site. Isolates belonging to this study are given in red.

Figure 3.10 Phylogenetic tree generated by maximum likelihood analysis (RAxML) of FOSC based on the combined *rpb2*, *tef1* and *tub2* sequence data

Figure 3.10 The tree is rooted with *Fusarium foetens* (CBS 120665) and *Fusarium udum* (CBS 177.31). The best-scoring RAxML tree with a final likelihood value of -4987.801452 is presented. The matrix had 199 distinct alignment patterns, with 0.90% of undetermined characters or gaps. Estimated base frequencies were as follows: A = 0.251044, C = 0.269288, G = 0.238899, T = 0.240769; substitution rates AC = 1.155437, AG = 2.887244, AT = 0.424595, CG = 0.728892, CT = 5.651969, GT = 1.000000; gamma distribution shape parameter α = 1.022063. ML bootstrap support values ≥50% and Bayesian posterior probabilities (BYPP)≥0.95 are given near the nodes. The scale bar indicates 0.02 changes per site. Isolates belonging to this study are given in red.

3.2.2.3 Morphological observation

Morphological characteristics were shown in Figure 3.11, Table 3.2 and Table 3.3. Based on cultural and morphological characters, *Fusarium* isolates were consistent with *F. compactum*, *F. ipomoeae*, *F. luffae*, *F. citri*, *F. nygamai*, *F. lateritium*

and *F. curvatum* as previously described (Leslie & Summerell, 2006; Wang et al., 2019; Lombard et al., 2019).
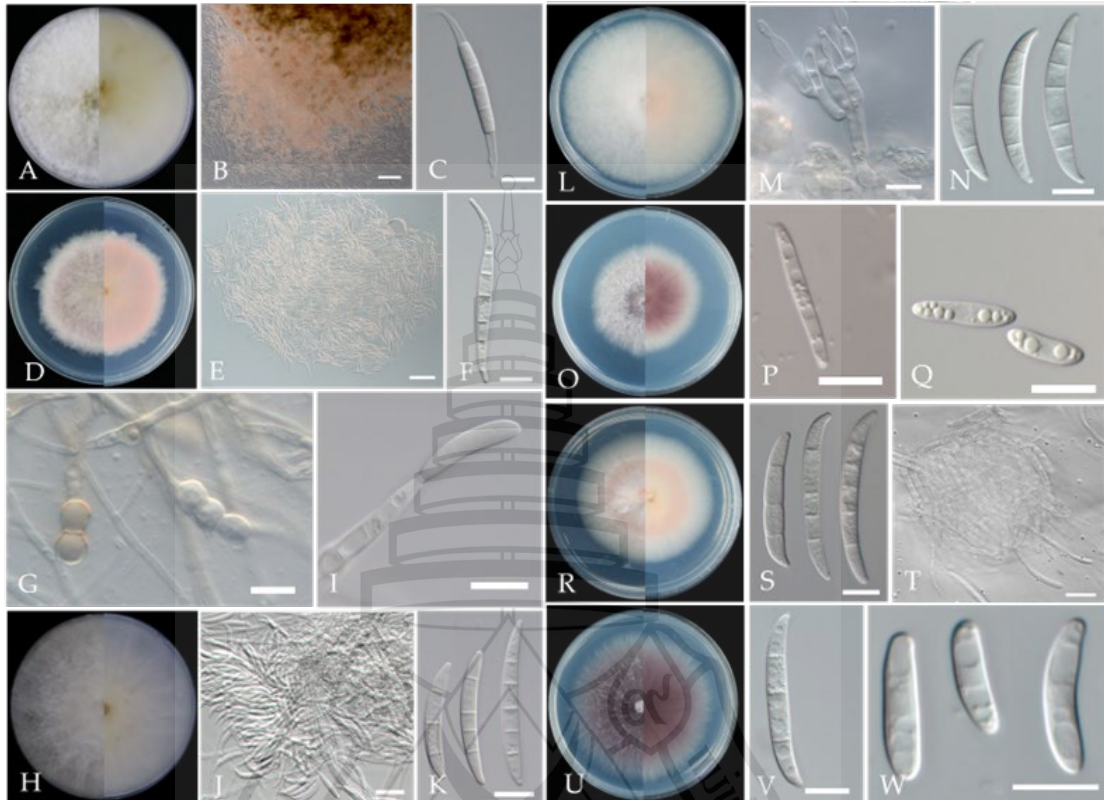
Figure 3.11 Morphological characteristics of *Fusarium* species isolated from cherry leaf spot

Figure 3.11 A Colony of *F. compactum*. B Sporodochia of *F. compactum* on carnation leaf C Macroconidia of *F. compactum* on CLA. D Colony of *F. ipomoeae*. E Sporodochia of *F. ipomoeae*. F Macroconidia of *F. ipomoeae*. G Chlamydospores of *F. ipomoeae*. H Colony of *F. luffae*; I Conidiophore of *F. luffae* on aerial hyphae. J Sporodochia of *F. luffae*. K Macroconidia of *F. luffae*. L Colony of *F. citri*. M Conidiogenous cells of *F. citri* formed on sporodochia. N Macroconidia of *F. citri*. O Colony of *F. nygamai*. P Macroconidia of *F. nygamai*. Q Microconidia of *F. nygamai* R Colony of *F. lateritium*. S Macroconidia of *F. lateritium*. T Sporodochia of *F. lateritium*. U Colony of *F. curvatum*. V Macroconidia of *F. curvatum*. W Microconidia of *F. curvatum*. Scale bars: A, C, D, F–I, K–S, U–W = 10 µm; J, T = 20 µm; B, E = 100 µm.

Table 3.2 Characteristics of colonies of *Fusarium* fungi cultivated on PDA

Species	Average diameter of colony (range) on 5 d, mm	Type and colour of aerial mycelium	Reverse pigmentation
F. compactum	79–85	White mycelia with brown pigments produced in the agar	White to pale yellow
F. ipomoeae	59–65	Colony margin lobate, pinkish white	Pale pink
F. luffae	67–73	Aerial mycelia dense, colony white	White to pale yellow
F. citri	78–80	Aerial mycelia dense, colony margin entire, white	Pinkish white
F. nygamai	53–56	Mycelia violet, with violet pigments produced in the agar	Violet with white margin
F. lateritium	45–54	Mycelia sparse, pale orange or pale pink	Pale orange or pale pink with white margin
F. curvatum	68–70	Mycelia violet, with violet pigments produced in the agar	Dark violet

Table 3.3 Description of conidia of *Fusarium* fungi cultivated on CLA

Species	Macroconidia		Microconidia	
	Shape, number of septa	Average size (range)	Shape, number of septa	Average size (range)
F. compactum	Strong dorsiventral curvature, apical cell elongate and tapering that is often needle like in appearance, basal cell foot-shaped, usually 5-septate	43.04–62.05 × 4.02–5.13 μm (avg.=54.08 × 4.50 μm, n=50)	Not observed	
F. ipomoeae	Dorsiventral curvature, smooth, hyaline, apical cell hooked to tapering, basal cell foot-shaped. Usually 5-septate	40.72–66.64 × 3.67–4.65 μm (avg.=56.60 × 4.16 μm, n=50)	Not observed	

Table 3.3 (continued)

Species	Macroconidia		Microconidia	
	Shape, number of septa	Average size (range)	Shape, number of septa	Average size (range)
F. luffae	Falcate, slender, slightly curved, smooth to slightly rough, hyaline, apical cell blunt or hooked, basal cell barely notched, 3–5-septate	26.18–42.88 × 3.75–4.69 μm (avg.=33.69 × 4.17 μm, n=50)	Not observed	
F. citri	Falcate, hyaline, apical cell papillate to hooked, basal cell distinctly notched to foot-shaped, 3–5-septate	24.23–48.42 × 4.05–5.39 μm (avg.=36.54 × 4.86 μm, n=50)	Not observed	
F. nygamai	Slender, thin walled, hyaline, straight to slightly curved, apical cell short and tapered, basal cell notched or foot-shaped, usually 3-septate	21.08–36.30 × 2.36–3.91 μm (avg.=25.81 × 2.36 μm, n=30)	Oval to elliptical, usually 0-septate	10.06–16.18 × 2.23–3.86 μm (avg.=12.88 × 3.02 μm, n=30)
F. lateritium	Falcate to relatively straight, with parallel walls, apical cell hooked or beaked, basal cell foot-shaped or notched, 3–5-septate, usually 5-septate	38.81–59.69 × 4.31–5.60 μm (avg.=49.10 × 4.88 μm, n=50)	Not observed	

3.2.2.4   Pathogenicity test

Three days post inoculation, all *Fusarium* isolates were pathogenic to **detached** cherry leaves, resulting in lesions similar to the disease symptoms observed in the field (Figure 3.12). The disease incidences [(symptomatic sites/ total inoculated sites) × 100%] and lesion diameter of wounded and unwounded leaves of each species are reported in Table 3.4. No symptoms were observed on the control leaves. According to the result, *F. compactum*, *F. luffae* and *F. ipomoeae* were the most aggressive and caused lesion diameters of more than 10 mm. The other species were relatively less virulent, with lesion diameters varying from 7 mm to 10 mm, and lesion diameters did not differ significantly. The disease incidence of wounded leaves was slightly higher than that of unwounded leaves, while unwounded leaves of some species appeared to form larger lesion diameters. The fungi were re-isolated from the lesions successfully and identified using morphology and molecular analyses.
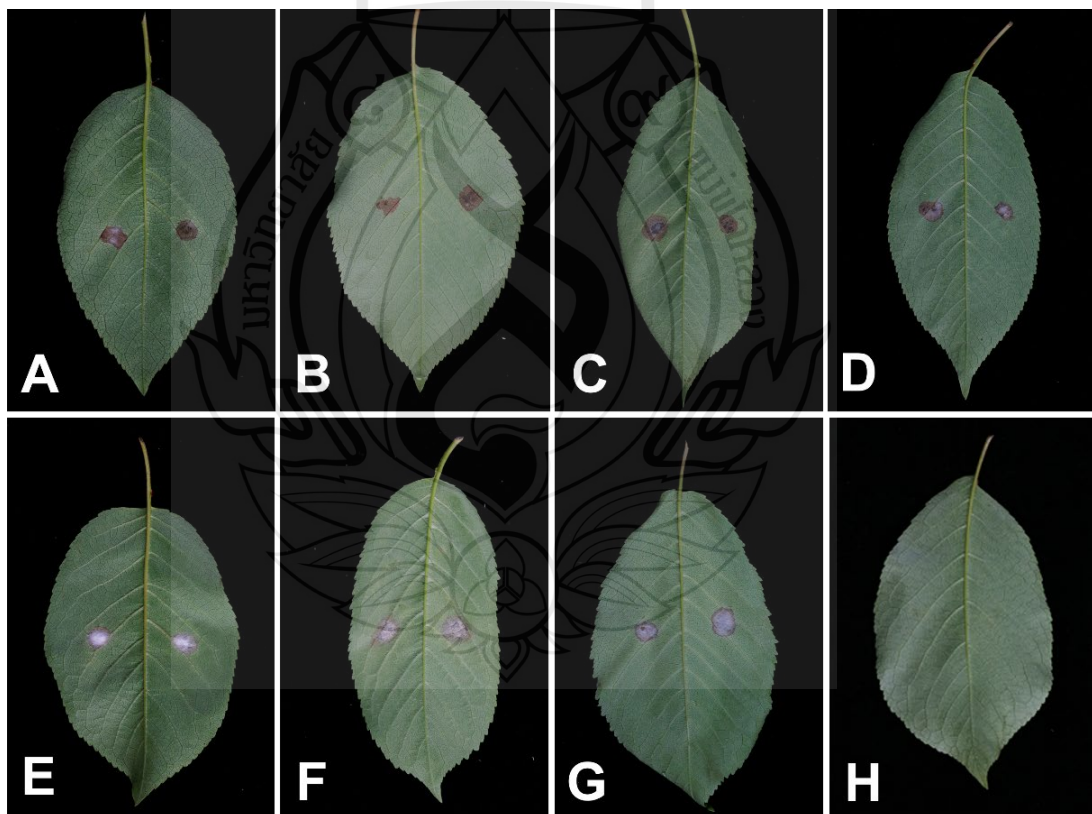
Figure 3.12 The pathogenicity test of *Fusarium* spp. on detached cherry leaves (cv. 'Tieton') three days post inoculation

Figure 3.12 A–G Detached leaves inoculation of *F. luffae*, *F. lateritium*, *F. compactum*, *F. nygamai*, *F. citri*, *F. ipomoeae and F. curvatum*, respectively. Left side of the leaf was wounded before inoculation, right side was unwounded. H Control.

Table 3.4 Disease incidence and lesion diameter of inoculated leaves 3 days post inoculation

Species	Disease incidence (%)		Lesion diameter (mm)	
	Wounded	**Unwounded**	**Wounded**	**Unwounded**
F. compactum	95	95	13.5 ± 0.3 a	14.0 ± 0.3 a
F. ipomoeae	95	75	11.8 ± 0.3 ab	12.8 ± 0.3 a
F. luffae	100	95	12.8 ± 0.4 ab	14.5 ± 0.5 a
F. citri	100	75	8.3 ± 0.1 b	8.8 ± 0.1 b
F. nygamai	100	95	8.3 ± 0.1 b	7.5 ± 0.1 b
F. lateritium	80	90	9.3 ± 0.1 ab	7.0 ± 0.2 b
F. curvatum	100	100	10.0 ± 0.1 ab	7.5 ± 0.1 b

Notes lowercase letters indicate the significant differences for lesion diameters (p < 0.05).

3.2.2.5 Summary

A new type of leaf spot disease was reported, with purplish-brown circular lesions. Twenty-four *Fusarium* isolates were identified as seven species, belonging to four species complexes. Except for *F. lateritium* that has been reported as the pathogen causing trunk diseases in Australia (Cook & Dubé, 1989), the other six species are new host records on cherry. *Fusarium compactum* had been regarded as a saprophyte, while being reported as the pathogen of corm and root rot of banana, a fatal canker on Italian cypress, and a wilt and root rot of peanuts (Frisullo et al., 1994; Madar et al., 1996; Saleh et al., 1997). *Fusarium ipomoeae*, *F. luffae* and *F. citri* were introduced in the study reported from *Fusarium incarnatum-equiseti* complex from China (Wang et al., 2019). Afterwards, *F. ipomoeae* was reported to cause leaf spots on peanut and *Bletilla striata* (Xu et al., 2021; Zhou et al., 2021), *F. luffae* was reported to cause fruit rot on muskmelon in China (Zhang et al., 2022), and *F. citri* was initially isolated from *Citrus* (Wang et al., 2019). *Fusarium nygamai* was first observed on a basal stalk and root rot

of grain sorghum (Trimboli & Burgess, 1985) and can also cause root rot on other crops including cotton, maize, millet, rice and sorghum (Leslie & Summerell, 2006). *Fusarium lateritium* can cause wilt, tip or branch dieback, or cankers on many woody trees and shrubs, including some important fruit trees and coffee (Leslie & Summerell, 2006). The pathogenicity test showed that the analysed strains of all species could produce lesions on detached cherry leaves, and specifically, *F. compactum*, *F. luffae* and *F. ipomoeae* showed relatively high virulence. Therefore, *Fusarium* was proven to be a pathogen of cherry leaf spots in China.

3.2.3 Morphological and Molecular Characterization of *Cladosporium* Species On Sweet Cherry in Beijing, China

3.2.3.1 Sample collection and isolation

A total of 21 isolates were obtained from leaf samples exhibiting leaf spot symptoms in Tongzhou, Fangshan and Haidian districts, Beijing. The leaf spots appear as dark pinpoint lesions, which enlarge to brown spots. As the disease progresses, some lesions merge and become irregular blights, and the diseased area becomes yellow (Figure 3.13).
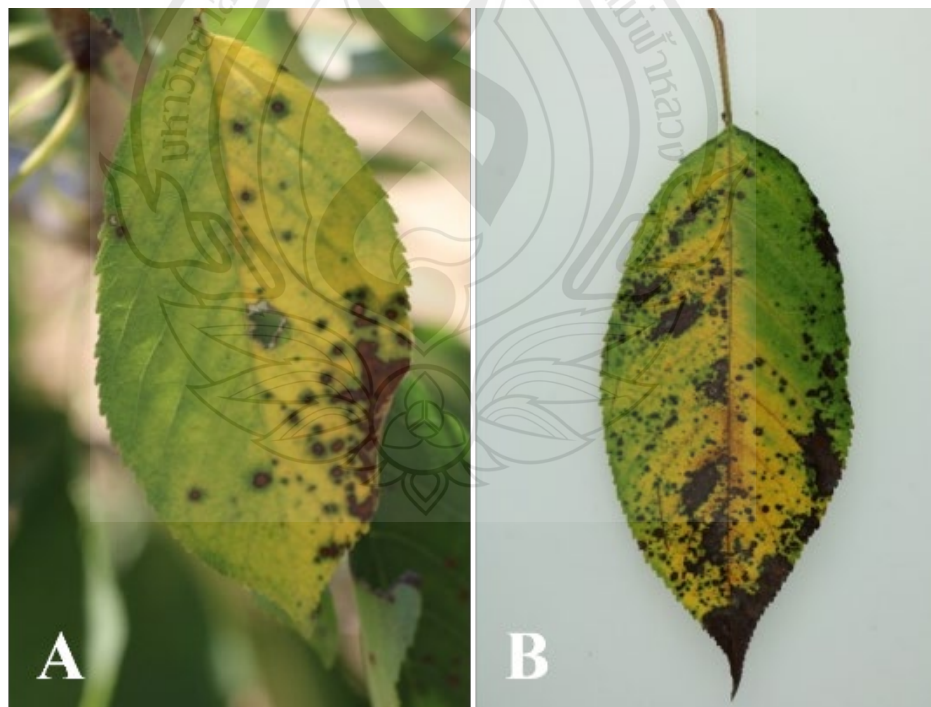
Note A Symptoms in the field. B Diseased cherry leaf sample.

Figure 3.13 Symptoms of *Cladosporium* cherry leaf spot

3.2.3.2 Phylogenetic analysis

The phylogenetic tree comprised 75 taxa with *Toxicocladosporium banksiae* (CBS 128215) as the outgroup. The best-scoring RAxML tree is shown in Figure 3.14 with a final ML optimization likelihood value of -8376.206813. The matrix had 377 distinct alignment patterns, with 4.98% of undetermined characters or gaps. Estimated base frequencies are as follows: A=0.226153, C=0.294242, G=0.248026, and T=0.231579; substitution rates AC= 2.599833, AG= 5.856880, AT= 2.798124, CG= 1.716334, CT=9.962494, and GT=1.000000; proportion of invariable sites I= 0.574301, gamma distribution shape parameter α=0.595053. The Bayesian analysis resulted in 15,000 trees after 2,000,000 generations. The ML and BI trees were similar in topology and did not differ significantly. The 21 isolates from this study clustered within six clades as *C. anthropophilum*, *C. asperulatum*, *C. cladosporioides*, *C. ramotenellum*, *C. rectoides* and *C. tenuissimum* The sequences generated in this study were deposited in GenBank.
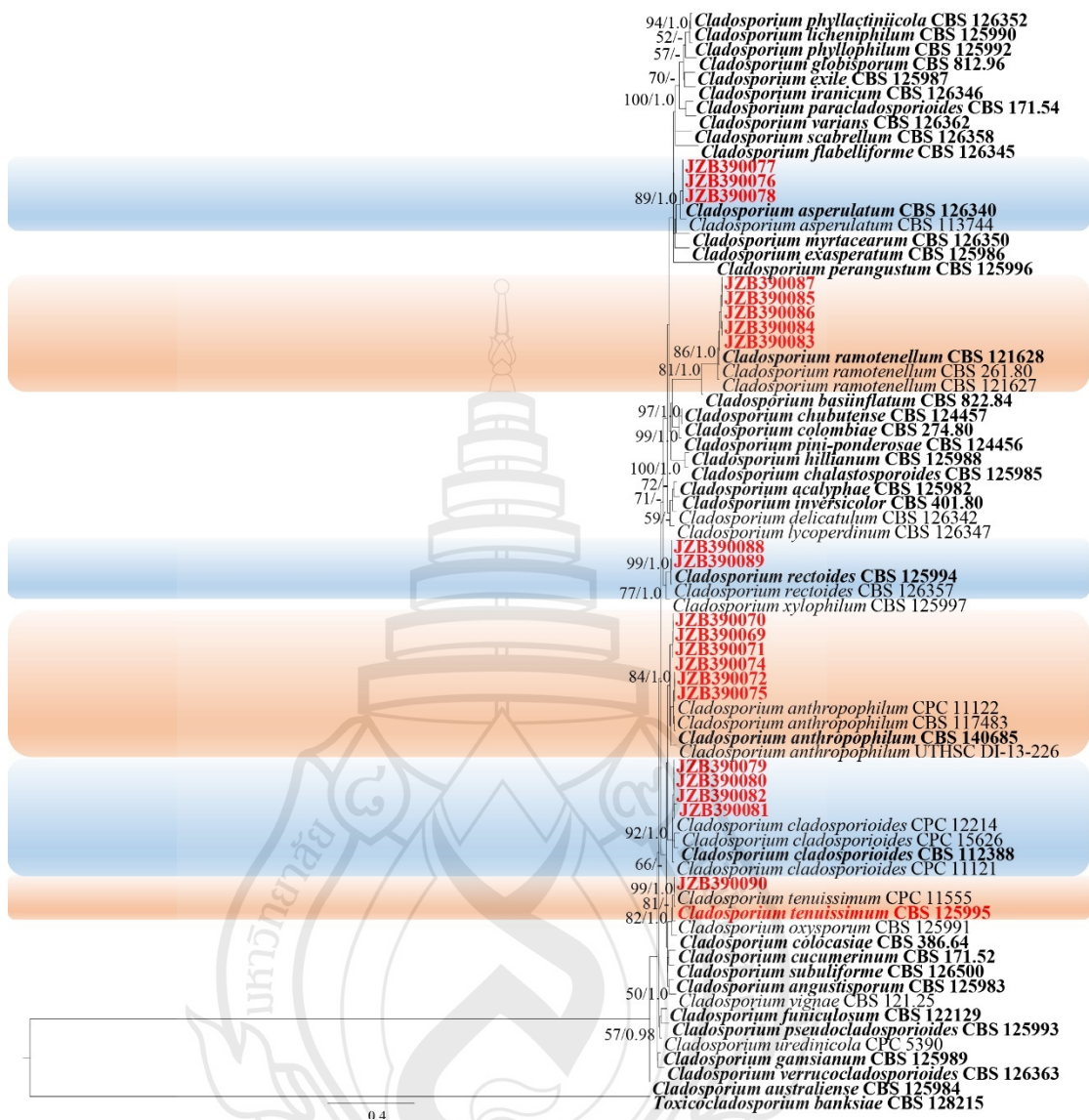
Figure 3.14 Phylogenetic tree generated by maximum likelihood analysis of combined ITS, *tef1*, and *act* sequence data of *Cladosporium* species

Figure 3.14 *Toxicocladosporium banksiae* (CBS 128215) was used as the outgroup. ML bootstrap support values ≥50% (BT) and Bayesian posterior probabilities ≥0.90 (BYPP) are shown near the nodes. The scale bar indicates 0.007 changes per site. Isolates from the current study are in red, and type specimens are in bold.

3.2.3.3 Taxonomy

Cladosporium anthropophilum Sand.-Den., Gené & Wiederh., in Sandoval-Denis, Gené, Sutton, Wiederhold, Cano-Lira & Guarro, Persoonia 36: 290 (2016)

Asexual morph: Hyphomycetous. Mycelium superficial and immersed. Hyphae 2–4 μm wide, septate, unbranched or branched, subhyaline to pale olivaceous, smooth, thick-walled. Conidiophores up to 207 μm long, 2–4 μm wide, macro- and semi-macronematous, erect, cylindrical, sometimes geniculate, septate, branched or unbranched, pale olivaceous brown, non-nodulose, thick-walled. Conidia forming short branched chains with up to four conidia in the terminal unbranched part of the chain, small terminal conidia 4–7 × 2–4 μm ($\bar{x}$ = 5.4 × 3.0 μm, n = 30), ovoid or ellipsoid; intercalary conidia 5–12 × 2–4 μm ($\bar{x}$ = 7.1 × 2.9 μm, n = 30), limoniform to ellipsoidal, aseptate. Secondary ramoconidia 9–27 × 2.5–3.5 μm ($\bar{x}$ = 14.0 × 3.0 μm, n = 30), ellipsoid to subcylindrical, often attenuated at the centre, 0–2-septate, smooth or finely roughened, subhyaline or pale olivaceous (Figure 3.15). **Sexual morph:** Not observed.

Culture characteristics – Colonies on PDA reaching 43–50 mm diam. after ten days at 25°C, entire margined, flat, velvety, aerial mycelium abundant, grey olivaceous to olivaceous, reverse leaden grey with white margin. Colonies on SNA reaching 34–40 mm diam. after ten days at 25°C, margin regular, flat, cottony, aerial mycelium loose diffuse, olivaceous, reverse olivaceous brown (Figure 3.15).

Material examined – China, Beijing, Tongzhou district, isolated from diseased leaves of *Prunus avium*, 11 July, 2019, Yueyan Zhou (JZBH390069–JZBH390072), living cultures JZB390069–JZB390072; *ibid.*, Fangshan district, isolated from diseased leaves of *Prunus avium*, September 22, 2021, Yueyan Zhou (JZBH390074), living cultures JZB390074; *ibid.*, Haidian district, isolated from diseased leaves of *Prunus avium*, September 27, 2022, Yueyan Zhou (JZBH390075), living cultures JZB390075.

Notes – Six new isolates (JZB390069–JZB390072, JZB390074–JZB390075) were clustered with the ex-type of *C. anthropophilum* (CBS 140685) with 84% ML bootstrap value and 1.0 BYPP. And the morphological characters of the isolates resembled the description of the ex-type (Sandoval-Denis et al., 2016). *Cladosporium anthropophilum* was first introduced in 2016 as a common saprobic fungus and then frequently isolated from clinical samples and indoor environments (Sandoval-Denis et al., 2016; Bensch et al., 2018). This is the first report of *C. anthropophilum* on sweet cherry.
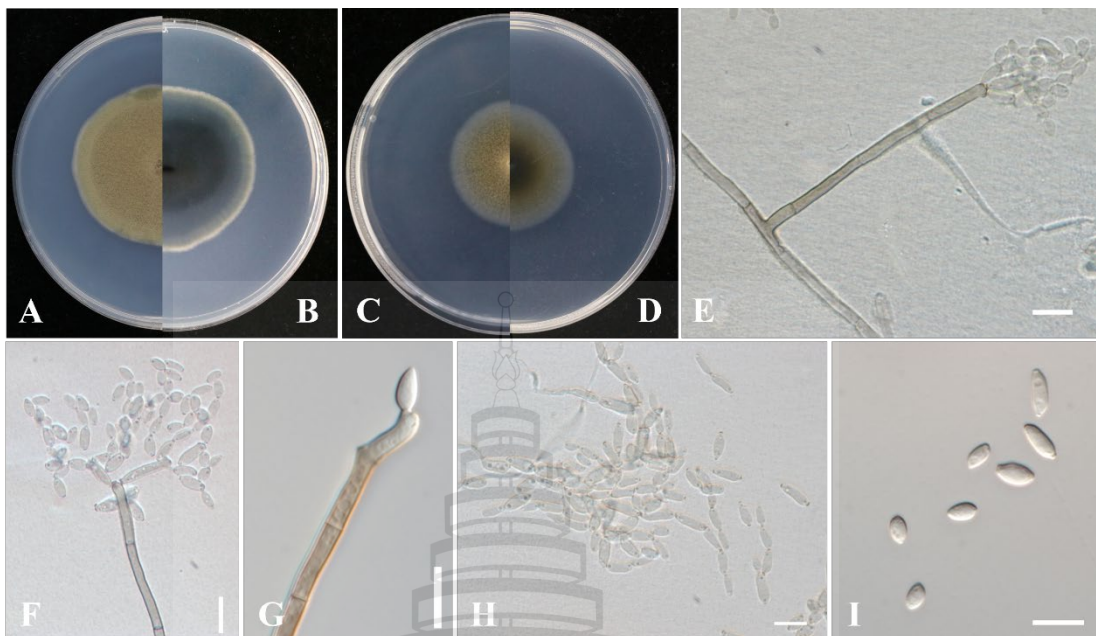
Figure 3.15 *Cladosporium anthropophilum* (JZB390070)

Figure 3.15 A–B Culture on PDA from above (A) and reverse (B). C–D Culture on SNA from above (C) and reverse (D). E–G Conidiophores. H Conidial chains. (I) Conidia. Scale bars: E–I = 10 μm.

Cladosporium asperulatum Bensch, Crous & U. Braun, Stud. Mycol. 67: 21 (2010)

Asexual morph: Hyphomycetous. Mycelium immersed. Hyphae 2.5–4 μm wide, septate, unbranched, subhyaline to pale or medium olivaceous-brown, smooth to minutely verruculose or irregularly verrucose, walls not thickened or almost so, sometimes forming ropes. Conidiophores up to 182 μm long, 3–5 μm wide, macro- and micronematous, erect, cylindrical-oblong, sometimes slightly geniculate towards the apex, septate, unbranched, occasionally branched, pale to medium olivaceous-brown, non-nodulose, smooth to asperulate or minutely verruculose, walls slightly thickened. Conidia catenate, in branched chains, up to ten conidia in the terminal unbranched part of the chain; small terminal conidia 5–8.5 × 2–4 μm (x̄ = 6.3 × 3.1 μm, n = 30), ovoid; intercalary conidia 6–13 × 2.5–4 μm (x̄ = 8.5 × 3.3 μm, n = 30), ovoid, fusiform to ellipsoid, aseptate. Secondary ramoconidia 10–20 × 3.5–5 μm (x̄ = 15.5 × 3.9 μm, n = 30), ellipsoid, fusiform, subcylindrical, not constricted at septa, smooth to minutely

verruculose, subhyaline to pale olivaceous brown (Figure 3.16). **Sexual morph:** Not observed.

Culture characteristics – Colonies on PDA reaching 31–32 mm diam. after ten days at 25°C, entire margined, flat or folded, fluffy, aerial mycelium dense, grey olivaceous with white margin, reverse leaden-grey to iron-grey. Colonies on SNA reaching 24–25 mm diam. after ten days at 25°C, margin regular, flat, cottony, aerial mycelium abundant, pale-olivaceous, reverse olivaceous to olivaceous-brown (Figure 3.16).

Material examined – China, Beijing, Tongzhou district, isolated from diseased leaves of *Prunus avium*, 11 July, 2019, Yueyan Zhou (JZBH390076, JZBH390077), living cultures JZBH390076, JZBH390077; *ibid.*, Fangshan district, isolated from diseased leaves of *Prunus avium*, September 22, 2021, Yueyan Zhou (JZBH390078), living cultures JZB390078.

Notes – Three new isolates (JZBH390076–JZBH390078) were clustered with the ex-type of *C. asperulatum* (CBS 126340) with 89% ML bootstrap value and 1.0 BYPP. Morphologically, the isolates conformed to the description of the ex-type (Bensch et al., 2010). *Cladosporium asperulatum* was introduced in 2010 from plant materials (Bensch et al., 2010), while its effects on the plants have not been specifically reported. This is the first report of *C. asperulatum* on sweet cherry.
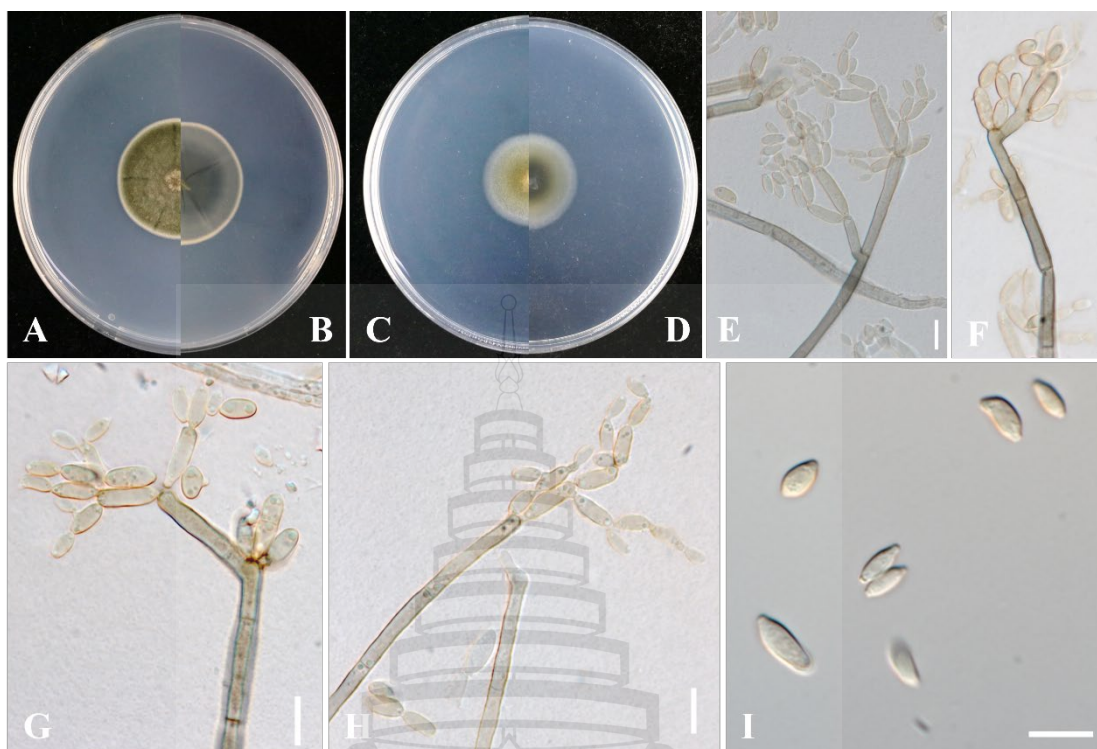
Figure 3.16 *Cladosporium asperulatum* (JZB390077)

Figure 3.16 A–B Culture on PDA from above (A) and reverse (B). C–D Culture on SNA from above (C) and reverse (D). E–G Conidiophores. H Conidial chains. I Conidia. Scale bars: E–I = 10 μm.

Cladosporium cladosporioides (Fresen.) G.A. de Vries, Contrib. Knowledge of the Genus Cladosporium Link ex Fries: 57 (1952)

Description — see Bensch et al. (2012).

Culture characteristics – Colonies on PDA reaching 47–50 mm diam. after ten days at 25°C, margin regular, flat to low convex, velvety to floccose, aerial mycelium dense, grey olivaceous, reverse leaden grey. Colonies on SNA reaching 32–33 mm diam. after ten days at 25°C, margin regular, flat, floccose, aerial mycelium loose to somewhat dense, light grey olivaceous, reverse olivaceous brown (Figure 3.17).

Material examined – China, Beijing, Tongzhou district, isolated from diseased leaves of *Prunus avium*, 11 July, 2019, Yueyan Zhou (JZBH390079, JZBH390080), living cultures JZB390079, JZB390080; *ibid.*, Fangshan district, isolated from diseased leaves of *Prunus avium*, 22 September, 2021, Yueyan Zhou (JZBH390081), living cultures

JZB390081; *ibid.*, Haidian district, isolated from diseased leaves of *Prunus avium*, 27 September, 2022, Yueyan Zhou (JZBH390082), living cultures JZB390082.

Notes – Four new isolates (JZBH390079–JZB390082) were clustered with the ex-type of *C. cladosporioides* (CBS 112388) with 92% ML bootstrap value and 1.0 BYPP. And their morphological characters conformed to the description of the ex-type (Bensch et al., 2012). *Cladosporium cladosporioides* is one of the most common saprophytic species, widely distributed in plants, air, soil, food and numerous other materials worldwide, and exists as an endophyte or secondary invader on faded or necrotic parts of many host plants (Bensch et al., 2012). The species was reported to cause leaf scab disease on papaya (Chen et al., 2009), blossom blight of red powder puff (Mukhtar et al., 2021), and fruit rot of grapes (Liu et al., 2021), and it was found to be the primary pathogens causing the core browning and moldy core of apples (Gao et al., 2013). In addition, it also has the potential to be a biocontrol agent. Köhl et al. (2015) found that the antagonistic strain of *C. cladosporioides* could reduce apple scab in leaves and fruits, which reached the same control levels as commercial fungicides. On cherry, *C. cladosporioides* was isolated from imported buds by Bensch et al. (2012).
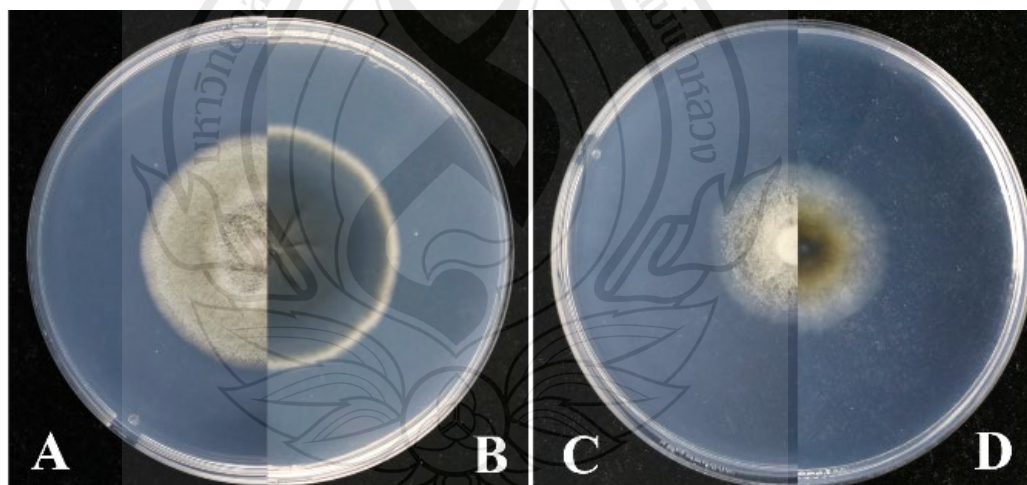
Figure 3.17 *Cladosporium cladosporioides* (JZB390081)

Figure 3.17 A–B Culture on PDA from above (A) and reverse (B). C–D Culture on SNA from above (C) and reverse (D).

Cladosporium ramotenellum K. Schub., Zalar, Crous & U. Braun, in Schubert, Groenewald, Braun, Dijksterhuis, Starink, Hill, Zalar, de Hoog & Crous, Stud. Mycol. 58: 137 (2007)

Asexual morph: Hyphomycetous. Mycelium superficial. Hyphae 2–4.5 μm wide, septate, unbranched, hyaline or subhyaline, smooth, walls not thickened. Conidiophores up to 251 μm long, 2.5–5 μm wide, macro- and micronematous, erect, cylindrical, septate, usually unbranched, subhyaline to pale olivaceous or brown, non-nodulose, smooth to minutely verruculose, walls not thickened. Conidia numerous, forming short branched chains with up to six conidia in the terminal unbranched part of the chain; small terminal conidia 3–7 × 2–4 μm ($\bar{x}$ = 4.5 × 3.0 μm, n = 30), globose, subglobose or ovoid, obovoid or limoniform, aseptate; intercalary conidia 6–12 × 3–4 μm ($\bar{x}$ = 8.6 × 3.6 μm, n = 30), ellipsoid, limoniform to subcylindrical. Secondary ramoconidia 8–28 × 2.5–5 μm, ellipsoid, subcylindrical to cylindrical-oblong, 0–3-septate, minutely verruculose, subhyaline to pale olivaceous ($\bar{x}$ = 16.7 × 3.8 μm, n = 30) (Figure 3.18). **Sexual morph:** Not observed.

Culture characteristics – Colonies on PDA reaching 40–57 mm diam. after ten days at 25℃, the margin slightly undulate, flat, powdery, olivaceous, reverse leaden grey. Colonies on SNA reaching 25–27 mm after ten days at 25℃, margin entire or slightly undulate, flat, aerial mycelium sparse, diffuse, olivaceous to olivaceous brown, reverse olivaceous brown (Figure 3.18).

Material examined – China, Beijing, Tongzhou district, isolated from diseased leaves of *Prunus avium*, 11 July 2019, Yueyan Zhou (JZBH390083–JZBH390085), living cultures JZB390083–JZB390085; *ibid.*, Tongzhou district, isolated from diseased leaves of *Prunus avium*, 20 October 2020, Yueyan Zhou (JZBH390086), living cultures JZB390086; *ibid.*, Fangshan district, isolated from diseased leaves of *Prunus avium*, 22 September 2021, Yueyan Zhou (JZBH390087), living cultures JZB390087.

Notes – Five new isolates (JZB390083–JZB390087) were clustered with the ex-type of *C. ramotenellum* (CBS 121628) with 86% ML bootstrap value and 1.0 BYPP. The isolates showed similar morphological characters to the original description of *C. ramotenellum* (Schubert et al., 2007). *Cladosporium ramotenellum* was initially isolated from indoor environments and water (Schubert et al., 2007). As a common

saprobic species, it has been reported to occur on various substrates with a wide geographic distribution (Bensch et al., 2015), and reported as a clinically relevant fungus in the United States (Sandoval-Denis et al., 2015). This is the first report of *C. ramotenellum* on sweet cherry.
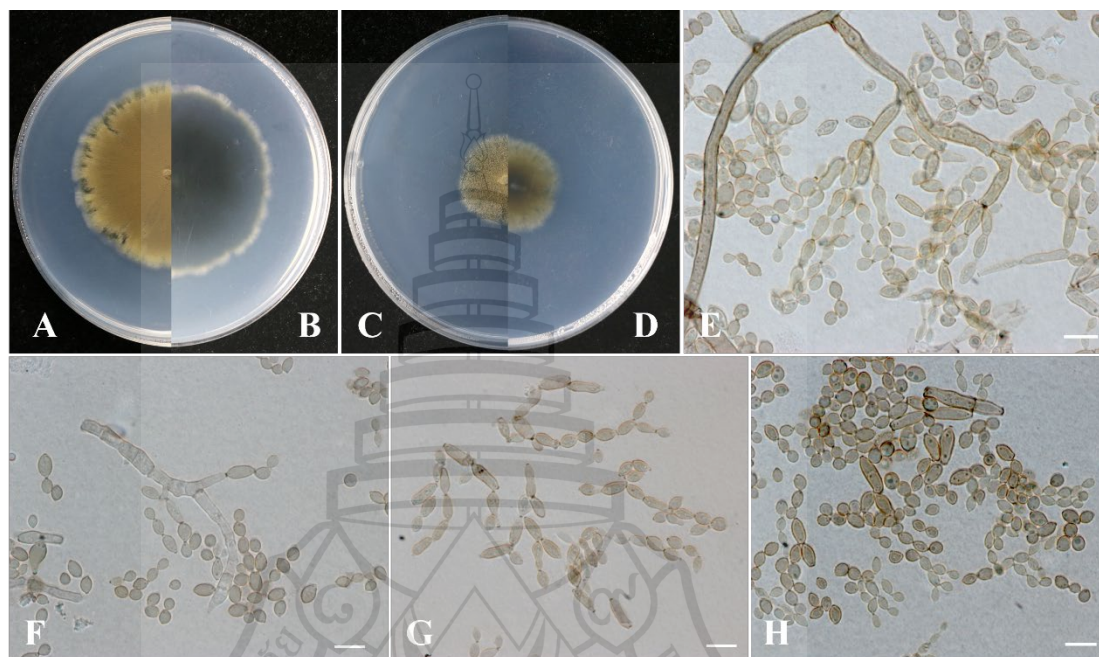
Figure 3.18 *Cladosporium ramotenellum* (JZB390084)

Figure 3.18 A–B Culture on PDA from above (A) and reverse (B). C–D Culture on SNA from above (C) and reverse (D). (E, F) Conidiophores. (G) Conidial chains. (H) Conidia. Scale bars: E–H = 10 μm.

Cladosporium rectoides Bensch, H.D. Shin, Crous & U. Braun, Stud. Mycol. 67: 73 (2010)

Description — see Bensch et al., (2012).

Culture characteristics – Colonies on PDA reaching 54–56 mm diam. after ten days at 25°C, margin regular, somewhat furrowed or wrinkled, velvety to floccose, aerial mycelium dense, olivaceous-grey to iron-grey, reverse leaden grey to olivaceous-black. Colonies on SNA reaching 31–35 mm diam. after ten days at 25°C, margin regular, flat, woolly-floccose, aerial mycelium loosely to densely floccose, olivaceous brown with a white margin, reverse brownish (Figure 3.19).

Material examined – China, Beijing City, Tongzhou district, isolated from diseased leaves of *Prunus avium*, 11 July 2019, Yueyan Zhou (JZBH390088, JZBH390089), living cultures JZB390088–JZB390089.

Notes – Two new isolates (JZBH390088 and JZBH390089) were clustered with the ex-type of *C. rectoides* (CBS 125994) with 99% ML bootstrap value and 1.0 BYPP. Morphologically, the isolates resembled the ex-type of *C. rectoides* (Bensch et al., 2010). *Cladosporium rectoides* was introduced from unknown plant materials, while the lifestyle was not provided (Bensch et al., 2010). This is the first report of *C. rectoides* on sweet cherry.
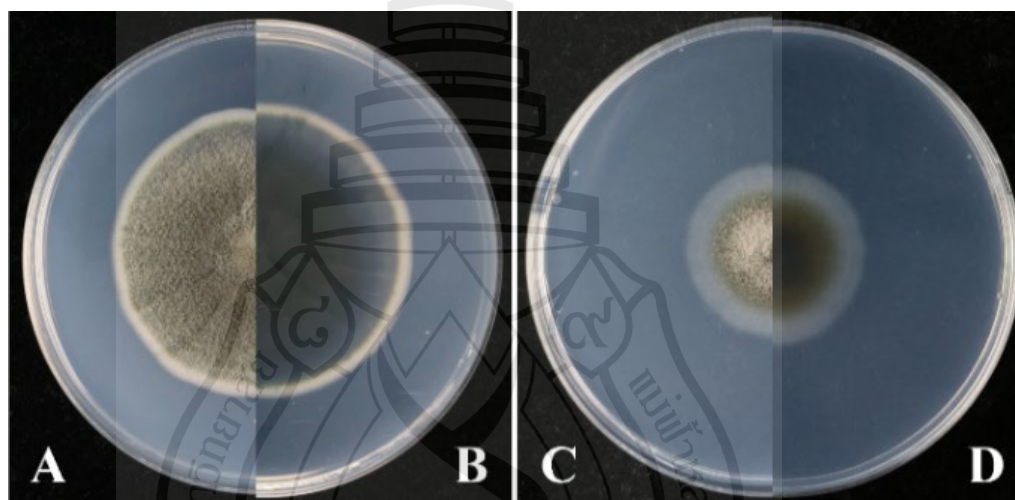
Figure 3.19 *Cladosporium rectoides* (JZB390089)

Figure 3.19 C*ladosporium rectoides* (JZB390089). A–B Culture on PDA from above (A) and reverse (B). C–D Culture on SNA from above (C) and reverse (D).

Cladosporium tenuissimum Cooke, Grevillea 6(no. 40): 140 (1878)

Asexual morph: Hyphomycetous. Mycelium immersed and superficial. Hyphae 2–4 μm wide, septate, branched, subhyaline to pale or medium brown, smooth to sometimes minutely verruculose, walls unthickened. Conidiophores up to 175 μm long, 2.5–4 μm wide, macronematous and micronematous, cylindrical-oblong to almost filiform, sometimes slightly to distinctly geniculate towards the apex, unbranched or branched, pale to medium brown or olivaceous-brown, non-nodulose or subnodulose, smooth, walls somewhat thickened. Conidia abundant, catenate, forming in densely branched chains with up to six conidia in the upper unbranched part; small terminal

conidia 3.5–6 × 2–3 μm (x̄ = 4.5 × 2.5 μm, n = 30), subglobose, obovoid, limoniform, sometimes globose, aseptate; intercalary conidia 4–14 × 2–4 μm (x̄ = 6.4 × 2.9 μm, n = 30), ovoid, ellipsoid or subcylindrical, aseptate. Secondary ramoconidia 13–22 × 3.5–5 μm (x̄ = 15.5 × 4.0 μm, n = 30), ellipsoid, fusiform to subcylindrical or cylindrical, 0-2 septate, smooth, pale brown or pale olivaceous-brown. **Sexual morph:** Not observed.

Culture characteristics – Colonies on PDA reaching 49–51 mm diam. after ten days at 25°C, margin regular, flat, powdery, grey olivaceous to dull green, reverse leaden grey to olivaceous black. Colonies on SNA reaching 26–30 mm after ten days at 25°C, margin regular, flat, floccose, aerial mycelium dense, olivaceous brown (Figure 3.20).

Material examined – China, Beijing City, Haidian district, isolated from diseased leaves of *Prunus avium*, 27 September 2022, Yueyan Zhou (JZBH390090), living cultures JZBH390090.

Notes – One new isolate (JZB390090) was clustered with the ex-type of *C. tenuissimum* (CBS 12995) with 82% ML bootstrap value and 1.0 BYPP. Morphologically, the isolate showed similar characteristics to *C. tenuissimum* (Bensch et al., 2010). This species is phenotypically similar to *C. cladosporioides* and often confused with the latter; thereby, the two species were divided based on the differences in genes and morphology, such as conidiophores, conidiogenous cells, conidial chains and secondary ramoconidia (Bensch et al., 2010; Bensch et al., 2012). *Cladosporium tenuissimum* is a common saprobe on numerous substrates and also a pathogen causing leaf spots on several hosts, including carnation (Xie et al., 2022), alfalfa (Han et al., 2019), and peanut (Geng et al., 2022). The species was also reported as one of the main pathogens causing the core browning and mouldy core of apples (Gao et al., 2013). This is the first report of *C. tenuissimum* on sweet cherry.
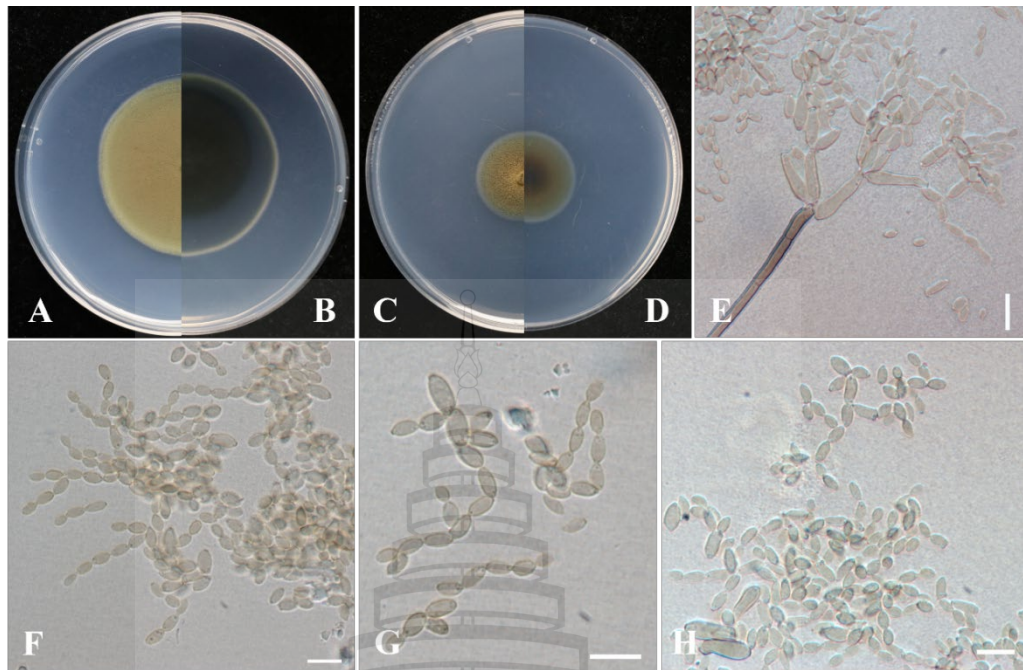
Figure 3.20 *Cladosporium tenuissimum* (JZB390090)

Figure 3.20 A–B Culture on PDA from above (A) and reverse (B). C–D Culture on SNA from above (C) and reverse (D). E Conidiophores. F–G Conidial chains. H Conidia. Scale bars: E–H = 10 μm.

3.2.3.4 Summary

Cladosporium is a monophyletic genus in Cladosporiaceae with a wide ecological distribution and host range. It is one of the largest genera of dematiaceous hyphomycetes with a coronate structure, conidia in acropetal chains (David, 1997; Bensch et al., 2010). In this study, six *Cladosporium* species associated with cherry leaf spots were identified and characterized, among which *C. anthropophilum* is dominant (28.6%). Except for *C. cladosporioides* has been reported from cherry buds, *C. anthropophilum*, *C. asperulatum*, *C. ramotenellum*, *C. rectoides,* and *C. tenuissimum* are new host records on sweet cherry. Their pathogenicity on cherry needs to be further studied.

3.2.4 Two Additional Species from Cherry Leaf Spot

During fungal isolation of cherry leaf spot, except for the above main genera, one additional new host record species and one new species were identified.

Diaporthe beijingensis Y.Y. Zhou, W. Zhang & J.Y. Yan. ***sp. nov.***

Index Fungorum number: IF902257; Facesoffungi number: FoF 15928 Figure 3.21

Etymology – 'beijingensis' refers to Beijing in China, from which it was isolated.

Associated with leaf spots of *Prunus avium* leaves. **Sexual morph:** Produced on 30 days old PDA culture. *Perithecia* 220–397 μm diam., subglobose, black, solitary to scattered, ostiolate. *Perithecial necks* 38–103 μm., black, subcylindrical, tapering towards the apex. *Asci* 25.6–37.2 × 5–8 μm ($\bar{x}$ = 31.8 × 6.7 μm, n = 30), unitunicate, 8-spored, sessile, ellipsoid to clavate, widest at centre and rounded towards the apices. *Ascospores* 5.6–8.5 × 2–3 μm ($\bar{x}$ = 6.5 × 2.6 μm, n = 50), hyaline, often biguttulate, ellipsoid to fusoid, **Asexual morph:** *Conidiomata* 180–350 μm diam., pycnidial, globose or irregular, scattered, orange cream conidial drops exuded from the ostioles. *Alpha conidia* 5–7.5 × 1.5–3 μm ($\bar{x}$ = 6.9 × 2.7 μm, n = 60), hyaline, biguttulate, fusoid to ellipsoid, *Beta* and *Gamma* conidia not observed.

Culture characteristics – Colonies on PDA entirely white both on surface and reverse. Reverse become amber with time. Aerial mycelium felty, colonies reaching 75 mm diam. after 4 days in room temperature.

Material examined – China, Beijing, on leaf spot of *Prunus avium* L. (*Rosaceae*), 27 September 2022, Yueyan Zhou and Wei Zhang 22-HD-2-5a (JZBH320260, **holotype**), ex-type JZB320260.

Notes – *Diaporthe beijingensis* forms a distinct clade within *Diaporthe* and is sister to *D. caulivora* (Figure 3.22). It forms an independent branch with 100% ML support. The morphological characters of our new collection are similar to *D. caulivora* (CBS 127268, ex-neotype). However, base pair showed 2.1% (11/536) differences in ITS, 4.4% (15/343) in *tef*, 1.6% (7/429 bp) in *act*, 2.2% (8/356) in *cal*, and 3.2% (15/475) in *his* between *D. beijingensis* (JZB320260) and *D. caulivora* (CBS 127268). Therefore, we introduce *Diaporthe beijingensis* as a new species.
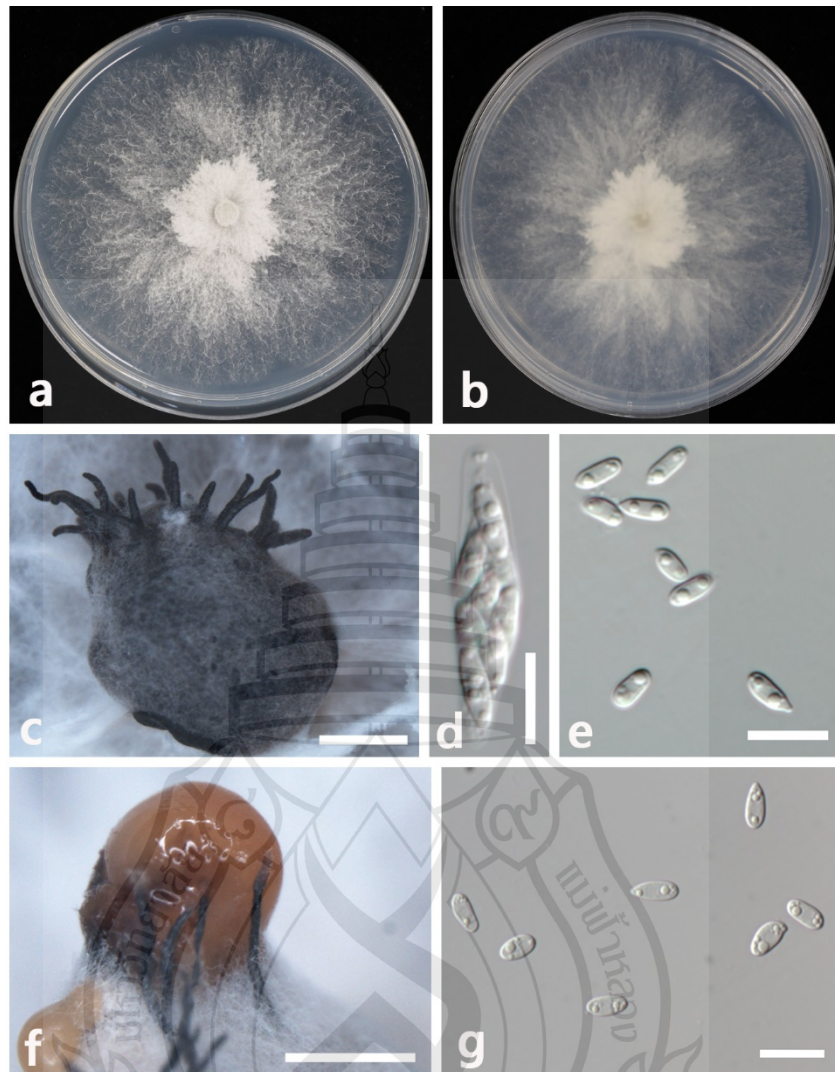
Figure 3.21 Morphological characters of *Diaporthe beijingensis* (JZB320260, holotype)

Figure 3.21 a Surface, b Reverse view of 4-days old colony on PDA. c Ascomata. d Asci. e Ascospores. f Conidiomata. g Conidia. Scale bars: c=20 μm; d, e=10 μm; f=100 μm; g=10 μm.

Figure 3.22 Phylogram of *Diaporthe* generated from maximum likelihood analysis based on combined ITS, *tef*, *tub*, *cal* and *his* sequence data

Figure 3.22 142 taxa were included in the combined analyses, which comprised 2151 characters in the alignment. Bootstrap support values equal or greater than for ML ≥ 60% and BYPP ≥ 0.95 are given above the nodes. The tree is rooted with *Diaporthe sojae* (FAU635) and *D. actinidiae* (ICMP 13683). The ex–type strains are indicated in bold. The newly generated sequence is indicated in red.

Neopestalotiopsis rosae Maharachch., K.D. Hyde & Crous, in Maharachchikumbura, Hyde, Groenewald, Xu & Crous, Stud. Mycol. 79: 147 (2014)

Index Fungorum number: IF809777; Facesoffungi number: FoF03890; Figure 3.23

Associated with the leaf spot of *Prunus avium*. **Sexual morph:** Not observed. **Asexual morph**: *Conidiomata* globose, solitary, black, 200–500 μm diam. *Conidiophores* indistinct, often reduced to conidiogenous cells. *Conidiogenous cells* discrete, cylindrical, hyaline, 7–20 × 3–5 μm. *Conidia* fusoid, ellipsoid, straight or slightly curved, 4-septate, 22–31 × 5–9 μm ($\overline{x}$ = 25.8 × 7.3 μm, n = 50); basal cell conic to obconic with a truncate base, hyaline, 4–6 μm long; three median cells doliiform, brown, septa and periclinal walls darker than the rest of the cell, 16–18.5 μm long (second cell from base 4–6 μm long; third cell 4.5–6.5 μm long; fourth cell 4–7 μm long); apical cell 3–5 μm long, cylindrical, hyaline, with 2–4 tubular appendages, filiform, 21–35 μm long; basal appendage single, tubular, unbranched, centric, 4.5–10 μm long.

Material examined – China, Beijing, Fangshan District, on the leaf spot of *Prunus avium*, 22 September 2021, Yueyan Zhou, JZB340092.

Notes – The morphologies of the asexual morph of our fungal collection are similar to the holotype of *N. rosae* isolated from a stem lesion in *Rosa* sp. (Maharachchikumbura et al., 2014). According to the phylogenetic analyses, our collection (JZB340092) clustered with the ex-type strain of *N. rosae* (CBS 101057) with 77% ML and 0.91 BYPP bootstrap supports (Figure 3.24). The species has been reported on a wide range of hosts, including *Eucalyptus* spp. (Belisário et al., 2020; Santos et al., 2020), *Fragaria × ananassa* (Essa et al., 2018; Rebollar-Alviter et al., 2020; Wu et al., 2020), *Paeonia suffruticosa* (Maharachchikumbura et al., 2014), *Persea americana* (Fiorenza et al., 2022), *Prunus avium* (this study), *Punica granatum* L. (Xavier et al., 2020), *Rosa* sp. (Maharachchikumbura et al., 2014), *Vaccinium corymbosum* (Rodríguez-Gálvez et al., 2020; Santos et al., 2022) and *Vitis vinifera* (Cosseboom & Hu, 2021; Zhou et al., 2023). The current study presents new host records of *N. rosae* on *Prunus avium* in China.
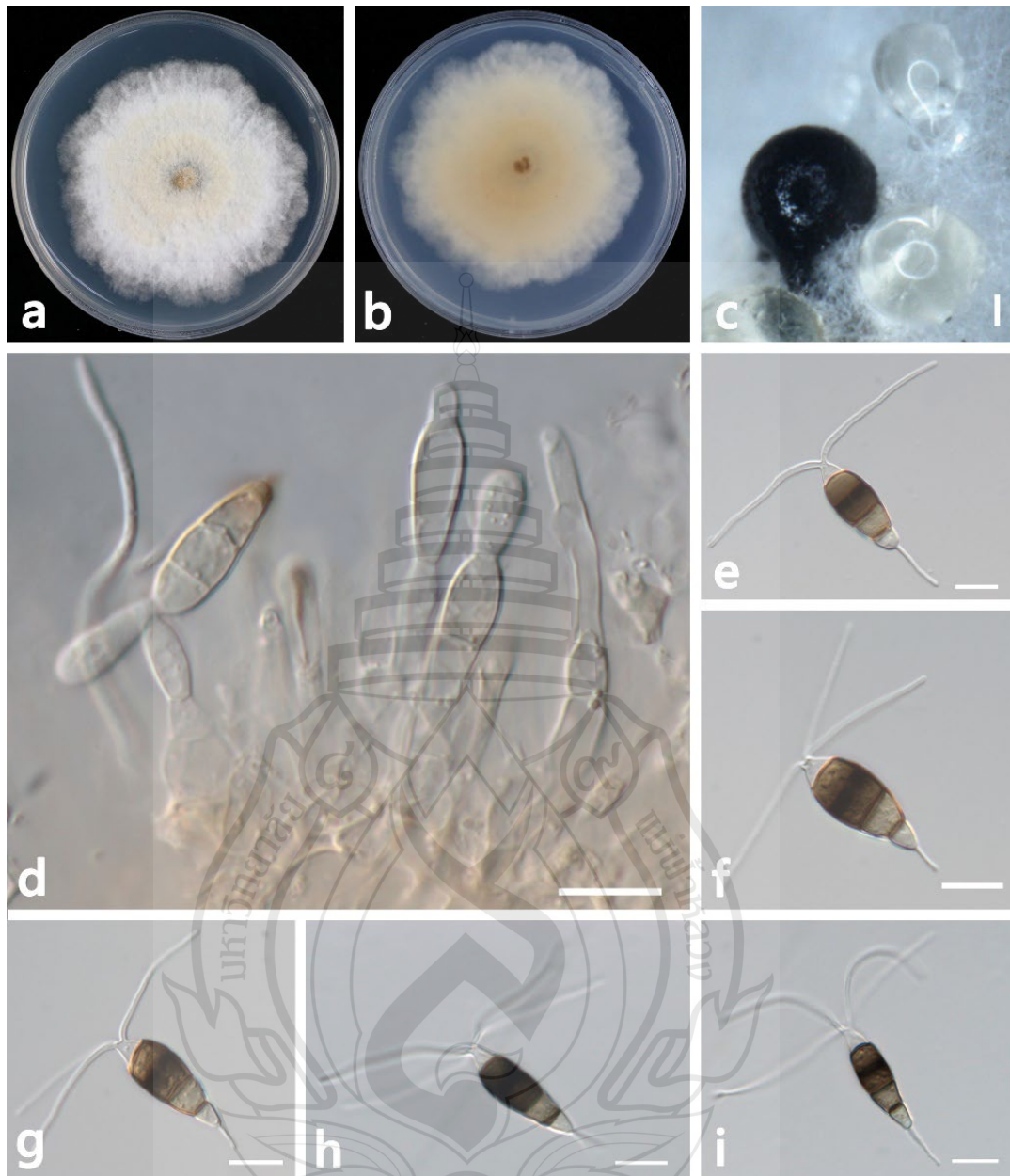
Figure 3.23 Morphological characters of *Neopestalotiopsis rosae* (JZB340092)

Figure 3.23 a the top view of a 5-day colony on PDA. b the bottom view of a 5-day colony on PDA. c Conidioma formed on PDA. d Conidiogenous cells. e–i Conidia. Scale bars: c = 100 μm, d–i = 10 μm.
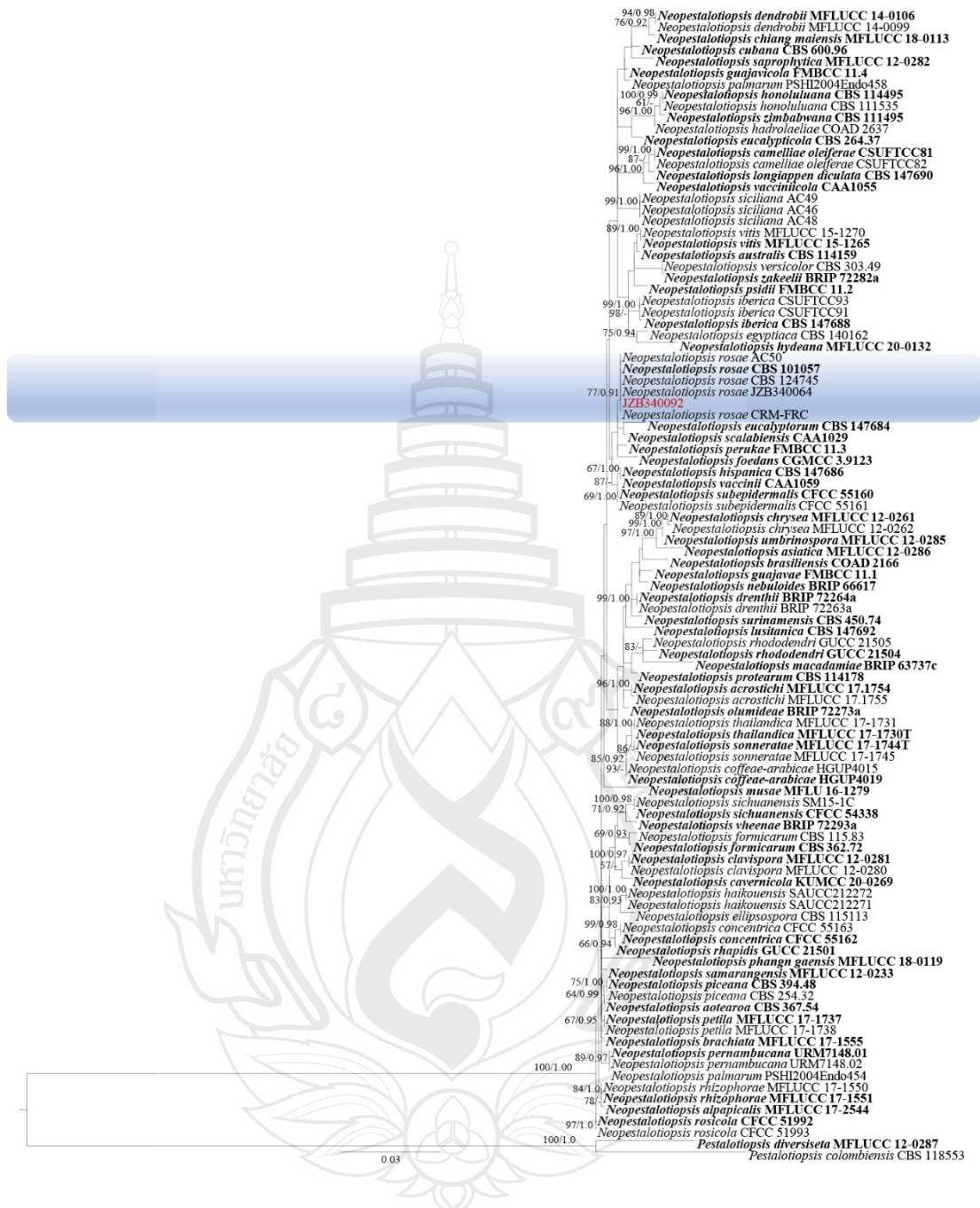
Figure 3.24 Phylogram generated from the maximum likelihood analysis based on the combined ITS, *tub* and *tef1-α* sequence data of the genus *Neopestalotiopsis*

Figure 3.24 101 strains are included in the combined analyses. Tree topology of the maximum likelihood analysis is similar to the Bayesian analysis. The best RAxML tree with a final likelihood value of -5269.182443 is presented. The matrix had 386 distinct alignment patterns, with 4.32% of undetermined characters or gaps. Bootstrap

support values for ML greater than 60% and Bayesian posterior probabilities greater than 0.90 are given near nodes, respectively. The tree was rooted with *Pestalotiopsis colombiensis* (CBS 118553) and *Pestalotiopsis diversiseta* (MFLUCC 12-0287). Ex-type strains are in bold. The newly generated sequences are indicated in red.

3.2.5 A Summary of Fungal Species Associated with Cherry Leaf Spot Disease Around the World

The checklist is based on publications and a current study (Table 3.5). The current name is used according to Index Fungorum (2024) and the classification follows Hyde et al. (2024). Up to now, a total of forty-five species have been reported from cherry leaf spots.

Table 3.5 Records of fungal species associated with cherry leaf spot disease around the world

Species	Life mode	Disease name	Locality	Identification method	Reference
Alternaria alternata	Pathogen	Cherry leaf spot/ cherry black spot	China (BJ, GS, LN, QH); Greece	Morphology + multi-gene phylogeny	Thomidis and Tsipouridis (2006), Chethana et al. (2019), Liu et al. (2020), Yang et al. (2020), Zhao et al. (2013)
Alternaria cerasi	Pathogen	Cherry leaf spot	China (GS)	Morphology	Zhu & Chang (2004)
Alternaria tenuissima	Pathogen	Cherry leaf spot/ cherry black spot	China (GS, QH)	Morphology + multi-gene phylogeny	Liu et al. (2020), Yang et al. (2020)
Alternaria pseudoeichhorniae	Pathogen	Cherry leaf spot	China (BJ)	Morphology + multi-gene phylogeny	Chethana et al. (2019)
Botryosphaeria dothidea	Pathogen	Cherry leaf spot	China (BJ, LN, SD)	Morphology + multi-gene phylogeny	Zhou et al. (2021)
Blumeriella jaapii	Pathogen	Cherry leaf spot	Australia, India, Italy, South Africa, USA	-	Cook and Dub (1989), Annesi et al. (1997), Doidge (1950), Garcia and Jones (1993), Khan et al. (2014)
Cladosporium anthropophilum	Undetermined	Cherry leaf spot	China (BJ)	Morphology + multi-gene phylogeny	This study
Cladosporium asperulatum	Undetermined	Cherry leaf spot	China (BJ)	Morphology + multi-gene phylogeny	This study
Cladosporium cladosporioides	Undetermined	Cherry leaf spot	China (BJ)	Morphology + multi-gene phylogeny	This study

Table 3.5 (continued)

Species	Life mode	Disease name	Locality	Identification method	Reference
Cladosporium ramotenellum	Undetermined	Cherry leaf spot	China (BJ)	Morphology + multi-gene phylogeny	This study
Cladosporium rectoides	Undetermined	Cherry leaf spot	China (BJ)	Morphology + multi-gene phylogeny	This study
Cladosporium tenuissimum	Undetermined	Cherry leaf spot	China (BJ)	Morphology + multi-gene phylogeny	This study
Colletotrichum aenigma	Pathogen	Cherry leaf spot/ anthracnose	China (BJ)	Morphology + multi-gene phylogeny	Chethana et al. (2019), Zhou et al. (2023)
Colletotrichum conoides	Pathogen	Cherry leaf spot/ anthracnose	China (BJ, SC, SD, LN)	Morphology + multi-gene phylogeny	Zhou et al. (2023)
Colletotrichum dematium	Pathogen	Cherry leaf spot/ anthracnose	China (BJ, SC, SD, LN)	Morphology + multi-gene phylogeny	Zhou et al. (2023)
Colletotrichum fructicola	Pathogen	Cherry leaf spot/ anthracnose	China (ZJ)	Morphology + multi-gene phylogeny	Tang et al. (2022), Zhou et al. (2023)
Colletotrichum gloeosporioides	Pathogen	Cherry leaf spot/ anthracnose	China (BJ, SC, SD, LN)	Morphology + multi-gene phylogeny	Zhou et al. (2023)
Colletotrichum hebeiense	Pathogen	Cherry leaf spot/ anthracnose	China (BJ, SC, SD, LN)	Morphology + multi-gene phylogeny	Zhou et al. (2023)
Colletotrichum incanum	Pathogen	Cherry leaf spot/ anthracnose	China (BJ, SC, SD, LN)	Morphology + multi-gene phylogeny	Zhou et al. (2023)

Table 3.5 (continued)

Species	Life mode	Disease name	Locality	Identification method	Reference
Colletotrichum karstii	Pathogen	Cherry leaf spot/ anthracnose	China (BJ, SC, SD, LN)	Morphology + multi-gene phylogeny	Zhou et al. (2023)
Colletotrichum plurivorum	Pathogen	Cherry leaf spot/ anthracnose	China (BJ, SC, SD, LN)	Morphology + multi-gene phylogeny	Zhou et al. (2023)
Colletotrichum pseudotheobromicola	Pathogen	Cherry leaf spot/ anthracnose	China (BJ)	Morphology + multi-gene phylogeny	Chethana et al. (2019)
Colletotrichum siamense	Pathogen	Cherry leaf spot/ anthracnose	China (BJ, SC, SD, LN)	Morphology + multi-gene phylogeny	Zhou et al. (2023)
Colletotrichum sojae	Pathogen	Cherry leaf spot/ anthracnose	China (BJ, SC, SD, LN)	Morphology + multi-gene phylogeny	Zhou et al. (2023)
Colletotrichum temperatum	Pathogen	Cherry leaf spot/ anthracnose	China (BJ, SC, SD, LN)	Morphology + multi-gene phylogeny	Zhou et al. (2023)
Colletotrichum truncatum	Pathogen	Cherry leaf spot/ anthracnose	China (BJ, SC, SD, LN)	Morphology + multi-gene phylogeny	Zhou et al. (2023)
Diaporthe beijingensis	Undetermined	Cherry leaf spot	China (BJ)	Morphology + multi-gene phylogeny	This study
Diaporthe eres	Pathogen	Cherry leaf spot	China (BJ, LN, SD)	Morphology + multi-gene phylogeny	Zhou et al. (2022)
Diaporthe sojae	Pathogen	Cherry leaf spot	China (LN, SC)	Morphology + multi-gene phylogeny	Zhou et al. (2022)

Table 3.5 (continued)

Species	Life mode	Disease name	Locality	Identification method	Reference
Epicoccum nigrum	Pathogen	Brown leaf spot	China (SC)	Morphology + ITS, *tub2*, *rpb2* sequence (BLAST)	Zhang et al. (2024)
Epicoccum pseudokeratinophilum	Pathogen	Cherry leaf spot	China (BJ)	Morphology + multi-gene phylogeny	Chethana et al. (2019)
Fusarium citri	Pathogen	Cherry leaf spot	China (BJ, SD)	Morphology + multi-gene phylogeny	This study
Fusarium compactum	Pathogen	Cherry leaf spot	China (BJ, LN)	Morphology + multi-gene phylogeny	This study
Fusarium curvatum	Pathogen	Cherry leaf spot	China (LN)	Morphology + multi-gene phylogeny	This study
Fusarium ipomoeae	Pathogen	Cherry leaf spot	China (BJ)	Morphology + multi-gene phylogeny	This study
Fusarium lateritium	Pathogen	Cherry leaf spot	China (SD)	Morphology + multi-gene phylogeny	This study
Fusarium luffae	Pathogen	Cherry leaf spot	China (BJ, SD)	Morphology + multi-gene phylogeny	This study
Fusarium nygamai	Pathogen	Cherry leaf spot	China (BJ)	Morphology + multi-gene phylogeny	This study
Nothophoma pruni	Pathogen	Cherry leaf spot	China (BJ)	Morphology + multi-gene phylogeny	Chethana et al. (2019)

Table 3.5 (continued)

Species	Life mode	Disease name	Locality	Identification method	Reference
Nothophoma quercina	Pathogen	Cherry leaf spot	China (BJ)	Morphology + multi-gene phylogeny	Chethana et al. (2019)
Neopestalotiopsis rosae	Undetermined	Cherry leaf spot	China (BJ)	Morphology + multi-gene phylogeny	This study
Pruniphilomyces circumscissus	Pathogen	Cherry leaf spot	China (SD), Israel, Italy, South Africa, Spain; USA	Morphology + ITS, tef sequences (BLAST)	Saccardo (1886), Saccardo (1902), Doidge (1950), Sztejnberg (1986), López-Carbonell et al. (1998), Sun et al. (2017), Sun et al. (2022)
Pseudocercospora pruni-persicicola	Pathogen	Cherry leaf spot	Korea	Morphology + ITS sequence (BLAST)	Choi et al. (2014)
Stagonosporopsis citrulli	Pathogen	Cherry leaf spot	China (BJ)	Morphology + multi-gene phylogeny	Chethana et al. (2019)

Note BJ-Beijing City; GS-Gansu Province; LN-Liaoning Province; QH-Qinghai Province; SC-Sichuan Province; SD: Shandong Province; SN: Shaanxi Province

3.3 Discussion

Leaf spot is one of the most common and widespread diseases of sweet cherry. Though the disease was well-known to be caused by *Blumeriella jaapi* and *Pruniphilomyces circumscissus*, more findings of other species records are proving that the disease is caused by a mixed infection of various pathogens. As members of the top five groups of fungi associated with cherry leaf spot, *Colletotrichum*, *Fusarium* and *Cladosporium* species were identified in this study.

Colletotrichum is a well-known pathogen infecting a wide range of hosts, and there are emerging records of *Colletotrichum* species causing cherry leaf spot in recent years (Chethana et al., 2019; Tang et al., 2022; Zhou et al., 2023). Zhou et al. (2023) collected *Colletotrichum* isolates from different regions in China, among thirteen *Colletotrichum* species identified, C. *aenigma*, C. *gloeosporioides,* and C. *fructicola* accounted for the largest portion, suggesting that they could be dominant pathogens of anthracnose leaf spot. In this study, *Colletotrichum* isolates from Beijing were identified as the above species, which could add to the evidence of the importance of the three species. Zhou et al. (2023) found C. *aenigma* is ranked fourth in virulence on cherry leaves (cv. 'Tieton' and 'Summit') among thirteen species, following C. *conoides*, C. *dematium,* and C. *gloeosporioides*. However, C. *aenigma* inhibited low pathogenicity in this study, which only caused lesions on wounded leaves (cv. Caihong). The record of this species on sweet cherry was first reported by Chethana et al. (2019). In the pathogenicity test, it showed a significant difference in virulence on three cultivars, which reflected in producing much larger lesions on 'Summit' than 'Tieton' and 'Sunburst'. Also, the pathogenicity showed differences between isolates. This phenomenon could explain that the pathogenicity result is influenced by varieties and fungal strains.

Fusarium is one of the most renowned genera, which includes a large number of saprotrophs, endophytes or pathogens (Sandoval-Denis et al., 2018). As a common plant pathogen, *Fusarium* spp. can cause many diseases with a wide range of hosts, usually causing wilts, blights, rots, and cankers (Ma et al., 2013). *Fusarium* can also be the causal agent of leaf spot disease in several plants, including Dracaena, mango, peanut and *Bletilla striata* (Baka & Krzywinski, 1996; Guo et al., 2021; Xu et al., 2021;

Zhou et al., 2021). *Fusarium* species reported on sweet cherry are usually associated with trunk disease. *Fusarium oxysporum* has been reported as the pathogen of cherry root and crown rot in Canada (Úrbez-Torres et al., 2016), and *F. lateritium* was reported to cause trunk diseases in Australia (Cook & Dubé, 1989). Five *Fusarium* species have also been reported to cause postharvest rot on Chinese cherry (Wang et al., 2021). However, the occurrence of *Fusarium* on cherry leaf spot has not been reported before in the world. In this study, *Fusarium* species were identified as causal agents of cherry leaf spot for the first time. All seven species showed obvious pathogenicity on cherry leaves, and these species all have records as pathogens on other hosts (see 3.2.2.5 Summary); therefore, attention should be paid to Fusarium leaf spot on sweet cherry, which may cause severe damage in some conditions.

Cladosporium is a ubiquitous fungal genus distributed on a wide range of substrates, including plants, soil, food, clinical and other samples, as well as outdoor and indoor air (Bensch et al., 2012; Sandoval-Denis et al., 2016; Bensch et al., 2018). Members of *Cladosporium* exist on numerous plants as saprobes, endophytes and pathogens (Bensch et al., 2012). Leaf spots caused by *Cladosporium* species have been observed in many plants, including vegetables like spinach (du Toit et al., 2012), ornamental crops like carnation (Xie et al., 2022), and forage crops like alfalfa (Han et al., 2019). In addition, some of the species showed antagonistic potential against phytopathogens. For example, *C. cladosporioides* could reduce apple scab in leaves and fruits (Köhl et al., 2015), and *C. herbarum* has the biocontrol ability of Eutypa dieback of grapevine (Munkvold & Marois 1993). Though it is a widespread fungus, few reports of *Cladosporium* were on sweet cherry. Only *C. cladosporioides* and *C. phyllophilum* were reported to be isolated from imported buds of sweet cherry (Bensch et al., 2012). Six *Cladosporium* species were generated from cherry leaf spot in the current study. Several records of *C. cladosporioides* and *C. tenuissimum* on different hosts are associated with foliar, blossom and fruit diseases in China, while other species were usually reported as saprobes or environmental fungi. Their virulence on cherry leaves needs to be further studied to confirm that these *Cladosporium* species act as the main pathogens of this type of leaf spot, as secondary pathogens or only common saprobes.

The results also showed that different fungal genera were related to different symptoms. *Colletotrichum* is associated with circular to subcircular brown spots with dark-brown or purple margins, or brown leaf blights; *Fusarium* causes circular or irregular, purple-brownish to grey-brownish spots or necrotic lesions; and *Cladosporium* was isolated from leaf spots, including pinpoint lesions or irregular blights. However, the relationship between fungi and disease symptoms is still a preliminary speculation based on limited samples. In the field, it is usually difficult to distinguish the specific pathogen under the circumstances of mixed infection. Further research is necessary to understand the occurrence of pathogens in cherry diseases.

Different from the main fungal genera such as *Colletotrichum*, *Fusarium* and *Cladosporium*, some other fungi were occasionally found in cherry leaf spot. Two *Diaporthe* species have been reported to cause cherry leaf spot by Zhou et al. (2022), and a new species of *Diaporthe* was introduced in the current study. Additionally, *Neopestalotiopsis rosae*, which is a common pathogen on other hosts, was first reported in this study. Even though, there are only three isolates of *Diaporthe beijingensis* and one isolate of *Neopestalotiopsis rosae* were generated, they have not been related to the symptom types; Therefore, whether they are pathogenic on cherry leaves needs to be further studied.

This study also listed all the fungal species associated with cherry leaf spot, which provided a summary of the current research advances on fungal pathogens of the disease. Most pathogens previously identified only based on morphology or ITS sequence, phylogenetic analyses have been used in several recent papers, while some research still use the BLAST of single or several gene sequences for molecular identification. Compared with other important fruit crops, such as grape and strawberry, research on cherry disease is still limited.

In conclusion, the present study expands the knowledge, as well as provides a systematic review of fungal species associated with cherry leaf spot disease worldwide. These findings can serve as a valuable insight into the research on the occurrence regularity and management strategies of cherry leaf spot disease.

CHAPTER 4

IDENTIFICATION OF FUNGAL SPECIES ASSOCIATED WITH GRAPEVINE TRUNK DISEASE

4.1 Introduction

Among all woody agricultural plants, *Vitis vinifera* is known as the host that is affected by the widest variety of pathogens, especially fungal pathogens. According to statistics, *V. vinifera* is susceptible to 29 fungal diseases. Grapevine trunk diseases (GTDs) are among the most destructive diseases worldwide and have drawn considerable attention during the last few decades (Gramaje et al., 2018; Reis et al., 2019). They reduce vineyard longevity, productivity and quality, and the worldwide loss caused by the diseases is estimated to be $1.5 billion annually (Hofstetter et al., 2012; Dissanayake et al., 2015a). Grapevine trunk diseases are a group of diseases causing necrosis and discoloration of wood and vascular tissue, even the death of the tree, including five types: Esca complex, Eutypa dieback, Botryosphaeria dieback, Black foot and Phomopsis (Diaporthe) dieback (Mondello et al., 2018; Ye et al., 2021a). Grapevine trunk diseases in fields are usually a mix of different disease types caused by various pathogens rather than a single one. Up to 2018, 133 fungal species belonging to 34 genera have been reported to be associated with grapevine trunk diseases (Gramaje et al., 2018). These fungi mainly act as latent pathogens, which can develop symptoms several years after the infection (Hrycan et al., 2020).

Esca disease complex is one of the oldest and most severe trunk diseases caused by *Phaeomoniella chlamydospora*, *Phaeoacremonium minimum* and a few other *Phaeoacremonium* spp. in all grapevine-growing areas worldwide. The history of the disease is possible as long as vine cultivation (Gramaje et al., 2018). Furthermore, some basidiomycete fungi like *Fomitiporia* species were also reported to cause Esca diseases (Clorte et al., 2015). In 2021, Ye and colleagues provided the first detailed report on the Esca complex in China, confirming that both *F. punicata* and *P. minimum* are the

causal agents of the Esca complex on Chinese grapevines (Ye et al., 2021b). This study also provided the first host record for *F. punicata* on the grapevine worldwide.

Botryosphaeria dieback is another important grapevine trunk disease reported in most grape-growing countries (Yan et al., 2013). More than 20 species from the Botryosphaeriaceae have been reported to cause Botryosphaeria dieback, including *Botryosphaeria* spp., *Diplodia* spp., *Dothiorella* spp., *Lasiodiplodia* spp., *Neofusicoccum* spp., *Neoscytalidium* spp., *Phaeobotryosphaeria* spp. and *Spencermartinsia* spp. (Gramaje et al., 2018). In China, Yan et al. (2013) first reported Botryosphaeria dieback in detail with its causative agents, *Botryosphaeria dothidea*, *Diplodia seriata*, *Lasiodiplodia theobromae*, and *Neofusicoccum parvum*. In addition, *Neofusicoccum mangiferae* and *Lasiodiplodia citricola* were also reported as pathogens of grapevine dieback in subsequent studies (Dissanayake et al., 2015b; Wu et al., 2021).

The black foot disease is a worldwide devastating grapevine trunk disease caused by *Cylindrocarpon*-like fungi, mainly in grapevine nurseries and young plantations and is commonly associated with species belonging to *Campylocarpon*, *Cylindrocladiella*, *Dactylonectria*, *Ilyonectria*, *Neonectria*, *Pleiocarpon* and *Thelonectria* (Gramaje et al., 2018; Lawrence et al., 2019). Ye et al. (2021c) first reported the black foot disease in China caused by five pathogens, *Cylindrocladiella lageniformis*, *Dactylonectria alcacerensis*, *D. macrodidyma*, *D. torresensis* and *Neonectria* sp. Recent studies have identified other fungi, such as *Campylocarpon fasciculare*, as causative agents of black foot disease on young grapevines in China (Abeywickrama et al., 2021). In addition, *Ilyonectria liriodendri* (former *Neonectria liriodendri*) has been reported as the pathogen of the black foot of grapevines in many countries (Jayawardena et al., 2018).

Furthermore, Diaporthe dieback is another disease categorised in the grapevine trunk disease complex worldwide. Currently, around 30 *Diaporthe* species have been identified as causal organisms of Diaporthe dieback in grape-producing countries, of which ten were reported in China (*D. eres*, *D. guangxiensis*, *D. hongkongensis*, *D. hubeiensis*, *D. gulyae*, *D. pescicola*, *D. phaseolorum*, *D. sojae*, *D. unshiuensis*, *D. viniferae*), and *Diaporthe eres* proved to be the most commonly isolated species in both studies in 2015 and 2019 (Dissanayake et al., 2015a; Guarnaccia et al., 2018; Manawasinghe et al., 2019).

Eutypa dieback has been one of the most damaging diseases in Australia, France and California since the 1970s. To date, no effective measures are available to control this disease (Mondello et al., 2018). Among the 24 Diatrypaceae species that cause this disease, *Eutypa lata* is the most virulent and common (Gramaje et al., 2018). Eutypa dieback was first reported in China in 2007 with *Eutypella vitis* as the pathogen, but this has not been proved by Koch's postulates (Ye et al., 2021a).

Due to the complexity of the disease and the lack of the most effective chemical products, managing grapevine trunk diseases is difficult (Gramaje et al., 2018). It is well-accepted that grapevine trunk diseases should be managed by an integrated disease management strategy, including biological control (Gramaje et al., 2018).

4.2 Results

4.2.1 Field Sampling and Fungal Isolation

In 2021, grapevine trunk diseases were investigated in 14 grapevine orchards in Beijing, Fujian, Hebei, Hubei, Ningxia, Shaanxi, Shanxi and Yunnan Provinces, China (Figure 4.1).
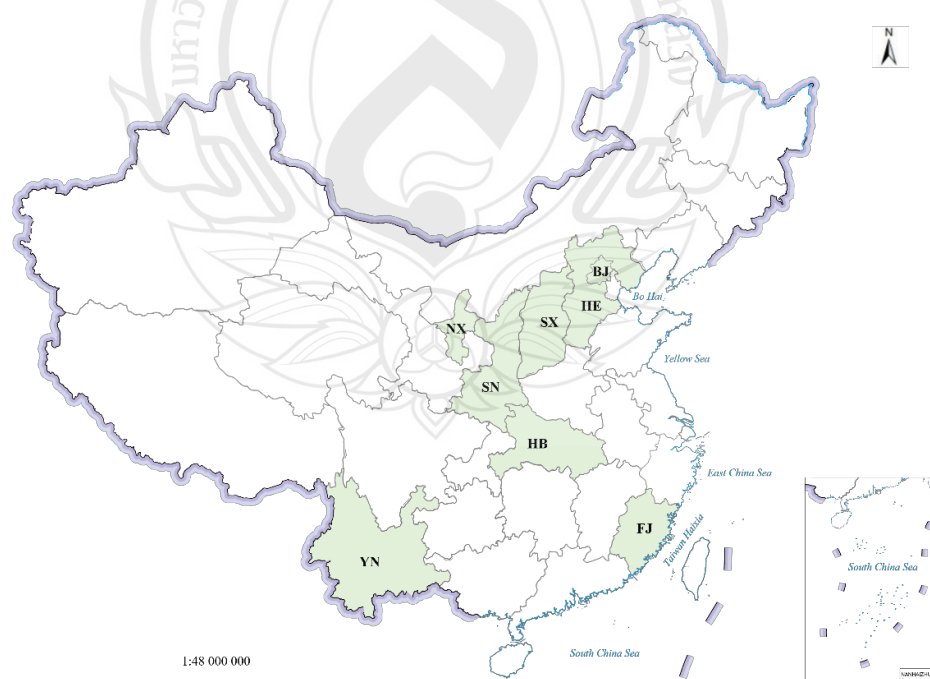
Figure 4.1 Sample collection sites of grapevine trunk diseases in eight provinces in China

Figure 4.1 A–C leaf symptoms in the field. D–F leaf spot samples. Sample collection sites of grapevine trunk diseases in eight provinces in China. BJ: Beijing. FJ: Fujian. HB: Hubei. HE: Hebei. NX: Ningxia. SN: Shaanxi. SX: Shanxi. YN: Yunnan.

Diseased grapevines exhibited several symptoms (Figure 4.2):

1. Weak tree vigour: low growth, stunt sprout, small leaves and short internodes. Leaves discoloured or appear tiger-striped symptoms. Berries poorly developed or uneven ripening;

2. Dieback: usually evident in early spring, the tree cannot sprout normally, and branches are dried-up, even the whole plant wilting or dead. The trunk shows discoloured vascular tissues in a cross-section, sometimes appears canker lesions or black fruit bodies, and/or roots poorly developed;

3. Fruits shrivelled or dry rotted, stem brown and wilting, sometimes appears black fruit bodies on the surface.

The investigation results showed that plant decline, dieback, fruit shirking and fall-off are the major symptoms of grapevine trunk diseases in China, which lead to the reduction of productivity and life span of grapes. Grapevine trunk diseases were observed in nearly 20% of orchards, and the proportion of diseased plants was about 10% in the investigated fields, up to 100% in severe cases. Main grapevine trunk diseases including black foot, Botryosphaeria dieback and Diaporthe dieback were observed in this investigation.

Figure 4.2 Symptoms of grapevine trunk diseases

Figure 4.2 a Stunted growth of plants. b Dried-up and discoloured leaves. c Dead grapevine. d Tiger striped leaves. e Shrivelled berries. f Uneven ripening of berries. g Withered shoot with fruiting bodies. h Necrotic root. i–j Internal symptoms of the diseased trunk. k Rotted berry with fruiting bodies. l Conidiomata on the necrotic trunk.

4.2.2 Isolation Results of Grapevine Trunk Disease Samples

A total of 199 purified fungal isolates were obtained from 68 samples collected from eight provinces. Further, these isolates were identified into 40 species across 21 genera and ten families. Among them, 22 species were reported as new geographical records in China, and 12 were new host records (Table 4.1). *Diaporthe* was the most dominant (19.6%), followed by *Dactylonectria* (14.1%), *Fusarium* (10.6%), and *Botryosphaeria* (8.5%). Most Botryosphaeriaceae, *Pestalotiopsis*-like and *Colletotrichum* species were isolated from the trunk, while most *Dactylonectria* species were isolated from the root. *Diaporthe* and *Fusarium* were isolated from both trunk and root. *Dactylonectria*, *Botryosphaeria* and *Bartalinia* were widely distributed in China. Sequences generated in this study were deposited in the GenBank.

Table 4.1 Details of fungal taxa and sources

No.	Family (count)	Genus (count)	Species	Count	Isolation source	Records on grapevine in China	Records on grapevine in other countries around the world
1	Botryosphaeriaceae (37)	*Botryosphaeria* (17)	*B. dothidea*	17	HB (T), YN (T, R), BJ (T), HE (T, TB)	Yan et al. (2012)	More than 20 countries
2		*Lasiodiplodia* (9)	*L. citricola*	4	HE (TB)	Wu et al. (2021)	Italy (Carlucci et al., 2015), Australia (Burgess et al., 2019)
3			*L. pseudotheobromae*	3	YN (T, R)	Dissanayake et al. (2015c)	Brazil (Correia et al., 2016), Tunisia (Rezgui et al., 2018), Australia (Burgess et al., 2019)
4			*L. theobromae*	2	HB (T)	Yan et al. (2013)	More than 15 countries (Farr & Rossman, 2023)
5		*Diplodia* (3)	*D. seriata*	3	HE (T)	Yan et al. (2013)	More than 10 countries (Farr & Rossman, 2023)
6		*Neofusicoccum* (2)	*N. parvum*	2	YN (T, R)	Yan et al. (2013)	More than 15 countries (Farr & Rossman, 2023)
7		*Phaeobotryon* (6)	*P. rhois*	6	NX (T, R)	**First report**	**First report**
8	Nectriaceae (72)	*Dactylonectria* (28)	*D. novozelandica*	12	YN (R), HE (TB, R), BJ (R)	Tan et al. (2022)	USA (Lawrence et al., 2019), New Zealand (Lawrence et al., 2019), South Africa (Lombard et al., 2014), Spain (Berlanas et al., 2020)
9			*D. alcacerensis*	10	SX (R), BJ (TB, R), HE (R)	Ye et al. (2021a)	USA (Lawrence et al., 2019), Portugal (Carlucci et al., 2017), South Africa (Langenhoven et al., 2018), Spain (Berlanas et al., 2020), Turkey (Güngör-Savaş et al., 2020)

Table 4.1 (continued)

No.	Family (count)	Genus (count)	Species	Count	Isolation source	Records on grapevine in China	Records on grapevine in other countries around the world
10			*D. torresensis*	3	HE (R), NX (R)	Ye et al. (2021a)	More than 5 countries (Farr & Rossman, 2023)
11			*D. macrodidyma*	3	BJ (TB), YN (R)	Ye et al. (2021a)	USA (Lawrence et al., 2019), France (Pintos et al., 2018), Portugal (Carlucci et al., 2017), South Africa (Lombard et al., 2014), Spain (Berlanas et al., 2020)
12		*Ilyonectria* (7)	*I. liriodendri*	7	SX (R), NX (T), BJ (TB)	**First report**	More than 10 countries (Farr & Rossman, 2023)
13		*Cylindrocladiella* (3)	*C. viticola*	3	YN (R)	**First report**	South Africa (van Coller et al., 2005)
14		*Fusarium* (21)	*F. oxysporum*	9	HE (R, T), YN (R), FJ (R)	Jayawardena et al. (2018)	Australia, Brazil, South Africa, Spain (Jayawardena et al., 2018), Italy (Lorenzini & Zapparoli, 2015), Egypt (Ziedan et al., 2011)
15			*F. brachygibbosum*	4	BJ (R)	**First report**	**First report**
16			*F. acuminatum*	4	NX (T); SX (T)	**First report**	Spain (Jayawardena et al., 2018)
17			*F. hainanense*	2	YN (T)	**First report**	**First report**
18			*F. lacertarum*	1	SN (R)	**First report**	**First report**
19			*F. compactum*	1	YN (T)	**First report**	**First report**
20		*Neocosmospora* (11)	*N. falciformis*	7	SN (R), NX (T), BJ (R)	**First report**	**First report**
21			*N. solani*	4	HE (R), FJ (R)	**First report**	Brazil, India (Jayawardena et al., 2018)

Table 4.1 (continued)

No.	Family (count)	Genus (count)	Species	Count	Isolation source	Records on grapevine in China	Records on grapevine in other countries around the world
22		*Bisifusarium* (2)	*B. delphinoides*	2	HE (R)	**First report**	India (on *Plasmopara viticola*) (Ghule et al., 2018)
23	Diaporthaceae (39)	*Diaporthe* (39)	*D. eres*	37	BJ (T, R), HE (T, TB, R)	Manawasinghe et al. (2019)	More than 10 countries (Farr & Rossman, 2023)
24			*D. unshiuensis*	2	FJ (T)	Manawasinghe et al. (2019)	
25	Togniniaceae (2)	*Phaeoacremonium* (2)	*P. iranianum*	2	HE (T)	**First report**	More than 5 countries (Farr & Rossman, 2023)
26	Schizoparmaceae (7)	*Coniella* (7)	*C. vitis*	7	BJ (T), HE (T, R)	Chethana et al. (2017)	
27	Sporocadaceae (16)	*Pestalotiopsis* (6)	*P. kenyana*	3	FJ (T)	**First report**	**First report**
28			*P. rhodomyrtus*	2	FJ (T)	**First report**	**First report**
29			*P. adusta*	1	FJ (R)	**First report**	**First report**
30		*Neopestalotiopsis* (2)	*N. rosae*	2	YN (T, R)	**First report**	USA (Cosseboom & Hu, 2021)
31		*Bartalinia* (8)	*B. kevinhydei*	8	YN (T), NX (T), HE (T), BJ (T)	**First report**	**First report**
32	Glomerellaceae (10)	*Colletotrichum* (10)	*C. viniferum*	6	FJ (S), BJ (T)	Yan et al. (2015)	Brazil (Echeverrigaray et al., 2020), Japan (Yokosawa et al., 2020), Korea (Oo & Oh, 2017)
33			*C. nymphaeae*	3	FJ (S, T)	Liu et al. (2016)	Brazil (Echeverrigaray et al., 2020)
34			*C. kahawae*	1	YN (T)	**First report**	Brazil (Echeverrigaray et al., 2020)
35	Pleosporaceae (8)	*Alternaria* (8)	*A. alternata*	6	SX (T), HE (T, TB)	Jayawardena et al. (2018)	More than 10 countries (Farr & Rossman, 2023)
36			*A. longipes*	2	FJ (T)	**First report**	**First report**

Table 4.1 (continued)

No.	Family (count)	Genus (count)	Species	Count	Isolation source	Records on grapevine in China	Records on grapevine in other countries around the world
37	Hypocreaceae (6)	*Trichoderma* (6)	*T. asperellum*	3	YN (T, R)	**First report**	Italy (Lorenzini et al., 2016)
38			*T. guizhouense*	2	BJ (R)	**First report**	**First report**
39			*T. virens*	1	HE (R)	**First report**	Bruez et al. (2016)
40	Cladosporiaceae (2)	*Cladosporium* (2)	*C. tenuissimum*	2	FJ (T)	Jayawardena et al. (2018)	
Total	**10**	**21**	**40**	**199**		**22 first records**	**12 first records**

Note T-trunk; R-root; TB-trunk base.
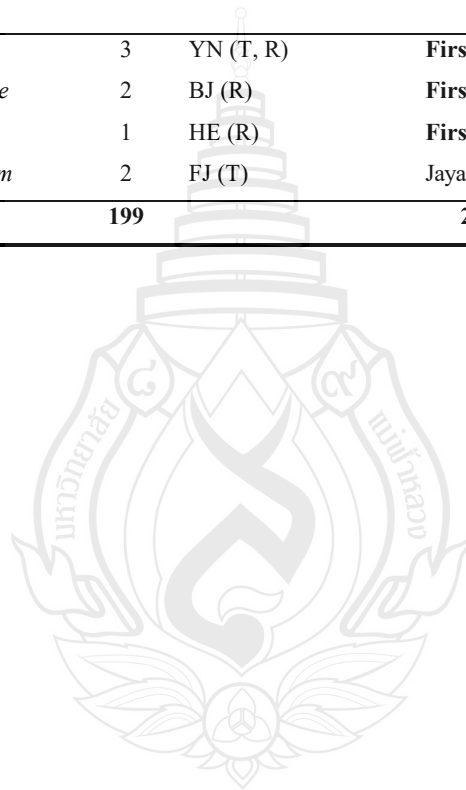
4.2.3 Phylogenetic Analysis and Morphological Characterization

Botryosphaeriaceae Theiss. & Syd [as 'Botryosphaeriacae'], Annls mycol. 16(1/2): 16 (1918)

The Botryosphaeriaceae comprises a wide range of species as pathogens, endophytes or saprobes mainly on woody hosts. They are also known as opportunistic pathogens with changing environmental conditions and weak tree vigour (Phillips et al., 2013; Chethana et al., 2016). Botryosphaeriaceae comprises 22 genera based on morphology and multi-gene phylogeny (Wijayawardene et al., 2021; Zhang et al., 2021), and eight genera have been reported to associate with grapevine trunk diseases (Gramaje et al., 2018).

In this study, thirty-seven isolates of Botryosphaeriaceae were obtained, belonging to *Botryosphaeria*, *Diplodia*, *Lasiodiplodia*, *Neofusicoccum* and *Phaeobotryon*, representing seven species. For taxonomic treatments of Botryosphaeriaceae, we follow Zhang et al. (2021).

Botryosphaeria Ces. & De Not., Comm. Soc. crittog. Ital. 1 (fasc. 4): 211 (1863)

Botryosphaeria dothidea (Moug.: Fr.) Ces. & De Not., Comm. Soc. crittog. Ital. 1 (fasc. 4): 212 (1863)

Index Fungorum number: IF183247; Facesoffungi number: FoF 03512

Description – see Phillips et al., (2013)

Material examined – China, Hubei Province, Wuhan City, on the trunk of *Vitis vinifera*, 28 April 2021, Linna Wu and Xinghong Li, living cultures JZB310204, JZB310205; *ibid*., Yunnan Province, Binchuan County, on the trunk of *Vitis vinifera*, 23 July 2021, Linna Wu and Xinghong Li, living cultures JZB310206, JZB310211–JZB310214; *ibid*., on the root of *Vitis vinifera*, 23 July 2021, Linna Wu and Xinghong Li, living cultures JZB310207; *ibid*., Beijing city, on the trunk of *Vitis vinifera*, 25 August 2021, Linna Wu and Xinghong Li, living cultures JZB310208–JZB310210; *ibid*., 11 September 2021, Linna Wu and Xinghong Li, living cultures JZB310215, JZB310216; *ibid*., Hebei Province, Qinhuangdao City, Changli County, on the trunk of *Vitis vinifera*, 18 October 2021, Linna Wu and Xinghong Li, living cultures JZB310217, JZB310218; *ibid*., on the trunk-base of *Vitis vinifera*, 13 November 2021, Linna Wu and Xinghong Li, living cultures JZB310219, JZB310220.

Notes – In the multi-locus phylogenetic analyses, 17 isolates clustered with *B. dothidea* with 69% ML bootstrap value and 0.95 BYPP (Figure 4.3). *Botryosphaeria dothidea* is an opportunistic pathogen with a wide host range (Marsberg et al., 2017). Yan et al. (2013) have mentioned that *B. dothidea* was distributed in 18 provinces from north to south throughout China and took up 65% of all isolates among *Botryosphaeria* dieback pathogens in China (Yan et al., 2013).
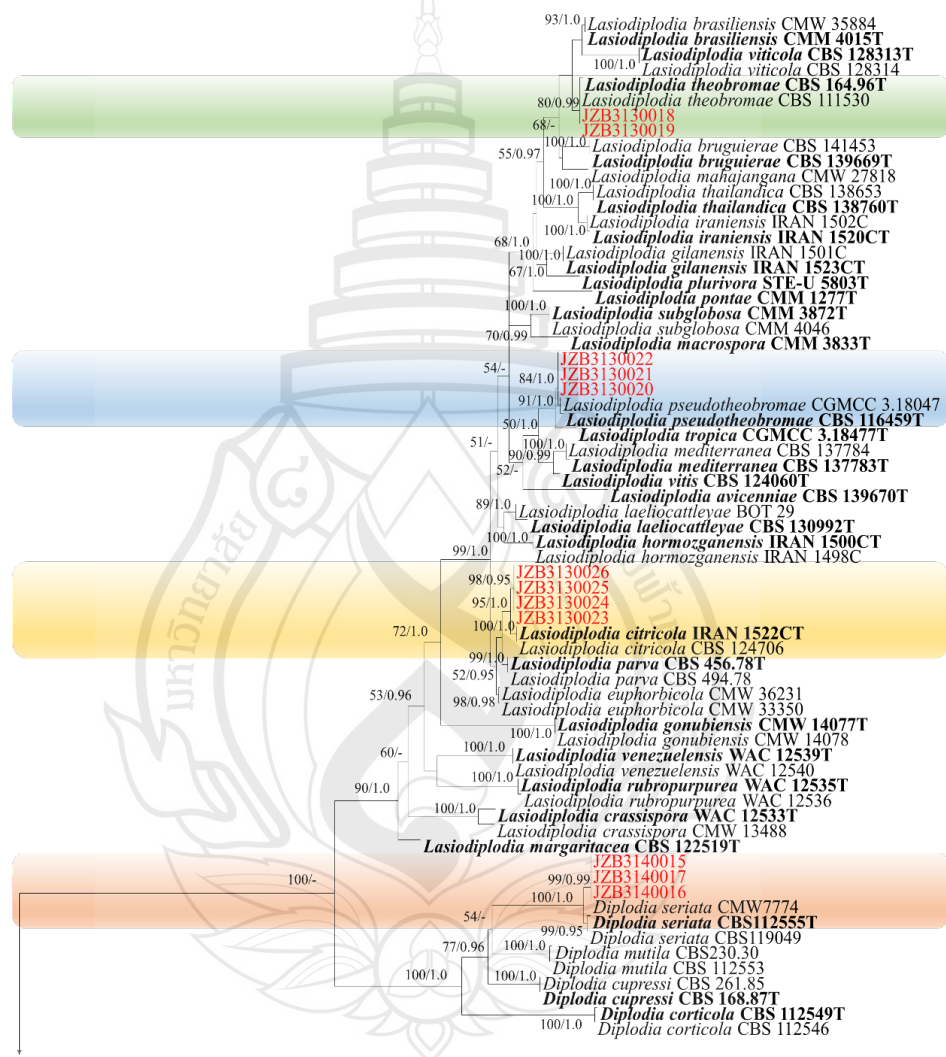
Figure 4.3 Phylogenetic tree generated by maximum likelihood analysis of combined ITS, *tef1* and *tub2* sequence data of *Botryosphaeria*, *Lasiodiplodia*, *Neofusicoccum* and *Diplodia* species
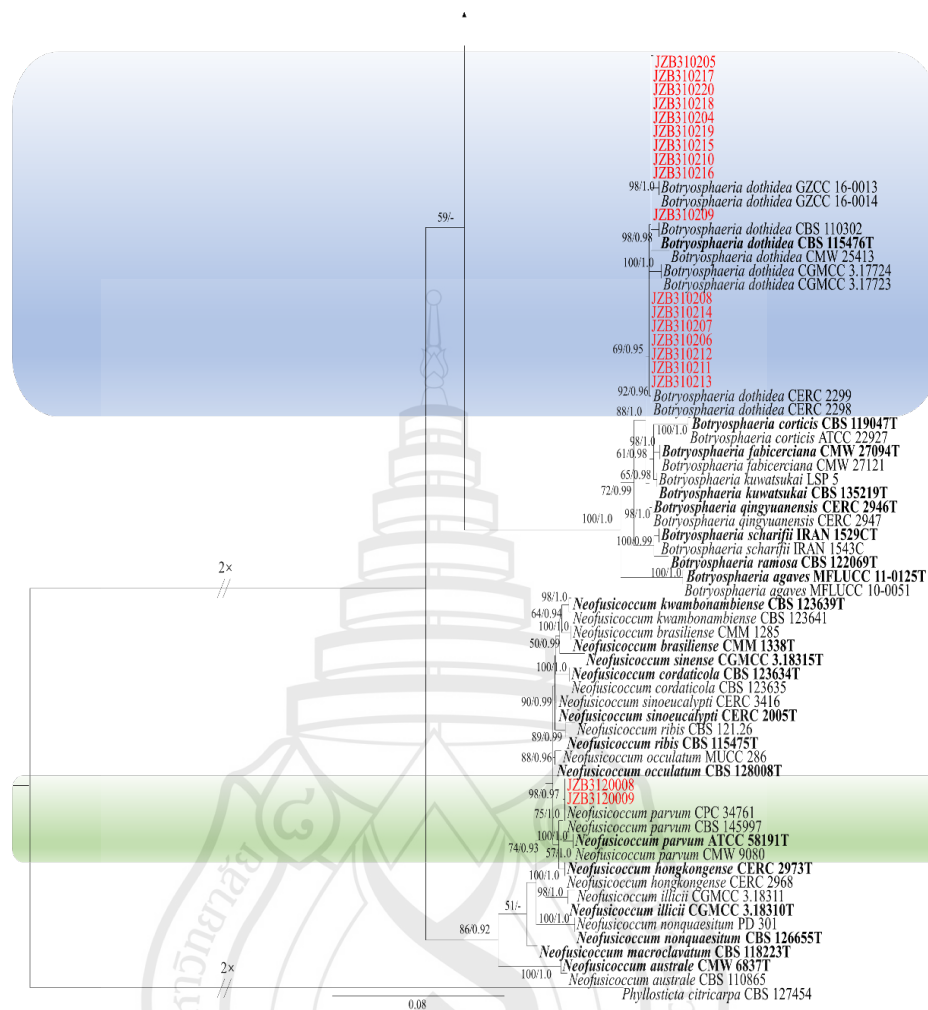
Figure 4.3 (Continued)

Figure 4.3 *Phyllosticta citricarpa* (CBS 127454) was used as the outgroup taxon. The best scoring RAxML tree with a final likelihood value of –8506.960370 was presented. The matrix had 695 distinct alignment patterns, with 19.31% of undetermined characters or gaps. Estimated base frequencies were as follows: A = 0.209952, C = 0.307342, G = 0.257379, T = 0.225327; substitution rates AC = 0.761022, AG = 2.876149, AT = 1.271062, CG = 1.067796, CT = 4.612694, GT = 1.000000; gamma distribution shape parameter α = 0.659641. ML bootstrap support values ≥50% (BT) and Bayesian posterior probabilities ≥0.90 (PP) are shown near the nodes. The scale bar indicates 0.08 changes per site. Isolates from the current study are in red and type specimens are in bold.

Diplodia Fr., in Montagne, Annls Sci. Nat., Bot., sér. 2 1: 302 (1834)

Diplodia seriata De Not., Mém. R. Accad. Sci. Torino, Ser. 2 7: 26 (1845)

Index Fungorum number: IF180468; Facesoffungi number: FoF 03596

Description – see Phillips et al. (2013)

Material examined – China, Hebei Province, Zhangjiakou City, Huailai County, on the trunk of *Vitis vinifera*, 22 August 2020, Linna Wu and Xinghong Li, living cultures JZB3140015–JZB3140017.

Notes – In the multi-locus phylogenetic analysis, three isolates clustered with *D. seriata* with 100% bootstrap value and 1.0 BYPP (Figure 4.3). The species were shown to be weakly pathogenic to grapevines in California (Úrbez-Torres & Gubler, 2009). In China, *D. seriata* was first reported by Yan et al. (2011b) on grapevine and its pathogenicity was also shown moderate virulence on most grapevine cultivars in China (Yan et al., 2013).

Lasiodiplodia Ellis & Everh., Bot. Gaz. 21: 92 (1896)

Lasiodiplodia citricola Abdollahz., Javadi & A.J.L. Phillips, Persoonia 25: 4 (2010)

Index Fungorum number: IF516777; Facesoffungi number: FoF 09503

Description – see Phillips et al. (2013)

Material examined – China, Hebei Province, Qinhuangdao City, Changli County, on the trunk base of *Vitis vinifera*, 13 November 2021, Linna Wu and Xinghong Li, living cultures JZB3130023–JZB3130026.

Notes – In the multi-locus phylogenetic analysis, four isolates clustered with *L. citricola* with 95% ML bootstrap value and 1.0 BYPP (Figure 4.3). *Lasiodiplodia citricola* was first reported on the grapevine in Italy in 2015 and showed aggressive pathogenicity (Carlucci et al., 2015). In 2020, it was first reported in China (Wu et al., 2021), causing severe symptoms or death of grapevine.

Lasiodiplodia pseudotheobromae A.J.L. Phillips, A. Alves & Crous, Fungal Diversity 28: 8 (2008)

Index Fungorum number: IF510941; Facesoffungi number: FoF 00166

Description – see Phillips et al. (2013)

Material examined – China, Yunnan Province, Binchuan County, on the trunk of *Vitis vinifera*, 23 July 2021, Linna Wu and Xinghong Li, living cultures JZB3130020; *ibid*., on the root of *Vitis vinifera*, 23 July 2021, Linna Wu and Xinghong Li, living cultures JZB3130021, JZB3130022.

Notes – In the multi-locus phylogenetic analysis, three isolates clustered with *L. pseudotheobromae* with 84% ML bootstrap value and 1.0 BYPP (Figure 4.3). *Lasiodiplodia pseudotheobromae* was first reported to cause the grapevine decline in Brazil (Correia et al., 2013) and was reported to cause pedicel and peduncle discolouration of grapes in China (Dissanayake et al., 2015c).

Lasiodiplodia theobromae (Pat.) Griffon & Maubl., Bull. Soc. mycol. Fr. 25: 57 (1909)

Index Fungorum number: IF188476; Facesoffungi number: FoF 00167

Description – see Phillips et al. (2013)

Material examined – China, Hubei Province, Wuhan City, on the trunk of *Vitis vinifera*, 13 November 2021, Linna Wu and Xinghong Li, living cultures JZB3130018, JZB3130019.

Notes – In the multi-locus phylogenetic analyses, two isolates clustered with *L. theobromae* with 80% ML bootstrap value and 0.99 BYPP (Figure 4.3). *Lasiodiplodia theobromae* is one of the most aggressive causal agents of Botryosphaeria dieback, especially in regions with hot climates (Úrbez-Torres & Gubler, 2009; Paolinelli-Alfonso et al., 2016). In 2011, this species was first reported to cause severe grapevine decline in China and was shown to be the most virulent among Botryosphaeriaceae species on grapevines (Yan et al., 2011a, 2013).

Neofusicoccum Crous, Slippers & A.J.L. Phillips, Stud. Mycol. 55: 247 (2006)

Neofusicoccum parvum (Pennycook & Samuels) Crous, Slippers & A.J.L. Phillips, in Crous, Slippers, Wingfield, Rheeder, Marasas, Phillips, Alves, Burgess, Barber & Groenewald, Stud. Mycol. 55: 248 (2006)

Index Fungorum number: IF500879; Facesoffungi number: FoF 02411

Description – see Phillips et al. (2013)

Material examined – China, Yunnan Province, Binchuan County, on the root of *Vitis vinifera*, 23 July 2021, Linna Wu and Xinghong Li, living cultures JZB3120008; *ibid*., on the trunk of *Vitis vinifera*, 23 July 2021, Linna Wu and Xinghong Li, living cultures JZB3120009.

Notes – In the multi-locus phylogenetic analysis, two isolates clustered with *N. parvum* with 75% bootstrap value and 1.0 BYPP (Figure 4.3). *Neofusicoccum parvum* is one of the most aggressive Botryosphaeria dieback pathogens worldwide. This species can cause internal cankers in the permanent woody structure of the vine (Úrbez-Torres & Gubler, 2009; Massonnet et al., 2017). In China, *N. parvum* was first reported as a grapevine Botryosphaeria dieback pathogen in 2013 while it showed weak pathogenicity on grapevines (Yan et al., 2013).

Phaeobotryon Theiss. & Syd., Annls mycol. 13(5/6): 664 (1915)

Phaeobotryon rhois C.M. Tian, X.L. Fan & K.D. Hyde, in Fan, Hyde, Liu, Liang & Tian, Phytotaxa 205(2): 95 (2015)

Index Fungorum number: IF 811599; Facesoffungi number: FoF 00596

Asexual morph: *Conidiomata* stromatic, globose. *Conidiophores* reduced to conidiogenous cells. *Conidiogenous cells* hyaline, smooth, formed from the cells lining the inner walls of the locules. *Conidia* 19–28 × 11–15 μm, ($\bar{x} \pm SD = 23.5 \pm 1.8 \times 12.5 \pm 1.0$ μm, n = 50), ellipsoid or ovoid, verruculose, initially hyaline, aseptate, and become brown with the time, 1-septate when mature (Figure 4.4). Sexual morph: Not observed.

Culture characteristics – Colonies on PDA were initially white with fluffy aerial mycelium, and later produced dark green to black pigments (Figure 4.4). Colonies reached 8.0 cm in diameter after 2 days at 25ºC.

Material examined – China, Ningxia Province, Yinchuan City, on the trunk of *Vitis vinifera*, 15 September 2021, Linna Wu and Xinghong Li (Inactive dry cultures JZBH3600001–JZBH3600003), living cultures JZB3600001–JZB3600003; *ibid*., on the root of *Vitis vinifera*, 15 September 2021, Linna Wu and Xinghong Li (Inactive dry cultures JZBH3600004–JZBH3600006), living cultures JZB3600004–JZB3600006.

Notes – In the multi-locus phylogenetic analysis, six isolates clustered with *P. rhois* with 99% bootstrap value and 1.0 BYPP (Figure 4.5). This species was reported to cause dieback and canker disease on *Rhus typhina* in China (Fan et al., 2015), as well

as *Dioscorea nipponica*, *Platycladus orientalis* and *Rhamnus dahuricus* in China (Pan et al., 2019). This is the first report of *P. rhois* associated with grapevine trunk diseases in China.
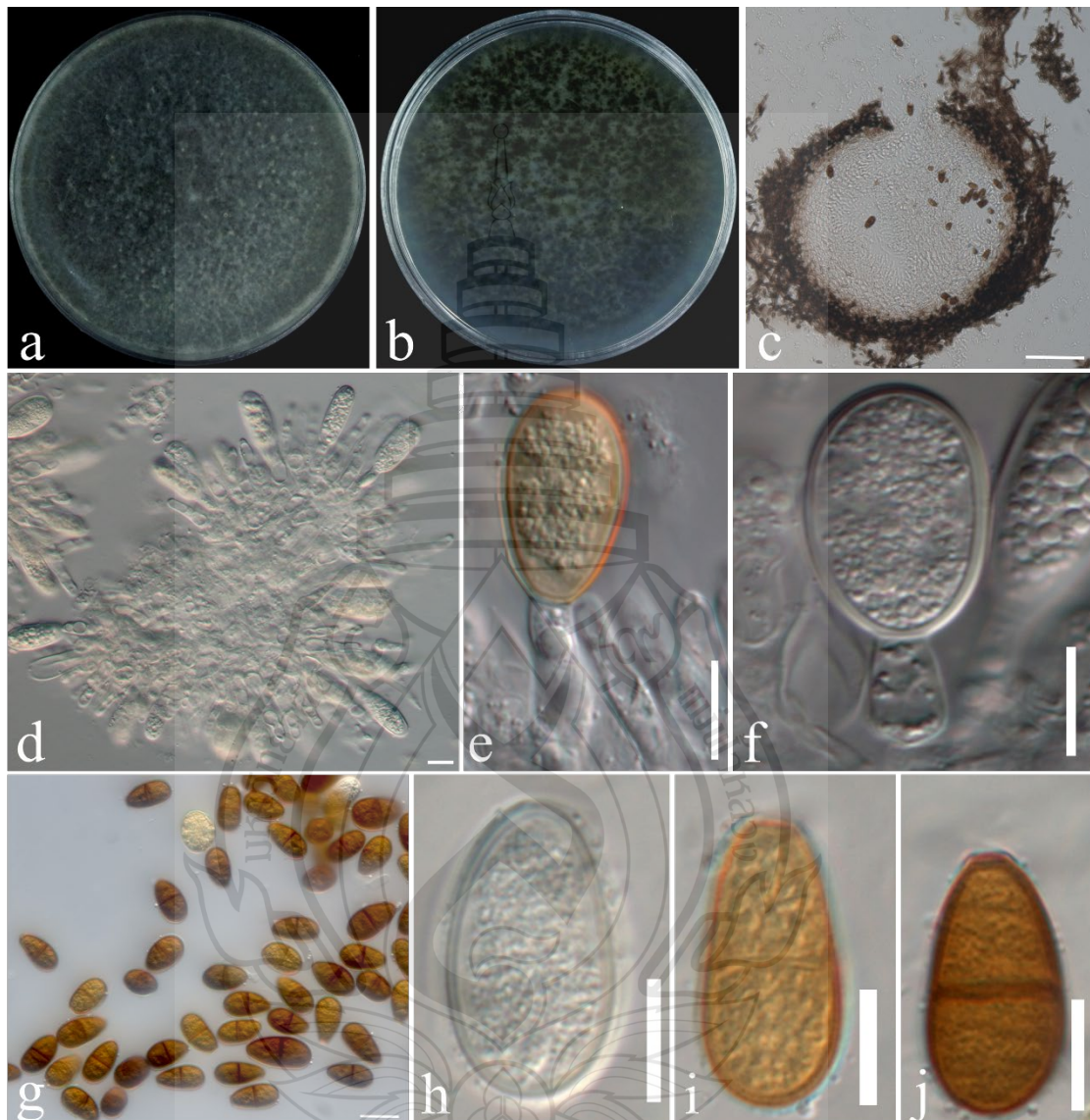
Figure 4.4 Morphological characterization of *Phaeobotryon rhois* (JZB3600005)

Figure 4.4 a Upper view of the colony on PDA. b Reverse view of the colony on PDA. c A cross section of a conidioma. d–f Conidiophores and conidiogenous cells. g–j Mature and immature conidia. Scale bars: c = 100 μm, d–f, h–j = 10 μm, g = 20 μm.

Phaeobotryon rhois CFCC 89662
Phaeobotryon rhois CFCC 89663
***Phaeobotryon rhois* CFCC 52448T**
JZB3600001
JZB3600002
JZB3600004
JZB3600003
JZB3600006
JZB3600005
99/1.0
100/1.0 *Phaeobotryon mamane* CPC 12440
Phaeobotryon mamane CPC 12443
Phaeobotryon mamane CPC 12442
53/-
100/1.0 *Phaeobotryon rhoinum* CFCC 52451
***Phaeobotryon rhoinum* CFCC 52449T**
65/1.0 *Phaeobotryon rhoinum* CFCC 52450
100/1.0 *Phaeobotryon cupressi* IRAN 1455C
Phaeobotryon cupressi IRAN 1456C
Phaeobotryon cupressi IRAN 1458C
76/0.95 *Phaeobotryon negundinis* CAA 798
85/1.0 100/1.0 *Phaeobotryon negundinis* CAA 799
Phaeobotryon negundinis MFLUCC 15-0436
98/1.0 ***Phaeobotryon aplospora* CFCC 53774T**
Phaeobotryon aplospora CFCC 53776
Phaeobotryon aplospora CFCC 53775
***Barriopsis fusca* CBS 174.26T**
0.007

Figure 4.5 Phylogenetic tree generated by maximum likelihood analysis of combined ITS, *tef1* and LSU sequence data of *Phaeobotryon* species

Figure 4.5 *Barriopsis fusca* (CBS 174.26) was used as the outgroup taxon. The best-scoring RAxML tree with a final likelihood value of -3653.517425 was presented. The matrix had 185 distinct alignment patterns, with 23.97% of undetermined characters or gaps. Estimated base frequencies were as follows: A = 0.230084, C = 0.261877, G = 0.279321, T = 0.228718; substitution rates AC = 1.390053, AG = 2.937002, AT = 0.769951, CG = 0.806736, CT = 7.065592, GT = 1.000000; gamma distribution shape parameter α = 0.839033. ML bootstrap support values ≥50% (BT) and Bayesian posterior probabilities ≥0.90 (BYPP) are shown near the nodes. The scale bar indicates 0.007 changes per site. Isolates from the current study are in red and type specimens are in bold.

Nectriaceae Tul. & C. Tul. [as 'Nectriei'], Select. fung. carpol. (Paris) 3: 3 (1865)

***Cylindrocarpon*-like fungi**

Cylindrocarpon-like species are widely distributed, soil-borne fungi around the world, including *Campylocarpon*, *Cylindrocladiella*, *Cylindrodendrum*, *Dactylonectria*, *Ilyonectria*, *Neonectria*, *Pleiocarpon* and *Thelonectria* (Capote et al., 2022). This group is considered as saprophytic or pathogenic causing cankers, root rot and decay of grapevines and many other plants (Jankowiak et al., 2016; Capote et al., 2022). Among them, all genera except *Cylindrodendrum* have been reported on the grapevines (Ye et al., 2021a). In this study, thirty-nine isolates representing six species belonging to *Dactylonectria*, *Ilyonectria* and *Cylindrocladiella* were identified. For taxonomic treatments, we follow Lu et al. (2020) and Ye et al. (2021a).

Dactylonectria novozelandica L. Lombard & Crous, in Lombard, van der Merwe, Groenewald & Crous, Phytopath. Mediterr. 53(3): 523 (2014)

Index Fungorum number: IF810150; Facesoffungi number: FoF 14330

Description – see Lombard et al., (2014)

Material Examined – China, Yunnan Province, Binchuan County, on the root of *Vitis vinifera*, 23 July 2021, Linna Wu and Xinghong Li, living cultures JZB3310031–JZB3310034; China, Hebei Province, Qinhuangdao City, Changli County, on the trunk-base of *Vitis vinifera*, 13 November 2021, Linna Wu and Xinghong Li, living cultures JZB3310035, JZB3310036; *ibid.*, on the root of *Vitis vinifera*, 13 November 2021, Linna Wu and Xinghong Li, living cultures JZB3310037, JZB3310038; China, Beijing City, on the root of *Vitis vinifera*, 11 September 2021, Linna Wu and Xinghong Li, living cultures JZB3310039–JZB3310042.

Notes – In the multi-locus phylogenetic analysis, twelve isolates clustered with *D. novozelandica* with 96% bootstrap value and 0.95 BYPP (Figure 4.6). *Dactylonectria novozelandica* has been reported to cause black foot disease from grapevines in China (Tan et al., 2022).

Figure 4.6 Phylogenetic tree generated by maximum likelihood analysis of combined ITS, *tef1*, *tub2* and *his* sequence data of *Dactylonectria* species

Figure 4.6 *Campylocarpon pseudofasciculare* (CBS 112679) and *C. fasciculare* (CBS 112613) were used as the outgroup taxon. The best- scoring RAxML tree with a final likelihood value of -7792.518531 was presented. The matrix had 599 distinct alignment patterns with 14.58% of undetermined characters or gaps. Estimated base frequencies were as follows: A = 0.221125, C = 0.327854, G = 0.223902, T = 0.227119; substitution rates AC = 1.748995, AG = 3.677564, AT = 1.718751, CG = 0.886389, CT = 6.913553, GT = 1.000000; gamma distribution shape parameter α = 0.715661. ML bootstrap support values ≥50% (BT) and Bayesian posterior probabilities ≥0.90 (BYPP) are shown near the nodes. The scale bar indicates 0.04 changes per site. Isolates from the current study are in red and type specimens are in bold.

Dactylonectria alcacerensis (A. Cabral, H. Oliveira & Crous) L. Lombard & Crous, in Lombard, van der Merwe, Groenewald & Crous, Phytopath. Mediterr. 53(3): 525 (2014)

Index Fungorum number: IF810143; Facesoffungi number: FoF 14331

Description – see Cabral et al. (2012)

Material Examined – China, Shanxi Province, Linfen City, on the root of *Vitis vinifera*, 23 June 2021, Linna Wu and Xinghong Li, living cultures JZB3310021–JZB3310024; China, Beijing City, on the root of *Vitis vinifera*, 11 September 2021, Linna Wu and Xinghong Li, living cultures JZB3310025, JZB3310026; *ibid*., 27 April 2021, Haiyun Hai and Xinghong Li, living cultures JZB3310029, JZB3310030; China, Hebei Province, Qinhuangdao City, Changli County, on the root of *Vitis vinifera*, 18 October 2021, Linna Wu and Xinghong Li, living cultures JZB3310027, JZB3310028.

Notes – In the multi-locus phylogenetic analysis, ten isolates clustered with *D. alcacerensis* with 99% bootstrap value and 1.0 BYPP (Figure 4.6). *Dactylonectria alcacerensis* has been reported as a pathogen causing the black foot disease of grapevines in China (Ye et al., 2021a).

Dactylonectria torresensis (A. Cabral, Rego & Crous) L. Lombard & Crous, in Lombard, van der Merwe, Groenewald & Crous, Phytopath. Mediterr. 53(3): 528 (2014)

Index Fungorum number: IF810153; Facesoffungi number: FoF 14332

Description – see Lombard et al. (2014)

Material Examined – China, Hebei Province, Huailai County, on the root of *Vitis vinifera*, 9 July 2021, Linna Wu and Xinghong Li, living cultures JZB3310046, JZB3310047; China, Ningxia Province, Yinchuan City, on the root of *Vitis vinifera*, 15 September 2021, Linna Wu and Xinghong Li, living cultures JZB3310048.

Notes – In the multi-locus phylogenetic analysis, three isolates clustered with *D. torresensis* with 99% bootstrap value and 1.0 BYPP (Figure 4.6). *Dactylonectria torresensis* has been reported to cause the black foot disease of grapevines in China (Ye et al., 2021a).

Dactylonectria macrodidyma (Halleen, Schroers & Crous) L. Lombard & Crous, in Lombard, van der Merwe, Groenewald & Crous, Phytopath. Mediterr. 53(3): 527 (2014)

Index Fungorum number: IF810147; Facesoffungi number: FoF 14333

Description – see Halleen et al. (2004)

Material Examined – China, Yunnan Province, Binchuan County, on the trunk of *Vitis vinifera*, 23 July 2021, Linna Wu and Xinghong Li, living cultures JZB3310043, JZB3310044; China, Beijing City, on the transition region between trunk and root of *Vitis vinifera*, 27 April 2021, Haiyun Tan and Xinghong Li, living cultures JZB3310045.

Notes – In the multi-locus phylogenetic analysis, three isolates clustered with *D. macrodidyma* with 100% bootstrap value and 1.0 BYPP (Figure 4.6). *Dactylonectria macrodidyma* is one of the causal agents of the black foot disease of grapevine in China and was verified to be the most aggressive on detached green shoots among five species associated with black foot disease of grapevine (*C. lageniformis*, *D. alcacerensis*, *D. macrodidyma*, *D. torresensis* and *Neonectria* sp. 1) (Ye et al., 2021a).

Ilyonectria P. Chaverri & Salgado, in Chaverri, Salgado, Hirooka, Rossman & Samuels, Stud. Mycol. 68: 69 (2011)

Ilyonectria liriodendri (Halleen, Rego & Crous) P. Chaverri & Salgado, in Chaverri, Salgado, Hirooka, Rossman & Samuels, Stud. Mycol. 68: 71 (2011)

Index Fungorum number: IF518561; Facesoffungi number: FoF 14355

Asexual morph: *Macroconidia* predominating, 1–3-septate, straight to slightly curved, cylindrical, 3-septate macroconidia 24–40 × 4–7 μm ($\bar{x} \pm SD = 29.0 \pm 3.7 \times 5.1 \pm 0.5$ μm, n = 50). *Microconidia* ellipsoidal, subcylindrical to ovoid, 0–1-septate, 6–14 × 3–4 μm, ($\bar{x} \pm SD = 9.2 \pm 1.7 \times 3.5 \pm 0.4$ μm, n = 50) (Figure 4.7). Sexual morph: Not observed.

Culture characteristics – Colonies on PDA white with sparse aerial mycelium, reverse pale orange (Figure 4.7), colonies reached 4.5 cm diam after 6 d.

Material Examined – China, Shanxi Province, Linfen City, on the root of *Vitis vinifera*, 23 June 2021, Linna Wu and Xinghong Li (Inactive dry cultures JZBH3610001, JZBH3610002), living cultures JZB3610001, JZB3610002; China, Ningxia Province, Yinchuan City, on the trunk of *Vitis vinifera*, 15 September 2021, Linna Wu and Xinghong Li (Inactive dry cultures JZBH3610003–JZBH3610006), living cultures JZB3610003–JZB3610006; China, Beijing City, on the transition region between trunk and root of *Vitis vinifera*, 27 April 2021, Haiyun Tan and Xinghong Li (Inactive dry cultures JZBH3610007), living cultures JZB3610007.

Notes – In the multi-locus phylogenetic analysis, seven isolates clustered with *I. liriodendri* with 98% ML bootstrap value and 1.0 BYPP (Figure 4.8). *Ilyonectria liriodendri* (former *Neonectria liriodendri*) has been reported as the pathogen of black foot of grapevines in many countries (Jayawardena et al., 2018). This is the first report of *I. liriodendri* on grapevines in China.

Figure 4.7 Morphological characterization of *Ilyonectria liriodendri* (JZB3610001)

Figure 4.7 a Upper view of the colony on PDA. b Reverse view of the colony on PDA. c, d Macroconidia and microconidia. Scale bars: c, d = 10 μm.
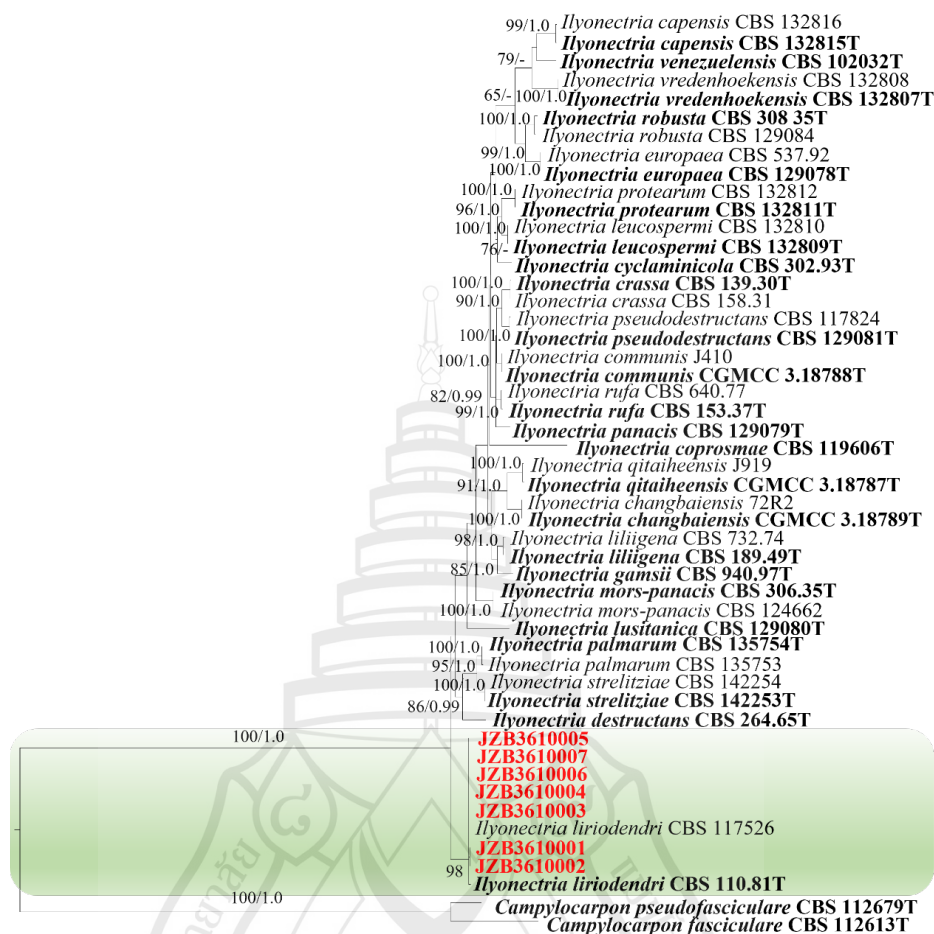
Figure 4.8 Phylogenetic tree generated by maximum likelihood analysis of combined ITS, *tef1*, *tub2* and *his* sequence data of *Ilyonectria* species

Figure 4.8 *Campylocarpon pseudofasciculare* (CBS 112679) and *C. fasciculare* (CBS 112613) were used as the outgroup taxon. The best scoring RAxML tree with a final likelihood value of -8714.157328 was presented. The matrix had 555 distinct alignment patterns, with 9.38% of undetermined characters or gaps. Estimated base frequencies were as follows: A = 0.218130, C = 0.328229, G = 0.229365, T = 0.224276; substitution rates AC = 1.504760, AG = 3.527434, AT = 1.562501, CG = 0.619652, CT = 6.790122, GT = 1.000000; gamma distribution shape parameter α = 0.587098. ML bootstrap support values ≥50% (BT) and Bayesian posterior probabilities ≥0.90 (BYPP) are shown near the nodes. The scale bar indicates 0.05 changes per site. Isolates from the current study are in red and type specimens are in bold.

Cylindrocladiella Boesew., Can. J. Bot. 60 (11): 2289 (1982)

Cylindrocladiella viticola Crous & Van Coller, in van Coller, Denman, Groenewald, Lamprecht & Crous, Australas. Pl. Path. 34(4): 493 (2005)

Index Fungorum: IF500187; Facesoffungi number: FoF 14356

Asexual morph: *Conidiophores* penicillate and subverticillate, hyaline. *Conidia* cylindrical, straight, rounded at both ends, straight, 1-septate, 8–16 × 2–3 μm (x̄ ± SD = 12.1 ± 1.4 × 2.7 ± 0.3 μm, n = 50). *Chlamydospores* arranged in chains (Figure 4.9). Sexual morph: Not observed.

Culture characteristics – Colonies on PDA raised, cottony, yellow to umber, colonies reached 6.4 cm diam after 6 d (Figure 4.9).

Material Examined – China, Yunnan Province, Binchuan County, on the root of *Vitis vinifera*, 23 July 2021, Linna Wu and Xinghong Li (Inactive dry cultures JZBH3320005, JZBH3320006, JZBH3320007), living cultures JZB3320005, JZB3320006, JZB3320007.

Notes – In the multi-locus phylogenetic analysis, three isolates clustered with *C. viticola* with 100% ML bootstrap value and 0.97 BYPP (Figure 4.10). *Cylindrocladiella viticola* was reported to cause cutting rot on grapevine in South Africa (van Coller et al., 2005). This is the first report of *C. viticola* associated with grapevine trunk diseases in China.
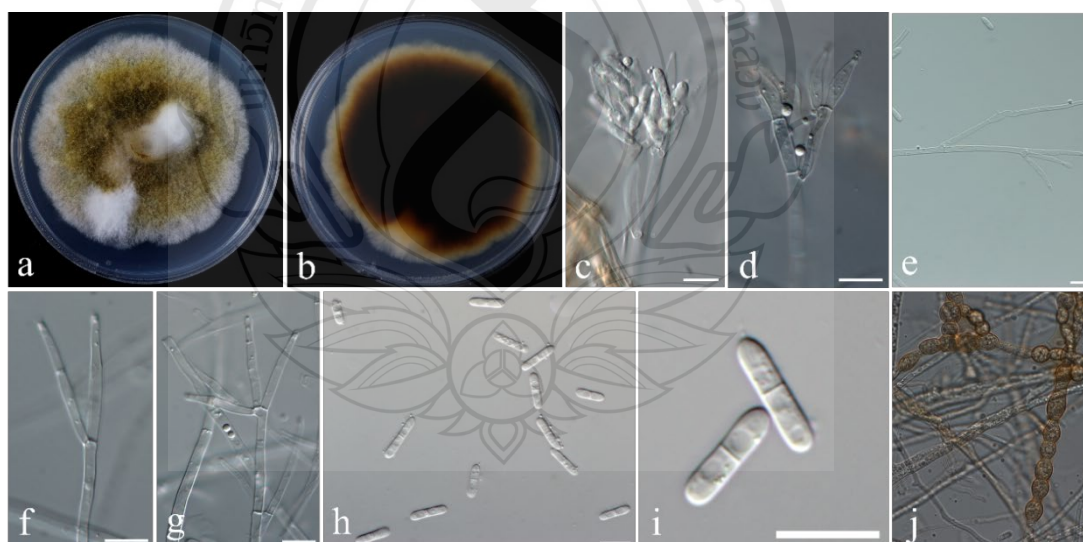
Figure 4.9 Morphological characterization of *Cylindrocladiella viticola* (JZB3320006)

Figure 4.9 a Upper view of the colony on PDA. b Reverse view of the colony on PDA. c, d Penicillate conidiophore. e-g Subverticillate conidiophore. h, i Conidia. j Chlamydospores. Scale bars: c–j =10 μm.

Figure 4.10 Phylogenetic tree generated by maximum likelihood analysis of combined ITS, *tef1* and *tub2* sequence data of *Cylindrocladiella* species

Figure 4.10 *Gliocladiopsis sagariensis* (CBS 199.55) was used as the outgroup taxon. The best scoring RAxML tree with a final likelihood value of -7461.214703 was presented. The matrix had 539 distinct alignment patterns, with 14.16% of undetermined characters or gaps. Estimated base frequencies were as follows: A = 0.224070, C = 0.307547, G = 0.220194, T = 0.248188; substitution rates AC = 1.015860, AG = 3.279433, AT = 0.995371, CG = 0.438164, CT = 4.326124, GT = 1.000000; gamma distribution shape parameter α = 0.505492. ML bootstrap support values ≥50% (BT) and Bayesian posterior probabilities ≥0.90 (BYPP) are shown near the nodes. The scale bar indicates 0.05 changes per site. Isolates from the current study are in red and type specimens are in bold.

Fusarium **and allied fusarioid genera**

Fusarium includes a large number of species as saprobes, endophytes or pathogens (Sandoval-Denis et al., 2018). Among them, *F. graminearum* and *F. oxysporum* are ranked as the top 10 fungal pathogens with scientific and economic importance (Dean et al., 2012). *Neocosmospora*, previously known as *F. solani* species complex (FFSC), includes the most important and ubiquitous groups of pathogens (Sandoval-Denis et al., 2019). *Bisifusarium* is a new genus proposed in recent years, encompasses species previously included in the *Fusarium dimerum* species complex (Sandoval-Denis et al., 2018).

In this study, thirty-four isolates from seven species belonging to *Fusarium*, *Neocosmospora* and *Bisifusarium* were identified (Figure 4.11). For taxonomic treatments, we followed Crous et al. (2021).

Figure 4.11 Phylogenetic tree generated by maximum likelihood analysis of combined
tef1 and *rpb2* sequence data of *Fusarium, Neocosmospora* and *Bisifusarium*
species
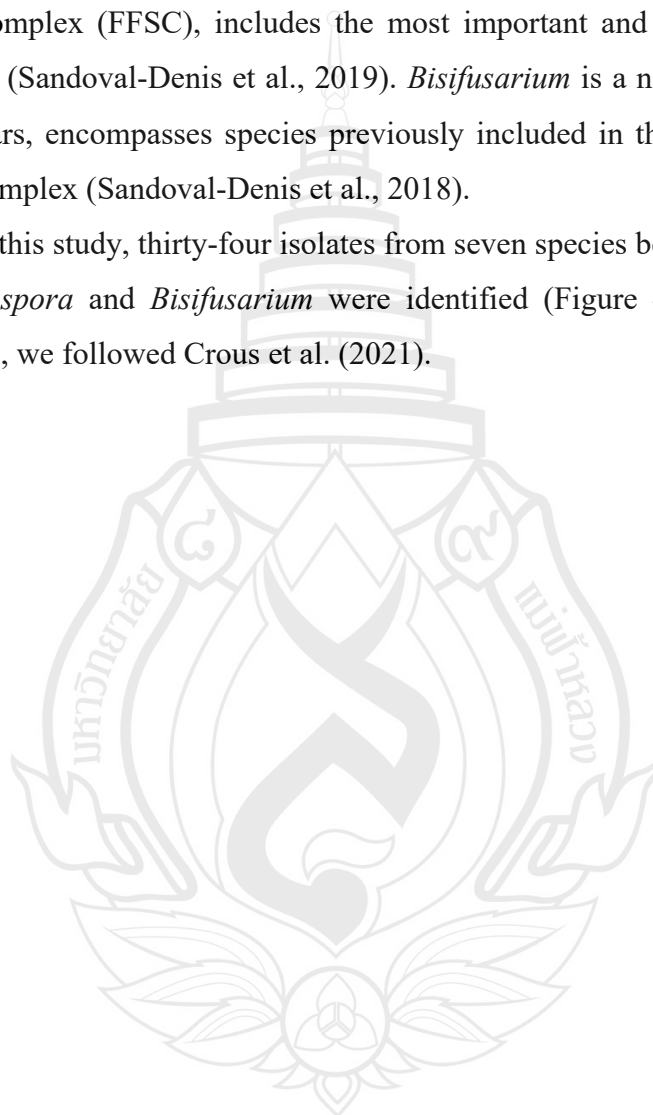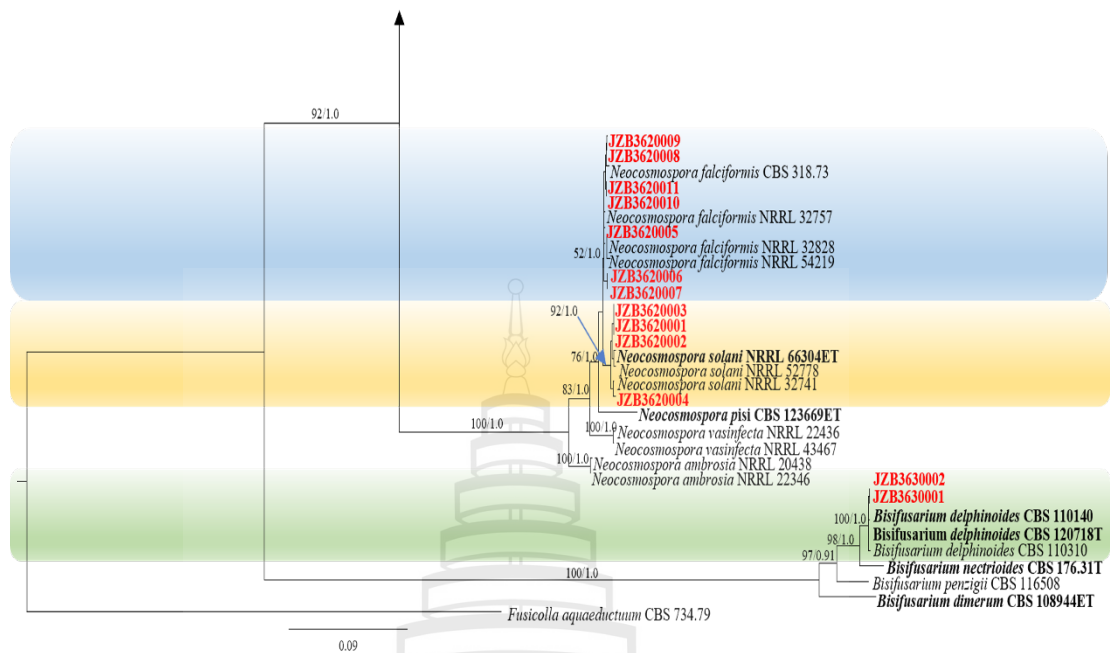
Figure 4.11 (Continued)

Figure 4.11 *Fusicolla aquaeductuum* (CBS 734.79) was used as the outgroup taxon. The best-scoring RAxML tree with a final likelihood value of -18302.824510 was presented. The matrix had 945 distinct alignment patterns, with 15.67% of undetermined characters or gaps. Estimated base frequencies were as follows: A = 0.251509, C = 0.269104, G = 0.244341, T = 0.235046; substitution rates AC = 1.483783, AG = 4.460272, AT = 1.757600, CG = 0.850730, CT = 9.879030, GT = 1.000000; gamma distribution shape parameter α = 1.224492. ML bootstrap support values ≥50% (BT) and Bayesian posterior probabilities ≥0.90 (BYPP) are shown near the nodes. The scale bar indicates 0.09 changes per site. Isolates from the current study are in red and type specimens are in bold.

Fusarium Link, Mag. Gesell. naturf. Freunde, Berlin 3(1-2): 10 (1809)

Fusarium acuminatum Ellis & Everh., Proc. Acad. nat. Sci. Philad. 47: 441 (1895)

Index Fungorum: IF219366; Facesoffungi number: FoF 14334

Description – See Leslie and Summerell (2006)

Material Examined – China, Ningxia Province, Yinchuan City, on the trunk of *Vitis vinifera*, 15 September 2021, Wei Zhang and Xinghong Li, living cultures JZB3110195, JZB3110196; China, Shanxi Province, Linfen City, on the trunk of *Vitis vinifera*, 23 June 2021, Linna Wu and Xinghong Li, living cultures JZB3110197, JZB3110198.

Notes – In the multi-locus phylogenetic analysis, four isolates clustered with *F. acuminatum* with 98% bootstrap value and 1.0 BYPP (Figure 4.11). *Fusarium acuminatum* has been reported as a pathogen of grapevine wilt in Spain (Jayawardena et al., 2018). This is the first report of *F. acuminatum* associated with grapevine trunk diseases in China.

Fusarium brachygibbosum Padwick, Mycol. Pap. 12: 11 (1945)

Index Fungorum: IF286508; Facesoffungi number: FoF 11683

Asexual morph: *Macroconidia* formed in orange sporodochia on the carnation leaf agar (CLA), slightly curved, with wide central cells, slightly sharp apical cell and distinct foot basal cells, usually have 5 septa, 23–59 × 5–6 μm ($\overline{x}$ ± SD = 44.8 ± 5.9 × 5.7 ± 0.4 μm, n = 50). *Spherical chlamydospores* were produced from mycelium (Figure 4.12). Sexual morph: Not observed.

Culture characteristics – Colonies on PDA were initially white with abundant aerial mycelium, turning light orange in the centre, reverse orange (Figure 4.12). Colonies reached 7.7 cm in diameter after 4 days at 25ºC.

Material Examined – China, Beijing City, on the root of *Vitis vinifera*, 11 September 2021, Linna Wu and Xinghong Li (Inactive dry cultures JZBH3110191– JZBH3110194), living cultures JZB3110191–JZB3110194.

Notes – In the multi-locus phylogenetic analysis, four isolates clustered with *F. brachygibbosum* with 100% bootstrap value and 1.0 BYPP (Figure 4.11). *Fusarium brachygibbosum* was reported to cause root rot of soybean, tobacco and maize stalk rot in China (Shan et al., 2017; Wang et al., 2021; Qiu et al., 2021). This is the first report of *F. brachygibbosum* associated with grapevine trunk diseases in China.
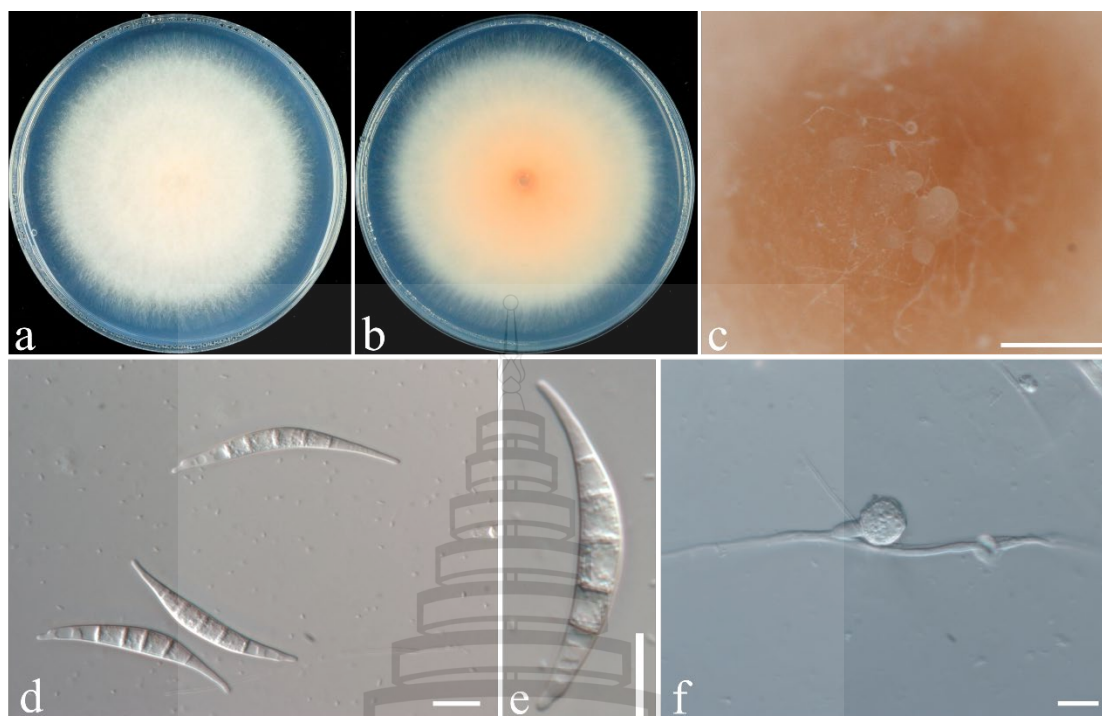
Figure 4.12 Morphological characterization of *Fusarium brachygibbosum* (JZB3110191)

Figure 4.12 a Upper view of the colony on PDA. b Reverse view of the colony on PDA. c Sporodochia formed on the surface of carnation leaves. d, e Macroconidia. f Chlamydospore. Scale bars: c = 50 μm, d–f = 10 μm.

Fusarium compactum (Wollenw.) Raillo, Fungi of the Genus *Fusarium*: 180 (1950)

Index Fungorum: IF297537; Facesoffungi number: FoF 14337

Asexual morph: Orange *sporodochia* formed on the CLA. *Macroconidia* produced from monophialides on branched conidiophores in sporodochia, have strong dorsi-ventral curvature with a pronounced foot cell and tapering elongate apical cell that is often needle like in appearance, usually 5-septate, 41–91 × 3–7 μm ($\bar{x} \pm SD = 66.7 \pm 11.8 \times 5.0 \pm 0.6$ μm, n = 50) (Figure 4.13). Sexual morph: Not observed.

Culture characteristics – Colonies on PDA were white with cottony, dense mycelium, and then turned light orange in centre, reverse orange (Figure 4.13). Colonies reached 6.9 cm in diameter after 4 days at 25ºC.

Material Examined – China, Yunnan Province, Binchuan County, on the trunk of *Vitis vinifera*, 23 July 2021, Linna Wu and Xinghong Li (Inactive dry cultures JZBH3110190), living cultures JZB3110190.

Notes – In the multi-locus phylogenetic analysis, one isolate clustered with *F. compactum* with 100% bootstrap value and 1.0 BYPP (Figure 4.11). *Fusarium compactum* was reported to cause wheat root and crown rot in Turkey (Tunali et al., 2008), or saprotroph on apples in Croatia (Sever et al., 2012). This is the first report of *F. compactum* associated with grapevine trunk diseases in the world.

Figure 4.13 Morphological characterization of *Fusarium compactum* (JZB3110190)

Figure 4.13 a Upper view of the colony on PDA. b Reverse view of the colony on PDA. c Sporodochia formed on the surface of carnation leaves. d Conidiophores. e, f Macroconidia. Scale bars: c = 50 μm, d–f = 10 μm.

Fusarium hainanense M.M. Wang, Qian Chen & L. Cai, in Wang, Chen, Diao, Duan & Cai, Persoonia 43: 82 (2019)

Index Fungorum: IF829536; Facesoffungi number: FoF 14335

Asexual morph: *Sporodochia* light orange on CLA. *Conidiophores* unbranched. *Macroconidia* fusiform to falcate, straight to slightly curved, sometimes with constricted septa, have barely- to distinctly- notched basal cell and blunt to papillate apical cell, 1–5-septate, 17–39 × 3–5 μm, ($\bar{x} \pm SD = 27.6 \pm 6.8 \times 4.1 \pm 0.5$ μm, n = 50) (Figure 4.14). Sexual morph: Not observed.

Culture characteristics – Colonies on PDA were white with scant aerial mycelia, reverse pale orange in the centre, white at the margin. Colonies reached 8.1 cm diam after 4 days at 25ºC (Figure 4.14).

Material Examined – China, Yunnan Province, Binchuan County, on the trunk of *Vitis vinifera*, 23 July 2021, Linna Wu and Xinghong Li (Inactive dry cultures JZBH3110199, JZBH3110200), living cultures JZB3110199, JZB3110200.

Notes – In the multi-locus phylogenetic analysis, two isolates clustered with *F. hainanense* with 100% bootstrap value and 1.0 BYPP (Figure 4.11). *Fusarium hainanense* was first isolated from rice as an endophyte in China (Wang et al., 2019). This is the first host report of *F. hainanense* associated with grapevine trunk diseases in China.

Figure 4.14 Morphological characterization of *Fusarium hainanense* (JZB3110199)

Figure 4.14 a Upper view of the colony on PDA. b Reverse view of the colony on PDA. c Sporodochia formed on the surface of carnation leaves. d Conidiophores. e–i Macroconidia. Scale bars: c = 50 μm, d–i = 10 μm.

Fusarium lacertarum Subrahm. [as 'laceratum'], Mykosen 26 (9): 478 (1983)

Index Fungorum: IF534970; Facesoffungi number: FoF 14336

Asexual morph: On CLA, *conidiophores* branched or unbranched. *Macroconidia* variable in size, fusiform to falcate, straight to slightly curved, with foot-shaped basal cells, tapering to hooked apical cells, 2–5-septate, 19–36 × 3–5 μm ($\bar{x} \pm$ SD = 27.8 ± 4.2 × 4.2 ± 0.5 μm, n = 50) (Figure 4.15). *Chlamydospores* were in abundance and present in chains. Sexual morph: Not observed.

Culture characteristics – Colonies on PDA were white with floccose aerial mycelium, turning pale buff in the centre. Colonies reached 7.4 cm diam after 4 days at 25ºC (Figure 4.15).

Material Examined – China, Shannxi Province, Weinan City, on the root of *Vitis vinifera*, 29 June 2021, Wei Zhang (Inactive dry cultures JZBH3110201), living cultures JZB3110201.

Notes – In the multi-locus phylogenetic analysis, one isolate clustered with *F. lacertarum* with 78% bootstrap value and 0.97 BYPP (Figure 4.11). *Fusarium lacertarum* was isolated from *Capsicum* in China (Wang et al., 2019) and reported to cause cladode rot in *Nopalea cochenillifera* in Brazil (Santiago et al., 2018) and the head blight on sorghum in North Carolina (Beacorn & Thiessen, 2021). This is the first report of *F. lacertarum* associated with grapevine trunk diseases in the world.
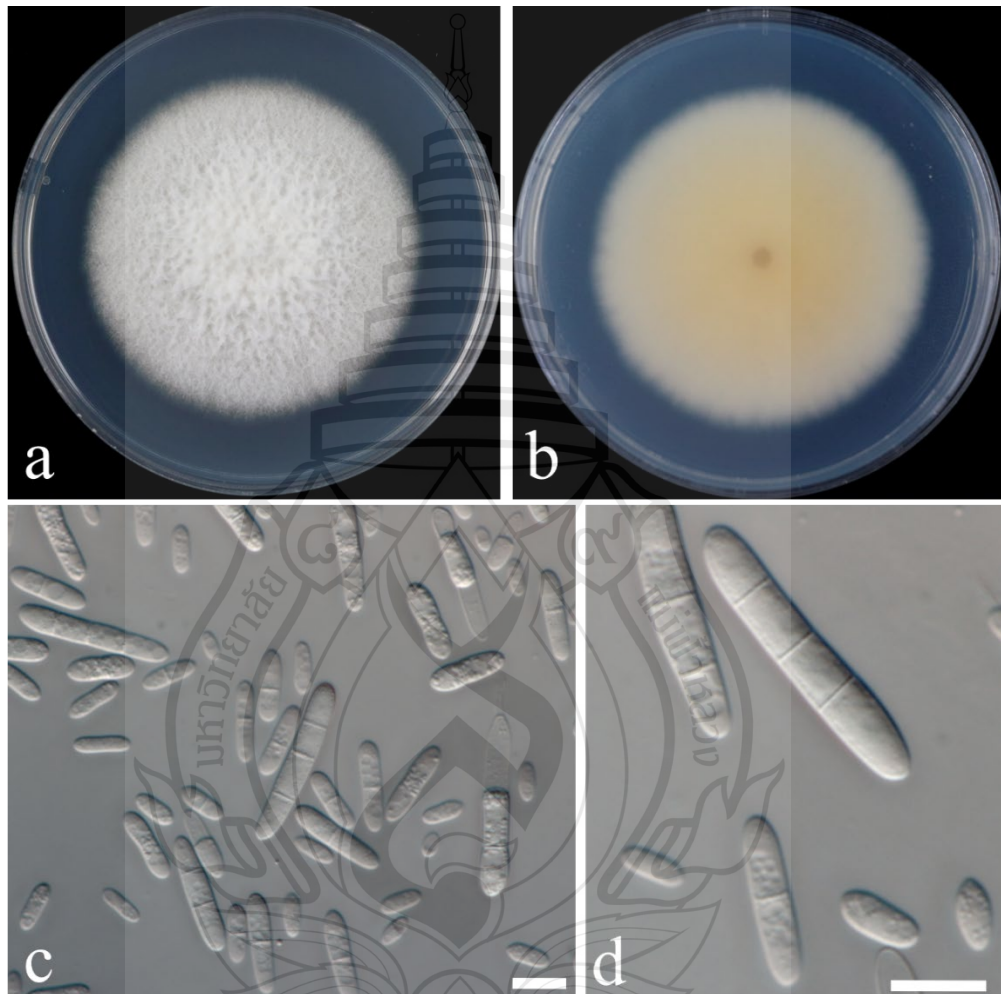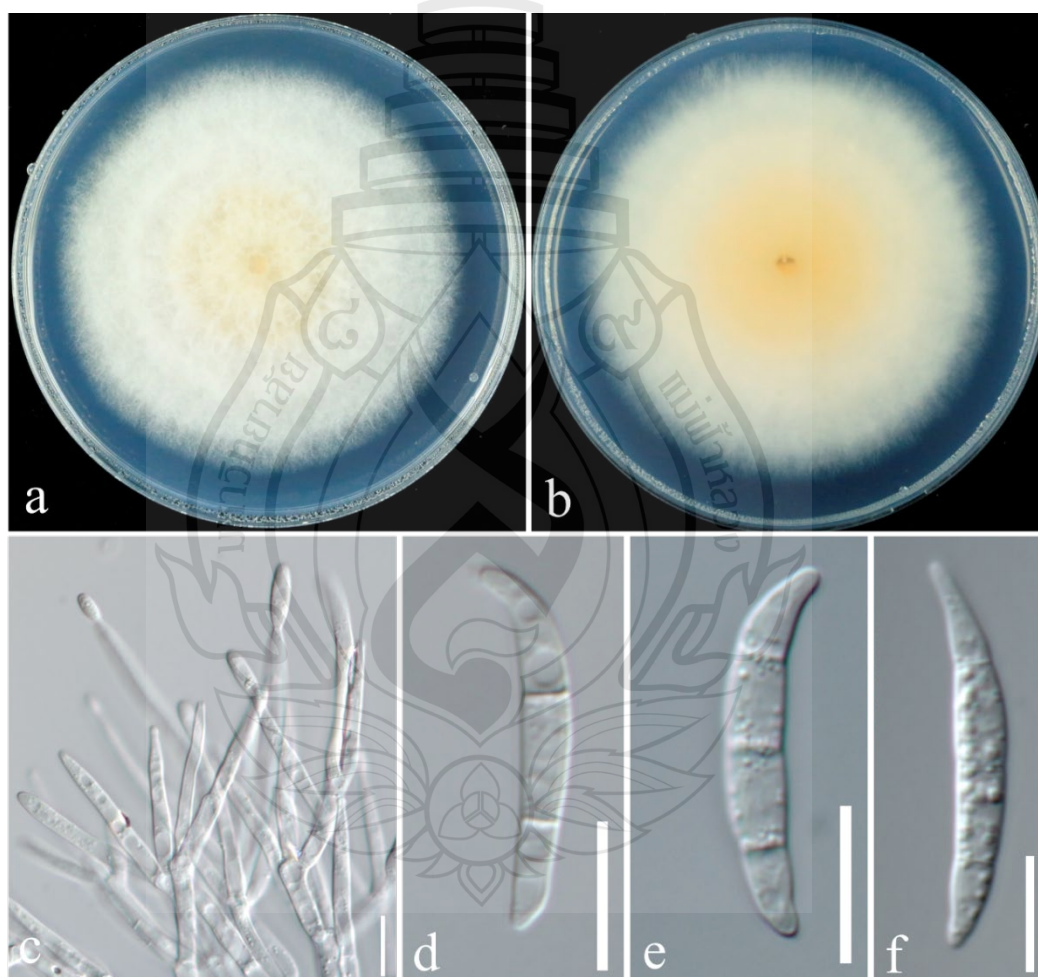

Figure 4.15 Morphological characterization of *Fusarium lacertarum* (JZB3110201)

Figure 4.15 a Upper view of the colony on PDA. b Reverse view of the colony on PDA. c Conidiophores. d–f Macroconidia. Scale bars: c = 20 μm, d–f = 10 μm.

Fusarium oxysporum Schltdl., Fl. berol. (Berlin) 2: 139 (1824)

Index Fungorum: IF218372; Facesoffungi number: FoF 03824

Description – see Lombard et al. (2019)

Material Examined – China, Hebei Province, Qinhuangdao City, Changli County, on the root of *Vitis vinifera*, 18 October 2021, Linna Wu and Xinghong Li, living cultures JZB3110181, JZB3110184; *ibid*., on the root of *Vitis vinifera*, 13 November 2021, Linna Wu and Xinghong Li, living cultures JZB3110185, JZB3110186; *ibid*., on the trunk of *Vitis vinifera*, 18 October 2021, Linna Wu and Xinghong Li, living cultures JZB3110182, JZB3110183; China, Yunnan Province, Binchuan County, on the root of *Vitis vinifera*, 23 July 2021, Linna Wu and Xinghong Li, living cultures JZB3110187; China, Fujian Province, Longyan City, Shanghang County, on the root of *Vitis vinifera*, 19 January 2022, Linna Wu and Xinghong Li, living cultures JZB3110188, JZB3110189.

Notes – In the multi-locus phylogenetic analysis, nine isolates clustered with *F. oxysporum* with 100% ML bootstrap value and 1.0 BYPP (Figure 4.11). *Fusarium oxysporum* is reported to be associated with grapevine decline and dieback in Australia (Highet & Nair, 1995; Castillo-Pando et al., 2001), vascular wilt in Egypt (Ziedan et al., 2011) and withered rotten grapes in Italy (Lorenzini & Zapparoli, 2015), or as an endophyte in Spain (González & Tello, 2011), and saprotrophic fungi in China (Jayawardena et al., 2018).

Neocosmospora E.F. Sm., Bull. U.S. Department of Agriculture 17: 45 (1899)

Neocosmospora falciformis (Carrión) L. Lombard & Crous, Stud. Mycol. 80: 227 (2015)

Index Fungorum: IF810958; Facesoffungi number: FoF 14357

Asexual morph: *Sporodochia* formed abundantly on CLA. *Conidiophores* verticillately branched; phialides subcylindrical to doliiform, smooth- and thin-walled. *Macroconidia* slightly fusoid to falcate, with blunt apical cells and barely notched basal cell, 2–5-septate, 25–46 × 5–8 μm, ($\bar{x}$ ± SD = 39.4 ± 4.7 × 5.9 ± 0.7 μm, n = 50). *Microconidia* ellipsoidal to subcylindrical, straight or gently curved, 0–1-septate. *Chlamydospores* were globose to subglobose, single-celled, terminal and rough-walled (Figure 4.16). Sexual morph: Not observed.

Culture characteristics – Colonies on PDA were white to pale-cream with sparse floccose aerial mycelium, growing in concentric rings, reverse beige. Colonies reached 4.9 cm diam. after 4 days at 25ºC (Figure 4.16).

Material Examined – China, Shaanxi Province, Weinan City, on the root of *Vitis vinifera*, 29 June 2021, Wei Zhang (Inactive dry cultures JZBH3620005), living cultures JZB3620005; China, Ningxia Province, Yinchuan City, on the trunk of *Vitis vinifera*, 15 September 2021, Weizhang and Xinghong Li (Inactive dry cultures JZBH3620006, JZBH3620007), living cultures JZB3620006, JZB3620007; China, Beijing City, on the root of *Vitis vinifera*, 11 September 2021, Linna Wu and Xinghong Li (Inactive dry cultures JZBH3620008–JZBH3620011), living cultures JZB3620008– JZB3620011.

Notes – In the multi-locus phylogenetic analysis, seven isolates clustered with *N. falciformis* with 52% ML bootstrap value and 1.0 BYPP (Figure 4.11). *Neocosmospora falciformis* (former *Fusarium falciforme*) was reported to cause root rot in *Weigela florida* and *Dioscorea polystachya* in China (Shen et al., 2020; Zhang et al., 2020), foot rot and wilt in tomatoes and maize stalk rot in Mexico (Vega-Gutiérrez et al., 2019; Douriet-Angulo et al., 2019). This is the first report of *N. falciformis* associated with grapevine trunk diseases in the world.
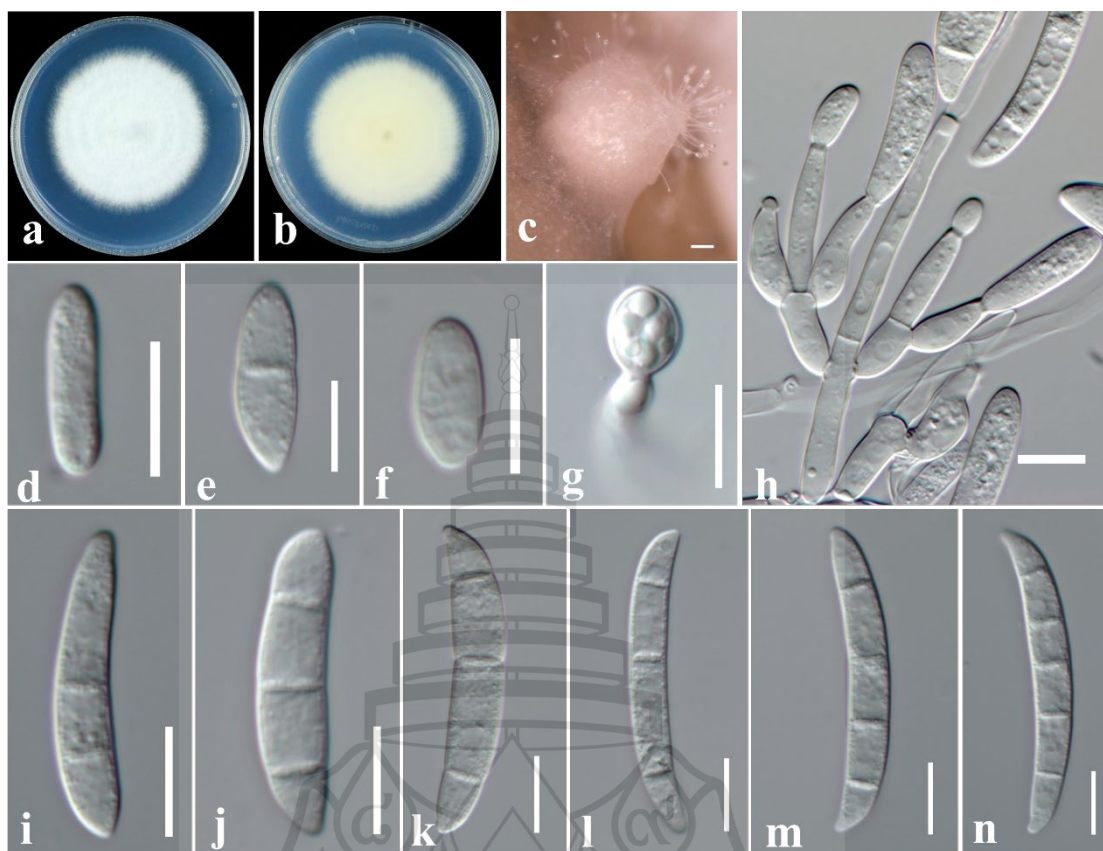
Figure 4.16 Morphological characterization of *Neocosmospora falciformis* (JZB3620005)

Figure 4.16 a Upper view of the colony on PDA. b Reverse view of the colony on PDA. c Sporodochia formed on the surface of carnation leaves. d–f Microconidia. g Chlamydospore. h Conidiophores and phialides. i–n Macroconidia. Scale bars: c–n = 10 μm.

Neocosmospora solani (Mart.) L. Lombard & Crous, in Lombard, van der Merwe, Groenewald & Crous, Stud. Mycol. 80: 228 (2015)

Index Fungorum: IF810964; Facesoffungi number: FoF 14358

Asexual morph: Cream sporodochia formed abundantly on CLA. *Conidiophores* branched. *Macroconidia* are relatively wide falcate or fusoid, straight or slightly curved with blunt apical cells and notched or round basal cell, 3–5-septate, 25–58 × 5–7 μm ($\bar{x} \pm SD = 47.5 \pm 6.4 \times 6.1 \pm 0.5$ μm, n = 50) (Figure 4.17). Sexual morph: Not observed.

Culture characteristics – Colonies on PDA were white to cream with sparse aerial mycelium, growing in concentric rings. Colonies reached 4.5 cm diam after 4 days at 25ºC (Figure 4.17).

Material Examined – China, Fujian Province, Longyan City, Shanghang County, on the root of *Vitis vinifera*, 19 January 2022, Linna Wu and Xinghong Li (Inactive dry cultures JZBH3620001–JZBH3620003), living cultures JZB3620001–JZB3620003; China, Hebei Province, Qinhuangdao City, Changli County, on the root of *Vitis vinifera*, 13 November 2021, Linna Wu and Xinghong Li (JZBH3620004), living cultures JZB3620004.

Notes – In the multi-locus phylogenetic analysis, four isolates clustered with *N. solani* with 92% ML bootstrap support values and 1.0 BYPP (Figure 4.11). *Neocosmospora solani* (former *Fusarium solani*) is an important pathogen and the most common species with a wide host range (Sandoval-Denis et al., 2019). This species was isolated from grapevine in Brazil and India (Jayawardena et al., 2018). This is the first report of *N. solani* associated with grapevine trunk diseases in China.
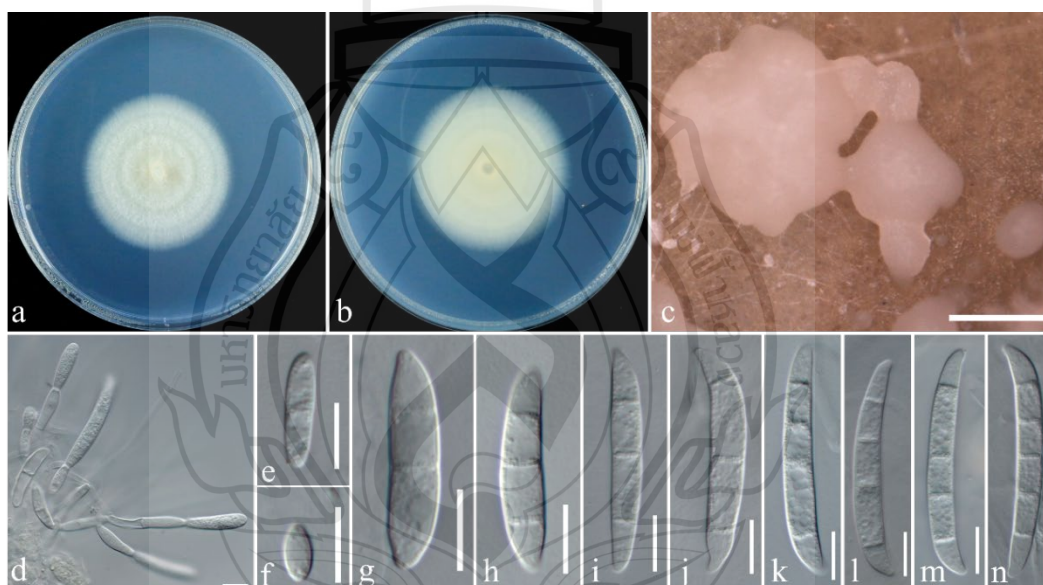
Figure 4.17 Morphological characterization of *Neocosmospora solani* (JZB3620004)

Figure 4.17 a Upper view of the colony on PDA. b Reverse view of the colony on PDA. c Sporodochia formed on the surface of carnation leaves. d Conidiophores. e, f Microconidia. g–n Macroconidia. Scale bars: c = 100 μm, d–n = 10 μm.

Bisifusarium L. Lombard, Crous & W. Gams, in Lombard, van der Merwe, Groenewald & Crous, Stud. Mycol. 80: 223 (2015)

Bisifusarium delphinoides (Schroers, Summerb., O'Donnell & Lampr.) L. Lombard & Crous, in Lombard, van der Merwe, Groenewald & Crous, Stud. Mycol. 80: 224 (2015)

Index Fungorum: IF810228; Facesoffungi number: FoF 14364

Description – See Schroers (2009)

Material Examined – China, Hebei Province, Zhangjiakou City, Huailai County, on the root of *Vitis vinifera*, 9 July 2021, Linna Wu and Xinghong Li (Inactive dry cultures JZBH3630001, JZBH3630002), living cultures JZB3630001, JZB3630002.

Notes – In the multi-locus phylogenetic analysis, two isolates clustered with *B. delphinoides* with 100% ML bootstrap value and 1.0 BYPP (Figure 4.11). The species was isolated from *Citrus* in the USA (Schroers et al., 2009), oriental melon (nonpathogenic) in Korea (Seo & Kim, 2017), and as putative mycoparasites of *Plasmopara viticola*, which cause downy mildew in grapevines (Ghule et al., 2018). This is the first report of *B. delphinoides* associated with grapevine trunk diseases in China.

Diaporthaceae Höhn. ex Wehm., Am. J. Bot. 13: 638 (1926)

Diaporthe Fuckel, Fungi rhenani exsic., suppl., fasc. 5: no. 1988 (1867)

The genus *Diaporthe* comprises pathogenic, endophytic and saprobic species with wide host ranges and geographic distributions (Norphanphoun et al., 2022). The taxonomy of the species in this genus is complicated because of cryptic diversification and phenotypic plasticity within the genus (Udayanga et al., 2014). In this study, 39 isolates belonging to *Diaporthe* species were identified. For taxonomic treatments, we follow Norphanphoun et al. (2022).

Diaporthe eres Nitschke, Pyrenomyc. Germ. 2: 245 (1870)

Index Fungorum: IF172054; Facesoffungi number: FoF 02182

Description – See Udayanga et al. (2014)

Material Examined – China, Beijing City, on the trunk of *Vitis vinifera*, 11 September 2021, Linna Wu and Xinghong Li, living cultures JZB320221–JZB320228, JZB320232–JZB320235; *ibid.*, on the root of *Vitis vinifera*, 11 September 2021, Linna Wu and Xinghong Li, living cultures JZB320229–JZB320231, JZB320236; China, Hebei

Province, Qinhuangdao City, Changli County, on the trunk of *Vitis vinifera*, 13 November 2021, Linna Wu and Xinghong Li, living cultures JZB320237–JZB320239; *ibid.*, Changli County, on the trunk base of *Vitis vinifera*, 13 November 2021, Linna Wu and Xinghong Li, living cultures JZB320240, JZB320241; *ibid.*, on the root of *Vitis vinifera*, 13 November 2021, Linna Wu and Xinghong Li, living cultures JZB320242–JZB320244; *ibid.*, Zhangjiakou City, Huailai County, on the trunk of *Vitis vinifera*, 22 August 2021, Linna Wu and Xinghong Li, living cultures JZB320245–JZB320247; *ibid.*, on the trunk of *Vitis vinifera*, 24 October 2020, Linna Wu and Xinghong Li, living cultures JZB320248–JZB320251; *ibid.*, on the trunk of *Vitis vinifera*, 25 July 2020, Linna Wu and Xinghong Li, living cultures JZB320252; *ibid.*, on the root of *Vitis vinifera*, 9 July 2021, Linna Wu and Xinghong Li, living cultures JZB3202513–JZB3202567.

Notes – In the multi-locus phylogenetic analysis, forty-four isolates clustered with two clades of *D. eres* (Figure 4.18). *Diaporthe eres* was regarded as the most prominent and widespread species associated with grapevine dieback in China (Manawasinghe et al., 2019).
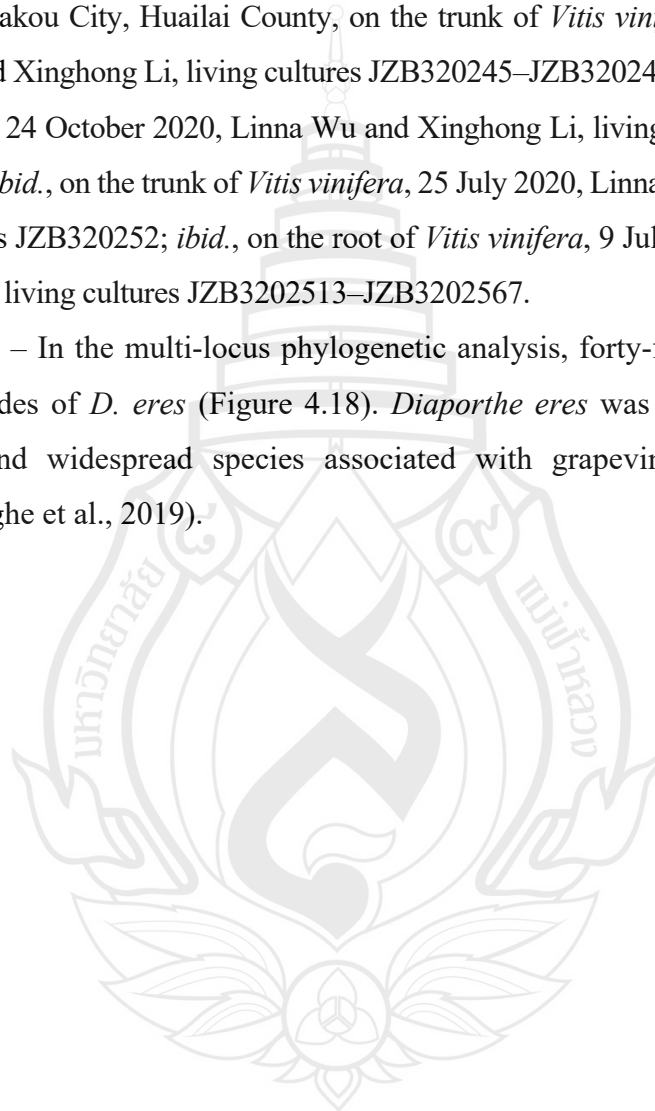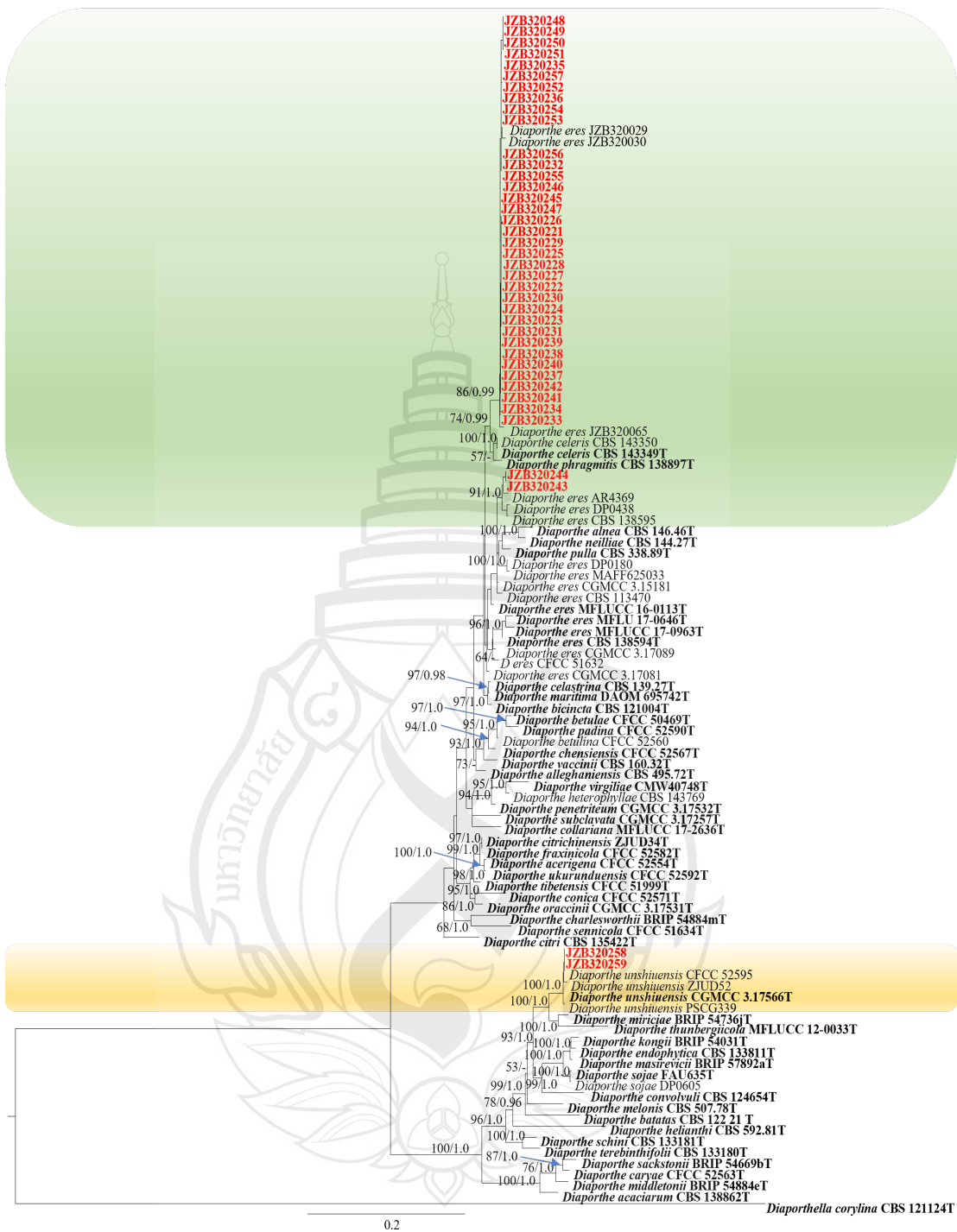
Figure 4.18 Maximum likelihood analysis of combined ITS, *tub2*, *cal* and *tef1* sequence
data of *Diaporthe* species

Figure 4.18 *Diaporthella corylina* (CBS 121124) was used as the outgroup taxon. The best scoring RAxML tree with a final likelihood value of -17167.323573 was presented here. The matrix had 1137 distinct alignment patterns, with 18.64% undetermined characters or gaps. Estimated base frequencies were as follows: A = 0.216280, C = 0.316586, G = 0.241042, T = 0.226092; substitution rates AC = 1.266614, AG = 3.539624, AT = 1.228789, CG = 1.147037, CT = 4.911515, GT = 1.000000; gamma distribution shape parameter α = 0.721142. ML bootstrap support values ≥50% (BT) and Bayesian posterior probabilities ≥0.90 (BYPP) are shown near the nodes. The scale bar indicates 0.2 changes per site. Isolates from the current study are in red and type specimens are in bold.

Diaporthe unshiuensis F. Huang, K.D. Hyde & Hong Y. Li, in Huang, Udayanga, Mei, Fu, Hyde & Li, Fungal Biology 119(5): 344 (2015)

Index Fungorum: IF810845; Facesoffungi number: FoF 09422

Description – See Huang et al. (2015)

Material Examined – China, Fujian Province, Longyan City, Shanghang County, on the trunk of *Vitis vinifera*, 19 January 2022, Linna Wu and Xinghong Li, living cultures JZB320258, JZB320259.

Notes – In the multi-locus phylogenetic analysis, two isolates clustered with *D. unshiuensis* with 100% ML bootstrap value and 1.0 BYPP (Figure 4.18). *Diaporthe unshiuensis* has been recorded to be associated with Diaporthe dieback in China (Manawasinghe et al., 2019).

Togniniaceae Réblová, L. Mostert, W. Gams & Crous, Stud. Mycol. 50(2): 540 (2004)

Phaeoacremonium W. Gams, Crous & M.J. Wingf., Mycologia 88 (5): 789 (1996)

Phaeoacremonium spp. are common pathogens on stems and branches on a wide range of woody hosts, especially on grapevine (Gramaje et al., 2015). In 2021, *Phaeoacremonium minimum* was first reported as a pathogen of Esca disease in China (Ye et al., 2020). In this study, we follow Ye et al. (2021b) for taxonomic treatments.

Phaeoacremonium iranianum L. Mostert, Gräfenhan, W. Gams & Crous, in Mostert, Groenewald, Summerbell, Gams & Crous, Stud. Mycol. 54: 83 (2006)

Index Fungorum: IF500227; Facesoffungi number: FoF 14338

Asexual morph: *Conidiophores* unbranched, erect. *Phialides* mostly monophialidic, have three types: type I phialides the shortest, cylindrical; type II phialides medium sized, elongate-ampulliform to navicular; type III phialides were long, subcylindrical to navicular, some tapering towards the apex to form a thin neck. *Conidia* oblong-ellipsoidal, 4–9 × 2–3 μm ($\overline{x} \pm$ SD = 6.1 ± 1.2 × 2.3 ± 0.3 μm, n = 50) (Figure 4.19). Sexual morph: Not observed.

Culture characteristics – Colonies on PDA felty, olive-brown, in reverse dark brown. Colonies reached 7.7 cm diam after 28 days at 25ºC (Figure 4.19).

Material Examined – China, Hebei Province, Changli County, on the trunk of *Vitis vinifera*, 18 October 2021, Linna Wu and Xinghong Li (Inactive dry cultures JZBH3190013, JZBH3190014), living cultures JZB3190013, JZB3190014.

Notes – In the multi-locus phylogenetic analysis, two isolates clustered with *P. iranianum* with 100% ML bootstrap value and 1.0 BYPP (Figure 4.20). *Phaeoacremonium iranianum* was initially isolated form kiwi fruit and grapevines in Iran and Italy (Mostert et al., 2006) and reported to cause Esca disease of grapevine in Canada, Italy, South Africa and Spain (Gramaje et al., 2015). This is the first report of *P. iranianum* associated with grapevine trunk diseases in China.
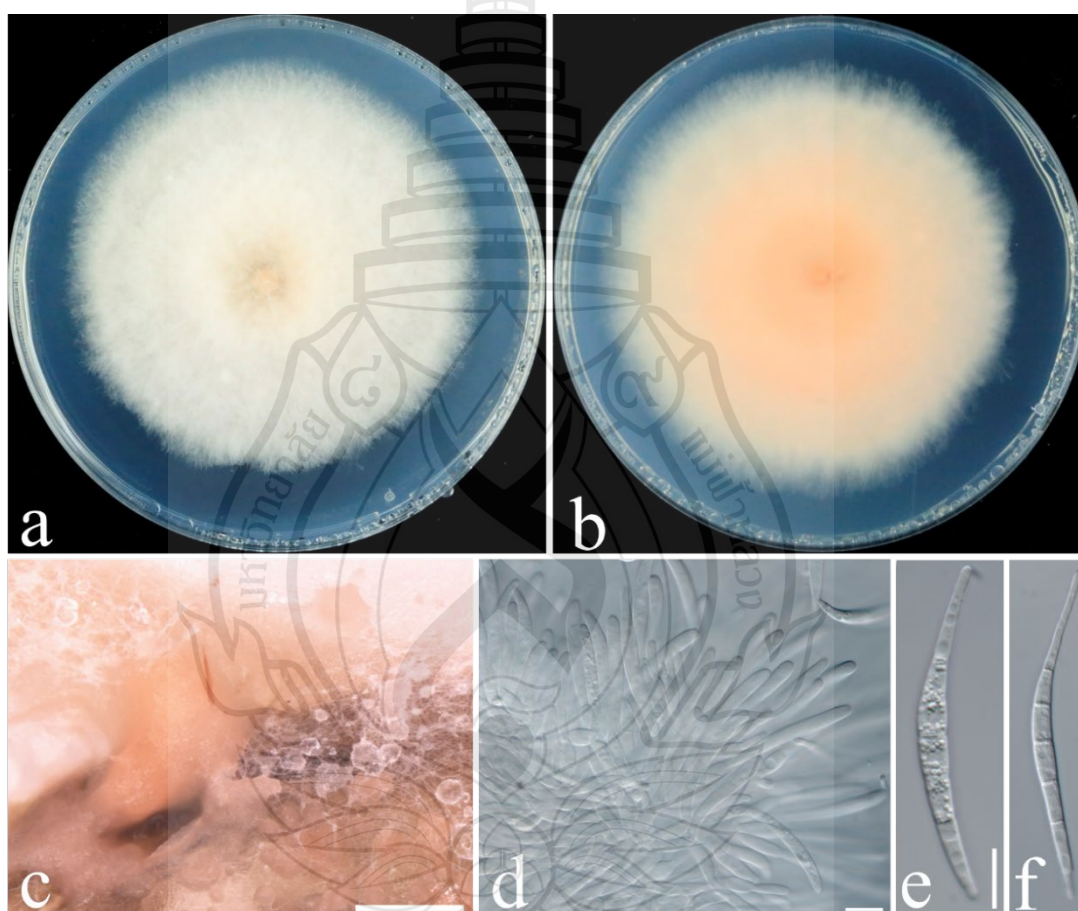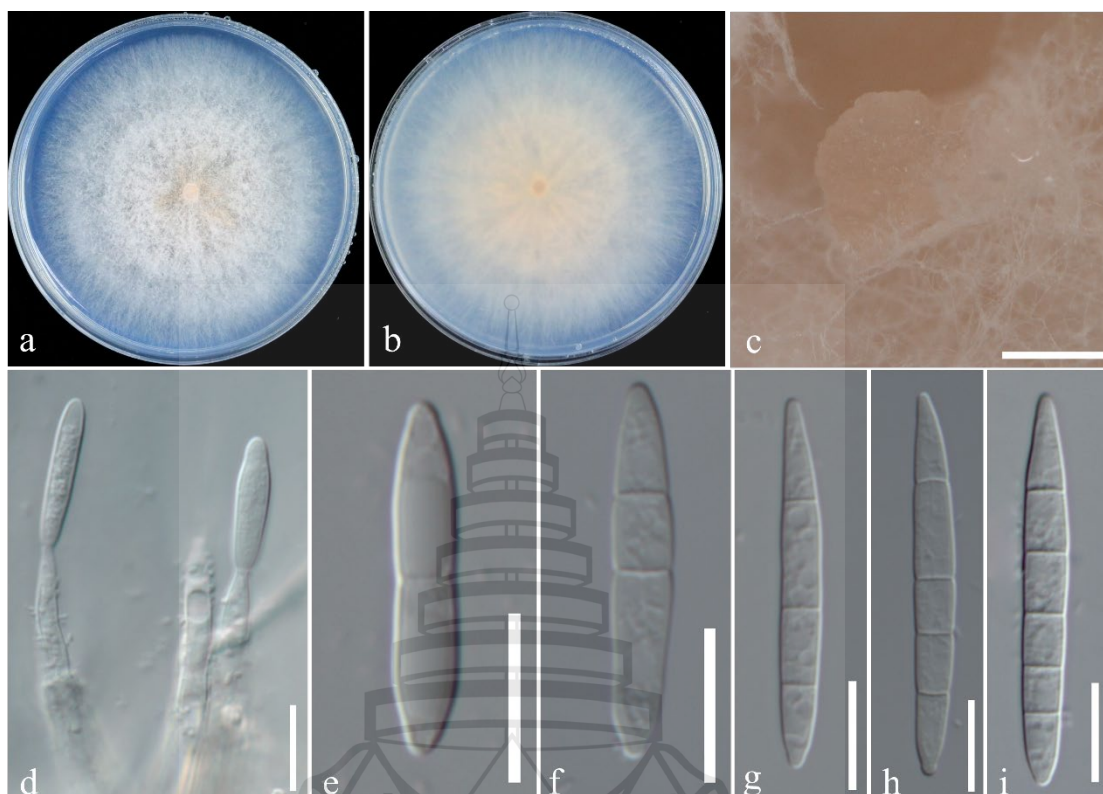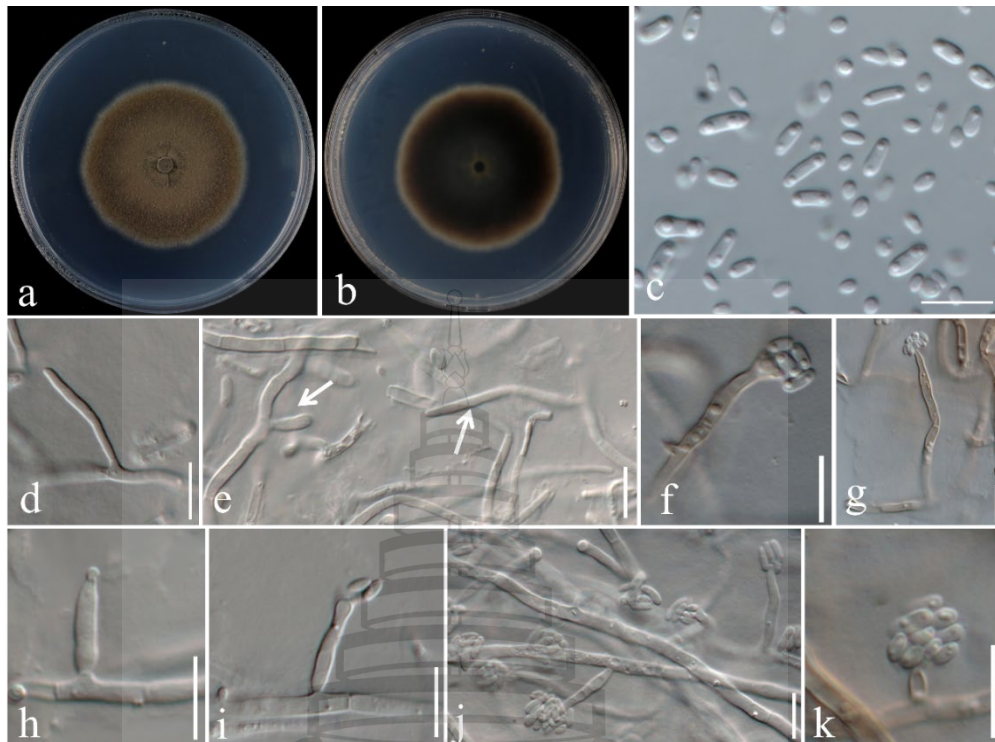
Figure 4.19 Morphological characterization of *Phaeoacremonium iranianum* (JZB3190014)

Figure 4.19 a Upper view of the colony on PDA. b Reverse view of the colony on PDA. c Conidia. d, e Conidiophore. f, g Type III phialides. h, i Type II Phialides. j, k Type I phialides. Scale bars: c–k = 10 μm.

Figure 4.20 Phylogenetic tree generated by maximum likelihood analysis of combined *act* and *tub2* sequence data of *Phaeoacremonium* species

Figure 4.20 *Pleurostoma richardsiae* (CBS 270.33) was used as the outgroup taxon. The best scoring RAxML tree with a final likelihood value of -10031.367491 was presented. The matrix had 622 distinct alignment patterns, with 12.24% of undetermined characters or gaps. Estimated base frequencies were as follows: A = 0.216115, C = 0.316660, G = 0.225016, T = 0.242209; substitution rates AC = 1.424857, AG = 5.577572, AT = 1.486155, CG = 1.182568, CT = 5.200674, GT = 1.000000;

gamma distribution shape parameter α = 2.279586. ML bootstrap support values ≥50% (BT) and Bayesian posterior probabilities ≥0.90 (BYPP) are shown near the nodes. The scale bar indicates 0.07 changes per site. Isolates from the current study are in red and type specimens are in bold.

Schizoparmaceae Rossman, D.F. Farr & Castl. [as 'Schizoparmeaceae'], Mycoscience 48 (3): 137 (2007)

Coniella Höhn., Ber. dt. bot. Ges. 36 (7): 316 (1918)

For taxonomic treatments, we follow Chethana et al. (2017).

Coniella vitis Chethana, J.Y. Yan, X.H. Li & K.D. Hyde, in Chethana, Zhou, Zhang, Liu, Xing, Hyde, Yan & Li, Pl. Dis. 101 (12): 2129 (2017)

Index Fungorum: IF819365; Facesoffungi number: FoF 02722

Description – See Chethana et al. (2017)

Material Examined – China, Beijing City, on the trunk of *Vitis vinifera*, 11 September 2021, Linna Wu and Xinghong Li, living cultures JZB3700081, JZB3700082; China, Hebei Province, Changli County, on the trunk of *Vitis vinifera*, 18 October 2021, Linna Wu and Xinghong Li, living cultures JZB3700083, JZB3700084; *ibid*., on the root of *Vitis vinifera*, 18 October 2021, Linna Wu and Xinghong Li, living cultures JZB3700085–JZB3700087.

Notes – In the multi-locus phylogenetic analysis, seven isolates clustered with *C. vitis* with 85% ML bootstrap values and 0.97 BYPP (Figure 4.21). *Coniella vitis* was described as a novel species causing white rot in grapevine berries in China (Chethana et al., 2017).
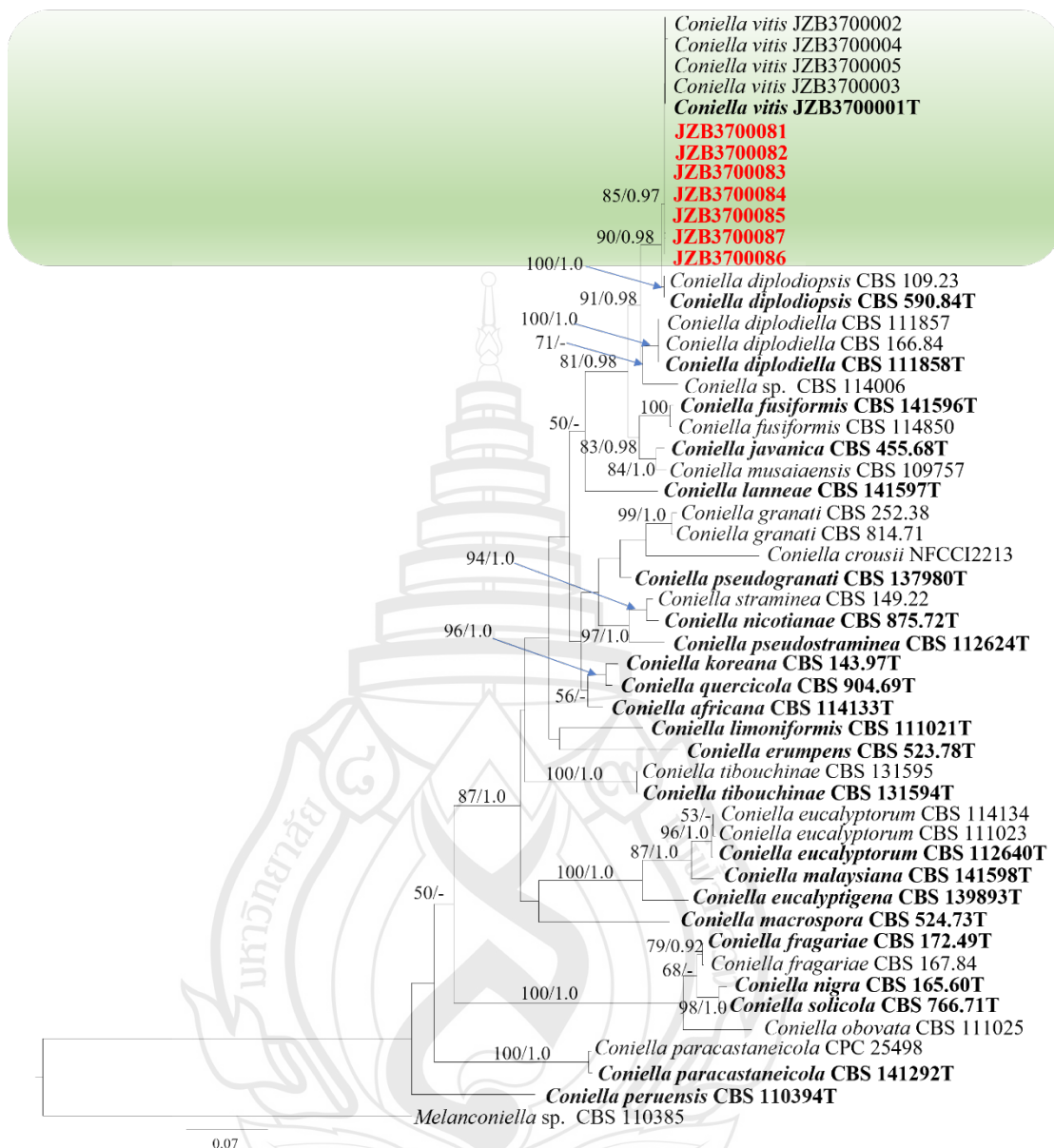
Figure 4.21 Phylogenetic tree generated by maximum likelihood analysis of combined ITS, *his*, LSU and *tef1* sequence data of *Coniella* species

Figure 4.21 A–C leaf symptoms in the field. D–F leaf spot samples. *Melanconiella* sp. (CBS 110385) was used as the outgroup taxon. The best-scoring RAxML tree with a final likelihood value of -12111.406531 was presented. The matrix had 688 distinct alignment patterns, with 21.86% of undetermined characters or gaps. Estimated base frequencies were as follows: A = 0.245494, C = 0.247696, G = 0.255443, T = 0.251367; substitution rates AC = 1.306162, AG = 2.579472, AT = 1.571029, CG = 0.884497,

CT = 5.752512, GT = 1.000000; gamma distribution shape parameter α = 0.397636. ML bootstrap support values ≥50% (BT) and Bayesian posterior probabilities ≥0.90 (BYPP) are shown near the nodes. The scale bar indicates 0.07 changes per site. Isolates from the current study are in red and type specimens are in bold.

Sporocadaceae Corda [as 'Sporocadeae'], Icon. fung. (Prague) 5: 34 (1842)

Species of Sporocadaceae are endophytes, phytopathogens or saprobes with a wide host range, which are characterized by producing appendaged conidia (Liu et al., 2019). *Neopestalotiopsis* and *Pestalotiopsis*, generally known as Pestalotioid fungi, are important pathogens causing postharvest fruit rot and trunk diseases on grapevines in many countries (Jayawardena et al., 2015; Maharachchikumbura et al., 2016). In this study, sixteen isolates were obtained from Sporocadaceae belonging to *Pestalotiopsis*, *Neopestalotiopsis* and *Bartalinia*, representing five species. For taxonomic treatments of Sporocadaceae, we follow Tibpromma et al. (2020) and Li et al. (2021).

Pestalotiopsis Steyaert, Bull. Jard. bot. État Brux. 19: 300 (1949)

Pestalotiopsis kenyana Maharachch., K.D. Hyde & Crous, in Maharachchikumbura, Hyde, Groenewald, Xu & Crous, Stud. Mycol. 79: 166 (2014)

Index Fungorum: IF809741; Facesoffungi number: FoF 06981

Asexual morph: *Conidiogenous* cells discrete, lageniform to subcylindrical, hyaline. *Conidia* fusoid to subcylindrical, straight to slightly curved, 4-septate, 23–29 × 7–9 μm ($\overline{x}$ ± SD = 25.2 ± 1.7 × 7.7 ± 0.5 μm, n = 50); basal cell conic to obconic, hyaline; three median cells doliiform, wall verruculose concolourous, brown, septa darker than the rest of the cell; apical cell subcylindrical, hyaline, with two to three tubular appendages arising from the apex of the apical cell, one filiform, basal appendage (Figure 4.22). Sexual morph: Not observed.

Culture characteristics – Colonies on PDA white with wavy edge. Colonies reached 6.7 cm diam after 5 days at 25°C (Figure 4.22).

Material Examined – China, Fujian Province, Longyan City, Shanghang County, on the trunk of *Vitis vinifera*, 4 January 2022, Linna Wu and Xinghong Li (Inactive dry cultures JZBH340076–JZBH340078), living cultures JZB340076–JZB340078.

Notes – In the multi-locus phylogenetic analysis, three isolates clustered with *P. kenyana* with 94% ML bootstrap value and 1.0 BYPP (Figure 4.23). *Pestalotiopsis*

kenyana was reported on *Camellia sinensis* in China (Liu et al., 2017). This is the first report of this species associated with grapevine trunk diseases in the world.
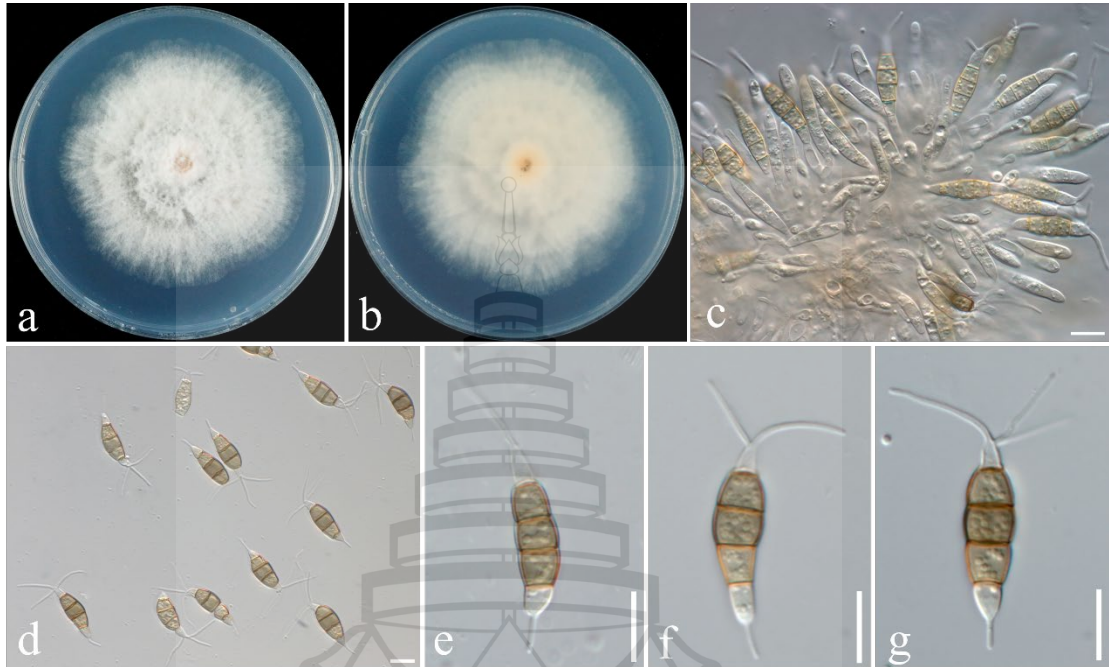
Figure 4.22 Morphological characterization of *Pestalotiopsis kenyana* (JZB340076)

Figure 4.22 a Upper view of the colony on PDA. b Reverse view of the colony on PDA. c Conidiogenous cells and conidia. d–g Conidia. Scale bars: c–g =10 μm.
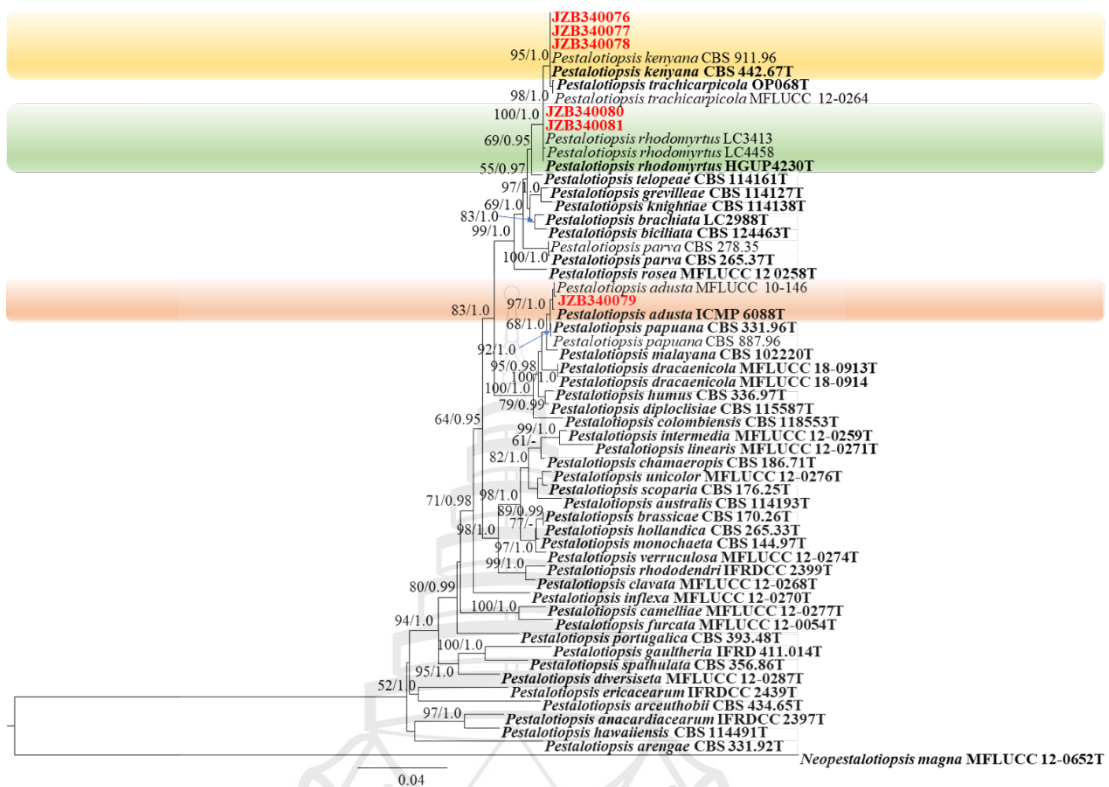
Figure 4.23 Phylogenetic tree generated by maximum likelihood analysis of combined ITS, *tub2* and *tef1* sequence data of *Pestalotiopsis* species

Figure 4.23 *Neopestalotiopsis magna* (MFLUCC 12-0652) was used as the outgroup taxon. The best-scoring RAxML tree with a final likelihood value of -9698.046952 was presented. The matrix had 733 distinct alignment patterns, with 15.42% of undetermined characters or gaps. Estimated base frequencies were as follows: A = 0.239513, C = 0.293756, G = 0.215210, T = 0.251521; substitution rates AC = 1.226778, AG = 3.764525, AT = 1.325866, CG = 1.211293, CT = 5.305853, GT = 1.000000; gamma distribution shape parameter α = 0.597712. ML bootstrap support values ≥50% (BT) and Bayesian posterior probabilities ≥0.90 (BYPP) are shown near the nodes. The scale bar indicates 0.04 changes per site. Isolates from the current study are in red and type specimens are in bold.

Pestalotiopsis rhodomyrtus Y. Song, K. Geng, K.D. Hyde & Yong Wang, Phytotaxa 126: 27. 2013.

Index Fungorum: IF846110; Facesoffungi number: FoF 09398

Asexual morph: *Conidiomata* scattered, black. *Conidiogenous cells* discrete, filiform, hyaline. *Conidia* fusoid, straight or slightly curved, 4-septate, 25–32 × 5–7 μm ($\overline{x} \pm SD = 28.6 \pm 1.9 \times 6.0 \pm 0.5$ μm, n = 50); basal cell conic to obconic, hyaline; three median cells doliiform, concolorous, brown, septate and periclinal walls darker than the rest of the cell, verruculous; apical cell subcylindrical to obconic, hyaline, with 2–3 tubular appendages arising from the apex of the apical cell, with one filiform, basal appendage (Figure 4.24). Sexual morph: Not observed.

Culture characteristics – Colonies on PDA were white with crenate edge, reverse light orange with white margin (Figure 4.24). Colonies reached 6.9 cm diam after 5 days at 25°C.

Material Examined – China, Fujian Province, Longyan City, Shanghang County, on the trunk of *Vitis vinifera*, 19 January 2022, Linna Wu and Xinghong Li (Inactive dry cultures JZBH340080–JZBH340081), living cultures JZB340080–JZB340081.

Notes – In the multi-locus phylogenetic analysis, two isolates clustered with *P. rhodomyrtus* with 100% ML bootstrap value and 1.0 BYPP (Figure 4.23). *Pestalotiopsis rhodomyrtus* was reported on *Rhodomyrtus tomentosa* and *Camellia sinensis* in China (Liu et al., 2017; Song et al., 2013). This is the first report of this species associated with grapevine trunk diseases in the world.

Figure 4.24 Morphological characterization of *Pestalotiopsis rhodomyrtus* (JZB340080)

Figure 4.24 a Upper view of the colony on PDA. b Reverse view of the colony on PDA. c Conidiomata sporulating on PDA. d, e Conidiogenous cells and conidia. f–i Conidia. Scale bars: c = 100 μm, d–i = 10 μm.

Pestalotiopsis adusta (Ellis & Everh.) Steyaert, Trans. Br. mycol. Soc. 36(2): 82 (1953)

Index Fungorum: IF302600; Facesoffungi number: FoF 14323

Asexual morph: *Conidiomata* globose, black. *Conidiogenous cells* discrete, filiform, hyaline. *Conidia* fusiform to ellipsoid, straight or slightly curved, 4-septate, 17–27 × 5–7 μm ($\bar{x} \pm SD = 21.7 \pm 2.0 \times 5.8 \pm 0.6$ μm, n = 50); basal cell obtuse, hyaline; three median cells doliiform, concolorous, olivaceous, septate and periclinal walls

darker than the rest of the cell, verruculose; apical cell obconic, hyaline, with 2–3 tubular appendages arising from the apex of the apical cell, with one filiform, basal appendage (Figure 4.25). Sexual morph: Not observed.

Culture characteristics – Colonies on PDA white with undulate edge, reverse orange (Figure 4.25). Colonies reached 8.0 cm diam. after 5 days at 25°C.

Material Examined – China, Fujian Province, Longyan City, Shanghang County, on the root of *Vitis vinifera*, 4 January 2022, Linna Wu and Xinghong Li (Inactive dry cultures JZBH340079), living cultures JZB340079.

Notes – In the multi-locus phylogenetic analysis, one isolate clustered with *P. adusta* with 99% ML bootstrap value and 1.0 BYPP (Figure 4.23). *Pestalotiopsis adusta* was reported to cause leaf spot on raspberry and mongo in China (Yan et al., 2019; Shu et al., 2020). This is the first report of the species associated with grapevine trunk diseases in the world.
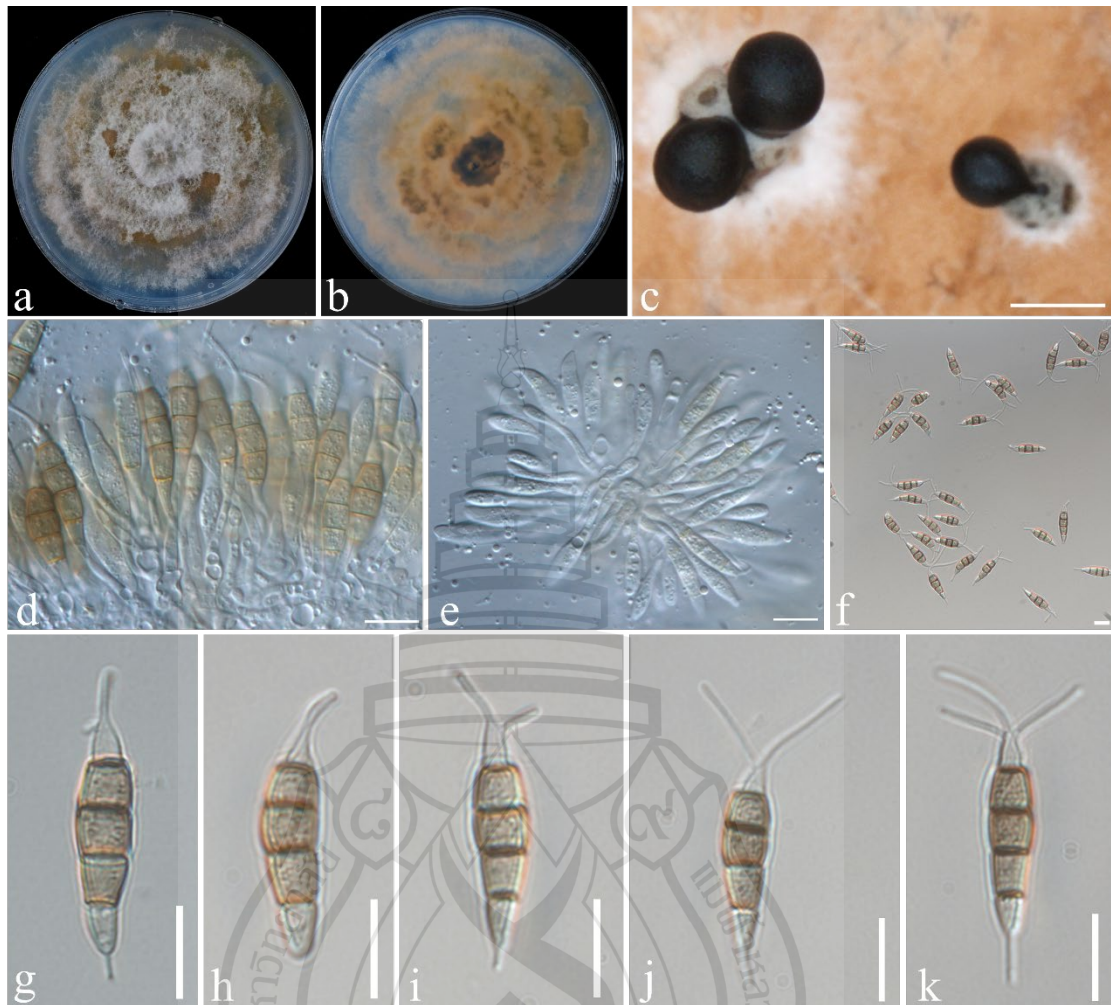
Figure 4.25 Morphological characterization of *Pestalotiopsis adusta* (JZB340079)

Figure 4.25 a Upper view of the colony on PDA. b Reverse view of the colony on PDA. c Conidiomata sporulating on PDA. d, e Conidiogenous cells and conidia. f–k Conidia. Scale bars: c = 100 μm, d–k = 10 μm.

Neopestalotiopsis Maharachch., K.D. Hyde & Crous, in Maharachchikumbura, Hyde, Groenewald, Xu & Crous, Stud. Mycol. 79: 135 (2014)

Neopestalotiopsis rosae Maharachch., K.D. Hyde & Crous, in Maharachchikumbura, Hyde, Groenewald, Xu & Crous, Stud. Mycol. 79: 147 (2014)

Index Fungorum: IF809777; Facesoffungi number: FoF 03890

Description – See Maharachchikumbura et al. (2014)

Material Examined – China, Yunnan Province, Binchuan County, on the trunk of *Vitis vinifera*, 23 July 2021, Linna Wu and Xinghong Li, living culture JZB340082; *ibid*., on the root of *Vitis vinifera*, 23 July 2021, Linna Wu and Xinghong Li, living culture JZB340083.

Notes – In the multi-locus phylogenetic analysis, two isolates clustered with *N. rosae* with 70% ML bootstrap value and 1.0 BYPP (Figure 4.26). The morphological characteristics of these isolates were similar to the type of *N. rosae* (CBS 101057) (Maharachchikumbura et al., 2014). *Neopestalotiopsis rosae* was reported to cause grape rot in the USA (Cosseboom & Hu, 2021). This is the first report of *N. rosae* associated with grapevine trunk diseases in China.
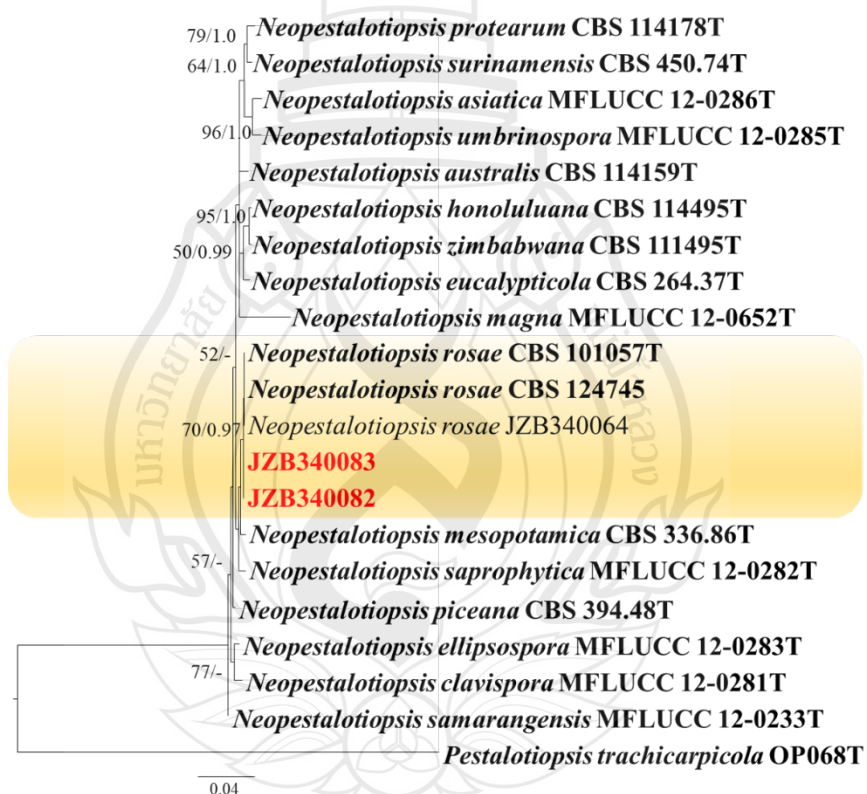
Figure 4.26 Phylogenetic tree generated by maximum likelihood analysis of combined ITS, *tub2* and *tef1* sequence data of *Neopestalotiopsis* species

Figure 4.26 *Pestalotiopsis trachicarpicola* (OP068T) was used as the outgroup taxon. The best-scoring RAxML tree with a final likelihood value of -4690.057697 was presented. The matrix had 220 distinct alignment patterns, with 9.61% of undetermined characters or gaps. Estimated base frequencies were as follows: A = 0.237087, C =

0.273572, G = 0.213431, T = 0.275910; substitution rates AC = 0.728700, AG = 4.270377, AT = 1.372478, CG = 0.528762, CT = 5.131524, GT = 1.000000; gamma distribution shape parameter α = 0.791052. ML bootstrap support values ≥50% (BT) and Bayesian posterior probabilities ≥0.90 (BYPP) are shown near the nodes. The scale bar indicates 0.04 changes per site. Isolates from the current study are in red and type specimens are in bold.

Bartalinia Tassi, Bulletin Labor. Orto Bot. de R. Univ. Siena 3: 4 (1900)

Bartalinia kevinhydei Doilom, Tibpromma & D.J. Bhat, in Tibpromma, Karunarathna, Mortimer, Xu, Doilom & Lumyong, Phytotaxa 474(1): 32 (2020)

Index Fungorum: IF557718; Facesoffungi number: FoF 08146

Asexual morph: *Conidiomata* subglobose. *Conidiogenous cells* ampulliform to subcylindrical, hyaline. *Conidia* subcylindrical, straight or slightly curved, 4-septate, 19–26 × 3–6 μm ($\bar{x} \pm SD = 21.4 \pm 1.7 \times 4.7 \pm 0.6$ μm, n = 50); basal cell conic, hyaline, sometimes pale brown, paler than second to fourth cells; three median cells doliiform, concolorous, pale brown, septate with periclinal walls darker than the rest of the cell; apical cell conical, hyaline, with 3 tubular appendages arising from the apex of the apical cell with one filiform, basal appendage (Figure 4.27). Sexual morph: Not observed.

Culture characteristics – Colonies on PDA were yellow-brown in the centre and cream color at edge (Figure 4.27). Colonies reached 6.2 cm diam after 5 days at 25°C.

Material Examined – China, Yunnan Province, Binchuan County, on the trunk of *Vitis vinifera*, 23 July 2021, Linna Wu and Xinghong Li (Inactive dry cultures JZBH3640001, JZBH3640002), living cultures JZB3640001, JZB3640002; *ibid.*, Ningxia Province, Yinchuan City, on the trunk of *Vitis vinifera*, 15 September 2021, Linna Wu and Xinghong Li (Inactive dry cultures JZBH3640003, JZBH3640004), living cultures JZB3640003, JZB3640004; *ibid.*, Hebei Province, Changli County, on the trunk of *Vitis vinifera*, 18 October 2021, Linna Wu and Xinghong Li (Inactive dry cultures JZBH3640005, JZBH3640006), living cultures JZB3640005, JZB3640006; *ibid.*, Beijing City, Fangshan District, on the trunk of *Vitis vinifera*, 11 September 2021, Linna Wu and Xinghong Li (Inactive dry cultures JZBH3640007, JZBH3640008), living cultures JZB3640007, JZB3640008.

128

Notes – In the multi-locus phylogenetic analysis, eight isolates clustered with *B. kevinhydei* with 67% ML bootstrap value and 1.0 BYPP (Figure 4.28). *Bartalinia kevinhydei* is a new leaf-spot causing fungus on teak from Northern Thailand (Tibpromma et al., 2020). This is the first report of *B. kevinhydei* associated with grapevine trunk diseases in the world.

Figure 4.27 Morphological characterization of *Bartalinia kevinhydei* (JZB3640003)

Figure 4.27 a Upper view of the colony on PDA. b Reverse view of the colony on PDA. c Conidiomata sporulating on PDA. d, e Conidiogenous cells and conidia. f, g Conidia. Scale bars: c = 100 μm, d–g = 10 μm.

JZB3640001
JZB3640008
JZB3640006
JZB3640003
JZB3640004
JZB3640007
JZB3640005
Bartalinia kevinhydei **MFLUCC 12-0384BT**
Bartalinia kevinhydei **MFLUCC 12-0384AT**
JZB3640002
Bartalinia pini CFCC 54574
Bartalinia pini **CBS 143891T**
Bartalinia lateripes HKUCC 6654
Bartalinia rosicola MFLUCC 17-0645
Bartalinia laurina HKUCC 6537
Bartalinia pondoensis CMW 31067
Bartalinia robillardoides CBS 122686
Bartalinia robillardoides **CBS 122705T**
Bartalinia robillardoides CNUFC-CNUP1-2
Bartalinia robillardoides CNUFC-CNUP1-1
Bartalinia kunmingensis **KUMCC 18-0178T**
Bartalinia bischofiae HKUCC 6534
Pestalotiopsis malayana **CBS 102220T**
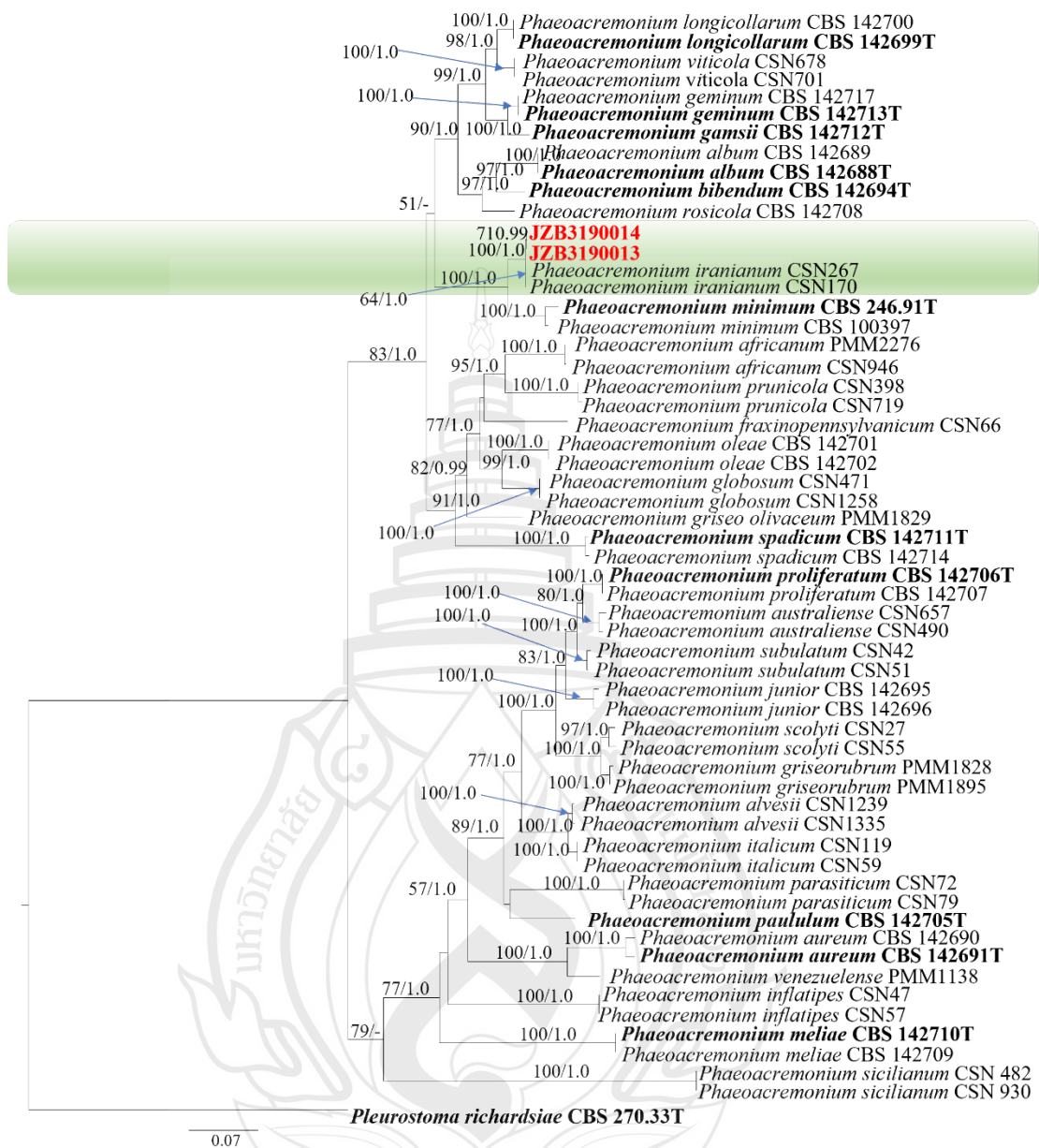
70/-
56/-
67/1.0
72/1.0
56/0.94
53/-
74/-
0.009

Figure 4.28 Phylogenetic tree generated by maximum likelihood analysis of combined ITS and LSU sequence data of *Bartalinia* species

Figure 4.28 *Pestalotiopsis malayana* (CBS 102220) was used as outgroup taxon. The best scoring RAxML tree with a final likelihood value of -2455.231222 was presented. The matrix had 64 distinct alignment patterns, with 9.62% of undetermined characters or gaps. Estimated base frequencies were as follows: A = 0.259785, C = 0.205067, G = 0.256605, T = 0.278543; substitution rates AC = 0.000100, AG = 6.135642, AT = 5.163560, CG = 7.199006, CT = 22.594137, GT = 1.000000; gamma distribution shape parameter α = 1000.000000. ML bootstrap support values ≥50% (BT) and Bayesian posterior probabilities ≥0.95 (BYPP) are shown near the nodes. The scale bar indicates 0.009 changes per site. Isolates from the current study are in red and type specimens are in bold.

Glomerellaceae Locq. ex Seifert & W. Gams, in Zhang, Castlebury, Miller, Huhndorf, Schoch, Seifert, Rossman, Rogers, Kohlmeyer, Volkmann-Kohlmeyer & Sung, Mycologia 98(6): 1083 (2007) [2006]

Colletotrichum Corda, in Sturm, Deutschl. Fl., 3 Abt. (Pilze Deutschl.) 3(12): 41 (1831)

Colletotrichum is the only genus in Glomerellaceae and is regarded as one of the top 10 phytopathogenic fungal genera in the world, causing anthracnose on leaves, fruits, stems and other more organs (Dean et al., 2012; Liu et al., 2022). In this study, we follow Liu et al. (2022) for taxonomic treatments.

Colletotrichum viniferum Li J. Peng, L. Cai, K.D. Hyde & Zi Y. Ying, Mycoscience 54(1): 36 (2013)

Index Fungorum: IF563086; Facesoffungi number: FoF 03600

Description – See Peng et al. (2013)

Material Examined – China, Fujian Province, Longyan City, Shanghang County, on the shoot of *Vitis vinifera*, 20 May 2021, Linna Wu and Xinghong Li, living cultures JZB330319–JZB330322; *ibid.*, Beijing City, on the trunk of *Vitis vinifera*, 11 September 2021, Linna Wu and Xinghong Li, living cultures JZB330323, JZB330324.

Notes – In the multi-locus phylogenetic analysis, six isolates clustered with *C. viniferum* with 100% ML bootstrap value and 1.0 BYPP (Figure 4.29). *Colletotrichum viniferum* was reported to cause fruit anthracnose and leaf lesions of grapevines in China (Peng et al., 2013; Yan et al., 2015).
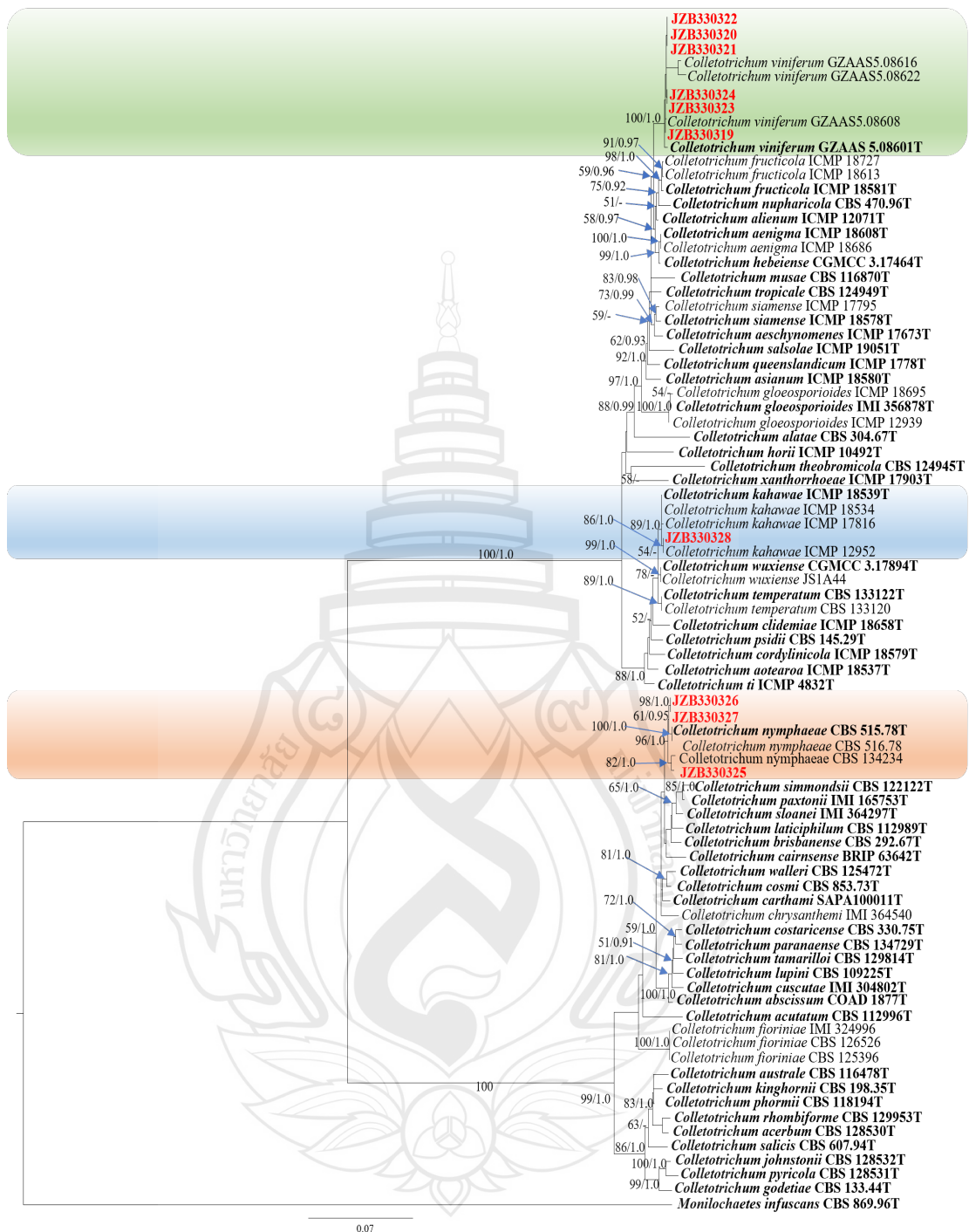
Figure 4.29 Phylogenetic tree generated by maximum likelihood analysis of combined ITS, *gapdh*, *act*, *chs* and *tub2* sequence data of *Colletotrichum* species

Figure 4.29 *Monilochaetes infuscans* (CBS 869.96) was used as the outgroup taxon. The best scoring RAxML tree with a final likelihood value of -11791.239474 was presented. The matrix had 941 distinct alignment patterns, with 13.45% of

undetermined characters or gaps. Estimated base frequencies were as follows: A = 0.232433, C = 0.302405, G = 0.240309, T = 0.224853; substitution rates AC = 1.238239, AG = 3.563826, AT = 1.094851, CG = 0.802739, CT = 5.163031, GT = 1.000000; gamma distribution shape parameter α = 0.983971. ML bootstrap support values ≥50% (BT) and Bayesian posterior probabilities ≥0.95 (BYPP) are shown near the nodes. The scale bar indicates 0.07 changes per site. Isolates from the current study are in red and type specimens are in bold.

Colletotrichum nymphaeae (Pass.) Aa, Netherlands Journal of Plant Pathology, Supplement 1 84(3): 110 (1978)

Index Fungorum: IF311502; Facesoffungi number: FoF 14339

Description – See Damm et al. (2012)

Material Examined – China, Fujian Province, Longyan City, Shanghang County, on the shoot of *Vitis vinifera*, 20 May 2021, Linna Wu and Xinghong Li, living cultures JZB330325; *ibid.*, on the trunk of *Vitis vinifera*, 4 January 2022, Linna Wu and Xinghong Li, living cultures JZB330326, JZB330327.

Notes – In the multi-locus phylogenetic analysis, three isolates clustered with *C. nymphaeae* with 96% ML bootstrap value and 1.0 BYPP (Figure 4.29). *Colletotrichum nymphaeae* was reported to cause twig anthracnose on grapevines in China (Liu et al., 2016).

Colletotrichum kahawae J.M. Waller & Bridge, Mycol. Res. 97(8): 993 (1993)

Index Fungorum: IF360355; Facesoffungi number: FoF 14359

Asexual morph: *Conidiophores* hyaline, one-celled, not branching. *Conidia* cylindrical, 10–15 × 5–8 μm (x̄ ± SD = 12.8 ± 1.1 × 6.5 ± 0.6 μm, n = 50). *Appressoria* spherical, ovoid or slightly irregular (Figure 4.30). Sexual morph: Not observed.

Culture characteristics – Colonies on PDA white to pale grey, reverse dark gray with white margin. Colonies reached 6.5 mm diam. after 5 days at 25ºC (Figure 4.30).

Material Examined – China, Yunnan Province, Mile City, on the trunk of *Vitis vinifera*, 9 September 2020, Linna Wu and Xinghong Li (Inactive dry cultures JZBH330328), living cultures JZB330328.

Notes – In the multi-locus phylogenetic analysis, one isolate clustered with *C. kahawae* with 89% ML bootstrap value and 1.0 BYPP (Figure 4.29). *Colletotrichum kahawae* was reported to cause grape ripe rot disease in Brazil (Echeverrigaray et al.,

2020). This is the first repot of *C. kahawae* associated with grapevine trunk disease in China.
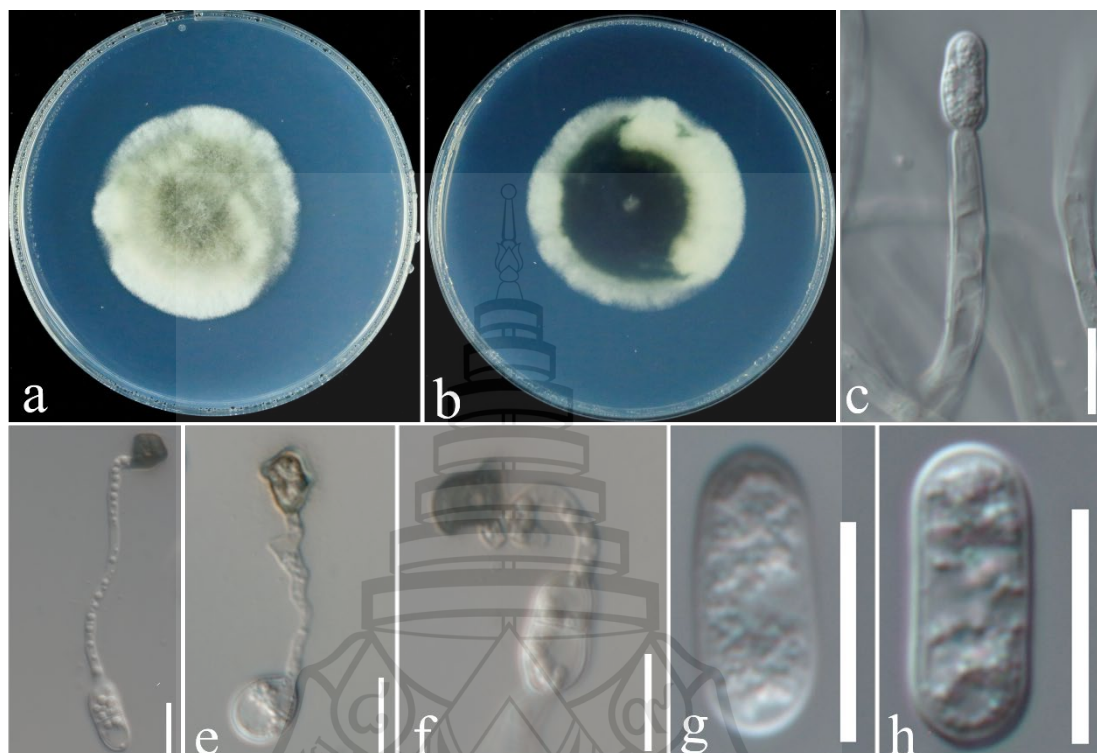
Figure 4.30 Morphological characterization of *Colletotrichum kahawae* (JZB330328)

Figure 4.30 a Upper view of the colony on PDA. b Reverse view of the colony on PDA. c Conidiophores. d–f Appressoria. g, h Conidia. Scale bars: c–h = 10 μm.

Pleosporaceae Nitschke, Verh. naturh. Ver. preuss. Rheinl. 26: 74 (1869)

Alternaria Nees, Syst. Pilze (Würzburg): 72 (1816) [1816-17]

Alternaria widely distributed in various substrates as saprobes, endophytes and pathogens, and has numerous hosts including grapevine (Woudenberg et al., 2013; Tao et al., 2014). In this study, eight isolates belonging to two *Alternaria* species were identified. For taxonomic treatments, we follow Woudenberg et al. (2013).

Alternaria alternata (Fr.) Keissl., Beih. bot. Zbl., Abt. 2 29: 434 (1912)

Index Fungorum: IF119834; Facesoffungi number: FoF 03825

Description – See Woudenberg et al. (2013)

Asexual morph: China, Shanxi Province, Linfen City, on the trunk of *Vitis vinifera*, 23 June 2021, Linna Wu and Xinghong Li, living cultures JZB3180127, JZB3180128; *ibid.*, Hebei Province, Zhangjiakou City, Huailai County, on the trunk of

Vitis vinifera, 9 July 2021, Linna Wu and Xinghong Li, living cultures JZB3180129, JZB3180130; *ibid.*, Qinhuangdao City, Changli County, on the trunk of *Vitis vinifera*, 13 November 2021, Linna Wu and Xinghong Li, living cultures JZB3180131; *ibid.*, Fujian Province, Longyan City, Shanghang County, on the trunk of *Vitis vinifera*, 4 January 2022, Linna Wu and Xinghong Li, living culture JZB3180132.

Notes – In the multi-locus phylogenetic analysis, six isolates clustered in two clades of *A. alternata* with 97% ML bootstrap value and 1.0 BYPP (Figure 4.31). *Alternaria* is a widespread fungus, which includes saprobic, endophytic and pathogenic species. *Alternaria alternata* is a well-known plant pathogen around the world, and is reported to cause grapevine fruit rot and also act as endophytes and saprotrophs on grapevine (Jayawardena et al., 2018).
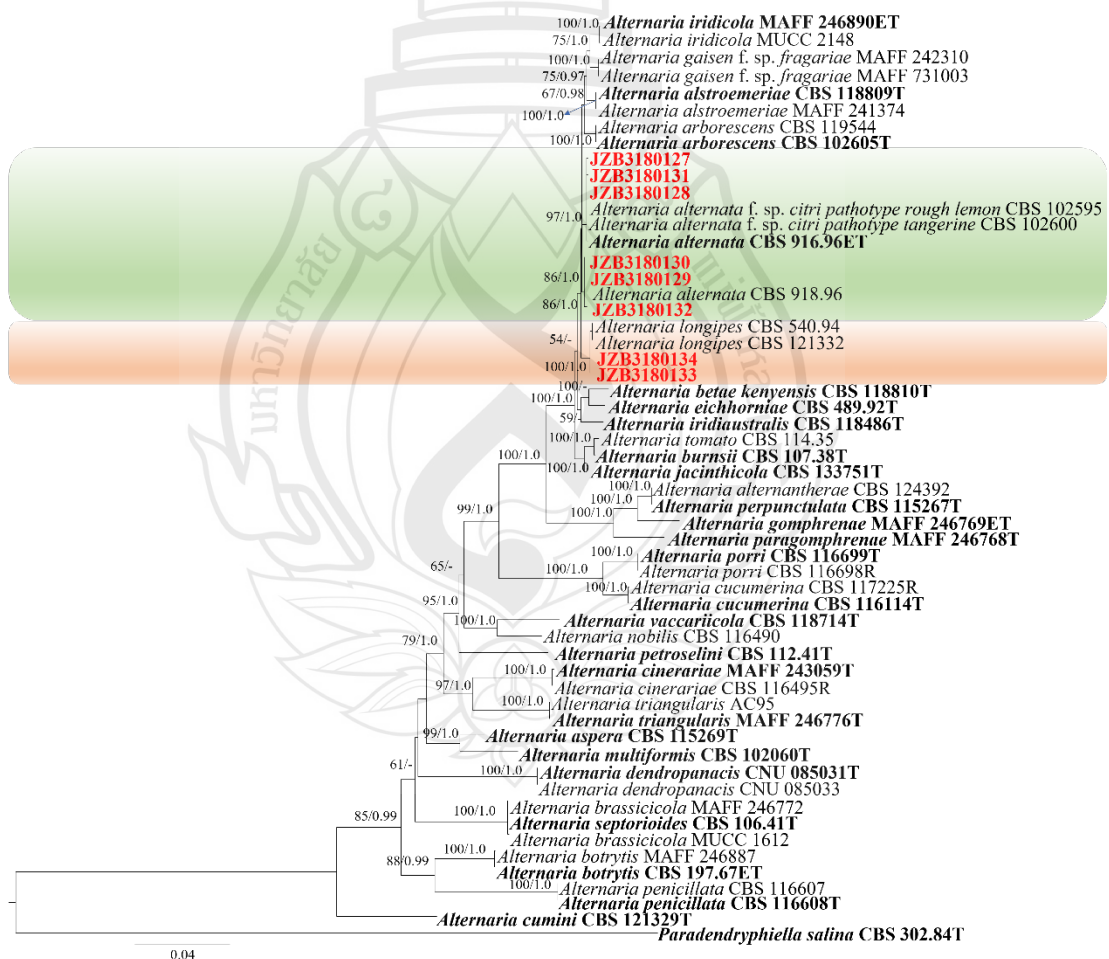
Figure 4.31 Phylogenetic tree generated by maximum likelihood analysis of combined ITS, *tef1*, *rpb2* and *gapdh* sequence data of *Alternaria* species

Figure 4.31 *Paradendryphiella salina* (CBS 302.84) was used as the outgroup taxon. The best scoring RAxML tree with a final likelihood value of -11419.172816 was presented. The matrix had 820 distinct alignment patterns, with 11.89% of undetermined characters or gaps. Estimated base frequencies were as follows: A = 0.241820, C = 0.277132, G = 0.247459, T = 0.233589; substitution rates AC = 1.364113, AG = 4.480928, AT = 1.081367, CG = 0.860134, CT = 10.450729, GT = 1.000000; gamma distribution shape parameter α = 0.900455. ML bootstrap support values $\geq$50% (BT) and Bayesian posterior probabilities $\geq$0.95 (BYPP) are shown near the nodes. The scale bar indicates 0.04 changes per site. Isolates from the current study are in red and type specimens are in bold.

Alternaria longipes (Ellis & Everh.) E.W. Mason, Annot. Acct Fungi rec'd Bur. Mycol. 2(1): 19 (1928)

Index Fungorum: IF269712; Facesoffungi number: FoF 14360

Asexual morph: *Conidiophores* light to dark brown with one or a few regular septa, mostly unbranched. *Conidia* obclavate, brown, with three to eight transverse and zero to two longitudinal or oblique septa, 10–32 × 6–14 μm ($\bar{x}$ ± SD = 20.0 ± 5.3 × 10.7 ± 2.0 μm, n = 50), and concatenated in long, sometimes branched chains (Figure 4.32). Sexual morph: Not observed.

Culture characteristics – Colonies on PDA were initially white and became grayish brown over time, reverse dark brown with white margin (Figure 4.32). Colonies reached 6.5 mm diam. after 6 days at 25ºC.

Material Examined – China, Fujian Province, Longyan City, Shanghang County, on the trunk of *Vitis vinifera*, 4 January 2021, Linna Wu and Xinghong Li (Inactive dry cultures JZBH3180133, JZBH3180134), living cultures JZB3180133, JZB3180134.

Notes – In the multi-locus phylogenetic analysis, two isolates clustered with *A. longipes* with 100% ML bootstrap value and 1.0 BYPP (Figure 4.31). *Alternaria longipes* hasbeen reported to cause leaf spot disease in tea and some medicinal plants in China (Tan et al., 2012; Yin et al., 2021). This is the first report of *A. longipes* associated with grapevine trunk disease in the world.
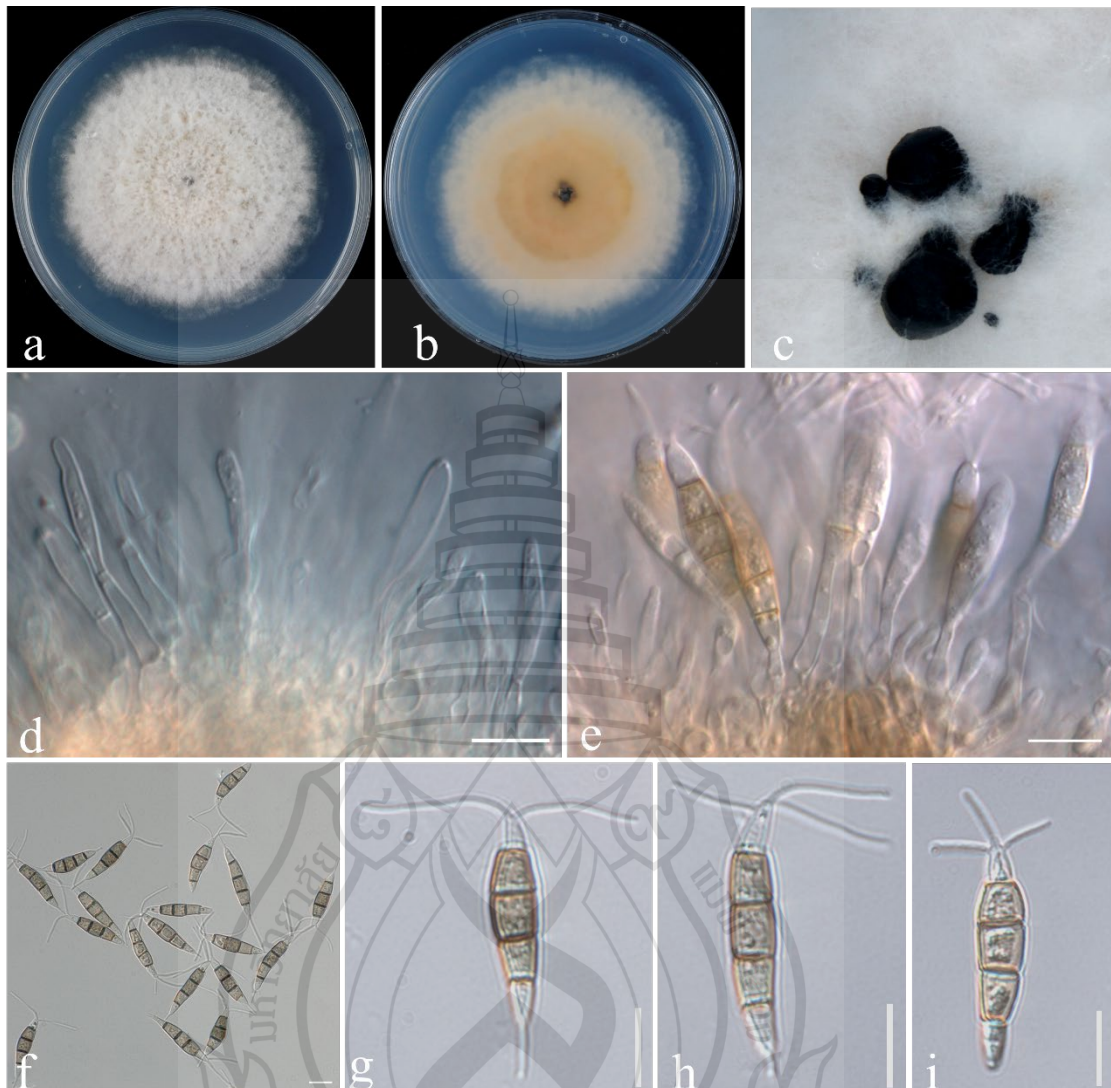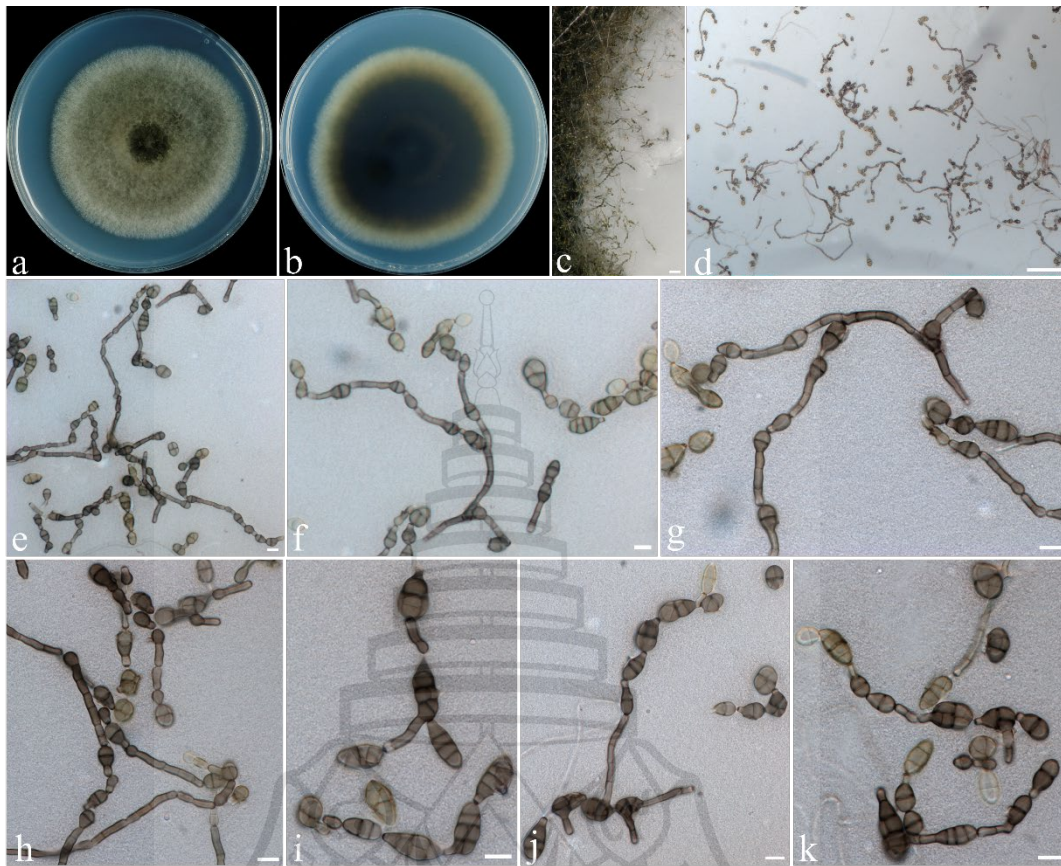
Figure 4.32 Morphological characterization of *Alternaria longipes* (JZB3180133)

Figure 4.32 a Upper view of the colony on PDA. b Reverse view of the colony on PDA. c–k Conidia and conidiophores. Scale bars: c = 500 μm, d = 100 μm, e–k = 10 μm.

Hypocreaceae De Not. [as 'Hypocreacei'], G. bot. ital. 2(1): 48 (1844)

Trichoderma Pers., Neues Mag. Bot. 1: 92 (1794)

Trichoderma is a widespread genus with abilities or potentials to be developed as biocontrol agents, for their potent degradative machinery for decomposition of heterogeneous substrates (Schuster & Schmoll, 2010). In this study, six isolates belonging to three *Trichoderma* species were identified. For taxonomic treatments, we follow Cai et al. (2022).

Trichoderma asperellum Samuels, Lieckf. & Nirenberg, Sydowia 51(1): 81 (1999)

Index Fungorum: IF461012; Facesoffungi number: FoF 14361

Asexual morph: *Conidiophores* tree-like, with repeated, paired branching with a main central branch. Phialides flask-shaped, enlarged in the middle. *Conidia* globose

to oval, green, smooth, 3–4 × 2–3 μm ($\overline{x}$ ± SD = 3.2 ± 0.2 × 2.8 ± 0.2 μm, n = 50). *Chlamydospores* elliptic or round (Figure 4.33). Sexual morph: Not observed.

Culture characteristics – Colonies on PDA initially whitish, downy, gradually green sporulation spread throughout the whole plate, reverse grayish with the formation of concentric rings (Figure 4.33). Colonies reached 6.0 mm diam. after 2 days at 25ºC.

Material Examined – China, Yunnan Province, Binchuan County, on the trunk of *Vitis vinifera*, 23 July 2021, Linna Wu and Xinghong Li (Inactive dry cultures JZBH3360013), living culture JZB3360013; *ibid.*, on the root of *Vitis vinifera*, 23 July 2021, Linna Wu and Xinghong Li (Inactive dry cultures JZBH3360014, JZBH3360015), living cultures JZB3360014, JZB3360015.

Notes – In the multi-locus phylogenetic analysis, three isolates clustered with *T. asperellum* with 98% ML bootstrap value and 1.0 BYPP (Figure 4.34). *Trichoderma asperellum* was reported to isolate from withered grape in Italy (Lorenzini et al., 2016). This is the first repot of *T. asperellum* associated with grapevine trunk disease in China.
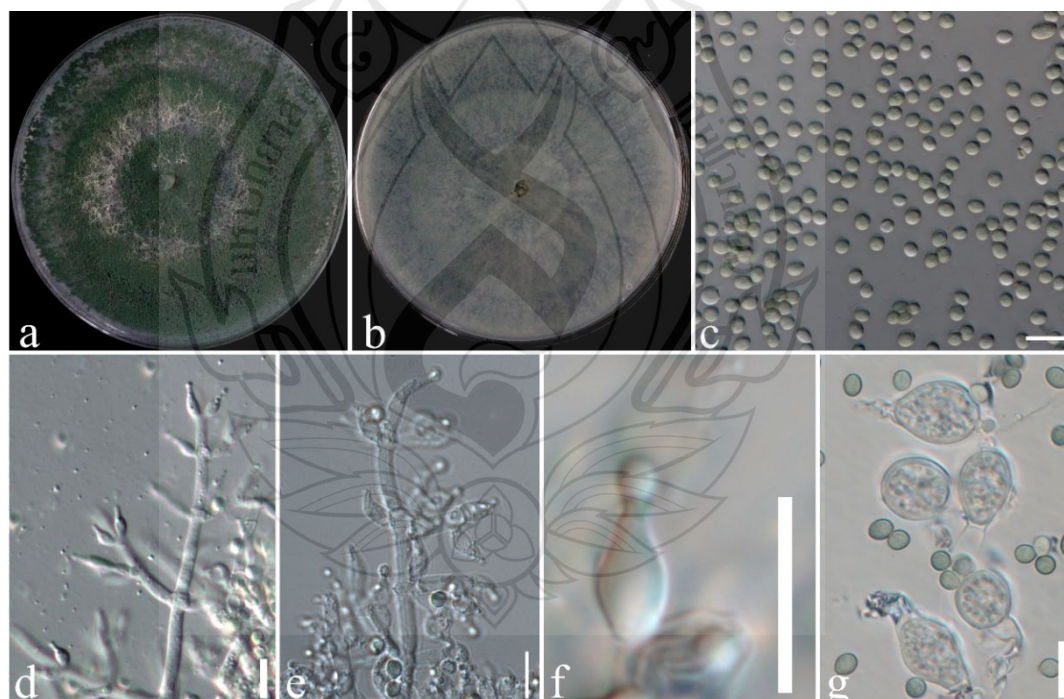
Figure 4.33 Morphological characterization of *Trichoderma asperellum* (JZB3360013)

Figure 4.33 a Upper view of the colony on PDA. b Reverse view of the colony on PDA. c Conidia. d, e Conidiophores. f phialide. g Chlamydospores. Scale bars: c–g = 10 μm.
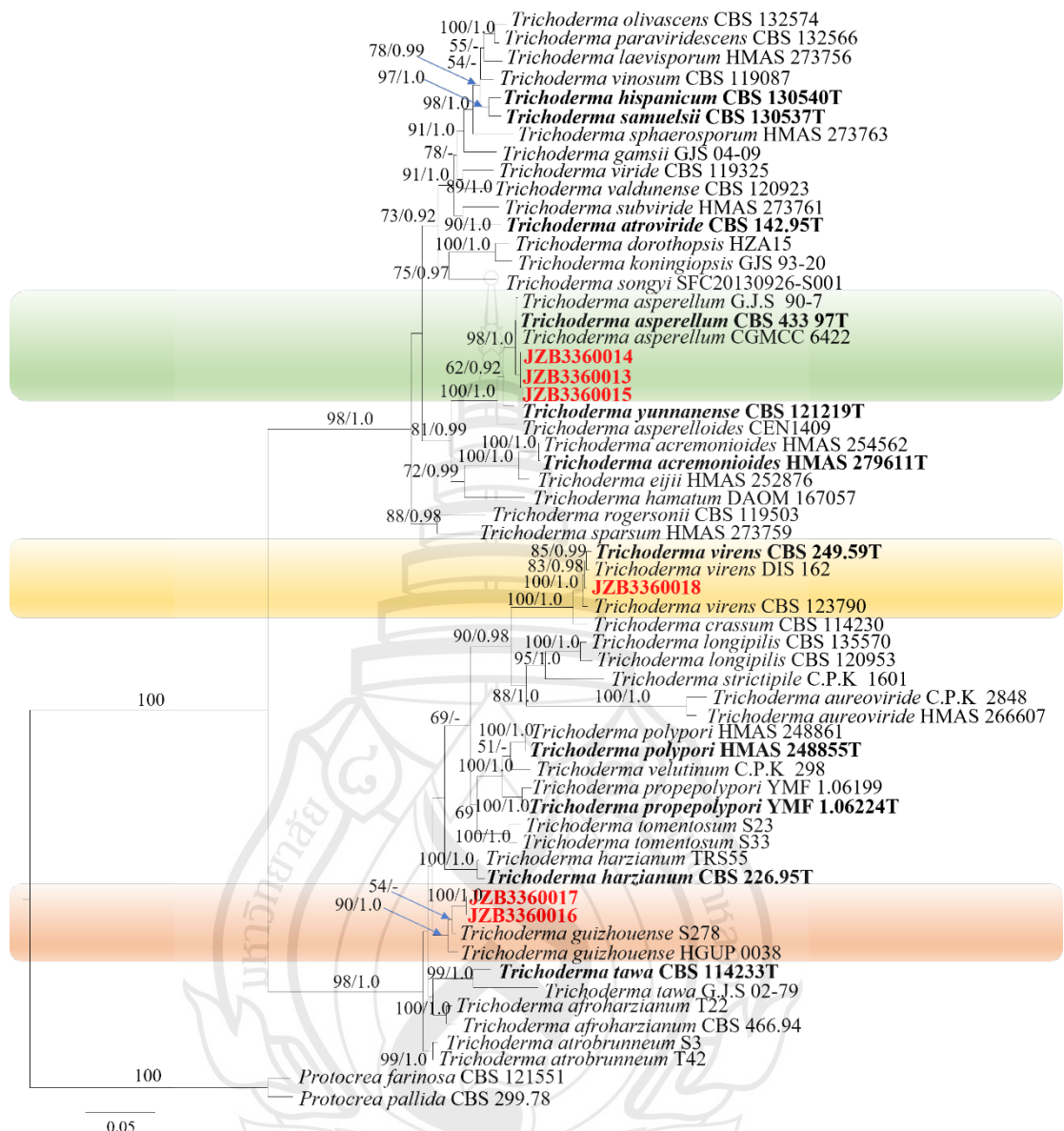
Figure 4.34 Phylogenetic tree generated by maximum likelihood analysis of combined *tef1* and *rpb2* sequence data of *Trichoderma* species

Figure 4.34 *Protocrea farinose* (CBS 121551) and *Protocrea pallida* (CBS 299.78) were used as the outgroup taxa. The best-scoring RAxML tree with a final likelihood value of -16356.159894 was presented. The matrix had 916 distinct alignment patterns, with 17.53% of undetermined characters or gaps. Estimated base frequencies were as follows: A = 0.235351, C = 0.280622, G = 0.241553, T = 0.242473;

substitution rates AC = 0.812912, AG = 3.702497, AT = 1.233164, CG = 0.719097, CT = 5.223883, GT = 1.000000; gamma distribution shape parameter α = 1.063259. ML bootstrap support values ≥50% (BT) and Bayesian posterior probabilities ≥0.95 (BYPP) are shown near the nodes. The scale bar indicates 0.05 changes per site. Isolates from the current study are in red and type specimens are in bold.

Trichoderma guizhouense Q.R. Li, McKenzie & Yong Wang bis, in Li, Tan, Jiang, Hyde, McKenzie, Bahkali, Kang & Wang, Mycol. Progr. 12(2): 170 (2012) [2013]

Index Fungorum: IF563664; Facesoffungi number: FoF 07838

Asexual morph: *Conidiophores* verticillate. *Phialides* ampulliform to lageniform, mostly in whorls of 2–3. *Conidia* oval to globose, yellow-green, smooth, 3–4 × 2–3 μm ($\bar{x}$ ± SD = 3.2 ± 0.2 × 2.8 ± 0.2 μm, n = 50). *Chlamydospores* elliptic or round, terminal (Figure 4.35). Sexual morph: Not observed.

Culture characteristics – Colonies on PDA cottony, dark green, forming concentric rings. Colonies reached 6.8 mm diam. after 2 days at 25ºC (Figure 4.35).

Material Examined – China, Beijing City, on the root of *Vitis vinifera*, 11 September 2021, Linna Wu and Xinghong Li (Inactive dry cultures JZBH3360016, JZBH3360017), living cultures JZB3360016, JZB3360017.

Notes – In the multi-locus phylogenetic analysis, two isolates clustered with *T. guizhouense* with 90% ML bootstrap value and 1.0 BYPP (Figure 4.34). *Tritroderma guizhouense* was initially isolated from soil in Guizhou Province, China (Li et al., 2013). This is the first report of *T. guizhouense* associated with grapevine trunk diseases.
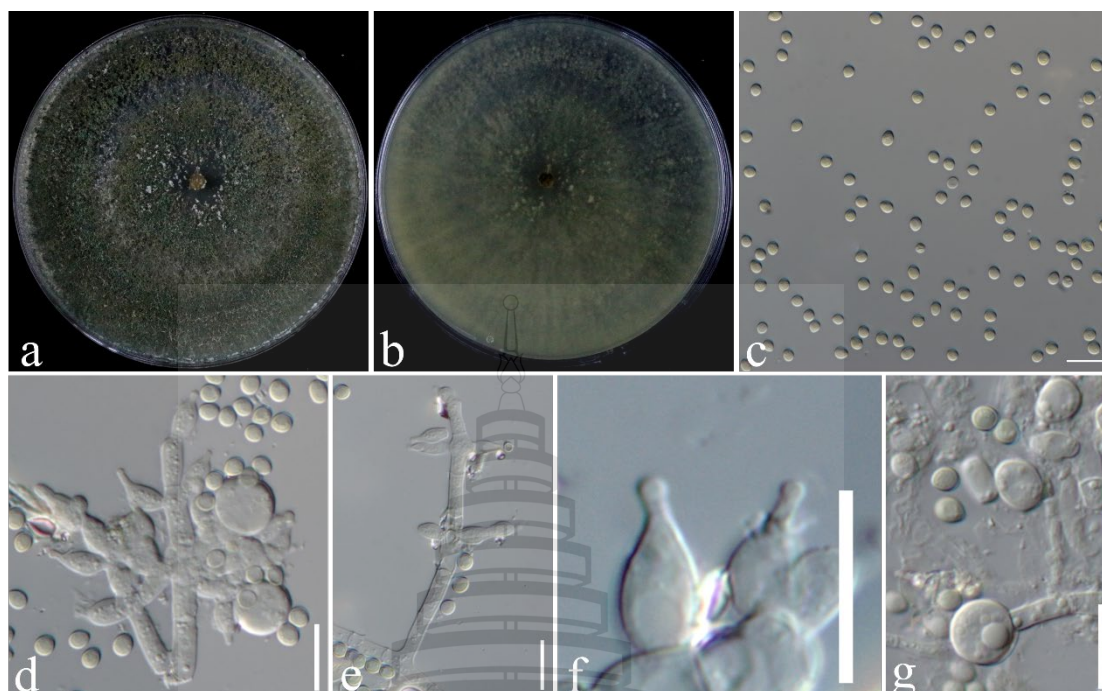
Figure 4.35 Morphological characterization of *Trichoderma guizhouense* (JZB3360016)

Figure 4.35 a Upper view of the colony on PDA. b Reverse view of the colony on PDA. c Conidia. d, e Conidiophores. f phialide. g Chlamydospores. Scale bars: c–g = 10 μm.

Trichoderma virens (J.H. Mill., Giddens & A.A. Foster) Arx, Beih. Nova Hedwigia 87: 288 (1987)

Index Fungorum: IF128198; Facesoffungi number: FoF 14362

Asexual morph: *Conidiophores* erect, asymmetrical branched. *Phialides* flask-shaped to ampulliform. *Conidia* sub-globose to elliptical, green, smooth, 4–6 × 3–5 μm ($\bar{x} \pm SD = 4.5 \pm 0.4 \times 3.8 \pm 0.3$ μm, n = 50). *Chlamydospores* elliptic or round (Figure 4.36). Sexual morph: Not observed.

Culture characteristics – Colonies on PDA initially whitish, gradually became deep green, reverse grayish. Colonies reached 5.9 mm diam. after 2 days at 25°C (Figure 4.36).

Material Examined – China, Hebei Province, Qinhuangdao City, Changli County, on the root of *Vitis vinifera*, 13 November 2021, Linna Wu and Xinghong Li (Inactive dry cultures JZBH3360018), living cultures JZB3360018.

Notes – In the multi-locus phylogenetic analysis, one isolate clustered with *T. virens* with 100% ML bootstrap value and 1.0 BYPP (Figure 4.34). *Trichoderma virens* was commonly isolated from the soil, and also reported as an endophyte of sugarcane and coffee (Romão-Dumaresq et al., 2016; Rodríguez et al., 2021). *Trichoderma virens* was isolated from a 42-year-old grapevine free of grapevine trunk disease symptoms in France (Bruez et al., 2016). This is the first report of *T. virens* associated with grapevine trunk disease in China.
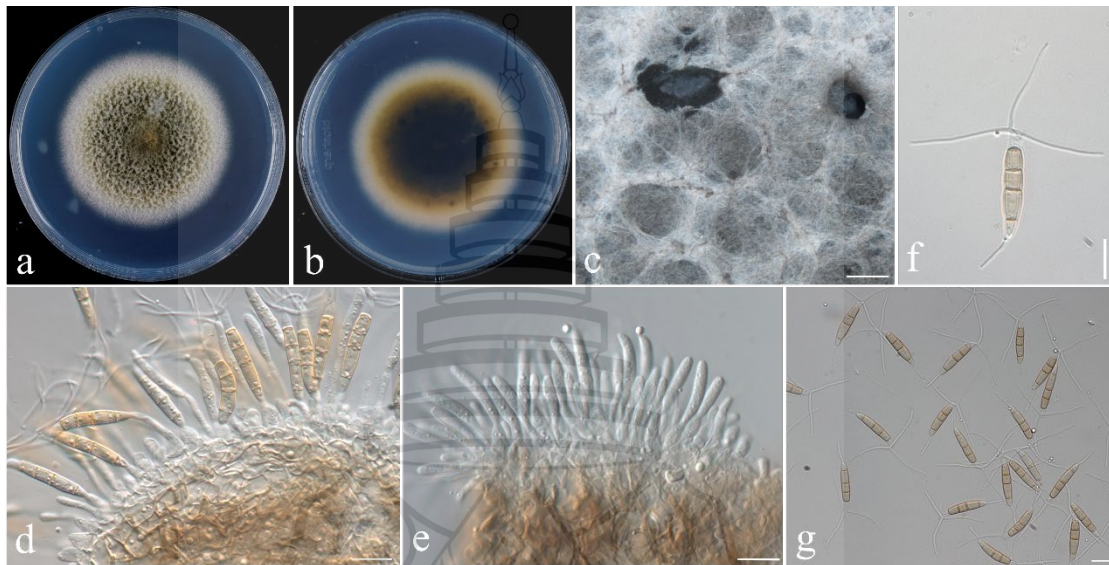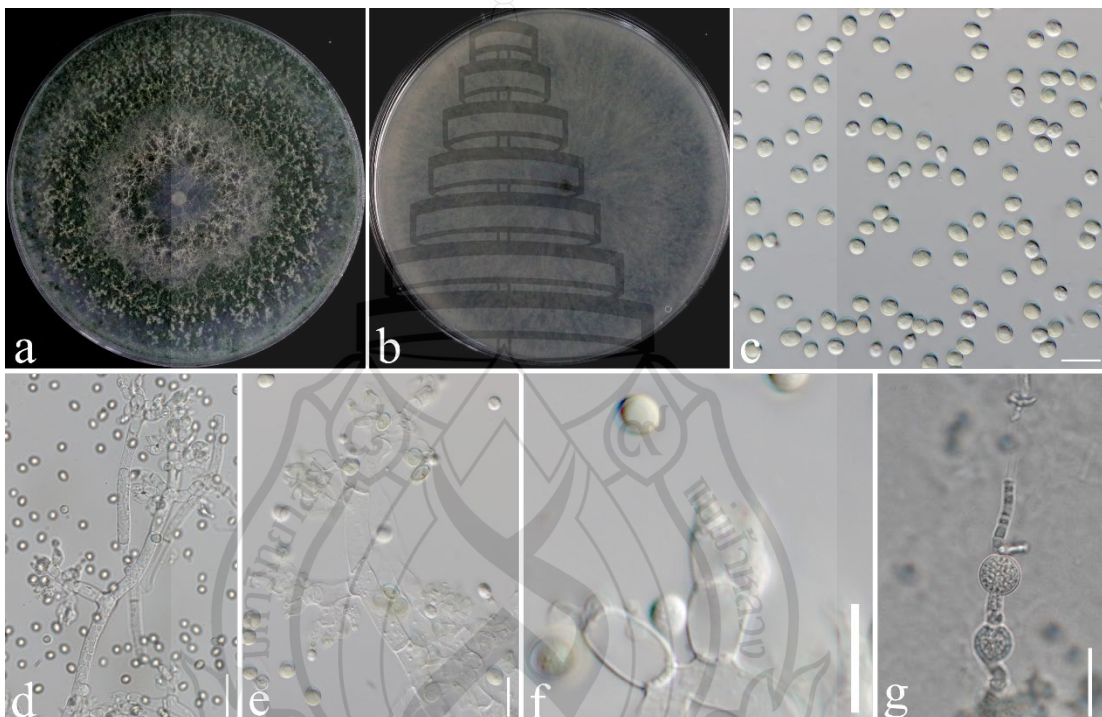

Figure 4.36 Morphological characterization of *Trichoderma virens* (JZB3360018)

Figure 4.36 a Upper view of the colony on PDA. b Reverse view of the colony on PDA. c Conidia. d, e Conidiophores. f phialide. g Chlamydospores. Scale bars: c–g = 10 μm.

Cladosporiaceae Chalm. & R.G. Archibald, Yearbook of Tropical Medicine and Hygiene: 25 (1915)

Cladosporium Link, Mag. Gesell. naturf. Freunde, Berlin 7: 37 (1816) [1815]

Cladosporium is a ubiquitous genus with small conidia in large numbers, spread easily over long distances. *Cladosporium* species are common endophytes, and also

could be secondary invaders after other plant pathogens, causing leaf spots (Bensch et al., 2012). In this study, we follow Bensch et al. (2012) for taxonomic treatments.

Cladosporium tenuissimum Cooke, Grevillea 6(no. 40): 140 (1878)

Index Fungorum: IF145672; Facesoffungi number: FoF 09313

Description – See Bensch et al. 2012

Material Examined – China, Fujian Province, Longyan City, Shanghang County, on the trunk of *Vitis vinifera*, 4 January 2021, Linna Wu and Xinghong Li, living cultures JZB390038, JZB390039.

Notes – In the multi-locus phylogenetic analysis, eight isolates clustered with *C. tenuissimum* with 99% ML bootstrap value and 1.0 BYPP (Figure 4.37). *Cladosporium tenuissimum* was reported as a pathogen causing grapevine fruit rot and/or as an endophytic fungus on grapevines in China (Dissanayake et al., 2018; Jayawardena et al., 2018).
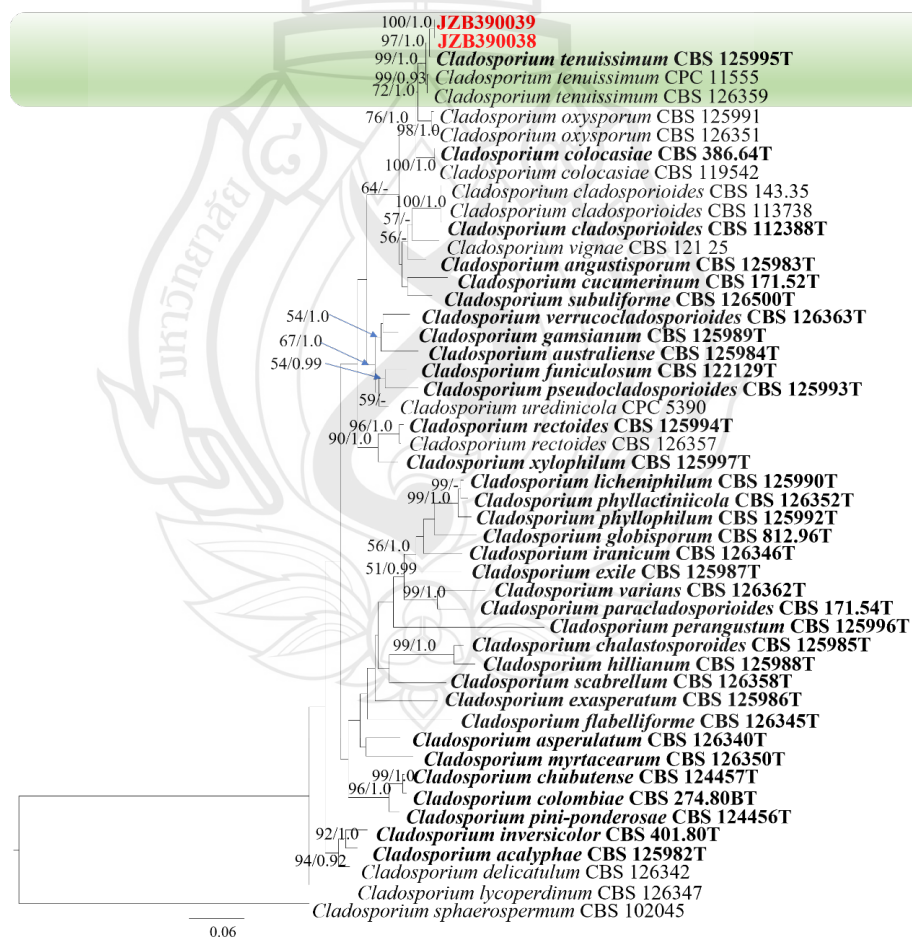
Figure 4.37 Phylogenetic tree generated by maximum likelihood analysis of combined ITS, *tef1* and LSU sequence data of *Cladosporium* species

Figure 4.37 A–C leaf symptoms in the field. D–F leaf spot samples. *Cladosporium sphaerospermum* (CBS 102045) was used as the outgroup taxon. The best scoring RAxML tree with a final likelihood value of -6579.450688 was presented. The matrix had 293 distinct alignment patterns, with 4.16% of undetermined characters or gaps. Estimated base frequencies were as follows: A = 0.224955, C = 0.297835, G = 0.240548, T = 0.236662; substitution rates AC = 2.713837, AG = 5.914225, AT = 2.658810, CG = 1.741064, CT = 8.493258, GT = 1.000000; gamma distribution shape parameter α = 0.651559. ML bootstrap support values ≥50% (BT) and Bayesian posterior probabilities ≥0.95 (BYPP) are shown near the nodes. The scale bar indicates 0.06 changes per site. Isolates from the current study are in red and type specimens are in bold.

4.3 Discussion

Grapevine trunk diseases are a huge threat to the sustainable development of the viticulture and viniculture industries, resulting in reduced yields and limited vineyard lifespans (Úrbez-Torres et al., 2020). At the same time, multiple fungal taxa have been recognized to be associated with a specific disease, and field symptoms are complex due to the mixed infection of different pathogens (Patanita et al., 2022). Roles of potential pathogens, effects of endophyte and saprobes, and their interactions among the fungal communities remain unclear. In this study, a total of 40 species belonging to 21 genera in 10 families were identified based on muti-locus phylogenetic analyses and morphological observations. Among them, 22 were first reports on grapevine in China and 12 species were first recorded on grapevine in the world. The top three taxa, *Diaporthe* (19.6%), *Cylindrocarpon*-like fungi (19.1%) and Botryosphaeriaceae (18.6%) accounted for more than half of the total isolates, which are well-established as pathogens causing grapevine trunk disease.

Diaporthe is an important fungal pathogen of grapevine trunk disease around the world, and extensive research has been done on the disease; Diaporthe dieback. In China, *Diaporthe eres* was proved to be the most commonly isolated species in both

studies in 2015 and 2019 (Dissanayake et al., 2015a; Manawasinghe et al., 2019). Thus, the result from the present study also accepts this conclusion. Black foot disease is a devastating grapevine trunk disease caused by *Cylindrocarpon*-like fungi, which are common in nurseries and young plantations worldwide (Lawrence et al., 2019). In this study, six *Cylindrocarpon*-like fungal species, belonging to *Dactylonectria*, *Ilyonectria* and *Cylindrocladiella* were identified. Ye et al. (2021a) reported *D. alcacerensis*, *D. torresensis*, *D. macrodidyma* for the first time in China, and *D. novozelandica* has been recently proven to be grapevine pathogens (Tan et al., 2022). *Ilyonectria liriodendri* and *Cylindrocladiella viticola* are common pathogens in many countries, however they have never been reported in China from grapevine previously.

Botryosphaeriaceae encompasses diverse members of pathogens and are regarded as plant opportunistic fungal pathogens (Phillips et al., 2013; Chethana et al., 2016). These species are important pathogens on grapevine and are associated with a series of diseases including leaf spots, shoot dieback, perennial cankers, vascular discoloration and fruit rots (Úrbez-Torres, 2011). More than 20 species from Botryosphaeriaceae have been reported to cause Botryosphaeria dieback (Gramaje et al., 2018). Most Botryosphaeriaceae species isolated and identified in this study have been proven to cause Botryosphaeria dieback in China (Yan et al., 2013; Jayawardena et al., 2018; Wu et al., 2021). *Phaeobotryon rhois* which belongs to Botryosphaeriaceae, has not reported for causing diseases on grapevine. However, this species has been reported to cause branch wilt of *Ulmus pumila* L. and *Rubus crataegifolius* Bge in China (Liu et al., 2020; Zhu et al., 2020).

In addition, two *Phaeoacremonium iranianum* isolates were identified in this study. *Phaeoacremonium* has been reported worldwide for its association with Esca disease, which has become a major concern in all grape-growing countries during the past decades (Hofstetter et al., 2012). However, *Phaeoacremonium iranianum* has not been reported from grapevine in China before. Therefore, based on our collection, this species might be also Esca pathogen which required further confirmation with pathogenicity tests. Pestalotiopsis-like fungi can also cause grapevine trunk disease showing wedge-shaped cankers and bleached canes with slitting (Jayawardena et al., 2015), while species in the current study (*P. kenyana*, *P. rhodomyrtus* and *P. adusta*) have not been reported from grapevine in the world yet.

In addition to the grapevine trunk diseases, several species isolated from this study are associated with grapevines causing different diseases. *Coniella* and *Colletotrichum* are commonly known as grape-fruit pathogens. *Coniella vitis* first reported in 2017 as a novel species causing white rot in China (Chethana et al., 2017). *Colletotrichum* species, including *C. nymphaeae* and *C. viniferum* reported in this study, were reported to cause anthracnose with symptoms of fruit ripe rot and twig dieback (Yan et al., 2015; Liu et al., 2016). *Pestalotiopsis*-like species were also reported to cause fruit rot (Jayawardena et al., 2015). This may prove that the grapevine pathogens not only exist in the main tissues, but also infect other tissues. The roles of these pathogenic taxa on the trunk and root need to be further explored.

Fusarium-like genera comprise many taxa with economic importance, acting as pathogens, saprophytes or endophytes, as well as secondary pathogens (Leslie & Summerell, 2006; Crous et al., 2021). In 1995, *Fusarium oxysporum* was isolated from the roots of declining grapevine in Australia (Highet & Nair, 1995). Recent studies have also identified *Fusarium* species in grapevine nurseries and vineyards. Several *Fusarium* species have been reported as pathogens on grapevines, indicating that *Fusarium* can transfer to being weak or latent pathogens in grapevines from endophytic phases under favourable conditions (Úrbez-Torres et al., 2020). In this study, nine *Fusarium*-like species were identified, belonging to *Fusarium*, *Neocosmospora* and *Bisifusarium*. Except for *F. oxysporum*, other species have not been reported on grapevines in China (Jayawardena et al., 2018). However, the exact life mode and pathogenicity mechanisms of these isolates need to be further explored.

According to the above results, theses isolated fungal taxa may have different effects on the grapevine. Grapevine wood is a highly competitive habitat, with the simultaneous presence of plant pathogens and beneficial, potentially protective fungi (Kraus et al., 2019). Pathogenic fungi can change the biotrophic mode from pathogenic to saprotrophic, and become active again once the conditions become favourable, being the primary source of inoculant in a vineyard (Jayawardena et al., 2018). On the other hand, the effect of endophytes on plant disease can be antagonistic, and fungal endophytes diversity can influence the severity of plant diseases (Busby et al., 2016). Thus, the roles of saprotroph, endophyte, and pathogen need to be clarified by pathogenicity tests, and interactions between different communities need to be explored.

Rather than focus on one of the grapevine trunk diseases, our study conducted an extensive survey on the diverse fungi that covered the main grapevine trunk disease symptoms in China in recent years. This results not only reported new records on the grapevine but also expanded the isolation source of some species compared to previous studies in China (Yan et al., 2013; Ye et al., 2021a, 2021b). For example, *Botryosphaeria dothidea*, *Dactylonectria novozelandica*, *D. macrodidyma*, *Lasiodiplodia pseudotheobromae* and *Neofusicoccum parvum* were first recorded in Yunnan Province; *Alternaria alternata*, *Cladosporium tenuissimum*, *Colletotrichum nymphaeae*, *C. viniferum* and *Diaporthe unshiuensis* were first reported in Fujian Province; *Dactylonectria alcacerensis* and *D. macrodidyma* were first recorded in Beijing; *Dactylonectria alcacerensis* and *L. pseudotheobromae* were first recorded in Hebei Province; and *D. torresensis* was first recorded in Ningxia Province. This may be because of the increase of investigated regions, the transfer of fungi between hosts, as well as the transportation of seedlings carrying pathogens (Manawasinghe et al., 2018). In addition to the parts of sampling and collection site, their distribution, diversity and proportion of fungal taxa may be influenced by climate, environment, and management practices (Mondello et al., 2018). The previous research on the geographical distribution of Botryosphaeriaceae species causing grapevine dieback in China showed that *L. theobromae* was isolated primarily from subtropical monsoon climate regions of China, *Diplodia seriata* isolated primarily from temperate monsoon climate regions, *Neofusicoccum parvum* primarily isolated from central and south China, and *Botryosphaeria dothidea* was isolated from north to south throughout China (Yan et al., 2013). Our results also support these conclusions. Furthermore, these infections may occur through the wounds made during the grapevine planting, or the propagation process, including pruning, retraining, trimming, and de-suckering (Gramaje et al., 2018; Berlanas et al., 2020). To determine the occurrence dynamics of the fungi associated with grapevine trunk disease throughout China, the field of investigation should further enlarge, and more samples should be collected.

The grapevine trunk diseases in fields are usually a mix of different disease types caused by various pathogens rather than a single one. Due to the complexity of the disease and the lack of the most effective chemical products, the management of grapevine trunk diseases is difficult (Gramaje et al., 2018). For pathogens inhabiting vascular tissues, chemical sprays and dips used for controlling surface pathogens could

hardly penetrate dormant grapevine cuttings sufficiently (Waite & May, 2005). It is well-accepted that grapevine trunk diseases should be managed by an integrated disease management strategy, including biological control (Gramaje et al., 2018). *Trichoderma* species are capable of efficient utilization of neighbouring substrates, as well as competitive aggression by secreting antibiotic metabolites and enzymes. With their antagonistic ability, some species have successfully been used in the commercial biological control of fungal pathogens (Schuster & Schmoll, 2010; Lopes et al., 2012). The control efficiency of *Trichoderma* on fungi associated with grapevine trunk disease was demonstrated in the field and nurseries (Kraus et al., 2019). For example, *T. atroviride* and *T. harzianum* applied to the control of Esca caused by *Phaeomoniella chlamydospora* and *Phaeoacremonium* species in nurseries (Pertot et al., 2016; Marco & Osti, 2007), and *T. harzianum* was applied to prevent infection of *Eutypa lata* on grapevine pruning wounds (John et al., 2005). In the current study, three *Trichoderma* species were identified. *Trichoderma virens* is one of the most common biological control agents (BCAs). It has excellent control compared to other fungicides against *Pythium ultimum* infecting cotton and *Rhizoctonia solani* infecting tobacco (Benítez et al., 2004) and was observed to have mediate resistance in tomatoes against Fusarium wilt (Jogaiah et al., 2018). *Trichoderma asperellum* also showed inhibitory activities against *R. solani* on maize and rice, *Sclerotium oryzae* on rice, *A. alternata* on apple, as well as *C. musae* and *F. oxysporum* causing banana fruit rot (Adebesin et al., 2009, Hariharan et al., 2022). Galarza et al. (2015) have assessed the antagonistic activities of *Trichoderma* species against the phytopathogenic fungi from Ecuador and Japan. They have found *T. virens* and *T. asperellum* showing strong inhibitory activities against some *Fusarium*, *Moniliophthora* and *Rosellinia* species (Galarza et al., 2015). *Trichoderma guizhouense* showed a significant effect on root rot of *Vigna unguiculata* caused by *R. solani* (Wang & Zhuang, 2019). *Trichoderma guizhouense* isolates from Italy were evaluated for their potential activity as BCAs in vitro against the canker-causing fungi *Diplodia seriata*, *Eutypa lata* and *Neofusicoccum parvum* (Úrbez-Torres et al., 2020). Interestingly, the isolation results showed that *Cylindrocarpon*-like fungi were sometimes isolated simultaneously with *Trichoderma* isolates. The three *Trichoderma* species in this study, namely *Trichoderma guizhouense*, *T. virens* and *T. asperellum*, may also have the promising ability to become as biocontrol agents for

grapevine trunk diseases. According to the former study by Munkvold and Marois (1993), *Fusarium* and *Cladosporium* showing the antagonistic effect on grapevine trunk disease pathogens. However, antagonistic activities and biocontrol potential of *Alternaria*, *Cladosporium* and *Fusarium* species reported in this study need to be further studied.

In conclusion, this study provides new insights into the diversity of fungi on symptomatic grapevine trunks and roots, including typical grapevine trunk disease agents, a pathogen associated with other diseases, endophytes with biocontrol potential and others. The relevant results reveal common fungal species associated with grapevine trunk diseases in China and establish the basis for research on the occurrence and management strategies of the grapevine trunk diseases worldwide.
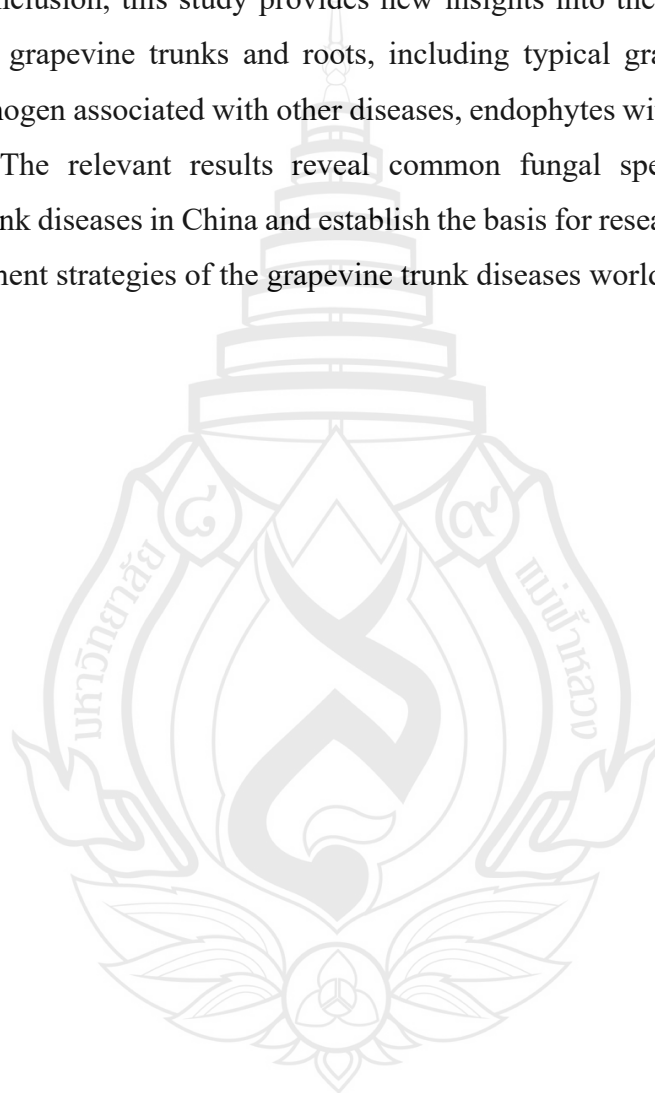
CHAPTER 5

IDENTIFICATION ON FUNGAL SPECIES ASSOCIATED WITH BLUEBERRY DISEASE

5.1 A Review of Blueberry Fungal Diseases

5.1.1 The Occurrence of Blueberry Fungal Diseases

Fungal diseases are main threat on blueberry from growing period to shelf life, which cause considerable production and economic losses worldwide (Malarczyk et al., 2019). According to the infected organ and symptoms, fungal diseases are mainly divided into four types including fruit rot, stem blight, leaf spot and root rot, and there are also some minor diseases such as powdery mildew and sooty blotch (Polashock, 2017). Compared with the main fruit crops, the cultivation history of blueberry is relatively short (Janick, 2005). Most researches on blueberry diseases were concentrated in the past two decades, and especially a large number of pathogens were reported in the recent five years. The range of blueberry pathogens is extensive, despite many studies have been conducted on blueberry diseases, many fungal pathogens affecting blueberries may still be undiscovered, and the knowledge on blueberry diseases is still building up.

5.1.2 Blueberry Fruit Rot

Blueberry fruits are perishable as they are susceptible to mechanical damage and infectious diseases for their delicate cell walls, proximity to moist soil, and exposure to rainfall (Malarczyk et al., 2019; Duan et al., 2022). Fruit rot diseases caused by fungi, especially Botrytis fruit rot and anthracnose fruit rot, significantly influence the yield and fruit quality pre- and post-harvest (Neugebauer et al., 2024). *Botrytis cinerea* is the predominant causal agent of Botrytis fruit rot, causing blights of flowers, leaves, twigs and decay of fruits, also known as grey mould (Rivera et al., 2013; Bell et al., 2021). Alongside *B. cinerea*, *B. pseudocinerea* and *B. californica* have also been reported to cause grey mould on blueberries (Saito et al., 2014; Li et al., 2023). Anthracnose fruit rot is caused by *Colletotrichum* spp., mainly *C. acutatum*, *C. gloeosporioides* and *C. fioriniae* (Wharton et

al., 2008; Eaton et al., 2021). These pathogens can infect blueberries from flowering to harvest and can also be present latent infection and show symptoms in postharvest period. Diseased fruits show sunken lesions with pink or salmon conidial masses (Bell et al., 2021). Anthracnose fruit rot has been reported to cause 10–20% yield loss, and the loss caused by Botrytis fruit rot can reach 30%–40% (Polashock et al., 2017). Another fruit rot, caused by *Alternaria* spp., also named Alternaria fruit rot, commonly occurs as an important post-harvest disease during transport and storage, characterized by sunken lesions with white to olivaceous mycelium (Neugebauer et al., 2024; Bell et al., 2021). In addition, *Monilinia vaccinii-corymbosi* and *Exobasidium maculosum* infect young fruits in the early season, causing mummy fruit and fruit spots, respectively (Ingram et al., 2019; Alvarez Osorio et al., 2022). And there are also minor blueberry fruit diseases without specific names, such as the fruit rots caused by *Diaporthe vaccinii*, *Pestalotia vaccinii*, *Phyllosticta vaccinii* and some yeast species (Neugebauer et al., 2024). Although diseases caused by specific pathogens have different names, a single plant can be infected by multiple pathogens. Since most fruit diseases lead to rotting fruit, they are collectively referred to as fruit rot disease (Neugebauer et al., 2024; Polashock et al., 2017). However, the use of specific names, like Botrytis fruit rot, Alternaria fruit rot, or anthracnose rot, helps in identifying the most effective management strategies against each particular fungal pathogen.

5.1.3 Blueberry Leaf Spot

Blueberry leaf diseases showed different symptom types including leaf spot, leaf blight, leaf rust, anthracnose and powdery mildew (Lai et al., 2022; Phillips et al., 2022). Typical leaf spot present round to irregular lesions with dark purple to brown border on leaf surface, when visible bright yellow-orange pustules of spores produced on the underside of leaves, the symptoms named leaf rust, while leaf blight refers to the shrivel, curl, or fall off of the leaves (Lai et al., 2022; Phillips et al., 2022). And anthracnose and powdery mildew refer in particular to leaf diseases caused by *Colletotrichum* and *Erysiphe* species respectively (Xu et al., 2013; Bradshaw et al., 2025). As the most common leaf disease type caused by various pathogens, leaf spot is emphasized in this study. Septoria leaf spot was reported on highbush blueberry in USA in the early stage, caused by *Septoria albopunctata* (Alfieri, 1991). The disease was not only causing premature defoliation, but also reductions in photosynthesis of leaves (Roloff et al., 2004). Subsequently the dynamics of Septoria leaf spot was studied on

rabbiteye blueberry, which showed that the occurrence of the disease started between late April and mid-June, and the severity increased severity until late September (Ojiambo et al., 2007). *Alternaria alternata* (=*Alternaria tenuissima*) was also reported to cause blueberry leaf spot in Argentina and South Korea (Wright et al., 2004; Kwon et al., 2014). In addition, *Calonectria*, *Diaporthe*, *Nigrospora*, *Sphaerulina* and *Exobasidium* were also once recorded (Wright et al., 2008; Ingram et al., 2019; Ali et al., 2021; Chen et al., 2023; Lai et al., 2023). In China, *Pestalotiopsis* species were more frequently reported on blueberry leaves, including *Neopestalotiopsis clavispora*, *Pestalotiopais adusta*, *P. chamaeropis*, *P. photiniae* and *P. trachicarpicola* (Luan et al., 2007; Chen et al., 2010; Zheng et al., 2023). The occurrence of leaf spot is often present as compound symptom together with fruit and stem disease, such as leaf spot, twig blight, and fruit rot of blueberry caused by *Alternaria alternata* (=*Alternaria tenuissima*) (Wright et al., 2004), leaf and fruit spot caused by *Exobasidium maculosum* (Ingram et al., 2019), as well as leaf spot and stem blight on blueberry caused by *Calonectria pseudoreteaudii* (Chen et al., 2023).

5.1.4 Blueberry Stem Blight

Stem blight is one of the most common and severe disease among blueberry diseases, resulting in reduced production and economic losses (Martino et al., 2024). In New Zealand, the disease incidence has reached 18%, causing $500,000 in annual losses (Sammonds et al., 2009); in Chile, the incidence rate ranges from 15 to 45% (Espinoza et al., 2009). As the top producer of blueberries, China also suffered 10% to 25% of crop damage from the disease (Zhao et al., 2019). Stem blight is caused by several fungal pathogens that infect plants through wounds or natural openings, leading to vascular damage, wood discoloration, and even the death of the plant (Martino et al., 2024; Ru et al., 2023). As a general term, stem blight is also known as stem canker or dieback. Typical symptoms of the disease are reddish-brown to grey-brown lesions on stems, shoots, or twigs (Hilário et al., 2021; Zhao et al., 2022; Zheng et al., 2023). *Pestalotiopsis*-like (*Pestalotiopsis* and *Neopestalotiopsis*) species, *Diaporthe* and many genera of Botryosphaeriaceae (*Botryosphaeria*, *Neofusicoccum* and *Lasiodiplodia*) are major causal agents of stem blight worldwide (Ru et al., 2023; Hilário et al., 2021; Zheng et al., 2023). Canker or dieback usually refer to diseases caused by Botryosphaeriaceae species on other hosts such as grapevine (Úrbez-Torres et al., 2009;

Yan et al., 2013), while on blueberry, though Botryosphaeriaceae species were also reported to cause dieback and cankers (Castillo et al., 2013; Tennakoon et al., 2018), these disease names are not strictly related to specific pathogens, but also sometimes related to *Diaporthe* and *Pestalotiopsis* species (Elfar et al., 2013; Zheng et al., 2023; Blagojević et al., 2024). These may because of the symptoms caused by different pathogens are difficult to distinguish. Additionally, some disease names are more emphasize on specific parts like twig blight or branch blight (Wright et al., 2014; Chen et al., 2016). For stem blight is the most commonly used name, here these names are collectively called stem blight. In addition to above fungal groups, *Calonectria*, *Colletotrichum*, *Nigrospora* and *Sphaerulina* species have been reported to cause stem blight on blueberries (Wright et al., 2008; Xu et al., 2013; Ali et al., 2021; Chen et al., 2023). The diversity of pathogens contributing to stem blight highlights its nature as a disease complex, making it difficult to distinguish based on field symptoms.

5.1.5 Blueberry Root Rot

Blueberry root rots are caused by fungi (Ascomycota and Basidiomycota), and fungus-like organisms (Oomycota). *Phytophthora cinnamomi*, one of the top 10 oomycete pathogens infecting huge number of plant hosts, is an important pathogen causing Phytophthora root rot on blueberry (Kamoun et al., 2015; Huarhua et al., 2018). Records of fungal pathogens are more scattered, including *Calonectria ilicicola* in China (Fei et al., 2018), *Fusarium commune* in China (Li et al., 2023), *Fusarium proliferatum* in Argentina (Pérez et al., 2011), *Fusarium oxysporium* in China (Liu et al., 2014), *Neocosmospora solani* in Argentina (Pérez et al., 2007), *Neopestalotiopsis clavispora* in China (Xue et al., 2018) and *Armillaria* species in Italy (Prodorutti et al., 2009). Root rots usually present symptoms of leaf chlorosis, dark brown to black rot of the root and stem base, and the withered and died of the whole plant in severe case (Fei et al., 2018; Huarhua et al., 2018; Li et al., 2023). Compared with fruit, stem and leaf diseases, records on blueberry root rots are relatively fewer, while the infection on roots usually cause the symptoms of the whole plants and harder to detected from overground part. With regard to the profound impact of root disease on plant health, and more root pathogens recorded in China than other countries, more attention should be paid on root rot disease.

5.1.6 Common Fungal Pathogens on Blueberry

      5.1.6.1 *Neopestalotiopsis* and *Pestalotiopsis* species. Among multiple pathogens, members of *Pestalotiopsis sensu lato* (pestalotioid fungi) are distributed throughout temperate and tropical regions (Maharachchikumbura et al., 2014; Liu et al., 2019). *Pestalotiopsis* and *Neopestalotiopsis* are the main pathogenic genera causing twig blight, stem cankers, and dieback on blueberry plants, as well as leaf diseases (Santos et al., 2022). Many studies documented the presence of pestalotioid fungi associated with blueberries disease in Argentina (leaf spots and branch cankers) (Fernández et al., 2015), Brazil (leaf spot) (Araujo et al., 2023), Chile (canker and twig Dieback) (Espinoza et al., 2008), China (leaf spot, root rot) (Luan et al., 2008; Xue et al., 2018), Czech Republic (stem blight and dieback) (Spetik et al., 2023), Korea (twig dieback) (Lee et al., 2019), Mexico (leaf rust) (Rebollar-Alviter et al., 2011), Peru (stem blight and dieback) (Rodríguez-Gálvez et al., 2020), Portugal (twig blight and dieback) (Santos et al., 2022), Spain (canker and twig dieback) (Borrero et al., 2018), Turkey (leaf spot and branch blight) (Dil et al., 2013) and Uruguay (twig and branch dieback) (González et al., 2012). And the most-reported pestalotioid species on blueberry plants are *Neopestalotiopsis clavispora* (syn. *Pestalotiopsis clavispora*) (González et al., 2012; Borrero et al., 2018; Xue et al., 2018; Lee et al., 2019), *N. rosae* (Rodríguez-Gálvez et al., 2020; Santos et al., 2022), *Pestalotiopsis microspora* (Jin et al., 2021) and *P. neglecta* (Espinoza et al., 2008). In China, *P. clavispora* has been reported to cause leaf spot, twig blight, stem canker and root rot (Luan et al., 2008; Chen et al., 2016; Xue et al., 2018; Zheng et al., 2023). In addition, *P. trachicarpicola*, *P. chamaeropis*, *P. adusta* and *P. photiniae* were also reported to cause stem canker and leaf spot (Chen et al., 2010; Zheng et al., 2023).

      5.1.6.2 Botryosphaeriaceae species. Botryosphaeriaceae is also a dominant pathogen causing stem disease in blueberries (Scarlett et al., 2019). A large number of *Botryosphaeriaceae* species have been found to associate with stem blight and cankers of blueberry plants in Australia (stem blight and dieback) (Scarlett et al., 2019), Chile (stem canker and dieback) (Espinoza et al., 2009), China (stem blight) (Xu et al., 2015), Korea (bark dieback) (Choi, 2011), Mexico (stem blight and dieback) (Boyzo-Marin et al., 2016), New Zealand (dieback) (Tennakoon et al., 2018), Peru (stem blight and dieback) (Rodríguez-Gálvez et al., 2020), Portugal (stem blight and dieback) (Hilário

et al., 2020), Spain (stem canker and dieback) (Castillo et al., 2013) and the United States (stem blight) (Wright & Harmon, 2010). Botryosphaeria stem blight is the most destructive disease affecting blueberry production worldwide, caused by more than 20 species in the genera *Botryosphaeria*, *Neofusicoccum*, *Lasiodiplodia* and *Macrophomina* (González et al., 2012; Zhao et al., 2019; Wang et al., 2021; Ru et al., 2023). To date, *Botryosphaeria dothidea*, *Neofusicoccum parvum*, *N. vaccinii*, *N. vitifusiforme*, *Lasiodiplodia clavispora*, *L. fujianensis*, *L. henanica*, *L. nanpingensis*, *L. paraphysoides*, *L. pseudotheobromae*, *L. theobromae*, *L. vaccinii*, *L. chinensis* and *Macrophomina vaccinii* have been reported to cause infections of blueberries in China (Kong et al., 2010; Yu et al., 2012b; Xu et al., 2015; Zhao et al., 2019, 2022; Wang et al., 2021).

5.1.6.3 *Diaporthe* species. *Diaporthe* is also a causal agent frequently reported, causing stem blight (Hilário et al., 2021), postharvest rot (Yu et al., 2018) and leaf spot (Lai et al., 2023). *Diaporthe eres* (=*Diaporthe vaccinii*) which is considered a concern to blueberry production worldwide, has been widely reported in South America, North America, Europe and Asia (Hilário et al., 2021). In addition, *Diaporthe ambigua*, *D. amygdali*, *D. crousii*, *D. foeniculina*, *D. hybrida*, *D. leucospermi*, *D. passiflorae* (=*D. malorum*) and *D. rudis* (=*D. australafricana*) were reported to cause stem diseases in Chile, Poland, Portugal, Serbia (Elfar et al., 2013; Hilário et al., 2021; Michalecka et al., 2023; Blagojević et al., 2024). Hilário et al. (2022) sequenced and analysed the genomes of *D. amygdali* (CAA958) and *D. eres* (CBS 160.32), identifying cellular transporters associated with the transport of toxins, ions, sugars, and effectors, as well as genes linked to pathogenicity in genomes of the both species. In China, leaf spot disease caused by *Diaporthe phoenicicola* (Lai et al., 2023), postharvest rot by *Diaporthe nobilis* (Yu et al., 2018) and stem canker by *Diaporthe sojae* (Li et al., 2023d) have been reported.

5.1.6.4 *Fusarium*. Researches on *Fusarium* from blueberry is relatively limited. The genus usually as the causal agent of wilt, root rot and fruit rot disease. *Neocosmospora solani* and *F. proliferatum* were reported to cause root rot of blueberry in Argentina (Pérez et al., 2007; Pérez et al., 2011), *F. acuminatum* was reported to cause stem blight in Argentina and postharvest fruit rot in China respectively (Wright et al., 2014; Wang et al., 2016). Fusarium wilt caused by *F. oxysporum* was reported in

China and Chile (Liu et al., 2014; Moya-Elizondo et al., 2019). Additionally, *Fusarium commune* was reported to cause blueberry root rot in China (Li et al., 2023).

       5.1.6.5 Other pathogens. In addition to the above dominant pathogens, *Botrytis*, *Colletotrichum* and *Alternaria* species are also common pathogens (Wright et al., 2004; Kwon et al., 2011; Liu et al., 2020). And some other genera such as *Calonectria*, *Nigrospora*, *Septoria*, *Truncatella* and *Thekopsora*, were also found to be associated with blueberry diseases (Roloff et al., 2004; Espinoza et al., 2008; Rebollar-Alviter et al., 2011; Zhang et al., 2019b; Chen et al., 2023b).

       5.1.6.6 Blueberry pathogens in China. Currently forty-seven species belonging to ten family have been reported to associated with blueberry disease in China. The information of the species including blueberry species, associated diseases, locality, and identification methods are provided in table 5.1. The summary shows that stem blight (canker/dieback) is most common reported in China. *Botryosphaeria dothidea* is the most widely distributed (eight provinces), followed by *Neofusicoccum parvum* (six provinces) and *Neopestalotiopsis clavispora* (five provinces). The occurrence of other species are only in one to three regions. In addition, though the phylogenetic analyses have become widespread, fungal identification in many studies still based on morphology and single gene alignment. Therefore, to get more knowledge on disease diagnosis and management, more researches are necessary on the identification and distribution of fungi associated with blueberry diseases.

Table 5.1 Recorded fungal species associated with blueberry disease in China

Family	Species	Host species	Associated disease	Locality	Identification method	Reference
Apiosporaceae	*Nigrospora oryzae*	*Vaccinium corymbosum*	Leaf spot	Shanghai	Morphology+ sequence BLAST	Zhang et al. (2019)
Botryosphaeriaceae	*Botryosphaeria dolichospermatii*	*Vaccinium uliginosum*	Stem canker	Fujian	Morphology + multi-locus phylogeny	Chu et al. (2021)
	Botryosphaeria dothidea	*Vaccinium corymbosum*	Stem blight and dieback	Fujian, Jiangsu, Liaoning, Shandong, Shanghai, Sichuan, Yunnan, Zhejiang	Morphology+ sequence BLAST/ multi-locus phylogeny	Yu et al. (2012), Xu et al. (2015)
	Botryosphaeria fujianensis	*Vaccinium uliginosum*	Stem canker	Fujian	Morphology + multi-locus phylogeny	Chu et al. (2021)
	Lasiodiplodia chinensis	*Vaccinium corymbosum*	Twig blight	Shandong	Morphology + multi-locus phylogeny	Wang et al. (2016)
	Lasiodiplodia clavispora	*Vaccinium uliginosum*	Stem blight (unverified)	Fujian	Morphology + multi-locus phylogeny	Wang et al. (2021)
	Lasiodiplodia fujianensis	*Vaccinium uliginosum*	Stem blight (unverified)	Fujian	Morphology + multi-locus phylogeny	Wang et al. (2021)
	Lasiodiplodia henanica	*Vaccinium uliginosum*	Stem blight (unverified)	Shandong	Morphology + multi-locus phylogeny	Wang et al. (2021)
	Lasiodiplodia nanpingensis	*Vaccinium uliginosum*	Stem blight (unverified)	Fujian	Morphology + multi-locus phylogeny	Wang et al. (2021)
	Lasiodiplodia paraphysoides	*Vaccinium uliginosum*	Stem blight (unverified)	Shandong	Morphology + multi-locus phylogeny	Wang et al. (2021)
	Lasiodiplodia pseudot heobromae	*Vaccinium corymbosum*	Twig blight	Shandong	Morphology + multi-locus phylogeny	Wang et al. (2016)

Table 5.1 (continued)

Family	Species	Host species	Associated disease	Locality	Identification method	Reference
	Lasiodiplodia theobromae	*Vaccinium corymbosum*	Stem blight	Zhejiang, Sichuan	Morphology + multi-locus phylogeny	Xu et al. (2015)
	Lasiodiplodia vaccinii	*Vaccinium corymbosum*	Stem blight	Beijing	Morphology + multi-locus phylogeny	Zhao et al. (2019a)
	Macrophomina vaccinii	*Vaccinium corymbosum*	Stem blight	Fujian	Morphology + multi-locus phylogeny	Zhao et al. (2019b)
	Neofusicoccum parvum	*Vaccinium corymbosum,* *V. virgatum*	Stem blight and dieback	Fujian, Guizhou, Shanghai, Sichuan, Yunnan, Zhejiang	Morphology + multi-locus phylogeny	Xu et al. (2015), Zhao et al. (2022)
	Neofusicoccum vaccinii	*Vaccinium corymbosum* and *V. virgatum*	Stem blight and dieback	Fujian, Guizhou, Shandong	Morphology + multi-locus phylogeny	Zhao et al. (2022)
	Neofusicoccum vitifusiforme	*Vaccinium corymbosum*	Bud and branch blight	Yunnan	Morphology + sequence BLAST	Kong et al. (2010)
Diaporthaceae	*Diaporthe eres* (=*D. nobilis*, *D. vaccinii*)	*Vaccinium* sp.	Bud blight, stem blight, twig blight, postharvest rot	Guizhou, Liaoning, Shandong	Morphology+ sequence BLAST/ single gene phylogeny/ multi-locus phylogeny	Yue et al. (2013), Yan et al. (2015), Zhang et al. (2016), Yu et al. (2018)
	Diaporthe hongkongensis (=*D. australiana*)	*Vaccinium* sp.	Stem canker, branch blight	Fujian, Zhejiang	Morphology+ multi-locus phylogeny	Li et al. (2017a), Zhang et al. (2023)
	Diaporthe phaseolorum	*Vaccinium* sp.	Stem canker	Fujian, Heilongjiang, Liaoning	Morphology+ multi-locus phylogeny	Li et al. (2017b)

Table 5.1 (continued)

Family	Species	Host species	Associated disease	Locality	Identification method	Reference
	Diaporthe phoenicicola	*Vaccinium virgatum*	Leaf spot	Jiangxi	Morphology+ multi-locus phylogeny	Lai et al. (2023)
	Diaporthe sojae	*Vaccinium corymbosum*	Stem canker	Anhui	Morphology+ multi-locus phylogeny	Li et al. (2023)
Nectriaceae	*Calonectria colhounii* (=*Cylindrocladium colhounii*)	*Vaccinium corymbosum*	Leaf spot	Liaoning, Yunnan	Morphology+ sequence BLAST/ multi-locus phylogeny	Luan et al. (2007), Yang et al. (2022)
	Calonectria ilicicola	*Vaccinium* sp.	Root rot	Yunnan	Morphology+ multi-locus phylogeny	Fei et al. (2018)
	Calonectria pseudoreteaudii	*Vaccinium corymbosum*	Stem blight	Guangdong	Morphology + multi-locus phylogeny	Chen et al. (2023)
	Fusarium commune	*Vaccinium uliginosum*	Root rot	Guizhou	Morphology+ sequence BLAST	Li et al. (2023)
	Fusarium oxysporum	*Vaccinium corymbosum*	Wilt (crown)	Zhejiang	Morphology+ sequence BLAST (ITS)	Liu et al. (2014)
Glomerellaceae	*Colletotrichum acutatum*	*Vaccinium corymbosum*	Anthracnose (stem)	Liaoning	Morphology + sequence BLAST	Xu et al. (2013)
	Colletotrichum aenigma	*Vaccinium corymbosum*	Anthracnose (leaf)	Jiangsu	Morphology+ multi-locus phylogeny	Feng et al. (2024)
	Colletotrichum fructicola	*Vaccinium corymbosum*	Anthracnose (leaf)	Jiangsu, Sichuan	Morphology+ multi-locus phylogeny	Liu et al. (2020), Feng et al. (2024)
	Colletotrichum gloeosporioides	*Vaccinium* sp.	Anthracnose (stem and leaf)	Liaoning	Morphology + sequence BLAST	Xu et al. (2013)

Table 5.1 (continued)

Family	Species	Host species	Associated disease	Locality	Identification method	Reference
	Colletotrichum kahawae	*Vaccinium corymbosum*	Anthracnose	Sichuan	Morphology+ multi-locus phylogeny	Liu et al. (2020)
	Colletotrichum karstii	*Vaccinium corymbosum*	Anthracnose	Sichuan	Morphology+ multi-locus phylogeny	Liu et al. (2020)
	Colletotrichum nymphaeae	*Vaccinium corymbosum*	Anthracnose	Sichuan	Morphology+ multi-locus phylogeny	Liu et al. (2020)
	Colletotrichum siamense	*Vaccinium corymbosum*	Anthracnose	Sichuan	Morphology+ multi-locus phylogeny	Liu et al. (2020)
	Colletotrichum sichuaninese	*Vaccinium corymbosum*	Anthracnose	Sichuan	Morphology+ multi-locus phylogeny	Liu et al. (2020)
Peronosporaceae	*Phytophthora cinnamomi*	*Vaccinium corymbosum*	Root and stem rot	Fujian	Morphology + sequence BLAST	Lan et al. (2016)
Pleosporaceae	*Alternaria alternata* (=*A. tenuissima*)	*Vaccinium corymbosum*	Leaf spot	Guizhou, Liaoning, Shandong, Yunnan	Morphology + sequence BLAST	Luan et al. (2007), Yan et al. (2014), Yu et al. (2015), Luo et al. (2023)
Schizoparmaceae	*Coniella castaneicola*	*Vaccinium virgatum*	Leaf blight	Jiangxi	Morphology + sequence BLAST	Lai et al. (2022)
Sclerotiniaceae	*Botrytis californica*	*Vaccinium corymbosum*	Grey mould (fruit)	Jiangsu	Morphology + multi-locus phylogeny	Li et al. (2023)
	Botrytis cinerea	*Vaccinium* sp.	Grey mould (fruit, leaf)	Liaoning	Morphology	Dai et al. (2011)
Sporocadaceae	*Neopestalotiopsis chrysea*	*Vaccinium virgatum*	Twig blight	Fujian	Morphology + multi-locus phylogeny	Shi et al. (2017)

Table 5.1 (continued)

Family	Species	Host species	Associated disease	Locality	Identification method	Reference
	Neopestalotiopsis clavispora (=*Pestalotiopsis clavispora*)	*Vaccinium corymbosum*, *Vaccinium virgatum*	Leaf spot/ stem canker/ twig dieback/ root rot	Anhui, Guizhou, Liaoning, Shandong, Sichuan	Morphology + sequence BLAST/ single gene phylogeny/ multi-locus phylogeny	Luan et al. (2008), Zhao et al. (2014), Chen et al. (2016), Xue et al. (2018), Chen et al. (2019), Zheng et al. (2023)
	Pestalotiopsis adusta	*Vaccinium corymbosum*	Stem canker	Sichuan	Morphology + multi-locus phylogeny	Zheng et al. (2023)
	Pestalotiopsis chamaeropis	*Vaccinium corymbosum*	Leaf spots and stem canker	Sichuan	Morphology + multi-locus phylogeny	Zheng et al. (2023)
	Pestalotiopsis photiniae	*Vaccinium angustifolium*	Leaf spot	Jilin	Morphology + sequence BLAST (ITS)	Chen et al. (2010)
	Pestalotiopsis trachicarpicola	*Vaccinium corymbosum*	Leaf spot, stem canker	Guangxi, Sichuan	Morphology + multi-locus phylogeny	Shi et al. (2017), Zheng et al. (2023)

5.2 Characterization of Fungal Pathogens Causing Blueberry Fruit Rot Disease in China

5.2.1 Disease Symptoms and Fungal Isolation

Fruit rot samples were collected from blueberry orchards in Fujian and Guizhou Provinces, China. Symptoms appeared during the green fruit stage, showing the gradual progression of decay. Diseased fruits dry-up, shrink, rot, and sometimes exude fluid. Stems turned brown, dry-out, and develop mould (Figure 5.1). Disease incidence was 2%-3%.

Sixteen isolates were generated from six samples, and were identified as seven species based on morphological characters and phylogenetic analyses. They include *Botryosphaeria dothidea*, *Botrytis cinerea*, *Cladosporium guizhouense*, *Colletotrichum fioriniae*, *Diaporthe anacardii*, *Fusarium annulatum* and *Neopestalotiopsis surinamensis*.
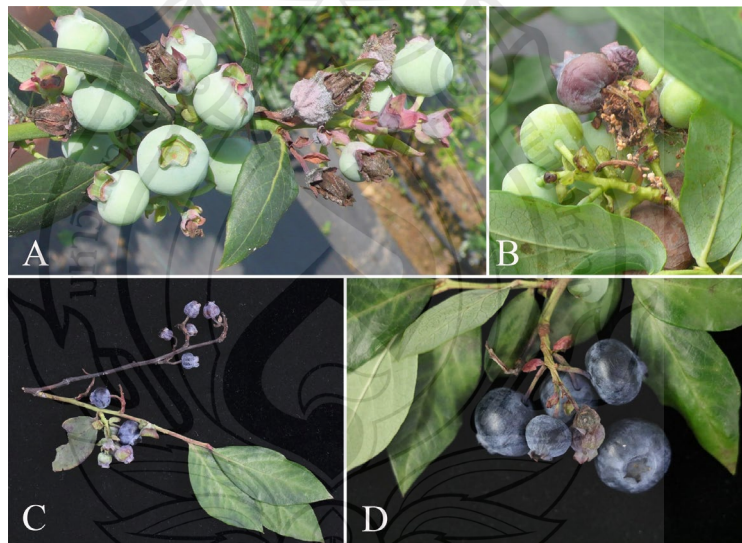
Figure 5.1 Symptoms of the blueberry fruit rot

Figure 5.1 A–B Field symptoms of blueberry fruit rot. C Died twigs with shrunken fruits. D Shrivelled fruit with mould.

5.2.2 Taxonomy

Botryosphaeria dothidea (Moug.: Fr.) Ces. & De Not., Comm. Soc. crittog. Ital. 1 (fasc. 4): 212 (1863).

Index Fungorum: IF 183247; Facesoffungi Number: FoF 03512.

Classification: Botryosphaeriaceae, Botryosphaeriales, Dothideomycetes, Ascomycota, Fungi (Hyde et al., 2024).

Pathogenic on fruits of *Vaccinium* sp. **Sexual morph:** Not observed. **Asexual morph:** *Conidiomata* produced on the PNA, pycnidial, solitary, globose, dark brown. *Conidiophores* 7–20 × 2–5 μm ($\bar{x}$ = 13.3 × 3.1 μm, n = 30), hyaline, smooth, cylindrical, or reduced to conidiogenous cells. *Conidiogenous cells* holoblastic, hyaline, subcylindrical. *Conidia* 19–31 × 5–9 μm ($\bar{x}$ = 25.2 × 6.9 μm, n = 50), hyaline, smooth with granular contents, aseptate, narrowly fusiform, with subtruncate to bluntly rounded base, apex sub-obtuse.

Culture characteristics – Colonies on PDA reaching 76 mm diam. after three days at 25°C, initially white, aerial mycelia fluffy with an irregular margin, subsequently becoming grey, reverse black, mycelial mat moderately dense.

Material examined – CHINA, Fujian Province, isolated from diseased fruit of *Vaccinium* spp., May 2023, Y. Y. Zhou and X. H. Li (dry cultures JZBH310277, JZBH310278), living cultures JZB310277, JZB310278.

Notes – As the type species of *Botryosphaeria* and one of the most common species in the order Botryosphaeriales, the taxonomy of *Botryosphaeria dothidea* has undergone large changes (Marsberg et al., 2017). The development of molecular technology resolved the problem of species concept among numerous morphologically similar specimens (Slippers et al., 2004). Subsequently, some taxa were separated from *B. dothidea*, and some were reduced to synonymy with *B. dothidea* (Zhang et al., 2021; Marsberg et al., 2017). In this study, we follow the taxonomy of Zhang et al. (2021). In the phylogenetic analyses, the two isolates (JZB310277 and JZB310278) clustered within the clade of *Botryosphaeria dothidea* with 66% ML bootstrap and 0.97 Bayesian probabilities (Figure 5.2), and they showed similar morphology (Figure 5.3) compared with the type description of *B. dothidea* (CBS 115476) (Phillips et al., 2013). *Botryosphaeria dothidea* is globally distributed, with a wide range of woody hosts, causing canker or dieback of twigs, branches and stems, fruit rots, and even death of

the plant in severe cases (Marsberg et al., 2017). In China, fruit rots caused by *Botryosphaeria dothidea* have been observed on kiwifruit, plum, pomegranate, as well as blueberry (Zhang et al., 2016; Gu et al., 2020; Wang et al., 2021; Yuan et al., 2024).

Figure 5.2 Phylogenetic tree generated by maximum likelihood (ML) analysis of combined ITS, *tef 1-α, β-tub* sequence data of *Botryosphaeria* species

Figure 5.2 The tree is rooted with *Cophinforma eucalypti* (CBS 134651). The matrix has 201 distinct alignment patterns, with 15.63% being undetermined characters or gaps. Estimated base frequencies are as follows: A = 0.211405; C = 0.307730; G = 0.252687; T = 0.228178. Substitution rates: AC = 0.564762; AG = 3.067476; AT = 0.831148; CG = 0.764470; CT = 5.328705; GT = 1.000000. Gamma distribution shape parameter: α = 1.261108. ML bootstrap support values ≥ 60% and Bayesian posterior probabilities (BYPP) ≥ 0.90 are given near the nodes. The scale bar indicates 0.009 changes. Arrows represents the value at nodes. The ex-type strains are in bold, and newly generated sequences are in red.
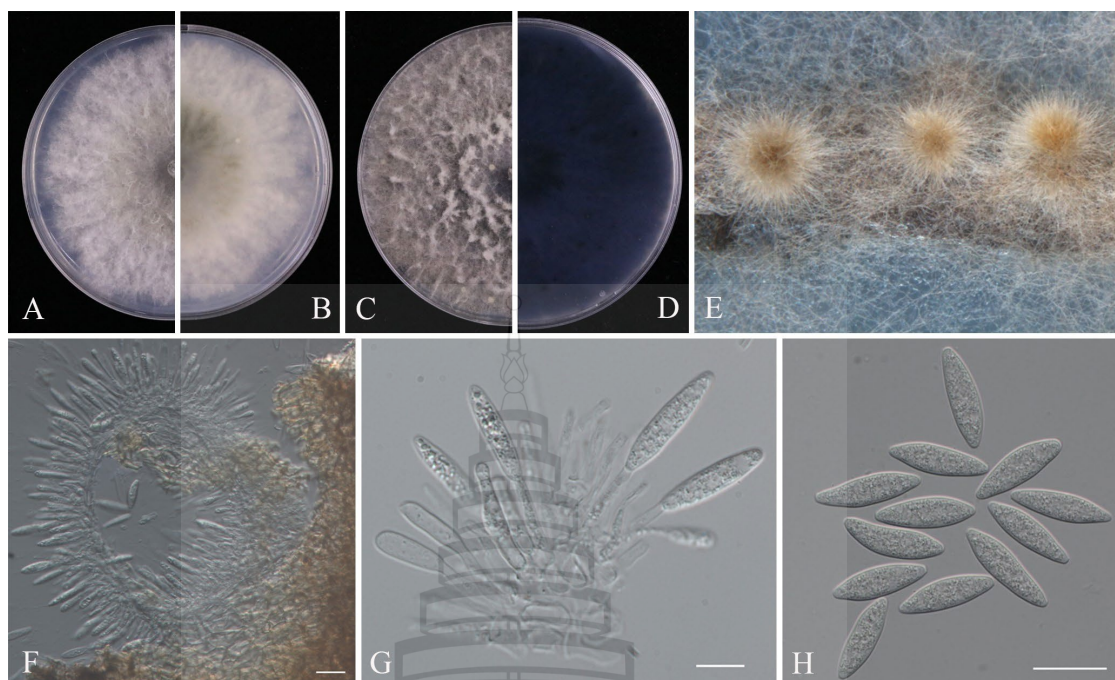
Figure 5.3 Morphological characters of *Botryosphaeria dothidea* (JZB310278)

Figure 5.3 A Upper view of the colony on PDA after three days; B Reverse view of the colony on PDA after three days; C Upper view of the colony on PDA after seven days; D Reverse view of the colony on PDA after seven days; E Colony sporulating on PNA; F, G Conidiogenous cells and developing conidia; H Conidia. Scale bars: F, H = 20 μm; G = 10 μm.

Botrytis cinerea Pers., Syn. meth. fung. (Göttingen) 2: 690 (1801).

Index Fungorum: IF 217312; Facesoffungi Number: FoF 03832.

Classification: Sclerotiniaceae, Helotiales, Leotiomycetes, Ascomycota, Fungi (Hyde et al., 2024).

Pathogenic on fruits of *Vaccinium* sp. For morphology, see the taxonomy description by Fillinger and Elad (2016) (description and illustration) and Bell et al. (2021) (record on blueberry fruit).

Material examined – CHINA, Guizhou Province, isolated from diseased fruits of *Vaccinium* spp., May 2023, Y. Y. Zhou and X. H. Li (dry cultures JZBH350048– JZBH350051), living cultures JZB350048–JZB350051.

Notes – Phylogenetic analyses of the combined multi-locus dataset shows that our four isolates (JZB350048–JZB350051) clustered together with the ex-type strain of

B. cinerea (MUCL87), with 90% ML bootstrap values and 1.00 Bayesian probabilities (Figure 5.4), and the isolates are morphologically identical to *Botrytis cinerea* (Figure 5.5). *Botrytis cinerea* is a cosmopolitan pathogen, infecting more than 200 plant species, including fruits, vegetables, and ornamental plants, leading to significant losses (Dean et al., 2012). The species has been reported as a major pathogen causing pre- and postharvest fruit rot on blueberry (Neugebauer et al., 2024).
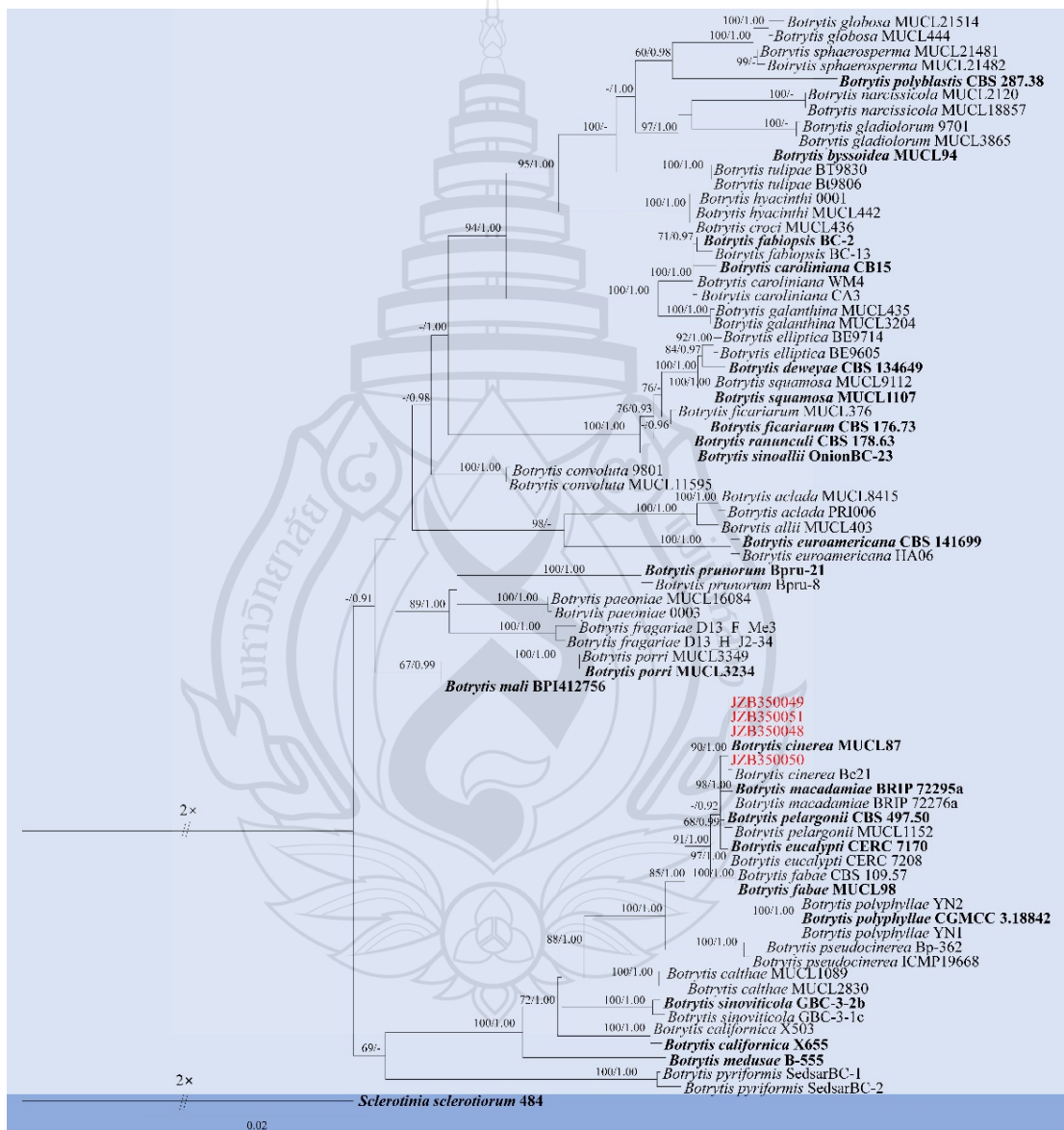
Figure 5.4 Phylogenetic tree generated by maximum likelihood (ML) analysis of combined *rpb2*, *gapdh*, *hsp60* sequence data of *Botrytis* species

Figure 5.4 The tree is rooted with *Sclerotinia sclerotiorum* (484). The matrix had 700 distinct alignment patterns, with 2.36% of characters or gaps undetermined. Estimated base frequencies were as follows: A = 0.271469, C = 0.237560, G = 0.235321, T = 0.255650; substitution rates AC = 1.400180, AG = 4.179758, AT = 1.216816, CG = 0.677408, CT = 10.830994, GT = 1.000000. Gamma distribution shape parameter α = 0.770821. ML bootstrap support values ≥ 60% and Bayesian posterior probabilities (BYPP) ≥ 0.90 are given near the nodes. The scale bar indicates 0.02 changes. The ex–type strains are in bold and newly generated sequences are in red.
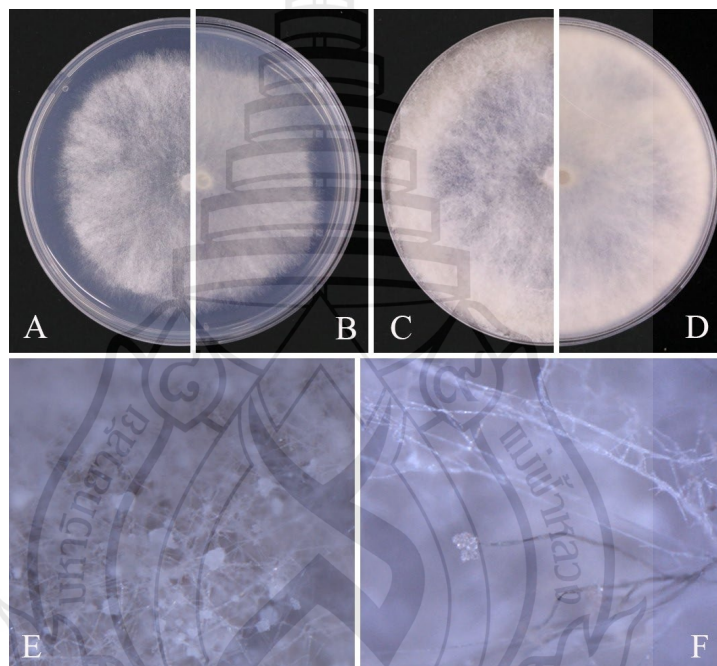
Figure 5.5 Morphological characters of *Botrytis cinerea* (JZB350048)

Figure 5.5 A Upper view of the colony on PDA after three days. B Reverse view of the colony on PDA after three days. C Upper view of the colony on PDA after seven days. D Reverse view of the colony on PDA after seven days. E Mycelia. F Sporulation of *B. cinerea*.

Cladosporium guizhouense S.Y. Wang, Yong Wang bis & Yan Li, MycoKeys 91: 160 (2021).

Index Fungorum: IF 842407; Facesoffungi Number: FoF 15881.

Classification: Cladosporiaceae, Cladosporiales, Dothideomycetes, Ascomycota, Fungi (Hyde et al., 2024).

Pathogenic on fruits of *Vaccinium* sp. **Sexual morph:** Not observed. **Asexual morph:** Hyphomycetous. *Mycelium* 1.7–4.2 μm wide, abundant, immersed, composed of septate, branched, pale olivaceous brown hyphae, smooth to slightly verruculose, with thin walls. *Conidiophores* 48–112 × 3–4 μm ($\bar{x}$ = 88.2 × 3.2 μm; n = 10), micro- to macronematous, solitary, formed laterally or terminally from hyphae, erect, branched, pale to medium olivaceous brown. *Conidia* 3–8 × 2–4 μm ($\bar{x}$ = 5.4 × 2.8 μm; n = 30), forming unbranched or branched acropetal chains, aseptate, pale olivaceous, smooth, thin-walled, ovoid, ellipsoid or subcylindrical. *Secondary ramoconidia* 6–20 × 3–5 μm ($\bar{x}$ = 12 × 3.5 μm; n = 30), aseptate, pale olivaceous, smooth, thin-walled, ellipsoid to subcylindrical.

Culture characteristics – Colonies on PDA reaching 39 mm diam. after seven days at 25°C, flat, aerial mycelium velvety to floccose, olivaceous, reverse dark grey with white margin.

Material examined – CHINA, Guizhou Province, isolated from diseased fruits of *Vaccinium* spp., May 2023, Y. Y. Zhou and X. H. Li (dry cultures JZBH390091, JZBH390092), living cultures JZB390091, JZB390092.

Notes – Two *Cladosporium* isolates generated in the present study (JZB390091, JZB390092) formed a sister clade with *C. guizhouense* strains with 100% ML bootstrap values and 1.0 Bayesian probabilities (Figure 5.6). Morphological characters of the two isolates (Figure 5.7) are similar to the original description of *C. guizhouense* (Wang et al., 2022). *Cladosporium guizhouense* was introduced as a saprobe on fallen leaves of *Eucommia ulmoides* by Wang et al. (2022) in Guizhou Province, China, and subsequently isolated from *citrus reticulata* (Yang et al., 2023). The species was also reported as a mycoparasite on rust fungi (Silva et al., 2023; Pereira et al., 2024). This is the first report of *C. guizhouense* on blueberry (*Vaccinium* spp.).
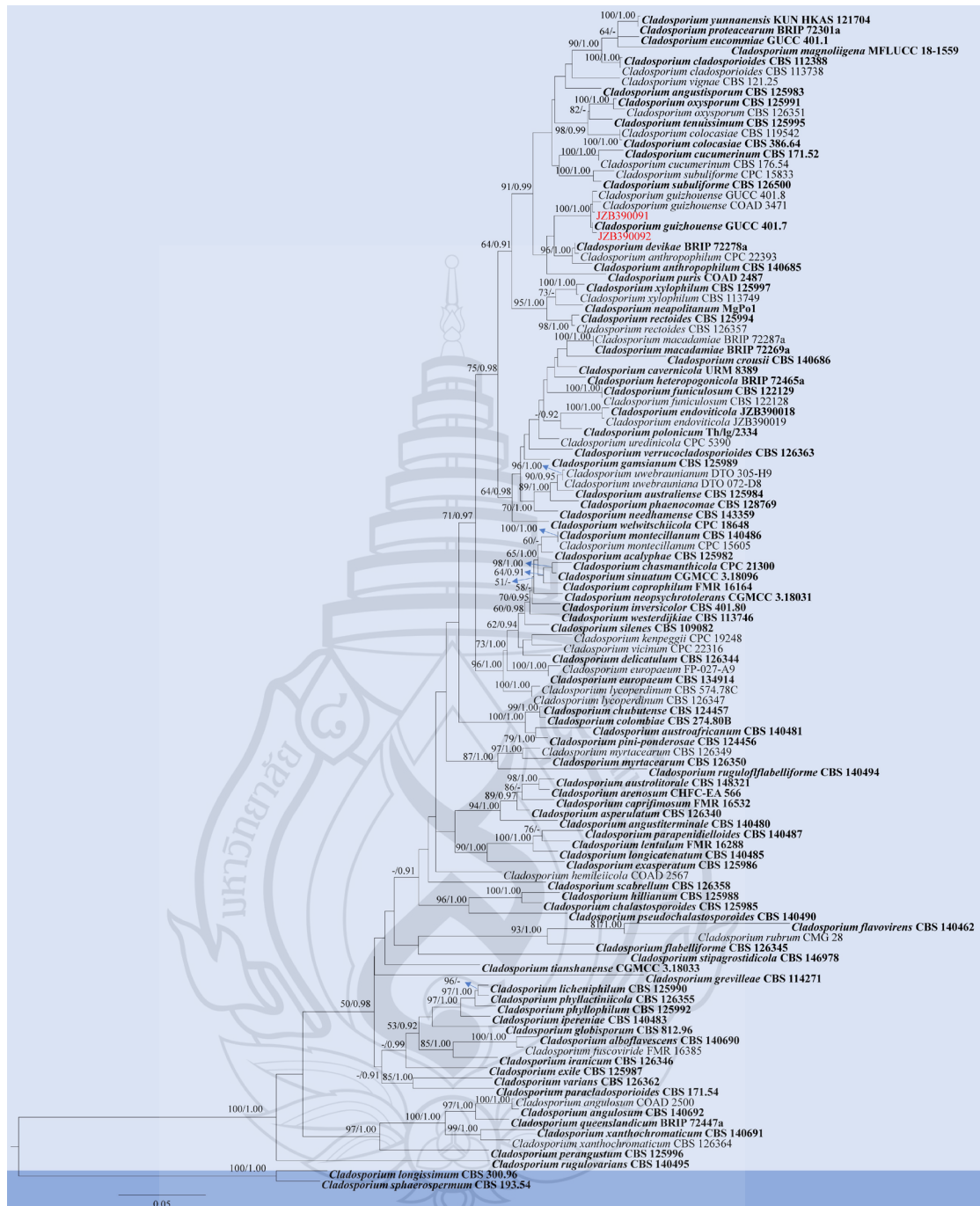
Figure 5.6 Phylogenetic tree generated by maximum likelihood (ML) analysis of combined ITS, *act*, *tef 1-α* sequence data of *Cladosporium cladosporioides* species complex

Figure 5.6 The tree is rooted with *Cladosporium longissimum* (CBS 300.96) and *Cladosporium sphaerospermum* (CBS 193.54). The matrix had 480 distinct alignment patterns, with 6.11% of undetermined characters or gaps. Estimated base frequencies

were as follows: A = 0.228323, C = 0.293145, G = 0.245258, T = 0.233274; substitution rates AC = 2.384560, AG = 5.066431, AT = 2.461368, CG = 1.411300, CT = 8.523585, GT = 1.000000; gamma distribution shape parameter α = 0.714986. ML bootstrap support values ≥ 50% and Bayesian posterior probabilities (BYPP) ≥ 0.90 are given near the nodes. The scale bar indicates 0.05 changes. Arrows represents the value at nodes. The ex–type strains are in bold and newly generated sequences are in red.
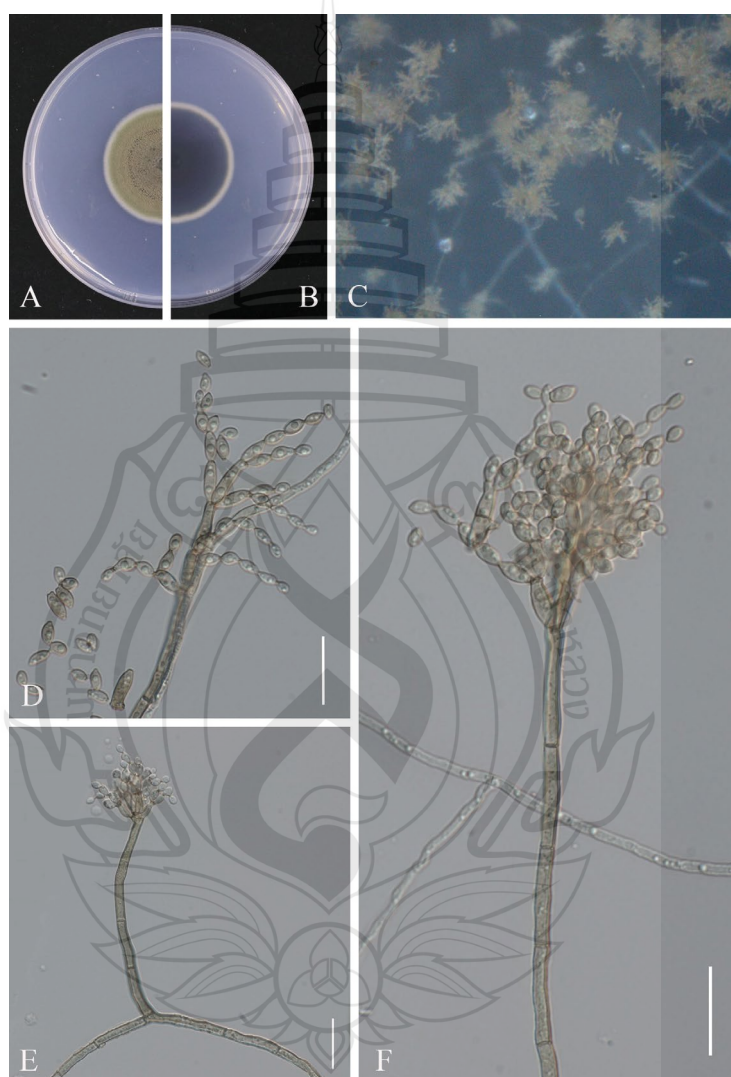
Figure 5.7 Morphological characters of *Cladosporium guizhouense* (JZB390091)

Figure 5.7 A Upper view of the colony on PDA after seven days; B Reverse view of the colony on PDA after seven days; C Mycelia and conidiophore on SNA; D–F Conidiophore, secondary ramoconidia and conidia. Scale bars: D–F = 20 μm.

Colletotrichum fioriniae (Moug.: Fr.) (Marcelino & Gouli) Pennycook, Mycotaxon 132(1): 150 (2017) [2016].

Index Fungorum: IF 553097; Facesoffungi Number: FoF 02891.

Classification: Glomerellaceae, Glomerellales, Sordariomycetes, Ascomycota, Fungi (Hyde et al., 2024).

Pathogenic on fruits of *Vaccinium* sp. For morphology, see description by Damm et al. (2012) (description and illustration) and Bell et al. (2022) (record on blueberry fruit).

Material examined – CHINA, Guizhou Province, isolated from diseased fruits of *Vaccinium* spp., May 2023, Y. Y. Zhou and X. H. Li (dry cultures JZBH330439, JZBH330440), living cultures JZB330439, JZB330440.

Notes – The two isolates obtained in this study (JZB330439, JZB330440) clustered with *C. fioriniae* strains in the phylogenetic analysis (100% ML bootstrap and 1.00 BYPP) (Figure 5.8), and share similar morphological characters (Figure 5.9) with the type description of *C. fioriniae* (Damm et al., 2012). *Colletotrichum fioriniae* is widely distributed around the world, especially in temperate regions (Talhinhas & Baroncelli, 2021). The species is one of the most common *Colletotrichum* species in China with more than 30 hosts and has been isolated from anthracnose fruit rot of litchi, peaches, and pears (Fu et al., 2019; Ling et al., 2021; Liu et al., 2022; Tan et al., 2022). This is the first report of *C. fioriniae* causing fruit rot on blueberry (*Vaccinium* spp.) in China.
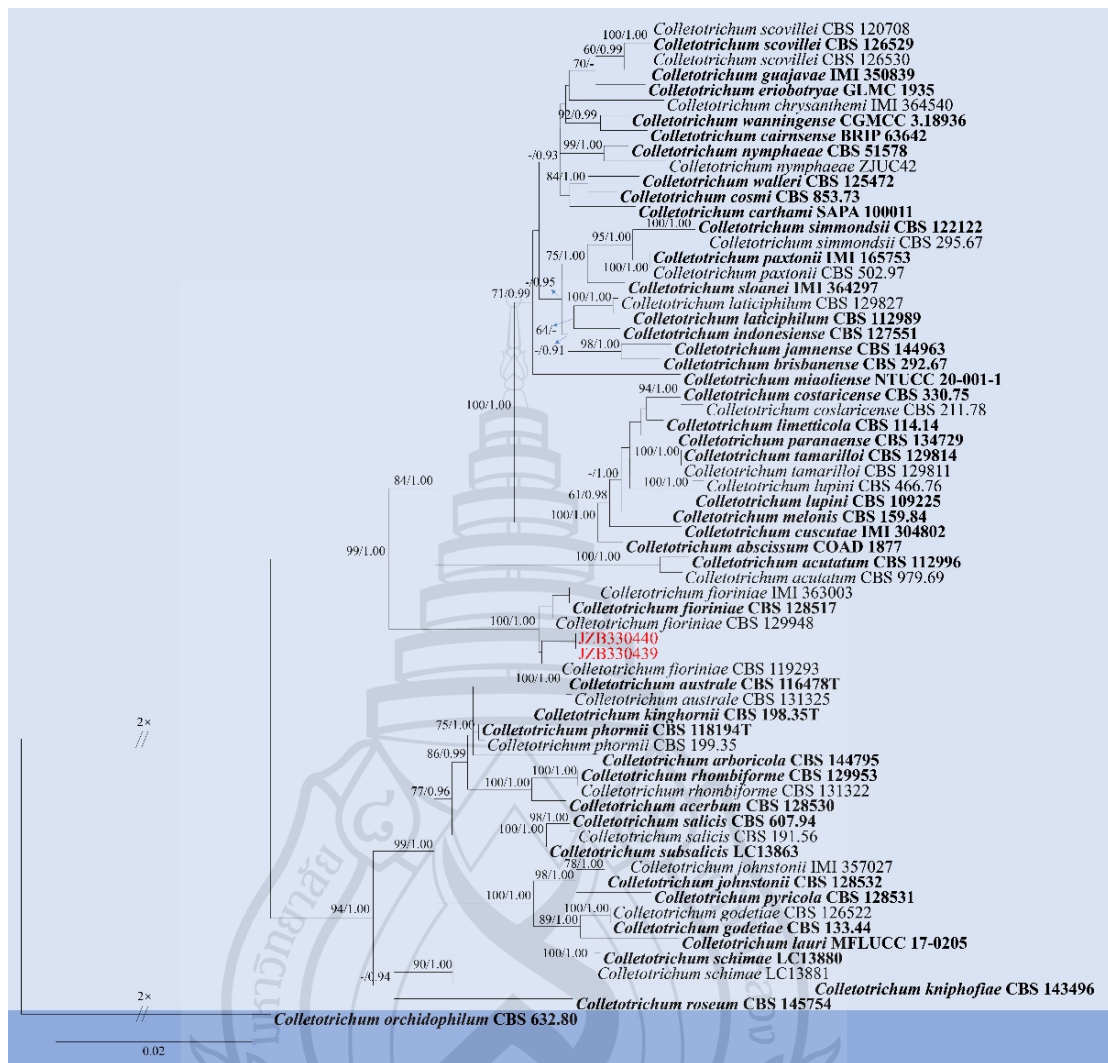
Figure 5.8 Phylogenetic tree generated by maximum likelihood (ML) analysis of combined ITS, *gapdh*, *chs*, *act*, *β-tub* sequence data of *Colletotrichum acutatum* species complex

Figure 5.8 The tree is rooted with *Colletotrichum orchidophilum* (CBS 632.80). The matrix had 542 distinct alignment patterns, with 3.67% of undetermined characters or gaps. Estimated base frequencies were as follows: A = 0.231239, C = 0.296836, G = 0.244083, T = 0.227842; substitution rates AC = 1.611674, AG = 4.644984, AT = 1.380603, CG = 0.638683, CT = 7.444475, GT = 1.000000; gamma distribution shape parameter α = 0.920840. ML bootstrap support values ≥ 50% and Bayesian posterior probabilities (BYPP) ≥ 0.90 are given near the nodes. The scale bar indicates 0.02

changes. Arrows represents the value at nodes. The ex–type strains are in bold and newly generated sequences are in red.
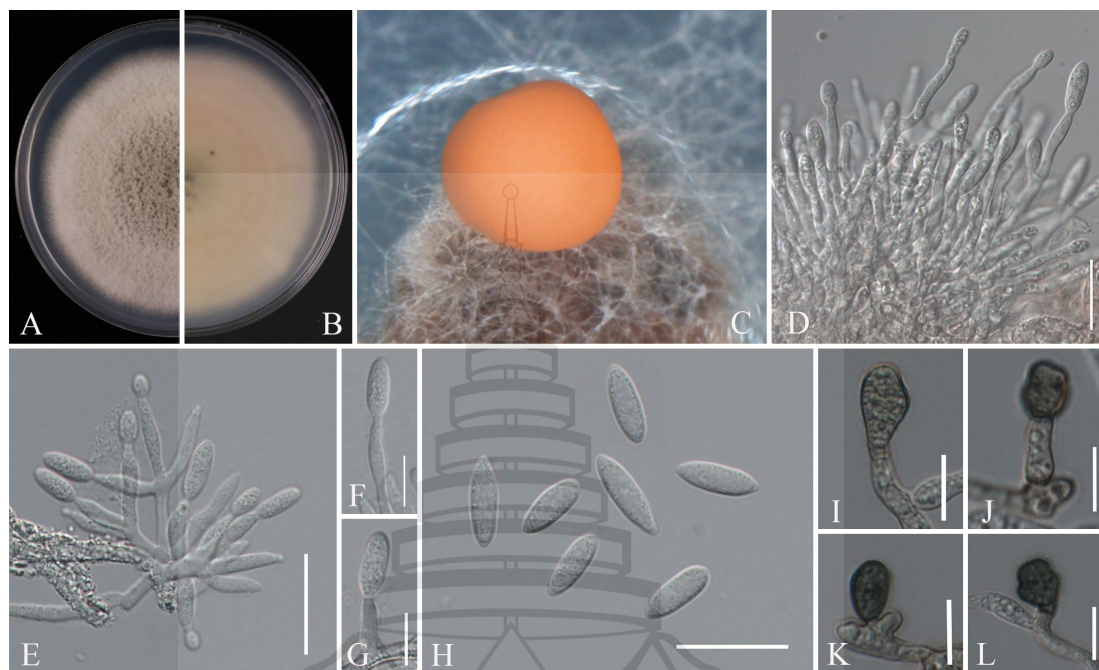
Figure 5.9 Morphological characters of *Colletotrichum fioriniae* (JZB330439)

Figure 5.9 A Upper view of the colony on PDA after seven days. B Reverse view of the colony on PDA after seven days. C Conidiomata on PNA. D–G Conidiophores. H Conidia. I–L Appressoria. Scale bars: D, E, H = 20 μm; F, G, I–L = 10 μm.

Diaporthe anacardii (Early & Punith.) R.R. Gomes, Glienke & Crous, Persoonia 31: 15 (2013).

Index Fungorum: IF 802923; Facesoffungi Number: FoF 16978.

Classification: Diaporthaceae, Diaporthales, Sordariomycetes, Ascomycota, Fungi (Hyde et al., 2024).

Pathogenic on fruits of *Vaccinium* sp. **Sexual morph:** Not observed. **Asexual morph:** *Conidiomata* pycnidial, globose, black. *Conidiophores* 10–21.5 × 1–2 μm ($\bar{x}$ = 15.1 × 1.4 μm; n = 30), densely aggregated, branched, straight to slightly sinuous, smooth, hyaline, cylindrical, slightly tapering towards the apex. *Alpha conidia* 6–9 × 2–3 μm ($\bar{x}$ = 7.6 × 2.8 μm; n = 50), straight, aseptate, bi-guttulate or multi-guttulate,

hyaline, fusoid to ellipsoid, slightly tapering towards both ends. Beta conidia not observed.

Culture characteristics – Colonies on PDA reaching 78 mm diam. after five days at 25°C, white with moderate, felted aerial mycelium, reverse yellowish to brownish at the centre.

Material examined – CHINA, Fujian Province, isolated from diseased fruits of *Vaccinium* spp., May 2023, Y. Y. Zhou and X. H. Li (dry cultures JZBH320308), living cultures JZB320308.

Notes – For the taxonomic treatment of *Diaporthe*, we followed the latest classification proposed by Norphanphoun et al. (2022) and Dissanayake et al. (2024). The phylogenetic analysis showed that our isolate JZB320308 clustered within the clade of *Diaporthe anacardii*, sister to CGMCC 3.18286 and LC4419 (=*D. velutina*) (Figure 5.10), and the morphology characters of JZB320308 (Figure 5.11) conformed to the description of *D. anacardii* (Gao et al., 2017). *Diaporthe anacardii* was introduced from *Anacardium occidentale* in Africa (as *Phomopsis anacardii*) (Early & Punithalingam, 1972), and was epitypified by Gomes et al. (2013). According to the new classification system, *D. acutispora*, *D. nebulae*, *D. phillipsii*, *D. portugallica* and *D. velutina* are reduced to synonymy with *D. anacardii* (Dissanayake et al., 2024). Among them *D. phillipsii* was originally introduced as a pathogen associated with blueberry twig blight and dieback in Portugal (Hilário et al., 2020). This is the first report of *D. anacardii* causing fruit rot on blueberry in China.
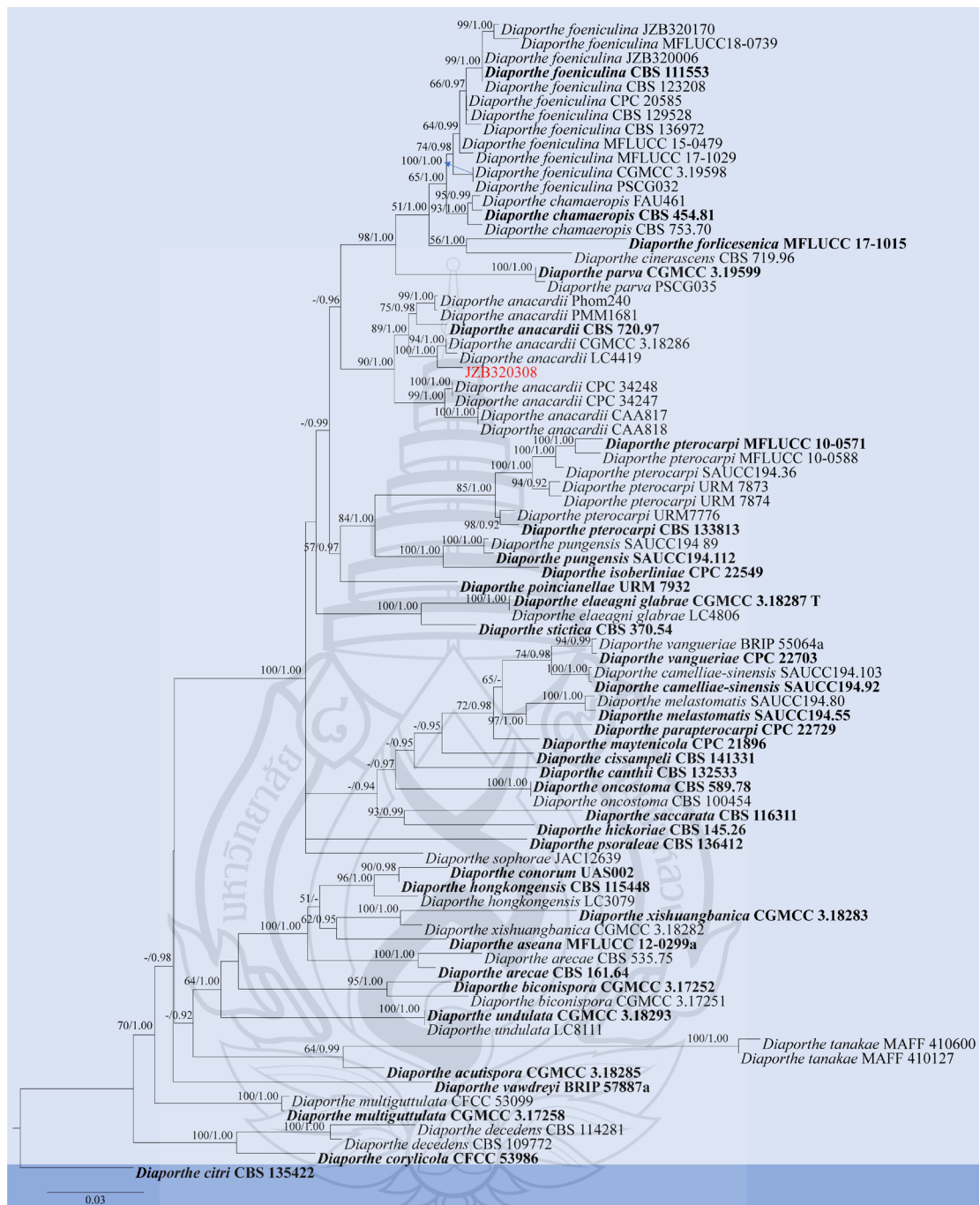
Figure 5.10 Phylogenetic tree generated by maximum likelihood (ML) analysis of combined ITS, *tef 1-α*, *β-tub*, *cal*, *his* sequence data of Section Foeniculina of *Diaporthe* species

Figure 5.10 The tree is rooted with *Diaporthe citri* (CBS 135422). The matrix had 1121 distinct alignment patterns, with 25.45% of undetermined characters or gaps. Estimated base frequencies were as follows: A = 0.214637, C = 0.324631, G =

0.237836, T = 0.222897; substitution rates AC = 1.200371, AG = 3.247133, AT = 1.039432, CG = 0.794522, CT = 4.498676, GT = 1.000000; gamma distribution shape parameter α = 0.912183. ML bootstrap support values ≥ 50% and Bayesian posterior probabilities (BYPP) ≥ 0.90 are given near the nodes. The scale bar indicates 0.03 changes. Arrows represents the value at nodes. The ex–type strains are in bold and newly generated sequences are in red.
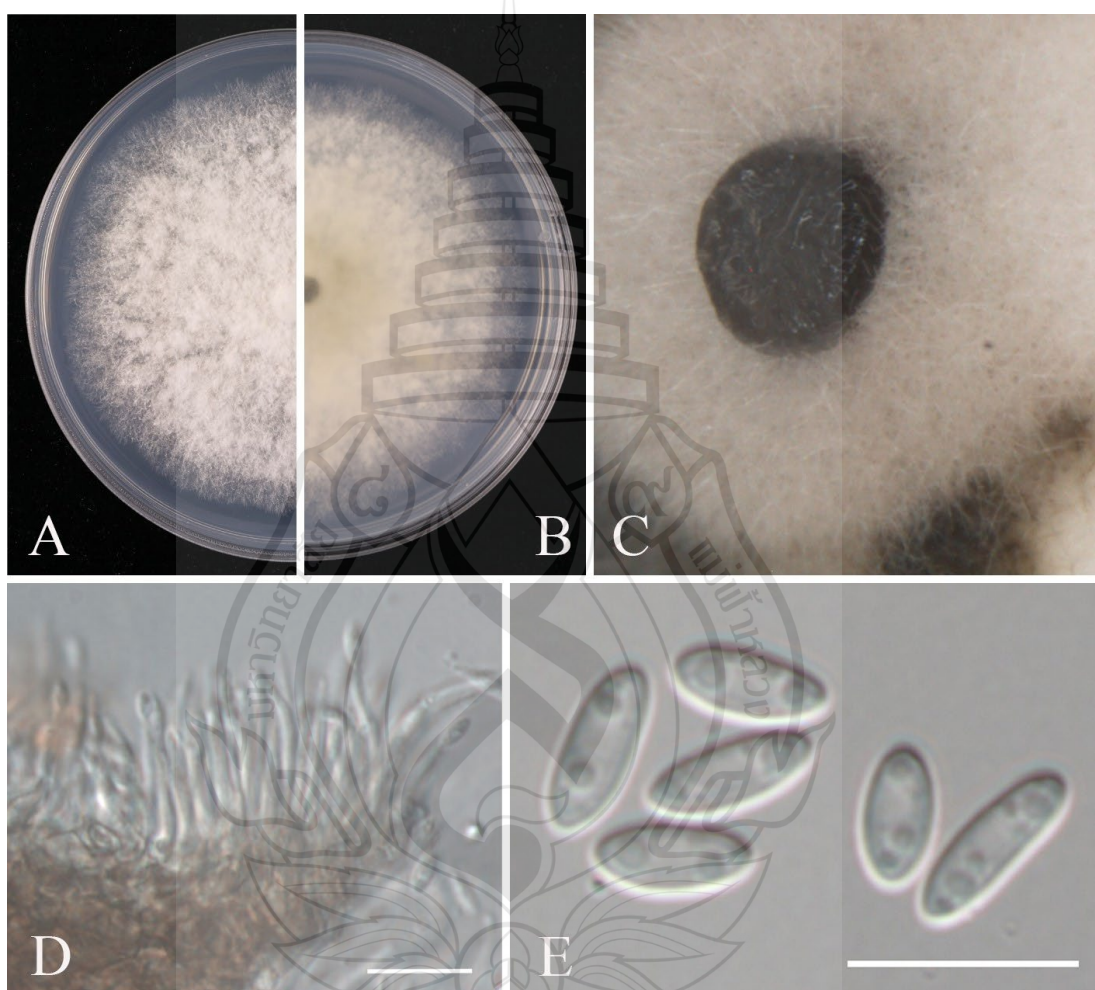
Figure 5.11 Morphological characters of *Diaporthe anacardii* (JZB320308)

Figure 5.11 A Upper view of the colony on PDA after five days. B Reverse view of the colony on PDA after three days. C Conidiomata on PNA. D Conidiophores. E Alpha conidia. Scale bars: D, E = 10 μm.

Fusarium annulatum Bugnic., Rev. gén. Bot. 59: 13 (1952).

Index Fungorum: IF 297536; Facesoffungi Number: FoF 16723.

Classification: Nectriaceae, Hypocreales, Sordariomycetes, Ascomycota, Fungi (Hyde et al., 2024).

Pathogenic on fruits of *Vaccinium* sp. **Sexual morph:** Not observed. **Asexual morph:** *Conidiophores* on CLA produced laterally on aerial mycelium and substrate mycelium, straight or flexuous, simple or more commonly sympodially to irregularly branched, or reduced to conidiogenous cells borne laterally on hyphae; *Conidiogenous cells* mono- and polyphialidic, subulate to cylindrical; *Microconidia* 5–10 × 2–3.5 μm ($\overline{x}$ = 7.0 × 2.6 μm; n = 50), formed on aerial conidiophores, hyaline, obovoid to ellipsoidal, smooth- and thin-walled, aseptate, forming a false head on phialides. *Macroconidia* 21.5–55.5 × 4–5.5 μm ($\overline{x}$ = 40.9 × 4.5 μm; n = 30), sparse, straight to slightly curved, tapering toward the basal part; apical cell blunt; basal cell barely notched, 2–4-septate, hyaline, thin- and smooth-walled. *Chlamydospores* absent.

Culture characteristics – Colonies on PDA reaching 75 mm diam. after six days at 25°C, flat, light purple to orange with abundant aerial mycelia.

Material examined – CHINA, Fujian Province, isolated from diseased fruits of *Vaccinium* spp., May 2023, Y. Y. Zhou and X. H. Li (dry cultures JZBH3110489, JZBH3110490), living cultures JZB3110489, JZB3110490.

Notes – According to the phylogenetic analyses, two isolates in this study (JZB3110489, JZB3110490) clustered within the clade of *Fusarium annulatum* (Figure 5.12). *Fusarium annulatum* was introduced by Bugnicourt (1952) from *Oryza sativa*, and was reported to infect multiple plant hosts under the name *F. proliferatum* (Seifert et al., 2003). Yilmaz et al. (2021) fixed the typification of *F. proliferatum* to a distinct phylogenetic clade, and provided an emended description of *F. annulatum*. *Fusarium annulatum* showed phylogenetic diversity and differentiation in morphology. According to the original description of the type strain (CBS 258.54) by Bugnicourt (1952), sporodochial conidia of *F. annulatum* are strongly curved and almost ring-shaped, and Nelson et al. (1983) regraded *F. annulatum* as *F. proliferatum* with strongly curved, sporodochial conidia (macroconidia), while Yilmaz et al. (2021) found that most *F. annulatum* isolates only produce straight, sporodochial conidia. Our study confirmed that macroconidia are straight to slightly curved (Figure 5.13). *Fusarium*

annulatum was reported to cause blight on *Bletilla striata*, maize, and *Rosa roxburghii* rot disease in China (Xu et al., 2022; Zhang et al., 2023; Zhang et al., 2024). This is the first report of *F. annulatum* causing fruit rot on blueberry (*Vaccinium* spp.).
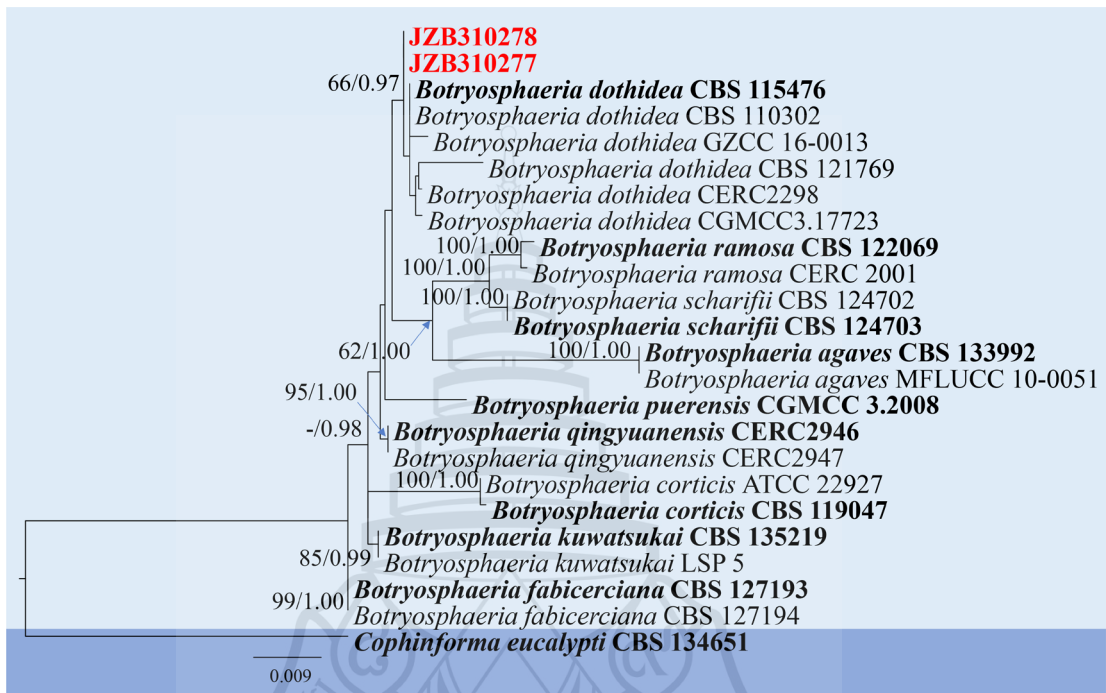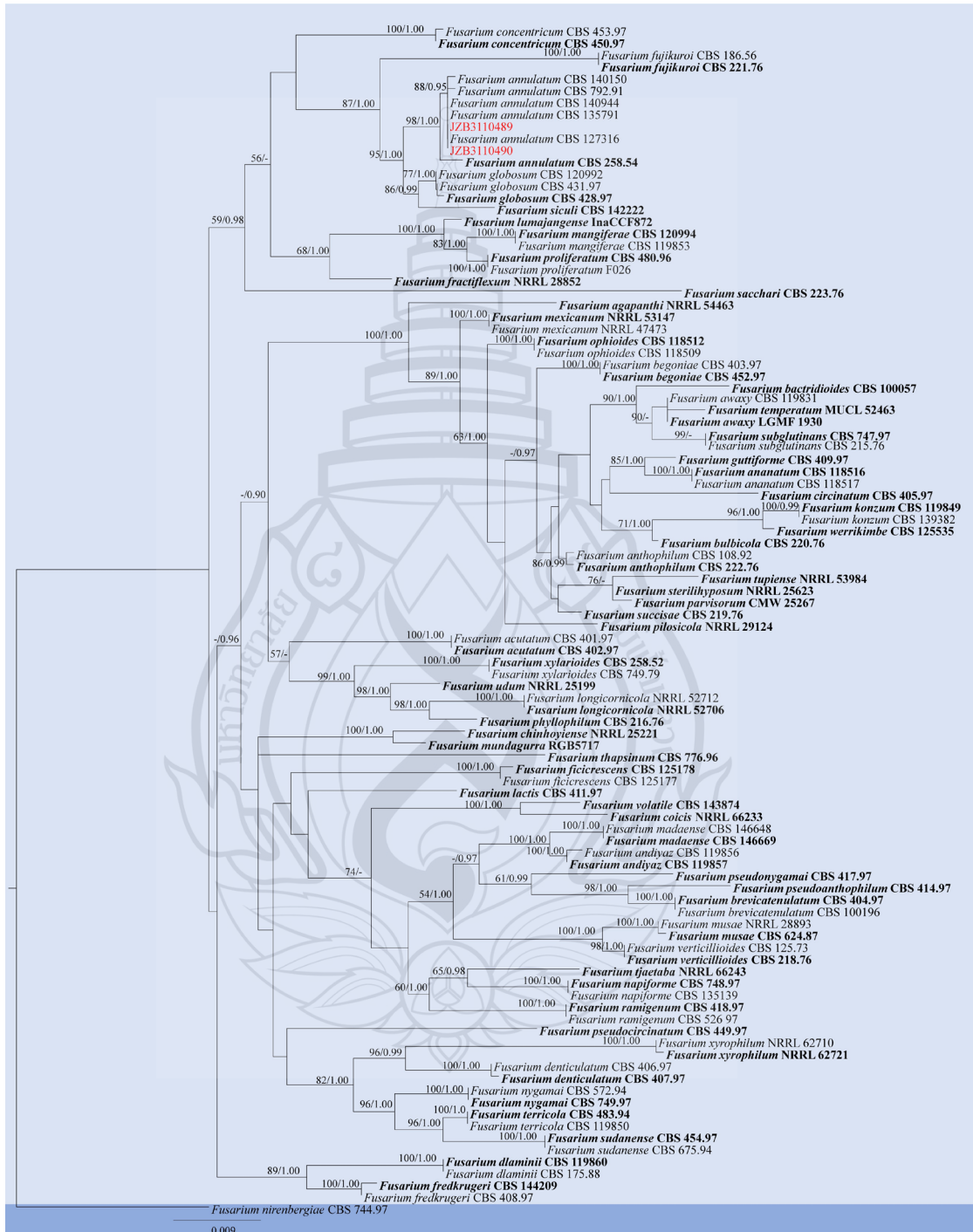

Figure 5.12 Phylogenetic tree generated by maximum likelihood (ML) analysis of combined *tef 1-α* and *rpb2* sequence data of *Fusarium* species

Figure 5.12 The tree is rooted with *Fusarium nirenbergiae* (CBS 744.97). The matrix had 421 distinct alignment patterns, with 3.70% of undetermined characters or gaps. Estimated base frequencies were as follows: A = 0.263854, C = 0.251445, G = 0.251382, T = 0.233319; substitution rates AC = 1.435916, AG = 6.155181, AT = 1.375277, CG = 0.854277, CT = 13.787190, GT = 1.000000; gamma distribution shape parameter α = 0.814503. ML bootstrap support values ≥ 50% and Bayesian posterior probabilities (BYPP) ≥ 0.90 are given near the nodes. The scale bar indicates 0.009 changes. The ex–type strains are in bold and newly generated sequences are in red.
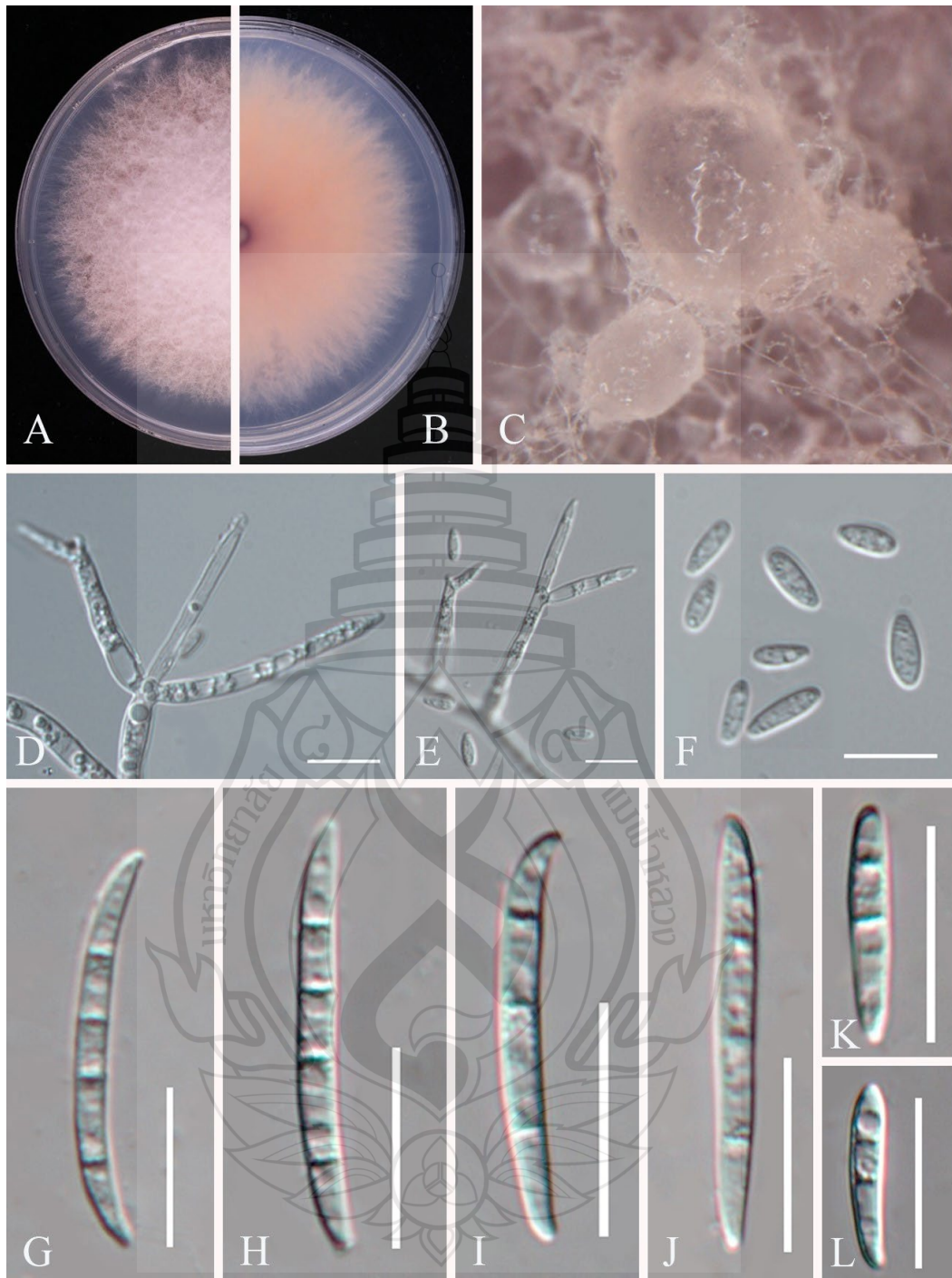
Figure 5.13 Morphological characters of *Fusarium annulatum* (JZB3110489)

Figure 5.13 A Upper view of the colony on PDA after six days. B Reverse view of the colony on PDA after six days. C Sporodochia formed on CLA. D, E Aerial conidiophores. F Microconidia. G–L Macroconidia. Scale bars: D–F = 10 μm; G–L = 20 μm.

Neopestalotiopsis surinamensis Maharachch., K.D. Hyde & Crous, in Maharachchikumbura, Hyde, Groenewald, Xu & Crous, Stud. Mycol. 79: 149 (2014).

Index Fungorum: IF 809781; Facesoffungi Number: FoF 16979.

Classification: Sporocadaceae, Amphisphaeriales, Sordariomycetes, Ascomycota, Fungi (Hyde et al., 2024).

Pathogenic on fruits of *Vaccinium* sp. **Sexual morph:** Not observed. **Asexual morph:** *Conidiomata* subglobose to globose, scattered or gregarious, semi-immersed or erumpent, exuding globose, black conidial masses. *Conidiophores* indistinct, often reduced to conidiogenous cells. *Conidiogenous cells* discrete, ampulliform, flask-shaped to subcylindrical, smooth-walled, hyaline. *Conidia* 20–27 × 7–9.5 μm ($\overline{x}$ = 23.0 × 8.1 μm; n = 30), fusoid, ellipsoid to subcylindrical, straight to slightly curved, 4-septate; basal cell 3.5–5 μm long, obconic with a truncate base, hyaline, rugose and thin-walled; three median cells 14–18.5 μm ($\overline{x}$ = 15.7 μm; n = 30) long, doliiform, wall rugose, versicolored, brown to pale brown, septa darker than the rest of the cell, second cell from the base 5–6 μm long, pale brown to brown; third cell 4.5–6 μm long, brown; fourth cell 4.5–6 μm long, brown; apical cell 3–4 μm long, hyaline, conical to subcylindrical, thin- and smooth-walled; apical appendages 2–4, 12.5–28.5 μm ($\overline{x}$ = 20.2 μm; n = 30) long, tubular, arising from the apical crest, unbranched, filiform; basal appendage 3.5–7.5 μm ($\overline{x}$ = 5.0 μm; n = 30) long, single, tubular, unbranched, centric.

Culture characteristics – Colonies on PDA reaching 79 mm diam. after five days at 25°C, raised with lobate margin, white, reverse pale yellow, aerial mycelia dense, flocculent.

Material examined – CHINA, Fujian Province, isolated from diseased fruits of *Vaccinium* spp., May 2023, Y. Y. Zhou and X. H. Li (dry cultures JZBH340093–JZBH340095), living cultures JZB340093–JZB340095.

Notes – In the phylogenetic tree of *Neopestalotiopsis*, three isolates from this study (JZB340093–JZB340095) grouped with the ex-type strain of *Neopestalotiopsis surinamensis* (CBS 450.74) and another strain (MFTU06-3) (Figure 5.14). Morphologically, isolates in this study (Figure 5.15) were similar to the original description of *N. surinamensis* by Maharachchikumbura et al. (2014). However, minor dimensional differences were observed in the size of basal cell and apical cell, which may be attributed to host differences. *Neopestalotiopsis surinamensis* was introduced

from soil under *Elaeis guineensis* in *Suriname* and living leaves of *Protea eximia* in Zimbabwe (Maharachchikumbura et al., 2014), and was reported as a pathogen causing guava scab (Solarte et al., 2018). This is the first report of *Neopestalotiopsis surinamensis* causing blueberry fruit rot.

Figure 5.14 Phylogenetic tree generated by maximum likelihood (ML) analysis of combined ITS, *tef 1-α* and *tub2* sequence data of *Neopestalotiopsis* species

Figure 5.14 The tree is rooted with *Pestalotiopsis spathulate* (CBS 356.86) and *Pestalotiopsis diversiseta* (MFLUCC 12-0287). The matrix had 606 distinct alignment patterns, with 13.33% of undetermined characters or gaps. Estimated base frequencies were as follows: A = 0.234657, C = 0.273247, G = 0.214726, T = 0.277370; substitution rates AC = 1.150331, AG = 1.150331, AT = 1.150331, CG = 0.850459, CT = 4.628454, GT = 1.000000; gamma distribution shape parameter α = 0.898468. ML bootstrap support values ≥50% and Bayesian posterior probabilities (BYPP) ≥0.90 are given near the nodes. The scale bar indicates 0.009 changes. Arrows represents the value at nodes. The ex–type strains are in bold and newly generated sequences are in red.
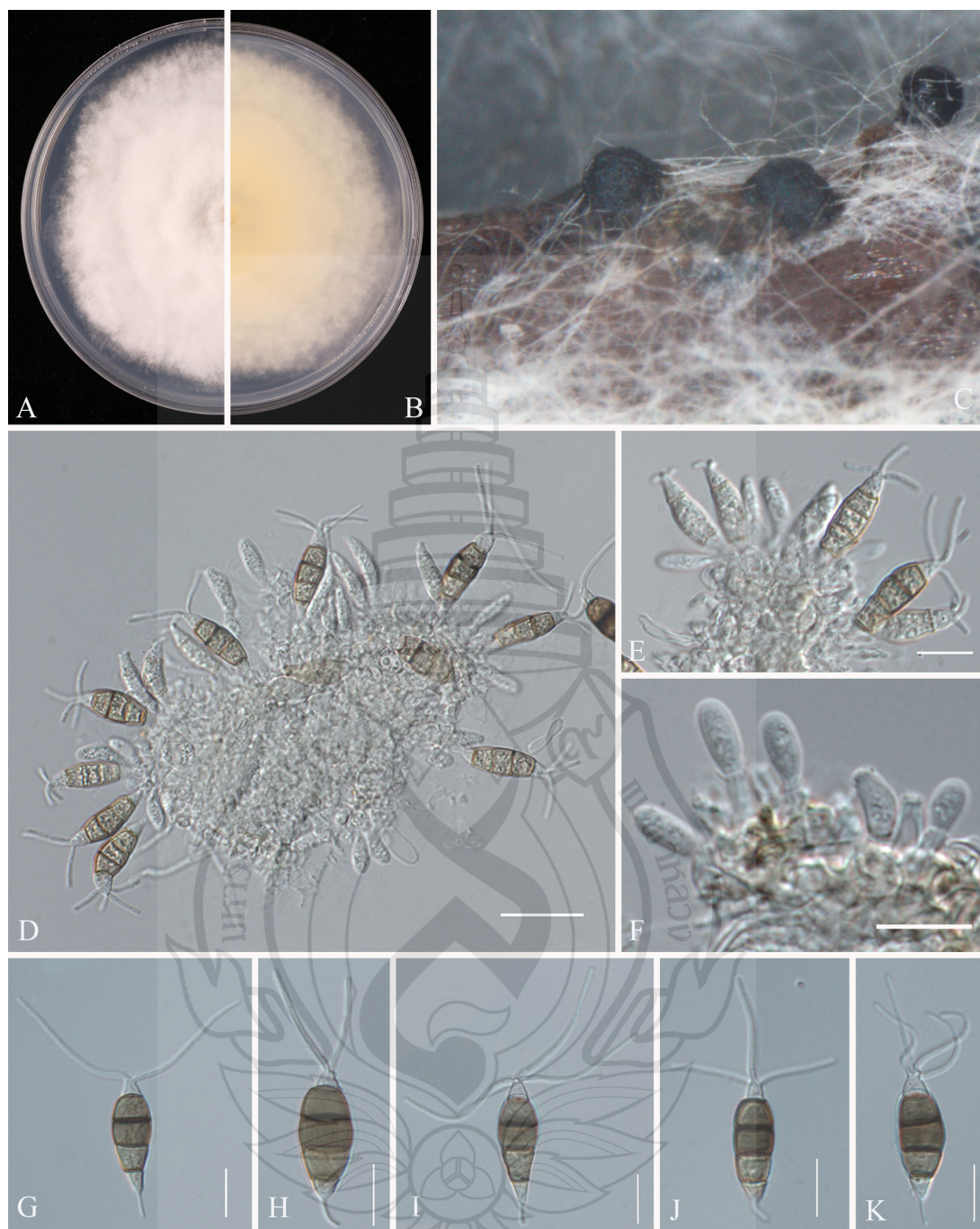
Figure 5.15 Morphological characters of *Neopestalotiopsis surinamensis* (JZB340093)

Figure 5.15 A Upper view of the colony on PDA after five days. B Reverse view of the colony on PDA after five days. C Conidiomata on PNA. D–F Conidiogenous cells. G–K Conidia. Scale bars: D = 20 μm; E–K = 10 μm.

5.2.3 Pathogenicity Test

Among the 16 isolates obtained from blueberry fruit rot, one representative isolate from each genus was selected for pathogenicity assay using spore suspensions. These include *Botryosphaeria dothidea* (JZB310278), *Botrytis cinerea* (JZB350048), *Cladosporium guizhouense* (JZB390091), *Colletotrichum fioriniae* (JZB330439), *Diaporthe anacardii* (JZB320308), *Fusarium annulatum* (JZB3110489) and *Neopestalotiopsis surinamensis* (JZB340093). All experimental isolates showed virulence on blueberry fruits with different symptoms (Figure 5.16). Fruits inoculated with *F. annulatum* formed white mycelia at the inoculation site; fruits inoculated with *D. anacardii* showed soft rot with a fluid exuded from the inoculation site; fruits inoculated with *B. cinerea* showed a rot surrounded by grey white mycelia; fruits inoculated with *C. fioriniae* secreted orange conidial mass; fruits inoculated with *B. dothidea* shrivelled and produced black globose conidiomata; fruits inoculated with *C. guizhouense* produced lesion with olive-green colony, and fruits inoculated with *N. surinamensis* produced a lesion shrivelled and formed white mycelia and black conidiomata. No symptoms were induced in the control fruits inoculated with sterile water. Fungal pathogens were re-isolated from lesions and confirmed by morphology and ITS sequence to prove Koch's postulates.
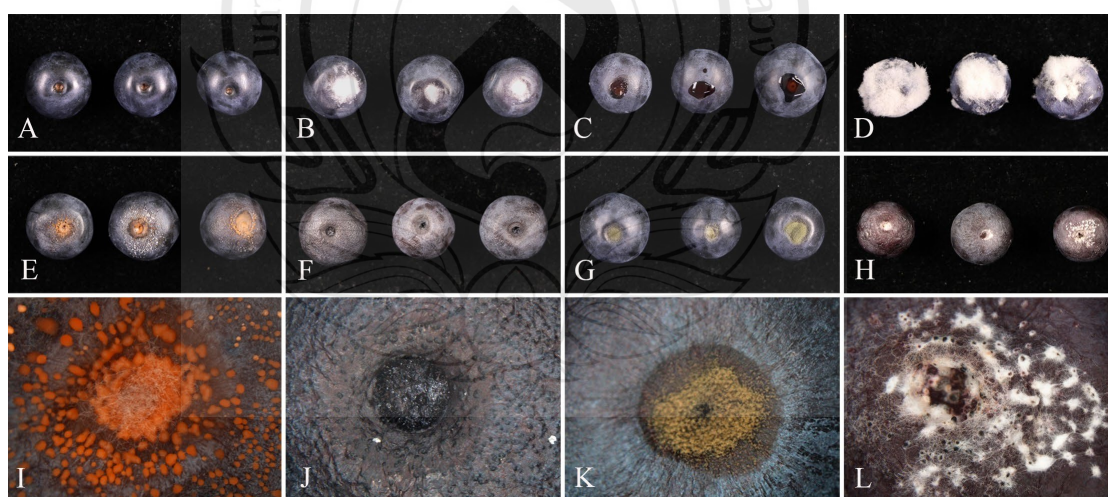
Figure 5.16 Detached fruit pathogenicity test for the fungal isolates on blueberry fruits five days post inoculation

Figure 5.16 A Control (sterilized water); B *Fusarium annulatum* (JZB3110489); C *Diaporthe anacardii* (JZB320308); D *Botrytis cinerea* (JZB350048); E, I *Colletotrichum fioriniae* (JZB330439); F J *Botryosphaeria dothidea* (JZB310278); G K *Cladosporium guizhouense* (JZB390091); H, L *Neopestalotiopsis surinamensis* (JZB340093).

5.2.4 Summary

In this section, seven fungal pathogens causing blueberry fruit rot disease in Guizhou and Fujian Provinces were identified and characterized, and their pathogenicity on fruits were confirmed. *Cladosporium guizhouense*, *Fusarium annulatum*, and *Neopestalotiopsis surinamensis* were reported for the first time on blueberry. The study demonstrated that fruit rot disease results from a mixed infection of multiple pathogens; and expanded the understanding of causal agents of blueberry fruit rot during the growth stage, highlighting their potential as latent pathogens that contribute to post-harvest losses. Relevant results provide a reference for the etiological research and disease management in blueberry fruit diseases.

5.3 Characterization of Micro-Fungi Associated with Blueberry Leaf, Stem and Root Diseases in China

5.3.1 Investigation, Sampling and Fungal Isolation

During the investigation of blueberry diseases in Fujian, Guizhou, Heilongjiang, Jilin and Liaoning from March to September in 2023, leaf spot, stem blight and root rot were found to be the most common diseases, with incidence rate from 1%–5%, and more than one symptom could appear on one plant (Figure 5.17):

1. Leaf spot: appear as pinpoint spots on leaves, enlarge to brown to purple lesion, and gradually expand and coalesce, until the wither and defoliation of leaves;

2. Stem blight: blight, dieback and canker were observed on twig, shoot and stem, here they are collectively called stem blight. Affected stems showed irregular, reddish-brown lesions that extended to both sides of the stem, and the tip became shrivelled and withered;

3. Root rot: main root or fibrous root showed brown and necrosis, plants affected by diseases usually short and poor-developed, with yellow leaves.

For typical symptoms, 94 diseased samples (25 leaf samples, 54 stem samples and 15 root samples) were collected, and 429 fungal isolates were generated by tissue isolation.

Figure 5.17 Field symptom of blueberry diseases

Figure 5.17 a poor-developed plants; b leaf spot; c stem blight; d withered branch with fruiting bodies; e stem canker; f brown vascular in diseased plant; g twig dieback; h rot on stem-base; i root rot

5.3.2 Composition and Information of Fungal Taxa

Isolates were preliminarily identified as forty genera, which are mostly belong to the class Sordariomycetes and Dothideomycetes. *Neopestalotiopsis* (15%), *Alternaria* (11%), *Fusarium* (11%), *Pestalotiopsis* (11%), *Botryosphaeria* (10%) are top five genera with highest proportion, accounting more than half of total isolate numbers (Figure 5.18).

A total of nighty species was identified by morphological characters and phylogenetic analysis, while there are additional twenty-one undetermined species, which need more morphological or molecular data. Species information was listed in Table 5.1, including classification (unidentified species were expressed by sp.), isolate

number, isolation source, isolation region and the records on blueberry. According to the results, seventy-eight species were newly recorded on blueberry worldwide (new host records), four species were first reported on blueberry in China (new host-geography association records), and three new species were proposed. The classification of fungi in this study followed Hyde et al. (2024).
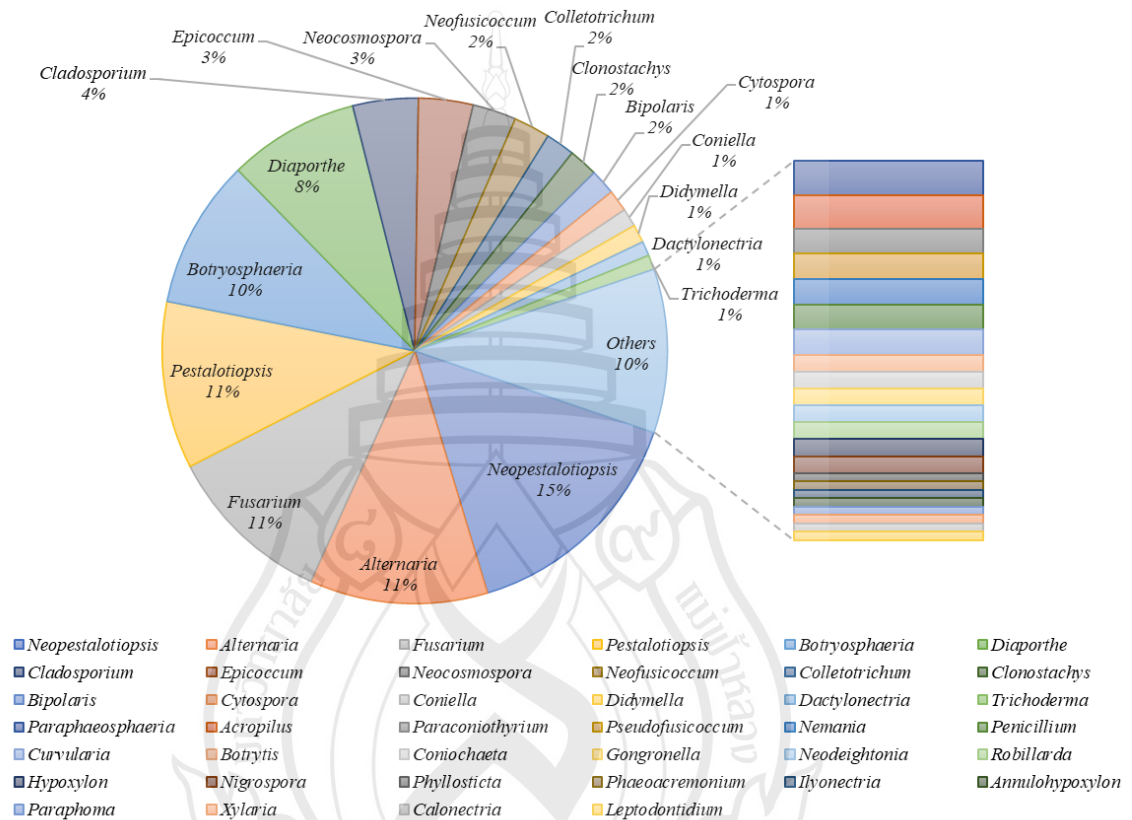
Figure 5.18 The proportion of isolate numbers divided by genera

Table 5.2 Species list in this study

Genus	Species	Number of isolates	Isolation source	Isolation region	Records on blueberry
1 Ascomycota					
1.1 Dothideomycetes					
1.1.1 Botryosphaeriales					
1.1.1.1 Botryosphaeriaceae					
Botryosphaeria (41 isolates, 1 species)	*B. dothidea*	41	Leaf (8)	FJ, GZ	Australia (Scarlett et al., 2019),
			Stem (30)	FJ, HLJ, JL, LN	China (Yu et al., 2012),
			Root (3)	LN	Portugal (Hilário et al., 2020),
					Korea (Choi 2011),
					USA (Phillips et al., 2006)
Neodeightonia (2 isolates, 1 species)	*N. subglobosa*	2	Leaf (2)	FJ	New host record
Neofusicoccum (10 isolates, 2 species)	*N. parvum*	9	Stem (9)	FJ, GZ	Australia (Scarlett et al., 2018),
					Chile (Espinoza et al., 2009),
					China (Xu et al., 2015),
					Czech Republic (Spetik et al., 2023),
					Mexico (Boyzo-Marin et al., 2016),
					New Zealand (Tennakoon et al., 2018),
					Portugal (Hilário et al., 2020),
					Spain (Castillo et al., 2013),
					USA (Koike et al., 2014)
	N. podocarpi	1	Stem (1)	FJ	New host record
1.1.1.2 Phyllostictaceae					
Phyllosticta (1 isolates, 1 species)	*Phyllosticta* sp.	1	Leaf (1)	FJ	New host record
Pseudofusicoccum (3 isolates, 1 species)	*P. violaceum*	3	Stem (3)	FJ	New host record

Table 5.2 (continued)

Genus	Species	Number of isolates	Isolation source	Isolation region	Records on blueberry
1.1.2 Cladosporiales					
1.1.2.1 Cladosporiaceae					
Cladosporium (18 isolates, 4 species)	*C. cladosporioides*	10	Leaf (4)	LN, FJ, GZ	New host record
			Stem (4)	LN	
			Root (2)	LN	
	C. perangustum	1	Leaf (1)	GZ	New host record
		2	Stem (2)	FJ, HLJ	
	C. ramotenellum	2	Stem (2)	HLJ	New host record
	C. tenuissimum	1	Leaf (1)	FJ	New host record
		2	Stem (2)	HLJ	
1.1.3 Pleosporales					
1.1.3.1 Didymellaceae					
Didymella (5 isolates, 3 species)	*D. glomerata*	1	Leaf (1)	JL	New host record
	D. pomorum	3	Leaf (1)	JL	New host record
			Stem (2)	JL	
	Didymella sp.	1	Stem (1)	JL	New host record
Epicoccum (15 isolates, 5 species)	*E. camelliae*	1	Stem (1)	JL	New host record
	E. dendrobii	7	Stem (7)	HLJ, JL	New host record
	E. djirangnandiri	2	Leaf (2)	FJ	New host record
	E. latusicollum	4	Stem (3)	FJ	New host record
			Root (1)	FJ	
	E. tritici	1	Leaf (1)	GZ	New host record

Table 5.2 (continued)

Genus	Species	Number of isolates	Isolation source	Isolation region	Records on blueberry
1.1.3.2 Didymosphaeriaceae					
Paraphaeosphaeria (4 isolates, 2 species)	*P. sporulosa*	2	Root (2)	LN	New host record
	P. neglecta	2	Stem (2)	JL	New host record
Paraconiothyrium (3 isolates, 1 species)	*P. brasiliense*	3	Stem (3)	GZ, JL	New host record
1.1.3.3 Phaeosphaeriaceae					
Paraphoma (1 isolates, 1 species)	*Paraphoma* sp.	1	Stem (1)	JL	New host record
1.1.3.4 Pleosporaceae					
Alternaria (49 isolates, 1 species)	*A. alternata*	49	Leaf (14)	GZ, JL, LN	China (Yan et al., 2014)
			Stem (32)	GZ, HLJ, JL, LN	
			Root (3)	LN	
Bipolaris (7 isolates, 2 species)	*B. sorokiniana*	5	Stem (5)	HLJ	New host record
	Bipolaris sp.	2	Stem (5)	HLJ	New host record
Curvularia (3 isolates, 2 species)	*C. moringae*	1	Stem (1)	JL	New host record
	C. austriaca	2	Stem (1)	JL	New host record
1.2 Eurotiomycetes					
1.2.1 Eurotiales					
1.2.1.1 Aspergillaceae					
Penicillium (3 isolates, 1 species)	*Penicillium* sp.	3	Stem (2)	JL, LN	New host record
			Root (1)	LN	
1.3 Leotiomycetes					
1.3.1 Helotiales					
1.3.1.1 Leptodontidiaceae					
Leptodontidium (1 isolates, 1 species)	*Leptodontidium* sp.	1	Stem (1)	JL	New host record

Table 5.2 (continued)

Genus	Species	Number of isolates	Isolation source	Isolation region	Records on blueberry
1.3.1.2 Sclerotiniaceae					
Botrytis (2 species, 1 isolates)	*Botrytis cinerea*	2	Leaf (2)	LN, GZ	Dai et al. (2011)
1.4 Sordariomycetes					
1.4.1 Amphisphaeriales					
1.4.1.1 Apiosporaceae					
Nigrospora (2 isolates, 2 species)	*Nigrospora* sp.	2	Leaf (1)	FJ	Undetermined
			Stem (1)	HLJ	
1.4.1.2 Sporocadaceae					
Neopestalotiopsis	*Neo. castanopsidis*	2	Stem (2)	FJ	New host record
(14 species, 65 isolates)	*Neo. chrysea*	8	Leaf (8)	FJ	China (Shi et al., 2017)
	Neo. collariata	2	Leaf (2)	FJ	New host record
	Neo. concentrica	4	Leaf (2)	FJ	New host record
			Stem (2)	FJ	
	Neo. haikouensis	4	Stem (4)	FJ, GZ	New host record
	Neo. iberica	3	Stem (3)	JL, LN	New host record
	Neo. jiangxiensis	2	Stem (2)	JL	New host record
	Neo. keteleeriae	2	Stem (2)	FJ	New host record
	Neo. photiniae	2	Leaf (2)	GZ	New host record
	Neo. protearum	2	Leaf (2)	FJ	New host record
	Neo. rosae	10	Leaf (1)	GZ	New host-geography association record
			Stem (5)	HLJ, LN	
			Root (4)	LN	
	Neo. scalabiensis	2	Stem (2)	JL, LN	New host-geography association record

Table 5.2 (continued)

Genus	Species	Number of isolates	Isolation source	Isolation region	Records on blueberry
	Neo. subepidermalis	2	Stem (1)	LN	New host record
			Root (1)	LN	
	Neo. vacciniicola	20	Leaf (1)	JL	New host-geography association
			Stem (19)	HLJ, JL	record
Pestalotiopsis (46 isolates, 13 species)	*Pes. caulicola* sp. nov	2	Stem (2)	FJ	New species
	Pes. fujianensis sp. nov	2	Leaf (2)	FJ	New species
	Pes. vaccinii sp. nov	3	Leaf (3)	FJ, GZ	New species
	Pes. anhuiensis	2	Stem (2)	LN	New host record
	Pes. clavata	2	Leaf (1)	FJ	New host record
			Stem (1)	GZ	
	Pes. foliicola	2	Stem (2)	GZ	New host record
	Pes. hainanensis	2	Stem (2)	GZ	New host record
	Pes. kenyana	17	Leaf (13)	FJ, GZ	New host record
			Stem (4)	FJ, GZ	
	Pes. rhodomyrti	7	Leaf (3)	FJ, GZ	New host record
			Stem (4)	JL	
	Pes. tumidia	2	Leaf (2)	JL	New host record
	Pestalotiopsis sp.1	1	Leaf (1)	FJ	Undetermined
	Pestalotiopsis sp.2	2	Leaf (2)	FJ	Undetermined
	Pestalotiopsis sp.3	2	Stem (2)	JL	Undetermined
Robillarda (2 isolates, 1 species)	*Robillarda* sp.	2	Stem (2)	JL	New host record

Table 5.2 (continued)

Genus	Species	Number of isolates	Isolation source	Isolation region	Records on blueberry
1.4.2 Coniochaetales					
1.4.2.1 Coniochaetaceae					
Coniochaeta (2 isolates, 1 species)	*C. velutina*	2	Leaf (1)	FJ	New host record
			Stem (1)	FJ	
1.4.3 Diaporthales					
1.4.3.1 Cytosporaceae					
Cytospora (6 isolates, 3 species)	*C. mali*	2	Stem (2)	JL	New host record
	Cytospora sp.1	3	Root (3)	FJ	Undetermined
	Cytospora sp.2	1	Stem (1)	JL	Undetermined
1.4.3.2 Diaporthaceae					
Diaporthe (8 species, 36 isolates)	*D. arecae*	1	Leaf (1)	FJ	New host record
	D. discoidispora	3	Leaf (3)	FJ	New host record
	D. eres	13	Leaf (4)	GZ, JL	China (Yan et al., 2015)
			Stem (7)	JL	
			Root (2)	LN	
	D. hongkongensis	11	Leaf (3)	FJ	China (Li et al., 2017a)
			Stem (6)	FJ, GZ	
			Root (2)	FJ	
	D. oraccinii	1	Leaf (1)	FJ	New host record
	D. sojae	4	Leaf (3)	FJ, GZ	China (Li et al., 2023)
			Stem (1)	JL	
	D. tulliensis	1	Stem (1)	GZ	New host record
	D. unshiuensis	2	Stem (2)	JL	New host record

Table 5.2 (continued)

Genus	Species	Number of isolates	Isolation source	Isolation region	Records on blueberry
1.4.3.3 Schizoparmaceae					
Coniella (5 isolates, 1 species)	*Coniella quercicola*	5	Leaf (3)	FJ	New host record
			Stem (2)	FJ	
1.4.4 Glomerellales					
1.4.4.1 Glomerellaceae					
Colletotrichum (8 isolates, 3 species)	*C. fructicola*	5	Leaf (5)	FJ	China (Liu et al., 2020)
	C. henanense	1	Leaf (1)	FJ	New host record
	C. temperatum	2	Stem (2)	LN	New host record
1.4.5 Hypocreales					
1.4.5.1 Bionectriaceae					
Clonostachys (8 isolates, 3 species)	*C. chloroleuca*	1	Root (1)	LN	New host record
	C. farinosa	6	Leaf (1)	JL	New host record
			Stem (4)	HLJ, JL, LN	
			Root (1)	LN	
	C. rosea	1	Stem (1)	HLJ	New host record
1.4.5.2 Hypocreaceae					
Trichoderma (3 isolates, 1 species)	*Trichoderma* sp.	3	Root (3)	LN	New host record
1.4.5.3 Nectriaceae					
Calonectria (1 isolates, 1 species)	*Calonectria* sp.	1	Root (1)	GZ	Undetermined
Dactylonectria (4 isolates, 2 species)	*D. palmicola*	3	Root (2)	LN	New host record
	D. pauciseptata	1	Root (1)	LN	New host record
Ilyonectria (1 isolates, 1 species)	*I. liriodendri*	1	Root (1)	LN	New host record
Fusarium (46 isolates, 9 species)	*F. annulatum*	2	Leaf (1)	LN	New host record
			Stem (1)	LN	

Table 5.2 (continued)

Genus	Species	Number of isolates	Isolation source	Isolation region	Records on blueberry
	F. commune	5	Root (5)	LN	Li et al. (2023)
	F. concentricum	2	Root (2)	LN	New host record
	F. diversisporum	2	Stem (2)	JL	New host record
	F. fujikuroi	2	Leaf (1)	FJ	New host record
			Stem (1)	GZ	
	F. nanum	2	Stem (2)	LN	New host record
	F. oxysporum	28	Leaf (2)	FJ, GZ	Liu et al. (2014)
			Stem (18)	GZ, HLJ, Jilin, LN	
			Root (8)	LN	
	F. pilosicola	1	Stem (1)	FJ	New host record
	F. redolens	2	Root (2)	LN	New host record
Neocosmospora (12 isolates, 4 species)	*N. falciformis*	2	Root (2)	LN	New host record
	N. parceramosa	2	Stem (2)	GZ	New host record
	N. solani	4	Root (3)	LN	New host-geography association
			Stem (1)	GZ	record
	Neocosmospora sp.	4	Leaf (3)	FJ	Undetermined
			Stem (1)	FJ	

1.4.6 Sordariales

1.4.6.1 Chaetomiaceae

Arcopilus (4 isolates, 1 species)	*Arcopilus* sp.	4	Stem (2)	GZ	New host record
			Root (2)	JL	

Table 5.2 (continued)

Genus	Species	Number of isolates	Isolation source	Isolation region	Records on blueberry
1.4.7 Togniniales					
1.4.7.1 Togniniaceae					
Phaeoacremonium (1 isolates, 1 species)	*Phaeoacremonium scolyti*	1	Stem (1)	LN	New host record
1.4.8 Xylariales					
1.4.8.1 Hypoxylaceae					
Annulohypoxylon (2 isolates, 1 species)	*Annulohypoxylon* sp.	1	Leaf (1)	FJ	New host record
Hypoxylon (2 isolates, 1 species)	*Hypoxylon* sp.	2	Stem (1)	FJ	New host record
			Leaf (1)	FJ	
1.4.8.2 Xylariaceae					
Nemania (3 isolates, 1 species)	*Nemania* sp.	3	Leaf (1)	FJ	New host record
			Stem (2)	FJ	
Xylaria (1 isolates, 1 species)	*Xylaria* sp.	1	Stem (1)	FJ	New host record
2 Mucoromycota					
2.1 Mucoromycetes					
2.1.1 Mucorales					
2.1.1.1 Cunninghamellaceae					
Gongronella (2 isolates, 1 species)	*Gongronella butleri*	2	Stem (2)	GZ	New host record

5.3.3 Prevalence of Fungal Genera Associated with Blueberry Diseases

5.3.3.1 Distribution of fungal genera by isolation source.

The 121 isolates from leaf sample belong to twenty-two genera, with *Pestalotiopsis* (22% isolation rate of the total isolates), *Neopestalotiopsis* (15%), *Diaporthe* (12%) and *Alternaria* (12%) as the dominant genera (Figure 5.19a). The 249 isolates from stem sample belong to thirty-two genera, with *Neopestalotiopsis* (17%), *Alternaria* (13%), *Botryosphaeria* (12%) and *Fusarium* (10%) as the dominant genera (Figure 5.19b). The 59 isolates from root sample belong to seventeen genera, with *Fusarium* (29%), *Neocosmospora* (8%), *Neopestalotiopsis* (8%), *Diaporthe* (7%) and *Dactylonectria* (7%) as the dominant genera (Figure 5.19c).

Among the forty genera generates, nine genera distributed simultaneously in the three parts: *Neopestalotiopsis*, *Alternaria*, *Fusarium*, *Botryosphaeria*, *Diaporthe*, *Cladosporium*, *Epicoccum*, *Neocosmospora*, *Clonostachys*. Four genera were only found in leaves: *Botrytis*, *Neodeightonia*, *Phyllosticta* and *Annulohypoxylon*. Ten genera, including *Bipolaris*, *Pseudofusicoccum* and *Curvularia* were only found in stems. *Dactylonectria*, *Trichoderma*, *Ilyonectria* and *Calonectria* were only found in roots (Figure 5.20).
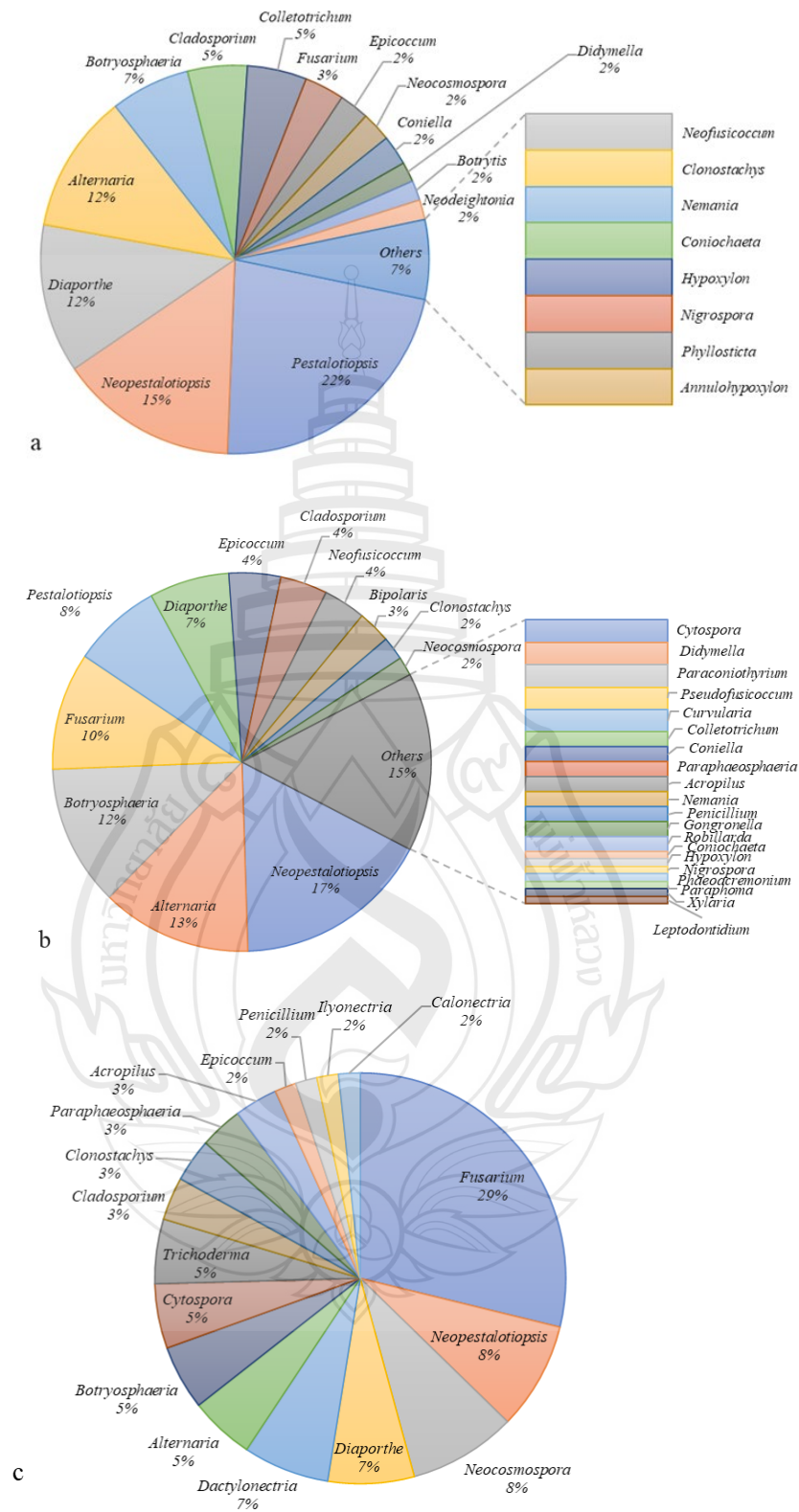
Note a leaf. b stem. c root.

Figure 5.19 Isolation rate (%) of genera from blueberry organs
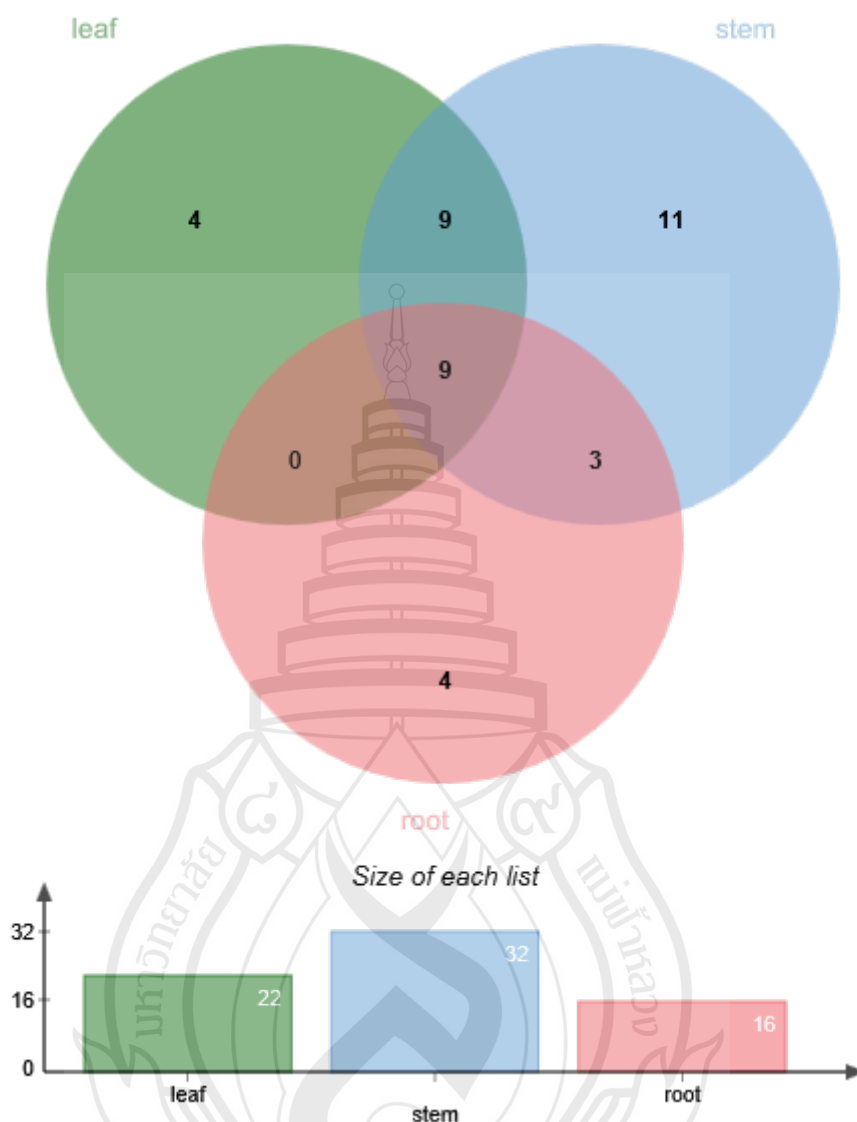
Figure 5.20 Distribution of fungal genera in blueberry leaf, stem and root

5.3.3.2 Distribution of fungal genera by collecting region.

In Fujian Province, 121 isolates belong to twenty-two genera were generated, with *Pestalotiopsis* (19%), *Neopestalotiopsis* (18%) and *Diaporthe* (13%) as dominant genera. In Guizhou Province, 59 isolates belong to fifteen genera were generated, with *Pestalotiopsis* (22%), *Fusarium* (12%) and *Diaporthe* (10%) as dominant genera. In Heilongjiang Province, 55 isolates belong to nine genera were generated, with *Alternaria* (27%), *Botryosphaeria* (27%) and *Bipolaris* (13%) as dominant genera. In Jilin Province, 101 isolates belong to nineteen genera were

generated, with *Neopestalotiopsis* (20%), *Alternaria* (18%) and *Diaporthe* (12%) as dominant genera.

   Neopestalotiopsis, *Fusarium* and *Botryosphaeria* species were the only three genera distributed in all the five regions. *Alternaria* was distributed in four regions except for Fujian Province, while *Coniella* was only found in Fujian. *Pestalotiopsis* and *Diaporthe* species were distributed in four regions except for Heilongjiang Province, while *Bipolaris* was only found in Heilongjiang (Figure 5.21).
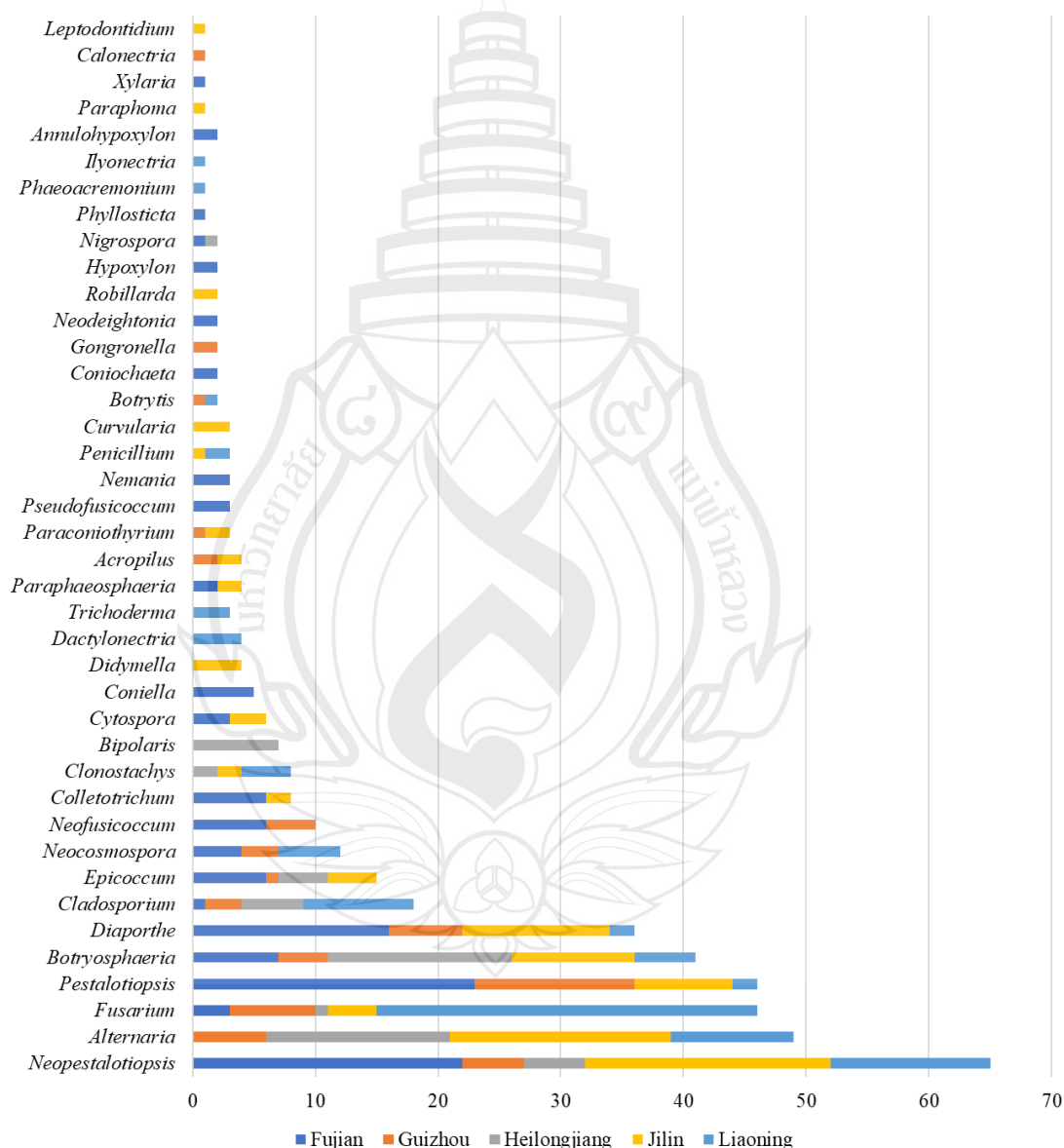
Figure 5.21 Distribution of fungal genera in five provinces of China

5.3.4 Characterization of Pestalotioid Fungi Associated with Blueberry Leaf, Stem and Root Diseases

Neopestalotiopsis Maharachch., K.D. Hyde & Crous, in Maharachchikumbura, Hyde, Groenewald, Xu & Crous, Stud. Mycol. 79: 135 (2014)

Classification: Sporocadaceae, Amphisphaeriales, Sordariomycetes, Ascomycota, Fungi (Hyde et al., 2024).

Notes: *Neopestalotiopsis*, typified by *Neopestalotiopsis protearum*, was proposed by Maharachchikumbura et al. (2014), distinguished from *Pestalotiopsis* by versicolourous median cells with indistinct conidiophores. As previously a portion of *Pestalotiopsis*, the genus *Neopestalotiopsis* is also common phytopathogens, endophytes and saprobes, and more and more new species have been observed in the recent years (Razaghi et al., 2024). Currently there are 119 epithets in the Index Fungorum (2024). Razaghi et al. (2024) made a re-evaluation on *Neopestalotiopsis*, and found that it is difficult to distinguish the two genera only based on morphology, because there are some morphological exceptions compared with previous recognized criterion, such as some members of *Neopestalotiopsis* and *Pestalotiopsis* produce more than 5-celled typical conidia, and distinct conidiophores and concolourous conidia were observed in many *Neopestalotiopsis* species. In addition, most Pestalotiopsis-like species are phylogenetically ambiguous, thus the type specimens of known species, especially species introduced by host-association, need to be further studied (Razaghi et al., 2024).

In this study, phylogenetic tree of *Neopestalotiopsis* was constructed based on ITS, *tef 1-α* and *β-tub* sequence data using ML and Bayesian analyses, with *Pseudopestalotiopsis cocos*, *Pseudopestalotiopsis indica* and *Pseudopestalotiopsis theae* as outgroups (Figure 5.22). New isolates from this study clustered into fourteen clades close to *Neo. castanopsidis*, *Neo. chrysea*, *Neo. collariata*, *Neo. concentrica*, *Neo. haikouensis Neo. jiangxiensis*, *Neo. keteleeriae*, *Neo. iberica*, *Neo. photiniae*, *Neo. protearum*, *Neo. rosae*, *Neo. scalabiensis*, *Neo. subepidermalis* and *Neo. vacciniicola*. Combined with morphological characters, sixty-five new collections were identified as fourteen species, including ten new host records.
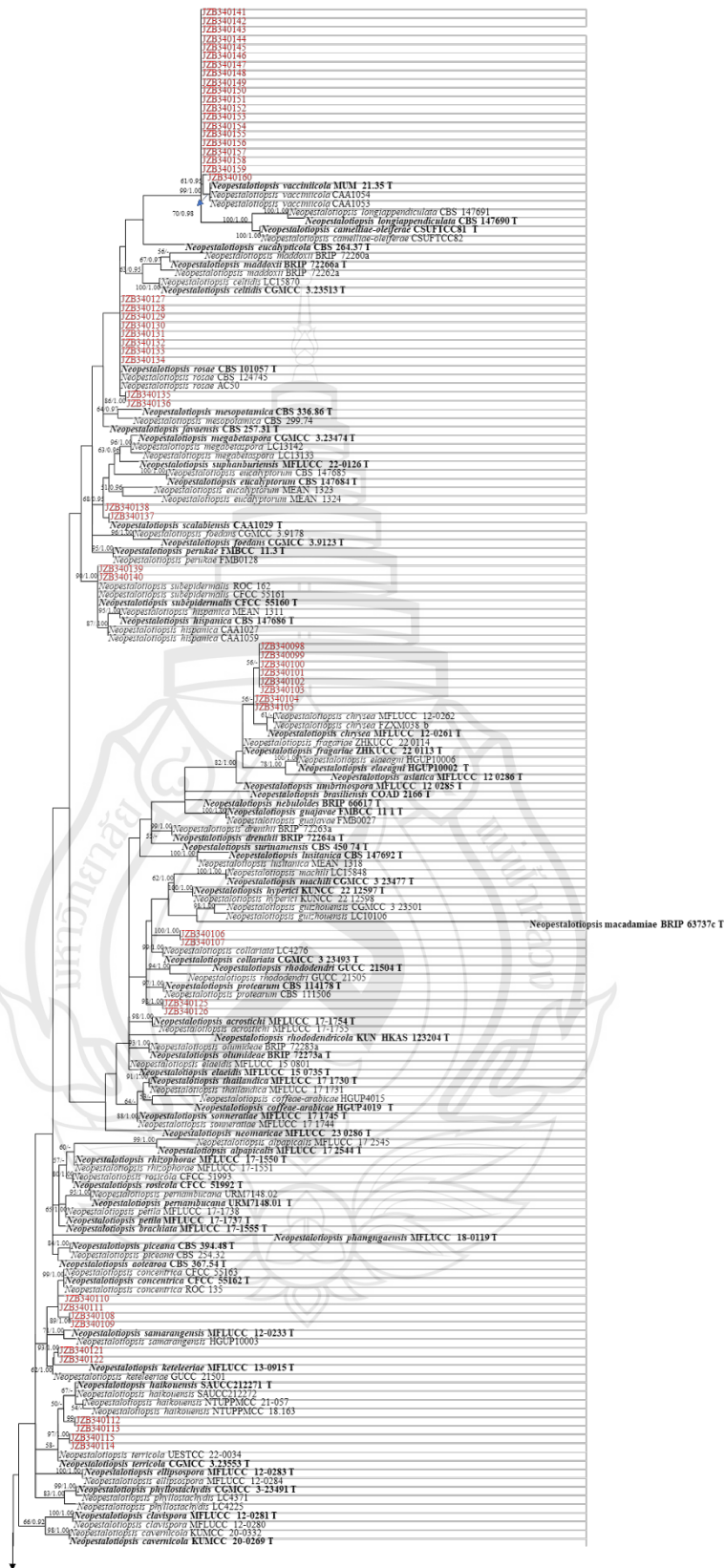
Figure 5.22 Phylogenetic tree generated from maximum likelihood (ML) analysis based on combined ITS, *tef 1-α* and *β-tub* sequence data of *Neopestalotiopsis*
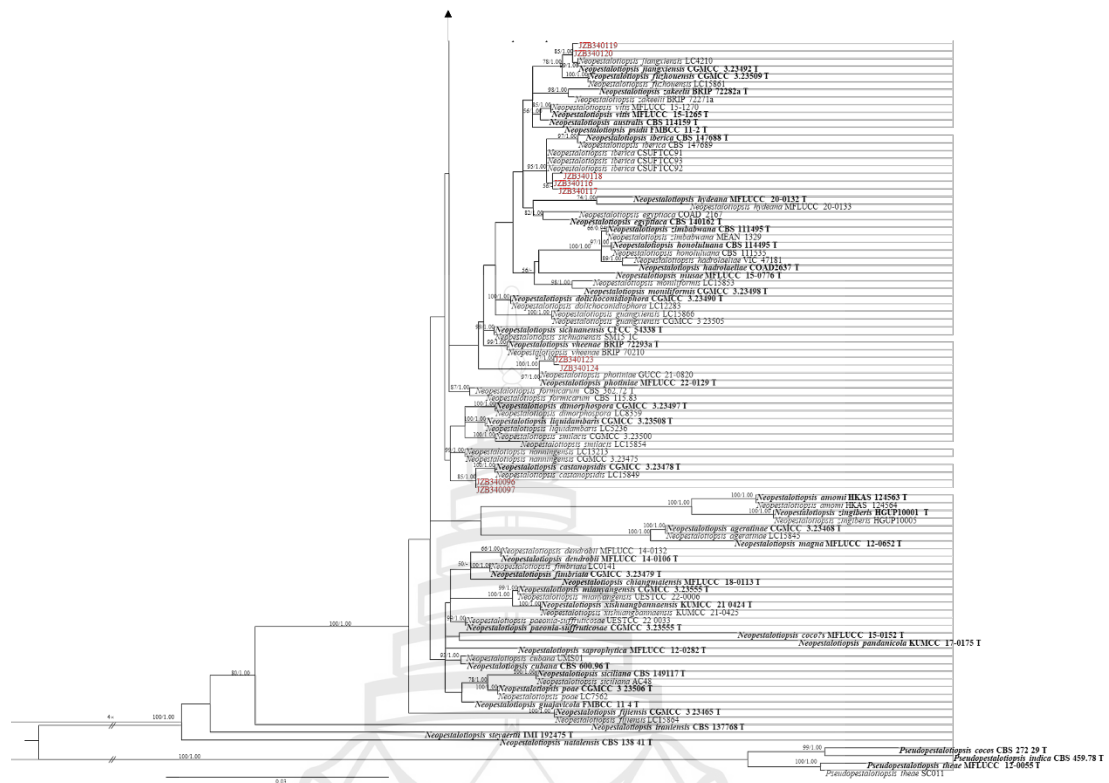
Figure 5.22 (continued)

Figure 5.22 The alignment comprises 1,785 characters with gaps. The tree is rooted with *Pseudopestalotiopsis cocos* (CBS 272.29), *Pseudopestalotiopsis indica* (CBS 459.78) and *Pseudopestalotiopsis theae* (MFLUCC 12-0055 and SC011). The tree topology of the ML analysis was similar to the Bayesian analysis. The best-scoring RAxML tree with a final likelihood value of -11172.378134 is presented. The matrix had 811 distinct alignment patterns, with 9.43% of undetermined characters or gaps. Estimated base frequencies were as follows: A = 0.234198, C = 0.273929, G = 0.213469, T = 0.278403; substitution rates AC = 0.945317, AG = 3.489706, AT = 1.239642, CG = 0.684809, CT = 4.846636, GT = 1.000000; gamma distribution shape parameter α = 0.640278. ML bootstrap support values ≥50% and Bayesian posterior probabilities (BYPP) ≥0.90 are given near the nodes. The scale bar indicates the number of nucleotide changes per site. Ex-type strains are indicated in bold and newly generated sequences are indicated in red.

Neopestalotiopsis castanopsidis P. Razaghi, F. Liu & L. Cai, in Razaghi, Raza, Han, Ma, Cai, Zhao, Chen, Phurbu & Liu, Stud. Mycol. 109: 214 (2024). Figure 5.23

Associated with stem blight of *Vaccinium corymbosum*. **Sexual morph:** Not observed. **Asexual morph:** *Conidiomata* globose, solitary or gregarious, semi-immersed or immersed, exuding globose, black conidial masses. *Conidiophores* indistinct, often reduced to conidiogenous cells. *Conidiogenous cells* discrete, ampulliform, flask-shaped or obclavate, hyaline, 9–14.5 × 2–5 μm ($\overline{x}$ = 12.9 × 3.2 μm, n = 30). *Conidia* fusoid to ellipsoid, straight to slightly curved, 4-septate, 20–23 × 7–9 μm ($\overline{x}$ = 21.5 × 8 μm, n = 30), L/W ratio = 2.7; basal cell obconic with a truncate base, hyaline, rugose and thin-walled, 3–4 μm long ($\overline{x}$ = 3.2 μm, n = 30); three median cells doliiform, 13–16 μm ($\overline{x}$ = 14.7 μm, n = 30) long, wall rugose, versicoloured, septa darker than the rest of the cell (second cell from the base pale brown, 4–5 μm long; third cell brown, 5–6 μm long; fourth cell brown, 4.5–5.5 μm long); apical cell 3–4.5 μm ($\overline{x}$ = 3.5 μm, n = 30) long, hyaline, conical to subcylindrical, thin- and smooth-walled, with 2–4 tubular apical appendages (mostly 3), arising from the apical crest, unbranched, filiform, flexuous, 17.5–38 μm ($\overline{x}$ = 24.5 μm, n = 30) long; basal appendage single, tubular, unbranched, centric, 4–7.5 μm ($\overline{x}$ = 6.1 μm, n = 30) long.

Culture characteristics – Colonies on PDA reaching 67 mm diam. after four days at 25°C, flat with lobate edge, concentric, white, aerial mycelium sparse, flocculence.

Material examined – China, Fujian Province, Longyan City, from diseased leaves of *Vaccinium corymbosum*, May 2023, X. H. Li and Y. Y. Zhou (dry cultures JZBH340096– JZBH340097), living cultures JZB340096– JZB340097.

Notes – The two new isolates from this study (JZB340096–JZB340097) phylogenetically close to the ex-type of *Neopestalotiopsis castanopsidis* (CGMCC 3.23478) with 85% ML bootstrap support and 1.00 Bayesian posterior probabilities. The morphology of the isolates is also similar to the description of the ex-type of *Neo. castanopsidis* (Razaghi et al., 2024). The two isolates are identified as *Neo. castanopsidis. Neopestalotiopsis castanopsidis* was introduced from *Castanopsis boisii* in China (Razaghi et al., 2024). This is the first report of *Neo. castanopsidis* on blueberry (*Vaccinium* spp.).

Figure 5.23 Morphological characters of *Neopestalotiopsis castanopsidis* (JZB340096)

Figure 5.23 a Colony on PDA after four days; b Colony on PDA after three weeks; c Conidiomata on PDA; d–f Conidiogenous cells; g–j Conidia; Scale bars: c=1000 μm; d=20 μm; e–j=10 μm

Neopestalotiopsis chrysea (Maharachch. & K.D. Hyde) Maharachch., K.D. Hyde & Crous, in Maharachchikumbura, Hyde, Groenewald, Xu & Crous, Stud. Mycol. 79: 138 (2014). Figure 5.24

Associated with leaf spot of *Vaccinium corymbosum*.

Sexual morph: Not observed. **Asexual morph:** *Conidiomata* globose, solitary or gregarious, semi-immersed or immersed, exuding globose, black conidial masses. *Conidiophores* indistinct, often reduced to conidiogenous cells. *Conidiogenous cells*

discrete, ampulliform, flask-shaped or obclavate, hyaline, 8.1–14.5 × 2.4–4.5 μm ($\overline{x}$ = 11.0 × 3.3 μm, n = 30). *Conidia* fusoid to ellipsoid, straight to slightly curved, 4-septate, 19.1–25.0 × 6.4–9.6 μm ($\overline{x}$ = 22.6 × 8.0 μm, n = 50), L/W ratio = 2.8; basal cell obconic with a truncate base, hyaline, rugose and thin-walled, 3.3–5.6 μm long ($\overline{x}$ = 4.2 μm, n = 20); three median cells doliiform, 13–17.4 μm ($\overline{x}$ = 15.2 μm, n = 20) long, wall rugose, versicoloured, septa darker than the rest of the cell (second cell from the base pale brown to brown, 3.7–5.4 μm long; third cell brown, 4.0–6.2 μm long; fourth cell brown, 3.9–5.5 μm long); apical cell 2.7–4.8 μm ($\overline{x}$ = 3.7 μm, n = 20) long, hyaline, conical to subcylindrical, thin- and smooth-walled, with 2–4 tubular apical appendages (mostly 3), arising from the apical crest, unbranched or branched at one appendage, filiform, flexuous, 11.2–37.0 μm ($\overline{x}$ = 22.4 μm, n = 30) long; basal appendage single, tubular, unbranched, centric, 3.0–11.6 μm ($\overline{x}$ = 5.6 μm, n = 30) long.

Culture characteristics – Colonies on PDA reaching 66–68 mm diam. after four days at 25°C, flat with lobate edge, concentric, colony from above white, becoming pale yellow after three weeks; colony from reverse pale yellow in centre, becoming rosy-buff after three weeks.

Material examined – China, Fujian Province, Longyan City, from diseased leaves of *Vaccinium corymbosum*, May 2023, X. H. Li and Y. Y. Zhou (dry cultures JZBH340098– JZBH340105), living cultures JZB340098–JZB340105.

Notes – In the phylogenetic tree of *Neopestalotiopsis*, eight new isolates from this study (JZB340098–JZB340105) clustered with *Neo. chrysea* with 56% ML bootstrap support. Sequences of JZB340098 and JZB340099 have 2 nucleotide differences (tub2: 2/520) from ex-type of *Neo. chrysea* (MFLUCC 12-0261), while sequences of JZB340100–JZB340105 have 3 nucleotide differences (tef1: 1/450; tub2: 2/520) from ex-type of *Neo. chrysea* (MFLUCC 12-0261). Morphology characters of our isolates are similar to *Neo. chrysea* except for smaller L/W ratio of conidia (2.8 vs. 3.7 in *Neo. chrysea*). In spite of this, the evidence is not sufficient to distinguish our isolates from *Neo. chrysea*. Based on phylogeny and morphology, we identified our new collections as *Neo. chrysea*. *Neopestalotiopsis chrysea* was originally introduced as *Pestalotiopsis chrysea* from dead plant material in China (Maharachchikumbura et al., 2012). Subsequently *Pes. chrysea* was transferred to *Neopestalotiopsis* as *Neopestalotiopsis chrysea* (Maharachchikumbura et al., 2014). *Neopestalotiopsis chrysea* has been reported to cause twig blight of rabbit-eye

blueberry (*Vaccinium virgatum*) in Fujian, China (Shi et al., 2017). Here we isolated the species in the same Province, on highbush blueberry (*Vaccinium corymbosum*).

In addition, we also compared the morphology of species adjacent to *Neo. chrysea*, including *Neo. fragariae*, *Neo. elaeagni*, *Neo. asiatica* and *Neo. umbrinospora*. As the comparation shown in table 5.3, their morphological characters are basically similar except for slight differences: the conidiogenous cells of *Neo. fragariae* is narrower, while the dimensions of conidiogenous cells of *Neo. chrysea* and *Neo. umbrinospora* are absent; and the number of apical appendages different among species. However, the differences are not distinct for the dimension ranges of conidiogenous cells, conidia and appendages are highly overlapped. If these species be synonymized need to be further studied.
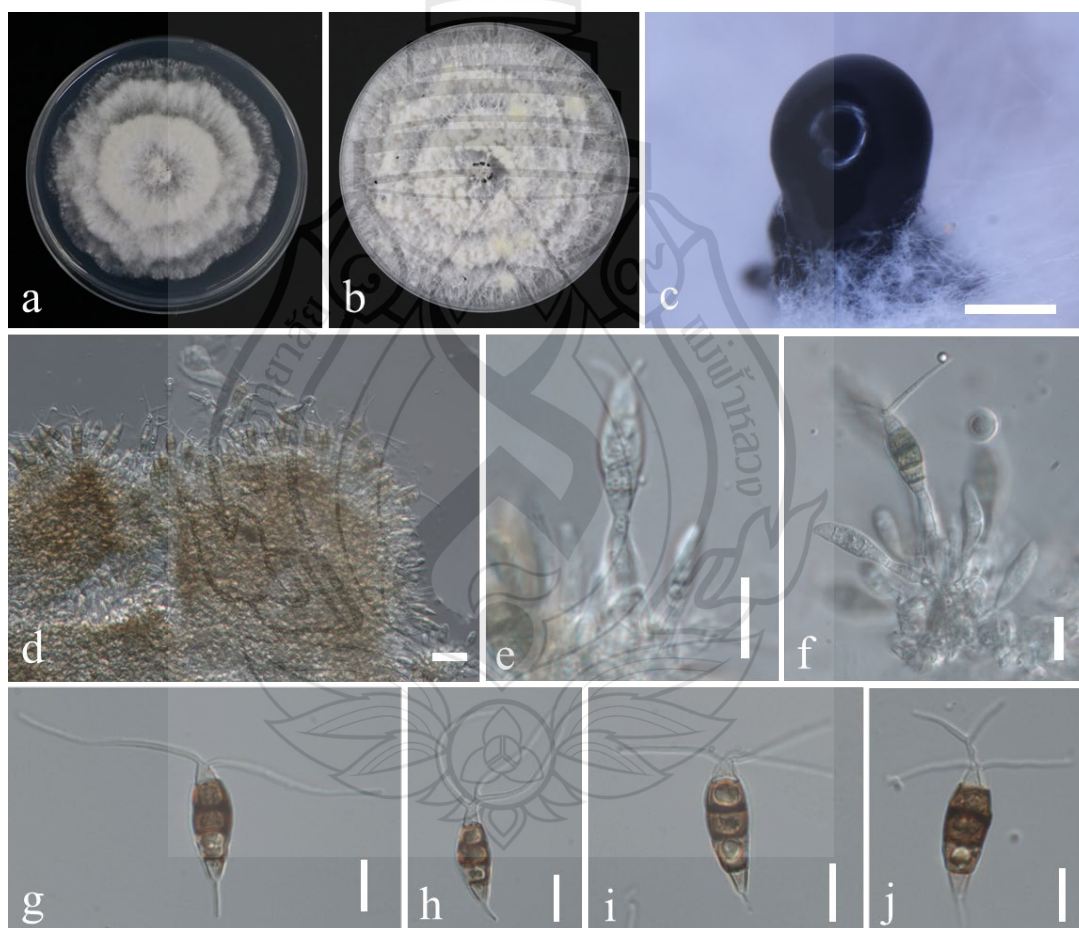
Figure 5.24 Morphological characters of *Neopestalotiopsis chrysea* (JZB340098)

Figure 5.24 a Colony on PDA after four days; b Colony on PDA after three weeks; c Conidiomata on PDA; d–f Conidiogenous cells; g–j Conidia; Scale bars: c=500μm; d=20 μm; e–j=10 μm

Table 5.3 Comparison of the conidial dimension of *Neopestalotiopsis* species related to this study

Species	Material examined	Conidiogenous cells (µm)	Conidial size (µm)	L/W ratio	Apical Appendages		Basal Appendage (µm)	Reference
					Number	Length (µm)		
	JZB340098	8.1–14.5 × 2.4–4.5	19.1–25.0 × 6.4–9.6	2.8	2–4 (mostly 3)	11.2–36.8	3.0–11.6	This study
Neo. chrysea	HMAS042855	-	20–24 × 5.5–7	3.7	3	22–30	3–6	Maharachchikumbura et al. (2012)
Neo. fragariae	ZHKUCC 22-0113	8–13 × 1–2	17–26 × 5–9	3.1	2–4 (mostly 3)	10.4–32.8	3.0–11.5	Prematunga et al. (2022)
Neo. elaeagni	GUCC 21002	8–13 × 2–3	19–25 × 4.5–7	-	1–3	13–30	5–7.5	He et al. (2022)
Neo. asiatica	MFLUCC 12–0286	3–12	20–26 × 5–7	3.6	2–4 (mostly 3)	20–30	4–8	Maharachchikumbura et al. (2012)
Neo. umbrinospora	MFLUCC 12–0285	-	19–25 × 6–8	3.3	1–3 (mostly 3)	22–35	5–7	Maharachchikumbura et al. (2012)
	JZB340113	6.2–17.6 × 2.0–5.2	19.8–24.7 × 6.7–9.4	2.8	2–4 (mostly 3)	15.0–33.0	2.1–5.7	This study
	JZB340114	7.5–18.2 × 2.2–4.9	15.9–23.2 × 5.6–8.2	2.7	2–3 (mostly 2)	13.2–26.7	2.5–7.2	This study
Neo. haikouensis	SAUCC212271	5.0–10.0 × 2.0–6.0	16.0–22.0 × 4.5–7.0	-	2–3 (mostly 3)	13.5–24.0	2.0–7.0	Zhang et al. (2022)
Neo. terricola	HKAS123213	2.5–3.5 × 2–3	20–23 × 8–9.5	2.5	3	15–23	4–6	Li et al. (2022)
	JZB340123	8.0–17.0 × 2.9–5.2	17.0–25.6 × 6.5–8.9	2.6	2–3 (mostly 3)	18.7–39.3	3.9–8.4	This study
Neo. photiniae	HKAS 125895	1–3 × 2–4	20–29 × 5–12	2.6	2–3	17–33	1–6	Sun et al. (2023)

Neopestalotiopsis collariata P. Razaghi, F. Liu & L. Cai, in Razaghi, Raza, Han, Ma, Cai, Zhao, Chen, Phurbu & Liu, Stud. Mycol. 109: 215 (2024). Figure 5.25.

Associated with leaf spot of *Vaccinium corymbosum*. **Sexual morph:** Not observed. **Asexual morph:** *Conidiomata* globose, solitary or gregarious, semi-immersed or immersed, exuding globose, black conidial masses. *Conidiophores* indistinct, often reduced to conidiogenous cells. *Conidiogenous cells* discrete, ampulliform, flask-shaped or obclavate, hyaline, 7.5–12.5 × 2–3 μm ($\overline{x}$ = 9.5 × 2.7 μm, n = 30). *Conidia* fusoid to ellipsoid, straight to slightly curved, 4-septate, 18–24 × 7.5–10 μm ($\overline{x}$ = 21.7 × 8.7 μm, n = 30), L/W ratio = 2.4; basal cell obconic with a truncate base, hyaline, rugose and thin-walled, 3.5–4 μm long ($\overline{x}$ = 4.0 μm, n = 30); three median cells doliiform, 15.5–19.5 μm ($\overline{x}$ = 18.0 μm, n = 30) long, wall rugose, versicoloured, septa darker than the rest of the cell (second cell from the base pale brown, 5–6 μm long; third cell brown, 5–7 μm long; fourth cell brown, 5.5–7 μm long); apical cell 3.5–5.5 μm ($\overline{x}$ = 4.7 μm, n = 30) long, hyaline, conical to subcylindrical, thin- and smooth-walled, with 2–4 tubular apical appendages (mostly 3), arising from the apical crest, unbranched, filiform, flexuous, 18.5–30 μm ($\overline{x}$ = 22.6 μm, n = 30) long; basal appendage single, tubular, unbranched, centric, 4.5–5.5 μm ($\overline{x}$ = 5.0 μm, n = 30) long.

Culture characteristics – Colonies on PDA reaching 67 mm diam. after four days at 25°C, flat with lobate edge, concentric, white, aerial mycelium sparse, flocculence.

Material examined – China, Fujian Province, Longyan City, from diseased leaves of *Vaccinium corymbosum*, May 2023, X. H. Li and Y. Y. Zhou (dry cultures JZBH340106–JZBH340107), living cultures JZB340106–JZB340107.

Notes – The two new isolates from this study (JZB340106–JZB340107) phylogenetically close to the ex-type of *Neopestalotiopsis collariata* (CGMCC 3.23493). The morphology of the isolates is also similar to the description of the ex-type of *Neo. collariata* (Razaghi et al., 2024). The two isolates are identified as *Neo. collariata*. *Neo. collariata* was introduced from *Rhododendron* (Ericaceae) and branches of *Diospyros kaki* in Jiangxi Province and Fujian Province in China (Razaghi et al., 2024). This is the first report of *Neo. collariata* on blueberry (*Vaccinium* spp.), which also suggesting the re-emergence of the species from Ericaceae host in Fujian Province, China.

Figure 5.25 Morphological characters of *Neopestalotiopsis collariata* (JZB340106)

Figure 5.25 a Colony on PDA after four days; b Colony on PDA after three weeks; c Conidiomata on PDA; d–f Conidiogenous cells; g–j Conidia; Scale bars: c=1000 μm; d=20 μm; e–j=10 μm.

Neopestalotiopsis concentrica C. Peng & C.M. Tian, in Peng, Crous, Jiang, Fan, Liang & Tian, Persoonia 49: 227 (2022)

Associated with leaf spot and stem blight of *Vaccinium corymbosum*. For morphological description, see Peng et al. (2022).

Material examined – China, Fujian Province, Longyan City, from leaf spot of *Vaccinium corymbosum*, May 2023, X. H. Li and Y. Y. Zhou (dried cultures JZBH340108–JZBH340109), living cultures JZB340108–JZB340109; *ibid.*, from stem blight of *Vaccinium corymbosum*, May 2023, X. H. Li and Y. Y. Zhou (dried cultures JZBH340110–JZBH340111), living cultures JZB340110–JZB340111.

Notes – In the phylogenetic analysis, four isolates obtained in the current study (JZB340108–JZB340111) clustered with ex-type of *Neopestalotiopsis concentrica* (CFCC 55162). And the morphological characters are similar to the ex-type isolate of *Neo. concentrica* (Peng et al., 2022). *Neopestalotiopsis concentrica* was introduced by Peng et al. (2022) from spines of *Rosa* spp. in China. And Zhang et al. (2024) isolated the species from leaf spots of *Rhapis excelsa*. This is the first report of *Neopestalotiopsis concentrica* on *Vaccinium* spp.

Neopestalotiopsis haikouensis Z.X. Zhang, J.W. Xia & X.G. Zhang, in Zhang, Liu, Liu, Mu, Zhang & Xia, MycoKeys 88: 181 (2022). Figure 5.26, Figure 5.27

Associated with stem blight of *Vaccinium corymbosum*.

Description from JZB340113 (Figure 5.26): **Sexual morph:** Not observed. **Asexual morph:** *Conidiomata* globose, solitary or gregarious, semi-immersed or immersed, exuding globose, black conidial masses. *Conidiophores* indistinct, often reduced to conidiogenous cells. *Conidiogenous cells* discrete, ampulliform, flask-shaped or cylindrical, hyaline, 6.2–17.6 × 2.0–5.2 μm ($\overline{x}$ = 11.6 × 3.7 μm, n = 25). *Conidia* fusoid to ellipsoid, straight to slightly curved, 4-septate, 19.8–24.7 × 6.7–9.4 μm ($\overline{x}$ = 21.7 × 7.8 μm, n = 40), L/W ratio = 2.8; basal cell obconic with a truncate base, hyaline, rugose and thin-walled, 2.6–4.8 μm long ($\overline{x}$ = 3.6 μm, n = 30); three median cells doliiform, 13.3–18.2 μm ($\overline{x}$ = 14.6 μm, n = 30) long, wall rugose, versicoloured, septa darker than the rest of the cell (second cell from the base pale brown to brown, 3.6–5.4 μm long; third cell brown, 4.7–6.8 μm long; fourth cell brown, 3.5–6.0 μm long); apical cell 3.0–5.0 μm ($\overline{x}$ = 3.9 μm, n = 30) long, hyaline, conical to subcylindrical, thin- and smooth-walled, with 2–4 tubular apical appendages (mostly 3), arising from the apical crest, unbranched or branched at one appendage, filiform, flexuous, 15.0–33.0 μm ($\overline{x}$ = 22.5 μm, n = 50) long; basal appendage single, tubular, unbranched, centric, 2.1–5.7 μm ($\overline{x}$ = 4.1 μm, n = 30) long.

Description from JZB340114 (Figure 5.27): **Sexual morph:** Not observed. **Asexual morph:** *Conidiomata* globose, solitary or gregarious, semi-immersed or superficial, exuding globose, black conidial masses. *Conidiophores* indistinct, often reduced to conidiogenous cells. *Conidiogenous cells* discrete, ampulliform, flask-shaped or obclavate, hyaline, 7.5–18.2 × 2.2–4.9 μm ($\overline{x}$ = 11.6 × 3.4 μm, n = 30). *Conidia* fusoid to ellipsoid, straight to slightly curved, 4-septate, 15.9–23.2 × 5.6–8.2

μm (x̄ = 19.0 × 6.9 μm, n = 40), L/W ratio = 2.7; basal cell obconic with a truncate base, hyaline, rugose and thin-walled, 2.6–5.8 μm long (x̄ = 3.6 μm, n = 30); three median cells doliiform, 11.1–14.9 μm (x̄ = 12.8 μm, n = 30) long, wall rugose, versicoloured, septa darker than the rest of the cell (second cell from the base pale brown to brown, 3.1–5.8 μm long; third cell brown, 3.5–6.3 μm long; fourth cell brown, 3.3–4.9 μm long); apical cell 2.4–5.2 μm (x̄ = 3.1 μm, n = 30) long, hyaline, conical to subcylindrical, thin- and smooth-walled, with 2–3 tubular apical appendages (mostly 2), arising from the apical crest, unbranched or branched at one appendage, filiform, flexuous, 13.2–26.7 μm (x̄ = 19.0 μm, n = 50) long; basal appendage single, tubular, unbranched, centric, 2.5–7.2 μm (x̄ = 4.7 μm, n = 30) long.

Culture characteristics – Colonies on PDA reaching 62–67 mm diam. after four days at 25°C with undulate edge, concentric, white, becoming buff after three weeks with dense felt mycelium, and produce abundant black conidiomata.

Material examined – China, Fujian Province, Longyan City, from diseased stems of *Vaccinium corymbosum*, May 2023, X. H. Li and Y. Y. Zhou (dry cultures JZBH340112–JZBH340113), living cultures JZB340112–JZB340113; Guizhou Province, Majiang County, from diseased leaves of *Vaccinium corymbosum*, May 2023, X. H. Li and Y. Y. Zhou (dry cultures JZBH340114–JZBH340115), living cultures JZB340114–JZB340115.

Notes – In the phylogenetic tree, four new isolates (JZB340112–JZB340115) formed two clades related to *Neo. haikouensis* and *Neo. terricola*. Sequences of JZB340112 and JZB340113 have 5 nucleotide differences (ITS: 1/550; tef1: 3/450; tub2:1/520) from *Neo. haikouensis*, and 3 nucleotide differences (tef1: 2/450; tub2: 1/520) from *Neo. terricola*; sequences of JZB340114 and JZB340115 have 5 nucleotide differences (ITS: 1/550; tub2: 4/520) from *Neo. haikouensis*, and 2 nucleotide differences (tub2: 2/520) from *Neo. terricola*. To confirm the relationship of the two clades, representative isolates (JZB340113 and JZB340114) was selected to observe morphology respectively. The comparison of morphological characters among *Neo. haikouensis*, *Neo. terricola* and the two clades was shown in table 3. The dimension of conidial size, apical appendages and basal appendages are similar, while the conidiogenous cells of *Neo. terricola* are shorter than the other three (2.5–3.5 × 2–3 μm vs. 5.0–10.0 × 2.0–6.0 μm in *Neo. haikouensis*, 6.2–17.6 × 2.0–5.2 μm in JZB340113

and 7.5–18.2 × 2.2–4.9 μm in JZB340114). The characters of culture are slightly different between JZB340113 and JZB340114, for the colony of JZB340113 showed more obvious concentric character in the early stage, it may because of the difference between isolates. The morphology between *Neo. haikouensis* and *Neo. terricola* was indistinguishable, while *Neo. haikouensis* (Zhang et al., 2022) was introduced before *Neo. terricola* (Li et al., 2022). Therefore, we identified all the four new isolates as *Neo. haikouensis*. Whether *Neo. terricola* will be synonymized under *Neo. haikouensis* need to be further studied. *Neo. haikouensis* was introduced by Zhang et al. (2022) from diseased leaves of *Ilex chinensis* in China. This is the first report of *Neo. haikouensis* on blueberry (*Vaccinium* spp.).
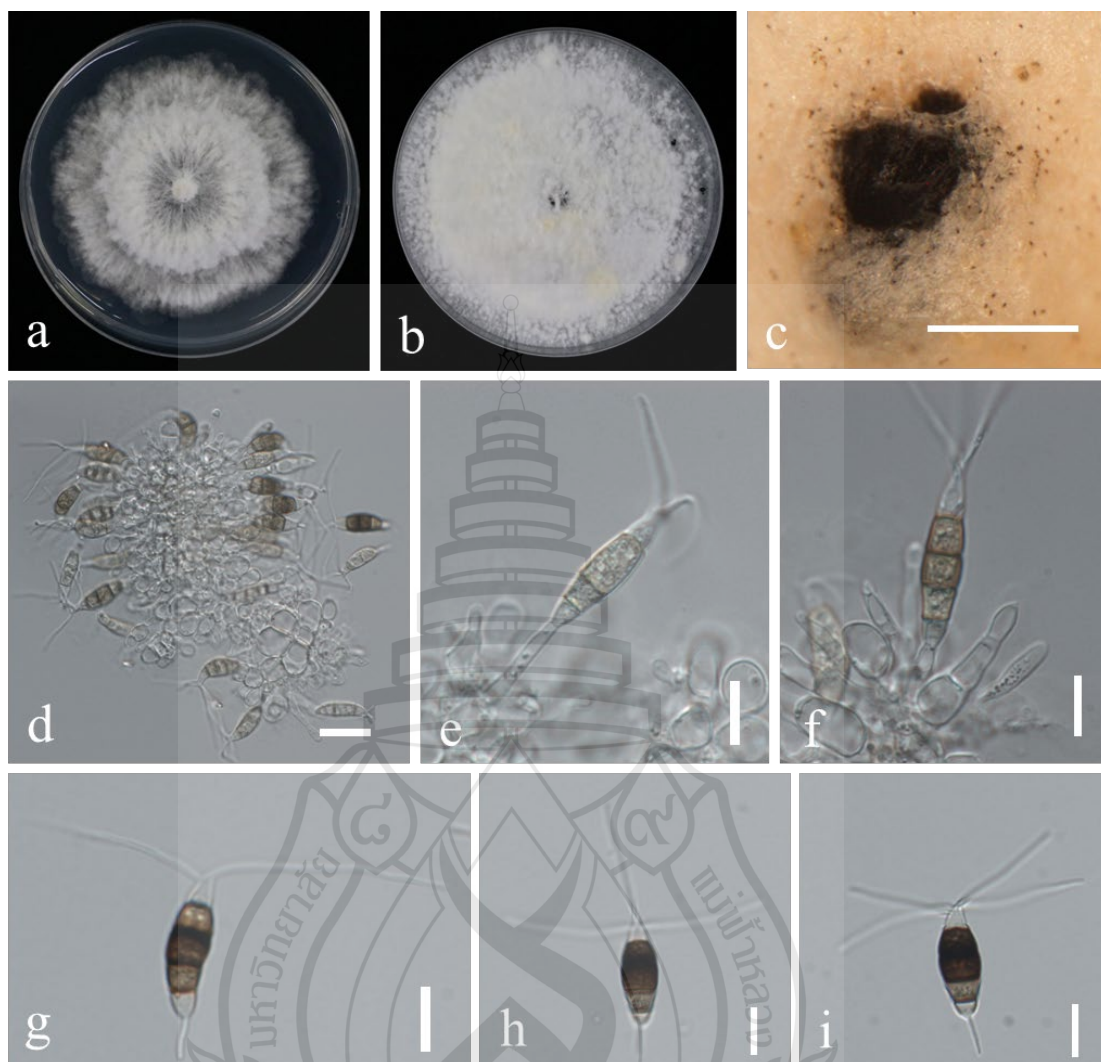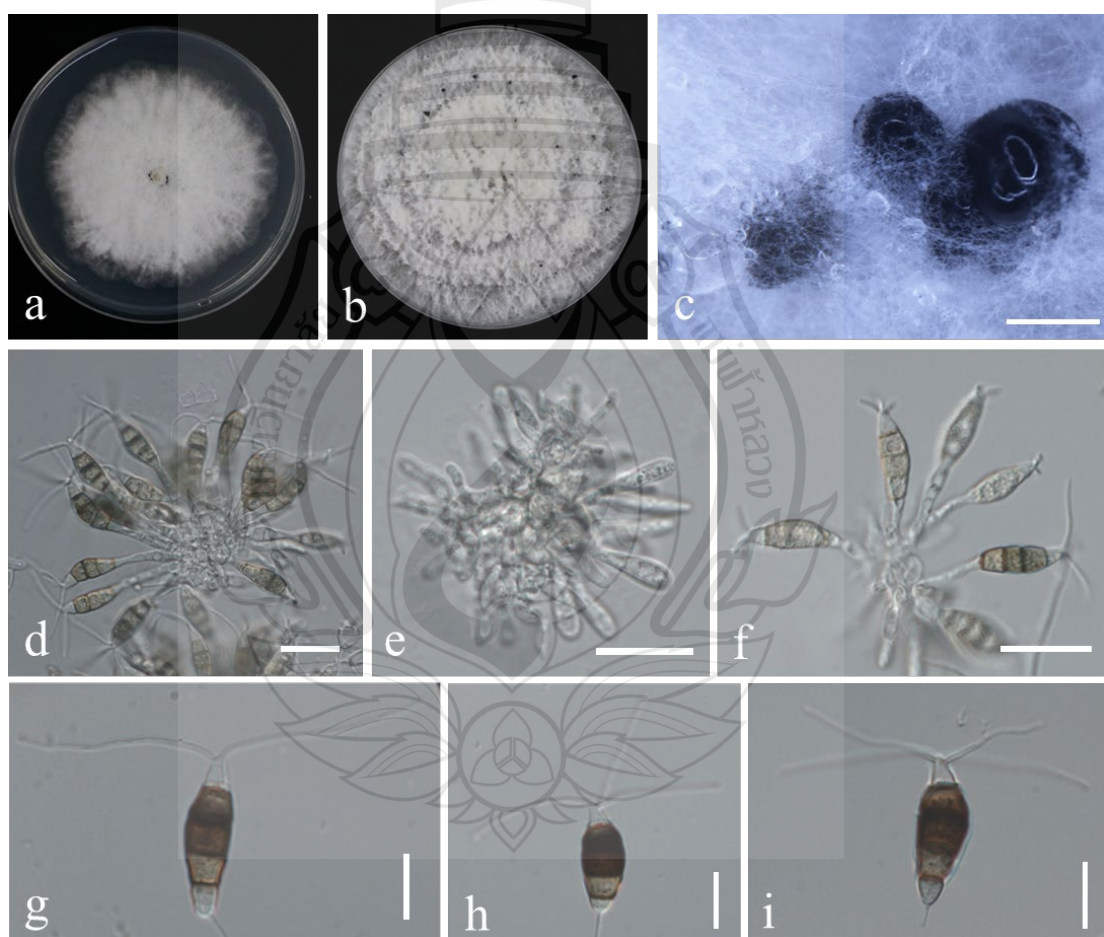

Figure 5.26 Morphological characters of *Neopestalotiopsis haikouensis* (JZB340113)

Figure 5.26 a Colony on PDA after four days; b Colony on PDA after three weeks; c Conidiomata on PDA; d–f Conidiogenous cells; g–i Conidia; Scale bars: c=1000 μm; d–f=20 μm; g–i=10 μm
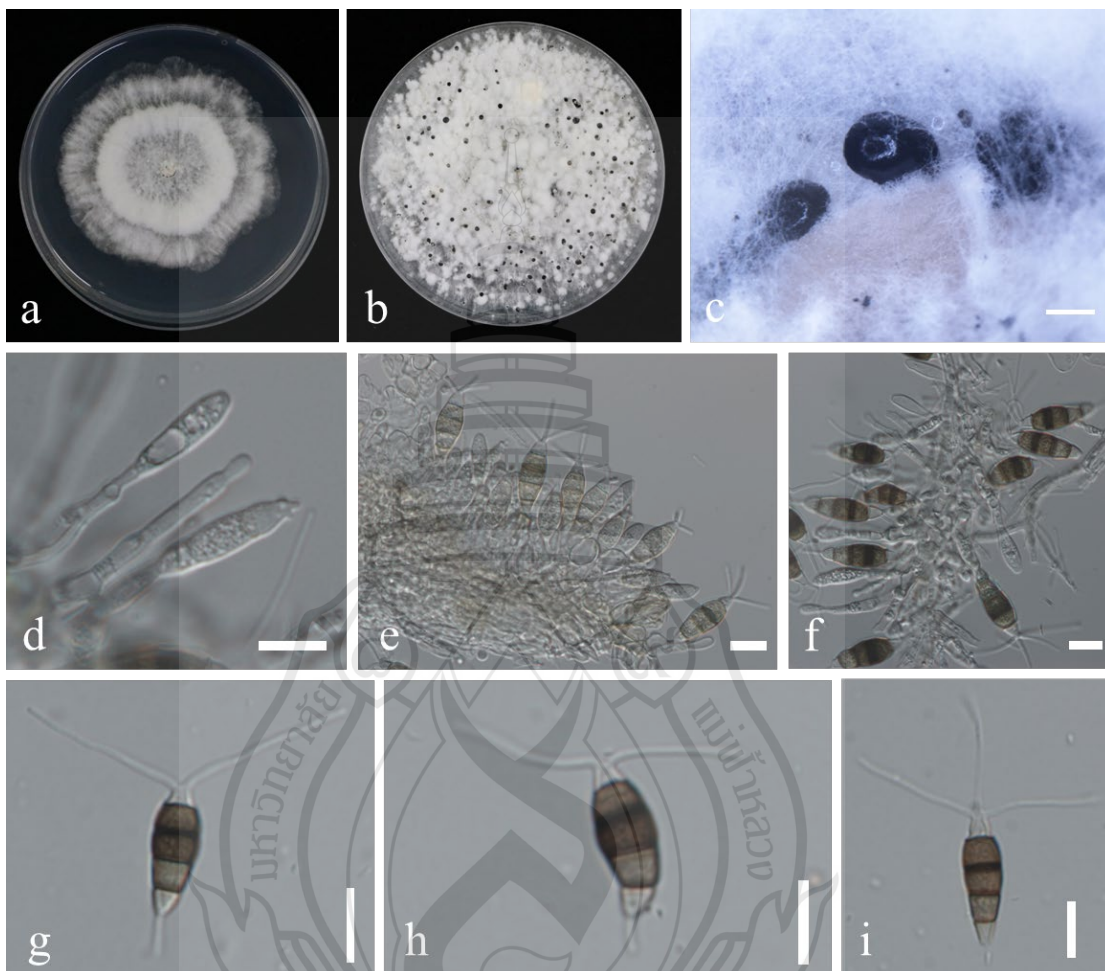
Figure 5.27 Morphological characters of *Neopestalotiopsis haikouensis* (JZB340114)

Figure 5.27 a Colony on PDA after four days; b Colony on PDA after three weeks; c Conidiomata on PDA; d–f Conidiogenous cells; g–j Conidia; Scale bars: d–f=10 μm.

Neopestalotiopsis iberica E. Diogo, M.H. Bragança & A.J.L. Phillips, in Diogo, Gonçalves, Silva, Valente, Bragança & Phillips, Mycol. Progr. 20(11): 1449 (2021).

Associated with stem blight of *Vaccinium* spp. For morphological description, see Diogo et al. (2021).

Material examined – China, Liaoning Province, Huludao City, from stem blight of *Vaccinium corymbosum*, April 2023, X. H. Li (dried culture JZBH340116–JZBH340117), living cultures JZB340116–JZB340117; *ibid.*, Jilin Province, Gongzhuling City, from stem blight of *Vaccinium angustifolium*, June 2023, X. H. Li, Y. Y. Zhou & P. Z. Chen (dried culture JZBH340118), living cultures JZB340118.

Notes – In the phylogenetic analysis, three isolates obtained in the current study (JZB340116–JZB340118) clustered together with reference isolates of *Neopestalotiopsis iberica* (including ex-type CBS 147688) with 95% ML bootstrap support and 1.00 Bayesian posterior probabilities. And the morphological characters of our isolates resemble to the type description of *Neo. iberica* (Diogo et al., 2021). *Neopestalotiopsis iberica* was introduced by Diogo et al. (2021) from diseased leaf and stem of *Eucalyptus globulus* in Portugal and Spain. In China, the species has been reported to cause leaf spots on *Camellia oleifera* and *Synsepalum dulcificum* (Li et al., 2021; You et al., 2024). The three isolates generated in this study were identified as *Neopestalotiopsis iberica* as a new host record on *Vaccinium* spp.

Neopestalotiopsis jiangxiensis P. Razaghi, F. Liu & L. Cai, in Razaghi, Raza, Han, Ma, Cai, Zhao, Chen, Phurbu & Liu, Stud. Mycol. 109: 226 (2024).

Associated with stem blight of *Vaccinium angustifolium*. For morphological description and illustration, see Razaghi et al. (2024).

Material examined – China, Jilin Province, Gongzhuling City, from stem blight of *Vaccinium angustifolium*, June 2023, X. H. Li, Y. Y. Zhou and P.Z. Chen (dried cultures JZBH340119–JZBH340120), living cultures JZB340119–JZB340120.

Notes – In the phylogenetic tree, two isolates obtained in the current study (JZB340119–JZB340120) clustered with the ex-type of *Neopestalotiopsis jiangxiensis* (CBS 114159) with 85% bootstrap support and 1.00 posterior probabilities. And the morphological characters are similar to description of *Neo. jiangxiensis* (Razaghi et al., 2024). *Neopestalotiopsis jiangxiensis* was introduced from *Rhododendron latoucheae* (Ericaceae) in China (Razaghi et al., 2024), and *R. latoucheae* was the only host

reported previously. This is the first report of *Neo. jiangxiensis* on *Vaccinium angustifolium*, which also belong to Ericaceae.

Neopestalotiopsis keteleeriae (Y. Song, K.D. Hyde & Yong Wang bis) P. Razaghi, F. Liu & L. Cai, in Razaghi, Raza, Han, Ma, Cai, Zhao, Chen, Phurbu & Liu, Stud. Mycol. 109: 229 (2024).

Associated with stem blight of *Vaccinium corymbosum*. For morphological description, see Song et al. (2014).

Material examined – China, Fujian Province, Longyan City, from stem blight of *Vaccinium corymbosum*, May 2023, X. H. Li and Y. Y. Zhou (dried culture JZBH340121–JZBH340122), living cultures JZB340121–JZB340122.

Notes – In the phylogenetic analysis, two isolates obtained in the current study (JZB340121 and JZB340122) clustered with reference isolates of *Neopestalotiopsis keteleeriae* (including ex-type MFLUCC 13-0915) with 62% bootstrap support and 1.00 posterior probabilities. The morphological characters of our isolates resemble to the type description of *Neo. keteleeriae* (Song et al., 2014). *Neopestalotiopsis keteleeriae* was introduced by Song et al. (2014) as '*Pestalotiopsis keteleeria*' from diseased leaves of *Keteleeria* in China. Soon after, Maharachchikumbura et al. (2014) proposed the genus *Neopestalotiopsis*, to accommodate segregates of *Pestalotiopsis*, comprising the clade in which '*Pestalotiopsis keteleeria*' located, while '*Pestalotiopsis keteleeria*' was not included in the data set. The species was referred to as '*Neopestalotiopsis keteleeria*' or '*Neo. keteleerie*' in the subsequent publications (Senanayake et al., 2020; Li et al., 2021; Yang et al., 2021). However, Razaghi et al. (2024) found that the sequence of transcription factor (tef) of ex-type (MFLUCC 13-0915) in these publications was inconsistent with that in the original publication. According to the latest classification, *Neopestalotiopsis keteleeriae* was officially established as a new combination, and *Neo. rhapidis* (introduced by Yang et al. in 2021 from leaf spots of *Rhapis excelsa* in China) was synonymised under *Neo. keteleeriae* (Razaghi et al., 2024). This is the first report of *Neopestalotiopsis keteleeriae* on *Vaccinium* spp.

Neopestalotiopsis photiniae Y.R. Sun & Yong Wang bis, in Sun, Jayawardena, Sun & Wang, Microbiology Spectrum: e03987-22, 6 (2023). Figure 5.28

Associated with leaf spot of *Vaccinium corymbosum*. **Sexual morph:** Not observed. **Asexual morph:** *Conidiomata* globose, gregarious, semi-immersed or superficial, exuding globose, black conidial masses. *Conidiophores* indistinct, often reduced to conidiogenous cells. *Conidiogenous cells* discrete, ampulliform, flask-shaped or obclavate, hyaline, 8.0–17.0 × 2.9–5.2 μm ($\overline{x}$ = 12.4 × 3.9 μm, n = 25). *Conidia* fusoid to ellipsoid, straight to slightly curved, 4-septate, 17.0–25.6 × 6.5–8.9 μm ($\overline{x}$ = 20.6 × 7.9 μm, n = 40), L/W ratio = 2.6; basal cell obconic with a truncate base, hyaline, rugose and thin-walled, 2.1–5.4 μm long ($\overline{x}$ = 3.4 μm, n = 30); three median cells doliiform, 11.6–16.8 μm ($\overline{x}$ = 14.6 μm, n = 30) long, wall rugose, versicoloured, septa darker than the rest of the cell (second cell from the base pale brown to brown, 2.9–5.9 μm long; third cell brown, 3.7–6.5 μm long; fourth cell brown, 3.0–5.9 μm long); apical cell 2.7–5.1 μm ($\overline{x}$ = 3.5 μm, n = 30) long, hyaline, conical to subcylindrical, thin- and smooth-walled, with 2–3 tubular apical appendages (mostly 3), arising from the apical crest, unbranched or branched at one appendage, filiform, flexuous, 18.7–39.3 μm ($\overline{x}$ = 23.5 μm, n = 50) long; basal appendage single, tubular, unbranched, centric, 3.9–8.4 μm ($\overline{x}$ = 5.7 μm, n = 30) long.

Culture characteristics – Colonies on PDA reaching 58 mm diam. after four days at 25°C, concentric with undulate edge, colony white, becoming pale yellow after three weeks.

Material examined – China, Guizhou Province, Majiang County, from diseased leaves of *Vaccinium corymbosum*, May 2023, X. H. Li and Y. Y. Zhou (dry cultures JZBH340123– JZBH340124), living cultures JZB340123– JZB340124.

Notes – In the phylogenetic tree, the two new isolates from this study (JZB340123 and JZB340124) clustered close to *Neopestalotiopsis photiniae* (MFLUCC 22-0129) with 100% ML bootstrap support and 1.00 Bayesian posterior probabilities. Sequences of the two new isolates have 3 nucleotide differences in tub2 from *Neo. photiniae*. The comparison of morphological characters between the new isolates and *Neo. photiniae* was shown in table 3. Most morphological characters of the isolates are similar to the description of the ex-type of *Neo. photiniae* except for longer conidiogenous cells (8.0–17.0 μm vs. 1–3 μm), and faster growth rate of the culture

(Sun et al., 2023). However, the phylogenetic relationship and other highly overlapped morphological characters could not support the establish of the new species. Therefore, we identify the two isolates as *Neo. photiniae*. *Neopestalotiopsis photiniae* was introduced from *Photinia serratifolia* leaf spot in Guizhou Province, China (Sun et al., 2023). This is the first report of *Neo. photiniae* on blueberry (*Vaccinium* spp.), also from leaf spot disease in Guizhou Province. Therefore, we speculate that *Neo. photiniae* could be a common plant pathogen in Guizhou Province in China.
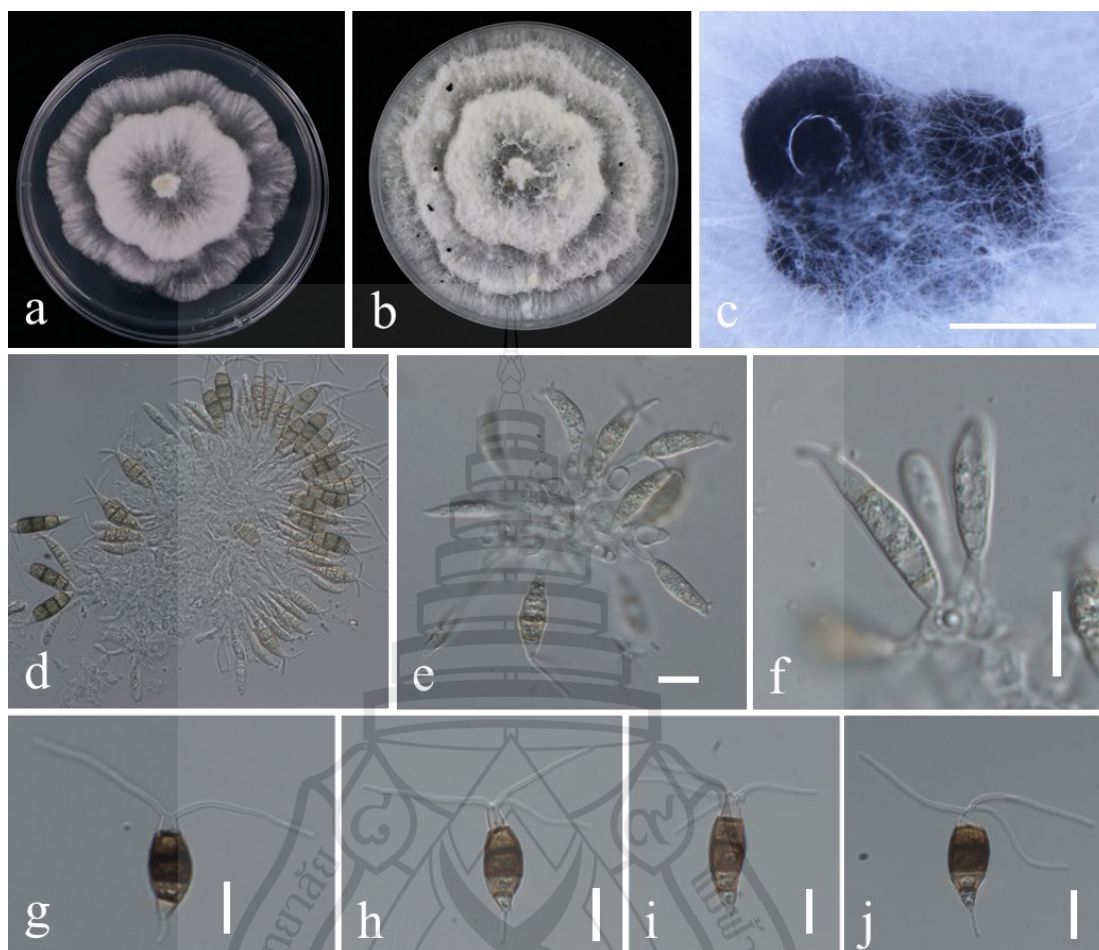

Figure 5.28 Morphological characters of *Neopestalotiopsis photiniae* (JZB340123)

Figure 5.28 a Colony on PDA after four days; b Colony on PDA after three weeks; c Conidiomata on PDA; d–f Conidiogenous cells; g–i Conidia; Scale bars: c = 500 μm; d–i = 10 μm

Neopestalotiopsis protearum (Crous & L. Swart) Maharachch., K.D. Hyde & Crous, in Maharachchikumbura, Hyde, Groenewald, Xu & Crous, Stud. Mycol. 79: 147 (2014). Figure 5.29

Associated with leaf spot of *Vaccinium corymbosum*. **Sexual morph:** Not observed. **Asexual morph:** *Conidiomata* globose, solitary or gregarious, semi-immersed or immersed, exuding globose, black conidial masses, 334–780 μm diam ($\overline{x}$ = 560 μm, n = 10). *Conidiophores* indistinct, often reduced to conidiogenous cells. *Conidiogenous cells* discrete, ampulliform, flask-shaped or obclavate, hyaline, 7.5–12 × 2–6 μm ($\overline{x}$ = 9.0 × 4.0 μm, n = 30). *Conidia* fusoid to ellipsoid, straight to slightly curved, 4-septate, 21–25 × 6.5–8 μm ($\overline{x}$ = 23.0 × 7.3 μm, n = 30), L/W ratio = 3.1; basal cell obconic with a truncate base, hyaline, rugose and thin-walled, 3–5 μm long ($\overline{x}$ = 4.0 μm, n = 30); three median cells doliiform, 15–16.5 μm ($\overline{x}$ = 15.7 μm, n = 30) long, wall rugose, versicoloured, septa darker than the rest of the cell (second cell from the base pale brown, 4–5 μm long; third cell brown, 5–6.5 μm long; fourth cell brown, 4.5–6 μm long); apical cell 3–5 μm ($\overline{x}$ = 4.0 μm, n = 30) long, hyaline, conical to subcylindrical, thin- and smooth-walled, with 3 tubular apical appendages, arising from the apical crest, unbranched, filiform, flexuous, 13–20 μm ($\overline{x}$ = 17.1 μm, n = 30) long; basal appendage single, tubular, unbranched, centric, 4.5–6.5 μm ($\overline{x}$ = 5.3 μm, n = 30) long.

Culture characteristics – Colonies on PDA reaching 67 mm diam. after four days at 25°C, flat with lobate edge, concentric, white, aerial mycelium sparse, flocculence.

Material examined – China, Fujian Province, Longyan City, from diseased leaves of *Vaccinium corymbosum*, May 2023, X. H. Li and Y. Y. Zhou (dry cultures JZBH340125– JZBH340126), living cultures JZB340125– JZB340126.

Notes – The two new isolates from this study (JZB340125 and JZB340126) phylogenetically close to the ex-type of *Neopestalotiopsis protearum* (CBS 114178). The morphology of the isolates is also similar to the description of the ex-type of *Neo. protearum* (Maharachchikumbura et al., 2014)*.* The two isolates are identified as *Neo. collariata. Neopestalotiopsis protearum* was originally introduced as *Pestalotiopsis protearum* from *Leucospermum cuneiforme* in Zimbabwe, associated with leaf spot (Crous et al., 2011). Subsequently *Pes. protearum* was transferred to *Neopestalotiopsis*,

and was assigned as the type species of *Neopestalotiopsis* (Maharachchikumbura et al., 2014). *Neopestalotiopsis protearum* has been also reported to cause seed rot on *Camellia oleifera* in China (Tang et al., 2021). This is the first report of *Neo. protearum* on blueberry (*Vaccinium* spp.).
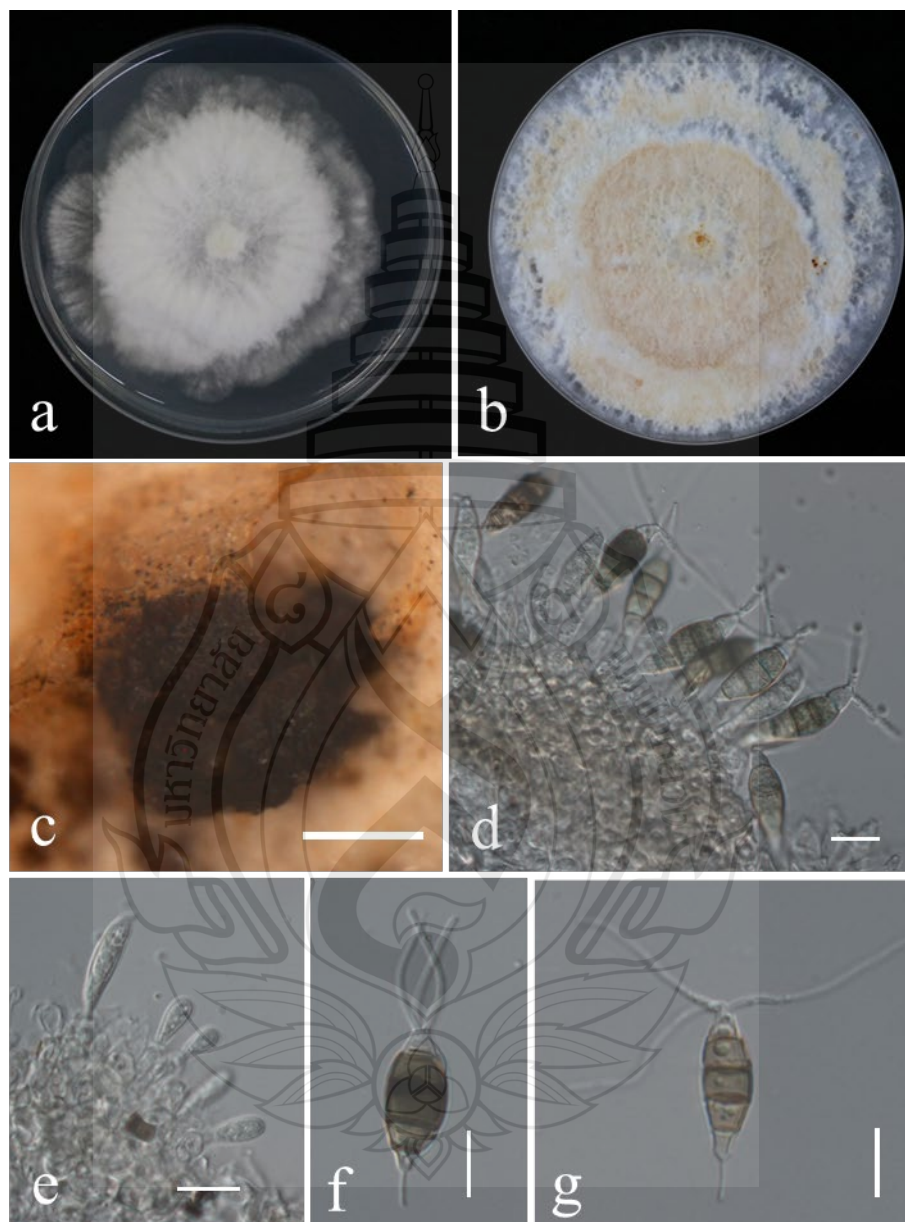
Figure 5.29 Morphological characters of *Neopestalotiopsis protearum* (JZB340126)

Figure 5.29 a Colony on PDA after four days; b Colony on PDA after three weeks; c Conidiomata on PDA; d–e Conidiogenous cells; f–g Conidia; Scale bars: c=500μm; d–g=10 μm.

Neopestalotiopsis rosae Maharachch., K.D. Hyde & Crous, in Maharachchikumbura, Hyde, Groenewald, Xu & Crous, Stud. Mycol. 79: 147 (2014).

Associated with leaf spot, stem blight and root rot of *Vaccinium* spp. For morphological description, see Maharachchikumbura et al. (2014).

Material examined – China, Liaoning Province, Dandong City, from stem blight of *Vaccinium* sp., March 2023, X. H. Li and L. N. Wu (dried culture JZBH340127), living cultures JZB340127; *ibid.*, from root rot of *Vaccinium* sp., March 2023, X. H. Li and L. N. Wu (dried culture JZBH340128– JZBH340129), living cultures JZB340128– JZB340129; *ibid.*, Huludao City, from root rot of *Vaccinium corymbosum*, April 2023, X. H. Li (dried culture JZBH340130– JZBH340131), living cultures JZB340130– JZB340131; *ibid.*, from stem blight of *Vaccinium corymbosum*, April 2023, X. H. Li (dried culture JZBH340132–JZBH340134), living cultures JZB340132–JZB340134; *ibid.*, Guizhou Province, Majiang County, from leaf spot of *Vaccinium virgatum*, May 2023, X. H. Li and Y. Y. Zhou (dried culture JZBH340135), living cultures JZB340135; *ibid.*, Heilongjiang Province, Harbin City, from stem blight of *Vaccinium* sp., June 2023, X. H. Li, Y. Y. Zhou and P. Z. Chen (dried culture JZBH340136), living cultures JZB340136.

Notes – In the phylogenetic analysis, seven isolates obtained in the current study (JZB340127– JZB340136) clustered with reference isolates of *Neopestalotiopsis rosae* (including ex-type CBS 101057). The morphological characters of our isolates resemble to the type description of *Neo. rosae* (Maharachchikumbura et al., 2014). *Neopestalotiopsis rosae* was initially isolated from stem lesion of *Rosa* sp. in New Zealand and stem of *Paeonia suffruticosa* in USA (Maharachchikumbura et al., 2014). In China, the species has been reported to cause root rot of strawberry (*Fragaria × ananassa*) (Sun et al., 2021) and leaf or fruit spot of pecan (*Carya illinoinensis*) (Gao et al., 2022), Shatangju (*Citrus reticulata*) (Ma et al., 2023) and honeysuckle (Lonicera caerulea) (Yan et al., 2024). While on blueberry (*Vaccinium* spp.), stem blight and dieback caused by *Neo. rosae* were only reported in Peru and in Portugal (Rodríguez-Gálvez et al., 2020; Santos et al., 2022). This is the first report of *Neopestalotiopsis rosae* on blueberry (*Vaccinium* spp.) in China.

Neopestalotiopsis scalabiensis J. Santos, S. Hilário & A. Alves, Eur. J. Pl. Path. 162: 547 (2021)

Associated with stem blight of *Vaccinium* spp. For morphological description, see Santos et al. (2022).

Material examined – China, Liaoning Province, Huludao City, from stem blight of *Vaccinium corymbosum*, April 2023, X. H. Li (dried culture JZBH340137), living cultures JZB340137; *ibid.*, Jilin Province, Gongzhuling City, from stem blight of *Vaccinium angustifolium*, June 2023, X. H. Li, Y. Y. Zhou & P. Z. Chen (dried culture JZBH340138), living cultures JZB340138.

Notes – In the phylogenetic analysis, two isolates obtained in the current study (JZB340137 and JZB340138) clustered with the ex-type of *Neo. scalabiensis* (CAA1029). Morphologically our isolates resemble to the description of *Neo. scalabiensis* (Santos et al., 2022). *Neopestalotiopsis scalabiensis* was introduced by Santos et al. (2022) from stem and twig blight of *Vaccinium corymbosum* in Portugal. This is the first report of *Neo. scalabiensis* on blueberry (*Vaccinium* spp.) in China.

Neopestalotiopsis subepidermalis C. Peng & C.M. Tian, in Peng, Crous, Jiang, Fan, Liang & Tian, Persoonia 49: 230 (2022)

Associated with stem blight and root rot of *Vaccinium* spp. For morphological description, see Peng et al. (2022).

Material examined – China, Dandong City, from stem blight of *Vaccinium* sp., March 2023, X. H. Li and L.N. Wu (dried culture JZBH340139), living cultures JZB340139; *ibid.*, Liaoning Province, Huludao City, from root rot of *Vaccinium corymbosum*, April 2023, X. H. Li (dried culture JZBH340140), living cultures JZB340140.

Notes – In the phylogenetic analysis, two isolates obtained in the current study (JZB340139 and JZB340140) clustered with reference isolates of *Neopestalotiopsis subepidermalis* (including ex-type CFCC 55160) with 90% bootstrap support and 1.00 posterior probabilities. The morphological characters of our isolates resemble to the type description of *Neo. subepidermalis* (Peng et al., 2022). *Neopestalotiopsis subepidermalis* was introduced by Peng et al. (2022) from spines and branches of *Rosa* spp. in China. This is the first report of *Neopestalotiopsis subepidermalis* on blueberry (*Vaccinium* spp.).

Neopestalotiopsis vacciniicola J. Santos, S. Hilário & A. Alves, Eur. J. Pl. Path. 162: 546 (2021)

Associated with leaf spot and stem blight of *Vaccinium* spp. For morphological description, see Santos et al. (2022).

Material examined – China, Heilongjiang Province, Harbin City, from stem blight of *Vaccinium* sp., June 2023, X. H. Li, Y. Y. Zhou and P. Z. Chen (dried culture JZBH340141– JZBH340144), living cultures JZB340141– JZB340144; *ibid.*, Jilin Province, Gongzhuling City, from stem blight of *Vaccinium angustifolium*, June 2023, X. H. Li, Y. Y. Zhou and P. Z. Chen (dried culture JZBH340145– JZBH340156), living cultures JZB340145– JZB340156; *ibid.*, Liaoning Province, Ji'an City, from leaf spot of *Vaccinium corymbosum*, September 2023, X. H. Li (dried culture JZBH340157), living cultures JZB340157; *ibid.*, from stem blight of *Vaccinium corymbosum*, September 2023, X. H. Li (dried culture JZBH340158– JZBH340160), living cultures JZB340158– JZB340160.

Notes – In the phylogenetic analysis, twenty isolates obtained in the current study (JZBH340141–JZBH340160) clustered with reference isolates of *Neopestalotiopsis vacciniicola* (including ex-type MUM 21.35) with 99% bootstrap support and 1.00 posterior probabilities. The morphological characters of our isolates resemble to the type description of *Neo. vacciniicola* (Santos et al., 2022). *Neopestalotiopsis vacciniicola* was introduced by Santos et al., (2022) from twigs of highbush blueberry (*Vaccinium corymbosum*) with blight symptom in Portugal, with moderate virulence on blueberry in the pathogenicity test. This is also the only record of the species. In the current study, we first reported *Neopestalotiopsis vacciniicola* on *Vaccinium* spp. in China. And the species takes the highest percentage among the *Neopestalotiopsis*.

Pestalotiopsis Steyaert, Bull. Jard. bot. État Brux. 19: 300 (1949)

Classification: Sporocadaceae, Amphisphaeriales, Xylariomycetidae, Sordariomycetes, Ascomycota, Fungi (Hyde et al., 2024).

Notes: *Pestalotiopsis* was introduced by Steyaert (1949) with *Pestalotiopsis guepinii* as type species. The genus is characterized by 5-celled conidia with apical appendages (Maharachchikumbura et al., 2014). However, the taxonomy of *Pestalotiopsis* is confusing, for the species were previously named according to host associations, and

cryptic species in the genus need to be resolved (Maharachchikumbura et al., 2012). Maharachchikumbura et al. (2014) segregated the genus into *Neopestalotiopsis*, *Pestalotiopsis* and *Pseudopestalotiopsis* based on the morphological characters especially conidiogenous cells and colour of median conidial cells, combined with DNA data. Current *Pestalotiopsis* was considered to produce conidia with concolourous median cells (Maharachchikumbura et al., 2014). *Pestalotiopsis* is widely distributed in tropical and temperate regions as important plant pathogens and common endophytes, and also can switch life modes (Maharachchikumbura et al., 2012). As phytopathogens, the genus causes various diseases on plant leaves, shoots and fruits with widely host range especially fruit crops (Maharachchikumbura et al., 2014).

In this study, phylogenetic tree of *Pestalotiopsis* was constructed based on ITS, *tef 1-α* and *β-tub* sequence data using ML and Bayesian analyses, with *Neopestalotiopsis cubana* (CBS 600.96), *Neopestalotiopsis protearum* (CBS 114178), *Pseudopestalotiopsis cocos* (CBS 272.29) and *Pseudopestalotiopsis indica* (CBS 459.78) as outgroups (Figure 5.30). New isolates from this study clustered into thirteen clades, including seven clades close to *P. anhuiensis*, *P. clavata*, *P. foliicola*, *P. hainanensis*, *P. kenyana*, *P. rhodomyrti*, *P. tumida*, three ambiguous clades, as well as three single clades. Combined with morphological characters, three new species *Pestalotiopsis caulicola*, *Pestalotiopsis fujianensis* and *Pestalotiopsis vaccinii* were introduced.

Figure 5.30 Phylogenetic tree generated from maximum likelihood (ML) analysis based on combined ITS, *tef 1-α, β-tub* sequence data of *Pestalotiopsis*
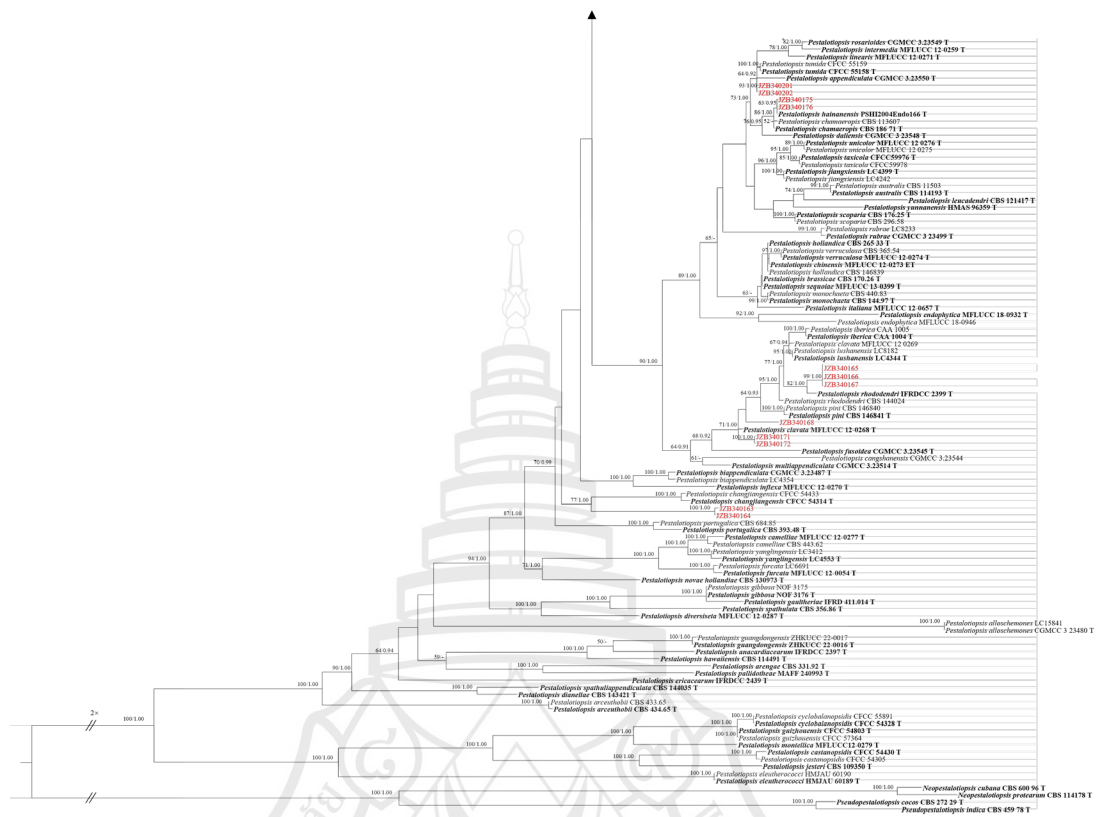
Figure 5.30 (continued)

Figure 5.30 The alignment comprises 1,676 characters with gaps. The tree is rooted with *Neopestalotiopsis cubana* (CBS 600.96), *Neopestalotiopsis protearum* (CBS 114178), *Pseudopestalotiopsis cocos* (CBS 272.29) and *Pseudopestalotiopsis indica* (CBS 459.78). The tree topology of the ML analysis was similar to the Bayesian analysis. The best-scoring RAxML tree with a final likelihood value of -19012.665673 is presented. The matrix had 905 distinct alignment patterns, with 9.20% of undetermined characters or gaps. Estimated base frequencies were as follows: A = 0.237741, C = 0.295298, G = 0.212298, T = 0.254663; substitution rates AC = 0.979184, AG = 3.599649, AT = 1.233153, CG = 1.000946, CT = 4.859047, GT = 1.000000; gamma distribution shape parameter α = 0.843840. ML bootstrap support values ≥50% and Bayesian posterior probabilities (BYPP) ≥0.90 are given near the nodes. The scale bar indicates the number of nucleotide changes per site. Ex-type strains are indicated in bold and newly generated sequences are indicated in red.

Pestalotiopsis caulicola sp. nov. Figure 5.31

Etymology – Named after the substrate origin from which it was isolated, stems.

Holotype – JZBH340161

Associated with stem blight of *Vaccinium corymbosum*. **Sexual morph:** Not observed. **Asexual morph:** *Conidiomata* in culture subglobose to globose, aggregated or solitary, black, epidermal to subepidermal, exuding black conidial masses. *Conidiophores* indistinct, often reduced to conidiogenous cells. *Conidiogenous cells* discrete, cylindrical to subcylindrical or ampulliform to lageniform, 7.7–15.5 × 2.2–3.2 µm ($\overline{x}$ = 11.0 × 2.7 µm, n = 30). *Conidia* fusoid to ellipsoid, straight to slightly curved, 4-septate, 20.2–25.1 × 5.3–6.6 µm ($\overline{x}$ = 22.3 × 5.9 µm, n = 40), L/W ratio = 3.8; basal cell obconic with a truncate base, hyaline, thin-walled, 3.6–5.3 µm long ($\overline{x}$ = 4.5 µm, n = 30); three median cells doliiform, 12.6–16.1 µm ($\overline{x}$ = 14.1 µm, n = 30) long, concolorous, pale brown (second cell from the base 4.1–5.5 µm long; third cell brown, 4.1–5.4 µm long; fourth cell brown, 4.0–5.3 µm long); apical cell 3.4–4.5 µm ($\overline{x}$ = 3.8 µm, n = 30) long, hyaline, conical to subcylindrical, thin- and smooth-walled, with 2–4 (mostly 3) tubular apical appendages, arising from the apical crest, unbranched or branched at one appendage, filiform, flexuous, 11.1–22.0 µm ($\overline{x}$ = 16.0 µm, n = 50) long; basal appendage single, tubular, unbranched, centric, 4.7–9.0 µm ($\overline{x}$ = 6.5 µm, n = 30) long.

Culture characteristic*s* – Colonies on PDA reaching 68 mm diam. after five days at 25°C, flat with entire edge, aerial mycelium sparse, pale yellow.

Typus – China, Fujian Province, Longyan City, from diseased stems of *Vaccinium corymbosum*, May 2023, X. H. Li and Y. Y. Zhou (holotype dry culture JZBH340161, ex-type living culture JZB340161).

Additional material examined – China, Fujian Province, Longyan City, from diseased stems of *Vaccinium corymbosum*, May 2023, X. H. Li and Y. Y. Zhou (dry culture JZBH340162, living culture JZB340162).

Notes – Three isolates of *Pestalotiopsis caulicola* (JZB340161 and JZB340162) formed a distinct clade close to *Pes. aggestorum*, *Pes. colombiensis* and *Pes. silvicola*, with 14 bp nucleotide differences (9 bp in tef, 5 bp in tub) from *Pes. aggestorum*; 10 bp nucleotide differences (1bp in ITS, 1 bp in tef; 8 bp in tub) from *Pes. colombiensis*; and 14 bp nucleotide differences (ITS: 1 bp; tef: 9 bp; tub: 4 bp) from *Pes. silvicola*.

Morphologically, *Pes. caulicola* differs from *Pes. aggestorum* by relatively shorter apical appendages (11.1–22.0 μm vs. 18–28.0 μm) and number of basal appendages (single vs. 1–2); from *Pes. colombiensis* by relatively longer basal appendages (4.7–9.0 μm vs. 2–5 μm); from *Pes. silvicola* by relatively thinner conidia (5.3–6.6 μm vs. 6(6.5)–7.5(–8.5) μm) and number of basal appendages (single vs. 1–2). Overall, differences of the morphology characters among the four species are not distinct. Combined phylogeny and morphology, we introduce *Pes. caulicola* as a new species.
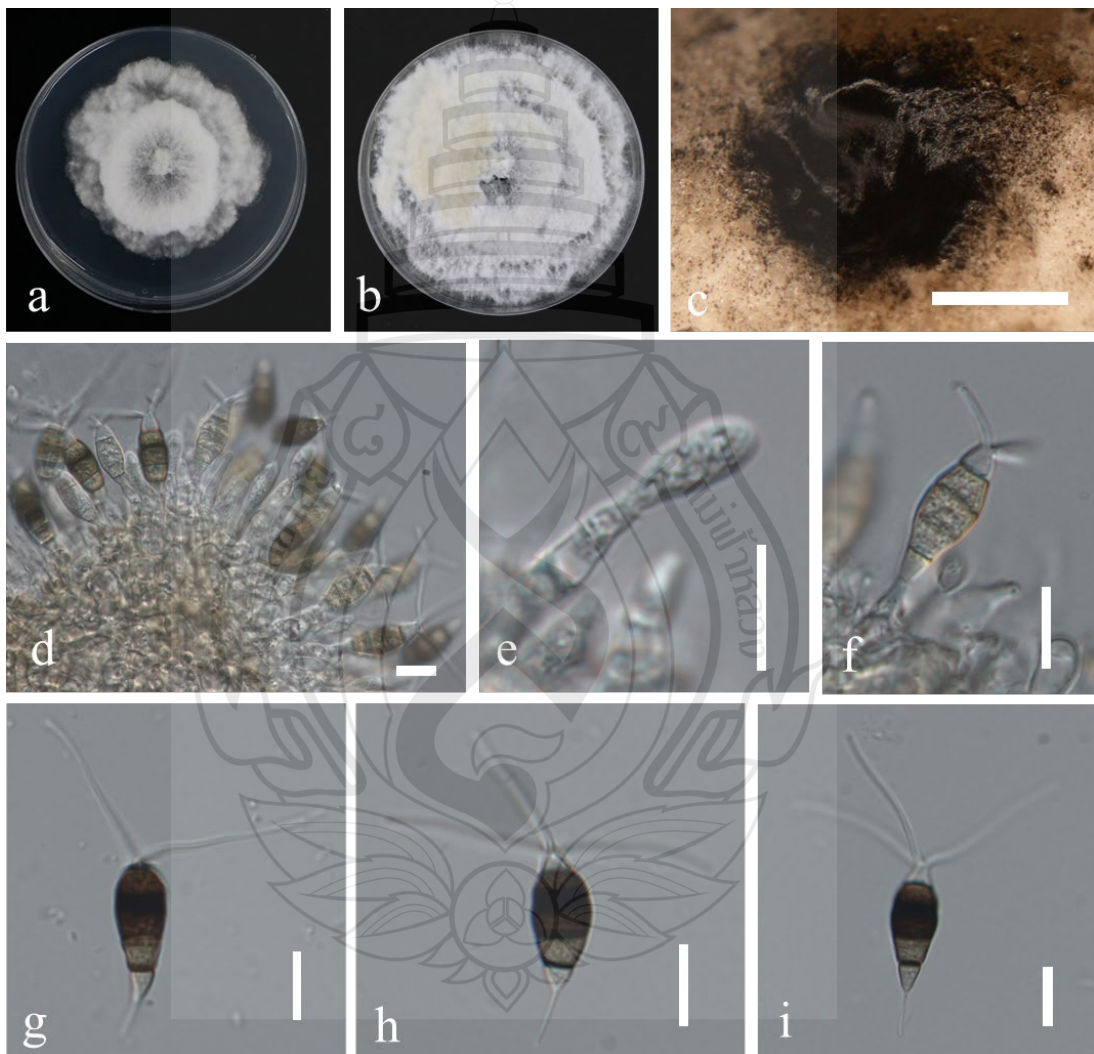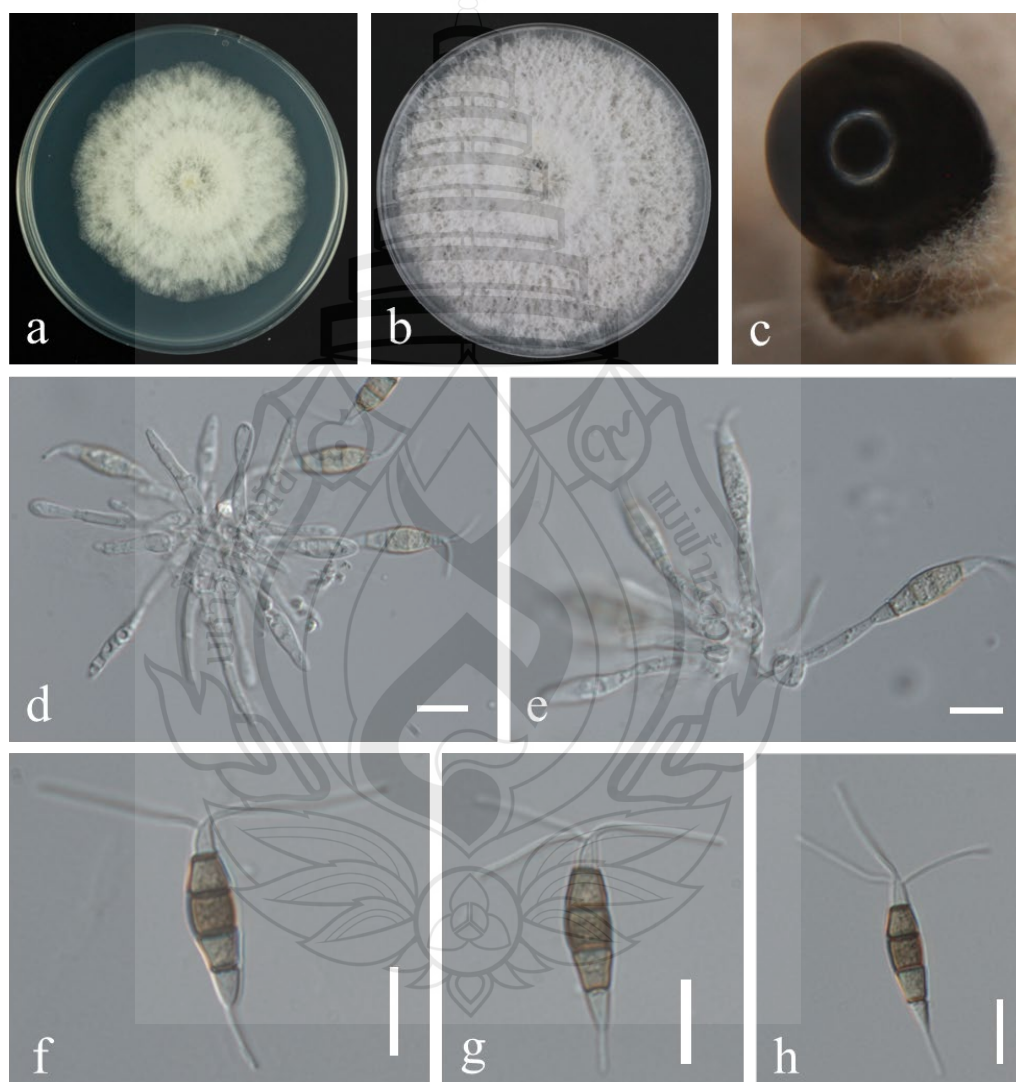

Figure 5.31 Morphological characters of *Pestalotiopsis caulicola* (JZB340161)

Figure 5.31 a Colony on PDA after four days; b Colony on PDA after three weeks; c Conidiomata on PDA; d–e Conidiogenous cells; f–h Conidia; Scale bars: d–h=10 μm.

Table 5.4 Comparison of the conidial dimension of *Pestalotiopsis* species related to this study

Species	Isolate number	Conidiogenous cells (µm)	Conidial size (µm)	L/W ratio	Apical Appendages		Basal Appendage (µm)	Reference
					number	Length (µm)		
	JZB340161	7.7–15.5 × 2.2–3.2	20.2–25.1 × 5.3–6.6	3.8	2–3 (mostly 3)	11.1–22.0	4.7–9.0	This study
Pes. aggestorum	CGMCC 3.18159	6–14.7 × 2–5.5	19–24.5 × 5–7	3.5	2–3 (mostly 3)	18–28	5–14 (1–2 basal appendages)	Liu et al. (2017)
Pes. colombiensis	CBS 118553	10–50 × 2–8	(19–)21–27(–28.5) × 5.5–7.5(–8)	3.8	2–3 (mostly 3)	(11–) 13–25(–28)	2–5	Maharachchikumbura et al. (2014)
Pes. silvicola	CFCC 55296	7.5–15 × 3–6	(20)21–24(26) × 6(6.5)–7.5(–8.5)	2.6–3.8	3	(12)12.5– 18.5(22.5)	(1–2 basal appendages) (3.5)4.5–7(8)	Jiang et al. (2022)
	JZB340163	8.8–14.1 × 2.5–4.3	18.9–25.5 × 6.1–8.8	3.1	2–4 (mostly 3)	16.5–26.2	5.1–11.2	This study
Pes. changjiangensis	CFCC 54314	3.5–6 × 2–5.5	19–24 × 7–8.5	2.4–3.3	indistinct	1.5–7	indistinct or absent	Jiang et al. (2022)
	48_B2_12_B1a	8.1–18.2 × 2.0–3.5	21.4–28.5 × 7.7–9.9	2.8	2–5 (mostly 3)	8.7–26.6	5.1–14.6	This study
Pes. rhododendri	IFRDCC 2399	-	(16)18–27(29) × 5–8	3.0	3	(5)7–15(18)	2–6	Zhang et al. (2013)
	JZB340168	7.1–14.0 × 2.7–4.6	23.0–31.4 × 5.8–7.6	4.0	2–3 (mostly 2)	9.7–23.5	1.8–6.3	This study
	JZB340171	8.2–16.0 × 2.3–4.2	21.4–28.6 × 7.2–9.9	2.9	2–3 (mostly 3)	10.3–26.1	(1–2 basal appendages) 1.8–8.4	This study

Table 5.4 (continued)

Species	Isolate number	Conidiogenous cells (μm)	Conidial size (μm)	L/W ratio	Apical Appendages number	Apical Appendages Length (μm)	Basal Appendage (μm)	Reference
Pes. clavata	HMAS047134	-	20–27 × 6.5–8	3.1	2–3 (mostly 3)	20–25	7–9	Maharachchikumbura et al. (2012)
	xs3	-	21.0–26.3 × 7.8–12.5 μm	2.2	2–4 (mostly 3)	8.3–28.4	4.7–11	Rui et al. (2025)
Pes. pini	MEAN 1094	12–25 × 2–4	(20.0–)23.3–24.6(–27.6) × (4.7–)7.4–7.8(–8.2)	3.2	3–4 (mostly 3)	(9.7–)18.4–19.8(–27.8)	1.4–7.6	Silva et al. (2020)
	JZB340201	7.3–10.8 × 3.1– 4.5	19.5–24.8 × 5.2–7.1	3.6	2–3 (mostly 2)	5.9–15.6	5.9–15.6	This study
Pes. tumida	BJFC-S1891	(7–)8–11.5(–12) × (1.5–)2– 4.5	(19–)19.5 – 23.5(–24) × 6.5–7.5	3.1	2–3 (mostly 3)	(10–)10.5–15.5(–16)	(1–2 basal appendages) (6.5–)7–19(–19.5)	Peng et al. (2022)
	CGMCC 3.23502	6.5–16(–20) × 2.5–6.5	18–25(–29) × 5–7	3.6	1–4 (mostly 1 and 2)	7–54	(1–3 basal appendages) 2.5–26	Razaghi et al. (2024)
Pes. appendiculata	KUN-HKAS 124571	-	19–24 × 5–6	4.2	2–3	8–15	3–5	Gu et al. (2022)

Pestalotiopsis fujianensis sp. nov. Figure 5.32

Etymology – Named after the province where the fungus was collected, Fujian Province.

Holotype – JZBH340163

Associated with leaf spot of *Vaccinium corymbosum*. **Sexual morph:** Not observed. **Asexual morph:** *Conidiomata* in culture subglobose to globose, aggregated or solitary, black, epidermal to subepidermal, exuding black conidial masses. *Conidiophores* indistinct, often reduced to conidiogenous cells. *Conidiogenous cells* discrete, cylindrical to subcylindrical or ampulliform to lageniform, 8.8–14.1 × 2.5–4.3 µm ($\bar{x}$ = 10.6 × 3.5 µm, n = 20). *Conidia* fusoid to ellipsoid, straight to slightly curved, 4-septate, 18.9–25.5 × 6.0–8.8 µm ($\bar{x}$ = 21.8 × 6.9 µm, n = 30), L/W ratio = 3.1; basal cell obconic with a truncate base, hyaline, thin-walled, 3.2–4.8 µm long ($\bar{x}$ = 4.0 µm, n = 30); three median cells doliiform, 12.1–15.2 µm ($\bar{x}$ = 13.3 µm, n = 30) long, concolorous, pale brown (second cell from the base 4.1–5.6 µm long; third cell brown, 4.5–5.8 µm long; fourth cell brown, 4.6–5.4 µm long); apical cell 3.6–3.9 µm ($\bar{x}$ = 3.7 µm, n = 30) long, hyaline, conical to subcylindrical, thin- and smooth-walled, with 2–4 (mostly 3) tubular apical appendages, arising from the apical crest, unbranched or branched at one appendage, filiform, flexuous, 16.5–26.2 µm ($\bar{x}$ = 20.8 µm, n = 30) long; basal appendage single, tubular, unbranched, centric, 5.1–11.2 µm ($\bar{x}$ = 8.5 µm, n = 30) long.

Culture characteristics – Colonies on PDA reaching 48 mm diam. after five days at 25°C, flat with entire edge, aerial mycelium sparse, pale yellow.

Typus – China, Fujian Province, Longyan City, from diseased stems of *Vaccinium corymbosum*, May 2023, X. H. Li and Y. Y. Zhou (holotype dry culture JZBH340163, ex-type living culture JZB340163).

Additional material examined – China, Fujian Province, Longyan City, from diseased leaves of *Vaccinium corymbosum*, May 2023, X. H. Li and Y. Y. Zhou (dry culture JZBH340164, living cultures JZB340164).

Notes – *Pestalotiopsis fujianensis* (JZB340163 and JZB340164) formed a distinct lineage and was sister to *Pes. changjiangensis* in the phylogenetic tree with 77% ML bootstrap value and 1.00 Bayesian posterior probabilities, with 51 bp different in sequences (ITS: 9bp; tef: 29bp; tub: 13bp). Morphologically, *P fujianensis* differs

from *Pes. changjiangensis* by longer conidiogenous cells (8.8–14.1 µm versus 3.5 to 6 mm), and longer apical appendages (16.5–26 µm versus 1.5 to 7 mm), as well as the existence and absent of basal appendage in *Pestalotiopsis fujianensis* and *Pes. changjiangensis* respectively (Jiang et al., 2022). The comparison was shown in Table 4. Therefore, we introduce *Pes. fujianensis* as a new species based on phylogeny and morphology.

Figure 5.32 Morphological characters of *Pestalotiopsis fujianensis* (JZB340163)

Figure 5.32 a Colony on PDA after four days; b Colony on PDA after three weeks; c Conidiomata on PDA; d–f Conidiogenous cells; g–j Conidia; Scale bars: c=500µm; d–j=20 µm.

Pestalotiopsis vaccinii sp. nov. Figure 5.33

Etymology – Named after the host species from which it was isolated, *Vaccinium* spp.

Holotype – JZBH340166

Associated with leaf spot of *Vaccinium* spp. **Sexual morph:** Not observed. **Asexual morph:** *Conidiomata* in culture subglobose to globose, aggregated or solitary, black, epidermal to subepidermal, exuding black conidial masses. *Conidiophores* indistinct, often reduced to conidiogenous cells. *Conidiogenous cells* discrete, cylindrical to subcylindrical or ampulliform to lageniform, 8.1–18.2 × 2.0–3.5 μm ($\bar{x}$ = 13.0 × 2.7 μm, n = 30). *Conidia* fusoid to ellipsoid, straight to slightly curved, 4-septate, 21.4–28.5 × 7.7–9.9 μm ($\bar{x}$ = 24.5 × 8.7 μm, n = 40), L/W ratio = 2.8; basal cell obconic with a truncate base, hyaline, thin-walled, 2.7–5.9 μm long ($\bar{x}$ = 4.5 μm, n = 30); three median cells doliiform, 14.6–18.2 μm ($\bar{x}$ = 16.4 μm, n = 30) long, concolorous, pale brown (second cell from the base 4.0–5.9 μm long; third cell brown, 4.8–6.2 μm long; fourth cell brown, 4.5–6.4 μm long); apical cell 3.0–5.5 μm ($\bar{x}$ = 3.8 μm, n = 30) long, hyaline, conical to subcylindrical, thin- and smooth-walled, with 2–5 (mostly 3) tubular apical appendages, arising from the apical crest, unbranched or branched at one appendage, filiform, flexuous, 8.7–26.6 μm ($\bar{x}$ = 16.7 μm, n = 50) long; basal appendage single, tubular, unbranched, centric, 5.1–14.6 μm ($\bar{x}$ = 8.1 μm, n = 30) long.

Culture characteristics – Colonies on PDA reaching 48 mm diam. after five days at 25°C, flat with entire edge, aerial mycelium sparse, pale yellow.

Typus – China, Guizhou Province, Majiang County, from diseased leaves of *Vaccinium corymbosum*, May 2023, X. H. Li and Y. Y. Zhou (holotype dry culture JZBH340166, ex-type living culture JZB340166).

Additional material examined – China, Fujian Province, Longyan City, from diseased leaves of *Vaccinium corymbosum*, May 2023, X. H. Li and Y. Y. Zhou (dry cultures JZBH340165, living cultures JZB340165); Guizhou Province, Majiang County, from diseased leaves of *Vaccinium virgatum*, May 2023, X. H. Li and Y. Y. Zhou (dry cultures JZBH340167, living cultures JZB340167).

Notes – In the phylogenetic analysis, *Pes. vaccinii* (JZB340165– JZB340167) closely related to *Pes. rhododendri*, with 3 nucleotide differences (2 bp in ITS and 3 bp in tub) to the ex-type of *Pes. rhododendri* (IFRDCC 2399). Morphologically, JZB340138 differs from *Pes. rhododendri* by relatively wider conidia (21.4–28.5 × 7.7–9.9 vs. (16)18–27(29) × 5–8 μm), and longer basal appendages (5.1–14.6 vs. 2–6), as well as the number of apical appendage (2–5 (mostly 3) vs. 3). The morphological comparison of the species in sister clade, *Pes. iberica* and *Pes. lushanensis*, was also provided in table 4. Here we introduced *Pes. vaccinii* as a new species combined phylogeny and morphology.
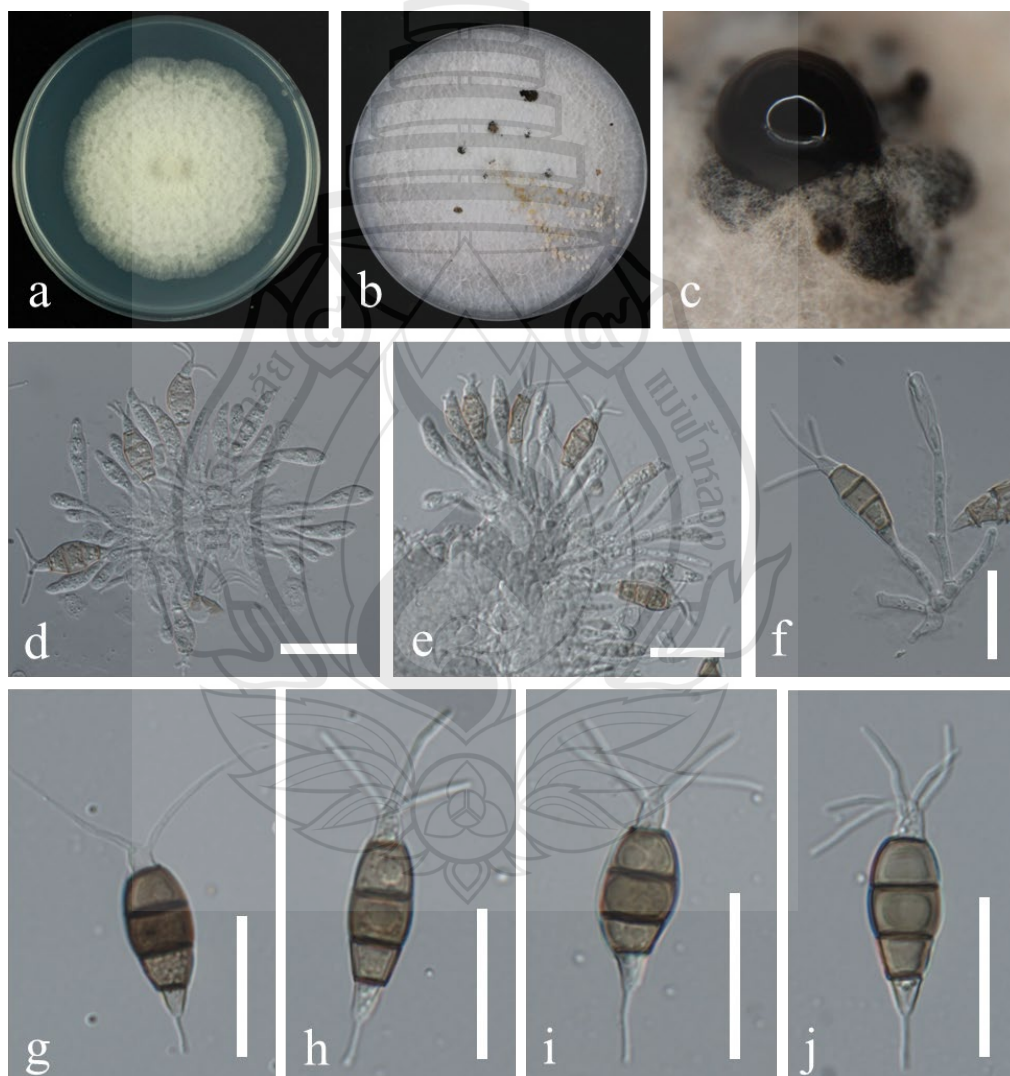
Figure 5.33 Morphological characters of *Pestalotiopsis vaccinii* (JZB340166)

Figure 5.33 a Colony on PDA after four days; b Colony on PDA after three weeks; c Conidiomata on PDA; d–f Conidiogenous cells; g–j Conidia; Scale bars: d–j =20 μm.

Pestalotiopsis **sp.1** Figure 5.34

Associated with leaf spot of *Vaccinium corymbosum*. **Sexual morph:** Not observed. **Asexual morph:** *Conidiomata* in culture subglobose to globose, aggregated or solitary, black, epidermal to subepidermal, exuding black conidial masses. indistinct, often reduced to conidiogenous cells. *Conidiogenous cells* discrete or integrated, ampulliform, cylindrical or subcylindrical, hyaline, 7.1–14.0 × 2.7–4.6 μm ($\overline{x}$ = 10.3 × 3.6 μm, n = 220). *Conidia* fusoid to ellipsoid, straight to slightly curved, 4-septate, 23.0–31.4 × 5.8–7.7 μm ($\overline{x}$ = 26.2 × 6.6 μm, n = 40), L/W ratio = 4.0; basal cell obconic with a truncate base, hyaline, thin-walled, 3.5–5.8 μm long ($\overline{x}$ = 4.6 μm, n = 30); three median cells doliiform, 13.0–17.5 μm ($\overline{x}$ = 15.3 μm, n = 30) long, concolorous, (second cell from the base pale brown to brown, 4.2–6.4 μm long; third cell brown, 4.7–6.6 μm long; fourth cell brown, 4.3–6.8 μm long); apical cell 3.5–5.7 μm ($\overline{x}$ = 4.3 μm, n = 30) long, hyaline, conical to subcylindrical, thin- and smooth-walled, with 2–3 (mostly 2) tubular apical appendages, arising from the apical crest, unbranched or branched at one appendage, filiform, flexuous, 9.7–23.5 μm ($\overline{x}$ = 16.7 μm, n = 50) long; basal appendage present or absent, tubular, unbranched, centric, 1.8–6.3 μm ($\overline{x}$ = 3.7 μm, n = 30) long.

Culture characteristics – Colonies on PDA reaching 61 mm diam. after five days at 25°C, flat with entire edge, aerial mycelium white, flocculent, forming black conidiomata with black conidial masses from colony centre; colony from reverse pale yellow in centre.

Material examined – China, Liaoning Province, Dandong City, from stems of *Vaccinium* sp. with blight symptoms, March 2023, X. H. Li and L. N. Wu (dry cultures JZBH340168), living cultures JZB340168.

Notes – In the phylogenetic analysis, the new isolate JZB340168formed a sister clade to *Pes. clavata* and *Pes. pini* with low bootstrap value, but differs from *Pes. clavata* (MFLUCC 12-0268) in 12 bp nucleotide differences (3 bp in ITS, 6 bp in tef and 3 bp in tub); differs from *Pes. pini* (CBS 146841) in 16 bp nucleotide differences (2 bp in ITS, 12 bp in tef and 2 bp in tub). Morphologically, JZB340138 differs from *Pes. clavata* in larger mean conidium length/width ratio (4.0 vs. 3.1), and smaller basal

appendage (1.8–6.3 vs. 7–9); differs from *Pes. pini* in relatively shorter conidiogenous cells (7.1–14.0 × 2.7–4.6 μm vs 12–25 × 2–4 μm), larger mean conidium length/width ratio (4.0 vs. 3.2), and the number of apical appendages (2–3, mostly 2 vs 3–4, mostly 3) (table 5.4). The isolate JZB340138 probably a new species, but for the low bootstrap value, and special clade of *P. clavata* (see notes under *P. clavata*), further study is needed to confirm that.

Figure 5.34 Morphological characters of *Pestalotiopsis* sp.1 (JZB340168)

Figure 5.34 a Upper view Colony on PDA after four days; b Colony on PDA after three weeks; c Conidiomata on PDA; d–e Conidiogenous cells; f–i Conidia; Scale bars: d–i =20μm.

Pestalotiopsis anhuiensis Ning Jiang, in Jiang, Voglmayr, Xue, Piao & Li, Persoonia: 10.1128/spectrum.03272-22, 6 (2022). Figure 5.34

Associated with stem blight of *Vaccinium* spp. **Sexual morph:** Not observed. **Asexual morph:** *Conidiomata* in culture subglobose to globose, solitary or gregarious, semi-immersed or immersed, exuding black conidial masses. *Conidiophores* indistinct, often reduced to conidiogenous cells. *Conidiogenous cells* discrete, cylindrical to ampulliform, hyaline, 6.2–13.3 × 2.4–5.8 μm ($\overline{x}$ = 9.3 × 3.3 μm, n = 20). *Conidia* fusoid to ellipsoid, straight to slightly curved, 4-septate, slightly constricted at the septa, 17.8–22.6 × 5.2–6.7 μm ($\overline{x}$ = 20.7 × 5.8 μm, n = 30), L/W ratio = 3.5; basal cell obconic with a truncate base, hyaline, thin-walled, 2.8–4.5 μm long ($\overline{x}$ = 3.6 μm, n = 30); three median cells doliiform, 12.7–15.5 μm ($\overline{x}$ = 14.4 μm, n = 30) long, concolorous, (second cell from the base pale brown to brown, 3.7–4.6 μm long; third cell brown, 4.4–6.0 μm long; fourth cell brown, 4.3–5.8 μm long); apical cell 2.9–3.5 μm ($\overline{x}$ = 3.3 μm, n = 30) long, hyaline, conical to subcylindrical, thin- and smooth-walled, with 2–3 tubular apical appendages, arising from the apical crest, unbranched or branched at one appendage, filiform, flexuous, 7.3–19.5 μm ($\overline{x}$ = 13.2 μm, n = 30) long; basal appendage single, tubular, unbranched, centric, 3.1–5.6 μm ($\overline{x}$ = 4.2 μm, n = 30) long.

Culture characteristics – Colonies on PDA reaching 60 mm diam. after five days at 25°C, flat with entire edge, aerial mycelium white, flocculent, forming black conidiomata with black conidial masses from colony centre; colony from reverse pale yellow in centre.

Material examined – China, Liaoning Province, Dandong City, from stem blight of *Vaccinium* sp., March 2023, X. H. Li and L. N. Wu (dry cultures JZBH340169–JZBH340170), living cultures JZB340169– JZB340170.

Notes – In the phylogenetic analysis, two new isolates of *Pes. anhuiensis* (JZB340169– JZB340170) clustered together with ex-type strain CFCC 54791. And morphological characters of the isolates are consistent with the description of *Pes. anhuiensis* (Jiang et al., 2022). *Pestalotiopsis anhuiensis* was introduced from *Cyclobalanopsis glauca* in China, associated with leaf diseases (Jiang et al., 2022). This is the first report of *Pes. anhuiensis* on blueberry (*Vaccinium* spp.).

Figure 5.35 Morphological characters of *Pestalotiopsis anhuiensis* (JZB340169)

Figure 5.35 a Colony on PDA after four days; b Colony on PDA after three weeks; c Conidiomata on PDA; d–e Conidiogenous cells; f–g Conidia; Scale bars: c=500 μm; d=20 μm; e–j=10 μm.

Pestalotiopsis clavata Maharachch. & K.D. Hyde, in Maharachchikumbura, Guo, Cai, Chukeatirote, Wu, Sun, Crous, Bhat, McKenzie, Bahkali & Hyde, Fungal Diversity 56(1): 108 (2012). Figure 5.36.

Associated with leaf spot and stem blight of *Vaccinium corymbosum*. **Sexual morph:** Not observed. **Asexual morph:** *Conidiomata* in culture subglobose to globose, aggregated or solitary, black, epidermal to subepidermal, exuding black conidial masses. *Conidiophores* cylindrical, branched at the base, hyaline. *Conidiogenous cells*

discrete or integrated, ampulliform, cylindrical or subcylindrical, hyaline, 8.2–16.0 × 2.3–4.2 μm ($\overline{x}$ = 12.8 × 3.0 μm, n = 30). *Conidia* fusoid to ellipsoid, straight to slightly curved, 4-septate, 21.4–28.6 × 7.1–9.8 μm ($\overline{x}$ = 24.2 × 8.3 μm, n = 40), L/W ratio = 2.9; basal cell obconic with a truncate base, hyaline, thin-walled, 3.2–6.0 μm long ($\overline{x}$ = 4.6 μm, n = 30); three median cells doliiform, 14.5–18.3 μm ($\overline{x}$ = 16.0 μm, n = 30) long, concolorous, (second cell from the base pale brown to brown, 4.0–6.7 μm long; third cell brown, 4.1–6.4 μm long; fourth cell brown, 4.5–5.9 μm long); apical cell 3.0–4.6 μm ($\overline{x}$ = 3.6 μm, n = 30) long, hyaline, conical to subcylindrical, thin- and smooth-walled, with 2–3 tubular apical appendages, arising from the apical crest, unbranched or branched at one appendage, filiform, flexuous, 10.3–26.1 μm ($\overline{x}$ = 18.2 μm, n = 50) long; basal appendage present or absent, 1–2, tubular, unbranched, centric, 1.8–8.4 μm ($\overline{x}$ = 5.1 μm, n = 30) long.

Culture characteristics – Colonies on PDA reaching 61 mm diam. after five days at 25°C, flat with entire edge, aerial mycelium white, flocculent, forming black conidiomata with black conidial masses from colony centre; colony from reverse pale yellow in centre.

Material examined – China, Fujian Province, Longyan City, from stems of *Vaccinium corymbosum* with blight symptoms, May 2023, X. H. Li and Y. Y. Zhou (dry cultures JZBH340171), living cultures JZB340171; China, Guizhou Province, Majiang County, from leaf spot of *Vaccinium corymbosum*, May 2023, X. H. Li and Y. Y. Zhou (dry cultures JZBH340172), living cultures JZB340172.

Notes – The two new isolates (JZB340171– JZB340172) phylogenetically formed a clade closely related to *Pes. clavata* (MFLUCC 12-0268) with 3 bp nucleotide differences (1 bp in ITS, 1 bp in tef and 1 bp in tub). Their morphological characters are mostly overlapping, while JZB340171 has relative wider conidia (21.4–28.6 × 7.2–9.9 μm vs. 20–27 × 6.5–8 μm), and larger dimension range of basal appendage (1.8–8.4 μm vs. 7–9 μm). We also compared with the character with the strain xs3 from another study (Rui et al., 2025), which have even wider conidia (7.8–12.5 μm). The difference in dimension may because of different hosts or substrates. For the phylogenetical and morphological differences between our isolates and *Pes. clavata* are relatively small, we identified the new isolates as *Pes. clavata*. It's worth noting that another strain of *Pes. clavata* (MFLUCC 12-0269), which was originally introduced as *Pes. clavata* together with the ex-type (MFLUCC 12-0268), was not clustered together

with the ex-type strain, but located between *Pes. iberica* and *Pes. lushanensis* in the phylogenetic tree. MFLUCC 12-0269 has 1 bp nucleotide difference in ITS sequences and 9 bp differences in tef-1α with the type strain. To resolve the phylogeny relationship of this branch, more approaches such as other informative gene loci are needed. *Pestalotiopsis clavata* was introduced as endophyte in living leaves of *Buxus* sp. and *Euonymus* sp. in China (Maharachchikumbura et al., 2012). Recently the species also reported as pathogen causing shoot blight on *Cedrus deodara* (Rui et al., 2025). In this study, *Pes. clavata* was first isolated from diseased stems on blueberry (*Vaccinium* spp.), which also be possible pathogen.
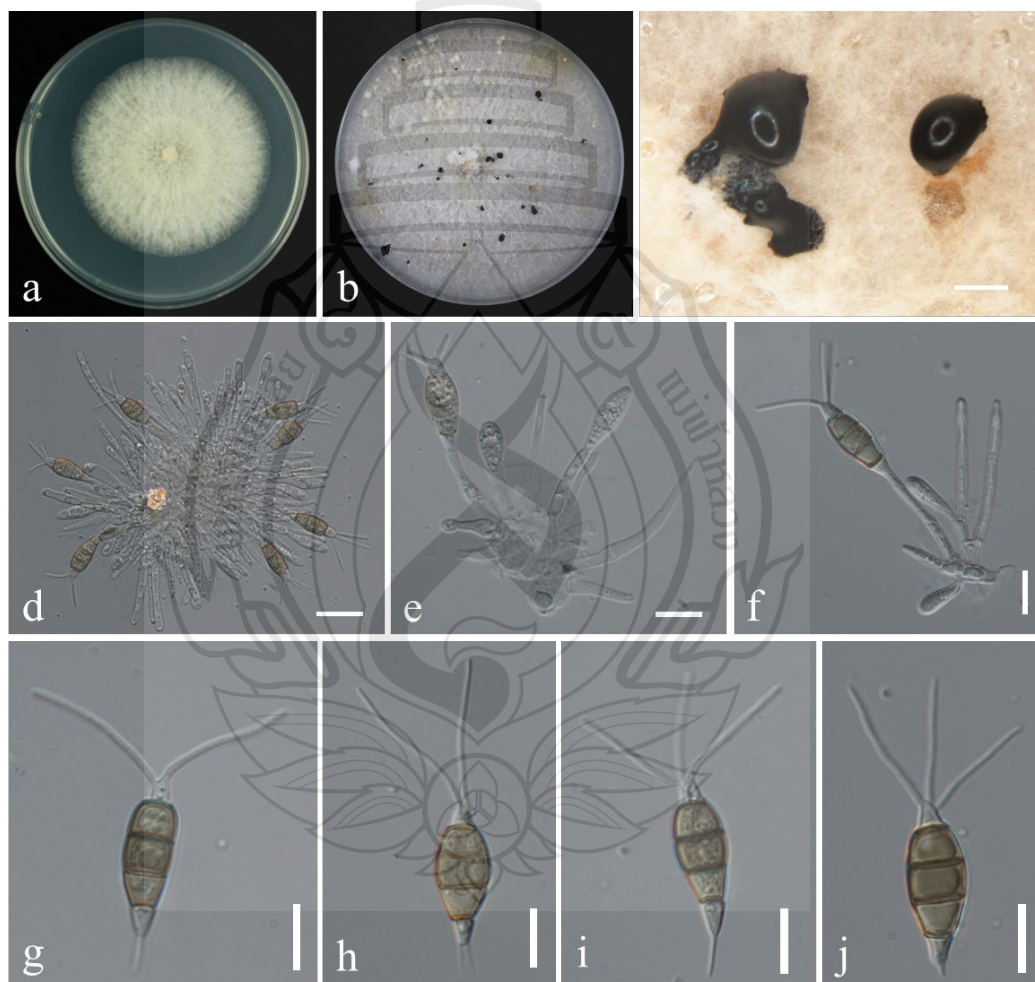
Figure 5.36 Morphological characters of *Pestalotiopsis clavata* (JZB340171)

Figure 5.36 a Colony on PDA after four days; b Colony on PDA after three weeks; c Conidiomata on PDA; d–f Conidiogenous cells; g–j Conidia; Scale bars: c=500μm; d=20μm; e–j=10 μm.

Pestalotiopsis foliicola Ning Jiang, in Jiang, Voglmayr, Xue, Piao & Li, Microbiology Spectrum: 10.1128/spectrum.03272-22, 13 (2022). Fig.5.37.

Associated with stem blight of *Vaccinium corymbosum*. **Sexual morph:** Not observed. **Asexual morph:** *Conidiomata* in culture subglobose to globose, solitary or gregarious, semi-immersed or immersed, exuding black conidial masses. *Conidiophores* indistinct, often reduced to conidiogenous cells. *Conidiogenous cells* discrete, cylindrical to ampulliform, hyaline, 8.2–19.0 × 2.0–3.3 μm (x̄ = 12.4 × 2.5 μm, n = 20). *Conidia* fusoid to ellipsoid, straight to slightly curved, 4-septate, slightly constricted at the septa, 19.6–24.1 × 7.5–10.0 μm (x̄ = 21.8 × 8.7 μm, n = 40), L/W ratio = 2.5; basal cell obconic with a truncate base, hyaline, thin-walled, 3.1–5.2 μm long (x̄ = 4.2 μm, n = 30); three median cells doliiform, 13.6–16.1 μm (x̄ = 14.8 μm, n = 30) long, concolorous, (second cell from the base pale brown to brown, 4.0–6.4 μm long; third cell brown, 4.1–6.0 μm long; fourth cell brown, 3.9–5.5 μm long); apical cell 2.7–4.1 μm (x̄ = 3.3 μm, n = 30) long, hyaline, conical to subcylindrical, thin- and smooth-walled, with 2–3 tubular apical appendages (mostly 3), arising from the apical crest, unbranched or branched at one appendage, filiform, flexuous, 9.3–28.8 μm (x̄ = 16.6 μm, n = 50) long; basal appendage single, tubular, unbranched, centric, 1.4–7.0 μm (x̄ = 3.8 μm, n = 30) long.

Culture characteristics – Colonies on PDA reaching 67 mm diam. after five days at 25°C, flat with entire edge, aerial mycelium white, flocculent, forming black conidiomata with black conidial masses from colony centre; colony from reverse pale yellow in centre.

Material examined – China, Fujian Province, Longyan City, from diseased stems of *Vaccinium corymbosum*, May 2023, X. H. Li and Y. Y. Zhou (dry cultures JZBH340173– JZBH340174), living cultures JZB340173– JZB340174.

Notes – In the phylogenetic analysis, two new isolates (JZB340173– JZB340174) are closely related to *Pes. foliicola*. And morphological characters of the isolates are consistent with the description of *Pes. foliicola* (Jiang et al., 2022). *Pestalotiopsis foliicola* was introduced from diseased leaves of *Castanopsis faberi* in China, associated with leaf diseases (Jiang et al., 2022). This is the first report of *Pes. foliicola* on blueberry (*Vaccinium* spp.), which isolated from disease stems. The species might be a pathogen on different hosts.
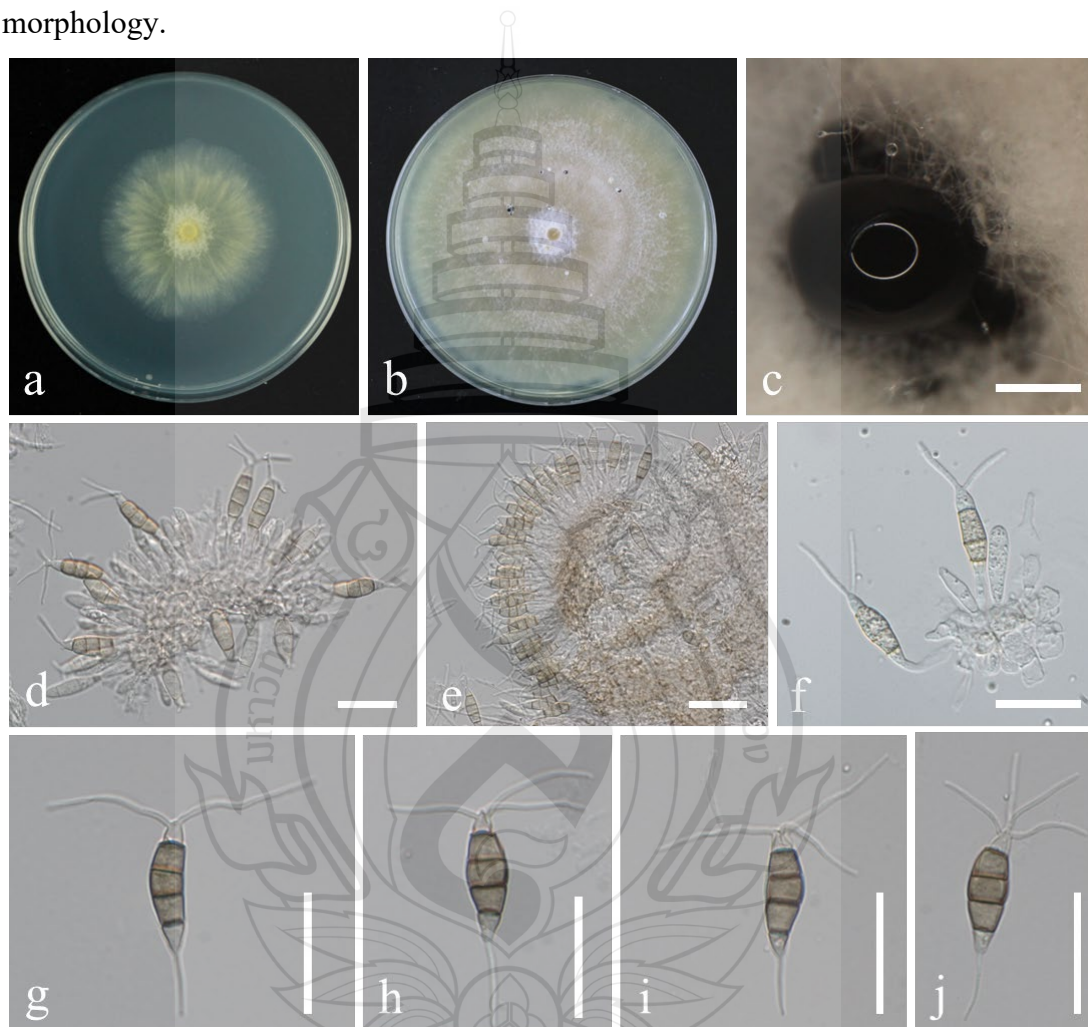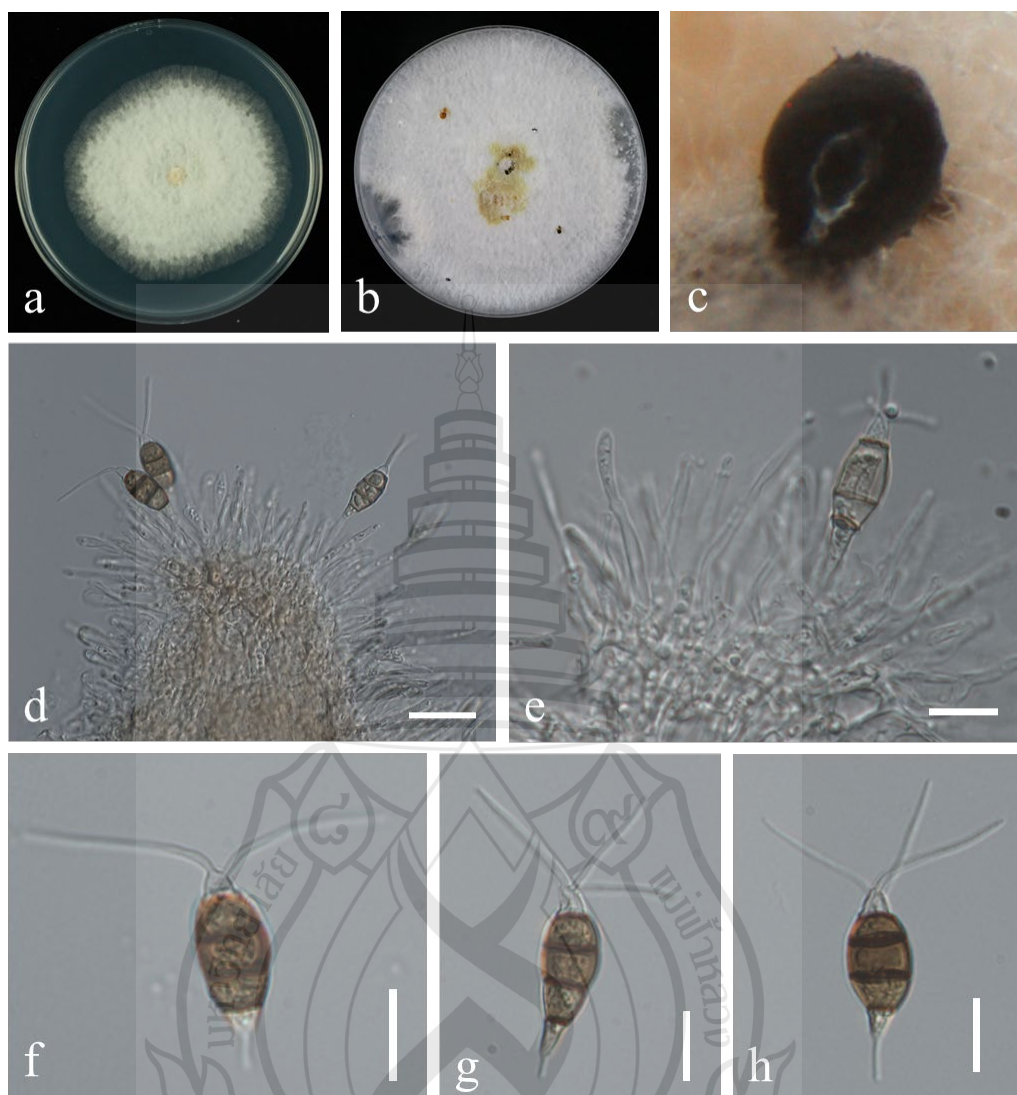
Figure 5.37 Morphological characters of *Pestalotiopsis foliicola* (JZB340174)

Figure 5.37 a Colony on PDA after four days; b Colony on PDA after three weeks; c Conidiomata on PDA; d–e Conidiogenous cells; f–h Conidia; Scale bars: d=20 µm; e–h=10 µm.

Pestalotiopsis hainanensis A.R. Liu, T. Xu & L.D. Guo, Fungal Diversity 24: 29 (2007)

Associated with stem blight of *Vaccinium corymbosum*.

Illustration and description: see Liu et al. (2013).

Material examined – China, Guizhou Province, Majiang County, from stem blight of *Vaccinium corymbosum*, May 2023, X. H. Li and Y. Y. Zhou (dried cultures JZBH340175– JZBH340176), living cultures JZB340175– JZB340176.

Notes – In the phylogenetic analysis, two isolates obtained in the current study (JZB340175–JZB340176) clustered with ex-type of *Pestalotiopsis hainanensis* (CNU060362) with 80% bootstrap support and 1.00 posterior probabilities. And the morphological characters are similar to the ex–type isolate of *Pes. hainanensis* (Liu et al., 2007). *Pestalotiopsis hainanensis* was introduced by Liu et al. (2007) as an endophyte from the stem of *Podocarpus macrophyllus* in China. This is the first report of *Pestalotiopsis hainanensis* on *Vaccinium* spp.

Pestalotiopsis kenyana Maharachch., K.D. Hyde & Crous, in Maharachchikumbura, Hyde, Groenewald, Xu & Crous, Stud. Mycol. 79: 166 (2014)

Associated with leaf spot and stem blight on *Vaccinium* spp. For morphological description, see Maharachchikumbura et al. (2014).

Material examined – China, Fujian Province, Longyan City, from leaf spot of *Vaccinium corymbosum*, May 2023, X. H. Li and Y. Y. Zhou (dried cultures JZBH340177– JZBH340187), living cultures JZB340177– JZB340187; *ibid.*, from stem blight of *Vaccinium corymbosum*, May 2023, X. H. Li and Y. Y. Zhou (dried cultures JZBH340188), living cultures JZB340188; China, Guizhou Province, Majiang County, from leaf spot of *Vaccinium corymbosum*, May 2023, X. H. Li and Y. Y. Zhou (dried cultures JZBH340189– JZBH340190), living cultures JZB340189– JZB340190; *ibid.*, from stem blight of *Vaccinium corymbosum*, May 2023, X. H. Li and Y. Y. Zhou (dried cultures JZBH340191), living cultures JZB340191; *ibid.*, from stem blight of *Vaccinium virgatum*, May 2023, X. H. Li and Y. Y. Zhou (dried cultures JZBH340192– JZBH340193), living cultures JZB340192– JZB340193.

Notes – In the phylogenetic analysis, seventeen isolates obtained in the current study (JZB340177– JZB340193) clustered with reference isolates of *Pestalotiopsis kenyana* (including ex-type CBS 442.67) with 91% bootstrap support and 1.00 posterior probabilities. And the morphological characters are similar to the ex-type isolate of *Pes. kenyana* (Maharachchikumbura et al., 2014). *Pestalotiopsis kenyana* was introduced by Maharachchikumbura et al., (2014) from the branch of *Coffea* sp. in Kenyana. Subsequently the species has been reported to cause leaf blight of bayberry (*Myrica rubra*), prickly ash (*Zanthoxylum schinifolium*) and tea (*Camellia sinensis*) (Wang et al., 2019; Liu et al., 2021; Xun et al., 2023), as well as stem-end rot of mango fruits

(Tao et al., 2024). This is the first report of *Pestalotiopsis kenyana* on blueberry (*Vaccinium* spp.), which also could be common pathogen on blueberry.

    Pestalotiopsis rhodomyrti Yu Song, K. Geng, K.D. Hyde & Yong Wang bis [as 'rhodomyrtus'], in Song, Geng, Zhang, Hyde, Zhao, Wei, Kang & Wang, Phytotaxa 126(1): 27 (2013)

    Associated with leaf spot and stem blight of *Vaccinium corymbosum*. For morphological description, see Song et al. (2013).

    Material examined – China, Fujian Province, Longyan City, from leaf spot of *Vaccinium corymbosum*, May 2023, X. H. Li and Y. Y. Zhou (dried cultures JZBH340194–JZBH340195), living cultures JZB340194– JZB340195; Guizhou Province, Majiang County, from leaf spot of *Vaccinium corymbosum*, May 2023, X. H. Li and Y. Y. Zhou (dried cultures JZBH340196), living cultures JZB340196; *ibid.*, Jilin Province, Ji'an City, from stem blight of *Vaccinium corymbosum*, September 2023, X. H. Li (dried cultures JZBH340197–JZBH340200), living cultures JZB340197–JZB340200.

    Notes – In the phylogenetic analysis, eight isolates obtained in the current study (JZB340194–JZB340200) clustered with ex-type of *Pestalotiopsis rhodomyrtus* (LC3413) with 100% bootstrap support and 1.00 posterior probabilities. And the morphological characters are similar to the ex-type isolate of *Pes. rhodomyrtus* (Song et al., 2013). *Pestalotiopsis rhodomyrtus* was introduced by Song et al. (2013) from asymptomatic leaves of *Rhodomyrtus tomentosa* in China, and also has been reported on diseased tea plants (Liu et al., 2017), as well as on *Rosa* spp. (Peng et al., 2022). This is the first report of *Pestalotiopsis rhodomyrtus* on *Vaccinium* spp.

    Pestalotiopsis tumida C. Peng & C.M. Tian, in Peng, Crous, Jiang, Fan, Liang & Tian, Persoonia 49: 235 (2022). Figure 5.38

    Associated with leaf spot of *Vaccinium angustifolium*. **Sexual morph:** Not observed. **Asexual morph:** *Conidiomata* in culture subglobose to globose, solitary or gregarious, semi-immersed or immersed, exuding black conidial masses. *Conidiophores* indistinct, often reduced to conidiogenous cells. *Conidiogenous cells* discrete, cylindrical to ampulliform, hyaline, 7.3–10.8 × 3.1–4.5 μm ($\bar{x}$ = 9.2 × 3.6 μm, n = 20). *Conidia* fusoid to ellipsoid, straight to slightly curved, 4-septate, slightly constricted at the septa, 19.5–24.8 × 5.3–7.1 μm ($\bar{x}$ = 22.1 × 6.2 μm, n = 30), L/W ratio

= 3.6; basal cell obconic with a truncate base, hyaline, thin-walled, 2.6–5.3 μm long ($\overline{x}$ = 3.6 μm, n = 30); three median cells doliiform, 14.5–17.3 μm ($\overline{x}$ = 15.7 μm, n = 30) long, concolorous, (second cell from the base pale brown to brown, 4.3–5.4 μm long; third cell brown, 4.4–5.8 μm long; fourth cell brown, 4.4–6.1 μm long); apical cell 3.2–5.8 μm ($\overline{x}$ = 4.2 μm, n = 30) long, hyaline, conical to subcylindrical, thin- and smooth-walled, with 2–3 tubular apical appendages (mostly 3), arising from the apical crest, unbranched, filiform, flexuous, 9.7–27.4 μm ($\overline{x}$ = 17.6 μm, n = 50) long; basal appendage single, tubular, unbranched, centric, 5.9–15.6 μm ($\overline{x}$ = 10.0 μm, n = 30) long.

Culture characteristics – Colonies on PDA reaching 60 mm diam. after five days at 25°C, flat with entire edge, aerial mycelium white, flocculent, forming black conidiomata with black conidial masses from colony centre; colony from reverse pale yellow in centre.

Material examined – China, Jilin Province, Gongzhuling City, from diseased leaves of *Vaccinium angustifolium*, June 2023, X. H. Li, Y. Y. Zhou and P. Z. Chen (dry cultures JZBH340201– JZBH340202), living cultures JZB340201– JZB340202.

Notes – Two new isolates (JZB340201– JZB340202) are phylogenetically close to *Pes. tumida* and *Pes. appendiculata*. We compared the morphological characters of two species (table 5.4), and found that the holotype of *Pes. tumida* (BJFC-S1891) have wider conidia than *Pes. appendiculata* (6.5–7.5 μm vs. 5–6 μm) and smaller L/W ratio (3.1 vs. 4.2), as well as more and longer basal appendage (1–2 basal appendages, (6.5 –)7–19(–19.5) μm vs. single appendages, 3–5 μm). However, additional strain of *Pes. tumida* (CGMCC 3.23502) described in by Razaghi (2024), have larger ranges of dimension, which have overlapped that of *Pes. appendiculata*. As two species were introduced at the same year (Gu et al., 2022; Peng et al., 2022) without compared with each other, we speculate that the two species have the possibility to be same. According the above information, we currently identify our isolates as *Pes. tumida*, which has been published earlier. Whether *Pes. appendiculata* be synonymized under *Pes. tumida* need to be further studied. *Pestalotiopsis tumida* was introduced from branches and spines of *Rosae chinensis* in China (Peng et al., 2022), which is also the only host reported. This is the first report of *Pes. tumida* on blueberry (*Vaccinium* spp.).
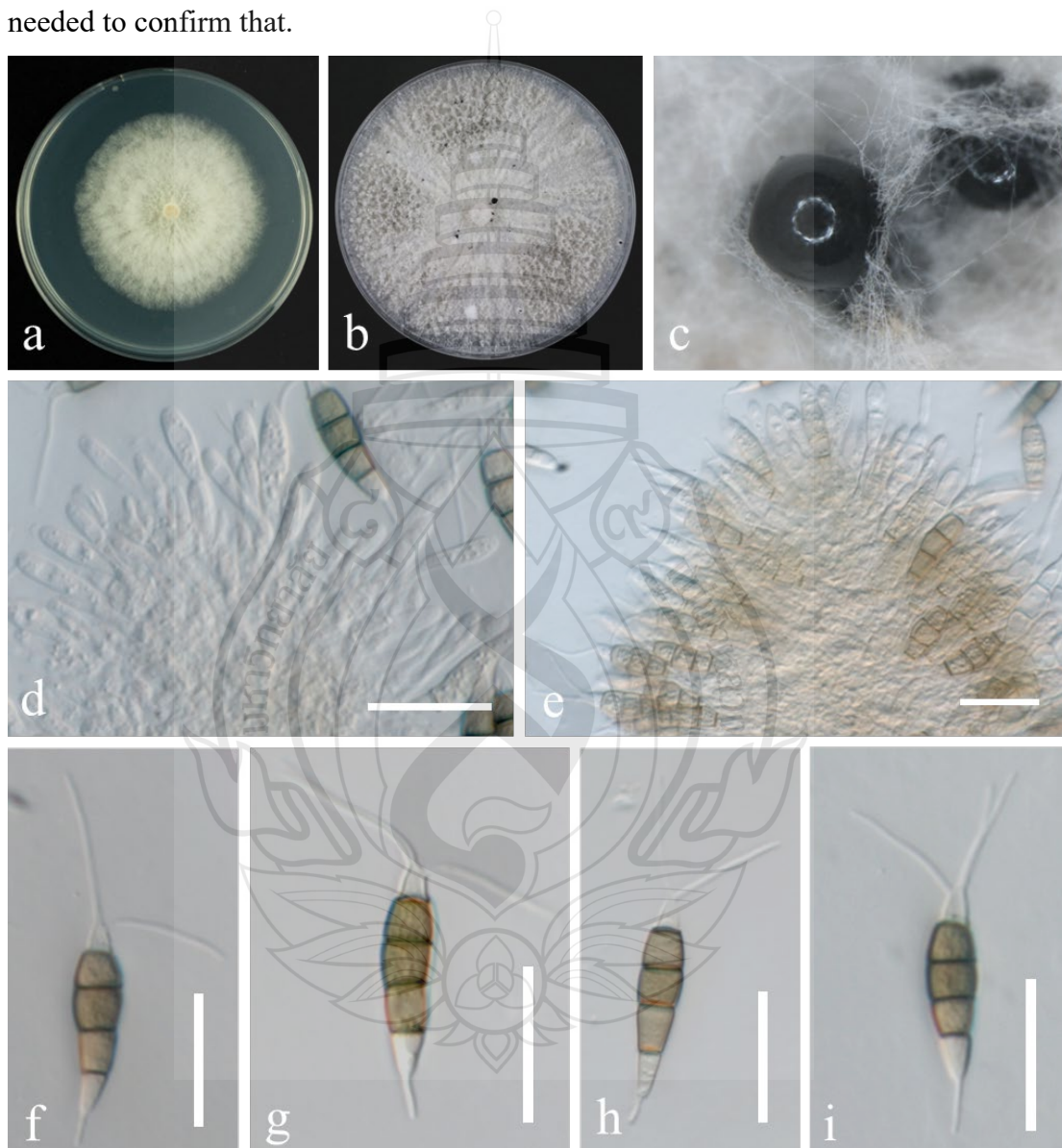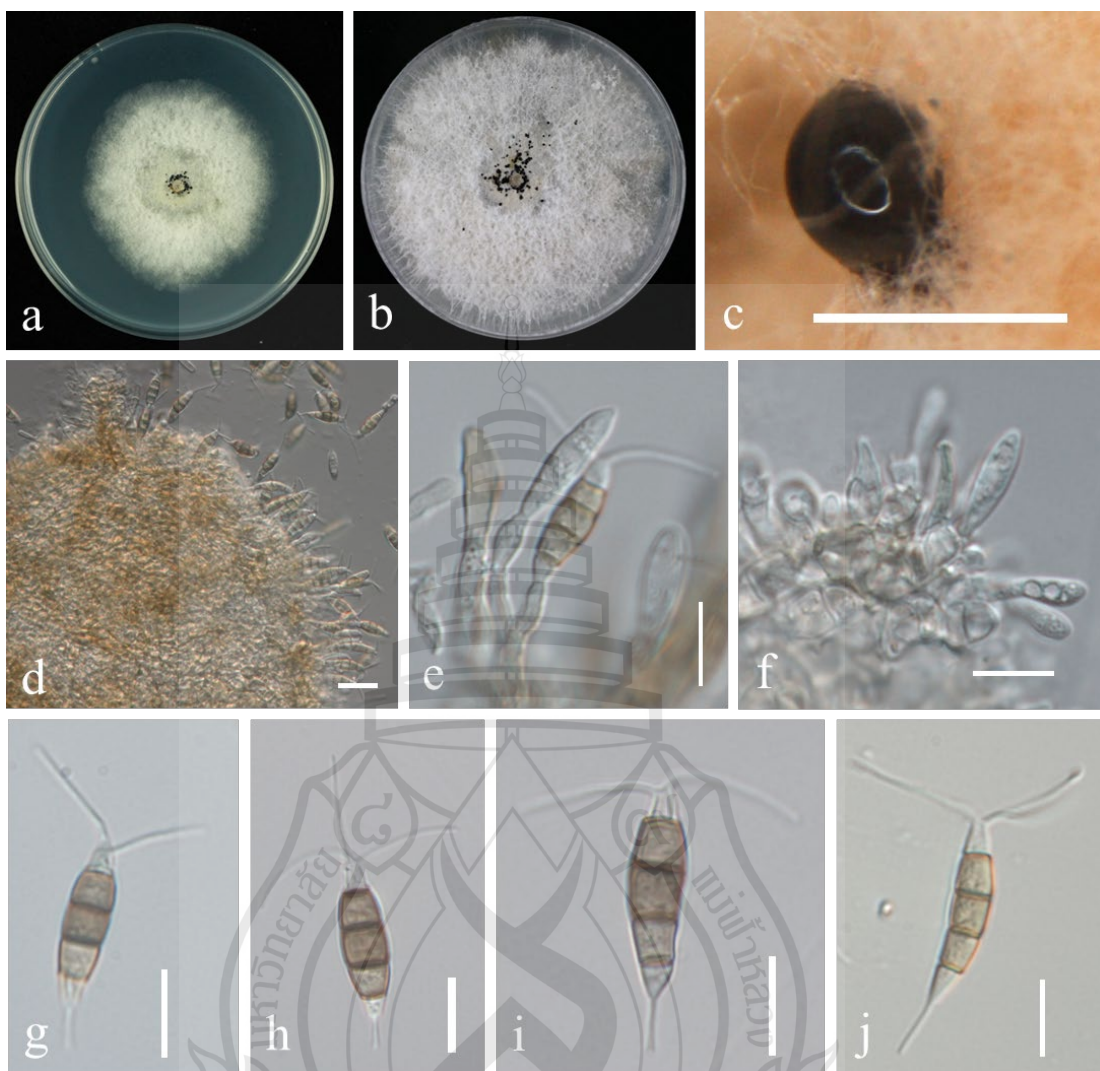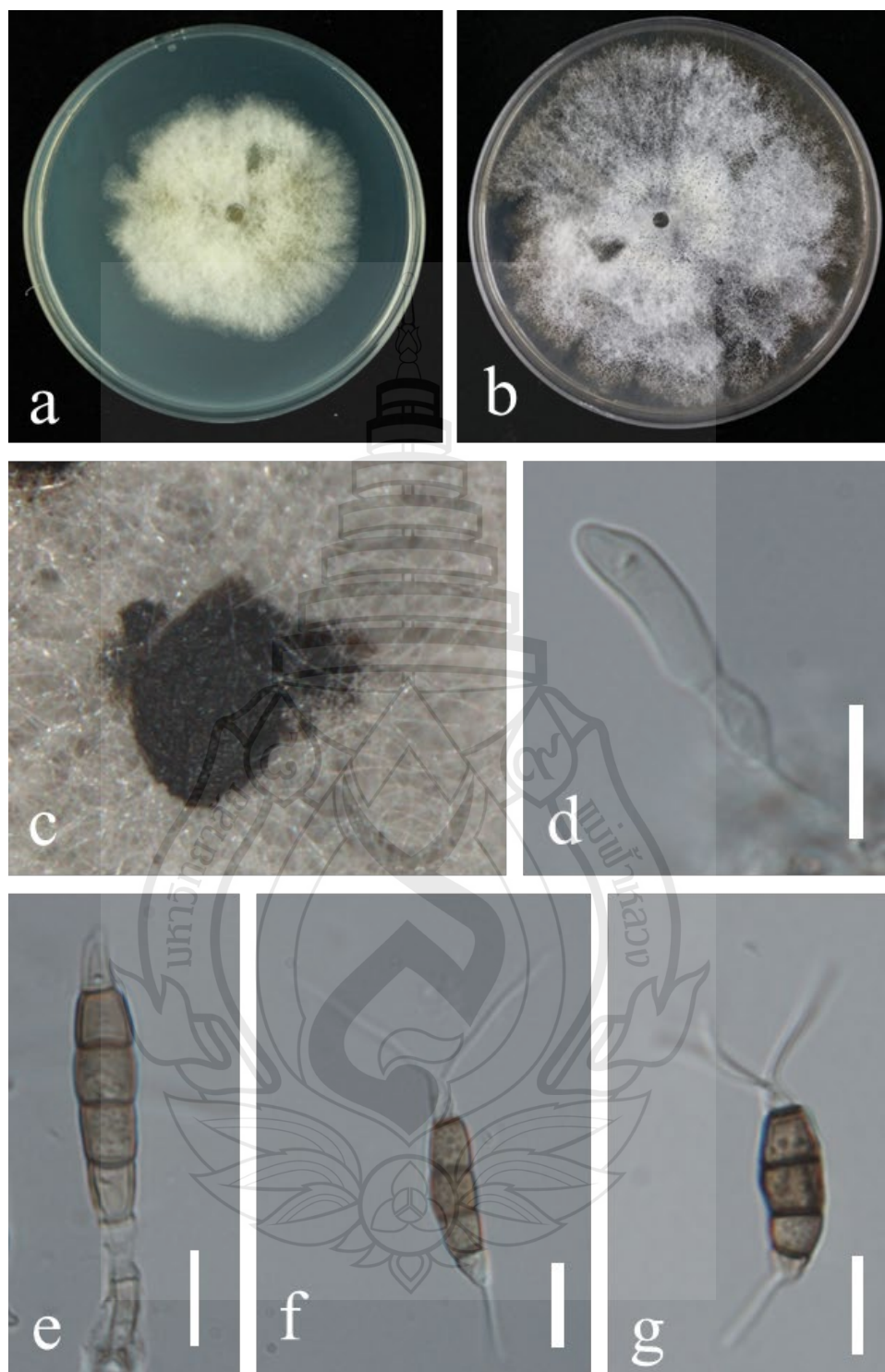
Figure 5.38 Morphological characters of *Pestalotiopsis tumida* (JZB340201)

Figure 5.38 a Colony on PDA after four days; b Colony on PDA after three weeks; c Conidiomata on PDA; d–e Conidiogenous cells; f–g Conidia. Scale bars: d–j=10 μm.

5.3.5 Characterization and Pathogenicity of Three New Host Records Associated with Blueberry Stem Blight

Among the 61 new host records generated from this study, some of them have been reported to cause important diseases on other hosts, while some others have not been reported on diseased plants. In spite of this, their pathogenicity needs to be verified on blueberry for the different susceptibility to pathogen of different hosts. In this study, three species *Colletotrichum temperatum*, *Curvularia austriaca*, and *Diaporthe unshiuensis* associated with blueberry stem blight were selected, their molecular and morphological characters were charactered, and pathogenicity test was conducted.

5.3.5.1 Taxonomy

Colletotrichum temperatum V.P. Doyle, P.V. Oudem. & S.A. Rehner, PLoS ONE 8(12): e51392, 17 (2013) Figure 5.39

Index Fungorum no: IF 801463; Facesoffungi Number: FoF 16980

Classification: Glomerellaceae, Glomerellales, Hypocreomycetidae, Sordariomycetes, Ascomycota, Fungi (Hyde et al., 2024)

Pathogenic on *Vaccinium corymbosum*. **Sexual morph** developed on PNA: *Ascomata* 156–387 × 147–347 μm ($\bar{x}$ = 259.7 × 222.6 μm, n = 15), solitary to clustered, subglobose to obpyriform, dark brown to black. *Asci* 38–64 × 8.5–13 μm ($\bar{x}$ = 49.2 × 10.7 μm, n = 30), 8-spored, obclavate, hyaline. *Ascospores* 15–25.5 × 4–5.5 μm ($\bar{x}$ = 19.0 × 4.90 μm, n=30), uniseriate to biseriate, reniform to lunate, aseptate, hyaline, with granular contents. **Asexual morph** developed on the blueberry stem. *Conidiomata* 295–478 × 213–371 μm ($\bar{x}$ = 390.6 × 290.1 μm, n = 15), acervular, semi-immersed, secreting orange conidial masses. Setae not observed. *Conidiophores* branched, hyaline, septate, smooth-walled. *Conidiogenous cells* 8–18 × 3–5 μm ($\bar{x}$ = 13.5 × 3.8 μm, n = 30), cylindrical to ampulliform, tapering toward the apex, hyaline. *Conidia* 13.5–17 × 5–6 μm ($\bar{x}$ = 15.4 × 5.4 μm, n = 30), subcylindrical, straight, hyaline, aseptate, rounded ends, while some conidia one end rounded and the other slightly acute. *Appressoria* 8–16.5 × 5.5–12.5 μm ($\bar{x}$ = 11.5 × 8.1 μm, n = 30), single, terminal, irregular, olivaceous.

Colony Characters — Colonies on PDA reach 85 mm diam. after six days, white to pale grey, flat with floccose aerial mycelium, reverse greyish white.

Material Examined — CHINA, Jilin Province, Ji'an City, on the diseased stem of *V. corymbosum*, 9 Sep. 2023, X.H. Li (dry cultures JZBH330443, JZBH330444), living cultures JZB330443, JZB330444.

Notes — In the phylogenetic tree of the *Colletotrichum gloeosporioides* species complex, isolates generated in this study (JZB330443, JZB330444) clustered with the ex-type of *Colletotrichum temperatum* (CBS 133122) with 85% ML bootstrap support and 1.00 BYPP (Figure 5.40). Morphologically, ascospore length of JZB330444 (15–25.5 μm, x̄ = 19.0 μm) cultured on PNA is larger than that of the ex-type (CBS 133122, 14.3–15.3 μm) of *C. temperatum* cultured on CMA, and the conidium width of JZB330444 (5–6 μm, x̄ = 5.4 μm) cultured on PNA is larger than that of the ex-type (CBS 133122, 4.5–4.7 μm) of *C. temperatum* cultured on CMA (Liu et al., 2022), the differences may be caused by the difference of the medium. *Colletotrichum temperatum* was introduced by Doyle and colleagues (Liu et al., 2022) from the decayed fruit of cranberry (*Vaccinium macrocarpon*) in the USA. This species has also been reported to be associated with grape fruit rot in the USA and cherry leaf spot in China (Bhunjun et al., 2024; Dean et al., 2012). This is the first report of *Colletotrichum temperatum* as a pathogen on *Vaccinium corymbosum*.
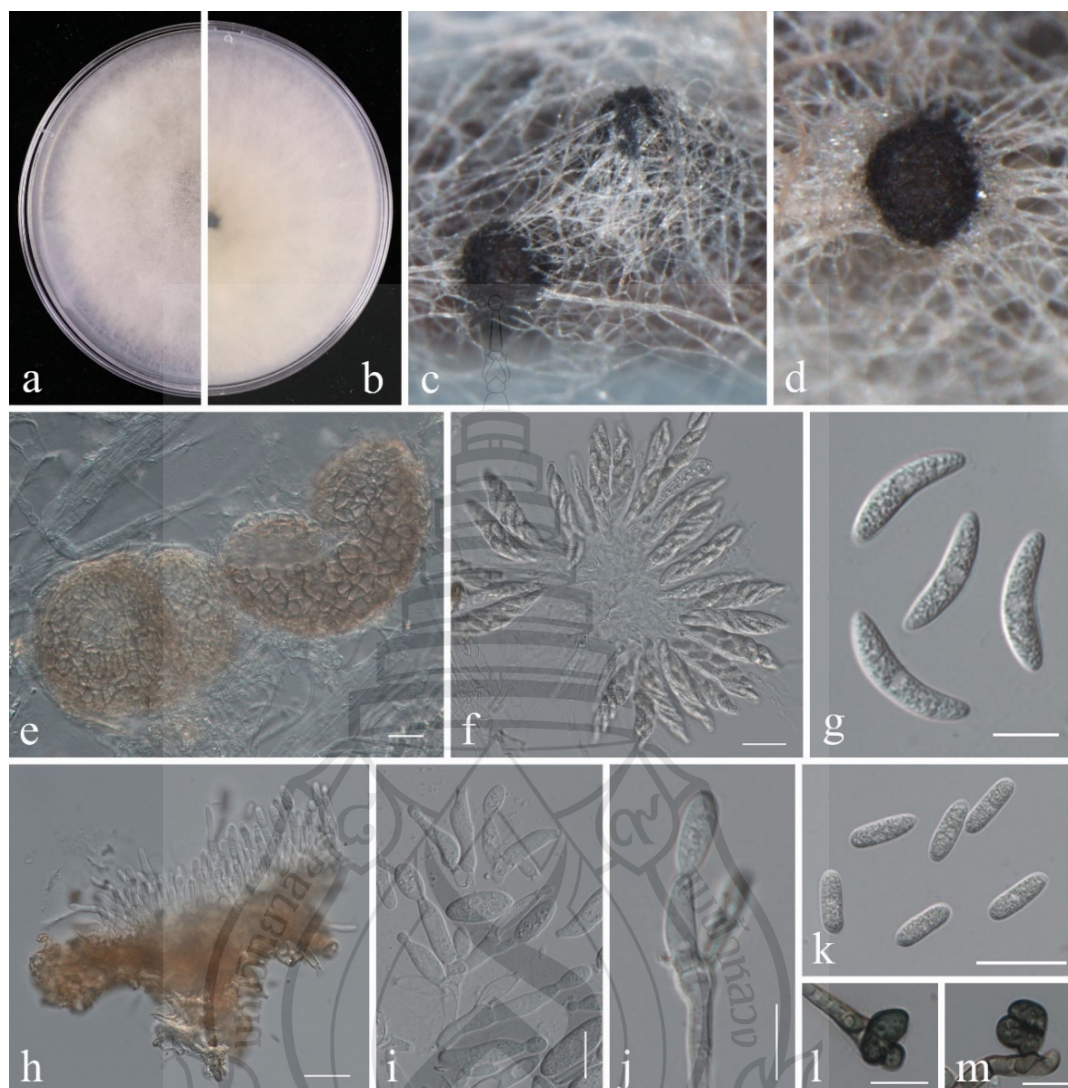
Figure 5.39 Morphological characters of *Colletotrichum temperatum* (JZB330444)

Figure 5.39 a An upper view of colonies on the PDA; b Reverse view of colonies on the PDA; c–e Ascomata; f Asci; g Ascospores; h Section view of acervulus; i–j Conidiophores; k Conidia; l–m Appressoria. Scale bars: e, f, h, k = 20 μm; g–j, l, m = 10 μm.
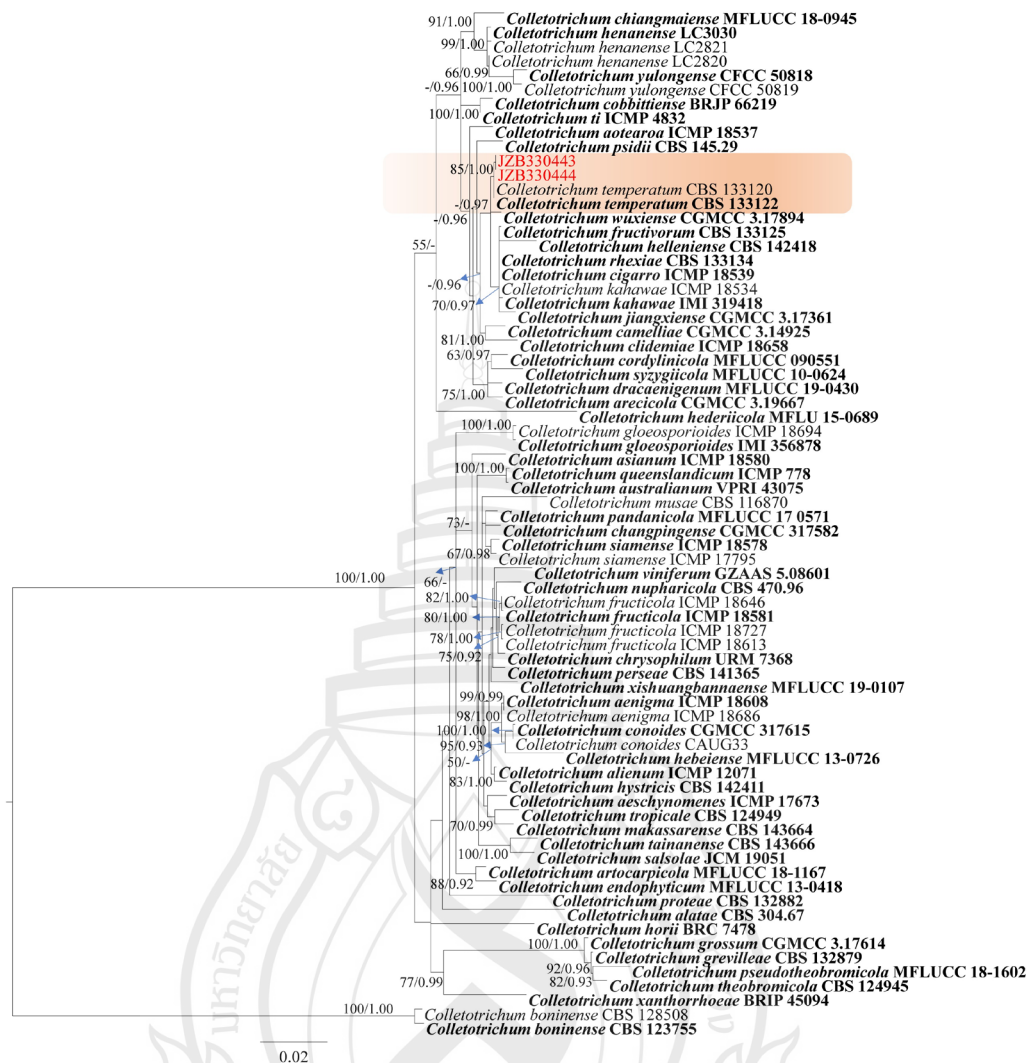
Figure 5.40 Phylogenetic tree generated by maximum likelihood (ML) analysis of the combined ITS, *gapdh*, *chs*, *act* and *tub* sequence data of species belonging to *Colletotrichum gloeosporioides* species complex

Figure 5.40 The tree is rooted with *Colletotrichum boninense* (CBS 123755 and CBS 128508). The tree topology of the ML analysis was similar to the Bayesian analysis. The best-scoring RAxML tree with a final likelihood value of -9965.268605 is presented (Figure 2). The matrix had 818 distinct alignment patterns, with 9.03% of undetermined characters or gaps. Estimated base frequencies were as follows: A = 0.226449, C = 0.302220, G = 0.238651, T = 0.232680; substitution rates AC = 1.012333, AG = 2.893451, AT = 1.007060, CG = 0.896810, CT = 4.881719, GT = 1.000000; gamma distribution shape parameter α = 1.066665. RAxML bootstrap support values

≥50% and Bayesian posterior probabilities ≥0.90 (BYPP) are shown near the nodes. The scale bar indicates 0.02 changes. The ex-type strains are in bold and isolates from the current study are in red.

Curvularia austriaca Y. Marín & Crous, in Marin-Felix, Hernández-Restrepo & Crous, Mycol. Progr. 19(6): 564 (2020) Figure 5.41

Index Fungorum no: IF 830045; Facesoffungi Number: FoF 16981

Classification: Pleosporaceae, Pleosporales, Pleosporomycetidae, Dothideomycetes, Ascomycota, Fungi (Hyde et al., 2024).

Pathogenic on *Vaccinium corymbosum*. **Sexual morph:** Not observed. **Asexual morph:** On PDA: *hyphae* 2–4 μm wide, branched, subhyaline to pale brown, septate. *Conidiophores* simple, rarely branched, straight to flexuous, often geniculate at the apex, pale brown, septate. *Conidiogenous cells* 6–14 × 3–5.5 μm ($\bar{x}$ = 10.0 × 4.0 μm, n = 10), terminal or intercalary, subcylindrical to slightly swollen, subhyaline to pale brown, smooth-walled. *Conidia* 21–29.5 × 7.5–12 μm ($\bar{x}$ = 25.5 × 9.7 μm, n = 30), straight or slightly curved, ellipsoidal to obovoid, middle cells slightly enlarged, smooth-walled to finely verruculose, apical and basal cells hyaline to pale brown, middle cells dark brown in matured conidia, 3 distoseptate, middle septa dark brown. *Hila* 1.5–2.5 μm wide, protruding, darkened, thickened. *Chlamydospores* not observed.

Culture characteristics — Colonies on PDA reach 85 mm diam. after 7 days, margin lobulate, luteous to orange, umber in the centre, aerial mycelium moderate, slightly cottony; reverse luteous to orange.

Material Examined — CHINA, Jilin Province, Ji'an City, on the diseased stem of *V. corymbosum*, 9 Sep. 2023, X.H. Li (dry cultures JZBH3720001, JZBH3720002), living cultures JZB3720001, JZB3720002.

Notes —Two isolates obtained from the blueberry stems in the present study (JZB3720001 and JZBH3720002) phylogenetically clustered with *Curvularia* strains (CBS 102694, UTHSC 08-2957 and UTHSC 09-3510), with 97% ML bootstrap support and 1.00 BYPP (Figure 5.42). The morphological characters of our isolates are in accordance with the description of *C. austriaca* type (Fu et al., 2019). This species was introduced by Marin-Felix and colleagues from a human (Fu et al., 2019), and no other records from plant hosts afterwards. This is the first report of *C. austriaca* associated with stem blight on *Vaccinium corymbosum*.
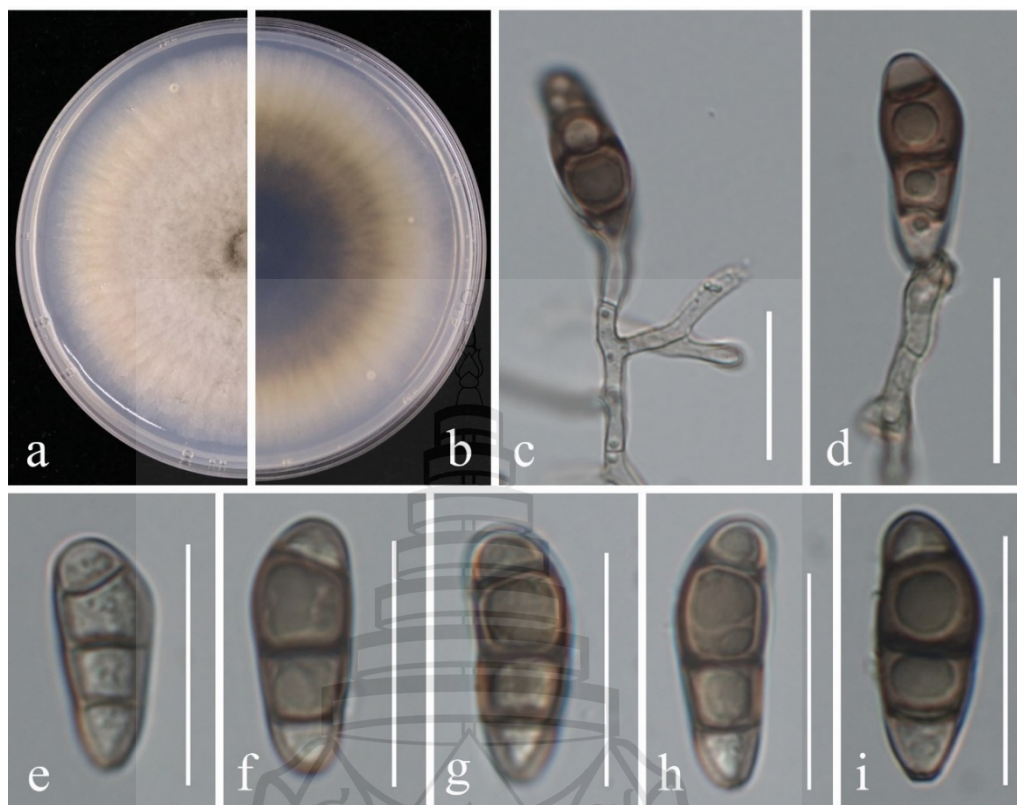
Figure 5.41 Morphological characters of *Curvularia austriaca* (JZB3720002)

Figure 5.41 a An upper view of colonies on the PDA; b Reverse view of colonies on the PDA; c–d Conidiogenous cells and conidia; e Immature conidia; f–i Mature conidia. Scale bars: c–i = 20 μm.
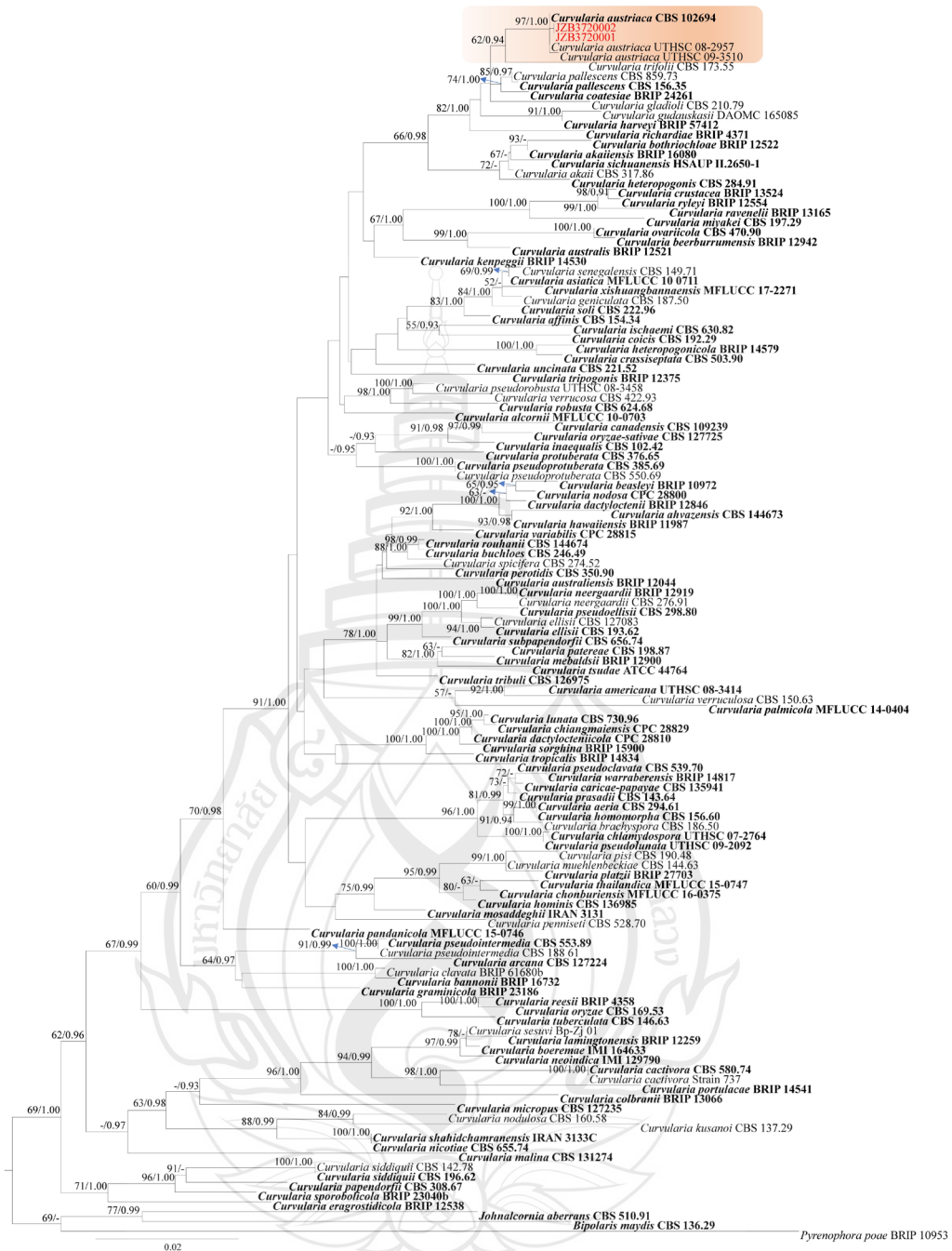
Figure 5.42 Phylogenetic tree generated by maximum likelihood analysis of the combined ITS, *gapdh* and *tef* sequence data of species belonging to *Curvularia*

Figure 5.42 The tree is rooted with *Bipolaris maydis* (CBS 136.29), *Johnalcornia aberrans* (CBS 510.91) and *Pyrenophora poae* (BRIP 10953). The ex-type strains are in bold and isolates from the current study are in red. The matrix had

655 distinct alignment patterns, with 17.23% of undetermined characters or gaps. Estimated base frequencies were as follows: A = 0.228223, C = 0.307112, G = 0.244933, T = 0.219732; substitution rates AC = 1.125622, AG = 4.404677, AT = 1.020378, CG = 1.429845, CT = 8.302359, GT = 1.000000; gamma distribution shape parameter α = 0.636951. RAxML bootstrap support values ≥50% and Bayesian posterior probabilities ≥0.90 (BYPP) are shown near the nodes. The scale bar indicates 0.02 changes.

Diaporthe unshiuensis F. Huang, K.D. Hyde & Hong Y. Li, in Huang, Udayanga, Mei, Fu, Hyde & Li, Fungal Biology 119(5): 344 (2015). Figure 5.43

Index Fungorum no: IF 810845; Facesoffungi Number: FoF 09422

Classification: Diaporthaceae, Diaporthales, Diaporthomycetidae, Sordariomycetes, Ascomycota, Fungi

Pathogenic on *Vaccinium corymbosum*. **Sexual morph:** Not observed. *Asexual morph*: On PNA: *Pycnidia* 103–371 × 80–285 μm (x̄ = 156.9 × 125.4 μm, n = 25), globose to subglobose, dark brown to black. *Conidiophores* were not observed. *Conidiogenous cells* were not observed. *Alpha conidia* 6–8.5 × 2–3 μm (x̄ = 6.7 × 2.7 μm, n = 50), straight to slightly curved, ellipsoidal to fusiform, sometimes with one end obtuse and the other acute, hyaline, smooth, aseptate, biguttulate. *Beta conidia* not observed.

Culture characteristics — Colonies on PDA reach 85 mm diam. after 4 days, white and turning to grey with ageing, reverse white or pale brown pigmentation at the centre.

Material Examined — CHINA, Jilin Province, Ji'an City, on the diseased stem of *V. corymbosum*, 9 Sep. 2023, X.H. Li (dry cultures JZBH320309, JZBH320310), living cultures JZB320309, JZB320310.

Notes — In the phylogenetic analysis, two isolates (JZB320309, JZB320310) obtained from this study formed a well-supported clade with the ex-type strain of *Diaporthe unshiuensis* (ZJUD52), with 100% ML bootstrap support and 1.00 BYPP (Figure 5.44). Morphologically, the two isolates are similar to the ex-type of *D. unshiuensis* (Gomes et al., 2013). *Diaporthe unshiuensis* was first reported by Huang and colleagues (Gomes et al., 2013) as an endophyte on the fruits of *Citrus unshiu* and on asymptomatic branches and twigs of *F. margarita* in China. Subsequently, the

species was also isolated from asymptomatic twigs of *Carya illinoensis* (Norphanphoun et al., 2022) and the healthy root of *M. officinalis* (Hongsanan et al., 2023). However, later it was found as a pathogen causing shoot blight, canker and dieback on fruit trees, including citrus, pear, kiwifruit, grapevine and peach (Dissanayake et al., 2024; Huang et al., 2025; Yang et al., 2018; Manawasinghe et al., 2019; Luo et al., 2022). The species was mostly distributed in China, and also reported from soybean in the USA (Guo et al., 2020). This is the first report of *D. unshiuensis* causing stem blight on *Vaccinium corymbosum*.
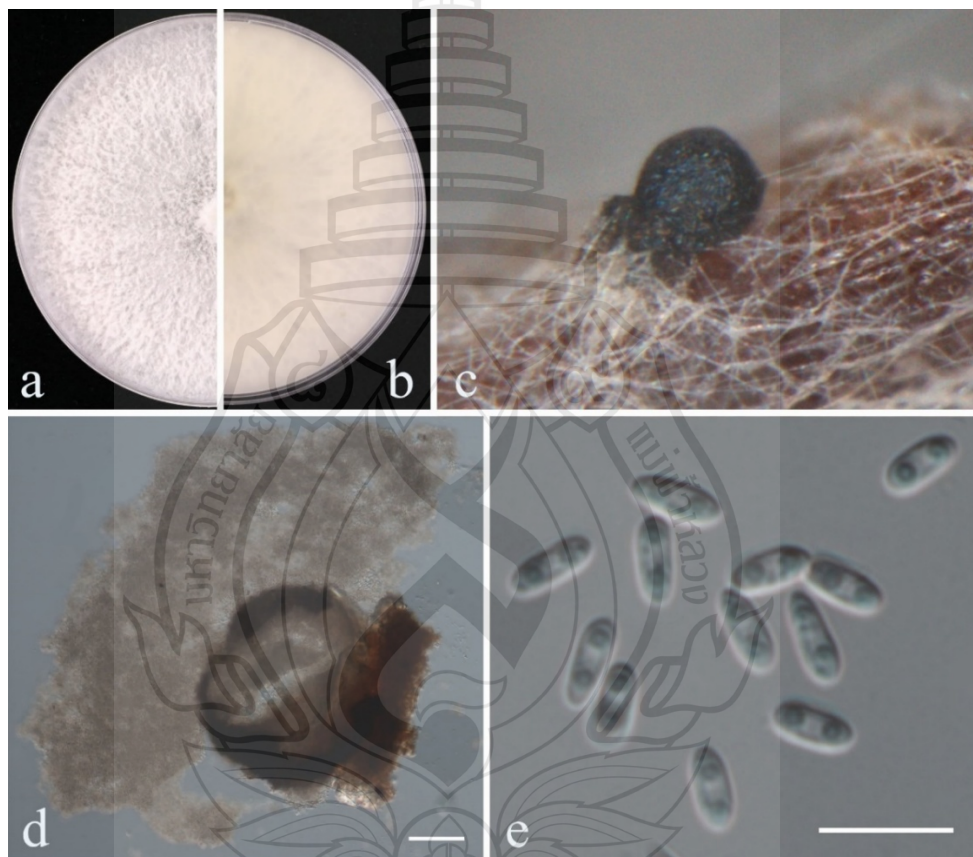
Figure 5.43 Morphological characters of *Diaporthe unshiuensis* (JZB320309)

Figure 5.43 a An upper view of colonies on the PDA; b Reverse view of colonies on the PDA; c Conidiomata sporulating on PNA; d Cross section of conidiomata; e Alpha conidia. Scale bars: d = 100 μm; e = 10 μm.
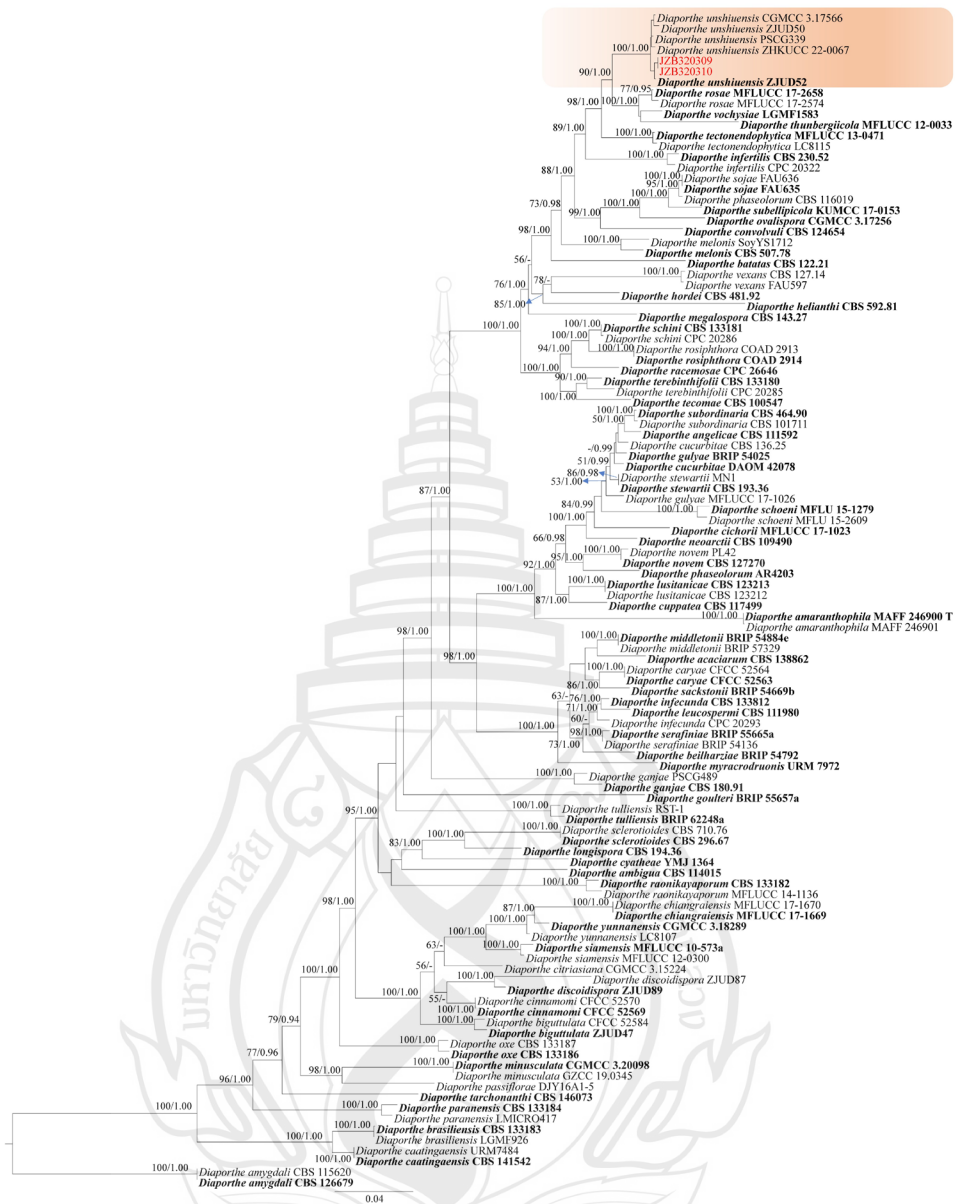
Figure 5.44 Phylogenetic tree generated by maximum likelihood analysis of combined ITS, *tef*, *tub*, *cal* and *his* sequence data of species belonging to *Diaporthe sojae* species complex

Figure 5.44 The tree is rooted with *D. amygdali* (CBS 126679 and CBS 115620). The tree topology of the ML analysis was similar to the Bayesian analysis. The best-scoring RAxML tree with a final likelihood value of -27986.001494 is presented (Figure 6). The matrix had 1208 distinct alignment patterns, with 19.34% of undetermined characters or gaps. Estimated base frequencies were as follows: A =

0.214688, C = 0.319197, G = 0.242643, T = 0.223473; substitution rates AC = 1.222391, AG = 3.869013, AT = 1.482265, CG = 1.021922, CT = 5.320754, GT = 1.000000; gamma distribution shape parameter α = 1.100460. RAxML bootstrap support values ≥50% and Bayesian posterior probabilities ≥0.90 (BYPP) are shown near the nodes. The scale bar indicates 0.04 changes. The ex-type strains are in bold and isolates from the current study are in red.

5.3.5.2 Pathogenetic assay

The virulence of *Colletotrichum temperatum* (JZB330444), *Curvularia austriaca* (JZB3720002), and *Diaporthe unshiuensis* (JZB320309) was assessed using a detached green shoots assay on *Vaccinium corymbosum* (Fig.5.45). Two weeks post-inoculation, necrotic lesions with dark brown margins were observed on all three treatments. The shoots inoculated with *D. unshiuensis* showed significant lesion development. Reddish-brown lesions extended upwards and downwards from the inoculation point, with the emergence of the brownish conidiomata that became black upon maturation, either solitary or clustered in groups of 3–5 conidiomata. On the shoots inoculated with *Colletotrichum* and *Curvularia*, lesions developed slowly, while dense black mycelia of *Curvularia* and fruiting bodies of *Colletotrichum* appeared at the inoculation point, leading to blight and necrosis of plant tissue. Interestingly, black ascomata and conidiomata secreting conidial masses of *Colletotrichum* appeared simultaneously. Twenty-one days after inoculation, *D. unshiuensis* developed the largest lesions (3.08 cm), while *C. temperatum* and *Curvularia austriaca* were less aggressive, with lesions of 0.75 and 0.65 cm, respectively. No lesions developed on the shoots inoculated with PDA discs. Koch's postulates were fulfilled by re-isolating original fungi from symptomatic stems.
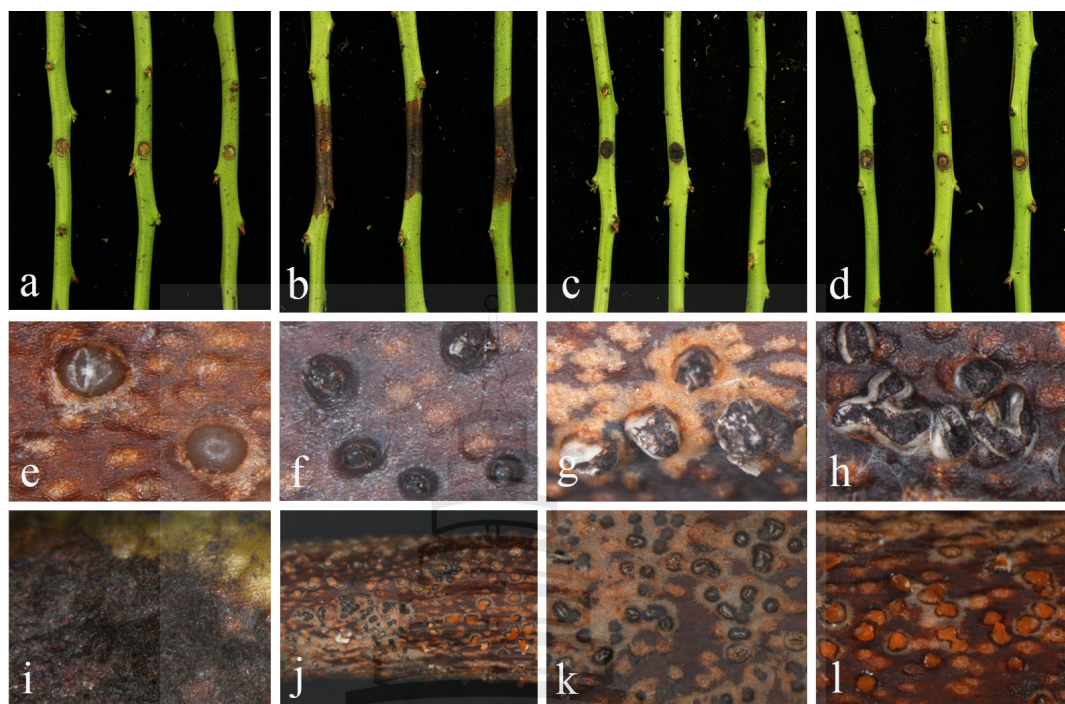
Figure 5.45 Pathogenicity assay on *Vaccinium corymbosum* shoots (cv. 'Duke')

Figure 5.45 a Control treatment, b Inoculated by *Diaporthe unshiuensis*, c Inoculated by *Curvularia austriaca*, d Inoculated by *Colletotrichum temperatum*, e–h Conidiomata of *Diaporthe unshiuensis* on the shoot lesions, i Mycelia of *Curvularia austriaca* on the shoot lesion, j Ascomata and conidiomata produced by *Colletotrichum temperatum* on the shoot lesion, k Ascomata of *Colletotrichum temperatum* on the shoot lesion, l Conidiomata of *Colletotrichum temperatum* on the shoot lesion.

5.3.6 Summary

In this section, micro-fungi associated with leaf, stem and root diseases from five provinces in China were identified and analysed. 429 isolates were identified to 90 species of 40 genera, the isolation source and collecting region of each species were listed. The isolation ratio of the genera among all the isolates was presented, and their distributions in different plant parts and collecting regions were further analysed. The dominant fungal group pestalotioid fungi, which accounted for more than 25% of the total isolates, were described, and species with ambiguous phylogeny or morphology were discussed. In addition, three new host record species of *Colletotrichum*, *Curvularia* and *Diaporthe* were described, and their virulence on blueberry stem was verified.

5.4 Discussion

The occurrence of blueberry diseases has been more frequent in recent years. Knowledge of the pathogens is crucial for understanding the occurrence, diagnosis and management of diseases. The current study provided insight into the communities of micro-fungi associated with fruit, leaf, stem and root diseases. The results showed that one disease type is associated with various fungi, suggesting the complexity of the pathogen groups.

5.4.1 Fungal Pathogens of Blueberry Fruit Rots

The perishable nature of blueberry fruits places a constant strain on industrial development. In the current study, among the seven species identified, *Botrytis cinerea* and *Colletotrichum fioriniae* have previously been recognized as important pathogens of blueberry fruit rot (Neugebauer et al., 2024). Grey mould caused by *Botrytis cinerea* could occur in open fields and greenhouses, affecting blueberries from the seedling stage to post-harvest. Rainfall and high humidity during the flowering period of blueberry were more conducive to the occurrence of severe grey mould (Zhai et al., 2024). In China, Dai et al. (2011) isolated *B. cinerea* from blueberry fruits and identified it by morphology. The current study confirmed the species by morphology and phylogeny. For *Colletotrichum fioriniae*, the pathogenicity on blueberry fruit was initially confirmed by MacKenzie et al. (2009) in Florida, USA, while the test strains were regarded as *C. acutatum*. Subsequently, Damm et al. (2012) accommodated those strains into *C. fioriniae*. Eaton et al. (2021) identified *Colletotrichum* causing fruit rots in mixed-fruit orchards in Kentucky, USA and found that all isolates from blueberry in the study belonged to *C. fioriniae*. In recent years, blueberry fruit disease caused by *C. fioriniae* has also been reported in Chile, Mexico, New Zealand and Poland (Pszczółkowska et al., 2016; Castro et al., 2023; Hosking et al., 2024; Covarrubias-Rivera et al., 2025), and the species is first reported in China in the current study. *Botryosphaeria dothidea* is usually reported as the causal agent of blueberry stem blight together with other Botryosphaeriaceae species (Xu et al., 2015). Zhang et al. (2016) investigated fruit rot in Guizhou Province in China, and the symptoms include rot and necrosis of the pedicel, with raised black spots on the fruit surface. The pathogen was

identified as *B. dothidea* by morphology. In this study, *B. dothidea* from fruit rot in Fujian Province was determined by morphology and phylogenetic analysis. *Diaporthe* is well-known as a genus comprising plant pathogens, endophytes or saprobes with a wide distribution and a range of hosts (Gomes et al., 2013; Norphanphoun et al., 2022; Hongsanan et al., 2023). On blueberry, the genus has been reported to cause stem blight and fruit rot or occur as endophytes or latent pathogens (Hilário et al., 2020). *Diaporthe vaccinii* can infect blueberry fruits throughout the entire growth period but often remains latent until the mature stages to harvest (Milholland & Daykin, 1983). Furthermore, *D. nobilis* was reported to cause postharvest rot of blueberry. Nevertheless, the two species were all synonymized under *D. eres* (Hilário et al., 2021). The isolates generated in this study clustered with *D. velutina*, which has been synonymized under *D. anacardii* (Dissanayake et al., 2024). Among the species reduced to synonymy with *D. anacardii*, *D. phillipsii* was introduced from blueberry, associated with stem dieback. According to the two studies, current *D. anacardii* could be a prevalent pathogen in blueberries. *Neopestalotiopsis* is one of the major causal agents of twig dieback, stem blight and canker, as well as leaf spot on blueberry (Santos et al., 2022), while there are rare records of *Neopestalotiopsis* on blueberry fruit diseases. However, *Neopestalotiopsis* spp. have been reported to cause fruit rots on various hosts such as strawberry, plum and avocado (Darapanit et al., 2021). *Fusarium* is a common pathogen on blueberry causing wilt and root rot (Liu et al., 2014; Li et al., 2023), and *F. acuminatum* was reported to cause postharvest fruit rot (Wang et al., 2016). *Cladosporium* is a cosmopolitan genus comprising phytopathogens, saprobes, endophytes and human pathogens (Bensch et al., 2012; Song et al., 2023). As fruit pathogens, *Cladosporium* spp. were reported on dekopon, grapevine, and raspberry (Briceño & Latorre 2008; Xiao et al., 2022; Delisle-Houde et al., 2024), and *Cladosporium cladosporioides* has been reported to cause blueberry fruit rot (Covarrubias-Rivera et al., 2024). Our species from the above three genera, *Cladosporium guizhouense*, *Fusarium annulatum* and *Neopestalotiopsis surinamensis*, are new host records on blueberry. Their pathogenicity on blueberry was confirmed by the appearance of obvious and commonly reported symptoms. Given the important role of the three genera among plant pathogens, these species could be prevalent or latent pathogens on blueberries.

Though many research have highlighted post-harvest management, many post-harvest diseases originate from infections in the field (Saito et al., 2016). Infections start at bloom but can remain latent until fruit ripening, or express symptoms during the postharvest period (Neugebauer et al., 2024). Latent pathogens can be activated by favourable conditions, environmental stresses and mechanical injuries (Neugebauer et al., 2024). Diseased fruits may be harvested together with healthy fruits in a cluster of blueberries, and cause persistent infection by contaminating healthy fruit, resulting in significant losses (Alvarez Osorio et al., 2022; Neugebauer et al., 2024). Thus, preharvest management, such as disease monitoring, agricultural and chemical control, is crucial for protecting fruit health (Saito et al., 2016; Neugebauer et al., 2024).

5.4.2 Fungi Associated with Blueberry Leaf, Stem and Root Diseases

Leaf, stem and root diseases of blueberry showed complexity and mixed infection of pathogens. This study took an overall look on the fungi associated with these diseases. Taken together, the data from the five provinces of this study, *Neopestalotiopsis*, *Pestalotiopsis*, *Alternaria*, *Fusarium*, *Botryosphaeria* and *Diaporthe* are the main fungal genera related to the diseases, which are consistent with previous studies (Barbu et al., 2018; Živković et al., 2021). The distributions of fungal genera in different plant parts and collecting regions were analysed, and the results showed that *Pestalotiopsis*, *Neopestalotiopsis* and *Fusarium* were the dominant genera associated with leaf, stem and root diseases, respectively. Stem samples comprised most genera, and nine genera existed in the three parts. Among the five provinces, Fujian showed the highest fungal diversity. *Neopestalotiopsis*, *Pestalotiopsis*, *Diaporthe*, and *Neofusicoccum* species were mostly distributed in Fujian Province, and isolates of nine genera were isolated only from Fujian Province.

Among all fungi identified, pestalotioid fungi are the predominant groups. However, the classification situation of *Pestalotiopsis* and *Neopestalotiopsis* was rather complicated. The differences in morphological characteristics and the nucleic acid between species are very small, which makes the delimitation of species boundaries very difficult (Razaghi et al., 2024). Though the recently established classification system of Sporocadaceae has promoted a better understanding of this group and facilitated species identification, many species are still difficult to identify when clustered into ambiguous clades. Pestalotioid fungi from this study were were described,

and some species with indistinct morphological and molecular differences were suggested to be synonymized.

As an important disease, blueberry stem blight has received special attention in recent years. Botryosphaeriaceae and *Pestalotiopsis*-like species have been recognized as major pathogens (Espinoza et al., 2009; Du et al., 2021), while reports of *Diaporthe* species as pathogens on blueberry have also emerged. To date, 23 *Diaporthe* species have been reported on blueberry, including *Diaporthe ambigua*, *D. amygdali*, *D. asheicola*, *D. australafricana*, *D. baccae*, *D. crousii*, *D. eres*, *D. foeniculina*, *D. hybrida*, *D. leucospermi*, *D. malorum*, *D. nobilis*, *D. oxe*, *D. passiflorae*, *D. phillipsii*, *D. phoenicicola*, *D. rossmaniae*, *D. rudis*, *D. sojae*, *D. sterillis*, *D. vaccinii*, *D. vacuae,* and *D. viticola* (Doyle et al., 2013; Elfar et al., 2013; Lombard et al., 2014; Sessa et al., 2018; Petrović et al., 2021; Wang et al., 2021; Zhao et al., 2019; Xiao et al., 2023). In this study, *Diaporthe unshiuensis* was reported on blueberry for the first time, while it has been reported to cause grapevine dieback and pear canker (Manawasinghe et al., 2019; Guo et al., 2020), so the species was selected for the pathogenicity test. *Colletotrichum* is also a ubiquitous pathogen. Diseases caused by *Colletotrichum*, usually known as anthracnose, lead to extensive yield and economic loss in agricultural production (Yu et al., 2018). On blueberry, *C. siamense*, *C. kahawae*, *C. karstii*, *C. nymphaeae* and *C. sichuaninese* have been reported to cause anthracnose symptoms on blueberry stems (Hilário et al., 2020). *Colletotrichum temperatum*, associated with grape fruit rot in the USA and cherry leaf spot in China (Bhunjun et al., 2024; Dean et al., 2012), was first recorded on blueberry. *Curvularia* is a filamentous fungus that contains many important plant pathogens causing leaf spots, blight, root rot, and other diseases on cereal crops (Tsushima & Shirasu., 2022; Li et al., 2023). The genus also comprises opportunistic pathogens of humans. *Curvularia austriaca*, identified in this study, was originally reported from humans by Marin-Felix and colleagues (Fu et al., 2019), and is now reported on blueberry for the first time in this study. In summary, *Diaporthe unshiuensis*, *Colletotrichum temperatum*, and *Curvularia austriaca* were selected as representative species for common stem pathogen, pathogen on other parts and new plant pathogen respectively. In the pathogenicity test, *Diaporthe unshiuensis* was confirmed to be pathogenic in blueberry, suggesting that it may become an emerging prevalent pathogen on blueberry. The other two species, *Colletotrichum*

temperatum and *Curvularia austriaca*, showed weak virulence on blueberry in the pathogenicity test, indicating that they may not be the major pathogens of stem blight. Nevertheless, their presence cannot be neglected as they may co-infect with *Diaporthe* on blueberry. Interspecies interactions of pathogenic microorganisms may enhance their impact on hosts (Liu et al., 2020). Additionally, the same species may exhibit different virulence on different host varieties (Bell et al., 2021). The pathogenicity of the above species among blueberry cultivars and the interplay between fungal species need to be further studied.

5.4.3 Research Significance and Application

The study provided a series of fungi associated with blueberry disease, with most of them are new host records. All species generated from fruits can cause different fruit rot symptoms, and three representative species from stem also showed pathogenicity. The result showed the potential of the new host record species as pathogen; thus, pathogenicity of all new collections needs to be studied. In addition, prevalence of blueberry fungi was preliminarily studied, some genera distributed widely, and some specially in one region. Their distributions need to be further verified.

The results of the current study contribute to the understanding of blueberry disease and provide a reference for the development of prevention and control strategies, such as the selection of target fungicide and formulation of calendar. Since the disease severity is affected by pathogens, climate factor and blueberry variety, further studies are necessary to explore the occurrence regularity of diseases, pathogen regional distribution, as well as virulence differences among host cultivars.

CHAPTER 6

CONCLUSIONS

6.1 Overall Conclusion

As important fruit crops in China and globally, cherry, grapevine, and blueberry serve as representative crops for understanding disease occurrence in fruit trees. In this study, cherry leaf spot, grapevine trunk disease, and blueberry diseases were investigated in major cultivation areas in China. Field symptoms were recorded and described, and micro-fungi associated with these diseases were comprehensively identified using morphological characters, phylogenetic analyses and pathogenicity tests. The isolation of known pathogens verified the re-emergence or prevalence of certain species, while the numerous new host records or newly described species may represent emerging pathogens that cause new disease types or aggravate the disease severity. Some of these fungi may also function as saprophytes or antagonists. The diversity of fungi associated with these diseases was revealed, and the relationship between fungi and symptoms, fungal communities and disease types, as well as fungal species distributions, was revealed. In addition, an updated list of pathogens was compiled by integrating the results from previous research with those of the current study.

6.1.1 Fungal Species Associated with Cherry Leaf Spot Disease

Though sweet cherry has a long cultivation history, research on cherry diseases was very limited in the early stages. In the current study, new collections of *Colletotrichum* species were identified, confirming the top three *Colletotrichum* species (*C. gloeosporioides*, *C. fructicola* and *C. aenigma*) causing leaf anthracnose. *Fusarium* species were found to be highly pathogenic to cherry leaves, and all species have been reported to cause diseases on other hosts, suggesting that they could be emerging pathogens for cherry. Furthermore, different symptoms caused by various pathogens were further confirmed. Infected leaves typically exhibit local, spotty necrosis, but the symptoms differ depending on the pathogen. For example, "brown spot" is caused by

Pruniphilomyces circumscissus, "black spot" by *Alternaria alternata*, and "anthracnose" by *Colletotrichum fructicola*. The current study also generated *Colletotrichum*, *Fusarium*, and *Cladosporium* isolates from distinctly different symptom types. While mixed infections of multiple pathogens are common in the field, understanding the differentiated symptoms could help in the preliminary identification of the main pathogen, thus accelerating the disease diagnosis and control. Additionally, *Pestalotiopsis rosae* was first recorded on cherry, as well as the new species *Diaporthe beijingensis*. Finally, all recorded fungal species associated with cherry leaf spot were summarized, along with their isolation regions and identification methods. Although there have been few new pathogen records in other countries in recent years, the pathogens associated with cherry leaf spot in China have shown increasing diversity. Since most pathogens have been reported in Beijing and a few other provinces like Shandong, Sichuan, Liaoning, and Gansu, the distribution of pathogens has not yet shown apparent regularity. Therefore, disease investigations and sample collections need to be conducted across more regions to gain a better understanding of pathogen distribution.

6.1.2 Fungal Species Associated with Grapevine Trunk Disease

Grapevine trunk diseases are constant concerns in nearly all grapevine cultivation areas worldwide. Currently, grapevine trunk diseases are divided into several types according to disease symptoms and pathogens, including Esca complex, Eutypa dieback, Botryosphaeria dieback, black foot and Phomopsis (Diaporthe) dieback (Azevedo-Nogueira et al., 2022). In this study, typical GTD samples were collected from eight main cultivation areas in China. A total of forty species were identified, belonging to twenty-one genera. The identification results could be interpreted from three aspects: Firstly, the GTD-associated fungi: Among the fungal genera generated, nine were recognized as GTD pathogens, associated with Botryosphaeria dieback (*Botryosphaeria*, *Lasiodiplodia*, *Diplodia*, *Neofusicoccum*), black foot disease (*Dactylonectria*, *Ilyonectria*, *Cylindrocladiella*), Phomopsis dieback (*Diaporthe*) and Esca complex (*Phaeoacremonium*). Twelve species (*Botryosphaeria dothidea*, *Lasiodiplodia citricola*, *Lasiodiplodia pseudotheobromae*, *Lasiodiplodia theobromae*, *Diplodia seriata*, *Neofusicoccum parvum*, *Dactylonectria novozelandica*, *Dactylonectria alcacerensis*, *Dactylonectria torresensis*, *Dactylonectria macrodidyma*,

Diaporthe eres, *Diaporthe unshiuensis*), which have been reported as important GTD pathogens in both China and globally, were identified, and three species (*Ilyonectria liriodendra*, *Cylindrocladiella viticola*, *Phaeoacremonium iranianum*) reported as GTD pathogens in other countries were recorded in China for the first time. The results verified the prevalent types of grapevine trunk diseases in China and encompassed most of the fungal genera that have been previously reported. However, the identified species showed differences compared to previous studies on GTD pathogens in China. For fungi associated with Botryosphaeria dieback, Botryosphaeriaceae species were highly overlapping with the study of Yan et al. (2013), except for *Neofusicoccum mangiferae*, which was not found at that time. The distribution of these species was in accord with that study. For fungi associated with black foot disease, all *Dactylonectria* species reported by Ye et al. (2021c) were discovered in this study, in addition to the *Ilyonectria liriodendra* and *Cylindrocladiella viticola* that were first identified in China. However, *Cylindrocladiella lageniformis* and *Neonectria* sp. 1 were not found in this study. Regarding fungi associated with Phomopsis dieback, among the ten species previously reported in China (Dissanayake et al., 2015a; Manawasinghe et al., 2019), only two species were identified in this study. For ESCA-associated fungi, only *Phaeoacremonium iranianum* was reported in this study, in contrast to *Fomitiporia punicata* and *Phaeoacremonium minimum*, which were previously reported by Ye et al. (2021b). The results showed the diversity and complexity of GTD pathogens.

Secondly, fungi associated with other diseases: Some species isolated from GTD samples are also common pathogens causing diseases in other parts of the grapevine, such as *Coniella vitis* causing white rot of fruits (Chethana et al., 2017), and *Colletotrichum nymphaeae* and *C. viniferum* causing fruit and twig anthracnose (Yan et al., 2015; Liu et al., 2016). Some species are new host records, while the genera to which they belong are common plant pathogens. For example, *Fusarium* is a common pathogen associated with grapevine decline (Úrbez-Torres et al., 2023). Li et al. (2023) found that *Fusarium* spp. caused similar symptoms to *Dactylonectria macrodidyma*, the pathogen of black foot disease, and can exacerbate the disease severity when co-inoculated with *Dactylonectria macrodidyma*. This phenomenon suggests that *Fusarium* spp. are related to grapevine trunk diseases. For the above fungi isolated from this study, further research is needed to determine whether they are associated with the

occurrence and severity of grapevine trunk disease. Finally, some species, such as *Phaeobotryon rhois* and *Bartalinia kevinhydei*, were reported for the first time on grapevine in this study. These fungi were previously known to cause dieback and leaf spot diseases on other hosts, respectively (Fan et al., 2015; Tibpromma et al., 2020). However, whether they act as pathogens on grapevine needs to be further studied. It is worth noting that although only eight isolates of *Bartalinia kevinhydei* were identified, they were found to be distributed across four provinces. Based on the above results, a diverse range of fungi were associated with grapevine trunk disease, including not only common pathogens but also many other fungi that could potentially be pathogens or saprobes. The impacts of these fungi on grapevine trunk disease remain unclear, and required further studies through pathogenicity tests and antagonistic studies. Additionally, broader and continued collections are needed to verify and expand the fungal list associated with the diseases.

6.1.3 Fungal Species Associated with Blueberry Disease

Currently, blueberry diseases are mainly divided into fruit rot, leaf spot, stem blight and root rot, with fruit rot and stem blight (canker, dieback). In China, though new pathogens continue emerging, most research consists of brief reports on a single new pathogen, and only a few studies have conducted comprehensive identification of groups of pathogens, such as Botryosphaeriaceae species associated with stem blight and *Colletotrichum* species associated with leaf and stem anthracnose. The current study provides an overall insight to the blueberry diseases in China for the first time, with emphasis on fruit rot, leaf spot, stem blight and root rot diseases, which summarized and updated the fungal pathogens. For fruit diseases, pre-harvest diseases were considered in this study, as they directly influence the production of fruits and can potentially serve as the source of postharvest diseases. Typical fruit pathogens like *Botrytis cinerea* and new host records such as *Neopestalotiopsis surinamensis* all showed strong virulence on blueberry fruits. For other diseases, among forty genera identified, *Alternaria*, *Botryosphaeria, Diaporthe*, *Fusarium*, *Neopestalotiopsis* and *Pestalotiopsis*, were the dominant genera, accounting for more than 60% of isolation ratio. From a family perspective, Botryosphaeriaceae (including *Botryosphaeria* and *Neofusicoccum*), Sporocadaceae (including *Neopestalotiopsis* and *Pestalotiopsis*), Diaporthaceae (including *Diaporthe*), and Pleosporaceae (including *Alternaria*)

covered the main pathogen groups associated with leaf spot and stem blight in previous studies. Similarly, Nectriaceae (including *Fusarium*, *Neocosmospora*, *Dactylonectria* and *Ilyonectria*) are more likely to be associated with root rot. Analysis of the fungal isolate information revealed certain patterns in fungal distribution. The isolation source (leaf, stem and root) indicated the fungal distribution across different plant parts, while the isolation region (Fujian and Guizhou representing subtropical areas; Heilongjiang, Jilin, and Liaoning representing temperate areas) reflected geographical distribution. *Botryosphaeria dothidea* was the only species widely distributed in all three plant parts and all five collecting areas. *Alternaria alternata* was present in all three plant parts and four collecting areas, except Fujian. *Diaporthe* species were distributed in all three plant parts and across three collecting areas. Certain fungi exhibited distinct regional characteristics. For example, *Bipolaris* species were only isolated from stem blight samples in Heilongjiang, while *Clonostachys* species were exclusive to the three northern provinces. Additionally, *Dactylonectria* and *Ilyonectria*, known black-foot pathogens in grapevines, were found only in root samples. Although these results provide insights into the occurrence of pathogens, they may be influenced by factors such as the selection of collection site, season and sample variability. The current conclusions need to be further verified by large-scale sampling.

As dominant pathogens of blueberry, Pestalotiopsis-like species, were described in detail, the isolates were carefully compared with closely related reference species based on both morphological and phylogenetic analyses. As a result, some species were suggested to be synonymized, though further evidence is required for confirmation.

In conclusion, this study represents the first intensive identification of micro-fungi associated with different diseases of blueberry. The results indicated the diversity of fungal species on blueberry, verified the previously recorded dominant fungal taxa, and expand the records of known fungi on blueberry. The dominant fungal communities identified in this study provide valuable references for future research on disease etiology and disease management.

6.1.4 The Comparison on Fungal Pathogens Between Cherry, Grapevine and Blueberry

Although cherry, grapevine, and blueberry have different growth cycles and distinct disease concerns, comparing dominant pathogens across these hosts enhances

the generalizability and reference value of the results. This study identified both common and host-specific pathogens among the three crops. There are some common pathogens, such as *Colletotrichum* spp. and *Fusarium* spp., in all three crops, though their distribution and species are varied. *Colletotrichum fructicola* was associated with leaf spot in both cherry and blueberry, whereas the *Colletotrichum* species recorded on grapevine trunk disease were not reported in the other two crops. *Fusarium compactum* was isolated from cherry leaves and grapevine trunks, while *F. oxysporum* was isolated in the roots and trunks (stems) of grapevine and blueberry. However, no *Fusarium* species were common to both cherry and blueberry. *Colletotrichum*, *Alternaria* and *Fusarium* were identified as cherry leaf spot pathogens, while *Neopestalotiopsis* and *Pestalotiopsis* species were the main pathogens causing blueberry leaf spot. Some woody pathogens were shared between grapevine and blueberry, including *Botryosphaeria dothidea*, *Neofusicoccum parvum*, and *Diaporthe eres*. Additionally, *Neocosmospora falciformis* and *Neocosmospora solani* were commonly isolated from the roots of both grapevine and blueberry. Pathogens associated with grapevine diseases, such as *Dactylonectria pauciseptata*, *Ilyonectria liriodendri* and *Phaeoacremonium scolyti*, which are linked to black foot and esca complex diseases, were also isolated from blueberry. In conclusion, most fungal pathogens are not strictly host-specific and may cause different disease types on different hosts. However, the dominant pathogens varied significantly across crops. Therefore, studying disease patterns in a crop needs long-term research, and targeted disease management strategies.

6.2 Research Advantages

6.2.1 This study enhanced the understanding of cherry leaf spot disease by identifying new disease types along with their associated pathogens and providing an updated summary of all known CLS pathogens. This represents the first comprehensive generalization of the disease, serving as an important reference for research on disease occurrence patterns and management practices.

6.2.2 This study provided a comprehensive overview of the occurrence of grapevine trunk disease and the diversity of fungi associated with it. Species identified

in the study were compared with previous studies in terms of their distribution and related disease types. Common GTD pathogens were verified, while additional pathogens and newly recorded species were also documented, expanding the current understanding of GTD-associated fungi.

6.2.3 This study represents the first comprehensive study on blueberry diseases and their associated fungal communities. It provides detailed information of fungal taxa identified from fruit rot, leaf spot, stem blight and root rot samples, linking them to the disease types. The study also clarifies fungal distribution patterns and dominant communities. Additionally, a pathogen list recorded in China was compiled, offering valuable insights for future research and disease management.

6.2.4 This study integrates plant disease research and fungal taxonomy, addressing the inconsistencies in pathogen identification. It provides a clarified framework for identifying fungal pathogens and offers a detailed interpretation of the latest classification of important pathogens.

6.3 Future Work

6.3.1 Continuous monitoring of the cherry leaf spot pathogens is essential to prevent disease outbreaks. Additionally, the development of rapid detection technologies is crucial for early and efficient field diagnosis. For other secondary CLS pathogens, such as *Diaporthe* and Didymellaceae species, further investigations are needed to confirm whether they represent emerging pathogens or occur incidentally. *Cladosporium*, a common genus associated with cherry leaf spot, has been linked to specific symptom types; however, its relationship with symptom expression requires further pathogenicity testing. *Pruniphilomyces circumscissus*, an early-recognized pathogen, has yet to be classified using multi-locus phylogenetic analysis. Although recent laboratory studies have identified this species, its pathogenicity remains unverified due to its difficulty in sporulation on artificial media. Future research will focus on clarifying its taxonomy and confirming its role in CLS development.

6.3.2 Grapevine trunk diseases (GTD) are a global concern with no effective control methods despite extensive research. Their underlying mechanisms remain

unclear. This study identified all fungi isolated from GTD samples, recording 12 new host associations and 22 new records on grapevine in China. For species previously reported as GTD pathogens in other countries but newly found in China, pathogenicity tests are needed to confirm their role. Other new host records can be categorized based on prior reports: potential pathogens require pathogenicity tests to assess virulence, while potential biocontrol fungi need antagonistic tests to evaluate their efficacy. Since many GTD pathogens are opportunistic, their infections are influenced by environmental factors and the microbiome. Studying co-infections among selected pathogens could help understand their interactions. Additionally, expanding disease surveys and sample collection across more regions in China will provide valuable reference data.

6.3.3 This study provides the dominant fungal communities identified, along with a summary of important pathogens previously reported on blueberry diseases. However, the findings are based on data from only one year and a limited range of collection sites. To ensure broader applicability, further investigations and additional sample collections are needed. Blueberry orchards should be selected from a wider range of regions, including other major cultivation areas and varying climate zones. When comparing fungal compositions across different regions, it is crucial to collect an adequate and equal number of samples within a similar timeframe. Future analyses will focus on how disease types, fungi, and community distribution change over time, as well as the correlation between symptoms and pathogens. Pathogenicity tests will be conducted on prevalent fungi, and species with high virulence will be inoculated on living plants, both alone and in combination with other pathogens. Additionally, leaf litter, rhizosphere soil, and adjacent plants will be sampled to study the life cycle of related fungi and the potential for host jump or host shift.

6.4 List of Publications

6.4.1 First Author

Yueyan Zhou et al., Micro-fungi associated with Blueberry diseases in China
[Manuscript preparation]. Mae Fah Luang University.

Zhou, Y., Wu, L., Ren, K., Wang, M., Wang, N., Tangtrakulwanich, K., . . . Yan, J.
(2025). Three new records of pathogens causing stem blight on *Vaccinium
corymbosum* in China. *Plants, 14*(5), 647.
https://doi.org/10.3390/plants14050647

Zhou, Y., Zhang, W., Chen, P., Chethana, K. W. T., Li, X., & Yan, J. (2024).
Morphological and molecular characterization of *Cladosporium* species on
sweet cherry in Beijing, China. *Acta Horticulturae, 1408*, 511–524.
https://www.actahort.org/books/1408/1408_68.htm

Zhou, Y., Zhang, W., Li, X., Ji, S., Chethana K. W. T., Hyde, K. D., . . . Yan, J.
(2022). *Fusarium* species associated with cherry leaf spot in China.
Plants, 11, 2760. https://doi.org/10.3390/plants11202760

Zhou, Y., Zhang, W., Wu, L., Chen, P., Li, X., Wen, G., . . . Yan, J. (2025).
Characterization of fungal pathogens causing blueberry fruit rot disease in
China. *Pathogens, 14*(2), 201. https://doi.org/10.3390/pathogens14020201

Zhou, Y., Zhang, W., Wu, L., Zhang, J., Tan, H., Chethana, K. W. T., . . . Yan, J.
(2023). Diversity of fungal communities associated with grapevine trunk
diseases in China. *Mycosphere, 14*(1), 1340–1435.
https://doi.org/10.5943/mycosphere/14/1/15

6.4.2 Co-author

Chen, P., Abeywickrama, P. D., Ji, S., Zhou, Y., Li, X., Zhang, W., . . . Yan, J.
(2023). Molecular identification and pathogenicity of *Diaporthe eres* and
D. hongkongensis (Diaporthales, Ascomycota) associated with cherry trunk
diseases in China. *Microorganisms, 11*(10), 2400.
https://doi.org/10.3390/microorganisms11102400

He, Z., Abeywickrama, P. D., Wu, L., Zhou, Y., Zhang, W., Yan, J., . . . Li, S. (2024). Diversity of *Cytospora* species associated with trunk diseases of *Prunus persica* (peach) in Northern China. *Journal of Fungi, 10*(12), 843. https://doi.org/10.3390/jof10120843

Jayawardena, R. S., Hyde, K. D., Aumentado, H. D. R., Abeywickrama, P. D., Avasthi, S., … Zhou, Y., . . . Wang, Y. (2025). One stop shop V: Taxonomic update with molecular phylogeny for important phytopathogenic genera: 101–125 (2024). *Fungal Diversity, 130*, 263–429. https://doi.org/10.1007/s13225-024-00542-x

Manawasinghe, I. S., Hyde, K. D., Wanasinghe, D. N., Karunarathna, S. C., Maharachchikumbura, S. S. N., … Zhou, Y., . . . Xu, B. (2024). Fungal diversity notes 1818–1918: Taxonomic and phylogenetic contributions on genera and species of fungi. *Fungal Diversity, 130*, 1–261. https://doi.org/10.1007/s13225-024-00541-y

Manawasinghe, I. S., Jayawardena, R. S., Li, H. L., Zhou, Y., Zhang, W., Phillips, A. J. L., . . . Yan, J. Y. (2021). Microfungi associated with *Camellia sinensis*: A case study of leaf and shoot necrosis on tea in Fujian, China. *Mycosphere, 12*(1), 430–518. https://doi.org/10.5943/mycosphere/12/1/6

Zhang, W., Chen, P., Zhou, Y., Manawasinghe, I. S., Ji, S., Li, X., . . . Yan, J. (2025). Morpho-molecular characterization and pathogenicity of fungi associated with sweet cherry (*Prunus avium*) trunk diseases in China. *Mycosphere, 16*(1), 169–244. https://doi.org/10.5943/mycosphere/16/1/3

REFERENCES

Abdullah, A. S., Moffat, C. S., Lopez-Ruiz, F. J., Gibberd, M. R., Hamblin, J., & Zerihun, A. (2017). Host–multi-pathogen warfare: Pathogen interactions in co-infected plants. *Frontiers in Plant Science, 8*, 1806. https://doi.org/10.3389/fpls.2017.01806

Abeywickrama, P. D., Zhang, W., Li, X. H, Jayawardena, R. S., Hyde, K. D., Yan, J. Y. (2021) *Campylocarpon fasciculare* (Nectriaceae, Sordariomycetes); Novel emergence of black-foot causing pathogen on young grapevines in China. *Pathogens, 10*(12), 1555. https://doi.org/10.3390/pathogens10121555

Adebesin, A. A., Odebode, C. A., & Ayodele, A. M. (2009). Control of postharvest rots of banana fruits by conidia and culture filtrates of *Trichoderma asperellum*. *Journal of Plant Protection Research, 49*(3), 302–308. https://doi.org/10.2478/v10045-009-0049-6

Akram, S., Ahmed, A., He, P. F., He, P. B., Liu, Y. L., Wu, Y. X., … He, Y. Q. (2023). Uniting the role of endophytic fungi against plant pathogens and their interaction. *Journal of Fungi, 9*(1), 72. https://doi.org/10.3390/jof9010072

Alfieri, S. A., Jr. (1991). *Septoria leaf spot of blueberry* (Plant Pathology Circular No. 340). Florida Department of Agriculture & Consumer Services, Division of Plant Industry. https://ccmedia.fdacs.gov/content/download/11347/file/pp340.pdf

Ali, S., Hildebrand, P. D., Renderos, W. E., & Abbasi, P. A. (2021). Identification and characterization of *Sphaerulina vaccinii* sp. nov. as the cause of leaf spot and stem canker in lowbush blueberry and its epidemiology. *Phytopathology, 111*(9), 1560–1570. https://doi.org/10.1094/PHYTO-04-20-0143-R

Alvarez Osorio, A. K., Miles, L. A., & Miles, T. D. (2022). Mummy berry of blueberry caused by *Monilinia vaccinii-corymbosi*: A diagnostic guide. *Plant Health Progress, 23*(3), 362–368. https://doi.org/10.1094/PHP-09-21-0120-DG

Alves, A., Crous, P. W., Correia, A. C. M., & Phillips, A. J. L. (2008). Morphological and molecular data reveal cryptic speciation in *Lasiodiplodia theobromae*. *Fungal Diversity, 28*, 1–13.

Andersen, K. L., Sebolt, A. M., Sundin, G. W., & Iezzoni, A. F. (2018). Assessment of the inheritance of resistance and tolerance in cherry (*Prunus* sp.) to *Blumeriella jaapii*, the causal agent of cherry leaf spot. *Plant Pathology, 67*(3), 682–691. https://doi.org/10.1111/ppa.12765

Annesi, T., Motta, E., & Forti, E. (1997). First report of *Blumeriella jaapii* teleomorph on wild cherry in Italy. *Plant Disease, 81*(10), 1214. https://doi.org/10.1094/PDIS.1997.81.10.1214A

Araujo, L., Ferreira Pinto, F. A. M., de Andrade, C. C. L., Mituti, T., Falkenbach, B. R., Gomes, L. B., Duarte, V. (2023). *Pestalotiopsis trachycarpicola* causes leaf spot disease on blueberry in Santa Catarina, Brazil. *Australasian Plant Disease Notes, 18*(1), 14. https://doi.org/10.1007/s13314-023-00500-7

Askari-Khorasgani, O., & Pessarakli, M. (2019). Fruit quality and nutrient composition of grapevines: A review. *Journal of Plant Nutrition, 42*(17), 2133–2150. https://doi.org/10.1080/01904167.2019.1643369

Atkinson, N. J., & Urwin, P. E. (2012). The interaction of plant biotic and abiotic stresses: From genes to the field. *Journal of Experimental Botany, 63*(10), 3523–3543. https://doi.org/10.1093/jxb/ers100

Azevedo-Nogueira, F., Rego, C., Gonçalves, H. M. R., Fortes, A. M., Gramaje, D., & Martins-Lopes, P. (2022). The road to molecular identification and detection of fungal grapevine trunk diseases. *Frontiers in Plant Science, 13*, 960289. https://doi.org/10.3389/fpls.2022.960289

Baka, Z. A. M., & Krzywinski, K. (1996). Fungi associated with leaf spots of *Dracaena ombet* (Kotschy and Peyr). *Microbiological Research*, *151*, 49–56. https://doi.org/10.1016/S0944-5013(96)80055-3

Beacorn, J. A., & Thiessen, L. D. (2021). First report of *Fusarium lacertarum* causing Fusarium head blight on sorghum in North Carolina. *Plant Disease, 105*(3), 699. https://doi.org/10.1094/PDIS-05-20-1012-PDN

Belisário, R., Aucique-Pérez, C. E., Abreu, L. M., Salcedo, S. S., Oliveira, W. M. D., & Furtado, G. Q. (2020). Infection by *Neopestalotiopsis* spp. occurs on unwounded eucalyptus leaves and is favoured by long periods of leaf wetness. *Plant Pathology, 69*(2), 194–204. https://doi.org/10.1111/ppa.13132

Bell, S. R., Hernández Montiel, L. G., González Estrada, R. R., & Gutiérrez Martínez, P. (2021). Main diseases in postharvest blueberries, conventional and eco-friendly control methods: A review. *LWT, 149*, 112046. https://doi.org/10.1016/j.lwt.2021.112046

Benítez, T., Rincón, A. M., Limón, M. C., & Codón, A. C. (2004). Biocontrol mechanisms of *Trichoderma* strains. *International Microbiology, 7*(4), 249–260.

Bensch, K., Braun, U., Groenewald, J. Z., & Crous, P. (2012). The genus *Cladosporium*. *Studies in Mycology, 72*, 1–401. https://doi.org/10.3114/sim0003

Bensch, K., Groenewald, J. Z., Braun, U., Dijksterhuis, J., de Jesús Yáñez-Morales, M., & Crous, P. W. (2015). Common but different: The expanding realm of *Cladosporium*. *Studies in Mycology, 82*, 23–74. https://doi.org/10.1016/j.simyco.2015.10.001

Bensch, K., Groenewald, J. Z., Dijksterhuis, J., Starink-Willemse, M., Andersen, B., Summerell, B. A., … Crous, P. W. (2010). Species and ecological diversity within the *Cladosporium cladosporioides* complex (Davidiellaceae, Capnodiales). *Studies in Mycology, 67*, 1–94. https://doi.org/10.3114/sim.2010.67.01

Bensch, K., Groenewald, J. Z., Meijer, M., Dijksterhuis, J., Jurjević, Ž., Andersen, B., … Samson, R. A. (2018). *Cladosporium* species in indoor environments. *Studies in Mycology, 89*, 177–301. https://doi.org/10.1016/j.simyco.2018.03.002

Berbee, M. L., Pirseyedi, M., & Hubbard, S. (1999). *Cochliobolus* phylogenetics and the origin of known, highly virulent pathogens, inferred from ITS and glyceraldehyde-3-phosphate dehydrogenase gene sequences. *Mycologia, 91*(6), 964–977. https://doi.org/10.1080/00275514.1999.12061106

Berlanas, C., Ojeda, S., López-Manzanares, B., Andrés-Sodupe, M., Bujanda, R., Martínez-Diz, M. D. P., & Gramaje, D. (2020). Occurrence and diversity of black-foot disease fungi in symptomless grapevine nursery stock in Spain. *Plant Disease, 104*(1), 94–104. https://doi.org/10.1094/PDIS-03-19-0484-RE

Bhunjun, C. S., Chen, Y. J., Phukhamsakda, C., Boekhout, T., Groenewald, J. Z., McKenzi, E. H. C., … Crous, P. W. (2024). What are the 100 most cited fungal genera? *Studies in Mycology, 108*, 1–412. https://doi.org/10.3114/sim.2024.108.01

Bhunjun, C. S., Phukhamsakda, C., Hyde, K. D., McKenzie, E. H. C., Saxena, R. K., & Li, Q. R. (2024). Do all fungi have ancestors with endophytic lifestyles? *Fungal Diversity, 125*, 73–98. https://doi.org/10.1007/s13225-023-00516-5

Blagojević, J., Aleksić, G., Vučurović, I., Starović, M., & Ristić, D. (2024). Exploring the phylogenetic diversity of *Botryosphaeriaceae* and *Diaporthe* species causing dieback and shoot blight of blueberry in Serbia. *Phytopathology, 114*(6), 1333–1345. https://doi.org/10.1094/PHYTO-04-23-0133-R

Blando, F., & Oomah, B. D. (2019). Sweet and sour cherries: Origin, distribution, nutritional composition and health benefits. *Trends in Food Science & Technology, 86*, 517–529. https://doi.org/10.1016/j.tifs.2019.02.052

Borrero, C., Castaño, R., & Avilés, M. (2018). First report of *Pestalotiopsis clavispora* (*Neopestalotiopsis clavispora*) causing canker and twig dieback on blueberry bushes in Spain. *Plant Disease, 102*(6), 1178. https://doi.org/10.1094/PDIS-10-17-1529-PDN

Børve, J., & Stensvand, A. (2008). Anthracnose – An emerging disease on sweet cherry. *Acta Horticulturae, 795*, 905–908. https://doi.org/10.17660/ActaHortic.2008.795.146

Boso, S., Alonso-Villaverde, V., Gago, P., Santiago, J. L., & Martínez, M. C. (2014). Susceptibility to downy mildew (*Plasmopara viticola*) of different *Vitis* varieties. *Crop Protection, 63*, 26–35. https://doi.org/10.1016/j.cropro.2014.04.018

Boyzo-Marin, J., Rebollar-Alviter, A., Silva-Rojas, H. V., & Ramirez-Maldonaldo, G. (2016). First report of *Neofusicoccum parvum* causing stem blight and dieback of blueberry in Mexico. *Plant Disease, 100*(12), 2524. https://doi.org/10.1094/PDIS-03-16-0381-PDN

Bradshaw, M., Ivors, K., Broome, J. C., Carbone, I., Braun, U., Yang, S., … Pfister, D. H. (2025). An emerging fungal disease is spreading across the globe and affecting the blueberry industry. *New Phytologist, 246*(1), 103–112. https://doi.org/10.1111/nph.20351

Briceño, E. X., & Latorre, B. A. (2008). Characterization of Cladosporium rot in grapevines, a problem of growing importance in Chile. *Plant Disease, 92*(12), 1635–1642. https://doi.org/10.1094/PDIS-92-12-1635

Bruez, E., Baumgartner, K., Bastien, S., Travadon, R., Guérin-Dubrana, L., & Fontaine, F. (2016). Various fungal communities colonise the functional wood tissues of old grapevines externally free from grapevine trunk disease symptoms. *Australian Journal of Grape and Wine Research, 22*(2), 288–295. https://doi.org/10.1111/ajgw.12209

Bugnicourt, F. (1952). Une espèce fusarienne nouvelle, parasite du riz. *Revue Générale de Botanique, 59*, 13–18.

Burgess, T. I., Tan, Y. P., Garnas, J., Edwards, J., Scarlett, K. A., Shuttleworth, L. A., . . . Jami, F. (2019). Current status of the Botryosphaeriaceae in Australia. *Australasian Plant Pathology, 48*(1), 35–44. https://doi.org/10.1007/s13313-018-0577-5

Busby, P. E., Ridout, M., & Newcombe, G. (2016). Fungal endophytes: Modifiers of plant disease. *Plant Molecular Biology, 90*(6), 645–655. https://doi.org/10.1007/s11103-015-0412-0

Cabral, A., Rego, C., Nascimento, T., Oliveira, H., Groenewald, J. Z., & Crous, P. W. (2012). Multi-gene analysis and morphology reveal novel *Ilyonectria* species associated with black foot disease of grapevines. *Fungal Biology, 116*(1), 62–80. https://doi.org/10.1016/j.funbio.2011.09.010

Cai, F., Dou, K., Wang, P., Chenthamara, K., Chen, J. & Druzhinina, I. S. (2022). The current state of *Trichoderma* taxonomy and species identification. In N. Amaresan, A. Sankaranarayanan, M. K. Dwivedi, & I. S. Druzhinina (Eds.), *Advances in Trichoderma biology for agricultural applications* (pp. 3–35). Springer.

Cannon, P., Buddie, A., & Bridge, P. D. (2008). The typification of *Colletotrichum gloeosporioides*. *Mycotaxon, 104*, 189–204.

Cao, J., Jiang, Q., Lin, J., Li, X., Sun, C., & Chen, K. (2015). Physicochemical characterisation of four cherry species (*Prunus* spp.) grown in China. *Food Chemistry, 173*, 855–863. https://doi.org/10.1016/j.foodchem.2014.10.094

Capella-Gutiérrez, S., Silla-Martínez, J. M., & Gabaldón, T. (2009). trimAl: A tool for automated alignment trimming in large-scale phylogenetic analyses. *Bioinformatics, 25*(15), 1972–1973. https://doi.org/10.1093/bioinformatics/btp348

Capote, N., Del Río, M., Herencia, J. F., & Arroyo, F. T. (2022). Molecular and pathogenic characterization of *Cylindrocarpon*-like anamorphs causing root and basal rot of almonds. *Plants, 11*(8), 984. https://doi.org/10.3390/plants11070984

Carbone, I., & Kohn, L. M. (1999). A method for designing primer sets for speciation studies in filamentous ascomycetes. *Mycologia, 91*(3), 553–556. https://doi.org/10.1080/00275514.1999.12061051

Carlucci, A., Cibelli, F., Lops, F., & Raimondo, M. L. (2015). Characterization of *Botryosphaeriaceae* species as causal agents of trunk diseases on grapevines. *Plant Disease, 99*(11), 1678–1688. https://doi.org/10.1094/PDIS-03-15-0286-RE

Carlucci, A., Lops, F., Mostert, L., Halleen, F., & Raimondo, M. (2017). Occurrence of fungi causing black foot on young grapevines and nursery rootstock plants in Italy. *Phytopathologia Mediterranea, 56*(1), 10–39. https://doi.org/10.14601/Phytopathol_Mediterr-18769

Carris, L. M., Little, C. R., & Stiles, C. M. (2012). *Introduction to fungi*. The Plant Health Instructor. https://doi.org/10.1094/PHI

Castillo, S., Borrero, C., Castaño, R., Rodríguez, A., & Avilés, M. (2013). First report of canker disease caused by *Neofusicoccum parvum* and *N. australe* on blueberry bushes in Spain. *Plant Disease, 97*(8), 1112. https://doi.org/10.1094/PDIS-11-12-1048-PDN

Castillo-Pando, M., Somers, A., Green, C. D., Priest, M., & Sriskanthades, M. (2001). Fungi associated with dieback of Semillon grapevines in the Hunter Valley of New South Wales. *Australasian Plant Pathology, 30*(1), 59–63. https://doi.org/10.1071/AP00068

Castro, J. F., Millas, P., Cisterna-Oyarce, V., Carrasco-Fernández, J., Santelices, C., Muñoz, V., … France, A. (2023). First report of *Colletotrichum fioriniae* causing anthracnose fruit rot on *Vaccinium corymbosum* in Chile. *Plant Disease, 107*(3), 959. https://doi.org/10.1094/PDIS-06-22-1340-PDN

Cheek, M., Nic Lughadha, E., Kirk, P., Lindon, H., Carretero, J., Looney, B., . . . Niskanen, T. (2020). New scientific discoveries: Plants and fungi. *Plants, People, Planet, 2*(5), 371–388. https://doi.org/10.1002/ppp3.10148

Chen, C. Q., Zhang, B., & Gao, J. (2010). Leaf spot disease of lowbush blueberry (*Vaccinium angustifolium*) caused by *Pestalotiopsis photiniae* newly reported in China. *New Disease Reports, 22*(1), 31. https://doi.org/10.5197/j.2044-0588.2010.022.031

Chen, C., Liang, X., Lin, Y., Hsiang, T., Xiang, M., & Zhang, Y. (2023). First report of leaf spot and stem blight on blueberry (*Vaccinium corymbosum* 'Bluerain') caused by *Calonectria pseudoreteaudii* in China. *Plant Disease, 107*(6), 1951. https://doi.org/10.1094/PDIS-09-22-2125-PDN

Chen, P. Z., Abeywickrama, P. D., Ji, S. X., Zhou, Y. Y., Li, X. H., Zhang, W., Yan, J. (2023). Molecular identification and pathogenicity of *Diaporthe eres* and *D. hongkongensis* (Diaporthales, Ascomycota) associated with cherry trunk diseases in China. *Microorganisms, 11*(10), 2400. https://doi.org/10.3390/microorganisms11102400

Chen, R. S., Wang, W. L., Li, J. C., Wang, Y. Y., & Tsay, J. G. (2009). First report of papaya scab caused by *Cladosporium cladosporioides* in Taiwan. *Plant Disease, 93*(4), 426. https://doi.org/10.1094/PDIS-93-4-0426C

Chen, Y., Zhang, A. F., Yang, X., Gu, C. Y., Kyaw, E. P., Yi, X. K., & Xu, Y. L. (2016). First report of *Pestalotiopsis clavispora* causing twig blight on highbush blueberry (*Vaccinium corymbosum*) in Anhui Province of China. *Plant Disease, 100*(4), 859. https://doi.org/10.1094/PDIS-04-15-0455-PDN

Chethana, K. W. T., Li, X., Zhang, W., Hyde, K. D., & Yan, J. Y. (2016). Trail of decryption of molecular research on *Botryosphaeriaceae* in woody plants. *Phytopathologia Mediterranea, 55*(2), 147–171. https://www.jstor.org/stable/44809324

Chethana, K. W. T., Manawasinghe, I. S., Hurdeal, V. G., Bhunjun, C. S., Appadoo, M. A., Gentekaki, E., … Hyde, K. D. (2021). What are fungal species and how to delineate them? *Fungal Diversity, 109*, 1–25. https://doi.org/10.1007/s13225-021-00483-9

Chethana, K. W. T., Zhou, Y., Zhang, W., Liu, M., Xing, Q. K., Li, X. H., … Hyde, K. D. (2017). *Coniella vitis* sp. nov. is the common pathogen of white rot in Chinese vineyards. *Plant Disease, 101*(12), 2123–2136. https://doi.org/10.1094/PDIS-12-16-1741-RE

Chethana, K. W. T., Jayawardena, R. S., Zhang, W., Zhou, Y. Y., Liu, M., Hyde, K. D., … Yan, J. Y. (2019). Molecular characterization and pathogenicity of fungal taxa associated with cherry leaf spot disease. *Mycosphere, 10*(1), 490–530. https://doi.org/10.5943/mycosphere/10/1/8

Choi, I. Y. (2011). First report of bark dieback on blueberry caused by *Botryosphaeria dothidea* in Korea. *Plant Disease, 95*(2), 227. https://doi.org/10.1094/PDIS-05-10-0371

Choi, I. Y., Braun, U., Park, J. H., & Shin, H. D. (2014). First report of leaf spot caused by *Pseudocercospora pruni-persicicola* on sweet cherry in Korea. *Plant Disease*, *98*(5), 693. https://doi.org/10.1094/PDIS-09-13-0968-PDN

Chu, R. T., Dou, Z. P., He, W., & Zhang, Y. (2021). Two novel species of *Botryosphaeria* causing stem canker of blueberries from China. *Mycosystema, 40*, 473–486. https://doi.org/10.13346/j.mycosystema.200333

Cloete, M., Fischer, M., Mostert, L., & Halleen, F. (2015). *Hymenochaetales* associated with esca-related wood rots on grapevine with a special emphasis on the status of esca in South African vineyards. *Phytopathologia Mediterranea, 54*(2), 299–312. https://doi.org/10.14601/Phytopathol_Mediterr-16364

Cook, R. P., & Dubé, A. J. (1989). *Host-pathogen index of plant diseases in South Australia*. South Australian Department of Agriculture.

Correia, K. C., Câmara, M. P. S., Barbosa, M. A. G., Sales Júnior, R., Agustí-Brisach, C. A., Gramaje, D., … Michereff, S. J. (2013). Fungal trunk pathogens associated with table grape decline in Northeastern Brazil. *Phytopathologia Mediterranea, 52*(2), 380–387. https://doi.org/10.14601/Phytopathol_Mediterr-11377

Correia, K. C., Silva, M. A., de Morais, M. A., Armengol, J., Phillips, A. J. L., Câmara, M. P. S., Michereff, S. J. (2016). Phylogeny, distribution and pathogenicity of *Lasiodiplodia* species associated with dieback of table grape in the main Brazilian exporting region. *Plant Pathology, 65*(1), 92–103. https://doi.org/10.1111/ppa.12388

Cosseboom, S. D., & Hu, M. (2021). Diversity, pathogenicity, and fungicide sensitivity of fungal species associated with late-season rots of wine grape in the Mid-Atlantic United States. *Plant Disease, 105*(10), 3101–3110. https://doi.org/10.1094/PDIS-01-21-0006-RE

Cosseboom, S. D., & Hu, M. (2022). Ontogenic susceptibility of grapevine clusters to ripe rot, caused by the *Colletotrichum acutatum* and *C. gloeosporioides* species complexes. *Phytopathology, 112*(10), 1956–1964. https://doi.org/10.1094/PHYTO-01-22-0004-R

Covarrubias-Rivera, L., Ragazzo-Sánchez, J. A., González-Gutiérrez, K. N., Narváez-Zapata, J. A., & Calderón-Santoyo, M. (2025). Isolation and identification of phytopathogenic fungi from blueberry (*Vaccinium corymbosum*) and their biocontrol by *Meyerozyma guilliermondii* LMA-Cp01. *Journal of Plant Pathology, 107*(1), 525–536. https://doi.org/10.1007/s42161-024-01793-y

Crous, P. W., Groenewald, J. Z., Risède, J. M., Simoneau, P. (2004), & Hywel-Jones, N. L. *Calonectria* species and their *Cylindrocladium* anamorphs: Species with sphaeropedunculate vesicles. *Studies in Mycology, 50*, 415–430.

Crous, P. W., Hawksworth, D. L., & Wingfield, M. J. (2015). Identifying and naming plant-pathogenic fungi: Past, present, and future. *Annual Review of Phytopathology, 53*, 247–267. https://doi.org/10.1146/annurev-phyto-080614-120245

Crous, P. W., Lombard, L., Sandoval-Denis, M., Seifert, K. A., Schroers, H. J., Chaverri, P., ... Thines, M. (2021). *Fusarium*: More than a node or a foot-shaped basal cell. *Studies in Mycology, 98*, 100116. https://doi.org/10.1016/j.simyco.2021.100116

Crous, P. W., Summerell, B. A., Swart, L., Denman, S., Taylor, J. E., Bezuidenhout, C. M., … Groenewald, J. Z. (2011). Fungal pathogens of Proteaceae. *Persoonia, 27*, 20–45. https://doi.org/10.3767/003158511X606239

Crous, P. W., Wingfield, M. J., Schumacher, R. K., Akulov, A., Bulgakov, T. S., Carnegie, A. J., … Groenewald, J. Z. (2020). New and interesting fungi. 3. *Fungal Systematics and Evolution, 6*(1), 157–231. https://doi.org/10.3114/fuse.2020.06.09

Crous, P., & Braun, U. (1996). Cercosporoid fungi from South Africa. *Mycological Research, 57*, 233–321.

da Silva, N. M. P., Guterres, D. C., Borges, L. S., Barreto, R. W., & Furtado, G. Q. (2023). Surveying potentially antagonistic fungi to myrtle rust (*Austropuccinia psidii*) in Brazil: Fungicolous *Cladosporium* spp. *Brazilian Journal of Microbiology, 54*, 1899–1914. https://doi.org/10.1007/s42770-023-01047-6

Dai, Q. D., & Li, G. X. (2011). Identification and biological characteristics of grey mould of blueberry. *China Fruits, 2011*(3), 46–48. https://doi.org/10.16626/j.cnki.issn1000-8047.2011.03.002

Damm, U., Cannon, P. F., Woudenberg, J. H. C., & Crous, P. W. (2012). The *Colletotrichum acutatum* species complex. *Studies in Mycology, 73*, 37–113. https://doi.org/10.3114/sim0010

Darapanit, A., Boonyuen, N., Leesutthiphonchai, W., Nuankaew, S., & Piasai, O. (2021). Identification, pathogenicity and effects of plant extracts on Neopestalotiopsis and Pseudopestalotiopsis causing fruit diseases. *Scientific Reports*, *11*(1), 22606. https://doi.org/10.1038/s41598-021-02113-5

David, J. C. (1997). *A contribution to the systematics of Cladosporium: Revision of the fungi previously referred to Heterosporium*. CABI Publishing. https://biotanz.landcareresearch.co.nz/references/1cb0defe-36b9-11d5-9548-00d0592d548c

Dean, R., Van Kan, J. A. L., Pretorius, Z. A., Hammond-Kosack, K. E., Di Pietro, A., Spanu, P. D., … Foster, G. D. (2012). The Top 10 fungal pathogens in molecular plant pathology. *Molecular Plant Pathology*, *13*(4), 414–430. https://doi.org/10.1111/j.1364-3703.2011.00783.x

Delisle-Houde, M., Dionne, A., Demers, F., & Tweddell, R. J. (2024). Cladosporium fruit rot of raspberry caused by *Cladosporium pseudocladosporioides* in the Québec Province. *Plant Disease, 108*(2), 526. https://doi.org/10.1094/PDIS-08-23-1657-PDN

Dil, T., Karakaya, A., & Çelik Oğuz, A. (2013). Blueberry fungal diseases in Rize, Turkey. In *Proceedings of the 24th International Scientific-Expert Conference of Agriculture and Food Industry* (pp. 409–413). Sarajevo, Bosnia and Herzegovina.

Diogo, E., Gonçalves, C. I., Silva, A. C., Valente, C., Bragança, H., & Phillips, A. J. L. (2021). Five new species of *Neopestalotiopsis* associated with diseased *Eucalyptus* spp. in Portugal. *Mycological Progress, 20*(11), 1441–1456. https://doi.org/10.1007/s11557-021-01741-5

Dissanayake, A. J., Liu, M., Zhang, W., Chen, Z., Udayanga, D., Chukeatirote, E., … Hyde, K. D. (2015). Morphological and molecular characterization of *Diaporthe* species associated with grapevine trunk disease in China. *Fungal Biology, 119*(5), 283–294. https://doi.org/10.1016/j.funbio.2014.11.003

Dissanayake, A. J., Purahong, W., Wubet, T., Hyde, K. D., Zhang, W., Xu, H. Y., … Yan, J. Y. (2018). Direct comparison of culture-dependent and culture-independent molecular approaches reveal the diversity of fungal endophytic communities in stems of grapevine (*Vitis vinifera*). *Fungal Diversity, 90*(1), 85–107. https://doi.org/10.1007/s13225-018-0399-3

Dissanayake, A. J., Zhang, W., Li, X. H., Zhou, Y., Chethana, T., Chukeatirote, E., … Zhao, W. S. (2015). First report of *Neofusicoccum mangiferae* associated with grapevine dieback in China. *Phytopathologia Mediterranea*, *54*(2), 414–419. https://doi.org/10.14601/Phytopathol_Mediterr-15159

Dissanayake, A. J., Zhang, W., Liu, M., Chukeatirote, E., Yan, J. Y., Li, X. H. & Hyde, K. D. (2015). *Lasiodiplodia pseudotheobromae* causes pedicel and peduncle discolouration of grapes in China. *Australasian Plant Disease Notes, 10*, 21. https://doi.org/10.1007/s13314-015-0170-5

Dissanayake, A. J., Zhu, J. T., Chen, Y. Y., Maharachchikumbura, S. S. N., Hyde, K. D., & Liu, J. K. (2024). A re-evaluation of *Diaporthe*: Refining the boundaries of species and species complexes. *Fungal Diversity, 126*(1), 1–125. https://doi.org/10.1007/s13225-024-00538-7

do Nascimento Nunes, M. C. (2008). Impact of environmental conditions on fruit and vegetable quality. *Stewart Postharvest Review, 4*(4), 1–14. https://doi.org/10.2212/spr.2008.4.4

Doidge, E. M. (1950). *The South African fungi and lichens to the end of 1945*. Government Printer.

Douriet-Angulo, A., López-Orona, C. A., López-Urquídez, G. A., Vega-Gutiérrez, T. A., Tirado-Ramírez, M. A., Estrada-Acosta, M. D., … Yáñez-Juárez, M. G. (2019). Maize stalk rot caused by *Fusarium falciforme* (FSSC 3 + 4) in Mexico. *Plant Disease, 103*, 2951. https://doi.org/10.1094/PDIS-05-19-1055-PDN

Doyle, V. P., Oudemans, P. V., Rehner, S. A., & Litt, A. (2013). Habitat and host indicate lineage identity in *Colletotrichum gloeosporioides* s.l. from wild and agricultural landscapes in North America. *PLoS ONE, 8*(5), e62394. https://doi.org/10.1371/journal.pone.0062394

du Toit, L. J., & Derie, M. L. (2012). First report of Cladosporium leaf spot of spinach caused by *Cladosporium variabile* in the winter spinach production region of California and Arizona. *Plant Disease, 96*(7), 1071. https://doi.org/10.1094/PDIS-03-12-0279-PDN

Du, Y. M., Wang, X. H., Guo, Y. S., Xiao, F., Peng, Y. H., Hong, N., & Wang, G. P. (2021). Biological and molecular characterization of seven *Diaporthe* species associated with kiwifruit shoot blight and leaf spot in China. *Phytopathologia Mediterranea, 60*, 177–198. https://doi.org/10.36253/phyto-12013

Duan, Y. M., Tarafdar, A., Chaurasia, D., Singh, A., Bhargava, P. C., Yang, J. F., … Awasthi, M. K. (2022). Blueberry fruit valorization and valuable constituents: A review. *International Journal of Food Microbiology, 381*, 109890. https://doi.org/10.1016/j.ijfoodmicro.2022.109890

Dugan, F., Glawe, D., Attanayake, R., & Chen, W. (2009). The importance of reporting new host–fungus records for ornamental and regional crops. *Plant Health Progress, 10*, 34. https://doi.org/10.1094/PHP-2009-0512-01-RV

Dwivedi, M., Singh, P., & Pandey, A. K. (2024). *Botrytis* fruit rot management: What have we achieved so far? *Food Microbiology, 122*, 104564. https://doi.org/10.1016/j.fm.2024.104564

Early, M. P., & Punithalingam, E. (1972). *Phomopsis anacardii* sp. nov. on *Anacardium occidentale*. *Transactions of the British Mycological Society, 59*, 345–347. https://doi.org/10.1016/S0007-1536(72)80030-5

Eaton, M. J., Edwards, S., Inocencio, H. A., Machado, F. J., Nuckles, E. M., Farman, M., … Vaillancourt, L. J. (2021). Diversity and cross-infection potential of *Colletotrichum* causing fruit rots in mixed-fruit orchards in Kentucky. *Plant Disease, 105*(4), 1115–1128. https://doi.org/10.1094/PDIS-06-20-1273-RE

Echeverrigaray, S., Scariot, F. J., Fontanella, G., Favaron, F., Sella, L., Santos, M. C., … Delamare, A. P. L. (2020). *Colletotrichum* species causing grape ripe rot disease in *Vitis labrusca* and *V. vinifera* varieties in the highlands of southern Brazil. *Plant Pathology, 69*(8), 1504–1512. https://doi.org/10.1111/ppa.13240

Edger, P. P., Iorizzo, M., Bassil, N. V., Benevenuto, J., Ferrão, L. F. V., Giongo, L., … Zalapa, J. (2022). There and back again; historical perspective and future directions for *Vaccinium* breeding and research studies. *Horticulture Research, 9*, uhac083. https://doi.org/10.1093/hr/uhac083

Elad, Y. (2016). Cultural and integrated control of *Botrytis* spp. In S. Fillinger & Y. Elad (Eds.), *Botrytis – the fungus, the pathogen and its management in agricultural systems* (pp. 149–164). Springer International Publishing.

El-Baky, N. A., & Amara, A. A. A. F. (2021). Recent approaches towards control of fungal diseases in plants: An updated review. *Journal of Fungi, 7*(11), 900. https://doi.org/10.3390/jof7110900

Elfar, K., Torres, R., Díaz, G. A., & Latorre, B. A. (2013). Characterization of *Diaporthe australafricana* and *Diaporthe* spp. associated with stem canker of blueberry in Chile. *Plant Disease, 97*(8), 1042–1050. https://doi.org/10.1094/PDIS-11-12-1030-RE

Ellis, M. A. (2016). *Cherry leaf spot*. https://ohioline.osu.edu/factsheet/plpath-fru-40

Espinoza, J. G., Briceño, E. X., Chávez, E. R., Úrbez-Torres, J. R., & Latorre, B. A. (2009). *Neofusicoccum* spp. associated with stem canker and dieback of blueberry in Chile. *Plant Disease, 93*(11), 1187–1194. https://doi.org/10.1094/PDIS-93-11-1187

Espinoza, J. G., Briceño, E. X., Keith, L. M., & Latorre, B. A. (2008). Canker and twig dieback of blueberry caused by *Pestalotiopsis* spp. and a *Truncatella* sp. in Chile. *Plant Disease, 92*(10), 1407–1414. https://doi.org/10.1094/PDIS-92-10-1407

Essa, T. A., Kamel, S., Ismail, A. M., & El-Ganainy, S. (2018). Characterization and chemical control of *Neopestalotiopsis rosae*, the causal agent of strawberry root and crown rot in Egypt. *Egyptian Journal of Phytopathology, 46*(1), 1–19. https://doi.org/10.21608/ejp.2018.87411

Fan, X. L., Hyde, K. D., Liu, J. K., Liang, Y. M., & Tian, C. M. (2015). Multigene phylogeny and morphology reveal *Phaeobotryon rhois* sp. nov. (Botryosphaeriales, Ascomycota). *Phytotaxa, 205*, 90–98. https://doi.org/10.11646/phytotaxa.205.2.2

Farr, D. F., & Rossman, A. Y. *Fungal databases, U.S. National Fungus Collections, ARS, USDA*. Retrieved February 19, 2023, from https://nt.ars-grin.gov/fungaldatabases/

Fedele, G., Armengol, J., Caffi, T., Languasco, L., Latinovic, N., Latinovic, J., … Rossi, V. (2024). *Diaporthe foeniculina* and *D. eres*, in addition to *D. ampelina*, may cause Phomopsis cane and leaf spot disease in grapevine. *Frontiers in Plant Science, 15*, 1446663. https://doi.org/10.3389/fpls.2024.1446663

Fei, N. Y., Qi, Y. B., Meng, T. T., Fu, J. F., & Yan, X. R. (2018). First report of root rot caused by *Calonectria ilicicola* on blueberry in Yunnan Province, China. *Plant Disease, 102*(5), 1036. https://doi.org/10.1094/PDIS-09-17-1337-PDN

Feng, H., Wang, C. L., He, Y. T., Tang, L., Han, P. L., Liang, J. H, & Huang, L. L. (2023). Apple Valsa canker: Insights into pathogenesis and disease control. *Phytopathology Research, 5*(1), 45. https://doi.org/10.1186/s42483-023-00200-1

Feng, W. K., Wang, C. H., Ju, Y. W., Chen, Z. X., Wu, X., & Fang, D. L. (2024). Identifying the biological characteristics of anthracnose pathogens of blueberries (*Vaccinium corymbosum* L.) in China. *Forests, 15*(1), 117. https://doi.org/10.3390/f15010117

Fernández, R., Rivera, M., Varsallona, B., & Wright, E. (2015). Disease prevalence and symptoms caused by *Alternaria tenuissima* and *Pestalotiopsis guepinii* on blueberry in Entre Ríos and Buenos Aires, Argentina. *American Journal of Plant Sciences, 6*(19), 3082–3090. https://doi.org/10.4236/ajps.2015.619301

Fillinger, S., & Elad, Y. (Eds.). (2016). *Botrytis—The fungus, the pathogen and its management in agricultural systems*. Springer.

Fiorenza, A., Gusella, G., Aiello, D., Polizzi, G., & Voglmayr, H. (2022). *Neopestalotiopsis siciliana* sp. nov. and *N. rosae* causing stem lesion and dieback on avocado plants in Italy. *Journal of Fungi, 8*(6), 562. https://doi.org/10.3390/jof8060562

Fisher, M. C., Gurr, S. J., Cuomo, C. A., Blehert, D. S., Jin, H., Stukenbrock, E. H., … Cowen, L. E. (2020). Threats posed by the fungal kingdom to humans, wildlife, and agriculture. *mBio, 11*(3), e00449-20. https://doi.org/10.1128/mBio.00449-20

Frisullo, S. A., Logrieco, A., Moretti, A., Grammatikaki, G., & Bottalico, A. (1994). Banana corm and root rot by *Fusarium compactum* in Crete. *Phytopathologia Mediterranea, 33*, 78–82.

Fu, M., Crous, P. W., Bai, Q., Zhang, P. F., Xiang, J., Guo, Y. S., … Wang, G. P. (2019). *Colletotrichum* species associated with anthracnose of *Pyrus* spp. in China. *Persoonia: Molecular Phylogeny and Evolution of Fungi, 42*(1), 1–35. https://doi.org/10.3767/persoonia.2019.42.01

Galarza, L., Akagi, Y., Takao, K., Kim, C. S., Maekawa, N., Itai, A., … Kodama, M. (2015). Characterization of *Trichoderma* species isolated in Ecuador and their antagonistic activities against phytopathogenic fungi from Ecuador and Japan. *Journal of General Plant Pathology, 81*, 201–210. https://doi.org/10.1007/s10327-015-0587-x

Gao, L. L., Zhang, Q., Sun, X. Y., Jiang, L., Zhang, R., Sun, G. Y., … Biggs, A. R. (2013). Etiology of moldy core, core browning, and core rot of Fuji apple in China. *Plant Disease, 97*(4), 510–516. https://doi.org/10.1094/PDIS-01-12-0024-RE

Gao, Y., Liu, F., Duan, W., Crous, P. W., & Cai, L. (2017). *Diaporthe* is paraphyletic. *IMA Fungus, 8*, 153–187. https://doi.org/10.5598/imafungus.2017.08.01.11

Gao, Y., Zhai, F. Y., Zhang, Y. B., Shu, J. P., Chang, J., Zhang, W., & Wang, H. J. (2022). *Neopestalotiopsis rosae* causing black spot on leaf and fruit of pecan (*Carya illinoinensis*) in China. *Plant Disease, 106*(7), 1995. https://doi.org/10.1094/PDIS-07-21-1541-PDN

Garcia, S. M. (1993). Influence of temperature on apothecial development and ascospore discharge by *Blumeriella jaapii*. *Plant Disease, 77*(8), 776. https://doi.org/10.1094/PD-77-0776

Garfinkel, A. R. (2021). The history of *Botrytis* taxonomy, the rise of phylogenetics, and implications for species recognition. *Phytopathology, 111*, 437–454. https://doi.org/10.1094/PHYTO-06-20-0211-IA

Geng, Y., Wang, J. G., Zhang, J. L., Chen, G., Yu, J. H., Li, Y. T., & Ma, L. G. (2022). First report of *Cladosporium tenuissimum* causing leaf spot of *Arachis hypogaea* in China. *Plant Disease, 106*(10), 2754. https://doi.org/10.1094/PDIS-11-21-2461-PDN

Ghule, M. R., Sawant, I. S., Sawant, S. D., Sharma, R., & Shouche, Y. S. (2018). Identification of *Fusarium* species as putative mycoparasites of *Plasmopara viticola* causing downy mildew in grapevines. *Australasian Plant Disease Notes, 13*, 16. https://doi.org/10.1007/s13314-018-0297-2

Glass, N. L., & Donaldson, G. C. (1995). Development of primer sets designed for use with the PCR to amplify conserved genes from filamentous ascomycetes. *Applied and Environmental Microbiology, 61*(4), 1323–1330. https://doi.org/10.1128/aem.61.4.1323-1330.1995

Goldschmidt, E. E. (2013). The evolution of fruit tree productivity: A review. *Economic Botany, 67*, 51–62. https://doi.org/10.1007/s12231-012-9219-y

Gomes, R. R., Glienke, C., Videira, S. I. R., Lombard, L., Groenewald, J. Z., & Crous, P. W. (2013). *Diaporthe*: A genus of endophytic, saprobic and plant pathogenic fungi. *Persoonia - Molecular Phylogeny and Evolution of Fungi, 31*(1), 1–41. https://doi.org/10.3767/003158513X666844

González, P., Alaniz, S., Montelongo, M. J., Rauduviniche, L., Rebellato, J., Silvera-Pérez, E., & Mondino, P. (2012). First report of *Pestalotiopsis clavispora* causing dieback on blueberry in Uruguay. *Plant Disease, 96*(6), 914. https://doi.org/10.1094/PDIS-12-11-1070-PDN

González, V., & Tello, M. L. (2011). The endophytic mycota associated with *Vitis vinifera* in central Spain. *Fungal Diversity, 47*, 29–42. https://doi.org/10.1007/s13225-010-0073-x

Goutam, E., Kumar, A., Tripathi, V., Bharti, Kumar, L., & Raj, A. (2024). Unveiling mechanisms for induced systemic resistance, resistance breeding and molecular marker-assisted breeding against Phomopsis blight of *Solanum melongena*. *Plant Pathology, 73*(4), 777–790. https://doi.org/10.1111/ppa.13860

Gramaje, D., Mostert, L., Groenewald, J. Z., & Crous, P. W. (2015). *Phaeoacremonium*: From esca disease to phaeohyphomycosis. *Fungal Biology, 119*, 759–783. https://doi.org/10.1016/j.funbio.2015.06.004

Gramaje, D., Úrbez-Torres, J. R., & Sosnowski, M. R. (2018). Managing grapevine trunk diseases with respect to etiology and epidemiology: Current strategies and future prospects. *Plant Disease, 102*(1), 12–39. https://doi.org/10.1094/PDIS-04-17-0512-FE

Gruber, B. R., Kruger, E. L., & McManus, P. S. (2012). Effects of cherry leaf spot on photosynthesis in tart cherry 'Montmorency' foliage. *Phytopathology, 102*(7), 656–661. https://doi.org/10.1094/PHYTO-12-11-0334

Gu, C. Y., Yang, X., Al-Attala, M. N., Abid, M., May Phyo, S. S., Zang, H. Y., … Chen, Y. (2020). First report of pomegranate fruit rot caused by *Botryosphaeria dothidea* in Anhui province of China. *Plant Disease, 104*, 2736. https://doi.org/10.1094/PDIS-04-20-0790-PDN

Gu, R., Bao, D. F., Shen, H. W., Su, X. J., Li, Y. X., & Luo, Z. L. (2022). Endophytic *Pestalotiopsis* species associated with *Rhododendron* in Cangshan Mountain, Yunnan Province, China. *Frontiers in Microbiology, 13*, 1016782. https://doi.org/10.3389/fmicb.2022.1016782

Guarnaccia, V., Groenewald, J. Z., Woodhall, J., Armengol, J., Cinelli, T., Eichmeier, A., … Crous, P. W. (2018). *Diaporthe* diversity and pathogenicity revealed from a broad survey of grapevine diseases in Europe. *Persoonia: Molecular Phylogeny and Evolution of Fungi, 40*, 135–153. https://doi.org/10.3767/persoonia.2018.40.06

Guarnaccia, V., Kraus, C., Markakis, E., Alves, A., Armengol, J., Eichmeier, A., . . . Gramaje, D. (2022). Fungal trunk diseases of fruit trees in Europe: Pathogens, spread and future directions. *Phytopathologia Mediterranea, 61*(3), 3. https://doi.org/10.36253/phyto-14167

Guerber, J. C., Liu, B., Correll, J. C., & Johnston, P. R. (2003). Characterization of diversity in *Colletotrichum acutatum* sensu lato by sequence analysis of two gene introns, mtDNA and intron RFLPs, and mating compatibility. *Mycologia, 95*, 872–895. https://doi.org/10.1080/15572536.2004.11833047

Güngör-Savaş, N., Akgül, D. S., Özarslandan, M., & Yıldız, M. (2020). First report of *Dactylonectria alcacerensis* and *Dactylonectria torresensis* associated with black foot disease of grapevine in Turkey. *Plant Disease, 104*, 2027. https://doi.org/10.1094/PDIS-02-20-0385-PDN

Guo, Y. S., Crous, P. W., Bai, Q., Fu, M., Yang, M. M., Wang, X. H., … Wang, G. P. (2020). High diversity of *Diaporthe* species associated with pear shoot canker in China. *Persoonia - Molecular Phylogeny and Evolution of Fungi, 45*(1), 132–162. https://doi.org/10.3767/persoonia.2020.45.05

Guo, Y., & Liu, X. (1992). Studies on the genus *Pseudocercospora* in China. *Acta Mycologica Sinica, 11*(3), 193–200.

Guo, Z. H., Yu, Z. H., Li, Q. L., Tang, L. H., Guo, T. X., Huang, S. P., … Luo, S. M. (2021). *Fusarium* species associated with leaf spots of mango in China. *Microbial Pathogenesis*, *150*, 104736. https://doi.org/10.1016/j.micpath.2021.104736

Hall, T. A. (1999). BioEdit: A user-friendly biological sequence alignment editor and analysis program for Windows 95/98/NT. *Nucleic Acids Symposium Series, 41*, 95–98.

Halleen, F., Schroers, H. J., Groenewald, J. Z., & Crous, P. W. (2004). Novel species of *Cylindrocarpon* (*Neonectria*) and *Campylocarpon* gen. nov. associated with black foot disease of grapevines (*Vitis* spp.). *Studies in Mycology, 50*, 431–455.

Han, Y. Z., Lu, Y. X., Wu, C. F., Fan, Z. W., Yang, Y. M., Shen, Q., … Zeng, B. (2019). First report of *Cladosporium tenuissimum* associated with leaf spot of alfalfa (*Medicago sativa*) in China. *Plant Disease, 103*(7), 1778. https://doi.org/10.1094/PDIS-12-18-2295-PDN

Hariharan, G., Rifnas, L. M., & Prasannath, K. (2022). Role of *Trichoderma* spp. in biocontrol of plant diseases. In A. Kumar (Ed.), *Microbial biocontrol: Food security and post harvest management* (pp. 39–78). Springer.

He, Y. K., Yang, Q., Sun, Y. R., Zeng, X. Y., Jayawardena, R. S., Hyde, K. D., & Wang, Y. (2022). Additions to *Neopestalotiopsis* (Amphisphaeriales, Sporocadaceae) fungi: Two new species and one new host record from China. *Biodiversity Data Journal, 10*, e90709. https://doi.org/10.3897/BDJ.10.e90709

Highet, A. S., & Nair, N. G. (1995). *Fusarium oxysporum* associated with grapevine decline in the Hunter Valley, NSW, Australia. *Australian Journal of Grape and Wine Research, 1*, 48–50. https://doi.org/10.1111/j.1755-0238.1995.tb00077.x

Hilário, S., Amaral, I. A., Gonçalves, M. F. M., Lopes, A., Santos, L., & Alves, A. (2022). *Diaporthe* species associated with twig blight and dieback of *Vaccinium* spp. in Portugal. *European Journal of Plant Pathology, 163*(1), 1–20. https://doi.org/10.1007/s10658-022-02503-1

Hilário, S., Amaral, I. A., Gonçalves, M. F. M., Lopes, A., Santos, L., & Alves, A. (2020). *Diaporthe* species associated with twig blight and dieback of *Vaccinium corymbosum* in Portugal, with description of four new species. *Mycologia, 112*(2), 293–308. https://doi.org/10.1080/00275514.2019.1698926

Hilário, S., Gonçalves, M. F. M., & Alves, A. (2021). Using genealogical concordance and coalescent-based species delimitation to assess species boundaries in the *Diaporthe eres* complex. *Journal of Fungi, 7*(7), 507. https://doi.org/10.3390/jof7070507

Hilário, S., Gonçalves, M. F. M., Fidalgo, C., Tacão, M., & Alves, A. (2022). Genome analyses of two blueberry pathogens: *Diaporthe amygdali* CAA958 and *Diaporthe eres* CBS 160.32. *Journal of Fungi, 8*(8), 804. https://doi.org/10.3390/jof8080804

Hilário, S., Lopes, A., Santos, L., & Alves, A. (2020). *Botryosphaeriaceae* species associated with blueberry stem blight and dieback in the Centre Region of Portugal. *European Journal of Plant Pathology, 156*(1), 31–44. https://doi.org/10.1007/s10658-019-01860-6

Hilário, S., Santos, L., & Alves, A. (2021). Diversity and pathogenicity of *Diaporthe* species revealed from a survey of blueberry orchards in Portugal. *Agriculture, 11*(12), 1271. https://doi.org/10.3390/agriculture11121271

Hofstetter, V., Buyck, B., Croll, D., Viret, O., Couloux, A., & Gindro, K. (2012). What if esca disease of grapevine were not a fungal disease? *Fungal Diversity, 54*, 51–67. https://doi.org/10.1007/s13225-012-0171-z

Holb, I. J. (2009). Some biological features of cherry leaf spot (*Blumeriella jaapii*) with special reference to cultivar susceptibility. *International Journal of Horticultural Science, 15*(1–2), 91-93. https://doi.org/10.31421/IJHS/15/1-2/818

Hongsanan, S., Norphanphoun, C., Senanayake, I. C., Jayawardena, R. S., Manawasinghe, I. S., Abeywickrama, P. D., … Bhunjun, C. S. (2023). Annotated notes on *Diaporthe* species. *Mycosphere, 14*(1), 918–1189. https://doi.org/10.5943/mycosphere/14/1/12

Hosking, J. E., Mesarich, C. H., Tarallo, M., de la Rosa, S., & Rivera, S. A. (2024). First report of *Colletotrichum fioriniae* and *Colletotrichum godetiae* causing anthracnose disease of blueberry (*Vaccinium corymbosum* L.) fruit in New Zealand. *Australasian Plant Pathology.* https://doi.org/10.1007/s13313-024-01002-5

Hrycan, J., Hart, M., Bowen, P., Forge, T., & Úrbez-Torres, J. R. (2020). Grapevine trunk disease fungi: Their roles as latent pathogens and stress factors that favour disease development and symptom expression. *Phytopathologia Mediterranea, 59*, 395–424.

Huang, F., Udayanga, D., Wang, X. H., Hou, X., Mei, X. F., Fu, Y. S., … Li, H. Y. (2015). Endophytic Diaporthe associated with Citrus: a phylogenetic reassessment with seven new species from China. *Fungal Biology*, *119*(5), 331–347. https://doi.org/10.1016/j.funbio.2015.02.006

Huarhua, M., Flores, J., Acuña, R., & Apaza, W. (2018). Morphological and molecular identification of *Phytophthora cinnamomi* Rands as causal agent of crown and root rot in blueberry (*Vaccinium corymbosum*) in Peru. *Peruvian Journal of Agronomy, 2*(2), 14–18. https://doi.org/10.21704/pja.v2i2.1202

Hyde, K. D., Alwasel, S., Aumentado, H. D. R., Boekhout, T., Bera, I., Khyaju, S., … Wanasinghe, D. N. (2024). Fungal numbers: Global needs for a realistic assessment. *Fungal Diversity, 128*, 1–25. https://doi.org/10.1007/s13225-023-00532-5

Hyde, K. D., Baldrian, P., Chen, Y. P., Chethana, K. W. T., De Hoog, S., Doilom, M., … Walker, A. (2024). Current trends, limitations and future research in the fungi. *Fungal Diversity, 125*(1), 1–71. https://doi.org/10.1007/s13225-023-00532-5

Hyde, K. D., Noorabadi, M. T., Thiyagaraja, V., He, M. Q., Johnston, P. R., Wijesinghe, S. N., … Zvyagina, E. (2024). The 2024 outline of fungi and fungus-like taxa. *Mycosphere, 15*(1), 5146–6239. https://doi.org/10.5943/mycosphere/15/1/25

Ingram, R. J., Ludwig, H. D., & Scherm, H. (2019). Epidemiology of Exobasidium leaf and fruit spot of rabbiteye blueberry: Pathogen overwintering, primary infection, and disease progression on leaves and fruit. *Plant Disease, 103*(6), 1293–1301. https://doi.org/10.1094/PDIS-09-18-1534-RE

Jain, A., Sarsaiya, S., Wu, Q., Lu, Y., & Shi, J. (2019). A review of plant leaf fungal diseases and its environment speciation. *Bioengineered, 10*(1), 409–424. https://doi.org/10.1080/21655979.2019.1649520

Jaklitsch, W. M., Komon, M., Kubicek, C. P., & Druzhinina, I. S. (2005). *Hypocrea voglmayrii* sp. nov. from the Austrian Alps represents a new phylogenetic clade in *Hypocrea/Trichoderma. Mycologia, 97*(6), 1365–1378. https://doi.org/10.1080/15572536.2006.11832743

Janick, J. (2005). The origins of fruits, fruit growing, and fruit breeding. In J. Janick (Ed.), *Plant breeding reviews* (Vol. 1, pp. 255–321). Wiley. https://doi.org/10.1002/9780470650301.ch8

Jankowiak, R., Stępniewska, H., Szwagrzyk, J., Bilański, P., & Gratzer, G. (2016). Characterization of *Cylindrocarpon*-like species associated with litter in the old-growth beech forests of central Europe. *Forest Pathology, 46*, 582–594. https://doi.org/10.1111/efp.12275

Jayawardena, R. S., Bhunjun, C. S., Hyde, K. D., Gentekaki, E., & Itthayakorn, P. (2021). *Colletotrichum*: Lifestyles, biology, morpho-species, species complexes and accepted species. *Mycosphere, 12*, 519–669. https://doi.org/10.5943/mycosphere/12/1/7

Jayawardena, R. S., Hyde, K. D., Chethana, K. W. T., Daranagama, D. A., Dissanayake, A. J., Goonasekara, I. D., … Yan, J. Y. (2018). Mycosphere Notes 102–168: Saprotrophic fungi on *Vitis* in China, Italy, Russia and Thailand. *Mycosphere, 9*(1), 1–114. https://doi.org/10.5943/mycosphere/9/1/1

Jayawardena, R. S., Hyde, K. D., De Farias, A. R. G., Bhunjun, C. S., Ferdinandez, H. S., Manamgoda, D. S., … Thines, M. (2021). What is a species in fungal plant pathogens?. *Fungal Diversity, 109*(1), 239–266. https://doi.org/10.1007/s13225-021-00484-8

Jayawardena, R. S., Purahong, W., Zhang, W., Wubet, T., Li, X. H., Liu, M., … Yan, J. Y. (2018). Biodiversity of fungi on *Vitis vinifera* L. revealed by traditional and high-resolution culture-independent approaches. *Fungal Diversity, 90*, 1–84. https://doi.org/10.1007/s13225-018-0398-4

Jayawardena, R. S., Zhang, W., Liu, M., Maharachchikumbura, S. S. N., Li, X., Zhou, Y., … Hyde, K. D. (2015). Identification and characterization of *Pestalotiopsis*-like fungi related to grapevine diseases in China. *Fungal Biology, 119*, 348–361. https://doi.org/10.1016/j.funbio.2014.11.001

Jermini, M., Blaise, P., & Gessler, C. (2010). Quantitative effect of leaf damage caused by downy mildew (*Plasmopara viticola*) on growth and yield quality of grapevine 'Merlot' (*Vitis vinifera*). *Vitis, 49*(2), 77–85.

Ji, T., Languasco, L., Li, M., & Rossi, V. (2021). Effects of temperature and wetness duration on infection by *Coniella diplodiella*, the fungus causing white rot of grape berries. *Plants, 10*(8), 8. https://doi.org/10.3390/plants10081696

Jiang, N., Voglmayr, H., Xue, H., Piao, C. G., & Li, Y. (2022). Morphology and phylogeny of *Pestalotiopsis* (Sporocadaceae, Amphisphaeriales) from Fagaceae leaves in China. *Microbiology Spectrum, 10*(6), e03272-22. https://doi.org/10.1128/spectrum.03272-22

Jin, Y. L., Jiang S. L., & Jiang X. L. (2021). Disease-resistant identification and analysis to transcriptome differences of blueberry leaf spot induced by beta-aminobutyric acid. *Archives of Microbiology, 203*(6), 3623–3632. https://doi.org/10.1007/s00203-021-02350-2

Jogaiah, S., Abdelrahman, M., Tran, L. S. P., & Ito, S. I. (2018). Different mechanisms of *Trichoderma virens*-mediated resistance in tomato against *Fusarium* wilt involve the jasmonic and salicylic acid pathways: *T. virens* resistance mechanism against *Fusarium*. *Molecular Plant Pathology, 19*, 870–882. https://doi.org/10.1111/mpp.12571

John, S., Wicks, T. J., Hunt, J. S., Lorimer, M. F., Oakey, H., & Scott, E. S. (2005). Protection of grapevine pruning wounds from infection by *Eutypa lata* using *Trichoderma harzianum* and *Fusarium lateritium*. *Australasian Plant Pathology, 34*, 569–575. https://doi.org/10.1071/AP05075

Joshua, J., & Mmbaga, M. T. (2015). Perpetuation of cherry leaf spot disease in ornamental cherry. *Journal of Phytopathology, 163*(3), 194–201. https://doi.org/10.1111/jph.12309

Kalt, W., Cassidy, A., Howard, L. R., Krikorian, R., Stull, A. J., Tremblay, F., & Zamora-Ros, R. (2020). Recent research on the health benefits of blueberries and their anthocyanins. *Advances in Nutrition, 11*(2), 224–236. https://doi.org/10.1093/advances/nmz065

Kamoun, S., Furzer, O., Jones, J. D. G., Judelson, H. S., Ali, G. S., Dalio, R. J. D., … Govers, F. (2015). The top 10 oomycete pathogens in molecular plant pathology. *Molecular Plant Pathology, 16*(4), 413–434. https://doi.org/10.1111/mpp.12190

Katoh, K., Rozewicki, J., & Yamada, K. D. (2019). MAFFT online service: Multiple sequence alignment, interactive sequence choice and visualization. *Briefings in Bioinformatics, 20*, 1160–1166. https://doi.org/10.1093/bib/bbx108

Kelley, D. S., Adkins, Y., & Laugero, K. D. (2018). A review of the health benefits of cherries. *Nutrients, 10*(3), 3. https://doi.org/10.3390/nu10030368

Khan, N. A., Bhat, M. A., Ahmad, K., & Qazi, N. A. (2014). First record of cherry leaf spot caused by *Cylindrosporium padi* (P. Karst.) from India. *Applied Biological Research, 16*(1), 122–123. https://doi.org/10.5958/0974-4517.2014.00059.7

Köhl, J., Scheer, C., Holb, I. J., Masny, S., & Molhoek, W. M. L. (2015). Toward an integrated use of biological control by *Cladosporium cladosporioides* H39 in apple scab (*Venturia inaequalis*) management. *Plant Disease, 99*(4), 535–543. https://doi.org/10.1094/PDIS-08-14-0836-RE

Koike, S. T., Rooney-Latham, S., & Wright, A. F. (2014). First report of stem blight of blueberry in California caused by *Neofusicoccum parvum*. *Plant Disease, 98*(9), 1280. https://doi.org/10.1094/PDIS-03-14-0325-PDN

Kong, C. S., Qiu, X. L., Yi, K. S., Yu, X. F., & Yu, L. (2010). First report of *Neofusicoccum vitifusiforme* causing blueberry blight of blueberry in China. *Plant Disease, 94*(11), 1373. https://doi.org/10.1094/PDIS-05-10-0393

Kraus, C., Voegele, R. T., & Fischer, M. (2019). Temporal development of the culturable, endophytic fungal community in healthy grapevine branches and occurrence of GTD-associated fungi. *Microbial Ecology, 77*, 866–876. https://doi.org/10.1007/s00248-018-1280-3

Krishna, P., Pandey, G., Thomas, R., & Parks, S. (2023). Improving blueberry fruit nutritional quality through physiological and genetic interventions: A review of current research and future directions. *Antioxidants, 12*(4), 810. https://doi.org/10.3390/antiox12040810

Kusai, N. A., Mior Zakuan Azmi, M., Zulkifly, S., Yusof, M. T., & Mohd Zainudin, N. A. I. (2016). Morphological and molecular characterization of *Curvularia* and related species associated with leaf spot disease of rice in Peninsular Malaysia. *Rendiconti Lincei. Scienze Fisiche e Naturali, 27*, 205–214. https://doi.org/10.1007/s12210-015-0458-6

Kwon, J. H., Cheon, M. G., Choi, O., & Kim, J. (2011). First report of *Botrytis cinerea* as a postharvest pathogen of blueberry in Korea. *Mycobiology, 39*(1), 52–53. https://doi.org/10.4489/MYCO.2011.39.1.052

Lai, J., Liu, B., Xiong, G., Liu, T., You, J., & Jiang, J. (2023). First report of *Diaporthe phoenicicola* causing leaf spot on blueberry (*Vaccinium virgatum*) in China. *Plant Disease, 107*(2), 569. https://doi.org/10.1094/PDIS-05-22-1007-PDN

Lai, J., Xiong, G., Liu, B., Kuang, W., & Song, S. (2022). First report of *Coniella castaneicola* causing leaf blight on blueberry (*Vaccinium virgatum*) in China. *Plant Disease, 106*(4), 1298. https://doi.org/10.1094/PDIS-05-21-1122-PDN

Lamichhane, J. R., & Venturi, V. (2015). Synergisms between microbial pathogens in plant disease complexes: A growing trend. *Frontiers in Plant Science, 6*, 385. https://doi.org/10.3389/fpls.2015.00385

Lan, C. Z., Ruan, H. C., & Yao, J. A. (2016). First report of *Phytophthora cinnamomi* causing root and stem rot of blueberry (*Vaccinium corymbosum*) in China. *Plant Disease, 100*(12), 2537. https://doi.org/10.1094/PDIS-03-16-0345-PDN

Langenhoven, S., Halleen, F., Spies, C. F. J., Stempien, E., & Mostert, L. (2018). Detection and quantification of black foot and crown and root rot pathogens in grapevine nursery soils in the Western Cape of South Africa. *Phytopathologia Mediterranea, 57*, 519–537. https://doi.org/10.14601/Phytopathol_Mediterr-23921

Lawrence, D. P., Nouri, M. T., & Trouillas, F. P. (2019). Taxonomy and multi-locus phylogeny of *Cylindrocarpon*-like species associated with diseased roots of grapevine and other fruit and nut crops in California. *Fungal Systematics and Evolution, 4*, 59–75. https://doi.org/10.3114/fuse.2019.04.06

Lee, Y., Kim, G. H., Kim, Y., Park, S. Y., & Koh, Y. J. (2019). First report of twig dieback caused by *Neopestalotiopsis clavispora* on blueberry in Korea. *Plant Disease, 103*(5), 1022. https://doi.org/10.1094/PDIS-10-18-1734-PDN

Leslie, J. F., & Summerell, B. A. (2006). *The Fusarium laboratory manual*. Blackwell Publishing.

Li, F. J., Yang, C., Li, M. Y., Liu, S., Xu, K., & Fu, X. J. (2025). Antifungal activity of genistein against phytopathogenic fungi *Valsa mali* through ROS-mediated lipid peroxidation. *Plants, 14*(1), 120. https://doi.org/10.3390/plants14010120

Li, L. L., Yang, Q., & Li, H. (2021). Morphology, phylogeny, and pathogenicity of pestalotioid species on *Camellia oleifera* in China. *Journal of Fungi, 7*, 1080. https://doi.org/10.3390/jof7121080

Li, Q. R., Tan, P., Jiang, Y. L., Hyde, K. D., McKenzie, E. H. C., Bahkali, A.H., … Wang, Y. (2013). A novel *Trichoderma* species isolated from soil in Guizhou, *T. guizhouense*. *Mycological Progress, 12*, 167–172. https://doi.org/10.1007/s11557-012-0821-2

Li, Q., Hou, Z. P., & Yu, J. P. (2023). First report of *Botrytis californica* causing gray mold on blueberry in China. *Plant Disease, 107*(10), 3318. https://doi.org/10.1094/PDIS-12-22-2881-PDN

Li, S. H. (2015). Grapevine breeding and genetics in China: History, current status and the future. *Acta Horticulturae, 1082*, 165–176. https://doi.org/10.17660/ActaHortic.2015.1082.22

Li, S., Hou, R., Zhang, F. M., & Shang, X. J. (2023). First report of *Fusarium commune* causing root rot of blueberry plants in Guizhou province, China. *Plant Disease, 107*(4), 1227. https://doi.org/10.1094/PDIS-06-22-1305-PDN

Li, W. L., Dissanayake, A. J., Zhang, T., Maharachchikumbura, S. S. N., & Liu, J. K. (2022). Identification and pathogenicity of pestalotiod fungi associated with woody oil plants in Sichuan Province, China. *Journal of Fungi, 8*(11), 1175. https://doi.org/10.3390/jof8111175

Li, Y. K., Hu, Y., Wu, Q. X., Wu, Y. Y., Zhang, Z. L., Yi, R., & Song, X. H. (2023). First report of *Diaporthe sojae* causing stem canker on blueberry in China. *Plant Disease, 107*(9), 2851. https://doi.org/10.1094/PDIS-02-23-0258-PDN

Li, Y., Shi L. B., Fei, N. Y., Meng, T. T., Fu, J. F., & Yan, X. R. (2021). Identification of *Diaporthe* species associated with cherry leaf spot disease in China. *Acta Phytopathologica Sinica*, *47*(6), 721–729.

Li, Z., dos Santos, R. F., Gao, L. L., Chang, P. P., & Wang, X. P. (2021). Current status and future prospects of grapevine anthracnose caused by *Elsinoe ampelina*: An important disease in humid grape-growing regions. *Molecular Plant Pathology, 22*(8), 899–910. https://doi.org/10.1111/mpp.13076

Limier, B., Ivorra, S., Bouby, L., Figueiral, I., Chabal, L., Cabanis, M., … Terral, J. F. (2018). Documenting the history of the grapevine and viticulture: A quantitative eco-anatomical perspective applied to modern and archaeological charcoal. *Journal of Archaeological Science, 100*, 45–61. https://doi.org/10.1016/j.jas.2018.10.001

Ling, J. F., Peng, A. T., Jiang, Z. D., Xi, P. G., Song, X. B., Cheng, B. P., … Chen, X. (2021). First report of anthracnose fruit rot caused by *Colletotrichum fioriniae* on litchi in China. *Plant Disease, 105*(5), 1225. https://doi.org/10.1094/PDIS-07-20-1539-PDN

Lino, L., Pacheco, I., Mercier, V., Faoro, F., Bassi, D., Bornard, I., & Quilot-Turion, B. (2016). Brown rot strikes *Prunus* fruit: An ancient fight almost always lost. *Journal of Agricultural and Food Chemistry, 64*(20), 4029–4047. https://doi.org/10.1021/acs.jafc.6b00104

Liu, A. R., Xu, T., & Guo, L. D. (2007). Molecular and morphological description of *Pestalotiopsis hainanensis* sp. nov., a new endophyte from a tropical region of China. *Fungal Diversity, 24*, 23–36.

Liu, B. Y., Zhang, W., Luan, B. H., & Wang, Y. Z. (2012). Identification of the pathogen and epidemic dynamics of brown spot of sweet cherry (*Prunus avium*). *Journal of Fruit Science, 29*(5), 765–771.

Liu, C., Luo, F. Y., Zhu, T. H., Han, S., & Li, S. J. (2021). Leaf spot disease caused by *Pestalotiopsis kenyana* on *Zanthoxylum schinifolium* in Sichuan Province, China. *Plant Disease, 105*(11), 3747. https://doi.org/10.1094/PDIS-10-20-2247-PDN

Liu, F., Bonthond, G., Groenewald, J. Z., Cai, L., & Crous, P. W. (2019). *Sporocadaceae*, a family of coelomycetous fungi with appendage-bearing conidia. *Studies in Mycology, 92*, 287–415. https://doi.org/10.1016/j.simyco.2018.11.001

Liu, F., Hou, L., Raza, M., & Cai, L. (2017). *Pestalotiopsis* and allied genera from *Camellia*, with description of 11 new species from China. *Scientific Reports, 7*, 866. https://doi.org/10.1038/s41598-017-00972-5

Liu, F., Ma, Z. Y., Hou, L. W., Diao, Y. Z., Wu, W. P., Damm, U., … Cai, L. (2022). Updating species diversity of *Colletotrichum*, with a phylogenomic overview. *Studies in Mycology, 101*, 1–56. https://doi.org/10.3114/sim.2022.101.01

Liu, J. R., Wang, Y. J., Liu, Z. X., Chen, J., Liu, X. F., & Dong, A. R. (2020). Molecular and morphological identification of branch wilt pathogen of *Rubus crataegifolius* (in Chinese). *Journal of Northeast Forestry University, 48*, 95–97+101.

Liu, M., Zhang, W., Zhou, Y., Liu, Y., Yan, J. Y., Li, X. H., … Hyde, K. D. (2016). First report of twig anthracnose on grapevine caused by *Colletotrichum nymphaeae* in China. *Plant Disease, 100*, 2530. https://doi.org/10.1094/PDIS-05-16-0632-PDN

Liu, Q., Ning, N., Ma, Y., & Guo, Q. (2020). Isolation and identification of the pathogen causing leaf spot on cherry in Qinghai Province. *Journal of Plant Protection, 47*(3), 12–18.

Liu, X., Zheng, X. J., Khaskheli, M. I., Sun, X., Chang, X. L., & Gong, G. S. (2020). Identification of *Colletotrichum* species associated with blueberry anthracnose in Sichuan, China. *Pathogens, 9*(9), 718. https://doi.org/10.3390/pathogens9090718

Liu, Y. H., Lin, T., Ye, C. S., & Zhang, C. Q. (2014). First report of Fusarium wilt in blueberry (*Vaccinium corymbosum*) caused by *Fusarium oxysporum* in China. *Plant Disease, 98*(8), 1158. https://doi.org/10.1094/PDIS-02-14-0167-PDN

Liu, Y. J., Whelen, S., & Hall, B. D. (1999). Phylogenetic relationships among ascomycetes: Evidence from an RNA polymerase II subunit. *Molecular Biology and Evolution, 16*(12), 1799–1808. https://doi.org/10.1093/oxfordjournals.molbev.a026092

Liu, Z., Jiao, R., Chen, S., Ren, Y., Zhang, L., Zhang, D., … Li, G. (2022). First report of fruit rot of grapes (*Vitis vinifera*) caused by *Cladosporium cladosporioides* in Xinjiang, China. *Plant Disease, 106*(1), 315. https://doi.org/10.1094/PDIS-01-21-0080-PDN

Lombard, L., Sandoval-Denis, M., Lamprecht, S. C., & Crous, P. W. (2019). Epitypification of *Fusarium oxysporum* – Clearing the taxonomic chaos. *Persoonia, 43*, 1–47. https://doi.org/10.3767/persoonia.2019.43.01

Lombard, L., van der Merwe, N., Groenewald, J. Z., & Crous, P. (2014). Lineages in *Nectriaceae*: Re-evaluating the generic status of *Ilyonectria* and allied genera. *Phytopathologia Mediterranea, 53*, 340–357. https://doi.org/10.14601/Phytopathol_Mediterr-14976

Lombard, L., van Leeuwen, G. C. M., Guarnaccia, V., Polizzi, G., van Rijswick, P. C. J., Rosendahl, K. C. H. M., … Crous, P. W. (2014). *Diaporthe* species associated with *Vaccinium*, with specific reference to Europe. *Phytopathologia Mediterranea, 53*, 287–299. https://doi.org/10.14601/Phytopathol_Mediterr-14034

Lopes, F. A. C., Steindorff, A. S., Geraldine, A. M., Brandão, R. S., Monteiro, V. N., Júnior M. L., … Silva, R. N. (2012). Biochemical and metabolic profiles of *Trichoderma* strains isolated from common bean crops in the Brazilian Cerrado, and potential antagonism against *Sclerotinia sclerotiorum*. *Fungal Biology, 116*, 815–824. https://doi.org/10.1016/j.funbio.2012.04.015

López-Carbonell, M., Moret, A., & Nadal, M. (1998). Changes in cell ultrastructure and zeatin riboside concentrations in *Hedera helix*, *Pelargonium zonale*, *Prunus avium*, and *Rubus ulmifolius* leaves infected by fungi. *Plant Disease*, *82*(8), 914–918. https://doi.org/10.1094/PDIS.1998.82.8.914

Lorenzini, M., & Zapparoli, G. (2015). Occurrence and infection of *Cladosporium*, *Fusarium*, *Epicoccum*, and *Aureobasidium* in withered rotten grapes during post-harvest dehydration. *Antonie van Leeuwenhoek*, *108*, 1171–1180. https://doi.org/10.1007/s10482-015-0570-8

Lorenzini, M, Cappello, M. S., Logrieco, A., & Zapparoli, G. (2016). Polymorphism and phylogenetic species delimitation in filamentous fungi from predominant mycobiota in withered grapes. *International Journal of Food Microbiology*, *238*, 56–62. https://doi.org/10.1016/j.ijfoodmicro.2016.08.039

Lu, X. H., Zhang, X. M., Jiao, X. L., Hao, J. J., Zhang, X. S., Luo, Y., & Guo, W. W. (2020). Taxonomy of fungal complex causing red-skin root of *Panax ginseng* in China. *Journal of Ginseng Research*, *44*(3), 506–518. https://doi.org/10.1016/j.jgr.2019.01.006

Luan, Y. S., Feng, L., & An, L. J. (2006). First report of blueberry leaf spot caused by *Cylindrocladium colhounii* in China. *Plant Disease, 90*(12), 1553. https://doi.org/10.1094/PD-90-1553A

Luan, Y. S., Feng, L., Xia, X. Y., & An, L. J. (2007). First report of *Alternaria tenuissima* causing disease on blueberry in China. *Plant Disease, 91*(4), 464. https://doi.org/10.1094/PDIS-91-4-0464A

Luan, Y. S., Shang, Z. T., Su, Q., Feng, L., & An, L. J. (2008). First report of a *Pestalotiopsis* sp. causing leaf spot of blueberry in China. *Plant Disease, 92*(1), 171. https://doi.org/10.1094/PDIS-92-1-0171A

Luo, M., Guo, W., Zhao, M. P., Manawasinghe, I. S., Guarnaccia, V., Liu, J. W., … You, C. P. (2022). Endophytic *Diaporthe* associated with *Morinda officinalis* in China. *Journal of Fungi, 8*(8), 806. https://doi.org/10.3390/jof8080806

Luo, Q. X., Yang, Y., Li, S., Zhang, R. X., & Xu, M. H. (2023). Identification and biological characteristics of the pathogen causing blueberry leaf spot disease. *Jiangsu Agricultural Sciences*, *51*(5), 146–154. https://doi.org/10.15889/j.issn.1002-1302.2023.05.020

Ma, L. J., Geiser, D. M., Proctor, R. H., Rooney, A. P., O'Donnell, K., Trail, F., … Kazan, K. (2013). *Fusarium* pathogenomics. *Annual Review of Microbiology*, *67*, 399–416. https://doi.org/10.1146/annurev-micro-092412-155650

Ma, X. M., Miao, J., Wang, J. F., Han, W., & Sun, Y. (2022). A novel, rapid and simple method for obtaining single-spore isolation of strongly parasitic fungi from diseased cherry leaves. *ScienceAsia*, *48*(6), 764–768. https://doi.org/10.2306/scienceasia1513-1874.2022.086

Ma, X. F., Qin, Y., Xiang, Y. Y., He, L. G., Song, F., Wang, Z. J., … Wu, L. M. (2023). First report of *Neopestalotiopsis rosae* causing leaf blight on Shatangju in southern China. *Plant Disease, 107*(8), 2535. https://doi.org/10.1094/PDIS-09-22-2066-PDN

MacKenzie, S. J., Peres, N. A., Barquero, M. P., Arauz, L. F., & Timmer, L. W. (2009). Host range and genetic relatedness of *Colletotrichum acutatum* isolates from fruit crops and leatherleaf fern in Florida. *Phytopathology, 99*(5), 620–631. https://doi.org/10.1094/PHYTO-99-5-0620

Madar, Z., Kimchi, M., & Solel, Z. (1996). Fusarium canker of Italian cypress (*Cupressus sempervirens*). *European Journal of Forest Pathology, 26*(2), 107–112. https://doi.org/10.1111/j.1439-0329.1996.tb00715.x

Maharachchikumbura, S. S. N., Guo, L. D., Cai, L., Chukeatirote, E., Wu, W. P., Sun, X., … Hyde, K. D. (2012). A multi-locus backbone tree for *Pestalotiopsis*, with a polyphasic characterization of 14 new species. *Fungal Diversity, 56*(1), 95–129. https://doi.org/10.1007/s13225-012-0198-1

Maharachchikumbura, S. S. N., Hyde, K. D., Groenewald, J. Z., Xu, J., & Crous, P. W. (2014). Pestalotiopsis revisited. *Studies in Mycology*, *79*(1), 121–186. https://doi.org/10.1016/j.simyco.2014.09.005

Maharachchikumbura, S. S. N., Larignon, P., Hyde, K. D., Al-Sadi, A. M., & Liu, Z. Y. (2017). Characterization of *Neopestalotiopsis*, *Pestalotiopsis* and *Truncatella* species associated with grapevine trunk diseases in France. *Phytopathologia Mediterranea*, *55*, 380–390. https://doi.org/10.14601/Phytopathol_Mediterr-18298

Malarczyk, D., Panek, J., & Frąc, M. (2019). Alternative molecular-based diagnostic methods of plant pathogenic fungi affecting berry crops—A review. *Molecules, 24*(7), 1200. https://doi.org/10.3390/molecules24071200

Manawasinghe, I. S., Dissanayake, A. J., Li, X. H., Liu, M., Wanasinghe, D. N., Xu, J. P., … Yan, J. Y. (2019). High genetic diversity and species complexity of *Diaporthe* associated with grapevine dieback in China. *Frontiers in Microbiology, 10*, 1936. https://doi.org/10.3389/fmicb.2019.01936

Manawasinghe, I. S., Phillips, A. J. L., Xu, J. P., Balasuriya, A., Hyde, K. D., Stępień, Ł., … Cheewangkoon R. (2021). Defining a species in fungal plant pathology: Beyond the species level. *Fungal Diversity, 109*, 267–282. https://doi.org/10.1007/s13225-021-00481-x

Manawasinghe, I. S., Zhang, W., Li, X. H., Zhao, W. S., Chethana, K. W. T., Xu, J. P., … Yan, J. Y. (2018). Novel microsatellite markers reveal multiple origins of *Botryosphaeria dothidea* causing the Chinese grapevine trunk disease. *Fungal Ecology, 33*, 134–142. https://doi.org/10.1016/j.funeco.2018.02.004

Marco, S. D., & Osti, F. (2007). Applications of *Trichoderma* to prevent *Phaeomoniella chlamydospora* infections in organic nurseries. *Phytopathologia Mediterranea*, *46*, 73–83. https://doi.org/10.36253/phyto-5204

Marin-Felix, Y., Hernández-Restrepo, M., & Crous, P. W. (2020). Multi-locus phylogeny of the genus *Curvularia* and description of ten new species. *Mycological Progress, 19*, 559–588. https://doi.org/10.1007/s11557-020-01576-6

Marsberg, A., Kemler, M., Jami, F., Nagel, J. H., Postma-Smidt, A., Naidoo, S., … Slippers, B. (2017). *Botryosphaeria dothidea*: A latent pathogen of global importance to woody plant health. *Molecular Plant Pathology, 18*, 477–488. https://doi.org/10.1111/mpp.12495

Martino, I., Lione, G., Garbelotto, M., Gonthier, P., & Guarnaccia, V. (2024). Modeling the effect of temperature on the severity of blueberry stem blight and dieback with a focus on *Neofusicoccum parvum* and cultivar susceptibility. *Horticulturae*, *10*(4), 4. https://doi.org/10.3390/horticulturae10040363

Massonnet, M., Figueroa-Balderas, R., Galarneau, E. R. A., Miki, S., Lawrence, D. P., Sun, Q., … Cantu, D. (2017). *Neofusicoccum parvum* colonization of the grapevine woody stem triggers asynchronous host responses at the site of infection and in the leaves. *Frontiers in Plant Science, 8*, 1117. https://doi.org/10.3389/fpls.2017.01117

McCook, S., & Vandermeer, J. (2015). The big rust and the Red Queen: Long-term perspectives on coffee rust research. *Phytopathology, 105*(9), 1164–1173. https://doi.org/10.1094/PHYTO-04-15-0085-RVW

Meng, Y. G., Xiao, Y. Z., Zhu, S., Xu, L. S., & Huang, L. L. (2024). VmSpm1: A secretory protein from Valsa mali that targets apple's abscisic acid receptor MdPYL4 to suppress jasmonic acid signaling and enhance infection. *New Phytologist, 244*(6), 2489–2504. https://doi.org/10.1111/nph.20194

Michalecka, M., Poniatowska, A., & Kałużna, M. (2023). Molecular identification and diversity of *Diaporthe* species associated with shoot dieback on highbush blueberry plants in Poland. *Journal of Phytopathology, 171*(1), e13185. https://doi.org/10.1111/jph.13185

Milholland, R. D. (1983). Blueberry fruit rot caused by *Phomopsis vaccinii*. *Plant Disease, 67*(3), 325–326. https://doi.org/10.1094/PD-67-325

Miller, M. A., Pfeiffer, W., & Schwartz, T. (2010). Creating the CIPRES Science Gateway for inference of large phylogenetic trees. In *Proceedings of the 2010 Gateway Computing Environments Workshop (GCE)* (pp. 1–8). IEEE. https://doi.org/10.1109/GCE.2010.5676129

Mondello, V., Songy, A., Battiston, E., Pinto, C., Coppin, C., Trotel-Aziz, P., … Fontaine, F. (2018). Grapevine trunk diseases: A review of fifteen years of trials for their control with chemicals and biocontrol agents. *Plant Disease, 102*(7), 1189–1217. https://doi.org/10.1094/PDIS-08-17-1181-FE

Mostert, L., Groenewald, J. Z., Summerbell, R. C., Gams, W., & Crous, P. W. (2006). Taxonomy and pathology of *Togninia* (Diaporthales) and its *Phaeoacremonium* anamorphs. *Studies in Mycology, 54*, 1–113. https://doi.org/10.3114/sim.54.1.1

Moya-Elizondo, E. A., Doussoulin, H., San Martin, J., Ruiz, B., & Del Valle, P. (2019). First report of *Fusarium oxysporum* causing Fusarium wilt on blueberry (*Vaccinium corymbosum*) in Chile. *Plant Disease, 103*(10), 2669–2669. https://doi.org/10.1094/PDIS-02-19-0275-PDN

Mukhtar, I., Ashraf, H. J., Khokhar, I., Huang, Q. H., Chen, B. Z., & Xie, B. G. (2021). First report of Cladosporium blossom blight caused by *Cladosporium cladosporioides* on *Calliandra haematocephala* in China. *Plant Disease, 105*(5), 1570. https://doi.org/10.1094/PDIS-07-20-1504-PDN

Munkvold, G. P., & Marois, J. J. (1993). Efficacy of natural epiphytes and colonizers of grapevine pruning wounds for biological control of Eutypa dieback. *Phytopathology, 83*(6), 624–629. https://doi.org/10.1094/Phyto-83-624

Myllys, L., Stenroos, S., & Thell, A. (2002). New genes for phylogenetic studies of lichenized fungi: Glyceraldehyde-3-phosphate dehydrogenase and beta-tubulin genes. *The Lichenologist, 34*(3), 237–246. https://doi.org/10.1006/lich.2002.0390

Nelson, P., Toussoun, T., & Marasas, W. F. O. (1983). *Fusarium species: An illustrated manual for identification*. Pennsylvania State University Press.

Neugebauer, K. A., Mattupalli, C., Hu, M., Oliver, J. E., VanderWeide, J., Lu, Y., … Miles, T. D. (2024). Managing fruit rot diseases of *Vaccinium corymbosum*. *Frontiers in Plant Science, 15*, 1428769. https://doi.org/10.3389/fpls.2024.1428769

Norphanphoun, C., Gentekaki, E., Hongsanan, S., Jayawardena, R., Senanayake, I., Manawasinghe, I., … Hyde, K. D. (2022). *Diaporthe*: Formalizing the species-group concept. *Mycosphere, 13*(1), 752–819. https://doi.org/10.5943/mycosphere/13/1/9

O'Donnell, K., & Cigelnik, E. (1997). Two divergent intragenomic rDNA ITS2 types within a monophyletic lineage of the fungus *Fusarium* are nonorthologous. *Molecular Phylogenetics and Evolution, 7*(1), 103–116. https://doi.org/10.1006/mpev.1996.0376

O'Donnell, K., Kistler, H. C., Cigelnik, E., & Ploetz, R. C. (1998). Multiple evolutionary origins of the fungus causing Panama disease of banana: Concordant evidence from nuclear and mitochondrial gene genealogies. *Proceedings of the National Academy of Sciences, 95*(5), 2044–2049. https://doi.org/10.1073/pnas.95.5.2044

O'Donnell, K., Nirenberg, H. I., Aoki, T., & Cigelnik, E. (2000). A multigene phylogeny of the *Gibberella fujikuroi* species complex: Detection of additional phylogenetically distinct species. *Mycoscience, 41*(1), 61–78. https://doi.org/10.1007/BF02464387

Ojiambo, P. S., Scherm, H., Brannen, P. M. (2007). Temporal dynamics of Septoria leaf spot of blueberry and its relationship to defoliation and yield. *Plant Health Progress, 8*, PHP-2007-0726-05-RS. https://doi.org/10.1094/PHP-2007-0726-05-RS

Oliver, R. (2024). *Agrios' plant pathology* (6th ed.). Academic Press.

Oo, M. M., & Oh, S. K. (2017). Identification and characterization of new record of grape ripe rot disease caused by *Colletotrichum viniferum* in Korea. *Mycobiology, 45*, 421–425. https://doi.org/10.5941/MYCO.2017.45.4.421

Pan, M., Zhu, H. Y., Bezerra, J. D. P., Bonthond, G., Tian, C. M. & Fan, X. L. (2019). Botryosphaerialean fungi causing canker and dieback of tree hosts from Mount Yudu in China. *Mycological Progress, 18*, 1341–1361. https://doi.org/10.1007/s11557-019-01532-z

Paolinelli-Alfonso, M., Villalobos-Escobedo, J. M., Rolshausen, P., Herrera-Estrella, A., Galindo-Sánchez, C., López-Hernández, J. F. & Hernandez-Martinez, R. (2016). Global transcriptional analysis suggests *Lasiodiplodia theobromae* pathogenicity factors involved in modulation of grapevine defensive response. *BMC Genomics, 17*, 615. https://doi.org/10.1186/s12864-016-2952-3

Patanita, M., Albuquerque, A., Campos, M. D., Materatski, P., Varanda, C. M. R., Ribeiro, J. A., Félix, M. d. R. (2022). Metagenomic assessment unravels fungal microbiota associated to grapevine trunk diseases. *Horticulturae, 8*(4), 288. https://doi.org/10.3390/horticulturae8040288

Peng, C., Crous, P. W., Jiang, N., Fan, X. L., Liang, Y. M., & Tian, C. M. (2022). Diversity of Sporocadaceae (pestalotioid fungi) from *Rosa* in China. *Persoonia - Molecular Phylogeny and Evolution of Fungi, 49*(1), 201–260. https://doi.org/10.3767/persoonia.2022.49.07

Peng, L. J., Sun, T., Yang, Y. L., Cai, L., Hyde, K. D., Bahkali, A. H., & Liu, Z. Y. (2013). *Colletotrichum* species on grape in Guizhou and Yunnan provinces, China. *Mycoscience, 54*, 29–41. https://doi.org/10.1016/j.myc.2012.07.006

Pereira, C. M., Sarmiento, S. S., Colmán, A. A., Belachew-Bekele, K., Evans, H. C., & Barreto, R. W. (2024). Mycodiversity in a micro-habitat: Twelve *Cladosporium* species, including four new taxa, isolated from uredinia of coffee leaf rust, *Hemileia vastatrix*. *Fungal Systematics and Evolution, 14*, 9–33. https://doi.org/10.3114/fuse.2024.14.02

Pérez, B. A., Berretta, M. F., Carrión, E., & Wright, E. R. (2011). First report of root rot caused by *Fusarium proliferatum* on blueberry in Argentina. *Plant Disease, 95*(11), 1478. https://doi.org/10.1094/PDIS-04-11-0307

Pérez, B. A., Murillo, F., Divo de Sesar, M., & Wright, E. R. (2007). Occurrence of *Fusarium solani* on blueberry in Argentina. *Plant Disease, 91*(8), 1053. https://doi.org/10.1094/PDIS-91-8-1053C

Pérez-Vicente, L. F. (2004). *Fusarium wilt (Panama disease) of bananas: An updating review of the current knowledge on the disease and its causal agent*. *Memorias de la XVI Reunión Internacional ACORBAT*, Havana, Cuba, January 2004, 1–14.

Pertot, I., Prodorutti, D., Colombini, A., & Pasini, L. (2016). *Trichoderma atroviride* SC1 prevents *Phaeomoniella chlamydospora* and *Phaeoacremonium aleophilum* infection of grapevine plants during the grafting process in nurseries. *BioControl, 61*, 257–267. https://doi.org/10.1007/s10526-016-9723-6

Pétriacq, P., López, A., & Luna, E. (2018). Fruit decay to diseases: Can induced resistance and priming help? *Plants, 7*(4), 77. https://doi.org/10.3390/plants7040077

Petrović, K., Skaltsas, D., Castlebury, L. A., Kontz, B., Allen, T. W., Chilvers, M. I., … Mathew, F. M. (2021). *Diaporthe* seed decay of soybean [*Glycine max* (L.) Merr.] is endemic in the United States, but new fungi are involved. *Plant Disease, 105*(6), 1621–1629. https://doi.org/10.1094/PDIS-03-20-0604-RE

Phillips, A. J. L., Alves, A., Abdollahzadeh, J., Slippers, B., Wingfield, M. J., Groenewald, J. Z., & Crous, P. W. (2013). The Botryosphaeriaceae: Genera and species known from culture. *Studies in Mycology, 76*, 51–167. https://doi.org/10.3114/sim0021

Phillips, A. J. L., Oudemans, P. V., & Correia, A. (2006). Characterisation and epitypification of *Botryosphaeria corticis*, the cause of blueberry cane canker. *Fungal Diversity, 21*, 141–155.

Phillips, D., Williamson, J., Lyrene, P., & Munoz, P. (2022). Southern highbush blueberry cultivars from the University of Florida. *EDIS, 2022*(5), 5. https://doi.org/10.32473/edis-hs1245-2022

Pintos, C., Redondo, V., Costas, D., Aguín, O., & Mansilla, P. (2018). Fungi associated with grapevine trunk diseases in nursery-produced *Vitis vinifera* plants. *Phytopathologia Mediterranea, 57*, 407–424. 10.14601/Phytopathol_Mediterr-22964

Polashock, J. J., Caruso, F. L., Averill, A. L., & Schilder, A. C. (2017). *Compendium of blueberry, cranberry, and lingonberry diseases and pests* (2nd ed.). APS Press.

Prematunga, C. J., You L. Q., Gomdola, D. Balasuriya, A., Yang Y. H., Jayawardena, R. S., & Luo, M. (2022). An addition to pestalotioid fungi in China: *Neopestalotiopsis fragariae* sp. nov. causing leaf spots on *Fragaria × ananassa*. *Asian Journal of Mycology, 5*(1), 188–197. https://doi.org/10.5943/ajom/5/2/10

Prihastuti, H., Cai, L., Chen, H., McKenzie, E. H. C., & Hyde, K. D. (2009). Characterization of *Colletotrichum* species associated with coffee berries in northern Thailand. *Fungal Diversity, 39*(1), 89–109.

Prodorutti, D., Vanblaere, T., Gobbin, D., Pellegrini, A., Gessler, C., & Pertot, I. (2009). Genetic diversity of *Armillaria* spp. infecting highbush blueberry in Northern Italy (Trentino region). *Phytopathology, 99*(6), 651–658. https://doi.org/10.1094/PHYTO-99-6-0651

Pszczółkowska, A., Okorski, A., Paukszto, Ł., & Jastrzębski, J. (2016). First report of anthracnose disease caused by *Colletotrichum fioriniae* on blueberry in western Poland. *Plant Disease, 100*(10), 2167. https://doi.org/10.1094/PDIS-04-16-0425-PDN

Qiu, R., Li, J., Zheng, W. M., Su, X. H., Xing, G. Z., Li, S. J., … Ping, W. L. (2021). First report of root rot of tobacco caused by *Fusarium brachygibbosum* in China. *Plant Disease, 105*, 4170. https://doi.org/10.1094/PDIS-01-21-0077-PDN

Rajan, R., Govindu, C., & Sravani, G. (2021). Advanced and modern fruit production techniques: A review. *Pharmaceutica Analytica Acta*, *10*(7), 938–943.

Ram, D., Devi, T. P., Koti, P. S., Jeevan, B., Kamil, D., Vanapalli, C. S., … Kashyap, A. S. (2024). Exploring the taxonomic classification of *Curvularia* genera: Enhancing understanding of phytopathogenic species in Poaceae through morphological and molecular approaches. *Journal of Plant Pathology, 106*, 539–551. https://doi.org/10.1007/s42161-023-01560-5

Rambaut, A. (2012). *FigTree* (Version 1.4.0). Available online: http://tree.bio.ed.ac.uk/software/Figtree/ (accessed on 1 January 2023).

Rayner, R. W. (1970). *A mycological colour chart*. British Mycological Society.

Razaghi, P., Raza, M., Han, S. L., Ma, Z. Y., Cai, L., Zhao, P., … Liu, F. (2024). Sporocadaceae revisited. *Studies in Mycology, 109*(3), 109030. https://doi.org/10.3114/sim.2024.109.03

Rebollar-Alviter, A., Minnis, A. M., Dixon, L. J., Castlebury, L. A., Ramírez-Mendoza, M. R., Silva-Rojas, H. V., & Valdovinos-Ponce, G. (2011). First report of leaf rust of blueberry caused by *Thekopsora minima* in Mexico. *Plant Disease, 95*(6), 772. https://doi.org/10.1094/PDIS-12-10-0885

Rebollar-Alviter, A., Silva-Rojas, H. V., Fuentes-Aragón, D., Acosta-González, U., Martínez-Ruiz, M., & Parra-Robles, B. E. (2020). An emerging strawberry fungal disease associated with root rot, crown rot and leaf spot caused by *Neopestalotiopsis rosae* in Mexico. *Plant Disease, 104*(8), 2054–2059. https://doi.org/10.1094/PDIS-11-19-2493-SC

Redkar, A., Sabale, M., Zuccaro, A., & Di Pietro, A. (2022). Determinants of endophytic and pathogenic lifestyle in root colonizing fungi. *Current Opinion in Plant Biology, 67*, 102226. https://doi.org/10.1016/j.pbi.2022.102226

Reeb, V., Lutzoni, F., & Roux, C. (2004). Contribution of RPB2 to multilocus phylogenetic studies of the euascomycetes (Pezizomycotina, Fungi) with special emphasis on the lichen-forming Acarosporaceae and evolution of polyspory. *Molecular Phylogenetics and Evolution, 32*(3), 1036–1060. https://doi.org/10.1016/j.ympev.2004.04.012

Rehner, S. A., & Buckley, E. (2005). A *Beauveria* phylogeny inferred from nuclear ITS and EF1-α sequences: Evidence for cryptic diversification and links to *Cordyceps* teleomorphs. *Mycologia, 97*(1), 84–98. https://doi.org/10.1080/15572536.2006.11832842

Rehner, S. A., & Samuels, G. J. (1994). Taxonomy and phylogeny of *Gliocladium* analysed from nuclear large subunit ribosomal DNA sequences. *Mycological Research, 98*(6), 625–634. https://doi.org/10.1016/S0953-7562(09)80409-7

Reis, P., Pierron, R., Larignon, P., Lecomte, P., Abou-Mansour, E., Farine, S., … Fontaine, F. (2019). Vitis methods to understand and develop strategies for diagnosis and sustainable control of grapevine trunk diseases. *Phytopathology, 109*, 916–931. https://doi.org/10.1094/PHYTO-09-18-0349-RVW

Rezgui, A., Vallance, J., Ben Ghnaya-Chakroun, A., Bruez, E., Dridi, M., Djidjou Demasse, … Sadfi-Zouaoui, N. (2018). Study of *Lasiodiplodia pseudotheobromae*, *Neofusicoccum parvum* and *Schizophyllum commune*, three pathogenic fungi associated with the grapevine trunk diseases in the North of Tunisia. *European Journal of Plant Pathology, 152*, 127–142. https://doi.org/10.1007/s10658-018-1458-z

Rivera, S. A., Zoffoli, J. P., & Latorre, B. A. (2013). Determination of optimal sulfur dioxide time and concentration product for postharvest control of gray mold of blueberry fruit. *Postharvest Biology and Technology, 83*, 40–46. https://doi.org/10.1016/j.postharvbio.2013.03.007

Rivera, S. A., Zoffoli, J. P., & Latorre, B. A. (2013). Infection risk and critical period for the postharvest control of gray mold (*Botrytis cinerea*) on blueberry in Chile. *Plant Disease, 97*(8), 1069–1074. https://doi.org/10.1094/PDIS-12-12-1112-RE

Rodríguez, M. D. C. H., Evans, H. C., de Abreu, L. M., de Macedo, D. M., Ndacnou, M. K., Bekele, K. B., & Barreto, R. W. (2021). New species and records of *Trichoderma* isolated as mycoparasites and endophytes from cultivated and wild coffee in Africa. *Scientific Reports, 11*, 5671. https://doi.org/10.1038/s41598-021-84111-1

Rodríguez-Gálvez, E., Hilário, S., Lopes, A., & Alves, A. (2020). Diversity and pathogenicity of *Lasiodiplodia* and *Neopestalotiopsis* species associated with stem blight and dieback of blueberry plants in Peru. *European Journal of Plant Pathology, 157*, 203–219. https://doi.org/10.1007/s10658-020-01983-1

Roloff, I., Scherm, H., & van Iersel, M. W. (2004). Photosynthesis of blueberry leaves as affected by Septoria leaf spot and abiotic leaf damage. *Plant Disease, 88*(4), 397–401. https://doi.org/10.1094/PDIS.2004.88.4.397

Romão-Dumaresq, A. S., Dourado, M. N., Fávaro, L. C. de L., Mendes, R., Ferreira, A., & Araújo, W. L. (2016). Diversity of cultivated fungi associated with conventional and transgenic sugarcane and the interaction between endophytic *Trichoderma virens* and the host plant. *PLOS ONE, 11*, e0158974. https://doi.org/10.1371/journal.pone.0158974

Ronquist, F., & Huelsenbeck, J. P. (2003). MrBayes 3: Bayesian phylogenetic inference under mixed models. *Bioinformatics, 19*(12), 1572–1574. https://doi.org/10.1093/bioinformatics/btg180

Rossman, A. Y., Adams, G. C., Cannon, P. F., Castlebury, L. A., Crous, P. W., Gryzenhout, M., … Walker, D. M. (2015). Recommendations of generic names in Diaporthales competing for protection or use. *IMA Fungus, 6*(1), 41–51. https://doi.org/10.5598/imafungus.2015.06.01.09

Rossman, A. Y., Seifert, K. A., Samuels, G. J., Minnis, A. M., Schroers, H. J., Lombard, L., … Chaverri, P. (2013). Genera in *Bionectriaceae*, *Hypocreaceae*, and *Nectriaceae* (Hypocreales) proposed for acceptance or rejection. *IMA Fungus, 4*(1), 41–51. https://doi.org/10.5598/imafungus.2013.04.01.05

Ru, S., Ding, S., Oliver, J. E., & Amodu, A. (2023). A review of *Botryosphaeria* stem blight disease of blueberry from the perspective of plant breeding. *Agriculture, 13*(1), 100. https://doi.org/10.3390/agriculture13010100

Ruan, R., Huang, K., Luo, H., Zhang, C., Xi, D., Pei, J., & Liu, H. (2023). Occurrence and characterization of *Sclerotinia sclerotiorum* causing fruit rot on sweet cherry in southern China. *Plants, 12*(24), 4165. https://doi.org/10.3390/plants12244165

Rui, L., Kong, W. L., Ye, J. R., & Wu, X. Q. (2025). First report of *Pestalotiopsis clavata*, *P. chamaeropis* and *P. lushanensis* causing shoot blight on *Cedrus deodara* in China. *Crop Protection, 190*, 107119. https://doi.org/10.1016/j.cropro.2025.107119

Saccardo, P. A. (1886). *Sylloge fungorum omnium hucusque cognitorum* (Vol. 4). Edwards Brothers.

Saito, S., Margosan, D., Michailides, T. J., & Xiao, C. L. (2016). *Botrytis californica*, a new cryptic species in the *B. cinerea* species complex causing gray mold in blueberries and table grapes. *Mycologia, 108*(2), 330–343. https://doi.org/10.3852/15-165

Saito, S., Michailides, T. J., & Xiao, C. L. (2014). First report of *Botrytis pseudocinerea* causing gray mold on blueberry in North America. *Plant Disease, 98*(12), 1743. https://doi.org/10.1094/PDIS-06-14-0573-PDN

Saito, S., Michailides, T. J., & Xiao, C. L. (2016). Fungicide resistance profiling in *Botrytis cinerea* populations from blueberry in California and Washington and their impact on control of gray mold. *Plant Disease, 100*(10), 2087–2093. https://doi.org/10.1094/PDIS-02-16-0229-RE

Saleh, O. I. (1997). Wilt, root rot and seed diseases of groundnut in El-Minia Governorate, Egypt. *Egyptian Journal of Phytopathology, 25*(1–2), 1–18.

Sammonds, J., Billones, R., Ridgway, H. J., Walter, M., & Jaspers, M. V. (2009). Survey of blueberry farms for *Botryosphaeria* dieback and crown rot pathogens. *New Zealand Plant Protection, 62*, 238–242. https://doi.org/10.30843/nzpp.2009.62.4826

Sandoval-Denis, M., Gené, J., Sutton, D. A., Wiederhold, N. P., Cano-Lira, J. F., & Guarro, J. (2016). New species of *Cladosporium* associated with human and animal infections. *Persoonia - Molecular Phylogeny and Evolution of Fungi, 36*(1), 281–298. https://doi.org/10.3767/003158516X691951

Sandoval-Denis, M., Guarnaccia, V., Polizzi, G., & Crous, P. W. (2018). Symptomatic citrus trees reveal a new pathogenic lineage in *Fusarium* and two new *Neocosmospora* species. *Persoonia - Molecular Phylogeny and Evolution of Fungi, 40*, 1–25. https://doi.org/10.3767/persoonia.2018.40.01

Sandoval-Denis, M., Lombard, L., & Crous, P. W. (2019). Back to the roots: A reappraisal of *Neocosmospora*. *Persoonia - Molecular Phylogeny and Evolution of Fungi, 43*, 90–185. https://doi.org/10.3767/persoonia.2019.43.04

Santiago, M. F., Santos, A. M. G., Inácio, C. P., Lira Neto, A. C., Assis, T. C., Neves, R. P., … Laranjeira, D. (2018). First report of *Fusarium lacertarum* causing cladode rot in *Nopalea cochenillifera* in Brazil. *Journal of Plant Pathology, 100*, 611. https://doi.org/10.1007/s42161-018-0120-0

Santos, G. S., Mafia, R. G., Aguiar, A. M., Zarpelon, T. G., Damacena, M. B., Barros, A. F., & Ferreira, M. A. (2020). Stem rot of eucalyptus cuttings caused by *Neopestalotiopsis* spp. in Brazil. *Journal of Phytopathology, 168*(6), 311–321. https://doi.org/10.1111/jph.12894

Santos, J., Hilário, S., Pinto, G., & Alves, A. (2022). Diversity and pathogenicity of pestalotioid fungi associated with blueberry plants in Portugal, with description of three novel species of *Neopestalotiopsis*. *European Journal of Plant Pathology, 162*(3), 539–555. https://doi.org/10.1007/s10658-021-02419-0

Scarlett, K. A., Shuttleworth, L. A., Collins, D., Rothwell, C. T., Guest, D. I., & Daniel, R. (2019). Botryosphaeriales associated with stem blight and dieback of blueberry (*Vaccinium* spp.) in New South Wales and Western Australia. *Australasian Plant Pathology, 48*(1), 45–57. https://doi.org/10.1007/s13313-018-0584-6

Schroers, H. J., O'Donnell, K., Lamprecht, S. C., Kammeyer, P. L., Johnson, S., Sutton, D. A., … Summerbell, R. C. (2009). Taxonomy and phylogeny of the *Fusarium dimerum* species group. *Mycologia*, *101*, 44–70. https://doi.org/10.3852/08-002

Schubert, K., Groenewald, J. Z., Braun, U., Dijksterhuis, J., Starink, M., Hill, C. F., … Crous, P. W. (2007). Biodiversity in the *Cladosporium herbarum* complex (Davidiellaceae, Capnodiales), with standardisation of methods for *Cladosporium* taxonomy and diagnostics. *Studies in Mycology*, *58*, 105–156. https://doi.org/10.3114/sim.2007.58.05

Schuster, A., & Schmoll, M. (2010). Biology and biotechnology of *Trichoderma*. *Applied Microbiology and Biotechnology*, *87*, 787–799. https://doi.org/10.1007/s00253-010-2632-1

Seifert, K. A., Aoki, T., Baayen, R. P., Brayford, D., Burgess, L. W., Chulze, S., … Waalwijk, C. (2003). The name *Fusarium moniliforme* should no longer be used. *Mycological Research, 107*(6), 643–644. https://doi.org/10.1017/S095375620323820X

Senanayake, I. C., Crous, P. W., Groenewald, J. Z., Maharachchikumbura, S. S. N., Jeewon, R., Phillips, A. J. L., … Hyde, K.D. (2017). Families of Diaporthales based on morphological and phylogenetic evidence. *Studies in Mycology*, *86*, 217–296. https://doi.org/10.1016/j.simyco.2017.07.003

Senanayake, I. C., Rathnayaka, A. R., Marasinghe, D. S., Calabon, M. S., Gentekaki, E., Lee, H. B., … Xiang, M. M. (2020). Morphological approaches in studying fungi: Collection, examination, isolation, sporulation and preservation. *Mycosphere, 11*(1), 2678–2754. https://doi.org/10.5943/mycosphere/11/1/20

Sessa, L., Abreo, E., & Lupo, S. (2018). Diversity of fungal latent pathogens and true endophytes associated with fruit trees in Uruguay. *Journal of Phytopathology, 166*(9), 633–647. https://doi.org/10.1111/jph.12726

Sever, Z., Ivić, D., Kos, T., & Miličević, T. (2012). Identification of *Fusarium* species isolated from stored apple fruit in Croatia. *Archives of Industrial Hygiene and Toxicology*, *63*, 463–470. https://doi.org/10.2478/10004-1254-63-2012-2227

Shan, L. Y., Cui, W. Y., Zhang, D. D., Zhang, J., Ma, N. N., Bao, Y. M., … Guo, W. (2017). First report of *Fusarium brachygibbosum* causing maize stalk rot in China. *Plant Disease*, *101*, 837. https://doi.org/10.1094/PDIS-10-16-1465-PDN

Shao, Y., & Li, D. (1995). Investigation and research on cherry brown spot disease. *Shandong Forestry Science and Technology*, 3, 37–38.

Sharon, A., & Shlezinger, N. (2013). Fungi infecting plants and animals: Killers, non-killers, and cell death. *PLoS Pathogens*, *9*(8), e1003517. https://doi.org/10.1371/journal.ppat.1003517

Shen, D. X., Song, Z. W., Lu, Y. M., & Fan, B. (2020). First report of *Fusarium falciforme* (FSSC 3+4) causing root rot in *Weigela florida* in China. *Plant Disease*, *104*, 981. https://doi.org/10.1094/PDIS-03-19-0521-PDN

Shi, L. B., Li, Y., Fei, N. Y., Fu, J. F., & Yan, X. R. (2017). First report of *Neopestalotiopsis chrysea* causing twig dieback of rabbiteye blueberry (*Vaccinium ashei*) in China. *Plant Disease, 101*(3), 506. https://doi.org/10.1094/PDIS-09-16-1282-PDN

Shu, J., Yu, Z., Sun, W. X., Zhao, J., Li, Q. L., Tang, L. H., … Luo, S. M. (2020). Identification and characterization of pestalotioid fungi causing leaf spots on mango in southern China. *Plant Disease*, *104*(4), 1207–1213. https://doi.org/10.1094/PDIS-03-19-0438-RE

Silva, A. C., Diogo, E., Henriques, J., Ramos, A. P., Sandoval-Denis, M., Crous, P. W., & Bragança, H. (2020). *Pestalotiopsis pini* sp. nov., an emerging pathogen on stone pine (*Pinus pinea* L.). *Forests, 11*(8), 8. https://doi.org/10.3390/f11080805

Slippers, B., Crous, P. W., Denman, S., Coutinho, T. A., Wingfield, B. D., & Wingfield, M. J. (2004). Combined multiple gene genealogies and phenotypic characters differentiate several species previously identified as *Botryosphaeria dothidea*. *Mycologia, 96*(1), 83–101. https://doi.org/10.1080/15572536.2005.11833000

Solarte, F., Muñoz, C. G., Maharachchikumbura, S. S. N., & Álvarez, E. (2018). Diversity of *Neopestalotiopsis* and *Pestalotiopsis* spp., causal agents of guava scab in Colombia. *Plant Disease*, 102(1), 49–59. https://doi.org/10.1094/PDIS-01-17-0068-RE

Song, Y. F., Zhang, C., Idrees, M., Yi, X. G., Wang, X. R., & Li, M. (2024). Molecular phylogenetics and biogeography reveal the origin of cherries (*Prunus* subg. *Cerasus*, Rosaceae). *Botanical Journal of the Linnean Society, 204*(4), 304–315. https://doi.org/10.1093/botlinnean/boad060

Song, Y., Geng, K., Hyde, K. D., Zhao, W. S., Wei, J. G., Kang, J. C., & Wang, Y. (2013). Two new species of *Pestalotiopsis* from Southern China. *Phytotaxa, 126*(1), 22–32. https://doi.org/10.11646/phytotaxa.126.1.2

Song, Y., Hu, S., de Hoog, S., Liu, X., Meng, X., Xue, R., … Gao, S. (2023). Medical *Fusarium*: Novel species or uncertain identifications? *Mycosphere, 14*(1), 2263–2283. https://doi.org/10.5943/mycosphere/14/1/27

Spetik, M., Cechova, J., & Eichmeier, A. (2023). First report of *Neofusicoccum parvum* causing stem blight and dieback of highbush blueberry in the Czech Republic. *Plant Disease, 107*(12), 4022. https://doi.org/10.1094/PDIS-03-23-0595-PDN

Srinidhi, V. V., Sahay, A., & Deeba, K. (2021). Plant pathology disease detection in apple leaves using deep convolutional neural networks: Apple leaves disease detection using EfficientNet and DenseNet. *In 2021 5th International Conference on Computing Methodologies and Communication (ICCMC)* (pp. 1119–1127). IEEE.

Staats, M., van Baarlen, P., & van Kan, J. A. L. (2004). Molecular phylogeny of the plant pathogenic genus *Botrytis* and the evolution of host specificity. *Molecular Biology and Evolution, 22*(2), 333–346. https://doi.org/10.1093/molbev/msi020

Stamatakis, A. (2014). RAxML version 8: A tool for phylogenetic analysis and post-analysis of large phylogenies. *Bioinformatics, 30*(9), 1312–1313. https://doi.org/10.1093/bioinformatics/btu033

Stamatakis, A., Hoover, P., & Rougemont, J. (2008). A rapid bootstrap algorithm for the RAxML web servers. *Systematic Biology, 57*(5), 758–771. https://doi.org/10.1080/10635150802429642

Steel, C. C., Blackman, J. W., & Schmidtke, L. M. (2013). Grapevine bunch rots: Impacts on wine composition, quality, and potential procedures for the removal of wine faults. *Journal of Agricultural and Food Chemistry, 61*(22), 5189–5206. https://doi.org/10.1021/jf400641r

Su, Y. Y., Qi, Y. L., & Cai, L. (2012). Induction of sporulation in plant pathogenic fungi. *Mycology, 3*(3), 195–200. https://doi.org/10.1080/21501203.2012.719042

Sun, L. P., Li, Y. G., Li, X. T., Ruan, X. Y., Zhao, Y. Y., Wen, R. D., … Gao, W. J. (2024). Cytological and ultrastructural investigation of pathogen infection pathway and host responses in asparagus stem infected by *Phomopsis asparagi. Phytopathology Research, 6*(1), 32. https://doi.org/10.1186/s42483-024-00252-x

Sun, Q., Harishchandra, D., Jia, J. Y., Zuo, Q., Zhang, G. Z., Wang, Q., … Li, X. H. (2021). Role of *Neopestalotiopsis rosae* in causing root rot of strawberry in Beijing, China. *Crop Protection, 147*, Article 105710. https://doi.org/10.1016/j.cropro.2021.105710

Sun, Y. R., Jayawardena, R. S., Sun, J. E., & Wang, Y. (2023). Pestalotioid species associated with medicinal plants in Southwest China and Thailand. *Microbiology Spectrum, 11*(1), e03987-22. https://doi.org/10.1128/spectrum.03987-22

Sun, Y., Han, W., Ma, X., & Miu, J. (2017). Identification and ITS sequence analysis of pathogen of cherry brown leaf spot in Shandong. *Northern Horticulture, 21*, 100–104.

Sun, Y., Han, W., Ma, X. M., Wang, J. F., Wei, G. Q., & Miu, J. (2022). Assessment of cherry cultivars for resistance to leaf spot caused by *Passalora circumscissa. HortScience, 57*(5), 624–628. https://doi.org/10.21273/HORTSCI16040-21

Sun, Y., Liu, B., Zhang, W., & Wang, Y. (2014). Advances on leaf brown spot disease of sweet cherry. *Journal of Fruit Science, 31*(2), 329–333.

Szabó, M., Csikász-Krizsics, A., Dula, T., Farkas, E., Roznik, D., Kozma, P., & Deák, T. (2023). Black rot of grapes (*Guignardia bidwellii*)—A comprehensive overview. *Horticulturae, 9*(2), 130. https://doi.org/10.3390/horticulturae9020130

Sztejnberg, A. (1986). Etiology and control of cherry leaf spot disease in Israel caused by *Cercospora circumscissa*. *Plant Disease, 70*(4), 349. https://doi.org/10.1094/PD-70-349

Tai, F. L. (Ed.). (1979). *Sylloge fungorum sinicorum*. Academia Sinica, Institute of Microbiology.

Talhinhas, P., & Baroncelli, R. (2021). *Colletotrichum* species and complexes: Geographic distribution, host range and conservation status. *Fungal Diversity, 110*, 109–198. https://doi.org/10.1007/s13225-021-00491-9

Tan, G. Y., Yuan, Z. L., Yang, Z. L., & Zhang, S. (2012). First report of leaf spot caused by *Alternaria longipes* on *Atractylodes macrocephala* in China. *Plant Disease*, *96*, 588. https://doi.org/10.1094/PDIS-11-11-0967

Tan, H. Y., Wu, L. N., Zhang, W., Chen, P. Z., Zhang, H. L., Wang, Y. Y., . . . Zhou, Y. Y. (2022). Identification of *Dactylonectria novozelandica* causing black foot disease of grapevine in China. *Acta Phytopathologica Sinica, 52*(3), 383–392.

Tan, Q., Schnabel, G., Chaisiri, C., Yin, L. F., Yin, W. X., & Luo, C. X. (2022). *Colletotrichum* species associated with peaches in China. *Journal of Fungi, 8*(3), 313. https://doi.org/10.3390/jof8030313

Tang, J., Lai, L. X., Du, Y. L., & Yang, Q. (2021). First report of *Neopestalotiopsis protearum* causing seed rot on *Camellia oleifera* in China. *Plant Disease, 105*(12), 4152. https://doi.org/10.1094/PDIS-12-20-2717-PDN

Tang, Z. Y., Lou, J., He, L. Q., Wang, Q. D., Chen, L. H., Zhong, X. T., … Wang, Z. Q. (2022). First report of *Colletotrichum fructicola* causing anthracnose on cherry (*Prunus avium*) in China. *Plant Disease, 106*(1), 317. https://doi.org/10.1094/PDIS-03-21-0544-PDN

Tao, R., Lin, L., Zhang, H. Y., Liu, Y. C., Duan, X. L., Li, H. Y., … Huang, M. (2024). First report of mango stem-end rot caused by *Pestalotiopsis kenyana* in Yunnan Province, China. *Plant Disease, 108*(10), 3190. https://doi.org/10.1094/PDIS-12-23-2766-PDN

Tao, W. C., Zhang, W., Yan, J. Y., Hyde, K. D., McKenzie, E. H. C., Li, X. H., & Wang, Y. (2014). A new *Alternaria* species from grapevine in China. *Mycological Progress*, *13*, 1119–1125. https://doi.org/10.1007/s11557-014-0999-6

Templeton, M. D., Rikkerink, E. H. A., Solon, S. L., & Crowhurst, R. N. (1992). Cloning and molecular characterization of the glyceraldehyde-3-phosphate dehydrogenase-encoding gene and cDNA from the plant-pathogenic fungus *Glomerella cingulata*. *Gene, 122*(1), 225–230. https://doi.org/10.1016/0378-1119(92)90055-T

Tennakoon, K. M. S., Ridgway, H. J., Jaspers, M. V., & Jones, E. E. (2018). Botryosphaeriaceae species associated with blueberry dieback and sources of primary inoculum in propagation nurseries in New Zealand. *European Journal of Plant Pathology, 150*(2), 363–374. https://doi.org/10.1007/s10658-017-1283-9

Terral, J. F., Tabard, E., Bouby, L., Ivorra, S., Pastor, T., Figueiral, I., … This, P. (2010). Evolution and history of grapevine (*Vitis vinifera*) under domestication: New morphometric perspectives to understand seed domestication syndrome and reveal origins of ancient European cultivars. *Annals of Botany, 105*(3), 443–455. https://doi.org/10.1093/aob/mcp298

Thomidis, T., & Tsipouridis, C. (2006). First report of *Alternaria* leaf spot on cherry trees in Greece. *Plant Disease, 90*(5), 680. https://doi.org/10.1094/PD-90-0680C

Tibpromma, S., Karunarathna, S. C., Mortimer, P. E., Xu, J., Doilom, M., & Lumyong, S. (2020). *Bartalinia kevinhydei* (Ascomycota), a new leaf-spot causing fungus on teak (*Tectona grandis*) from Northern Thailand. *Phytotaxa, 474*(1), 27–39. https://doi.org/10.11646/phytotaxa.474.1.3

Trimboli, D. S., & Burgess, L. W. (1985). Fungi associated with basal stalk rot and root rot of dryland grain sorghum in New South Wales. *Plant Protection Quarterly, 1*(1), 3–9.

Tsushima, A., & Shirasu, K. (2022). Genomic resources of *Colletotrichum* fungi: Development and application. *Journal of General Plant Pathology, 88*(6), 349–357. https://doi.org/10.1007/s10327-022-01097-y

Tunali, B., Nicol, J. M., Hodson, D., Uçkun, Z., Büyük, O., Erdurmuş, D., … Bağci, S. A. (2008). Root and crown rot fungi associated with spring, facultative, and winter wheat in Turkey. *Plant Disease*, *92*, 1299–1306. https://doi.org/10.1094/PDIS-92-9-1299

Turner, R. S. (2005). After the famine: Plant pathology, *Phytophthora infestans*, and the late blight of potatoes, 1845–1960. *Historical Studies in the Physical and Biological Sciences, 35*(2), 341–370. https://doi.org/10.1525/hsps.2005.35.2.341

U.S. Department of Agriculture. (2023). *China: Blueberry annual voluntary 2023*. https://fas.usda.gov/data/china-blueberry-annual-voluntary-2023

Udayanga, D., Castlebury, L. A., Rossman, A. Y., Chukeatirote, E., & Hyde, K. D. (2014). Insights into the genus *Diaporthe*: Phylogenetic species delimitation in the *D. eres* species complex. *Fungal Diversity, 67*, 203–229. https://doi.org/10.1007/s13225-014-0297-2

Udayanga, D., Liu, X. Z., Crous, P. W., McKenzie, E. H. C., Chukeatirote, E., & Hyde, K. D. (2012). A multi-locus phylogenetic evaluation of *Diaporthe* (*Phomopsis*). *Fungal Diversity, 56*(1), 157–171. https://doi.org/10.1007/s13225-012-0190-9

Udayanga, D., Liu, X. Z., McKenzie, E. H. C., Chukeatirote, E., Bahkali, A. H. A., & Hyde, K. D. (2011). The genus *Phomopsis*: Biology, applications, species concepts and names of common phytopathogens. *Fungal Diversity, 50*(1), 189–225. https://doi.org/10.1007/s13225-011-0126-9

Underwood, W., & Misar, C. G. (2024). Multiple forms of resistance to the *Phomopsis* stem canker pathogens *Diaporthe helianthi* and *D. gulyae* in sunflower. *Plant Disease, 108*(6), 1740–1749. https://doi.org/10.1094/PDIS-03-23-0610-RE

Úrbez-Torres, J. R. (2011). The status of *Botryosphaeriaceae* species infecting grapevines. *Phytopathologia Mediterranea, 50*(4), 5–45. https://doi.org/10.14601/Phytopathol_Mediterr-9316

Úrbez-Torres, J. R., & Gubler, W. D. (2009). Pathogenicity of *Botryosphaeriaceae* species isolated from grapevine cankers in California. *Plant Disease, 93*, 584–592. https://doi.org/10.1094/PDIS-93-6-0584

Úrbez-Torres, J. R., Boulé, J., Haag, P., Hampson, C., & O'Gorman, D. T. (2016). First report of root and crown rot caused by *Fusarium oxysporum* on sweet cherry (*Prunus avium*) in British Columbia. *Plant Disease*, *100*, 855. https://doi.org/10.1094/PDIS-08-15-0932-PDN

Úrbez-Torres, J. R., Tomaselli, E., Pollard-Flamand, J., Boulé, J., Gerin, D., & Pollastro, S. (2020). Characterization of *Trichoderma* isolates from southern Italy, and their potential biocontrol activity against grapevine trunk disease fungi. *Phytopathologia Mediterranea, 59*(3), 425–439.

Uyemoto, J. K., Ogawa, J. M., & Jaffee, B. A. (2018). Diseases of sweet cherry and sour cherry. In *APSnet Education Center* (American Phytopathological Society). https://www.apsnet.org/edcenter/resources/commonnames/Pages/Cherry.aspx

Van Coller, G. J., Denman, S., Groenewald, J. Z., Lamprecht, S. C., Korsten, L., & Crous, P. W. (2005). Characterization and pathogenicity of *Cylindrocladiella* spp. associated with root and cutting rot symptoms of grapevines in nurseries. *Australasian Plant Pathology, 34*, 489–498. https://doi.org/10.1071/AP05058

Vega-Gutiérrez, T. A., López-Orona, C. A., López-Urquídez, G. A., Velarde-Félix, S., Amarillas-Bueno, L. A., Martínez-Campos, A. R., & Allende-Molar, R. (2019). Foot rot and wilt in tomato caused by *Fusarium falciforme* (FSSC 3 + 4) in Mexico. *Plant Disease, 103*, 157. https://doi.org/10.1094/PDIS-06-18-1001-PDN

Vicente, A. R., Manganaris, G. A., Sozzi, G. O., & Crisosto, C. H. (2009). Nutritional quality of fruits and vegetables. In E. Yahia (Ed.), *Postharvest biology and technology of tropical and subtropical fruits* (Vol. 1, pp. 57–106). Woodhead Publishing.

Vignani, R., & Scali, M. (2024). Chapter one—Grapevine origin and diversity. In P. Martins-Lopes (Ed.), *Advances in Botanical Research* (Vol. 110, pp. 1–25). Academic Press.

Vignati, E., Lipska, M., Dunwell, J. M., Caccamo, M., & Simkin, A. J. (2022). Fruit development in sweet cherry. *Plants, 11*(12), 1531. https://doi.org/10.3390/plants11121531

Vilgalys, R., & Hester, M. (1990). Rapid genetic identification and mapping of enzymatically amplified ribosomal DNA from several *Cryptococcus* species. *Journal of Bacteriology, 172*(8), 4238–4246. https://doi.org/10.1128/jb.172.8.4238-4246.1990

Waite, H., & May, P. (2005). The effects of hot water treatment, hydration and order of nursery operations on cuttings of *Vitis vinifera* cultivars. *Phytopathologia Mediterranea, 44*(2), 144–152.

Wang, C., & Zhuang, W. Y. (2019). Evaluating effective *Trichoderma* isolates for biocontrol of *Rhizoctonia solani* causing root rot of *Vigna unguiculata*. *Journal of Integrative Agriculture, 18*, 2072–2079. https://doi.org/10.1016/S2095-3119(19)62593-1

Wang, C. W., Wang, Y., Wang, L., Li, X. F., Wang, M. Q., & Wang, J. M. (2021). *Fusarium* species causing postharvest rot on Chinese cherry in China. *Crop Protection, 141*, 105496. https://doi.org/10.1016/j.cropro.2020.105496

Wang, J. N., Zhao, H. H., Yu, Y. Y., Li, X. D., Liang, C., & Li, B. D. (2016). *The pathogen causing Lasiodiplodia twig blight of blueberry*. *Mycosystema*, 35, 657–665. https://doi.org/10.13346/j.mycosystema.150165

Wang, L., Hou, H., Zhou, Z. Q., Tu, H. T., & Yuan, H. B. (2021). Identification and detection of *Botryosphaeria dothidea* from kiwifruit (*Actinidia chinensis*) in China. *Plants*, 10, 401. https://doi.org/10.3390/plants10020401

Wang, M. M., Chen, Q., Diao, Y. Z., Duan, W. J., & Cai, L. (2019). *Fusarium incarnatum-equiseti* complex from China. *Persoonia - Molecular Phylogeny and Evolution of Fungi, 43*(1), 70–89. https://doi.org/10.3767/persoonia.2019.43.03

Wang, S. Y., Wang, Y., & Li, Y. (2022). *Cladosporium* spp. (Cladosporiaceae) isolated from *Eucommia ulmoides* in China. *MycoKeys*, 91, 151–168. https://doi.org/10.3897/mycokeys.91.87841

Wang, S., Li, X., Liu, C., Liu, L., Yang, F., Guo, Y., & Li, Y. (2021). First report of *Fusarium brachygibbosum* causing root rot on soybean in Northeastern China. *Plant Disease, 105*, 1560. https://doi.org/10.1094/PDIS-05-20-0941-PDN

Wang, X. H., Guo, Y. S., Du, Y. M., Yang, Z. L., Huang, X. Z., Hong, N., … Wang, G. P. (2021). Characterization of *Diaporthe* species associated with peach constriction canker, with two novel species from China. *MycoKeys*, 80, 77–90. https://doi.org/10.3897/mycokeys.80.63816

Wang, X., Shi, C. M., Gleason, M. L., & Huang, L. L. (2020). Fungal species associated with apple Valsa canker in East Asia. *Phytopathology Research, 2*(1), 35. https://doi.org/10.1186/s42483-020-00076-5

Wang, Y., Wang, C. W., Gao, J., & Yang, L. N. (2016). First report of *Fusarium acuminatum* causing postharvest fruit rot on stored *Vaccinium corymbosum* in China. *Plant Disease*, 100(12), 2527. https://doi.org/10.1094/PDIS-04-16-0529-PDN

Wang, Y., Xiong, F., Lu, Q., Hao, X., Zheng, M., Wang, L., … Yang, Y. (2019). Diversity of *Pestalotiopsis*-like species causing gray blight disease of tea plants (*Camellia sinensis*) in China, including two novel *Pestalotiopsis* species, and analysis of their pathogenicity. *Plant Disease*, 103(10), 2548–2558. https://doi.org/10.1094/PDIS-02-19-0264-RE

Wang, Y., Zhang, Y., Bhoyroo, V., Rampadarath, S., & Jeewon, R. (2021). Multigene phylogenetics and morphology reveal five novel *Lasiodiplodia* species associated with blueberries. *Life*, 11(7), Article 7. https://doi.org/10.3390/life11070657

Weir, B. S., Johnston, P. R., & Damm, U. (2012). The *Colletotrichum gloeosporioides* species complex. *Studies in Mycology, 73*, 115–180. https://doi.org/10.3114/sim0011

Wharton, P. S., & Schilder, A. C. (2008). Novel infection strategies of *Colletotrichum acutatum* on ripe blueberry fruit. *Plant Pathology*, 57(1), 122–134. https://doi.org/10.1111/j.1365-3059.2007.01698.x

Wharton, P. S., Iezzoni, A., & Jones, A. L. (2003). Screening cherry germ plasm for resistance to leaf spot. *Plant Disease, 87*(5), 471–477. https://doi.org/10.1094/PDIS.2003.87.5.471

White, T. J., Bruns, T., Lee, S., & Taylor, J. (1990). Amplification and direct sequencing of fungal ribosomal RNA genes for phylogenetics. In M. A. Innis, D. H. Gelfand, J. J. Sninsky, & T. J. White (Eds.), *PCR protocols: A guide to methods and applications* (pp. 315–322). Academic Press.

Wijayawardene, N. N., Hyde, K. D., Dai, D. Q., Sánchez-García, M., Goto, B. T., Saxena, R. K., . . . Thines, M. (2022). Outline of fungi and fungus-like taxa – 2021. *Mycosphere, 13*(1), 53–453. https://doi.org/10.5943/mycosphere/13/1/2

Wilcox, W. F., Gubler, W. D., & Uyemoto, J. K. (Eds.). (2015). *Compendium of grape diseases, disorders, and pests* (2nd ed.). The American Phytopathological Society.

Williamson-Benavides, B. A., & Dhingra, A. (2021). Understanding root rot disease in agricultural crops. *Horticulturae, 7*(2), 33. https://doi.org/10.3390/horticulturae7020033

Wingfield, M. J., De Beer, Z. W., Slippers, B., Wingfield, B. D., Groenewald, J. Z., Lombard, L., & Crous, P. W. (2012). One fungus, one name promotes progressive plant pathology. *Molecular Plant Pathology, 13*(6), 604–613. https://doi.org/10.1111/j.1364-3703.2011.00768.x

Woudenberg, J. H. C., Groenewald, J. Z., Binder, M., & Crous, P. W. (2013). *Alternaria* redefined. *Studies in Mycology, 75*, 171–212. https://doi.org/10.3114/sim0015

Wright, A. F., & Harmon, P. F. (2010). Identification of species in the *Botryosphaeriaceae* family causing stem blight on southern highbush blueberry in Florida. *Plant Disease*, 94(8), 966–971. https://doi.org/10.1094/PDIS-94-8-0966

Wright, E. R., Folgado, M., Rivera, M. C., Crelier, A., Vasquez, P., & Lopez, S. E. (2008). *Nigrospora sphaerica* causing leaf spot and twig and shoot blight on blueberry: A new host of the pathogen. *Plant Disease*, 92(1), 171. https://doi.org/10.1094/PDIS-92-1-0171B

Wright, E. R., Rivera, M. C., Esperón, J., Cheheid, A., & Rodríguez Codazzi, A. (2004). *Alternaria* leaf spot, twig blight, and fruit rot of highbush blueberry in Argentina. *Plant Disease*, 88(12), 1383. https://doi.org/10.1094/PDIS.2004.88.12.1383B

Wu, H. Y., Tsai, C. Y., Wu, Y. M., Ariyawansa, H. A., Chung, C. L., & Chung, P. C. (2021). First report of *Neopestalotiopsis rosae* causing leaf blight and crown rot on strawberry in Taiwan. *Plant Disease, 105*(2), 487. https://doi.org/10.1094/PDIS-05-20-1045-PDN

Wu, L. N., Li, X. H., Zhang, W., Zhou, Y. Y., & Yan, J. Y. (2020). Identification and biological characteristics of *Lasiodiplodia citricola* causing *Botryosphaeria* dieback of grapes in Beijing (in Chinese). *Acta Phytopathologica Sinica, 52*, 1003–1005.

Xavier, K. V., Yu, X., & Vallad, G. E. (2021). First report of *Neopestalotiopsis rosae* causing foliar and fruit spots on pomegranate in Florida. *Plant Disease, 105*(2), 504. https://doi.org/10.1094/PDIS-06-20-1282-PDN

Xiao, X. E., Liu, Y. D., Zheng, F., Xiong, T., Zeng, Y. T., Wang, W., … Li, H. Y. (2023). High species diversity in *Diaporthe* associated with *Citrus* diseases in China. *Persoonia*, 51, 229–256. https://doi.org/10.3767/persoonia.2023.51.06

Xiao, Y. S., Xie, Y. Y., Su, Q. N., Huo, G. H., & Cui, C. Y. (2022). First report of brown spot of dekopon fruit caused by *Cladosporium tenuissimum* in China. *Plant Disease*, 107(2), 559. https://doi.org/10.1094/PDIS-03-22-0529-PDN

Xie, X. W., Huang, Y. S., Shi, Y. X., Chai, A. L., Li, L., & Li, B. J. (2022). First report of *Cladosporium tenuissimum* causing leaf spots on carnation in China. *Plant Disease, 106*(4), 1300. https://doi.org/10.1094/PDIS-07-21-1437-PDN

Xu, C. N., Zhang, H. J., Zhou, Z. S., Hu, T. L., Wang, S. T., Wang, Y. N., & Cao, K. Q. (2015). Identification and distribution of Botryosphaeriaceae species associated with blueberry stem blight in China. *European Journal of Plant Pathology*, 143, 737–752. https://doi.org/10.1007/s10658-015-0724-6

Xu, C. N., Zhou, Z. S., Wu, Y. X., Chi, F. M., Ji, Z. R., & Zhang, H. J. (2013). First report of stem and leaf anthracnose on blueberry caused by *Colletotrichum gloeosporioides* in China. *Plant Disease*, 97(6), 845–845. https://doi.org/10.1094/PDIS-11-12-1056-PDN

Xu, C. N., Zhou, Z. S., Wu, Y. X., Chi, F. M., Ji, Z. R., & Zhang, H. J. (2013). First report of *Colletotrichum acutatum* associated with stem blight of blueberry plants in China. *Plant Disease*, 97(3), 422. https://doi.org/10.1094/PDIS-08-12-0738-PDN

Xu, J. P. (2022). Assessing global fungal threats to humans. *mLife, 1*(3), 223–240. https://doi.org/10.1002/mlf2.12036

Xu, M., Zhang, X., Yu, J., Guo, Z., Li, Y., Wu, J., & Chi, Y. (2021). First report of *Fusarium ipomoeae* causing peanut leaf spot in China. *Plant Disease, 105*(11), 3754. https://doi.org/10.1094/PDIS-01-21-0226-PDN

Xu, X., Zhang, L., Yang, X. L., Shen, G. J., Wang, S., Teng, H. L., … Xiang, W. S. (2022). *Fusarium* species associated with maize leaf blight in Heilongjiang Province, China. *Journal of Fungi*, 8(11), 1170. https://doi.org/10.3390/jof8111170

Xue, D. S., Lian, S., Li, B. H., & Wang, C. X. (2018). First report of *Pestalotiopsis clavispora* causing root rot on blueberry in China. *Plant Disease*, 102(8), 1655–1655. https://doi.org/10.1094/PDIS-01-18-0138-PDN

Xun, W., Wu, C., Wu, X., Bai, Q., Sun, Y., Xie, D., … Jin, L. (2023). First report of bayberry leaf blight caused by *Pestalotiopsis kenyana* in Zhejiang Province, China. *Plant Disease*, 107(9), 2860. https://doi.org/10.1094/PDIS-03-23-0450-PDN

Yan, H., Mi, Y., Jiao, T., Lv, P., Guo, L., Huo, J., … Cheng, Y. (2024). First report of leaf spot disease caused by *Neopestalotiopsis rosae* on *Lonicera caerulea* in Heilongjiang Province, China. *Plant Disease*, 108(9), 2918. https://doi.org/10.1094/PDIS-01-24-0158-PDN

Yan, J. Y., Jayawardena, M. M. R. S., Goonasekara, I. D., Wang, Y., Zhang, W., Liu, M., … Li, X.H. (2015). Diverse species of *Colletotrichum* associated with grapevine anthracnose in China. *Fungal Diversity, 71*(1), 233–246. https://doi.org/10.1007/s13225-014-0310-9

Yan, J. Y., Li, X. H., Kong, F. F., Wang, Z. Y., Gong, L. Z. & He, H. P. (2011a). Occurrence of grapevine trunk disease caused by *Botryosphaeria rhodina* in China.

Plant Disease, 95, 219. https://doi.org/10.1094/PDIS-02-10-0140

Yan, J. Y., Peng, Y. L., Xie, Y., Li, X. H., Yao, S. W., Tang, M. L. & Wang, Z. Y. (2011). First report of grapevine trunk disease caused by *Botryosphaeria obtusa* in China. *Plant Disease, 95*, 616. https://doi.org/10.1094/PDIS-11-10-0821

Yan, J. Y., Xie, Y., Yao, S. W., Wang, Z. Y., & Li, X. H. (2012). Characterization of *Botryosphaeria dothidea*, the causal agent of grapevine canker in China. *Australasian Plant Pathology, 41*, 351–357. https://doi.org/10.1007/s13313-012-0135-5

Yan, J. Y., Xie, Y., Zhang, W., Wang, Y., Liu, J. K., Hyde, K. D., … Li, X. H. (2013). Species of Botryosphaeriaceae involved in grapevine dieback in China. *Fungal Diversity*, 61(1), 221–236. https://doi.org/10.1007/s13225-013-0251-8

Yan, X. R., Meng, T. T., Qi, Y. B., Fei, N. Y., & Dai, H. P. (2019). First report of *Pestalotiopsis adusta* causing leaf spot on raspberry in China. *Plant Disease, 103*, 2688. https://doi.org/10.1094/PDIS-07-18-1135-PDN

Yan, X. R., Wang, X., Hu, M. Q., Dai, H. P., Fu, J. F., & Li, T. L. (2015). Identification and biological characteristic of blueberry *Diaporthe* bud blight pathogen. *Acta Phytopathologica Sinica*, 45(5), 556–560.

Yan, X. R., Zhou, Y., Zhao, R. J., Dai, H. P., & Fu, J. F. (2014). Identification on the pathogen of blueberry leaf shot hole disease and study on its biological characteristics. *Northern Horticulture*, 2014(16), 123–127.

Yang, L. P., Jin, M. J., Cui, L. X., Li, T. H., An, J., Wei, L. J., . . . Yang, C. D. (2020). Isolation and identification of the pathogen causing cherry black spot in Gansu Province. *Journal of Fruit Science*, *37*(10), 1316–1323.

Yang, Q., Fan, X. L., Guarnaccia, V., & Tian, C. M. (2018). High diversity of *Diaporthe* species associated with dieback diseases in China, with twelve new species described. *MycoKeys, 39*, 97–149. https://doi.org/10.3897/mycokeys.39.26914

Yang, Q., Zeng, X. Y., Yuan, J., Zhang, Q., He, Y. K., & Wang, Y. (2021). Two new species of *Neopestalotiopsis* from southern China. *Biodiversity Data Journal, 9*, e70446. https://doi.org/10.3897/BDJ.9.e70446

Yang, Y., Luo, W., Zhang, W., Mridha, M. A. U., Wijesinghe, S. N., McKenzie, E. H. C., & Wang, Y. (2023). *Cladosporium* species associated with fruit trees in Guizhou Province, China. *Journal of Fungi, 9*, 250. https://doi.org/10.3390/jof9020250

Ye, Q. T., Jia, J. Y., Manawasinghe, I. S., Li, X. H., Zhang, W., Mugnai, L., … Yan, J. Y. (2021). *Fomitiporia punicata* and *Phaeoacremonium minimum* associated with Esca complex of grapevine in China. *Phytopathology Research, 3*, 11. https://doi.org/10.1186/s42483-021-00087-w

Ye, Q. T., Li, Y. M., Zhou, Y. Y., Li, X. H., & Yan, J. Y. (2021c). Occurrence of grapevine trunk diseases caused by fungal pathogens in the domestic and overseas (in Chinese). *Journal of Fruit Science, 38*, 278–292.

Ye, Q. T., Manawasinghe, I. S., Zhang, W., Mugnai, L., Hyde, K. D., Li, X. H., & Yan, J. Y. (2020). First report of *Phaeoacremonium minimum* associated with grapevine trunk diseases in China. *Plant Disease, 104*, 1259. https://doi.org/10.1094/PDIS-08-19-1649-PDN

Ye, Q. T., Zhang, W., Jia, J. Y., Li, X. H., Zhou, Y. Y., Han, C. P., … Yan, J. Y. (2021). Fungal pathogens associated with black foot of grapevine in China. *Phytopathologia Mediterranea, 60*, 303–319. https://doi.org/10.36253/phyto-12353

Yilmaz, N., Sandoval-Denis, M., Lombard, L., Visagie, C. M., Wingfield, B. D., & Crous, P. W. (2021). Redefining species limits in the *Fusarium fujikuroi* species complex. *Persoonia, 46*, 129–162. https://doi.org/10.3767/persoonia.2021.46.05

Yin, Q. X., An, X. L., Wu, X., Dharmasena, D. S. P., Li, D. X., Jiang, S. L., … Chen, Z. (2021). First report of *Alternaria longipes* causing leaf spot on tea in China. *Plant Disease, 105*, 4167. https://doi.org/10.1094/PDIS-07-20-1583-PDN

Yin, W. X., Adnan, M., Shang, Y., Lin, Y., & Luo, C. X. (2018). Sensitivity of *Botrytis cinerea* from nectarine/cherry in China to six fungicides and characterization of resistant isolates. *Plant Disease, 102*(12), 2578–2585. https://doi.org/10.1094/PDIS-02-18-0244-RE

Yokosawa, S., Eguchi, N., & Sato, T. (2020). Characterization of the *Colletotrichum gloeosporioides* species complex causing grape ripe rot in Nagano Prefecture, Japan. *Journal of General Plant Pathology, 86*, 163–172. https://doi.org/10.1007/s10327-020-00907-5

You, L., Senanayake, I., Liu, J., Luo, M., Huang, Y., & Dong, Z. (2024). *Neopestalotiopsis iberica* induces leaf spots on *Synsepalum dulcificum* in China. *Journal of Phytopathology, 172*, e13258. https://doi.org/10.1111/jph.13258

Yu, C., Wu, C., Li, G., & Wang, C. (2018). First report of *Diaporthe nobilis* causing postharvest rot of blueberry in Shandong Province, China. *Plant Disease, 102*(9), 1856. https://doi.org/10.1094/PDIS-11-17-1816-PDN

Yu, H., Gu, Y., Jiang, Y., & He, S. (2012). An update on blueberry growing in China. *International Journal of Fruit Science, 12*(1–3), 100–105. https://doi.org/10.1080/15538362.2011.619128

Yu, L., Rarisara, I., Xu, S. G., Wu, X., & Zhao, J. R. (2012). First report of stem blight of blueberry caused by *Botryosphaeria dothidea* in China. *Plant Disease, 96*(11), 1697. https://doi.org/10.1094/PDIS-05-12-0500-PDN

Yu, L., Zhao, J. R., Xu, S. G., Rarisara, I., Su, Y., Pei, W. H., & Kong, C. S. (2015). Identification of the pathogen causing leaf spot on blueberry in Yunnan. *Acta Phytopathologica Sinica, 45*(2), 216–219. https://doi.org/10.13926/j.cnki.apps.2015.02.014

Yuan, B., Yue, F., Cui, Y., & Chen, C. (2022). The role of fine management techniques in relation to agricultural pollution and farmer income: The case of the fruit industry. *Environmental Research Letters, 17*(3), 034001. https://doi.org/10.1088/1748-9326/ac4654

Yuan, X. L., Qi, Y. T., Wu, Z., Yang, C. X., & Cui, C. Y. (2024). First report of *Botryosphaeria dothidea* causing postharvest fruit rot of plum in China. *Plant Disease, 108*, 1111. https://doi.org/10.1094/PDIS-12-23-2680-PDN

Yue, Q. H., Zhao, H. H., Liang, C., & Li, X. D. (2013). The pathogen causing Phomopsis twig blight of blueberry. *Mycosystema*, 32(6), 959–966. https://doi.org/10.1079/CABICOMPENDIUM.18747

Zakaria, L. (2023). *Fusarium species associated with diseases of major tropical fruit crops*. *Horticulturae, 9*(3), 322. https://doi.org/10.3390/horticulturae9030322

Zhai, H., Li, Y., Wu, N., Yao, M., Liu, H., & Cui, D. (2024). Occurrence and control of gray mold in blueberry. *Deciduous Fruits*, *56*(2), 85–86. https://doi.org/10.13855/j.cnki.lygs.2024.02.021

Zhang, G. H., Yang, Q., Li, X. Y., Song, S. Y., Ren, Y. Q., & Huang, S. H. (2016). Pathogens identification of twig blight and fruit rot disease and investigation on insect pests against *Vaccinium uliginosum* in Majiang County. *China Plant Protection*, *5*, 12–15.

Zhang, H., Sha, H. D., Chen, W. L., & Mao, B. Z. (2024). First report of *Fusarium annulatum* causing blight on *Bletilla striata* (Baiji) in China. *Plant Disease*, *108*, 800. https://doi.org/10.1094/PDIS-08-23-1715-PDN

Zhang, H., Zeng, Y., Wei, T. P., Jiang, Y. L., & Zeng, X. Y. (2023). Endophytic *Fusarium* and allied fungi from *Rosa roxburghii* in China. *Mycosphere*, *14*, 2092–2207. https://doi.org/10.5943/mycosphere/14/1/25

Zhang, J., Wang, D., Wei, T., Lai, X., Tang, G., Wang, L., … Liang, J. (2024). First report of *Epicoccum nigrum* causing brown leaf spot of sweet cherry (*Prunus avium*) in China. *Plant Disease, 108*(7), 2217. https://doi.org/10.1094/PDIS-10-23-2074-PDN

Zhang, K. C., Liu, Q. Z., Pan, F. R., & Yan, G. H. (2024). Cherries in China: Germplasm, history and current trends. *Acta Horticulturae, 1408*, 29–36. https://doi.org/10.17660/ActaHortic.2024.1408.4

Zhang, K. C., Yan, G. H., Zhang, X. M., Wang, J., & Duan, X. W. (2017). Cultivation history, production status and development suggestions of sweet cherry in China. *Deciduous Fruit Tree Science, 49*(6), 1–5.

Zhang, K., Li, T., & Yan, G. (eds.). (2024b). International society for horticultural science, & international society for horticultural science. In *Proceedings of the IX International Cherry Symposium: Beijing, China, May 21–25, 2023*. International Cherry Symposium, Leuven: ISHS.

Zhang, L. Q., Jiang, S., Meng, J. J., An, H. S., & Zhang, X. Y. (2019). First report of leaf spot caused by *Nigrospora oryzae* on blueberry in Shanghai, China. *Plant Disease, 103*(9), 2473. https://doi.org/10.1094/PDIS-02-19-0242-PDN

Zhang, L. Z., Zhang, Q., Yang, P., Niu, Y., & Niu, W. (2019). First report of gummosis disease of sweet cherry caused by *Botryosphaeria dothidea* in China. *Plant Disease, 103*(12), 3283. https://doi.org/10.1094/PDIS-07-19-1418-PDN

Zhang, T. (2010). The causes and control measures of cherry brown spot disease. *Journal of Fruit Science*, 27(3), 477–480.

Zhang, W., Groenewald, J. Z., Lombard, L., Schumacher, R. K., Phillips, A. J. L., & Crous, P. W. (2021). Evaluating species in Botryosphaeriales. *Persoonia*, *46*, 63–115. https://doi.org/10.3767/persoonia.2021.46.03

Zhang, W., Li, Y., Lin, L., Jia, A., & Fan, X. (2024). Updating the species diversity of pestalotioid fungi: Four new species of *Neopestalotiopsis* and *Pestalotiopsis*. *Journal of Fungi*, *10*(7), 7. https://doi.org/10.3390/jof10070475

Zhang, X. P., Cao, X. D., Dang, Q. Q., Liu, Y. G., Zhu, X. P., & Xia, J. W. (2022). First report of fruit rot caused by *Fusarium luffae* in muskmelon in China. *Plant Disease*, 106(6), 1763. https://doi.org/10.1094/PDIS-12-21-2666-PDN

Zhang, X. Y., Chen, X. H., Xie, L. X., Zhang, L. J., Zheng, S., & Li, T. (2023). Pathogen of branch blight on blueberry plants in Fujian. *Fujian Journal of Agricultural Sciences*, *38*(10), 1214–1219.

Zhang, X., Li, L. R., Yang, J. Y., Yan, H. F., & Liu, D. Q. (2020). Rot on rhizomes and adventitious root of *Dioscorea polystachya* caused by *Fusarium falciforme* in China. *Plant Disease, 104*, 1544. https://doi.org/10.1094/PDIS-12-19-2529-PDN

Zhang, Y. M., Maharachchikumbura, S. S. N., Tian, Q., & Hyde, K. D. (2013). Pestalotiopsis species on ornamental plants in Yunnan Province, China. *Phytotaxa, 126*(1), 45–62. https://doi.org/10.11646/phytotaxa.126.1.2

Zhang, Z., Liu, R., Liu, S., Mu, T., Zhang, X., & Xia, J. (2022). Morphological and phylogenetic analyses reveal two new species of Sporocadaceae from Hainan, China. *MycoKeys, 88*, 171–192. https://doi.org/10.3897/mycokeys.88.82229

Zhao, B., Ji, B., Yin, W., & Luo, C. (2023). First report of brown rot caused by *Monilia yunnanensis* on sweet cherry in China. *Plant Disease, 108*(1), 226. https://doi.org/10.1094/PDIS-09-23-1716-PDN

Zhao, L., Cai, J., He, W., & Zhang, Y. (2019). *Macrophomina vaccinii* sp. nov. causing blueberry stem blight in China. *MycoKeys, 55*, 1–14. https://doi.org/10.3897/mycokeys.55.35015

Zhao, L., Sun, W., Zhao, L., Zhang, L., Yin, Y., & Zhang, Y. (2022). *Neofusicoccum vaccinii*: A novel species causing stem blight and dieback of blueberries in China. *Plant Disease, 106*(9), 2338–2347. https://doi.org/10.1094/PDIS-09-21-2068-RE

Zhao, L., Wang, Y., He, W., & Zhang, Y. (2019). Stem blight of blueberry caused by *Lasiodiplodia vaccinii* sp. nov. in China. *Plant Disease, 103*(8), 2041–2050. https://doi.org/10.1094/PDIS-01-19-0079-RE

Zhao, Y. Z., Liu, Z. H., Li, Y. T., Zhou, S., & Huang, X. Y. (2013). Identification and pathogenicity study of the pathogen causing black spot disease on sweet cherry. *Journal of Horticultural Science*, *40*(8), 1560–1566.

Zheng, H., Qiao, M., Lv, Y., Du, X., Zhang, Y., Zhang, L., . . . Zhang, K. (2021). New species of *Trichoderma* isolated as endophytes and saprobes from Southwest China. *Journal of Fungi, 7*, 467. https://doi.org/10.3390/jof7060467

Zheng, X., Liu, X., Li, X., Quan, C., Li, P., Chang, X., … Gong, G. (2023). *Pestalotiopsis* species associated with blueberry leaf spots and stem cankers in Sichuan Province of China. *Plant Disease, 107*(1), 149–156. https://doi.org/10.1094/PDIS-07-21-1550-RE

Zheng, Y., Yu, J., Wen, H., Chen, Y., Lin, M., Lin, Y., … Lin, H. T. (2025). *Phomopsis longanae* Chi infection induces changes in the metabolisms of energy and respiration in relation to longan pulp breakdown. *Postharvest Biology and Technology, 219*, 113199. https://doi.org/10.1016/j.postharvbio.2024.113199

Zhou, L. Y., Yang, S. F., Wang, S. M., Lv, J. W., Wan, W. Q., Li, Y. H., . . . Zhou, H. (2021). Identification of *Fusarium ipomoeae* as the causative agent of leaf spot disease in *Bletilla striata* in China. *Plant Disease*, *105*, 1204. https://doi.org/10.1094/PDIS-09-20-1974-PDN

Zhou, Y. Y., Zhang, W., Li, X. H., Jia, J. Y., Wang, J., Zhang, K. C., . . . Yan, J. Y. (2021). Identification of *Botryosphaeria dothidea* associated with cherry leaf spot disease. *Acta Phytopathologica Sinica, 51*(4), 636–640.

Zhou, Y. Y., Zhang, W., Li, Y. M., Ji, S. X., Li, X. H., Hyde, K. D., … Yan, J. Y. (2023). Identification and characterization of *Colletotrichum* species associated with cherry leaf spot disease in China. *Plant Disease, 107*(2), 500–513. https://doi.org/10.1094/PDIS-11-21-2538-RE

Zhou, Y., Zhang, W., Li, X., Ji, S., Han, C., & Yan, J. (2022). Identification of *Diaporthe* species associated with cherry leaf spot in China. *Journal of Plant Protection, 49*(4), 1077–1084.

Zhu, J. L., & Chang, Y. Y. (2004). Identification and biological characteristics of the pathogen causing black ring spot of cherry. *China Fruits, 2004*(3), 44–45.

Zhu, W. B., Liu, J. R., Wang, Y., Peng, X. J., & Liu, X. F. (2020). Morphological identification of the branch wilt pathogen of *Ulmus pumila* L. *Forest Engineering, 36*, 19–24.

Ziedan, E. S. H., Embaby, E. S. M., & Farrag, E. S. (2011). First record of *Fusarium* vascular wilt on grapevine in Egypt. *Archives of Phytopathology and Plant Protection, 44*, 1719–1727. https://doi.org/10.1080/03235408.2010.522818

APPENDIX A

STRAINS USED IN PHYLOGENETIC ANALYSES

Table A1 Strains used in phylogenetic analysis with GenBank accession numbers

| Species | Isolate | GenBank accession numbers | | | | | | | | | |
		ITS	*tef1*	*tub2*	*rpb2*	LSU	*his*	*act*	*cal*	*gapdh*	*chs*
Botryosphaeria agaves	**MFLUCC 11-0125T**	JX646791	JX646856	JX646841							
B. agaves	MFLUCC 10-0051	JX646790	JX646855	JX646840							
B. corticis	**CBS 119047T**	DQ299245	EU017539	EU673107							
B. corticis	ATCC 22927	DQ299247	EU673291	EU673108							
B. dothidea (B. auasmontanum)	CMW 25413	EU101303	EU101348	N/A							
B. dothidea	**CBS 115476T**	AY236949	AY236898	AY236927							
B. dothidea	CBS 110302	AY259092	AY573218	EU673106							
B. dothidea (B. minutispermatia)	GZCC 16-0013	KX447675	KX447678	N/A							
B. dothidea (B. minutispermatia)	GZCC 16-0014	KX447676	KX447679	N/A							
B. dothidea (B. sinensia)	CGMCC 3.17723	KT343254	KU221233	KX197107							
B. dothidea (B. sinensia)	CGMCC 3.17724	KT343256	KU221234	KX197108							
B. dothidea (B. wangensis)	CERC2298	KX278002	KX278107	KX278211							
B. dothidea (B. wangensis)	CERC2299	KX278003	KX278108	KX278212							
B. fabicerciana	**CMW 27094T**	HQ332197	HQ332213	KF779068							
B. fabicerciana	CMW 27121	HQ332198	HQ332214	KF779069							
B. kuwatsukai	**CBS 135219T**	KJ433388	KJ433410	N/A							

Table A1 (continued)

Species	Isolate	GenBank accession numbers										
		ITS	*tef1*	*tub2*	*rpb2*	LSU	*his*	*act*	*cal*	*gapdh*	*chs*
B. kuwatsukai	LSP 5	KJ433395	KJ433417	N/A							
B. qingyuanensis	**CERC2946T**	KX278000	KX278105	KX278209							
B. qingyuanensis	CERC2947	KX278001	KX278106	KX278210							
B. ramosa	**CBS 122069T**	EU144055	EU144070	KF766132							
B. scharifii	**IRAN 1529CT**	JQ772020	JQ772057	N/A							
B. scharifii	IRAN 1543C	JQ772019	JQ772056	N/A							
Lasiodiplodia avicenniae	**CBS 139670T**	KP860835	KP860680	KP860758							
L. brasiliensis	**CMM 4015T**	JX464063	JX464049	N/A							
L. brasiliensis	CMW 35884	KU887094	KU886972	KU887466							
L. bruguierae	**CBS 139669T**	KP860833	KP860678	KP860756							
L. bruguierae	CBS 141453	KP860832	KP860677	KP860755							
L. citricola	**IRAN 1522CT**	GU945354	GU945340	KU887505							
L. citricola	CBS 124706	GU945353	GU945339	KU887504							
L. crassispora	**WAC 12533T**	DQ103550	DQ103557	KU887506							
L. crassispora	CMW 13488	DQ103552	DQ103559	KU887507							
L. euphorbicola	CMW 33350	KU887149	KU887026	KU887455							
L. euphorbicola	CMW 36231	KU887187	KU887063	KU887494							
L. gilanensis	**IRAN 1523CT**	GU945351	GU945342	KU887511							
L. gilanensis	IRAN 1501C	GU945352	GU945341	KU887510							
L. gonubiensis	**CMW 14077T**	AY639595	DQ103566	DQ458860							
L. gonubiensis	CMW 14078	AY639594	DQ103567	EU673126							
L. hormozganensis	**IRAN 1500CT**	GU945355	GU945343	KU887515							
L. hormozganensis	IRAN 1498C	GU945356	GU945344	KU887514							
L. iraniensis	**IRAN 1520CT**	GU945348	GU945336	KU887516							
L. iraniensis	IRAN 1502C	GU945347	GU945335	KU887517							
L. laeliocattleyae	**CBS 130992T**	JN814397	JN814424	KU887508							

Table A1 (continued)

| Species | Isolate | GenBank accession numbers | | | | | | | | | |
		ITS	*tef1*	*tub2*	*rpb2*	LSU	*his*	*act*	*cal*	*gapdh*	*chs*
L. laeliocattleyae	BOT 29	JN814401	JN814428	N/A							
L. macrospora	**CMM 3833T**	KF234557	KF226718	KF254941							
L. mahajangana	CMW 27818	FJ900596	FJ900642	FJ900631							
L. margaritacea	**CBS 122519T**	EU144050	EU144065	KU887520							
L. mediterranea	**CBS 137783T**	KJ638312	KJ638331	KU887521							
L. mediterranea	CBS 137784	KJ638311	KJ638330	KU887522							
L. parva	**CBS 456.78T**	EF622083	EF622063	KU887523							
L. parva	CBS 494.78	EF622084	EF622064	EU673114							
L. plurivora	**STE-U 5803T**	EF445362	EF445395	KP872421							
L. pontae	**CMM 1277T**	KT151794	KT151791	KT151797							
L. pseudotheobromae	**CBS 116459T**	EF622077	EF622057	EU673111							
L. pseudotheobromae	CGMCC 3.18047	KX499876	KX499914	KX499989							
L. rubropurpurea	**WAC 12535T**	DQ103553	DQ103571	EU673136							
L. rubropurpurea	WAC 12536	DQ103554	DQ103572	KU887530							
L. subglobosa	CMM 4046	KF234560	KF226723	KF254944							
L. subglobosa	**CMM 3872T**	KF234558	KF226721	KF254942							
L. thailandica	**CBS 138760T**	KJ193637	KJ193681	N/A							
L. thailandica	CBS 138653	KM006433	KM006464	N/A							
L. theobromae	CBS 111530	EF622074	EF622054	KU887531							
L. theobromae	**CBS 164.96T**	AY640255	AY640258	KU887532							
L. tropica	**CGMCC 3.18477T**	KY783454	KY848616	KY848540							
L. venezuelensis	**WAC 12539T**	DQ103547	DQ103568	KU887533							
L. venezuelensis	WAC 12540	DQ103548	DQ103569	KU887534							
L. viticola	**CBS 128313T**	HQ288227	HQ288269	HQ288306							
L. viticola	CBS 128314	HQ288228	HQ288270	HQ288307							
L. vitis	**CBS 124060T**	KX464148	KX464642	KX464917							

Table A1 (continued)

Species	Isolate	GenBank accession numbers									
		ITS	*tef1*	*tub2*	*rpb2*	LSU	*his*	*act*	*cal*	*gapdh*	*chs*
Diplodia corticola	CBS 112546	AY259090	EU673310	EU673117							
D. corticola	**CBS 112549T**	AY259100	AY573227	DQ458853							
D. cupressi	**CBS 168.87T**	DQ458893	DQ458878	DQ458861							
D. cupressi	CBS 261.85	DQ458894	DQ458879	DQ458862							
D. mutila	CBS 112553	AY259093	AY573219	DQ458850							
D. mutila	CBS 230.30	DQ458886	DQ458869	DQ458849							
D. seriata	CBS 119049	DQ458889	DQ458874	DQ458857							
D. seriata	**CBS 112555T**	AY259094	AY573220	DQ458856							
D. seriata	CMW 7774	AY236953	AY236902	AY236931							
Neofusicoccum australe	**CMW 6837T**	AY339262	AY339270	AY339254							
N. australe	CBS 110865	AY343408	KX464661	KX464937							
N. brasiliense	**CMM 1338T**	JX513630	JX513610	KC794031							
N. brasiliense	CMM 1285	JX513628	JX513608	KC794030							
N. cordaticola	**CBS 123634T**	EU821898	EU821868	EU821838							
N. cordaticola	CBS 123635	EU821903	EU821873	EU821843							
N. hongkongense	CERC 2968	KX278051	KX278156	KX278260							
N. hongkongense	**CERC 2973T**	KX278052	KX278157	KX278261							
N. illicii	**CGMCC 3.18310T**	KY350149	N/A	KY350155							
N. illicii	CGMCC 3.18311	KY350150	KY817756	KY350156							
N. kwambonambiense	**CBS 123639T**	EU821900	EU821870	EU821840							
N. kwambonambiense	CBS 123641	EU821919	EU821889	EU821859							
N. macroclavatum	**CBS 118223T**	DQ093196	DQ093217	DQ093206							
N. nonquaesitum	**CBS 126655T**	GU251163	GU251295	GU251823							
N. nonquaesitum	PD 301	GU251164	GU251296	GU251824							
N. occulatum	**CBS 128008T**	EU301030	EU339509	EU339472							
N. occulatum	MUCC 286	EU736947	EU339511	EU339474							

Table A1 (continued)

Species	Isolate	GenBank accession numbers									
		ITS	*tef1*	*tub2*	*rpb2*	LSU	*his*	*act*	*cal*	*gapdh*	*chs*
N. parvum	**ATCC 58191T**	AY236943	AY236888	AY236917							
N. parvum	CMW 9080	AY236942	AY236887	AY236916							
N. parvum	CBS 145997	MT587449	MT592159	MT592649							
N. parvum	CPC 34761	MT587452	MT592161	MT592652							
N. ribis	**CBS 115475T**	AY236935	AY236877	AY236906							
N. ribis	CBS 121.26	AF241177	AY236879	AY236908							
N. sinense	**CGMCC 3.18315T**	KY350148	KY817755	KY350154							
N. sinoeucalypti	**CERC 2005T**	KX278061	KX278166	KX278270							
N. sinoeucalypti	CERC 3416	KX278064	KX278169	KX278273							
Guignardia citricarpa	CBS 127454	JF343583	JF343604	N/A							
Phaeobotryon aplospora	**CFCC 53774T**	MN215836	MN205996			MN215871					
P. aplospora	CFCC 53775	MN215837	N/A			MN215872					
P. aplospora	CFCC 53776	MN215838	MN205997			MN215873					
P. cupressi	IRAN 1456C	FJ919670	FJ919659			N/A					
P. cupressi	IRAN 1458C	FJ919671	FJ919660			N/A					
P. cupressi	IRAN 1455C	FJ919672	FJ919661			N/A					
P. mamane	CPC 12442	EU673333	EU673299			DQ377899					
P. mamane	CPC 12440	KF766209	EU673298			EU673248					
P. mamane	CPC 12443	EU673334	EU673300			EU673249					
P. negundinis	CAA798	KX061514	KX061508			N/A					
P. negundinis	CAA799	KX061515	KX061509			N/A					
P. negundinis	MFLUCC 15-0436	KU820970	KU853997			KU820971					
P. rhoinum	**CFCC 52449T**	MH133923	MH133957			MH133940					
P. rhoinum	CFCC 52450	MH133924	MH133958			MH133941					
P. rhoinum	CFCC 52451	MH133925	MH133959			MH133942					
P. rhois	CFCC 89662	KM030584	KM030598			KM030591					

Table A1 (continued)

| Species | Isolate | GenBank accession numbers | | | | | | | | | |
		ITS	*tef1*	*tub2*	*rpb2*	LSU	*his*	*act*	*cal*	*gapdh*	*chs*
P. rhois	CFCC 89663	KM030585	KM030599			KM030592					
P. rhois	**CFCC 52448T**	MH133922	MH133956			MH133939					
Barriopsis fusca	**CBS 174.26T**	EU673330	EU673296			DQ377857					
Dactylonectria alcacerensis	**CBS 129087T**	JF735333	JF735819	N/A			JF735630				
D. alcacerensis	Cy134	JF735332	JF735818	N/A			JF735629				
D. alcacerensis	JZB3310007	MN988716	MN956381	MN958528			MN958539				
D. amazonica	**MUCL 55430T**	MF683706	MF683664	MF683643			MF683686				
D. anthuriicola	CBS 564.95	JF735302	JF735768	JF735430			JF735579				
D. ecuadoriensis	**MUCL 55424T**	MF683704	MF683662	MF683641			MF683684				
D. ecuadoriensis	MUCL 55425	MF683705	MF683663	MF683642			MF683684				
D. estremocencis	CPC 13539	JF735330	JF735816	JF735458			JF735627				
D. estremocencis	**CBS 129085T**	JF735320	JF735806	JF735448			JF735617				
D. hispanica	**CBS 142827T**	KY676882	KY676870	KY676876			KY676864				
D. hispanica	Cy228	JF735301	JF735767	JF735429			JF735578				
D. hordeicola	**CBS 162.89T**	AM419060	JF735799	AM419084			JF735610				
D. macrodidyma	CBS 112601	MH862898	JF735833	AY677229			JF735644				
D. macrodidyma	**CBS 112615T**	AY677290	JF268750	AY677233			JF735647				
D. macrodidyma	Cy258	JF735348	JF735845	JF735477			JF735656				
D. macrodidyma	CBS 112604	AY677284	JF735833	AY677229			JF735644				
D. novozelandica	CBS 112608	AY677288	JF735821	AY677235			JF735632				
D. novozelandica	**CBS 113552T**	JF735334	JF735822	AY677237			JF735633				
D. palmicola	**MUCL 55426T**	MF683708	MF683666	MF683645			MF683687				
D. pauciseptata	**CBS 120171T**	EF607089	JF735776	EF607066			JF735587				
D. pinicola	CBS 159.43	JF735318	JF735802	JF735446			JF735613				
D. pinicola	**CBS 173.37T**	JF735319	JF735803	JF735447			JF735614				
D. polyphaga	**MUCL 55209T**	MF683689	MF683647	MF683626			MF683668				

Table A1 (continued)

| Species | Isolate | GenBank accession numbers | | | | | | | | | |
		ITS	*tef1*	*tub2*	*rpb2*	LSU	*his*	*act*	*cal*	*gapdh*	*chs*
D. torresensis	CBS 119.41	JF735349	JF735846	JF735478			JF735657				
D. torresensis	Cyl124	KP823912	KP823881	KP823891			KP823900				
D. torresensis	**CBS 129086T**	JF735362	JF735870.1	JF735492			JF735681				
D. valentina	**CBS 142826T**	KY676881	KY676869	KY676875			KY676863				
D. vitis	**CBS 129082T**	JF735303	JF735769.1	JF735431			JF735580				
Ilyonectria capensis	**CBS 132815T**	JX231151	JX231119	JX231103			JX231135				
I. capensis	CBS 132816	JX231160	JX231128	JX231112			JX231144				
I. changbaiensis	**CGMCC 3.18789T**	MF350464	MF350491	MF350410			MF350437				
I. changbaiensis	72R2	MF350465	MF350492	MF350411			MF350438				
I. communis	**CGMCC 3.18788T**	MF350456	MF350483	MF350402			MF350429				
I. communis	J410	MF350457	MF350484	MF350403			MF350430				
I. coprosmae	**CBS 119606T**	JF735260	JF735694	JF735373			JF735505				
I. crassa	**CBS 139.30T**	JF735275	JF735723	JF735393			JF735534				
I. crassa	CBS 158.31	JF735276	JF735724	JF735394			JF735535				
I. cyclaminicola	**CBS 302.93T**	JF735304	JF735770	JF735432			JF735581				
I. destructans	**CBS 264.65T**	AY677273	JF735695	AY677256			JF735506				
I. europaea	**CBS 129078T**	JF735294	JF735756	JF735421			JF735567				
I. europaea	CBS 537.92	EF607079	JF735757	EF607064			JF735568				
I. gamsii	**CBS 940.97T**	AM419065	JF735766	AM419089			JF735577				
I. leucospermi	**CBS 132809T**	JX231161	JX231129	JX231113			JX231145				
I. leucospermi	CBS 132810	JX231162	JX231130	JX231114			JX231146				
I. liliigena	**CBS 189.49T**	JF735297	JF735762	JF735425			JF735573				
I. liliigena	CBS 732.74	JF735298	JF735763	JF735426			JF735574				
I. liriodendri	**CBS 110.81T**	DQ178163	JF735696	DQ178170			JF735507				
I. liriodendri	CBS 117526	DQ178164	JF735697	DQ178171			JF735508				
I. lusitanica	**CBS 129080T**	JF735296	JF735759	JF735423			JF735570				

Table A1 (continued)

| Species | Isolate | GenBank accession numbers | | | | | | | | | |
		ITS	*tef1*	*tub2*	*rpb2*	LSU	*his*	*act*	*cal*	*gapdh*	*chs*
I. mors-panacis	**CBS 306.35T**	JF735288	JF735746	JF735414			JF735557				
I. mors-panacis	CBS 124662	JF735290	JF735748	JF735416			JF735559				
I. palmarum	**CBS 135754T**	HF937431	HF922614	HF922608			HF922620				
I. palmarum	CBS 135753	HF937432	HF922615	HF922609			HF922621				
I. panacis	**CBS 129079T**	AY295316	JF735761	JF735424			JF735572				
I. protearum	**CBS 132811T**	JX231157	JX231125	JX231109			JX231141				
I. protearum	CBS 132812	JX231165	JX231133	JX231117			JX231149				
I. pseudodestructans	**CBS 129081T**	AJ875330	JF735752	AM419091			JF735563				
I. pseudodestructans	CBS 117824	JF735292	JF735751	JF735419			JF735562				
I. qitaiheensis	**CGMCC 3.18787T**	MF350472	MF350499	MF350418			MF350445				
I. qitaiheensis	J919	MF350473	MF350500	MF350419			MF350446				
I. robusta	**CBS 308.35T**	JF735264	JF735707	JF735377			JF735518				
I. robusta	CBS 129084	JF735273	JF735721	JF735391			JF735532				
I. rufa	**CBS 153.37T**	AY677271	JF735729	AY677251			JF735540				
I. rufa	CBS 640.77	JF735277	JF735731	JF735399			JF735542				
I. strelitziae	**CBS 142253T**	KY304649	KY304727	KY304755			KY304621				
I. strelitziae	CBS 142254	KY304651	KY304729	KY304757			KY304623				
I. venezuelensis	**CBS 102032T**	AM419059	JF735760	AY677255			JF735571				
I. vredenhoekensis	**CBS 132807T**	JX231155	JX231123	JX231107			JX231139				
I. vredenhoekensis	CBS 132808	JX231159	JX231127	JX231111			JX231143				
Campylocarpon fasciculare	**CBS 112613T**	AY677301	JF735691	AY677221			JF735502				
C. pseudofasciculare	**CBS 112679T**	AY677306	JF735692	KJ022328			JF735503				
Cylindrocladiella addiensis	**CBS 143794T**	MH111383		MH111388			N/A				
C. addiensis	CBS 143793	MH111385		MH111390			N/A				
C. arbusta	**CMW 47295T**	MH017015		MH016958			MH016996				
C. arbusta	CMW 47296	MH017016		MH016959			MH016997				

Table A1 (continued)

Species	Isolate	GenBank accession numbers									
		ITS	*tef1*	*tub2*	*rpb2*	LSU	*his*	*act*	*cal*	*gapdh*	*chs*
C. australiensis	**CBS 129567T**	JN100624		JN098747			JN098932				
C. brevistipitata	**CBS 142786T**	N/A		MF444926			N/A				
C. camelliae	IMI 346845	AF220952		AY793471			AY793509				
C. clavata	**CBS 129564T**	JN099095		JN098752			JN098858				
C. cymbiformis	**CBS 129553T**	JN099103		JN098753			JN098866				
C. elegans	**CBS 338.92T**	AY793444		AY793474			AY793512				
C. ellipsoidea	**CBS 129573T**	JN099094		JN098757			JN098857				
C. hahajimaensis	**MAFF 238172T**	JN687561		N/A			N/A				
C. hawaiiensis	**CBS 129569T**	JN100621		JN098761			JN098929				
C. horticola	**CBS 142784T**	MF444911		MF444924			N/A				
C. humicola	**CBS 142779T**	MF444906		MF444919			N/A				
C. infestans	**CBS 111795T**	AF220955		AF320190			AY793513				
C. kurandica	**CBS 129577T**	JN100646		JN098765			JN098953				
C. lageniformis	CBS 112898	AY793445		AY725652			AY725699				
C. lageniformis	**CBS 340.92T**	MH862360		AY793481			AY793520				
C. lanceolata	**CBS 129566T**	JN099099		JN098789			JN098862				
C. lateralis	**CBS 142788T**	MF444914		MF444928			N/A				
C. longiphialidica	**CBS 129557T**	JN100585		JN098790			JN098851				
C. longistipitata	**CBS 116075T**	AF220958		AY793506			AY793546				
C. malesiana	CBS 143549	MH017017		MH016960			MH016998				
C. microcylindrica	**CBS 111794T**	AY793452		AY793483			AY793523				
C. natalensis	**CBS 114943T**	JN100588		JN098794			JN098895				
C. nauliensis	**CBS 143792T**	MH111387		MH111392			N/A				
C. nauliensis	CBS 143791	MH111386		MH111391			N/A				
C. nederlandica	**CBS 152.91T**	JN100603		JN098800			JN098910				
C. novazelandica	**CBS 486.77T**	AF220963		AY793485			AY793525				

Table A1 (continued)

| Species | Isolate | GenBank accession numbers | | | | | | | | | |
		ITS	*tef1*	*tub2*	*rpb2*	LSU	*his*	*act*	*cal*	*gapdh*	*chs*
C. obpyriformis	**CMW 47194T**	MH017022		MH016965			MH017003				
C. parva	CBS 114524	AF220964		AY793486			AY793526				
C. parvispora	**CMW 47197T**	MH017025		MH016968			MH017006				
C. peruviana	**IMUR 1843T**	AF220966		AY793500			AY793540				
C. pseudocamelliae	**CBS 129555T**	JN100577		JN098814			JN098843				
C. pseudohawaiiensis	**CBS 210.94T**	JN099128		JN098819			JN098890				
C. pseudohawaiiensis	CBS 115610	JN100594		JN098820			JN098901				
C. pseudoinfestans	**CBS 114531T**	AF220957		AY793508			AY793548				
C. pseudoparva	**CBS 129560T**	JN100620		JN098824			JN098927				
C. queenslandica	**CBS 129574T**	JN099098		JN098826			JN098861				
C. reginae	**CBS 142782T**	MF444909		MF444922			N/A				
C. solicola	**CMW 47198T**	MH017021		MH016964			MH017002				
C. stellenboschensis	**CBS 110668T**	JN100615		JN098829			JN098922				
C. terrestris	**CBS 142789T**	MF444915		MF444929			N/A				
C. thailandica	**CBS 129571T**	JN100582		JN098834			JN098848				
C. variabilis	**CBS 129561T**	JN100643		JN098719			JN098950				
C. viticola	**CBS 112897T**	AY793468		AY793504			AY793544				
C. viticola	CPC 5620	AY793469		AY793505			AY793545				
C. vitis	**CBS 142517T**	KY979751		KY979918			N/A				
Gliocladiopsis sagariensis	**CBS 199.55T**	NR147628		JQ666141			JQ666031				
Fusarium acuminatum	NRRL 36147		GQ505420		GQ505484						
F. acuminatum	IBE000016		EF531240		N/A						
F. acuminatum	R-9382		FJ154733		N/A						
F. acuminatum	R-2165		FJ154735		N/A						
F. agapanthi	**NRRL 54463T**		KU900630		KU900625						
F. ananatum	NRRL 53131		HM347128		HM347213						

Table A1 (continued)

Species	Isolate	GenBank accession numbers									
		ITS	*tef1*	*tub2*	*rpb2*	LSU	*his*	*act*	*cal*	*gapdh*	*chs*
F. andiyazi	**CBS 119857T**		LT996092		LT996138						
F. anthophilum	NRRL 25214		KF466414		KU171696						
F. armeniacum	NRRL 6227		N/A		JX171560						
F. asiaticum	NRRL 13818		N/A		JX171573						
F. avenaceum	NRRL 25128		JF740751		JF741079						
F. begoniae	**CBS 403.97T**		AF160293		LT996140						
F. beomiforme	CBS 740.97		N/A		JX171619						
F. brachygibbosum	FRC R7630		MW233173		MW233517						
F. brachygibbosum	FRC R7637		MW233174		MW233518						
F. brachygibbosum	FRC R8851		MW233198		MW233542						
F. brachygibbosum	NRRL 20954		MW233075		MW233418						
F. bulbicola	**CBS 220.76T**		KF466415		KF466404						
F. burgessii	**CBS 125537T**		N/A		HQ646393						
F. circinatum	**CBS 405.97T**		KM231943		HM068354						
F. clavum	**CBS 126202T**		MN170456		MN170389						
F. coicis	**NRRL 66233T**		KP083251		KP083274						
F. commune	NRRL 52764		JF740838		JF741002						
F. compactum	CBS 185.31		GQ505646		GQ505824						
F. compactum	**CBS 186.31T**		GQ505648		GQ505826						
F. compactum	NRRL 28029		GQ505602		GQ505780						
F. concentricum	**CBS 450.97T**		AF160282		JF741086						
F. culmorum	NRRL 25475		N/A		JX171628						
F. denticulatum	CBS 735.97		AF160269		LT996143						
F. dlaminii	**CBS 119860T**		AF160277		KU171701						
F. equiseti	CBS 107.07		GQ505644		GQ505822						
F. flocciferum	CBS 831.85		N/A		JX171627						

Table A1 (continued)

Species	Isolate	GenBank accession numbers									
		ITS	*tef1*	*tub2*	*rpb2*	LSU	*his*	*act*	*cal*	*gapdh*	*chs*
F. fractiflexum	**NRRL 28852T**		AF160288		LT575064						
F. fujikuroi	**CBS 221.76T**		AF160279		MW834005						
F. gaditjirrii	NRRL 45417		N/A		KU171704						
F. globosum	**CBS 428.97T**		KF466417		KF466406						
F. graminearum	CBS 123657		AY452957		JX171644						
F. hainanense	CBS 131386		MN170510		MN170443						
F. hainanense	CBS 544.96		GQ505598		GQ505776						
F. hainanense	NRRL 28714		GQ505604		GQ505782						
F. hainanense	CGMCC3.19478		MK289581		MK289735						
F. hostae	NRRL 29889		N/A		JX171640						
F. incarnatum	**CBS 132.73NT**		MN170476		MN170409						
F. konzum	**CBS 119849T**		LT996098		LT996148						
F. lacertarum	NRRL 20423		GQ505593		JX171581						
F. lacertarum	**CBS 130185T**		GQ505593		GQ505771						
F. lacertarum	LC7927		MK289637		MK289791						
F. lacertarum	LC7942		MK289643		MK289797						
F. lactis	**CBS 411.97ET**		AF160272		LT996149						
F. lyarnte	NRRL 54252		N/A		JX171661						
F. mangiferae	**NRRL 25226T**		AF160281		JX171622						
F. mexicanum	NRRL 47473		GU737416		LR792615						
F. napiforme	**CBS 748.97T**		AF160266		EF470117						
F. nelsonii	NRRL 13338		GQ505402		JX171561						
F. nisikadoi	NRRL 25179		N/A		JX171620						
F. nygamai	**CBS 749.97T**		AF160273		EF470114						
F. oxysporum	**CBS 716.74T**		AF008479		JX171583						
F. oxysporum	NRRL 25387		HM347117		HM347209						

Table A1 (continued)

Species	Isolate	GenBank accession numbers									
		ITS	*tef1*	*tub2*	*rpb2*	LSU	*his*	*act*	*cal*	*gapdh*	*chs*
F. oxysporum	NRRL 22902		AF160312		LT575065						
F. phyllophilum	**CBS 216.76T**		KF466421		KF466410						
F. poae	NRRL 13714		N/A		JX171572						
F. proliferatum	NRRL 22944		AF160280		HM068352						
F. pseudocircinatum	**NRRL 22946T**		AF160271		N/A						
F. pseudonygamai	**CBS 417.97T**		AF160263		LT996152						
F. ramigenum	**CBS 418.98T**		KF466423		KF466412						
F. redolens	CBS 743.97		MT409452		JX171616						
F. sacchari	**CBS 223.76ET**		AF160278		JX171580						
F. sambucinum	NRRL 22187		MW834277		JX171606						
F. scirpi	NRRL 13402		GQ505592		JX171566						
F. sterilihyphosum	**NRRL 25623T**		AF160300		MN193897						
F. subglutinans	**NRRL 22016T**		AF160289		JX171599						
F. succisae	NRRL 13613		AF160291		LT996154						
F. thapsinum	NRRL 22045		AF160270		JX171600						
F. tjaetaba	**NRRL 66243T**		KP083263		KP083275						
F. torulosum	NRRL 22748		N/A		JX171615						
F. tricinctum	**NRRL 25481T**		HM068307		HM068327						
F. tupiense	**NRRL 53984T**		GU737404		LR792619						
F. udum	NRRL 22949		AF160275		LT996172						
F. venenatum	NRRL 22196		N/A		JX171607						
F. verticillioides	NRRL 22172		AF160262		EF470122						
Neocosmospora ambrosia	NRRL 20438		AF178332		JX171584						
N. ambrosia	NRRL 22346		FJ240350		EU329503						
N. falciformis	NRRL 32757		DQ247075		EU329614						
N. falciformis	NRRL 32828		DQ247135		EU329626						

Table A1 (continued)

Species	Isolate	GenBank accession numbers									
		ITS	*tef1*	*tub2*	*rpb2*	LSU	*his*	*act*	*cal*	*gapdh*	*chs*
N. falciformis	CBS 318.73		JX435158		JX435258						
N. falciformis	NRRL 54219		HQ401721		HQ401723						
N. pisi	**CBS 123669ET**		LR583636		LR583862						
N. solani	NRRL 52778		JF740846		JF741172						
N. solani	**NRRL 66304ET**		KT313611		KT313623						
N. solani	NRRL 32741		DQ247061		EU329608						
N. vasinfecta	NRRL 22436		AF178348		JX171610						
N. vasinfecta	NRRL 43467		EF452940		EF469979						
Bisifusarium delphinoides	CBS 110140		EU926302		HM347219						
B. delphinoides	**CBS 120718T**		EU926296		N/A						
B. delphinoides	CBS 110310		EU926307		N/A						
B. dimerum	**CBS 108944ET**		KR673912		HM347218						
B. nectrioides	CBS 176.31T		EU926312		JX171591						
B. penzigii	CBS 116508		EU926323		HM347217						
Fusicolla aquaeductuum	CBS 734.79		HQ897742		MW847905						
Diaporthe acaciarum	**CBS 138862T**	KP004460	N/A	KP004509					N/A		
D.acerigena	**CFCC 52554T**	MH121489	MH121531	N/A					MH121413		
D.alleghaniensis	**CBS 495.72T**	KC343007	KC343733	KC343975					KC343249		
D.alnea	**CBS 146.46T**	KC343008	KC343734	KC343976					KC343250		
D.batatas	**CBS 122.21T**	KC343040	KC343766	KC344008					KC343282		
D.betulae	**CFCC 50469T**	KT732950	KT733016	KT733020					KT732997		
D.betulina	CFCC 52560	MH121495	MH121537	MH121577					MH121419		
D.bicincta	**CBS 121004T**	KC343134	KC343860	KC344102					KC343376		
D.caryae	**CFCC 52563T**	MH121498	MH121540	MH121580					MH121422		
D.celastrina	**CBS 139.27T**	KC343047	KC343773	KC344015					KC343289		
D.celeris	**CBS 143349T**	MG281017	MG281538	MG281190					MG281712		

Table A1 (continued)

| Species | Isolate | GenBank accession numbers | | | | | | | | | |
		ITS	*tef1*	*tub2*	*rpb2*	LSU	*his*	*act*	*cal*	*gapdh*	*chs*
D.celeris	CBS 143350	MG281018	MG281539	MG281191					MG281713		
D.charlesworthii	**BRIP 54884mT**	KJ197288	KJ197250	KJ197268					N/A		
D.chensiensis	**CFCC 52567T**	MH121502	MH121544	MH121584					MH121426		
D.citri	**CBS 135422T**	KC843311	KC843071	KC843187					KC843157		
D.citrichinensis	**ZJUD34T**	JQ954648	JQ954666	KJ490396					KC357494		
D.collariana	**MFLUCC 17-2636T**	MG806115	MG783040	MG783041					MG783042		
D.conica	**CFCC 52571T**	MH121506	MH121548	MH121588					MH121428		
D.convolvuli	**CBS 124654T**	KC343054	KC343780	KC344022					KC343296		
D.endophytica	**CBS 133811T**	KC343065	KC343791	KC344033					KC343307		
D.eres	AR4369	JQ807440	JQ807366	KJ420813					KJ435005		
D.eres	**CBS 138594T**	KJ210529	KJ210550	KJ420799					KJ434999		
D.eres	CBS 138595	KJ210533	KJ210554	KJ420817					KJ435006		
D.eres	DP0180	JQ807453	JQ807384	KJ420804					KJ435029		
D.eres	DP0438	KJ210532	KJ210553	KJ420816					KJ435016		
D.eres	JZB320029	MK335717	MK523620	MK500177					MK500069		
D.eres	JZB320030	MK335718	MK523621	MK500178					MK500070		
D.eres	JZB320065	MK335749	MK523615	MK500208					MK500101		
D.eres (= D.biguttusis)	**CGMCC 3.17081T**	KF576282	KF576257	KF576306					N/A		
D.eres **(= D.camptothecicola)**	**CFCC 51632T**	KY203726	KY228887	KY228893					KY228877		
D.eres (= D.fukushii)	**MAFF625033T**	JQ807468	JQ807417	KJ420814					KJ435017		
D.eres (= D.longicicola)	**CGMCC 3.17089T**	KF576267	KF576242	KF576291					N/A		
D.eres (= D.lonicerae)	**MFLUCC 17-0963T**	KY964190	KY964146	KY964073					KY964116		
D.eres **(= D.mahothocarpus)**	**CGMCC 3.15181T**	KC153096	KC153087	KF576312					N/A		
D.eres (= D.momicola)	**MFLUCC 16-0113T**	KU557563	KU557631	KU557587					KU557611		

Table A1 (continued)

Species	Isolate	GenBank accession numbers									
		ITS	*tef1*	*tub2*	*rpb2*	LSU	*his*	*act*	*cal*	*gapdh*	*chs*
D.eres (= D.nobilis))	CBS 113470	KC343146	KC343872	KC344114					KC343388		
D.eres (= D.rosicola)	**MFLU 17-0646T**	MG828895	MG829270	MG843877					MG829274		
D.fraxinicola	**CFCC 52582T**	MH121517	MH121559	N/A					MH121435		
D.helianthi	**CBS 592.81T**	KC343115	KC343841	KC344083					KC343357		
D.heterophyllae	CBS 143769	MG600222	MG600224	MG600226					MG600218		
D.kongii	**BRIP 54031T**	JF431301	JN645797	N/A					N/A		
D.maritima	**DAOM 695742T**	KU552025	KU552023	KU574615					MN136126		
D.masirevicii	**BRIP 57892aT**	KJ197276	KJ197239	KJ197257					N/A		
D.melonis	**CBS 507.78T**	KC343142	KC343868	KC344110					KC343384		
D.middletonii	**BRIP 54884eT**	KJ197286	KJ197248	KJ197266					N/A		
D.miriciae	**BRIP 54736jT**	KJ197282	KJ197244	KJ197262					N/A		
D.neilliae	**CBS 144.27T**	KC343144	KC343870	KC344112					KC343386		
D.oraccinii	**CGMCC 3.17531T**	KP267863	KP267937	KP293443					N/A		
D.padina	**CFCC 52590T**	MH121525	MH121567	MH121604					MH121443		
D.penetriteum	**CGMCC 3.17532T**	KP714505	KP714517	KP714529					N/A		
D.phragmitis	**CBS 138897T**	KP004445	N/A	KP004507					N/A		
D.pulla	**CBS 338.89T**	KC343152	KC343878	KC344120					KC343394		
D.sackstonii	**BRIP 54669bT**	KJ197287	KJ197249	KJ197267					N/A		
D.schini	**CBS 133181T**	KC343191	KC343917	KC344159					KC343433		
D.sennicola	**CFCC 51634T**	KY203722	KY228883	KY228889					KY228873		
D.sojae	DP0605	KJ590707	KJ590750	KJ610863					KJ612104		
D.sojae	**FAU635T**	KJ590719	KJ590762	KJ610875					KJ612116		
D.subclavata	**CGMCC 3.17257T**	KJ490630	KJ490509	KJ490451					N/A		
D.terebinthifolii	**CBS 133180T**	KC343216	KC343942	KC344184					KC343458		
D.thunbergiicola	**MFLUCC 12-0033T**	KP715097	KP715098	N/A					N/A		
D.tibetensis	**CFCC 51999T**	MF279843	MF279858	MF279873					MF279888		

Table A1 (continued)

Species	Isolate	GenBank accession numbers									
		ITS	*tef1*	*tub2*	*rpb2*	LSU	*his*	*act*	*cal*	*gapdh*	*chs*
D.ukurunduensis	**CFCC 52592T**	MH121527	MH121569	N/A					MH121445		
D.unshiuensis	**CGMCC 3.17566T**	KJ490584	KJ490463	KJ490405					N/A		
D.unshiuensis	PSCG339	MK626928	MK654879	MK691300					MK691181		
D.unshiuensis	ZJUD52	KJ490587	KJ490466	KJ490408					N/A		
D.unshiuensis	CFCC 52595	MH121530	MH121572	MH121607					N/A		
D.vaccinii	**CBS 160.32T**	KC343228	KC343954	KC344196					KC343470		
D.virgiliae	**CMW40748T**	KP247566	N/A	KP247575					N/A		
Diaporthella corylina	**CBS 121124T**	KC343004	KC343730	KC343972					KC343246		
Phaeoacremonium africanum	CSN946			KY906773				KY906772			
P. africanum	PMM2276			KY906927				KY906926			
P. album	**CBS 142688T**			KY906885				KY906884			
P. album	CBS 142689			KY906925				KY906924			
P. alvesii	CSN1239			KY906785				KY906784			
P. alvesii	CSN1335			KY906801				KY906800			
P. aureum	CBS 142690			KY906799				KY906798			
P. aureum	**CBS 142691T**			KY906657				KY906656			
P. australiense	CSN490			KY906729				KY906728			
P. australiense	CSN657			KY906735				KY906734			
P. bibendum	**CBS 142694T**			KY906759				KY906758			
P. fraxinopennsylvanicum	CSN66			KY906681				KY906680			
P. gamsii	**CBS 142712T**			KY906741				KY906740			
P. geminum	**CBS 142713T**			KY906649				KY906648			
P. geminum	CBS 142717			KY906647				KY906646			
P. globosum	CSN471			KY906725				KY906724			
P. globosum	CSN1258			KY906797				KY906796			
P. griseo-olivaceum	PMM1829			KY906853				KY906852			

Table A1 (continued)

Species	Isolate	GenBank accession numbers									
		ITS	*tef1*	*tub2*	*rpb2*	LSU	*his*	*act*	*cal*	*gapdh*	*chs*
P. griseorubrum	PMM1828			KY906851				KY906850			
P. griseorubrum	PMM1895			KY906875				KY906874			
P. inflatipes	CSN47			KY906665				KY906664			
P. inflatipes	CSN57			KY906675				KY906674			
P. iranianum	CSN170			KY906695				KY906694			
P. iranianum	CSN267			KY906707				KY906706			
P. italicum	CSN59			KY906677				KY906676			
P. italicum	CSN119			KY906691				KY906690			
P. junior	CBS 142695			KY906651				KY906650			
P. junior	CBS 142696			KY906653				KY906652			
P. longicollarum	**CBS 142699T**			KY906689				KY906688			
P. longicollarum	CBS 142700			KY906879				KY906878			
P. meliae	CBS 142709			KY906705				KY906704			
P. meliae	**CBS 142710T**			KY906825				KY906824			
P. minimum	**CBS 246.91T**			AF246811				AY735497			
P. minimum	CBS 100397			AF246806				AY735498			
P. oleae	CBS 142701			KY906719				KY906718			
P. oleae	CBS 142702			KY906771				KY906770			
P. parasiticum	CSN72			KY906683				KY906682			
P. parasiticum	CSN79			KY906687				KY906686			
P. paululum	**CBS 142705T**			KY906881				KY906880			
P. proliferatum	**CBS 142706T**			KY906903				KY906902			
P. proliferatum	CBS 142707			KY906827				KY906826			
P. prunicola	CSN398			KY906717				KY906716			
P. prunicola	CSN719			KY906753				KY906752			
P. rosicola	CBS 142708			KY906831				KY906830			

Table A1 (continued)

Species	Isolate	GenBank accession numbers									
		ITS	*tef1*	*tub2*	*rpb2*	LSU	*his*	*act*	*cal*	*gapdh*	*chs*
P. scolyti	CSN27			KY906661				KY906660			
P. scolyti	CSN55			KY906671				KY906670			
P. sicilianum	CSN 482			KY906727				KY906726			
P. sicilianum	CSN 930			KY906769				KY906768			
P. spadicum	**CBS 142711T**			KY906839				KY906838			
P. spadicum	CBS 142714			KY906667				KY906666			
P. subulatum	CSN42			KY906663				KY906662			
P. subulatum	CSN51			KY906669				KY906668			
P. venezuelense	PMM1138			KY906835				KY906834			
P. viticola	CSN678			KY906745				KY906744			
P. viticola	CSN701			KY906749				KY906748			
Pleurostoma richardsiae	**CBS 270.33T**			AY579334				AY579271			
Coniella africana	**CBS 114133T**	AY339344	AY339364			AY339293	AY339309				
C. crousii	NFCCI2213	HQ264189	N/A			N/A	N/A				
C. diplodiella	**CBS 111858T**	AY339323	AY339355			AY339284	AY339297				
C. diplodiella	CBS 166.84	AY339325	AY339356			AY339285	AY339299				
C. diplodiella	CBS 111857	AY339331	AY339357			AY339286	AY339305				
C. diplodiopsis	**CBS 590.84T**	AY339334	AY339359			AY339288	AY339308				
C. diplodiopsis	CBS 109.23	AY339332	AY339358			AY339287	AY339306				
C. erumpens	**CBS 523.78T**	KX833533	KX833630			KX833361	N/A				
C. eucalyptigena	**CBS 139893T**	KR476725	N/A			KR476760	N/A				
C. eucalyptorum	**CBS 112640T**	AY339338	KX833637			AY339290	N/A				
C. eucalyptorum	CBS 114134	AY339339	AY339361			AY339289	N/A				
C. eucalyptorum	CBS 111023	AY339337	AY339360			KX833363	N/A				
C. fragariae	**CBS 172.49T**	AY339317	AY339352			AY339282	N/A				
C. fragariae	CBS 167.84	AY339318	KX833662			EU754149	N/A				

Table A1 (continued)

Species	Isolate	GenBank accession numbers									
		ITS	*tef1*	*tub2*	*rpb2*	LSU	*his*	*act*	*cal*	*gapdh*	*chs*
C. fusiformis	**CBS 141596T**	KX833576	KX833674			KX833397	N/A				
C. fusiformis	CBS 114850	KX833574	KX833672			KX833395	N/A				
C. granati	CBS 252.38	AY339342	AY339362			AY339291	N/A				
C. granati	CBS 814.71	KX833582	KX833682			AY408380	N/A				
C. javanica	**CBS 455.68T**	KX833583	KX833683			KX833403	N/A				
C. koreana	**CBS 143.97T**	KX833584	KX833684			AF408378	N/A				
C. lanneae	**CBS 141597T**	KX833585	KX833685			KX833404	N/A				
C. limoniformis	**CBS 111021T**	AY339346	KX833686			KX833405	AY339310				
C. macrospora	**CBS 524.73T**	AY339343	AY339363			AY339292	N/A				
C. malaysiana	**CBS 141598T**	KX833588	KX833688			KX833406	N/A				
C. musaiaensis	CBS 109757	KX833589	KX833689			AF408337	N/A				
C. nicotianae	**CBS 875.72T**	KX833590	KX833690			KX833407	N/A				
C. nigra	**CBS 165.60T**	AY339319	KX833691			KX833408	N/A				
C. obovata	CBS 111025	AY339313	KX833692			KX833409	N/A				
C. paracastaneicola	**CBS 141292T**	KX833591	KX833693			KX833410	N/A				
C. paracastaneicola	CPC 25498	KX833592	KX833694			KX833411	N/A				
C. peruensis	**CBS 110394T**	KJ710463	KX833695			KJ710441	N/A				
C. pseudogranati	**CBS 137980T**	KJ869132	N/A			KJ869189	N/A				
C. pseudostraminea	**CBS 112624T**	KX833593	KX833696			KX833412	N/A				
C. quercicola	**CBS 904.69T**	KX833595	KX833698			KX833414	N/A				
C. solicola	**CBS 766.71T**	KX833597	KX833701			KX833416	N/A				
C. sp.	CBS 114006	AY339347	KX833703			AY339295	AY339311				
C. straminea	CBS 149.22	AY339348	AY339366			AY339296	AY339312				
C. tibouchinae	**CBS 131594T**	JQ281774	JQ281778			JQ281776	N/A				
C. tibouchinae	CBS 131595	JQ281775	JQ281779			JQ281777	N/A				
C. vitis	**JZB3700001T**	KX890008	KX890058			KX890083	KX890033				

Table A1 (continued)

| Species | Isolate | GenBank accession numbers | | | | | | | | | |
		ITS	*tef1*	*tub2*	*rpb2*	LSU	*his*	*act*	*cal*	*gapdh*	*chs*
C. vitis	JZB3700002	KX889992	KX890042			KX890067	KX890017				
C. vitis	JZB3700003	KX889993	KX890043			KX890068	KX890018				
C. vitis	JZB3700004	KX889994	KX890044			KX890069	KX890019				
C. vitis	JZB3700005	KX889995	KX890045			KX890070	KX890020				
Melanconiella sp.	CBS 110385	KX833599	KX833707			KX833420	N/A				
Pestalotiopsis adusta	**ICMP 6088T**	JX399006	JX399070	JX399037							
P. adusta	MFLUCC 10-146	JX399007	JX399071	JX399038							
P. anacardiacearum	**IFRDCC 2397T**	KC247154	KC247156	KC247155							
P. arceuthobii	**CBS 434.65T**	KM199341	KM199516	KM199427							
P. arengae	**CBS 331.92T**	KM199340	KM199515	KM199426							
P. australis	**CBS 114193T**	KM199332	KM199475	KM199383							
P. biciliata	**CBS 124463T**	KM199308	KM199505	KM199399							
P. brachiata	**LC2988T**	KX894933	KX895150	KX895265							
P. brassicae	**CBS 170.26T**	KM199379	KM199558	N/A							
P. camelliae	**MFLUCC 12-0277T**	JX399010	JX399074	JX399041							
P. chamaeropis	**CBS 186.71T**	KM199326	KM199473	KM199391							
P. clavata	**MFLUCC 12-0268T**	JX398990	JX399056	JX399025							
P. colombiensis	**CBS 118553T**	KM199307	KM199488	KM199421							
P. diploclisiae	**CBS 115587T**	KM199320	KM199486	KM199419							
P. diversiseta	**MFLUCC 12-0287T**	NR120187	JX399073	JX399040							
P. dracaenicola	**MFLUCC 18-0913T**	MN962731	MN962732	MN962733							
P. dracaenicola	MFLUCC 18-0914	MN962734	MN962735	MN962736							
P. ericacearum	**IFRDCC 2439T**	KC537807	KC537814	KC537821							
P. furcata	**MFLUCC 12-0054T**	JQ683724	JQ683740	JQ683708							
P. gaultheria	**IFRD 411-014T**	KC537805	KC537812	KC537819							
P. grevilleae	**CBS 114127T**	KM199300	KM199504	KM199407							

Table A1 (continued)

Species	Isolate	GenBank accession numbers									
		ITS	*tef1*	*tub2*	*rpb2*	LSU	*his*	*act*	*cal*	*gapdh*	*chs*
P. hawaiiensis	**CBS 114491T**	KM199339	KM199514	KM199428							
P. hollandica	**CBS 265.33T**	KM199328	KM199481	KM199388							
P. humus	**CBS 336.97T**	KM199317	KM199484	KM199420							
P. inflexa	**MFLUCC 12-0270T**	JX399008	JX399072	JX399039							
P. intermedia	**MFLUCC 12-0259T**	JX398993	JX399059	JX399028							
P. kenyana	**CBS 442.67T**	KM199302	KM199502	KM199395							
P. kenyana	CBS 911.96	KM199303	KM199503	KM199396							
P. knightiae	**CBS 114138T**	KM199310	KM199497	KM199408							
P. linearis	**MFLUCC 12-0271T**	JX398992	JX399058	JX399027							
P. malayana	**CBS 102220T**	KM199306	KM199482	KM199411							
P. monochaeta	**CBS 144.97T**	KM199327	KM199479	KM199386							
P. papuana	**CBS 331.96T**	KM199321	KM199491	KM199413							
P. papuana	CBS 887.96	KM199318	KM199492	KM199415							
P. parva	**CBS 265.37T**	KM199312	KM199508	KM199404							
P. parva	CBS 278.35	KM199313	KM199509	KM199405							
P. portugalica	**CBS 393.48T**	KM199335	KM199510	KM199422							
P. rhododendri	**IFRDCC 2399T**	KC537804	KC537811	KC537818							
P. rhodomyrtus	**HGUP4230T**	KF412648	KF412645	KF412642							
P. rhodomyrtus	LC4458	KX895010	KX895228	KX895342							
P. rhodomyrtus	LC3413	KX894981	KX895198	KX895313							
P. rosea	**MFLUCC 12-0258T**	JX399005	JX399069	JX399036							
P. scoparia	**CBS 176.25T**	KM199330	KM199478	KM199393							
P. spathulata	**CBS 356.86T**	KM199338	KM199513	KM199423							
P. telopeae	**CBS 114161T**	KM199296	KM199500	KM199403							
P. trachicarpicola	MFLUCC 12-0264	JX399004	JX399068	JX399035							
P. trachicarpicola	**OP068T**	JQ845947	JQ845946	JQ845945							

Species	Isolate	GenBank accession numbers									
		ITS	*tef1*	*tub2*	*rpb2*	LSU	*his*	*act*	*cal*	*gapdh*	*chs*
P. unicolor	**MFLUCC 12-0276T**	JX398999	N/A	JX399030							
P. verruculosa	**MFLUCC 12-0274T**	JX398996	JX399061	N/A							
Neopestalotiopsis asiatica	**MFLUCC 12-0286T**	JX398983	JX399049	JX399018							
N. australis	**CBS 114159T**	KM199348	KM199537	KM199432							
N. clavispora	**MFLUCC 12-0281T**	JX398979	JX399045	JX399014							
N. ellipsospora	**MFLUCC 12-0283T**	JX398980	JX399047	JX399016							
N. eucalypticola	**CBS 264.37T**	KM199376	KM199551	KM199431							
N. honoluluana	**CBS 114495T**	KM199364	KM199548	KM199457							
N. magna	**MFLUCC 12-0652T**	KF582795	KF582791	KF582793							
N. mesopotamica	**CBS 336.86T**	KM199362	KM199555	KM199441							
N. piceana	**CBS 394.48T**	KM199368	KM199527	KM199453							
N. protearum	**CBS 114178T**	JN712498	KM199542	KM199463							
N. rosae	**CBS 101057T**	KM199359	KM199523	KM199429							
N. rosae	CBS 124745	KM199360	KM199524	KM199430							
N. rosae	JZB340064	MN495972	MN968328	MN968336							
N. samarangensis	**MFLUCC 12-0233T**	JQ968609	JQ968611	JQ968610							
N. saprophytica	**MFLUCC 12-0282T**	KM199345	KM199538	KM199433							
N. surinamensis	**CBS 450.74T**	KM199351	KM199518	KM199465							
N. umbrinospora	**MFLUCC 12-0285T**	JX398984	JX399050	JX399019							
N. zimbabwana	**CBS 111495T**	JX556231	KM199545	KM199456							
Pseudopestalotiopsis cocos	**CBS 272.29T**	KM199378	KM199553	KM199467							
Bartalinia bischofiae	HKUCC 6534	N/A				AF382367					
B. kevinhydei	**MFLUCC 12-0384AT**	MT477057				MT477059					
B. kevinhydei	**MFLUCC 12-0384BT**	MT477058				MT477060					
B. kunmingensis	**KUMCC 18-0178T**	MK353083				MK353085					
B. lateripes	HKUCC 6654	N/A				AF382368					

Table A1 (continued)

Species	Isolate	GenBank accession numbers									
		ITS	*tef1*	*tub2*	*rpb2*	**LSU**	*his*	*act*	*cal*	*gapdh*	*chs*
B. laurina	HKUCC 6537	AF405302				AF382369					
B. pini	**CBS 143891T**	MH554125				MH554330					
B. pini	CFCC 54574	MW364285				MW364276					
B. pondoensis	CMW 31067	NR153599				N/A					
B. robillardoides	CBS 122686	EU552102				N/A					
B. robillardoides	**CBS 122705T**	LT853104				N/A					
B. robillardoides	CNUFC-CNUP1-1	MH482847				MH482853					
B. robillardoides	CNUFC-CNUP1-2	MH482848				MH482854					
B. rosicola	MFLUCC 17-0645	MG828872				MG828988					
Colletotrichum abscissum	**COAD 1877T**	KP843126		KP843135				KP843141		KP843129	KP843132
C. acerbum	**CBS 128530T**	JQ948459		JQ950110				JQ949780		JQ948790	JQ949120
C. acutatum	**CBS 112996T**	JQ005776		JQ005860				JQ005839		JQ948677	JQ005797
C. aenigma	**ICMP 18608T**	JX010244		JX010389				JX009443		JX010044	JX009774
C. aenigma	ICMP 18686	JX010243		JX010390				JX009519		JX009913	JX009789
C. aeschynomenes	**ICMP 17673T**	JX010176		JX010392				JX009483		JX009930	JX009799
C. alatae	**CBS 304.67T**	JX010190		JX010383				JX009471		JX009990	JX009837
C. alienum	**ICMP 12071T**	JX010251		JX010411				JX009572		JX010028	JX009882
C. aotearoa	**ICMP 18537T**	JX010205		JX010420				JX009564		JX010005	JX009853
C. asianum	**ICMP 18580T**	FJ972612		JX010406				JX009584		JX010053	JX009867
C. australe	**CBS 116478T**	JQ948455		JQ950106				JQ949776		JQ948786	JQ949116
C. brisbanense	**CBS 292.67T**	JQ948291		JQ949942				JQ949612		JQ948621	JQ948952
C. cairnsense	**BRIP 63642T**	KU923672		KU923688				KU923716		KU923704	KU923710
C. carthami	**SAPA100011T**	AB696998		AB696992				N/A		N/A	N/A
C. chrysanthemi	IMI 364540	JQ948273		JQ949924				JQ949594		JQ948603	JQ948934
C. clidemiae	**ICMP 18658T**	JX010265		JX010438				JX009537		JX009989	JX009877
C. cordylinicola	**ICMP 18579T**	JX010226		JX010440				HM470235		JX009975	JX009864

Species	Isolate	GenBank accession numbers									
		ITS	*tef1*	*tub2*	*rpb2*	LSU	*his*	*act*	*cal*	*gapdh*	*chs*
C. cosmi	**CBS 853.73T**	JQ948274		JQ949925				JQ949595		JQ948604	JQ948935
C. costaricense	**CBS 330.75T**	JQ948180		JQ949831				JQ949501		JQ948510	JQ948841
C. cuscutae	**IMI 304802T**	JQ948195		JQ949846				JQ949516		JQ948525	JQ948856
C. fioriniae	CBS 125396	JQ948299		JQ949950				JQ949620		JQ948629	JQ948960
C. fioriniae	IMI 324996	JQ948301		JQ949952				JQ949622		JQ948631	JQ948962
C. fioriniae	CBS 126526	JQ948323		JQ949974				JQ949644		JQ948653	JQ948984
C. fructicola	**ICMP 18581T**	JX010165		JX010405				FJ907426		JX010033	JX009866
C. fructicola	ICMP 18613	JX010167		JX010388				JX009491		JX009998	JX009772
C. fructicola	ICMP 18727	JX010179		JX010394				JX009565		JX010035	JX009812
C. gloeosporioides	**IMI 356878T**	JX010152		JX010445				JX009531		JX010056	JX009818
C. gloeosporioides	ICMP 12939	JX010149		N/A				JX009462		JX009931	JX009747
C. gloeosporioides	ICMP 18695	JX010153		N/A				JX009494		JX009979	JX009779
C. godetiae	**CBS 133.44T**	JQ948402		JQ950053				JQ949723		JQ948733	JQ949063
C. hebeiense	**CGMCC 3.17464T**	KF156863		KF288975				KF377532		KF377495	KF289008
C. horii	**ICMP 10492T**	GQ329690		JX010450				JX009438		GQ329681	JX009752
C. johnstonii	**CBS 128532T**	JQ948444		JQ950095				JQ949765		JQ948775	JQ949105
C. kahawae subsp. ciggaro	**ICMP 18539T**	JX010230		JX010434				JX009523		JX009966	JX009800
C. kahawae subsp. ciggaro	ICMP 18534	JX010227		JX010427				JX009473		JX009904	JX009765
C. kahawae subsp. ciggaro	ICMP 12952	JX010214		JX010426				JX009431		JX009971	JX009757
C. kahawae subsp. kahawae	**IMI 319418T**	JX010231		JX010444				JX009452		JX010012	JX009813
C. kinghornii	**CBS 198.35T**	JQ948454		JQ950105				JQ949775		JQ948785	JQ949115
C. laticiphilum	**CBS 112989T**	JQ948289		JQ949940				JQ949610		JQ948619	JQ948950
C. lupini	**CBS 109225T**	JQ948155		JQ949806				JQ949476		JQ948485	JQ948816
C. musae	**CBS 116870T**	JX010146		HQ596280				JX009433		JX010050	JX009896
C. nupharicola	**CBS 470.96T**	JX010187		JX010398				JX009437		JX009972	JX009835
C. nymphaeae	**CBS 515.78T**	JQ948197		JQ949848				JQ949518		JQ948527	JQ948858

Table A1 (continued)

Species	Isolate	GenBank accession numbers									
		ITS	*tef1*	*tub2*	*rpb2*	LSU	*his*	*act*	*cal*	*gapdh*	*chs*
C. nymphaeae	CBS 134234	KC293582		KC293662				KY855974		KC293742	KY856139
C. nymphaeae	CBS 516.78	JQ948198		JQ949849				JQ949519		JQ948528	JQ948859
C. paranaense	**CBS 134729T**	KC204992		KC205060				KC205077		KC205026	KC205043
C. paxtonii	**IMI 165753T**	JQ948285		JQ949936				JQ949606		JQ948615	JQ948946
C. phormii	**CBS 118194T**	JQ948446		JQ950097				JQ949767		JQ948777	JQ949107
C. psidii	**CBS 145.29T**	JX010219		JX010443				JX009515		JX009967	JX009901
C. pyricola	**CBS 128531T**	JQ948445		JQ950096				JQ949766		JQ948776	JQ949106
C. queenslandicum	**ICMP 1778T**	JX010276		JX010414				JX009447		JX009934	JX009899
C. rhombiforme	**CBS 129953T**	JQ948457		JQ950108				JQ949778		JQ948788	JQ949118
C. salicis	**CBS 607.94T**	JQ948460		JQ950111				JQ949781		JQ948791	JQ949121
C. salsolae	**ICMP 19051T**	JX010242		JX010403				JX009562		JX009916	JX009863
C. siamense	**ICMP 18578T**	JX010171		JX010404				FJ907423		JX009924	JX009865
C. siamense	ICMP 17795	JX010162		JX010393				JX009506		JX010051	JX009805
C. simmondsii	**CBS 122122T**	JQ948276		JQ949927				JQ949597		JQ948606	JQ948937
C. sloanei	**IMI 364297T**	JQ948287		JQ949938				JQ949608		JQ948617	JQ948948
C. tamarilloi	**CBS 129814T**	JQ948184		JQ949835				JQ949505		JQ948514	JQ948845
C. temperatum	**CBS 133122T**	JX145159		JX145211				N/A		N/A	N/A
C. temperatum	CBS 133120	JX145135		JX145186				N/A		N/A	N/A
C. theobromicola	**CBS 124945T**	JX010294		JX010447				JX009444		JX010006	JX009869
C. ti	**ICMP 4832T**	JX010269		JX010442				JX009520		JX009952	JX009898
C. tropicale	**CBS 124949T**	JX010264		JX010407				JX009489		JX010007	JX009870
C. viniferum	**GZAAS 5.08601T**	JN412804		JN412813				JN412795		JN412798	N/A
C. viniferum	GZAAS5.08608	JN412802		JN412811				JN412793		JN412800	N/A
C. viniferum	GZAAS5.08616	JN412807		JN412809				JN412790		JN412799	N/A
C. viniferum	GZAAS5.08622	JN412806		JN412812				JN412791		JN412796	N/A
C. walleri	**CBS 125472T**	JQ948275		JQ949926				JQ949596		JQ948605	JQ948936

Species	Isolate	GenBank accession numbers									
		ITS	*tef1*	*tub2*	*rpb2*	LSU	*his*	*act*	*cal*	*gapdh*	*chs*
C. wuxiense	**CGMCC 3.17894T**	KU251591		KU252200				KU251672		KU252045	KU251939
C. wuxiense	JS1A44	KU251592		KU252201				KU251673		KU252046	KU251940
C. xanthorrhoeae	**ICMP 17903T**	JX010261		JX010448				JX009478		JX009927	JX009823
Monilochaefes infuscans	**CBS 869.96T**	JQ005780		JQ005864				JQ005843		JX546612	JQ005801
Alternaria alstroemeriae	MAFF 241374	AB678214	LC275050		LC275231					AB744034	
A. alstroemeriae	**CBS 118809T**	KP124297	KP125072		KP124765					KP124154	
A. alternantherae	CBS 124392	KC584179	KC584633		KC584374					KC584096	
A. alternata	**CBS 916.96ET**	AF347031	KC584634		KC584375					AY278808	
A. alternata	CBS 918.96	AF347032	KC584693		KC584435					AY278809	
A. alternata f. sp. citri pathotype rough lemon	CBS 102595	FJ266476	KC584666		KC584408					AY562411	
A. alternata f. sp. citri pathotype tangerine	CBS 102600	KP124331	KP125107		KP124799					KP124186	
A. arborescens species complex	**CBS 102605T**	AF347033	KC584636		KC584377					AY278810	
A. arborescens species complex	CBS 119544	KP124408	KP125186		KP124878					JQ646321	
A. aspera	**CBS 115269T**	KC584242	KC584734		KC584474					KC584166	
A. betae-kenyensis	**CBS 118810T**	KP124419	KP125197		KP124888					KP124270	
A. botrytis	MAFF 246887	LC440625	LC480252		LC476834					LC482047	
A. botrytis	**CBS 197.67ET**	KC584243	KC584736		KC584476					KC584168	
A. brassicicola	MAFF 246772	LC440585	LC480212		LC476792					LC482007	
A. brassicicola	MUCC 1612	LC440586	AB862981		AB862975					AB862969	
A. burnsii	**CBS 107.38T**	KP124420	KP125198		KP124889					JQ646305	
A. cinerariae	**MAFF 243059T**	AB906673	LC480247		LC476828					AB906670	
A. cinerariae	CBS 116495R	KC584190	KC584648		KC584389					KC584109	

Table A1 (continued)

| Species | Isolate | GenBank accession numbers | | | | | | | | | |
		ITS	*tef1*	*tub2*	*rpb2*	LSU	*his*	*act*	*cal*	*gapdh*	*chs*
A. cucumerina	CBS 117225R	KJ718154	KJ718502		KJ718327					KJ718001	
A. cucumerina	**CBS 116114T**	KJ718153	KJ718501		KJ718326					KJ718000	
A. cumini	**CBS 121329T**	KC584191	KC584650		KC584391					KC584110	
A. dendropanacis	**CNU 085031T**	HQ203210	KP877992		KP877985					KF516506	
A. dendropanacis	CNU 085033	N/A	KP877993		KP877986					KF516507	
A. eichhorniae	**CBS 489.92T**	KC146356	KP125204		KP124895					KP124276	
A. gaisen f. sp. fragariae	MAFF 242310	LC269973	LC275059		LC275239					LC270141	
A. gaisen f. sp. fragariae	MAFF 731003	LC164852	LC167150		LC169133					LC169127	
A. gomphrenae	**MAFF 246769ET**	LC440579	LC480206		LC476782					LC481999	
A. iridiaustralis	**CBS 118486T**	KP124435	KP125214		KP124905					KP124284	
A. iridicola	MUCC 2148	LC269974	LC275060		LC275240					LC270142	
A. iridicola	**MAFF 246890ET**	LC269975	LC275061		LC275241					LC270143	
A. jacinthicola	**CBS 133751T**	KP124438	KP125217		KP124908					KP124287	
A. longipes	CBS 540.94R	AY278835	KC584667		KC584409					AY278811	
A. longipes	CBS 121332R	KP124443	KP125222		KP124913					KP124292	
A. multiformis	**CBS 102060T**	FJ266486	KC584744		KC584484					KC584174	
A. nobilis	CBS 116490R	KC584208	KC584673		KC584415					KC584127	
A. paragomphrenae	**MAFF 246768T**	N/A	LC480207		LC476783					LC482000	
A. penicillata	**CBS 116608T**	FJ357311	KC584698		KC584440					FJ357299	
A. penicillata	CBS 116607	KC584229	KC584706		KC584447					KC584153	
A. perpunctulata	**CBS 115267T**	KC584210	KC584676		KC584418					KC584129	
A. petroselini	**CBS 112.41T**	KC584211	KC584677		KC584419					KC584130	
A. porri	**CBS 116699T**	KJ718218	KJ718564		KJ718391					KJ718053	
A. porri	CBS 116698R	DQ323700	KC584679		KC584421					KC584132	
A. septorioides	**CBS 106.41T**	KC584216	KC584685		KC584427					KC584136	
A. tomato	CBS 114.35	KP124446	KP125225		KP124916					KP124295	

Table A1 (continued)

Species	Isolate	GenBank accession numbers									
		ITS	*tef1*	*tub2*	*rpb2*	LSU	*his*	*act*	*cal*	*gapdh*	*chs*
A. triangularis	**MAFF 246776T**	LC440629	LC480255		LC476837					LC482050	
A. triangularis	AC95	LC440630	LC480256		LC476838					LC482051	
A. vaccariicola	**CBS 118714T**	KC584224	KC584697		KC584439					KC584147	
Paradendryphiella salina	**CBS 302.84T**	JN383486	KC584709		KC584450					JN383467	
Trichoderma acremonioides	**HMAS 279611T**		MH612375		MH612369						
T. acremonioides	HMAS 254562		MH612374		MH612368						
T. afroharzianum	CBS 466.94		KP008851		KP009150						
T. afroharzianum	T22		KP008850		KP009145						
T. asperelloides	CEN1409		MK696647		MK696808						
T. asperellum	CGMCC 6422		KF425756		KF425755						
T. asperellum	**CBS 433.97T**		AY376058		EU248617						
T. asperellum	G.J.S. 90-7		EU338333		EU338337						
T. atrobrunneum	T42		KX632629		KX632572						
T. atrobrunneum	S3		KJ665376		KJ665241						
T. atroviride	**CBS 142.95T**		AY376051		EU241500						
T. aureoviride	C.P.K. 2848		FJ860615		FJ860523						
T. aureoviride	HMAS 266607		KF923280		KF923306						
T. crassum	CBS 114230		JN133572		AY481587						
T. dorothopsis	HZA15		MK850837		MH647805						
T. eijii	HMAS 252876		KJ634775		KJ634742						
T. gamsii	GJS 04-09		DQ307541		JN133561						
T. guizhouense	S278		KF134799		KF134791						
T. guizhouense	**HGUP 0038**		JN215484		JQ901400						
T. hamatum	DAOM 167057		EU279965		AF545548						
T. harzianum	**CBS 226.95T**		AF534621		AF545549						
T. harzianum	TRS55		KP008803		KP009121						

Table A1 (continued)

| Species | Isolate | GenBank accession numbers | | | | | | | | | |
		ITS	*tef1*	*tub2*	*rpb2*	LSU	*his*	*act*	*cal*	*gapdh*	*chs*
T. hispanicum	**CBS 130540T**		JN715659		JN715600						
T. koningiopsis	GJS 93-20		DQ284966		EU241506						
T. laevisporum	HMAS 273756		KU529128		KU529139						
T. longipilis	CBS 120953		FJ860643		FJ860542						
T. longipilis	CBS 135570		KJ665556		KJ665292						
T. olivascens	CBS 132574		KC285624		KC285752						
T. paraviridescens	CBS 132566		KC285671		KC285764						
T. polypori	**HMAS 248855T**		KY688058		KY687994						
T. polypori	HMAS 248861		KY688059		KY688000						
T. propepolypori	**YMF 1.06224T**		MT070158		MT052181						
T. propepolypori	YMF 1.06199		MT070157		MT052182						
T. rogersonii	CBS 119503		FJ860690		FJ860583						
T. samuelsii	**CBS 130537T**		JN715651		JN715599						
T. songyi	SFC20130926-S001		KJ636525		KJ636518						
T. sparsum	HMAS 273759		KU529136		KU529147						
T. sphaerosporum	HMAS 273763		KU529134		KU529145						
T. strictipile	C.P.K. 1601		FJ860704		FJ860594						
T. subviride	HMAS 273761		KU529131		KU529142						
T. tawa	G.J.S 02-79		AY392003		AY391955						
T. tawa	**CBS 114233T**		AY392004		AY391956						
T. tomentosum	S23		KJ665759		KJ665351						
T. tomentosum	S33		KF134801		KF134793						
T. valdunense	CBS 120923		FJ860717		FJ860605						
T. velutinum	C.P.K. 298		KJ665769		KF134794						
T. vinosum	CBS 119087		N/A		KC285779						
T. virens	**CBS 249.59T**		AF534631		AF545558						

Table A1 (continued)

Species	Isolate	GenBank accession numbers									
		ITS	*tef1*	*tub2*	*rpb2*	LSU	*his*	*act*	*cal*	*gapdh*	*chs*
T. virens	DIS 162		FJ463367		FJ442696						
T. virens	CBS 123790		AY750894		EU341804						
T. viride	CBS 119325		DQ672615		EU711362						
T. yunnanense	**CBS 121219T**		GU198243		GU198274						
Protocrea farinosa	CBS 121551		EU703889		EU703935						
Protocrea pallida	CBS 299.78		EU703900		EU703948						
Cladosporium acalyphae	**CBS 125982T**	HM147994	HM148235					HM148481			
C. angustisporum	**CBS 125983T**	HM147995	HM148236					HM148482			
C. asperulatum	**CBS 126340T**	HM147998	HM148239					HM148485			
C. australiense	**CBS 125984T**	HM147999	HM148240					HM148486			
C. chalastosporoides	**CBS 125985T**	HM148001	HM148242					HM148488			
C. chubutense	**CBS 124457T**	FJ936158	FJ936161					FJ936165			
C. cladosporioides	**CBS 112388T**	HM148003	HM148244					HM148490			
C. cladosporioides	CBS 113738	HM148004	HM148245					HM148491			
C. cladosporioides	CBS 143.35	HM148011	HM148252					HM148498			
C. colocasiae	**CBS 386.64T**	HM148067	HM148310					HM148555			
C. colocasiae	CBS 119542	HM148066	HM148309					HM148554			
C. colombiae	**CBS 274.80BT**	FJ936159	FJ936163					FJ936166			
C. cucumerinum	**CBS 171.52T**	HM148072	HM148316					HM148561			
C. delicatulum	CBS 126342	HM148079	HM148323					HM148568			
C. exasperatum	**CBS 125986T**	HM148090	HM148334					HM148579			
C. exile	**CBS 125987T**	HM148091	HM148335					HM148580			
C. flabelliforme	**CBS 126345T**	HM148092	HM148336					HM148581			
C. funiculosum	**CBS 122129T**	HM148094	HM148338					HM148583			
C. gamsianum	**CBS 125989T**	HM148095	HM148339					HM148584			
C. globisporum	**CBS 812.96T**	HM148096	HM148340					HM148585			

Table A1 (continued)

Species	Isolate	GenBank accession numbers										
		ITS	*tef1*	*tub2*	*rpb2*	LSU	*his*	*act*	*cal*	*gapdh*	*chs*
C. hillianum	**CBS 125988T**	HM148097	HM148341					HM148586			
C. inversicolor	**CBS 401.80T**	HM148101	HM148345					HM148590			
C. iranicum	**CBS 126346T**	HM148110	HM148354					HM148599			
C. licheniphilum	**CBS 125990T**	HM148111	HM148355					HM148600			
C. lycoperdinum	CBS 126347	HM148112	HM148356					HM148601			
C. myrtacearum	**CBS 126350T**	HM148117	HM148361					HM148606			
C. oxysporum	CBS 125991	HM148118	HM148362					HM148607			
C. oxysporum	CBS 126351	HM148119	HM148363					HM148608			
C. paracladosporioides	**CBS 171.54T**	HM148120	HM148364					HM148609			
C. perangustum	**CBS 125996T**	HM148121	HM148365					HM148610			
C. phyllactiniicola	**CBS 126352T**	HM148150	HM148394					HM148639			
C. phyllophilum	**CBS 125992T**	HM148154	HM148398					HM148643			
C. pini-ponderosae	**CBS 124456T**	FJ936160	FJ936164					FJ936167			
C. pseudocladosporioides	**CBS 125993T**	HM148158	HM148402					HM148647			
C. rectoides	**CBS 125994T**	HM148193	HM148438					HM148683			
C. rectoides	CBS 126357	HM148194	HM148439					HM148684			
C. scabrellum	**CBS 126358T**	HM148195	HM148440					HM148685			
C. subuliforme	**CBS 126500T**	HM148196	HM148441					HM148686			
C. tenuissimum	**CBS 125995T**	HM148197	HM148442					HM148687			
C. tenuissimum	CBS 126359	HM148198	HM148443					HM148688			
C. tenuissimum	CPC 11555	HM148205	HM148450					HM148695			
C. uredinicola	CPC 5390	AY251071	HM148467					HM148712			
C. varians	**CBS 126362T**	HM148224	HM148470					HM148715			
C. verrucocladosporioides	**CBS 126363T**	HM148226	HM148472					HM148717			
C. vignae	CBS 121.25	HM148227	HM148473					HM148718			
C. xylophilum	**CBS 125997T**	HM148230	HM148476					HM148721			
C. sphaerospermum	CBS 102045	DQ780351	EU570262					EF101378			

APPENDIX B

ABSTRACT OF PUBLICATIONS

Article

Fusarium Species Associated with Cherry Leaf Spot in China

Yueyan Zhou [1,2], Wei Zhang [1], Xinghong Li [1], Shuxian Ji [1], Kandawatte Wedaralalage Thilini Chethana [2], Kevin David Hyde [2] and Jiye Yan [1,*]

[1] Beijing Key Laboratory of Environment Friendly Management on Fruit Diseases and Pests in North China, Institute of Plant Protection, Beijing Academy of Agriculture and Forestry Sciences, Beijing 100097, China
[2] Center of Excellence in Fungal Research, School of Science, Mae Fah Luang University, Chiang Rai 57100, Thailand
* Correspondence: jiyeyan@vip.163.com

Abstract: Sweet cherry is an important fruit crop in China with a high economic value. From 2019 to 2020, a leaf spot disease was reported, with purplish-brown circular lesions in three cultivating regions in China. Twenty-four *Fusarium* isolates were obtained from diseased samples and were identified based on morphological characteristics and multi-locus phylogenetic analyses. Seven species, including *F. luffae* (7 isolates), *F. lateritium* (6 isolates), *F. compactum* (5 isolates), *F. nygamai* (2 isolates), *F. citri* (2 isolates), *F. ipomoeae* (1 isolate) and *F. curvatum* (1 isolate) were identified. The pathogenicity test showed that analyzed strains of all species could produce lesions on detached cherry leaves. Therefore, *Fusarium* was proved to be a pathogen of cherry leaf spots in China. This is the first report of *F. luffae*, *F. compactum*, *F. nygamai*, *F. citri*, *F. ipomoeae* and *F. curvatum* on sweet cherry in China.

Keywords: *Prunus avium*; *Fusarium*; phylogeny; morphology; pathogenicity

1. Introduction

Sweet cherry (*Prunus avium* L.) is an economically important fruit crop widely planted in temperate regions worldwide. The cherry industry in China developed rapidly in the last decade, with 233,000 ha of cultivation area and a yield of 1,700,000 tons in 2019 [1,2]. Even with ideal conditions, various diseases occur on cherries, among which leaf spot is one of the most common and widespread [3]. Since the first report from the USA in 1878, the disease has spread quickly and occurred in most growing areas around the world [4]. The disease causes premature defoliation of leaves, the reduction of tree vigor and winter hardiness, and even tree death, leading to a bad quality of cherries [5]. *Blumeriella jaapii* was regarded as the causal agent of cherry leaf spot disease in Europe and North America [6]. In addition, several other associated fungi were reported. In Israel, the pathogen of cherry leaf spot was identified as *Cercospora circumscissa*, which caused a 40% yield loss in 1975 [7]. Additionally, *Alternaria alternata* and *Pseudocercospora pruni-persicicola* were reported as causing leaf spot in Greece and Korea, respectively [8,9]. In China, *Alternaria cerasi* and *Passalora circumscissa* were identified to cause "black spot" and "brown spot" of sweet cherry according to their morphology in the early days, respectively [10,11]. In recent years, more pathogenic species have been reported based on morphological characterization coupled with phylogenetic analysis, including four *Alternaria* species, three *Colletotrichum* species and four Didymellaceae species [3,12,13]. In this study, *Fusarium* spp. were isolated from cherry leaf spots for the first time, which supplemented the pathogen variety of the disease.

2. Results

2.1. Symptom Observation, Sample Collection and Fungal Isolation

Fifteen leaf spot samples were collected from sweet cherry trees cultured in open fields with the following symptoms, (1) small purple-brownish spots which may merge

Morphological and molecular characterization of *Cladosporium* species on sweet cherry in Beijing, China

Y.Y. Zhou[1,2,3], W. Zhang[1], P.Z. Chen[1], K.W. Thilini Chethana[2,3], X.H. Li[1] and J.Y. Yan[1,a]

[1]Beijing Key Laboratory of Environment Friendly Management on Diseases and Pests of North China Fruits, Institute of Plant Protection, Beijing Academy of Agriculture and Forestry Sciences, Beijing, China; [2]Center of Excellence in Fungal Research, Mae Fah Luang University, Chiang Rai, Thailand; [3]School of Science, Mae Fah Luang University, Chiang Rai, Thailand.

Abstract

Cladosporium is a ubiquitous fungal genus with a wide ecological distribution and host range, which plays different roles as pathogen, endophyte and saprobe. The objective of this study was to characterize *Cladosporium* species isolated from sweet cherry (*Prunus avium*) with leaf spot symptoms, using morphological characteristics and phylogenetic analyses based on the internal transcribed spacers (ITS), partial actin (*act*) and translation elongation factor-1α (*tef1*) gene regions. A total of six species, *C. anthropophilum*, *C. asperulatum*, *C. cladosporioides*, *C. ramotenellum*, *C. rectoides* and *C. tenuissimum*, were identified including five new host records except for *C. cladosporioides*. The present study enhances the knowledge of fungal species associated with sweet cherry.

Keywords: *Prunus avium*, *Cladosporium* species, morphology, phylogeny

INTRODUCTION

Cladosporium is a monophyletic genus in *Cladosporiaceae*. It is one of the largest genera of dematiaceous hyphomycetes with coronate structure, conidia in acropetal chains and *Davidiella* teleomorphs (David 1997; Bensch et al., 2010). Currently, there are 896 records of *Cladosporium* species in the Index Fungorum (https://www.indexfungorum.org/; accessed on 25 October 2023). Cladosporium species have been isolated from a wide range of substrates including plants, soil, food, clinical and other samples, as well as outdoor and indoor air (Bensch et al., 2012; Sandoval-Denis et al., 2016; Bensch et al., 2018).

Members of *Cladosporium* exist on various plants as saprobes, endophytes and pathogens (Bensch et al., 2012). Leaf spots caused by *Cladosporium* species have been observed in many plants, including vegetables like spinach (du Toit and Derie, 2012), ornamental crops like carnation (Xie et al., 2022), and forage crops like alfalfa (Han et al., 2019). In addition, some of the species showed antagonistic potential on phytopathogens. For example, *C. cladosporioides* could reduce apple scab in leaves and fruits (Köhl et al., 2015), and *C. herbarum* has the biocontrol ability of Eutypa dieback of grapevine (Munkvold and Marois, 1993).

Sweet cherry (*Prunus avium*) is a vital fruit crop cultivated widely in temperate regions of Asian, European, and American countries. Various fungi associated with sweet cherries have been reported as pathogens or endophytes (Aghdam and Fotouhifar, 2017; Chethana et al., 2019). However, few reports of *Cladosporium* were on sweet cherry. Only *C. cladosporioides* and *C. phyllophilum* were reported to be isolated from imported buds of sweet cherry (Bensch et al., 2012).

The current study focuses on *Cladosporium* species associated with sweet cherry by morphological observation and multi-locus phylogenetic analyses, revealing the re-occurrence of this taxa.

---

[a]E-mail: jiyeyan@vip.163.com

Diversity of Fungal Communities Associated with Grapevine Trunk Diseases in China

Zhou YY[1,2,3±], Zhang W[1±], Wu LN[1±], Zhang J[1], Tan HY[1], Chethana KWT[2,3], Manawasinghe IS[4], Liu M[1], Li XH[1] and Yan JY[1*]

[1]*Beijing Key Laboratory of Environment Friendly Management on Diseases and Pests of North China Fruits, Institute of Plant Protection, Beijing Academy of Agriculture and Forestry Sciences, Beijing 100097, China*
[2]*Center of Excellence in Fungal Research, Mae Fah Luang University, Chiang Rai 57100, Thailand*
[3]*School of Science, Mae Fah Luang University, Chiang Rai 57100, Thailand*
[4]*Innovative Institute for Plant Health, Zhongkai University of Agriculture and Engineering, Guangzhou 510225, China*

Abstract

Grapevine trunk diseases (GTDs) are one kind of the most common and destructive diseases worldwide which challenge the sustainable development of the grape industry and cause serious economic loss. From 2020 to 2022, grapevine trunk disease samples were collected from eight provinces in China and associated fungi were identified based on phylogenetic analyses and morphological observations. A total of 199 isolates were obtained, representing 40 species belonging to 21 genera in 10 families. Twenty-one species are reported as the first records in China and 13 as the first records on grapevine worldwide. *Diaporthe*, Botryosphaeriaceae, *Cylindrocarpon*-like and *Fusarium*-like genera were the most frequently isolated taxa. *Bartalinia*, *Botryosphaeria* and *Dactylonectria* species were widely distributed in China. The study provides an insight into the diversity of fungal species on the diseased grapevine, among which some may play the role of common or potential pathogens, endophytes, and saprobes. Relevant results provide the basis for further research on the interactions among fungal communities and strategies for managing grapevine trunk diseases.

Keywords – diversity – grapevine trunk diseases – morphology – new records – phylogenetic analyses

Introduction

Grapevine (*Vitis* spp.) is one of the most widely planted and economically important fruit crops in the world since historic times and served as table fruits or processed into vine and raisin (Gramaje et al. 2018). China ranks third among grape-cultivation countries, with a cultivation area of 783 Kha in 2021 (OIV 2022) with 15 million metric tons of annual production. However, *Vitis* species are susceptible to many fungal diseases. Among these, the grapevine trunk diseases (GTDs) are one of the most destructive diseases in the world, which have drawn considerable attention in the last decades (Reis et al. 2019). They reduce vineyard longevity, productivity and quality, and the loss caused is estimated to be $1.5 billion per year (Hofstetter et al. 2012, Dissanayake et al. 2015a). The grapevine trunk diseases include a group of diseases associated with diverse vascular

pathogens

MDPI

Article

Characterization of Fungal Pathogens Causing Blueberry Fruit Rot Disease in China

Yueyan Zhou [1,2,3], Wei Zhang [1], Linna Wu [1], Pengzhao Chen [1], Xinghong Li [1], Guangqin Wen [4], Khanobporn Tangtrakulwanich [3], Kandawatte Wedaralalage Thilini Chethana [2,3,*], Fatimah Al-Otibi [5], Kevin D. Hyde [2,5] and Jiye Yan [1,*]

1 Beijing Key Laboratory of Environment Friendly Management on Fruit Diseases and Pests in North China, Institute of Plant Protection, Beijing Academy of Agriculture and Forestry Sciences, Beijing 100097, China; 6471105009@lamduan.mfu.ac.th (Y.Z.); zhangwei@baafs.net.cn (W.Z.); guiwawa4567@outlook.com (L.W.); ppchen9609@outlook.com (P.C.); lixinghong@baafs.net.cn (X.L.)
2 Center of Excellence in Fungal Research, Mae Fah Luang University, Chiang Rai 57100, Thailand; kdhyde3@gmail.com
3 School of Science, Mae Fah Luang University, Chiang Rai 57100, Thailand; khanobporn.tan@mfu.ac.th
4 Botanical Garden of Guizhou Province, Guiyang 550025, China; lanmei8588@126.com
5 Department of Botany and Microbiology, College of Science, King Saud University, P.O. Box 22452, Riyadh 11495, Saudi Arabia; falotibi@ksu.edu.sa
* Correspondence: kandawatte.thi@mfu.ac.th (K.W.T.C.); yanjiye@baafs.net.cn (J.Y.)

Abstract: Blueberry has been a burgeoning fruit in China in recent years, but its perishable nature places a constant strain on industrial development. To determine the pathogens infecting blueberry fruits, diseased samples were collected from Guizhou and Fujian Provinces. Isolates from the samples were identified by morphological characterization and phylogenetic analyses. Pathogenicity assays were conducted on fresh blueberry fruits using spore suspensions. Sixteen isolates were identified as seven species, namely, *Botryosphaeria dothidea*, *Botrytis cinerea*, *Cladosporium guizhouense*, *Colletotrichum fioriniae*, *Diaporthe anacardii*, *Fusarium annulatum*, and *Neopestalotiopsis surinamensis*, and their pathogenicity on blueberry fruits were confirmed following Koch's postulates. The current study reported *Cladosporium guizhouense*, *Fusarium annulatum*, and *Neopestalotiopsis surinamensis* for the first time on blueberry. The study (1) demonstrated that fruit rot disease results from a mixed infection of multiple pathogens; and (2) expanded the understanding of causal agents of blueberry fruit rot during the growth stage, highlighting their potential as latent pathogens that contribute to post-harvest losses. Relevant results provide a reference for the etiological research and disease management in blueberry fruit diseases.

Keywords: *Vaccinium* spp.; new host records; phylogenetic analysis; pathogenicity

1. Introduction

Blueberry (*Vaccinium* spp.) has been cultivated for more than 100 years, and the industry has developed rapidly in the recent years, with the global production more than doubling in the last decade (U.S. Department of Agriculture 2021). As of 2023, the global cultivation area of blueberry comes up to 262,417 hectares, with a global production of 1.78 million tons, and China is ranked first, producing 0.56 million tons (International Blueberry Organization 2024). Blueberries are recognized as a "superfruit" for their rich nutrients, including vitamins (C and K), minerals (calcium, iron, magnesium, manganese, and zinc), dietary fiber (2.4–3.5% of fruit weight), and polyphenols (anthocyanins and flavonols) [1]. Specifically, anthocyanin flavonoids, which account for up to 60% of the total

plants

Article

Three New Records of Pathogens Causing Stem Blight on *Vaccinium corymbosum* in China

Yueyan Zhou [1,2,3], Linna Wu [2], Kaixuan Ren [2], Meng Wang [2], Nannan Wang [2], Khanobporn Tangtrakulwanich [1], Xinghong Li [2], Kandawatte Wedaralalage Thilini Chethana [1,3,*], Kevin D. Hyde [3], Wei Zhang [2,*] and Jiye Yan [2]

[1] School of Science, Mae Fah Luang University, Chiang Rai 57100, Thailand
[2] Beijing Key Laboratory of Environment Friendly Management on Fruit Diseases and Pests in North China, Institute of Plant Protection, Beijing Academy of Agriculture and Forestry Sciences, Beijing 100097, China
[3] Centre of Excellence in Fungal Research, Mae Fah Luang University, Chiang Rai 57100, Thailand
* Correspondence: kandawatte.thi@mfu.ac.th (K.W.T.C.); zhangwei@baafs.net.cn (W.Z.)

Abstract: Stem blight is a significant disease affecting blueberries worldwide, caused by various pathogens. This study investigated stem blight disease in Ji'an, Jilin Province, China. Fungi isolated from diseased stems were identified as *Colletotrichum temperatum*, *Curvularia austriaca*, and *Diaporthe unshiuensis* based on morphological characters and multi-locus phylogenetic analyses using the internal transcribed spacer (ITS) region, glyceraldehyde 3-phosphate dehydrogenase (*gapdh*), chitin synthase (*chs*), actin (*act*), β-tubulin (*tub2*), the translation elongation factor 1-alpha (*tef1-α*), calmodulin (*cal*), and histone 3 (*his3*) regions. Pathogenicity test was conducted on detached green blueberry shoots, all shoots inoculated by mycelium plugs presented necrotic lesions with dark brown margins, while the control (PDA plugs) group did not show any symptoms. Koch's postulates were confirmed by re-isolating the inoculated pathogen from the disease symptoms. The study provides three new host–pathogen records of fungi associated with blueberry stem blight.

Keywords: *Colletotrichum*; *Curvularia*; *Diaporthe*; morphology; phylogeny; Koch's postulates; new host records

1. Introduction

Blueberry (*Vaccinium* spp.), well known for its rich bioactive compounds that promote health, is widely recognized as a "super fruit" [1]. The high nutritional and economic value of blueberries has driven rapid development in the blueberry industry. Over the past five years, the global area under cultivation and blueberry yield increased from 198,817 ha and 1.28 million tons to 262,417 ha and 1.78 million tons, respectively [2]. In China, blueberries are now planted in 26 of 34 provinces [3].

Despite the high resilience of blueberries, various diseases inevitably emerge throughout their lifespan, including fruit rot, stem blight, leaf spot, powdery mildew, and root rot, which pose serious threats to plant health [4]. Among these various diseases, stem blight is both common and severe, resulting in reduced production and economic losses [5]. In New Zealand, the disease incidence has reached 18%, causing $500,000 in annual losses [6]; in Chile, the incidence rate ranges from 15 to 45% [7]. As the top producer of blueberries, China also suffered 10% to 25% of crop damage from the disease [8].

Stem blight is caused by several fungal pathogens that infect plants through wounds or natural openings, leading to vascular damage, wood discoloration, and even the death of the plant [5,9]. As a general term, stem blight is also known as stem canker or dieback. Typical symptoms of the disease are reddish-brown to gray-brown lesions on stems, shoots, or

CURRICULUM VITAE

NAME   Yueyan Zhou

EDUCATIONAL BACKGROUND

2018-2021   Master of Agriculture

Resource Utilization and Plant Protection

College of Plant Protection,

Agricultural University, China

2014-2018   Bachelor of Agriculture

Plant Protection

College of Agriculture,

Northeast Agricultural University, China

PUBLICATIONS

First Author

Yueyan Zhou et al., Micro-fungi associated with Blueberry diseases in China
    [Manuscript preparation]. Mae Fah Luang University.

Zhou, Y., Wu, L., Ren, K., Wang, M., Wang, N., Tangtrakulwanich, K., . . . Yan, J.
    (2025). Three new records of pathogens causing stem blight on *Vaccinium*
    corymbosum in China. *Plants, 14*(5), 647.
    https://doi.org/10.3390/plants14050647

Zhou, Y., Zhang, W., Chen, P., Chethana, K. W. T., Li, X., & Yan, J. (2024).
    Morphological and molecular characterization of *Cladosporium* species on
    sweet cherry in Beijing, China. *Acta Horticulturae, 1408*, 511–524.
    https://www.actahort.org/books/1408/1408_68.htm

Zhou, Y., Zhang, W., Li, X., Ji, S., Chethana K. W. T., Hyde, K. D., . . . Yan, J.
    (2022). *Fusarium* species associated with cherry leaf spot in China.
    Plants, 11, 2760. https://doi.org/10.3390/plants11202760

Zhou, Y., Zhang, W., Wu, L., Chen, P., Li, X., Wen, G., . . . Yan, J. (2025).
    Characterization of fungal pathogens causing blueberry fruit rot disease in
    China. *Pathogens, 14*(2), 201. https://doi.org/10.3390/pathogens14020201

Zhou, Y., Zhang, W., Wu, L., Zhang, J., Tan, H., Chethana, K. W. T., . . . Yan, J. (2023). Diversity of fungal communities associated with grapevine trunk diseases in China. *Mycosphere, 14*(1), 1340–1435. https://doi.org/10.5943/mycosphere/14/1/15

Co-author

Chen, P., Abeywickrama, P. D., Ji, S., Zhou, Y., Li, X., Zhang, W., . . . Yan, J. (2023). Molecular identification and pathogenicity of *Diaporthe eres* and *D. hongkongensis* (Diaporthales, Ascomycota) associated with cherry trunk diseases in China. *Microorganisms, 11*(10), 2400. https://doi.org/10.3390/microorganisms11102400

He, Z., Abeywickrama, P. D., Wu, L., Zhou, Y., Zhang, W., Yan, J., . . . Li, S. (2024). Diversity of *Cytospora* species associated with trunk diseases of *Prunus persica* (peach) in Northern China. *Journal of Fungi, 10*(12), 843. https://doi.org/10.3390/jof10120843

Jayawardena, R. S., Hyde, K. D., Aumentado, H. D. R., Abeywickrama, P. D., Avasthi, S., … Zhou, Y., . . . Wang, Y. (2025). One stop shop V: Taxonomic update with molecular phylogeny for important phytopathogenic genera: 101–125 (2024). *Fungal Diversity, 130*, 263–429. https://doi.org/10.1007/s13225-024-00542-x

Manawasinghe, I. S., Hyde, K. D., Wanasinghe, D. N., Karunarathna, S. C., Maharachchikumbura, S. S. N., … Zhou, Y., . . . Xu, B. (2024). Fungal diversity notes 1818–1918: Taxonomic and phylogenetic contributions on genera and species of fungi. *Fungal Diversity, 130*, 1–261. https://doi.org/10.1007/s13225-024-00541-y

Manawasinghe, I. S., Jayawardena, R. S., Li, H. L., Zhou, Y., Zhang, W., Phillips, A. J. L., . . . Yan, J. Y. (2021). Microfungi associated with *Camellia sinensis*: A case study of leaf and shoot necrosis on tea in Fujian, China. *Mycosphere, 12*(1), 430–518. https://doi.org/10.5943/mycosphere/12/1/6

Zhang, W., Chen, P., Zhou, Y., Manawasinghe, I. S., Ji, S., Li, X., . . . Yan, J. (2025). Morpho-molecular characterization and pathogenicity of fungi associated with sweet cherry (*Prunus avium*) trunk diseases in China. *Mycosphere, 16*(1), 169–244. https://doi.org/10.5943/mycosphere/16/1/3